Scenes from the Life of Moses, detail of the Daughters of Jethro by Sandro Botticelli *– Fresco in the Sistine Chapel 1480s. This exquisite scene depicts a young girl obviously in pain as is depicted by the facial expression and red glow in her cheeks, The girdle she wears consists of apples, the symbol of fertility and acorns symbolising slow growth and long duration. This is believed to depict and fend off infertility and chronic pelvic pain which are two of the most important manifestations of endometriosis.*

A study of Gene, Protein and miRNA alterations in women with Endometriosis

PhD Thesis

Submitted in partial fulfilment of the requirements of the Degree of Doctor of Philosophy

Student:
Dr. Christine Anna Maria Schembri Deguara

Academic Supervisor:
Professor Finbarr Cotter MB, BS, FRCP (UK), FRCPath, FRCP(I) PhD

Clinical Supervisor:
Mr. Colin Davis MBBS FRCOG MD

Patent information

Patent reference	**P063434GB**
Name, address and postcode of the applicant	Queen Mary University of London Mile End Road London E1 4NS United Kingdom
Title of the invention	Biomarkers for Endometriosis
Inventors	Dr. Christine Anna Maria Schembri Deguara Professor Finbarr Cotter MB, BS, FRCP (UK), FRCPath, FRCP(I) PhD Mr. Colin Davis MBBS FRCOG MD

Statement of originality

I, Christine Anna Maria Schembri Deguara, confirm that the research included within this thesis is my own work or that where it has been carried out in collaboration with, or supported by others, that this is duly acknowledged below and my contribution indicated. Previously published material is also acknowledged below.

I attest that I have exercised reasonable care to ensure that the work is original, and does not to the best of my knowledge break any UK law, infringe any third party's copyright or other Intellectual Property Right, or contain any confidential material.

I accept that the College has the right to use plagiarism detection software to check the electronic version of the thesis.

I confirm that this thesis has not been previously submitted for the award of a degree by this or any other university.

Signature: _____

Date:

Details of collaboration and publications:

2010-2011	Edited and updated Shaw's Textbook of Gynaecology on the following areas: • Surgery of other benign conditions of the uterine appendages including pelvic inflammatory disease • Treatment of ectopic pregnancy • Sterilisation Operations • Infertility
2011	First author: "Laparoscopic entry techniques" Current Opinion in Obstetrics & Gynaecology
2012	First author: "Does minimally invasive surgery for endometriosis improve pelvic symptoms and quality of life?" Current Opinion in Obstetrics & Gynaecology
2012	Second author: "Update on the surgical management of adenomyosis" Current Opinion in Obstetrics & Gynaecology
2013	First author: "Measured symptomatic and psychological outcomes in women undergoing laparoscopic surgery for endometriosis-A prospective study" Current Opinion in Obstetrics & Gynaecology

Abstract

The aim of this thesis was to improve understanding of the underlying genetic and proteomic alterations potentially contributing to endometriosis. Assessment of the genetic mechanisms and pathways controlling angiogenesis, apoptosis and inflammation allowed identification of potential aberrations contributing to disease.

Tissue miRNA expression experiments show that, the ebv-mir-BART2-5p is detected in endometriosis. Endometriosis cells contained higher levels of ebv-mir-BART2-5p compared to eutopic endometrium and this finding was confirmed by quantitative PCR. In situ hybridisation for EBV on tissue microarrays did not confirm the presence of active EBV within the endometriotic epithelial cells (Figure 4-24) but 5 of the 42 endometriotic samples on TMA-A gave a positive reading for EBV presence in some of the lymphocytes. PCR on the peripheral blood monocytes confirms overall higher levels of EBV DNA in the monocytes of people with endometriosis compared to controls (see Table 9-39 in the Appendix). There were no detected EBV levels in the surgically confirmed control patient samples. The presence of ebv-mir-BART2-5p is a permissive event for the development of endometriosis potentially acting as an initiator for engraftment of endometrial cells to the peritoneum causing the development of endometriosis. It also aids in disease development by suppressing T-cell function and encouraging adhesions and angiogenesis in affected tissues. Alterations in cellular genotype also enable the ectopic endometrial cells to evade NK cells and Lymphocytes, promoting proliferation and metastasis. Effects of genes on various stages of the cell cycle checkpoints and pathways have been explored as contributors to disease development.

Downstream proteins from EBV upregulation are also confirmed to be affected. Tissue microarray studies demonstrate the upregulation of Cyclin D1 (Figure 4-22) and downregulation of E-Cadherin, Maspin and BCLAF-1) (Figure 4-11, Figure 4-13 and Figure 4-15). Galectin 3 (a prominent anti-apoptotic and angiogenic member of the lectin family) proteins were also upregulated in endometriosis. Galectin-3 had already been shown to be a good therapeutic target in humans and may provide alternatives to current surgical or hormonally repressive therapy. A set of *in vitro* experiments have been performed and show effective disease repression with Galectin therapeutics (Galectin 3 inhibitor GCS-100), potentially opening a window for the development of novel therapeutics.

Serum was analysed for miRNA and antibody protein expression profiles. Pathways linked to identified biomarkers have been explored aiding in the understanding of disease development at a molecular level. Identified miRNAs are seen to interact with a number of important pathways listed below. There could potentially be effects on cellular mitosis and meiosis, cellular structure, intra and intercellular signalling, vesicular transport including exo and endocytosis and cellular apoptosis. All of these changes can result in endometriotic cells that replicate at accelerated rates, adhere to ectopic sites, enable angiogenesis and growth, evade normal apoptotic mechanisms and evade immune responses. Certain identified pathways act as tumour suppressors that could potentially explain the non-malignant properties in the majority of cases of endometriosis. These include the p38 MAPK[1] pathway and the p53 tumour suppressor genes[2]. Other pathways involved are known to be associated with tumorigenesis and have pro-oncogenic properties, these include the RAS, WNT, TRK receptors and MAPKKKK pathways. It is the fine balance

between tumour suppressors and oncogenes that probably control the transition between endometriosis and endometrial carcinomas. Identification of protein and miRNA expression profiles predicting the presence of endometriosis allowed us to work towards developing a panel of non-invasive biomarkers (Patent P063434GB) for earlier identification and treatment of disease and aids in unlocking new methods of molecular targeting as treatment.

Acknowledgements

I would like to express my special appreciation and thanks to my mentors and advisors Professor Finbarr Cotter and Mr. Colin Davis. It has been an honour to work side by side with two brilliant people who I look up to and greatly admire. You believed in me, taught me, encouraged and supported me throughout challenging times. For this I am forever grateful.

I would like to thank my colleagues Suzanne Mc Mahon, Sameena Iqbal, Andrew Clear and Jacek Marzek. You have always been there for me. You have offered support and guidance when I felt completely out of my depth and made my path smoother and more enjoyable. I thank you for the endless hours out of your free time which you gave up selflessly to provide me with the help I needed. You have thought me patiently and been at the end of a line at all hours. I will always regard you as not only some of the most intelligent and kind-hearted people I have had the pleasure of knowing but also as good friends. I hope life rewards your kindness.

Special thanks go to my family. Words cannot express how grateful I am to my parents and aunt for all of the sacrifices that you have made throughout my life. You have always instilled in me a sense of adventure and awe at the world around me. You have taught me to be inquisitive and you have always shown me that challenges make you a richer person and enable you to grow stronger. A special thank you goes to my father who spent endless hours proof-reading a thesis without giving up on me!

Finally, I would like express appreciation to my beloved husband Rudi. You are and have always been my rock. I thank you for all those lost weekends, holidays and sleepless nights you have given up selflessly to help me succeed. You have supported me through the rough patches of self-doubt and always encouraged me to go on, telling me how proud you were of what I was doing. I could not have gone through this without you.

Table of contents

Table of figures

Abbreviations

17β-HSD	17β-hydroxysteroid dehydrogenase type 2
2-DE gels	Two-dimensional gel electrophoresis
ABRA	Actin-binding rho-activating protein
ACO1	Cytoplasmic aconitate hydratase
ACSL6	Long-chain-fatty-acid-CoA ligase 6
ADCYAP1R1	Pituitary adenylate cyclase-activating polypeptide type I receptor
ADIPOR2	Adiponectin receptor protein 2
ALDOA	Aldolase A, Fructose-Bisphosphate
ANA	Antinuclear antibodies
ANOVA	Analysis of variance
AP-1	Activating protein-1
Apaf1	Apoptotic protease activating factor 1
ARA24	Androgen receptor
ARF	ADP-ribosylation factor
ASRM	American Society of Reproductive Medicine
ATF2	Activating transcription factor 2
ATXN3	Ataxin3
AUC	Area under curve
BAI2	Brain-specific angiogenesis inhibitor 2
BASP1	Brain acid soluble protein 1
Bax	The Bcl-2-associated X protein gene
BCAR1	Breast Cancer Anti-Oestrogen Resistance 1
Bcl-2	B-cell lymphoma 2
BCLAF	Bcl-2-associated transcription factor
BIRC2	Baculoviral inhibitor of apoptosis proteins repeat-containing 2
BLCAP	Bladder cancer-associated protein
BRG1	Brahma related gene 1
BSA	Bovine serum albumin
BTRC	F-box/WD repeat-containing protein 1A
C17orf48	Manganese-dependent ADP-ribose/CDP-alcohol diphosphatase
C19orf50	Chromosome 19 open reading frame 50
C1orf106	Uncharacterized protein C1orf106
C1q	Complement component C1
C6orf136	Uncharacterized protein C6orf136
CA	Carbonic anhydrase
CA 19-9	Cancer Antigen 19-9
CA-125	Cancer Antigen 125
CACNA2D2	Voltage-dependent calcium channel subunit alpha-2/delta-2
CAN5	Calpain-5
CARD	Caspase recruitment domain
CARMA1	Membrane-associated guanylate kinase protein 1
CASP10	Caspase 10, Apoptosis-Related Cysteine Peptidase
CASP6	Caspase 6
CAST	Calpastatin
CBFA2T1	Core-binding factor, runt domain, alpha subunit 2; translocated to,1
CCNB1IP1	Cyclin B1 Interacting Protein 1, E3 Ubiquitin Protein Ligase
CCR1	Cognate chemokine receptor-1
CD36	Cluster of differentiation 36
CD54	Cluster of Differentiation 54

CDC25B	Cell division cycle 25B
CDKs	Cyclin-dependent kinases
cDNA	Complimentary DNA
CENPP	Centromere protein P
CIP	Calf intestinal alkaline phosphatase
CLC4F	C-type lectin domain family 4 member F
CLIC4	Chloride intracellular channel protein 4
CMV	Cytomegalovirus
CNGB3	Cyclic nucleotide-gated cation channel beta-3
COCP	Combined Oral Contraceptive Pill
COPB1	Coatomer subunit beta
COX-2	Cyclo-oxygenase type 2
CPA6	Carboxypeptidase A6
CRD	Carbohydrate Binding Domain
CREB1	Cyclic AMP-responsive element-binding protein
CTH	Cystathionine gamma-lyase
CTNNB1	Catenin beta-1
CTXN2	Cortexin-2
CUX1	Homeobox protein cut-like 1
CV	Coefficient of variation
CXCL6	C-X-C motif chemokine 6
Cy3	Cyanine dye 3
CYTH2	Cytohesin-2
DAB	Diaminobenzidine
DCAF6	DDB1- and CUL4-associated factor 6
DES	Diethylstilbestrol
DISC	Death-inducing signalling complex
DMEM	Dulbecco's Modified Eagle Medium
DMSO	Dimethylsulphoxide
DNA	Deoxyribonucleic Acid
dNTP	Deoxynucleotide Solution Mix
DPX	Distyrene, tricresyl phosphate and xylene
DRP2	Dystrophin-related protein 2
dTTP	Deoxythymidine triphosphate
DUSP4	Dual specificity protein phosphatase 4
DYNC1LI2	Cytoplasmic dynein 1 light intermediate chain 2
DYRK1A	Dual specificity tyrosine-phosphorylation-regulated kinase 1A
EBNA	Epstein-Barr nuclear antigens
EBV	Epstein–Barr virus
EGF	Epidermal growth factor
EIF4EBP1	Eukaryotic translation initiation factor 4E binding protein 1
ELISA	Enzyme-linked immunosorbant assay
ENSA	Alpha-endosulfine
EP2	Prostaglandin E2 pathway
EPB41L5	Erythrocyte membrane protein band 4.1-like protein 5
EPF	Early-pregnancy factor
Erα	Estrogen receptor-α
Erβ	Estrogen receptor-β
ES	Endometriosis
ESHRE	European Society of Human Reproduction and Embryology
ESR1	Estrogen receptor 1
FADD	Fas Associated Via Death Domain

FAK	Focal adhesion kinase
FAM3C	Family with sequence similarity 3, member C1
FasL	Fas ligand
FBS	Foetal Bovine Serum
FC	Fold change
FCS	Fetal calf serum
FDR	False discovery rate
FNA	Fine needle aspiration
FNDC3B	Fibronectin type III domain-containing protein 3B
FSH	Follicle stimulating hormone
FYCO1	FYVE and coiled-coil domain-containing protein 1
GGPS1	Geranylgeranyl Diphosphate Synthase 1
GIT1	ARF GTPase-activating protein GIT1
GlcNAc	N-Acetylglucosamine
GMEB1	Glucocorticoid modulatory element binding protein 1
GnRH	Gonadotrophin Releasing Hormone
GOLGA3	Golgin subfamily A member 3
GOLGA8A	Golgin subfamily A member 8A
GOPD.	Gynaecology out-patient department
GP	General practitioner
GREB1	Growth Regulation By Estrogen In Breast Cancer
GSTM1	Glutathione S-transferase Mu 1
HLA-DR	Human leukocyte antigen DR receptor
HNF1	Hepatocyte nuclear factor 1
HPVs	Human papilloma viruses
HRP	Horseradish peroxidase
Hsp10	Heat shock 10 kDa protein 1
HSP60 or HSPD1	Heat shock protein 60
HSPD1	Heat Shock 60kDa Protein 1
HSPs	Heat shock proteins
IAP	Inhibitor of apoptosis proteins
IBS	Irritable Bowel Syndrome
IBS	Irritable bowel syndrome
ICAM	Intercellular Adhesion Molecule
ICSI	Intra-cytoplasmic sperm injection
IFIT5	Interferon-induced protein with tetratricopeptide repeats 5
IFN	Interferons
IGF-1	Insulin-like growth factor 1
IgG	Immunoglobulin G
IGSF5	Immunoglobulin superfamily member 5
IKK	I kappa B kinase
IL	Interleukin
IL-1β	Interleukin-1β
IL-6	Interleukin-6
IL7	Interleukin-7
IL-8	Interleukin-8
IMPA1	Inositol(Myo)-1(Or 4)-Monophosphatase
IMS	Industrial Methylated Spirit
IPO5	Importin-5
ITAMs	Immunoreceptor tyrosine-based activation motifs)
ITSN1	Intersectin-1
IVF	*In vitro* Fertilisation

IVP	Intravenous pyelography
JaK3	Janus activating kinase
JAK-STAT cascade	Janus kinase and signal transducer and activator of transcription
JNK	C-Jun N-terminal kinase
KCNC2	Potassium voltage-gated channel subfamily C member 2
KDM5C	Lysine-specific demethylase 5C
KLF3	Krueppel-like factor 3
KLH15	Kelch-like protein 15
KPNA1	Importin subunit alpha-1
KRAB box	Krüppel associated
K-Ras	Kirsten rat sarcoma viral oncogene homolog
LacNAc	N-acetyllactosamine
LBP	Lipopolysaccharide-binding protein
LDHB	Lactate dehydrogenase B
LFA-1	Lymphocyte function-associated antigen 1
LH	Lieutenising hormone
LMNB2	Lamin-B2
LMP	Latent membrane proteins
LNG-IUS	Levonorgestrel Intrauterine System
LNX1	Ligand-of-Numb protein X1
LOXL4	Lysyl oxidase homolog 4
LUNA	Laparoscopic Uterine Nerve Ablation
MACROD2	MACRO domain-containing protein 2
MADD	MAP kinase-activating death domain protein
MAGUK	Membrane-associated guanylate kinase
MALDI	Matrix-assisted laser desorption/ionization
MAP	Mitogen-activated protein
MAP2K6	Dual specificity mitogen-activated protein kinase kinase 6
MAP3K12	Mitogen-activated protein kinase kinase kinase 12
MAP3K7IP1/TAB1	TGF-Beta Activated Kinase 1/MAP3K7 Binding Protein 1
MAPK	Mitogen activated protein kinase
MAPK14	Mitogen-Activated Protein Kinase 14
MAX	MYC Associated Factor X
MCP-1	Monocyte chemotactic protein–1
MDM4	Protein Mdm4
MEF2C	Myocyte-specific enhancer factor 2C or MADS box transcription enhancer factor 2, polypeptide C
MHC	Major histocompatibility complex
MHC class 2	Major histocompatibility complex class 2
MICB	MHC Class I Polypeptide-Related Sequence B
miRNA	Micro Ribonucleic Acid
MKK3/6	Mitogen-activated protein kinase kinase 3 and 6
MMP-7	Matrix-metalloproteinase-7
MMPs	Matrix metalloproteinases
MPF	Maturation promoting factor or Mitosis promoting factor
MPZL1or PZR	Myelin protein zero-like protein 1
MRI	Magnetic Resonance Imaging
mRNA	Messenger RNA
MST3	Mammalian sterile 20-like kinase 3
MT1-MMP	Membrane type 1 metalloprotease complex
MTCH2	Mitochondrial carrier homolog 2
MTHFD2L	Methenyltetrahydrofolate cyclohydrolase
mTOR	Mammalian target of rapamycin

MYB	Transcriptional activator Myb
MYCBP	MYC binding protein or V-Myc Avian Myelocytomatosis Viral Oncogene Homolog
MYO18A	Myosin superfamily,
NAD and NADH	Nicotinamide adenine dinucleotide
NASBA	Nucleic acid sequence based amplification
NDED	NF-kappa B-inducible death effector domain containing protein
NE	Normal endometrium
NEUROD4	Neurogenic differentiation factor 4
NEUROD6	Neurogenic differentiation factor 6
NF-κB	Nuclear factor Kappa Beta
NICN1	Nicolin-1
NIPA2	Magnesium transporter NIPA2
NK cells	Natural killer cells
Nkt1	Natural killer t-cells
NOLC1	Nucleolar and coiled-body phosphoprotein 1
NP	Normal Peritoneum
NPEPPS	Puromycin-sensitive aminopeptidase
NRCAM	Neuronal cell adhesion molecule
NSAIDS	Non-steroidal anti-inflammatory drugs
OCLN	Occludin
OCP	Oral Contraceptive Pill
OGT	O-Linked N-Acetylglucosamine Transferase
ORC2	Origin recognition complex subunit 2
OvES	Ovarian Endometriosis
PANK1	Pantothenate kinase 1
PBS	Phosphate buffered saline
PCA	Principal Component Analysis
PCBD1	Pterin-4 alpha-carbinolamine dehydratase/dimerization cofactor of hepatocyte nuclear factor 1 alpha
PCDH9	Protocadherin-9
PCNA	Proliferating cell nuclear antigen
PCOS	Polycystic ovarian syndrome)
PCR	Polymerase Chain Reaction
PDCD4	Programmed cell death protein 4
Pdgfr-alpha	Platelet-derived growth factor receptor alpha polypeptide
PEX5	Peroxisomal targeting signal 1 receptor
PGE2	Prostaglandin-E2
PI 3-kinase	Phosphoinositide 3-kinase pathway
PI3K	Phosphatidylinositol 3-kinase
PID	Pelvic Inflammatory Disease
PIK3CA	Phosphoinositide-3-kinase, catalytic, alpha
PIQ-6	Pain Impact Questionnaire
PKN2	Serine/threonine-protein kinase N2
PLC gamma1	Phospholipase C gamma 1
PMAIP1	Phorbol-12-myristate-13-acetate-induced protein 1
POD	Pouch of Douglas
PPP1R3A	Protein phosphatase 1 regulatory subunit 3A
PR	Progesterone receptor
PRIC2	Prickle-like protein 2
pri-miRNA	Primary-sequence microRNA
PRKCZ	Protein kinase C Zeta
PRKG2	CGMP-dependent protein kinase 2

PRKRA	Interferon-inducible double stranded RNA-dependent protein kinase activator. A
PRSS16	Thymus-specific serine protease
PSIP1	PC4 and SFRS1-interacting protein
PTEN	Phosphatase and tensin homolog
PXMP4	Peroxisomal membrane protein 4
PYCR1	Pyrroline-5-carboxylate reductase 1
QC	Quality control
RAB5A	Ras-Related Protein Rab-5A
rAFS	Revised American Fertility Society
RAN	GTP-binding nuclear protein Ran
RanBP	Ran binding protein
RanGAP	Ran GTPase activating protein
RanGEF	Ran Guanine nucleotide exchange factor)
RANTES	Regulated upon activation, normal T cell expressed and secreted gene
RAPGEF2	Rap guanine nucleotide exchange factor 2
Ras	Rat sarcoma viral oncogene homolog
RASSF1A	Ras-association domain family member 1
Rb	Retinoblastoma
RBBP7	Histone-binding protein RBBP7
RBMXL2	RNA-binding motif protein, X-linked-like-2
RCOG	Royal College of Obstetricians and Gynaecologists
RFU	Relative fluorescence units
RFXAP	Regulatory factor X-associated protein
RGNEF	Rho-guanine nucleotide exchange factor
RGS20	Regulator of G-protein signalling 20
RHOBTB3	Rho-related BTB domain-containing protein 3
r-hTBP1	Recombinant human TNFRSF1A
RIMS1	Regulating synaptic membrane exocytosis protein 1
RIP1	Receptor-interacting protein 1
RISC	RNA-induced silencing complex
RMI	Risk of malignancy index
RNA	Ribonucleic Acid
RNase	Ribonuclease
RNASE3	Ribonuclease, RNase A Family, 3
ROC	Receiver Operator Characteristic
RPM	Revolutions per minute
RPMI	Roswell Park Memorial Institute medium
RUNX1T1	Runt-related transcription factor 1 translocated to 1 (cyclin D-related)
RYBP	RING1 and YY1-binding protein
SAB	Spiked assay buffer
SAMD12	Sterile alpha motif domain-containing protein 12
SATB1	Special AT-rich sequence binding protein 1
SCD5	Stearoyl-CoA desaturase 5
SCML4	Sex comb on midleg-like protein 4
SD	Standard deviation
SELDI-TOF-MS	Surface-enhanced laser desorption ionisation time-of-flight mass spectrometry
SEMA3A	Semaphorin-3A
Sept9	Septin 9
SESD1	SEC14 domain and spectrin repeat-containing protein 1
SF12	Short Form 12 questionnaire
SF36	Short Form 36 questionnaire

SH3	SRC Homology 3 Domain
SH3GL1	SH3-Domain GRB2-Like 1
sICAM-1	Soluble intracellular adhesion molecules
SIRT6	Sirtuin-6
SLC9A1	Solute Carrier family 9 Sodium/hydrogen exchanger 1
SMARCD2	SWI/SNF-related matrix-associated actin-dependent regulator of chromatin subfamily D member 2
SMC3	Structural maintenance of chromosomes protein 3
SMYD4	SET and MYND domain-containing protein 4
SND1	Staphylococcal nuclease domain-containing protein 1
snoRNAs	Small nucleolar RNAs
SNX21	Sorting nexin-21
SP1	Transcription factor Sp1
SPOCK2	Testican-2
SST	Serum separator vial
ST8SIA3	Sia-alpha-2,3-Gal-beta-1,4-GlcNAc-R:alpha 2,8-sialyltransferase
STAT	Signal transducers and activators of transcription
STI	Sexually Transmitted Infections
STK24	Serine/threonine-protein kinase 24
STUB1 or CHIP	E3 ubiquitin-protein ligase CHIP
SUN1	SUN domain-containing protein 1
SV2B	Synaptic vesicle glycoprotein 2B
SYNP2	Synaptopodin-2
SYT14	Synaptotagmin-14
TBC	Tubulin cofactors
TBS-T	Tris-buffered saline with tween
TENS1	Tensin-1
TGF beta	Tumour growth factor beta
TGF-βR2	Transforming growth factor-β receptor 2
TLR	Toll-like receptor
TMA	Tissue microarray
TMEM175	Transmembrane protein 175
TMEM30B	Cell cycle control protein 50B
TNF	Tumour necrosis factor
TNF α	Tumour Necrosis Factor Alpha
TNFAIP8	Tumour necrosis factor alpha-induced protein 8
TNFR	Tumour necrosis factor receptor
TNFRSF10A	Tumour necrosis factor receptor superfamily, member 10a
TNFRSF1A	Tumour necrosis factor receptor superfamily, member 1A
TNFRSF6	Tumour necrosis factor receptor superfamily, member 6
TNF-α	Tumour necrosis factor-alpha
TOF	Time-of-flight mass spectrometer
TOM1	Target of Myb1
TPM1	Tropomyosin alpha-1 chain
TPP1	Tripeptidyl-peptidase 1
TRAB2B	Transformer-2 protein homolog beta
TRADD	TNFRSF1A-Associated Via Death Domain
TRAF	Tumor necrosis factor receptor-associated factor
TRAIL	TNF-related apoptosis-inducing ligand
TSP-1	Thrombospondin-1
UBAP2L	Ubiquitin-associated protein 2-like
UBE2W	Ubiquitin-conjugating enzyme E2 W
UBXN4	UBX domain-containing protein 4

UCHL1	Ubiquitin carboxyl-terminal hydrolase isozyme L1
VEGF	Vascular endothelial growth factor
VEZF1	Vascular endothelial zinc finger 1
WNT5A	Wingless-Type MMTV Integration Site Family, Member 5A
WT1	Wilms tumour suppressor gene
WTAP	Wilms tumour 1 associated protein
XIAP.	X-Linked Inhibitor Of Apoptosis
ZFC3H1	Zinc finger C3H1 domain-containing protein
ZNF	Zinc finger protein
ZNF138	Zinc finger protein 138
ZNF257	Zinc finger protein 257
ZNF41	Zinc finger protein 41
ZNF430	Zinc Finger protein 430
ZNF493	Zinc finger protein 493

The aims and objectives of the research

This research aimed to analyse proteomic expression in endometriotic tissue from standardized pelvic sites. Assessment of the genetic mechanisms and pathways controlling angiogenesis, apoptosis and inflammation allowed identification and definition of aberrations that could affect control of the aforementioned processes causing or precipitating disease development. Comparative studies of proteomic expression from specific sites were carried out to assess for possible variations in pathophysiology of the disease processes. The identification of tissue and serum inflammatory gene expression profiles or micro ribonucleic acid (miRNA) expression profiles that potentially predict the severity and stage of endometriotic disease allowed us to work towards a panel of markers for the non-invasive identification and physiological classification of an as yet surgically classified disease.

Identification of pathways linked to endometriosis provided an insight into potential novel therapeutics and were tested successfully in *in vitro* experimentation.

1 Introduction

1.1 Definition and overview

Endometriosis is a common gynaecological disorder found almost exclusively in women of reproductive age, characterised by pelvic pain, dysmenorrhea and infertility causing numerous psychosocial co-morbidities and severely limiting the quality of patient's life[3]. It is a chronic oestrogen dependant condition with an average age at diagnosis of 25-29 years. Optimal treatment for endometriosis is as yet unclear with a delay in diagnosis of disease quoted at around 6.7 years in one multicentre trial[4]. US studies report an average delay in diagnosis of 11.7 years and UK studies estimate 8 years of diagnostic delay[5]. The disease in itself affects around 5%-15% of women in their reproductive age varying in prevalence between populations. It is estimated to affect over 70 million women worldwide[6]. Diagnostic incidence rates have been quoted in 26.4% (95% CI: 20-32.7%) of African to 54.5% (95% CI: 44.2-64.7%) in South American countries[7]. Endometriosis is prevalent in 0.5-5% of fertile women and 25-40% of infertile women making it a leading cause of infertility[8,9]. In one Norwegian study the lifetime prevalence was documented at 2.2%[10]. Pain experienced by women is not directly related to the classification of disease severity[11]. Characteristically, ectopic endometrial tissue is found outside its usual site in the uterus, within the pelvis and these respond to hormone changes during the menstrual cycle. Rarer cases of endometriosis in peripheral sites such as lung, brain and surgical incisions have been documented in medical literature[12,13].

There are no defined causative factors but risk factors associated with the disease vary. Suggestions as to age (rare before and after menarche and menopause respectively), social class and race[14] (increased incidence in higher social classes), in utero exposure to multiple pregnancies and Diethylstilbestrol[15], infertility[16], low parity[16], oral contraceptive use and age of commencement or stopping of OCP[17], family history[18,19], smoking[20], diet[9], exercise[21], body mass index[22], dioxin[23], a history of immune disorders[24], association with Non-Hodgkin's Lymphoma[25], association with pigmentary traits[26], links with Melanoma[27] and association with ovarian (serous, mucinous, endometroid, clear cell, other subtypes) and endometrial cancer have all been published. Most studies describing links to diet, exercise and familial inheritance show conflicting evidence and are by no means definitive.

Classic theories as to the origin of endometriosis will be reviewed in this document. They have however, failed to propose a precise pathogenetic mechanism, confirming the limited knowledge of the pathogenesis and pathophysiology of the disease[28]. Although endometriosis is a benign disorder, recent studies have suggested that it could be viewed as a neoplastic process[29]. Genetic factors and familial aggregation are associated with the disease process and the risk for first-degree relatives of women with severe endometriosis is six times higher than that for relatives of unaffected women[30]. The disease has been documented in medical literature for over 300 years; nevertheless, current diagnosis and treatment of patients has not progressed; treatment encompasses invasive, surgical solutions with limited outcomes and substantial side effects.

Endometriosis, be it superficial peritoneal or ovarian and its associated adhesions, is not always detectable by trans-vaginal scanning[31] and peritoneal endometriosis is only visible at surgery. The current gold standard diagnosis is laparoscopy. In this surgical procedure a rigid camera is inserted into the abdomen and pelvis usually through the umbilicus enabling pathology visualisation and treatment. This technique is invasive, and carries surgical and anaesthetic morbidity and mortality. Diagnosis of disease is based on the visualization of endometriotic lesions during surgery and is therefore operator dependant. No reliable serum marker is currently available. Over the last two decades, proteomic technologies have been used to identify molecules, serum markers and novel proteins as probable aetiological factors in endometriotic pathogenesis. While some molecules identified by proteomic technologies may have a relevant role in the pathogenesis of endometriosis, the research of potential serum markers for this condition is still in its early stages and far from any clinical application[32].

Current pharmacotherapy for endometriosis includes gonadotropin-releasing hormone (GnRH) agonists, oral contraceptives and progesterone receptor ligands[33]. Being able to use proteomic technologies and genetic analysis to flag molecular targets and disease patterns, would aid in unlocking new methods of molecular targeting as a treatment for this disease.

1.2 History of endometriosis

Three hundred and nineteen years ago in 1690, Daniel Christianus Schrön in his inaugural dissertation, *Disputatio inauguralis Medica de Ulceribus Ulceri*, described sores throughout the "stomach", bladder, intestines, and broad ligament which had a tendency to form adhesions that linked visceral areas together[34,35]. This is now believed to be the first documented description of endometriosis. Arguments against Schrön's identifying endometriosis lie in the fact that other lesions in his dissertation could also be attributed to alternate inflammatory or infective lesions. In truth, without the advent of microscopy the definite presence of ectopic endometrial tissue could not be confirmed in the 17th and 18th centuries. The description of these unknown lesions remained unchanged for the next 79 years until in 1769, Arthur Duff, a Scottish physician added an additional facet to this pathology, describing the intense pain and suffering of women with this condition. He described morbid symptoms that manifestly changed the disposition of the entire body[36]. Less than ten years later, in 1776 Roederer, Broughton, Tailford, Duff, Ludgers in the *De ulceribus utero molestis observationibus* described the disease of endometriosis and its symptoms.

In 1800, the advent of microscopy led to the visualisation of the endometriotic cells and in 1860 Carl von Rokitansky observed that this pathology involved the presence of endometrial glands not only in external pelvic sites but embedded within the uterine muscle (myometrium). A dissertation by Batt in 2008[37] describes three phenotypes from Carl von Rokitansky's observations. The first description, when lesions were seen invading the uterine muscle was labelled as *'Sarcoma adenoids uterinum'*. Where lesions were cystic in nature and associated with myometrial hypertrophy, they were called *'cystosarcoma adenoids uterinum'*. The second described phenotype, called '*cystosarcoma adenoids uterinum polyposum',* was observed in the invasion of the endometrial cavity forming a polyp. The third phenotype, called '*ovarian cystosarcom*'[38], described invasion of the ovary. Arguments have arisen as to the possible malignant nature of the described lesions, though Batt, maintained their benign nature, as asserted by Rokitansky. In

1896, Von Recklinghausen disputed Rokitansky's findings claiming that the 'Adenomyoma' lesions were displaced mesonephric or Wolffian tissues[39]. Up until the 19th and early 20th century pathologists refuted the hypothesis that observed glands originated endometrially. They were however unable to describe their origins in tissues.

Up to this point in history, little was known as to how this disease progressed. It was the surgeon Thomas Stephen Cullen in 1917 who researched the visualized 'mucosal invasion', noted to be a characteristic of this disease[40]. He observed that a uniformly enlarged uterus was caused by a diffuse myomal 'tumour' occupying the inner portion of the uterine wall. Studies of multiple specimens showed how the endometrial glands continued diffusing into the myometrium causing this pathology. He also noted that the stromal cells decidualised during pregnancy, providing proof of their endometrial origin. In 1920 Cullen depicted the commonest sites of adenomyotic lesions within the pelvis which included the myometrium, rectovaginal septum, fallopian tube, round ligament, ovarian surface and hilus, uterosacral ligaments, bowels, abdominal wall and umbilicus.

Until 1921, attention was focused on the deep sited endometriosis in the pelvis, referred to as *adenomyosis externa*. The disease, irrespective of the sites affected, was regarded as one pathology. In 1923, the surgeon Dr. John A. Sampson created the term 'endometriosis'; he noted during his operative procedures that the observed peritoneal lesions bled during menstruation similar to eutopic uterine endometrium[41]. Sampson's initial theory was that superficial endometriosis was caused by the rupture of an ovarian endometrioma. This theory was however altered when it was noted that the free superficial peritoneal implants reacted like eutopic endometrium, responding to hormonal stimulation. These implants were recognized as implants from menstrual blood regurgitated into the pelvic cavity. In 1926 he was the first to hypothesize the theory of disease causation by retrograde menstruation[42]. It was from that time that adenomyosis externa, ovarian endometriomas and peritoneal endometriosis came to be regarded as the multifaceted presentation of the same disease[43].

In the 1960's the advent of laparoscopic surgery, enabled direct visualisation and treatment of the pelvic lesions. As retrograde menstruation could not describe the localisation of all endometriotic lesions, especially the disseminated ones, theories of peritoneal metaplasia, lymphatic or vascular disease dissemination, embryonic remnants and stem cell or bone marrow transformation are all debated. Assessment of "normal" peritoneum at surgery often shows the presence of endometrial implants many of which resolve spontaneously leaving minor scarring [44]. As yet there is no definite cause triggering the development of these cells into the pathology of endometriosis. Studies have however hinted at a multifactorial aetiology in the peritoneum, uterus and endometrium of affected patients.

The current definition of Adenomyosis was given in 1972 by C. C. Bird who stated that 'Adenomyosis may be defined as the benign invasion of endometrium into the myometrium, producing a diffusely enlarged uterus microscopically exhibiting ectopic non-neoplastic, endometrial glands and stroma surrounded by the hypertrophic and hyperplastic myometrium'[45].

1.3 Symptoms and signs of endometriosis

Women suffering from endometriosis can range from being completely asymptomatic from the disease to having a range of non-specific ailments. Chronic pelvic pain, ovulatory/mid cycle pain, dysmenorrhea, perimenstrual symptoms involving bowel and/or bladder, fatigue and/or infertility have all been reported. It is estimated that 25%-70% of women and adolescents with chronic pelvic pain and/or dysmenorrhoea suffer from endometriosis[46-50]. Children as young as 10 years of age have been found to be suffering from the disease[47] with an incidence of 12%[50] in girls between 11 and 13 years of age. This variation in symptoms experienced by women serves to highlight the difficulties encountered when diagnosing the disease on clinical history alone. If clinically severe disease is suspected, the European Society of Human Reproduction and Embryology (ESHRE) advises early patient referral to tertiary centres where a multidisciplinary team approach is available[31].

Clinically, women may have unremarkable findings. Abdominal masses may indicate ovarian endometriomas and enlarged ovaries, whilst a fixed retroverted uterus with a tender pouch of Douglas (POD) and tender uterosacral ligaments are all suggestive of endometriosis. In severe cases, deeply infiltrating nodules of endometriosis can be seen in extrapelvic sites such as vagina or cervix[51]. Rarer manifestations of extrapelvic sites have also been reported in lungs, bowels and brain[52,53].

1.4 Historical developments

The first attempts at a classification system was performed by Sampson in 1921 where the retrograde theory of menstruation was proposed and categorisation of adhesions and haemorrhagic cysts was attempted[41]. Over the years, classification systems have aimed to look at and classify endometriosis from its histological and anatomical presentation. Attempts have been made to correlate the disease histopathology with findings at surgery and its clinical presentation of pain[54]. To date, there is no correlation between pain experienced by patients and the severity of diagnosed disease. In 1966, Beecham[55] claimed that there would be no purpose in creating a detailed classification for this disease, suggesting a simple four stage classification using operative findings and physical locations. In 1973, *Acosta et al.*[56] proposed a different classification system which tried to assess the probability of surgical success and pregnancy rates according to the site and distribution of the lesions. Most physicians rejected this latter classification arguing it failed to distinguish unilateral from bilateral disease and was not specific. *Kistner et al.* tried developing a classification which directly related endometriosis to infertility. None of the classification systems developed before 1978 received widespread acceptance.

In 1979, *Buttram et al.*[57] proposed an expanded classification over Acosta's, according to laparoscopic findings, malignancy lesions, lesion site and location as well as therapeutic response. These classification attempts failed to predict outcomes of infertility and pregnancy rates and were therefore criticised. The American Fertility Society (AFS) classification was then developed as a classification tool[58].

1.5 Classification of endometriosis

An ideal classification system has a good scientific basis, is unambiguous in its terms, is applicable for all cases, has a true reflection of the disease and is comprehensive and reproducible. It should aim to accurately translate physical findings into verbal descriptions which are easy to discuss with patients. Ideally it should standardise the disease irrespective of who is performing the assessment, be a reflection of disease severity, and be a good measure of the effect of treatment on disease[54]. Classification systems may be of value in the prognosis and management of infertility[59,60] but there are limitations to the use of these classification systems. Endometriotic lesions also have a wide spectrum of appearances varying from black/blue/brown puckered lesions termed, peritoneal or ovarian 'powder burn' or 'gunshot' lesions, to overt haemorrhagic cysts and nodules. Milder or more subtle lesions, which may be harder to spot, may look like red implants or serous clear vesicles. White plaques, as well as peritoneal discoloration may manifest when fibrosis is involved[31]. Lesions can cause extensive scarring involving the large and small bowel, the fallopian tubes and in rarer cases, other extraperitoneal locations such as the lung and brain. The depth of lesion infiltration is known to correlate with the type and symptom severity of patients[61-63]. Deep lesions will extend over 5mm beneath peritoneal surfaces. It is these deep infiltrative lesions that invade abdominal structures such as the bladder, ureters, the intestine, uterus, uterosacral ligaments and occasionally the vagina and cervix.

1.5.1 American Fertility Society classification

The American Fertility Society was the first society to propose a quantitative classification system in 1979[64]. It consisted of a paper document with defined classification points and the ability to be flexible for its use in varied cases of the disease. Its aim was to define the severity of disease by its location and extent. It did not however enable a correlation between disease severity and pregnancy rates so in 1982 *Guzick et al.*[65] proposed an amendment to the original classification by adding on a nonparametric monotonic estimator where a dose response relationship between AFS score (dose) and pregnancy post treatment (response) were used to improve the discriminatory power of the classification[65]. In 1982 attempts at the use of clustering techniques for the anatomical findings to predict pregnancy rates failed[66]. Other reviews within the same period provided additional recommendations to the classification system but recognised the failure and difficulties encountered in creating an "ideal" classification system partly due to the wide spectrum of disease[67,68]. The AFS classification[67] was revised in 1985 with additional details. These included quantification of ovarian adhesions, differentiation between superficial and deep lesions on the ovaries and peritoneum, recognition of minimal disease, creation of a tubal endometriosis category and the recording of the presence of other pathology[54]. In 1992, *Canis et al.* proposed an additional stage for endometriosis which he suggested could be added on to the AFS[69]. This Stage V classification was meant to be attributed to cases with severe bilateral disease that would require early *in vitro* fertilisation (IVF) intervention to achieve fertility. Irrespective, fertility itself is found to be reduced in severe disease[70]. In 1996, there was a re-publication of the classification system with illustrations for pelvic pain[58] and the AFS was renamed as The American Society for Reproductive Medicine (ASRM) classification system (Figure 1-1).

1.5.1.1 Limitations of the American Society for Reproductive Medicine (ASRM) classification

It is maintained that although the ASRM classification is useful in documentation of disease, it fails clinically to predict prognosis or management options for pain or infertility[54]. Identified limitations include wide scoring ranges, possible observer errors in recognising disease due to its variation in morphology[71], fluctuations in disease presentation according to hormonal stage of the cycle[72] and variations in reporting of disease depending on operative technique e.g. laparoscopy versus laparotomy[73]. Articles assessing the reproducibility of the ASRM system identify substantial intra observer staging, especially when assessing endometriosis within the pouch of Douglas or ovaries[74]. Disagreement in reporting multiple lesion types in the same patient make the classification and staging of disease difficult[75]. The ASRM (except in extensive disease) also correlates poorly with infertility[76] and there is also poor correlation with pelvic pain[77], dyspareunia, dysmenorrhoea and extent of disease[78]. The ASRM is therefore unable to encompass the role of a disease predictor or monitor of outcome of treatment.

Other classifications by *Chapron et al.* in 1993[59] looked at deeply infiltrating disease and its surgical implications. Alternate classification categories have tried to modify that of the ASRM by focusing on varied aspects such as pregnancy rates[79], pain levels[80], radiological, histological and morphological factors or biomarkers and genetic markers. Classification systems for disease affecting a particular location such as retrocervical endometriosis, were attempted in 1993 by *Adamyan et al.* and updated in 2001[81]. The multitude of attempts at classification reflects the broad spectrum of clinical presentations and symptoms.

The ESHRE have developed a guideline for the diagnosis and classification of endometriosis. Disease severity is assessed by describing surgical findings or using the standardised ASRM classification.

FIGURE 1-1

AMERICAN SOCIETY FOR REPRODUCTIVE MEDICINE
REVISED CLASSIFICATION OF ENDOMETRIOSIS

Patient's Name _____ Date _____

Stage I (Minimal) - 1-5
Stage II (Mild) - 6-15
Stage III (Moderate) - 16-40
Stage IV (Severe) - >40
Total _____

Laparoscopy _____ Laparotomy _____ Photography _____
Recommended Treatment _____
Prognosis _____

PERITONEUM	**ENDOMETRIOSIS**	<1cm	1-3cm	>3cm
	Superficial	1	2	4
	Deep	2	4	6
OVARY	R Superficial	1	2	4
	Deep	4	16	20
	L Superficial	1	2	4
	Deep	4	16	20
	POSTERIOR CULDESAC OBLITERATION	Partial	Complete	
		4	40	
OVARY	**ADHESIONS**	<1/3 Enclosure	1/3-2/3 Enclosure	>2/3 Enclosure
	R Filmy	1	2	4
	Dense	4	8	16
	L Filmy	1	2	4
	Dense	4	8	16
TUBE	R Filmy	1	2	4
	Dense	4*	8*	16
	L Filmy	1	2	4
	Dense	4*	8*	16

*If the fimbriated end of the fallopian tube is completely enclosed, change the point assignment to 16.

Denote appearance of superficial implant types as red [(R), red, red-pink, flamelike, vesicular blobs, clear vesicles], white [(W), opacifications, peritoneal defects, yellow-brown], or black [(B) black, hemosiderin deposits, blue]. Denote percent of total described as R___%, W___% and B___%. Total should equal 100%.

Additional Endometriosis: _____

Associated Pathology: _____

To Be Used with Normal Tubes and Ovaries

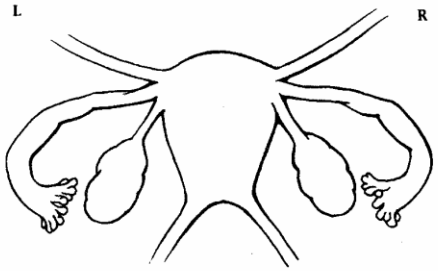

To Be Used with Abnormal Tubes and/or Ovaries

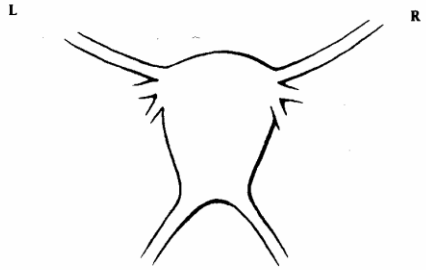

The American Society for Reproductive Medicine (ASRM) classification of endometriosis (1996)[58]

1.6 Theories of causation

Theories of causation vary with literature supporting or refuting each respectively. Theories include those of: in situ development, Müllerianosis[82], accentuation by genital tract anomalies[83], genetic predisposition[84], coelomic metaplasia[40], induction[85], transplantation[86], retrograde menstruation[42] with implantation and growth of endometrial cells, endometrial stem cells[87], physiological phenomenon[88], alterations in the endometrium[89], exogenous endometrial hormonal production[90], angiogenesis[91], the evasion of endometrial tissue from the immune system[92], cellular protection from apoptosis[93,94], the potential of endometrium to implant[95] and invade[96], and differences in peritoneal fluid[97]. Below is a summary of the historical theories of the causation of endometriosis (Table 1-1)[98]:

TABLE 1-1

In-situ development
a) Germinal epithelium of the ovary (Waldeyer, 1870)
b) Embryonic cell rests
Mesonephric (Wolffian knob, Wolffian duct) (Von Recklinghausen, 1895, Breus, 1894)
Paramesonephric (Müllerian ducts) (Cullen, 1896, Russell, 1899)
c) Coelomic metaplasia (Iwanoff, 1898, Meyer, 1903, Lauche, 1923)
d) Metaplasia by inflammation (Hueter, 1918, Meyer, 1919, Tobler, 1923)
e) Metaplasia by hormonal stimulation (Novak, 1931)
f) Metaplasia by induction (omnipotent blastema) (Levander, 1941, Merril, 1966)
g) Secondary Müllerian system (Lauchlan, 1972)
Transplantation
a) Implantation, retrograde menstruation (Sampson, 1921)
b) Implantation, mechanical transplantation (Greenhill, 1942)
c) Benign lymphogenous metastasis (hystero-adenosis metastatica) (Halban, 1924/1925, Javert, 1949)
Combination of in-situ development and endometrial transplantation and implantation

Theories on the pathogenesis of endometriosis (modified from Hingst, 1926 and Ridley, 1968)[98]

At first glance, the theories appear to contradict each other. Whereas one theory speculates the origin of endometriosis from the uterine endometrium that has refluxed back in to the pelvis at menstruation, others look at the De Novo origin of endometrial tissue from the peritoneal serosa. These theories can, however, be complimentary. Metaplasia and the growth of mullerin tissues can be induced experimentally with menstrual debris, supporting the theory of induction[99].

Studies assessing post-mortem human foetuses have shown the presence of ectopic endometrium at known sites of endometriosis including the posterior uterine wall, rectovaginal septum and pouch of Douglas (POD)[82]. These findings give support to further theories that endometriosis develops as result of abnormally dislocated primitive endometrial tissue during embryonic organogenesis.

1.6.1 Retrograde menstruation, endometrial implantation and growth

This is today the most widely accepted theory on the development of endometriosis. Initially in 1921, Sampson proposed that endometriosis arose from seedlings of diseased ovaries[41]. In 1927, his theory

changed and Sampson postulated that retrograde menstruation acted in the form of a vessel, causing metastatic like transport of endometrial cells intraperitoneally, resulting in endometriosis. Cells within the pelvis would be 'showered' by endometrial cells which were viable, would live on and grow in external peritoneal sites[42]. Another study related the causation of endometriosis to women with increased amounts of menstrual flow and factors influencing endogenous hormonal levels[100]. At the time when Sampson's theory was proposed, menstrual debris was regarded as being solely composed of dead tissue. Sampson's theory was therefore refuted due to the perceived lack of cellular viability. Over the years studies have shown viable epithelial endometrial cells within menstrual and peritoneal fluid[101] capable of growth and proliferation. Menstrual debris is now known to be composed of single viable cells as well as glandular structures[102]. Sampson's theory of retrograde menstruation therefore holds. During laparoscopic surgery in women who are menstruating[103], there is evidence of menstrual reflux within the pelvis. It has been noted in a study performed by Halme *et al.*, that in women with patent tubes, 90% had intrabdominal blood compared to 15% of women with occluded tubes[103]. A case report in the 1980's of a 31 year old lady who underwent the Estes procedure is also used to support Sampson's hypothesis where unilateral endometriosis was seen to develop at the site of ovarian implantation into the uterine window. This could be a human in vivo representation of other endometriosis inducing experiments in rhesus monkeys where intra-abdominal menstruation was induced[104]. Distribution of endometrial lesions within the pelvis are also in keeping with menstrual reflux patterns[105]. Peritoneal fluid flow is anticlockwise in pattern and diaphragmatic lesions are found more commonly on the right[106]. Left ovarian endometriomas are commoner than right sided ones. This is believed to be due to increased peritoneal fluid stasis on the left side due to the sigmoid colon[107]. Nevertheless, not all women progress to develop endometriosis and not all women develop the disease to the same extent.

1.6.2 Development in situ

A commonly believed theory in the formation of endometriosis is the development of ectopic tissue from local tissue. This theory encompasses the development of disease from ovarian or intraperitoneal tissue[108], metaplasia or embryonic Wolffian or Müllerian remnants[109].

1.6.3 Embryonic remnants

It has been proposed that the localisation of endometriosis in the uterosacral ligaments, broad ligaments or pouch of Douglas occurs due to aberrant differentiation or migration of the developing Müllerian system (derived from the coelomic epithelium) across the pelvic floor. Lauchlan *et al.* introduced the concept of a secondary Müllerian system[109] to describe epithelium (including endometriotic cells) disseminated throughout the peritoneum, over the ovaries and within the retroperitoneal space. Supporting this theory of 'Müllerianosis'[110] are observations that women with known Müllerian anomalies have an increased incidence of endometriosis[111]. There is another case report in the literature of a patient with complete uterine agenesis having endometriosis thereby promoting the metaplastic theory and refuting the theory of retrograde menstruation[112]. A further observation supporting the embryonic theory is the presence of ectopic uterine tissues expressing CA125 and oestrogen receptors in newly born female foetuses[82].

1.6.4 Coelomic metaplasia

Embryologically, the fallopian tubes, uterus, cervix and upper third of the vagina all develop from the Müllerian (or paramesonephric) ducts. The Müllerian ducts are themselves formed by invagination and proliferation of the coelomic epithelium[113]. The surface of the ovaries (germinal epithelial layer) is derived from the mesoderm during embryonic development and is closely related to the peritoneal mesothelium. In the theory of coelomic metaplasia, the germinal epithelium of the ovary and the peritoneal serosa transforms into endometrial tissue by metaplasia[114] secondary to chronic inflammation or hormonal stimulation[115]. Further studies supporting a metaplastic process within the peritoneal mesothelium have shown that the pelvic mesothelium itself develops characteristics similar to epithelial and Müllerian type structures[116]. Markers for epithelial differentiation (antibodies for Ber-EP4 antigen), and markers for Müllerian differentiation (oestrogen and progesterone receptors) were positive in peritoneal mesothelium and ovarian surface epithelium adjacent to endometriotic lesions but negative in otherwise sited tissue. Between normal ovarian surface epithelium and normal peritoneum, there was an increased frequency of Ber-EP4 positivity showing fundamental differences between tissues. This finding has also been suggested as an explanation for the increased prevalence of epithelial neoplasms in ovarian tissue[116]. The metaplastic theory of endometriosis would be able to explain endometriosis outside the pelvis such as the lungs, diaphragm or pleura[117]. It would also explain how endometriosis can be found in uterine or menstrual absence. Male cases that were reported to have endometriosis were found to be receiving high doses of unopposed oestrogen for prostatic carcinoma, and in these cases arguments against the pathology being classified as endometriosis exist.

There are a number of arguments against the metaplastic theory. If spontaneous alteration of peritoneal cells could occur, then its prevalence in males should increase. The disease, as with most metaplastic processes, would be expected to increase with age and affect peritoneal surfaces uniformly. Another counter-argument concerns embryological development, as the thoracic cavity is lined by the coelomic membrane, the disease should be more prevalent within the chest.

1.6.5 Transplantation theory

This theory postulates that endometrial fragments can be disseminated throughout the body either via lymphatic, haematogenous or iatrogenic spread. Iatrogenic transplantation is believed to be the development of disease secondary to intrabdominal implants left during a surgical procedure. These cells implant within the pelvis causing disseminated endometriosis. Case reports of women undergoing laparoscopic subtotal hysterectomies with ovarian conservation and the use of the morcellator as a means of removing the uterus have reported post-operative endometriosis. On analysis of operative techniques, the procedures themselves had no complications, no endometriosis was visualized at initial surgery, the abdomen and pelvis were irrigated at the end of the procedure and any possible endometrium remaining within the cervical stump had been cauterized. The histological specimen removed was reported as not having adenomyosis or endometriosis. Nevertheless, within eight months, patients reported new onset symptoms of cyclical pelvic pain, dysuria, dyspareunia and dyschesia lasting 5-8 days with a 20 day interval[118-121]. These symptoms were not responsive to antibiotics but did respond slightly to GnRH analogues. A repeat operative laparoscopic procedure confirmed disseminated, extensive visualised

endometriosis (also confirmed histologically) which was treated, leaving the patients asymptomatic. Alternate explanatory reasons for finding endometriosis include the possibility of missing pre-existing endometriosis at initial surgery. This theory is unlikely in view of the extensive lesions easily visualized at the second operative procedure. A second theory postulates that endometrial tissue within the cervical stump causes retrograde menstruation and endometriosis. Analysis of the operative technique in question shows that the stump was cauterized and covered by the peritoneal flap approximating the bladder. Should retrograde flow from this area be the only causative agent, then one would expect to find endometriosis in its proximity and expect the patient to complain of menstrual loss. Neither of these were reported.

Iatrogenic dissemination of endometriosis causing endometriomas at varied points within surgical scar tissue is reported in around 0.1% of women undergoing Caesarean section or other gynaecological surgery including laparoscopic ovarian cystectomies and one case of laparoscopic appendicectomy[122]. Other rare reported sites include the rectus abdominis[123] muscle. In case reports between 1948 and 2011 endometriosis is described in scar endometriomas. Most of these cases were initially confused with other surgical and dermatological pathologies presenting with cyclical pain and/or swelling. All lesions were confirmed radiologically and some by fine needle aspiration techniques (FNA)[121,124]. Fine needle aspiration has been documented as a fast and accurate method of diagnosing ectopic endometrial lesions where endometrial-like epithelial cells, stromal cells and evidence of decidualisation have been noted[125]. Excised lesions were then re-confirmed histologically and a 12 year post excision follow up showed no recurrence[126].

1.6.6 Induction theory

In this theory, uterine endometrium either releases biochemical substances into the blood or lymphatic system, or alternatively induces immunological responses within the patient causing undifferentiated cells within the body to differentiate. An early study with rabbit models in 1955[85] claimed that the implantation of dying endometrial tissue into the rabbit's abdominal cavity caused epithelial differentiation within 7 days. They based their findings on histological analysis. A similar study performed 41 years later by Merrill in 1996 using Millipore filters which prevented cellular dissemination from the implanted endometrial tissue showed the presence of endometrial-like glands adjacent to the implants. There was however no evidence of stromal presence and this did not enable the definitive diagnosis of newly formed endometriosis[127].

1.6.7 Familial inheritance and genetic predisposition

Some small scale studies have hinted at a genetic basis and familial inheritance of the disease[128] with endometriosis reported as being more severe in women with family members suffering from the same disease[18]. Women with family members who have endometriosis are susceptible to developing the disease[129]. A 79%-93% associated maternal lineage has been reported[129], with a stronger link to the mother compared to the sister. The overall incidence in first degree relatives with family members suffering from endometriosis has been estimated between 3.9%-4.9%[18,129]. Rates for second degree relatives such as aunts and grandmothers are reported around 3.1% to 4% respectively, whilst 4.8% of

sisters have been affected[18]. Further publications report an increased disease incidence in monozygotic twins[19], further supporting the theory of a genetic basis of the disease. Its mode of inheritance is however unknown[128].

1.6.8 Endometrial alterations

The endometrium is a unique tissue that undergoes transitions between the phases of proliferation, secretion, regeneration and regression in response to hormonal influences during menstruation. All these processes have complex mechanisms providing control and stability. It is possible that alterations, even subtle ones, can cause a dysregulation of this tight control and result in pathology. Differences have been noted in the eutopic endometrium of women who have disease and those who do not[130]. Endometrial cells have also been found to have stem cell properties proliferating at a rate significantly higher than umbilical cord stem cells which were used as controls. The mononuclear cells collected from menstrual blood also contained a population of adherent cells. This could explain the ability to adhere, differentiate and proliferate in ectopic sites[131]. The menstrual cycle, hormonal influences such as oestrogen and cyclical cellular shedding have been referred to as the triggering stimuli that activate the inflammatory and repair mechanisms stimulating cellular infiltration, adherence and implantation as endometriosis[132].

1.6.9 Hormonal stimuli

Endometrial cells are known to respond to hormonal influences throughout the menstrual cycle. Oestrogen is responsible for endometrial proliferation. Prolonged periods of unopposed oestrogens are associated with hyperplasia and malignant transformation[133,134]. Analysis of endometrial tissue in women with endometriosis has shown defects in 17β-hydroxysteroid dehydrogenase type 2 (17β-HSD) which hinders the conversion of the potent oestrogen 17β-estradiol into the weaker oestrogen estrone[135]. This increases the oestrogen within the endometrium acting as a stimulus for cellular hyperplasia. Menstrual fluid has also been found to have higher estradiol levels confirming these theories[136]. Reports of an activated positive feedback loop leads to the production of further oestrogen within the endometrium stimulating endometriosis[137]. Oestrogen stimulates the enzyme Cyclo-oxygenase type 2 (COX-2) and increases prostaglandin-E_2 (PGE_2) which in turn stimulates aromatase (P450 enzyme) activity[138]. This is the key enzyme for oestrogen biosynthesis. Endometriosis related pain as well as severe disease are seen to decrease when treated with an Aromatase inhibitor[139] with varying responses[140]. Limited long term data exists and these are not currently advised as treatment modalities[141].

1.6.10 Lymphatic spread

Surgical excision for improved quality of life, symptoms and pain reduction is well documented[24,142] especially in cases where post-surgical adjuvant treatment is not given. Recurrence post-surgery is not uncommon especially in severe cases with deep infiltrative disease[143]. Surgical recurrence figures of 25% increasing to 37% at 1 and 3 years post operatively with the figure reaching 40-50% at five years have been found[144]. In cases of deep infiltrating endometriosis, studies at re laparoscopy show recurrence of growth at the previous site of disease[145] or in the ipsilateral ovary[146]. Theories of recurrence solely due to retrograde menstruation have been contested as case reports of endometriosis recurrence after ablative

surgery or hysterectomy exist[147,148]. The involvement of lymph nodes in endometriosis was identified incidentally at the assessment of pericolic lymph nodes on patients with bowel endometriosis. The thickness of the primary lesion was directly associated with the extent of regional lymph node involvement[149]. Their current prevalence is estimated at 20-30%[149-153]. Microscopic implants are not visualised at surgery but are potential causes of disease recurrence and dissemination. Lymph node dissection itself entails significant morbidity including abscess formation, lymphoedema and cysts[154]. Up to date there is no indication for routine surgical node dissemination in the management of endometriosis.

1.6.11 Endometriosis and high risk human papilloma viruses (HPVs)

HPVs are the causative agents in all cases of cervical dysplasia or malignancy[155]. There are around 40 high risk subtypes which are associated with malignant development in the anogenital epithelium[156,157]. There is an 80% prevalence rate in sexually active women with the majority of infections eradicated within one year[158]. Studies looking at the miRNAs present in cervical dysplasia or cancer in patients who were HPV-16 positive have been published by *William et al.*[156](Table 1-2,Table 1-3).

TABLE 1-2

Overexpressed	**Fold change**
hsa_miR_124	58.2
hsa_miR_449a	35.3
hsa_miR_449b	30.5
hsa_miR_301b	24.3
hsa_miR_517c	22.4
hsa_miR_545	17.4
hsa_miR_223	14.2
hsa_miR_135b	11.1
hsa_miR_21	9.6
hsa_miR_512_3p	9.4
hsa_miR_542_3p	7.8
hsa_miR_181c	7.6
hsa_miR_517a	6.9
hsa_miR_518f	5
hsa_miR_106b	4.3
hsa_miR_192	3.8
hsa_miR_16	3.8
hsa_miR_141	2.8

TABLE 1-3

Underexpressed	**Fold change**
hsa_miR_433	-18.6
hsa_mir_218	-5.6

Tables showing miRNAs differentially expressed in cervical cancer tissue compared to normal cervical tissue ($P<0.05$)

In a study by Oppelt *et al.* an assessment for the presence of DNA of *Chlamydia trachomatis* and all 6 herpes virus family members was performed on the endometrium of patients with endometriosis[159]. The DNA was not found and they then looked for the presence of HPV via polymerase chain reaction (PCR). Controls were women without endometriosis but with a prior clinical bias for human papilloma infections including the presence of abnormal smear tests or cervical carcinomas. They then concluded that both high and medium-risk HPV types are associated with both endometriosis and control tissues[159]. They postulated that viral spreading or HPV infected endometrial cells occurs pelvically causing pathology. They also proposed that chronic HPV infection of endometriosis cells can contribute to malignant transformation.

Alterations in miRNA expression have been linked to the development of malignancies[160]. These changes are identified close to fragile chromosomal sites or integration of high risk viral strains such as HPV[161]. miRNAs have been shown to regulate the Ras and Bcl oncogenes and tumour suppressor genes pRb.

1.6.12 Immune system deregulation and altered cellular properties

Endometriosis has been described as an immune system disease. Autoimmune diseases are widely believed to occur as a result of genetic predisposition often triggered by environmental and other external factors[92,162]. When endometrial cells within menstrual fluid fall intraperitoneally, an inflammatory response is induced and activated proteloytic enzymes and phagocytes act on the cells to clear out the 'debris'[163]. This system may be deficient in women who develop endometriosis.

Studies assessing characteristics of these ectopic endometrial cells indicate that they are able to escape immune surveillance and phagocytosis, enabling them to implant and proliferate (Figure 1-2). During the inflammatory response CD56+ natural killer cells (NK cells) are the predominant cells present to clear out the debris. A smaller proportion of CD14+macrophages and CD3+ T cells are also present[164]. There is a reported defect in NK cell activity towards these autologous intraperitoneal cells[165,166]. Elevations of B cell levels are seen in women with endometriosis positive for antinuclear antibodies (ANA) antibodies. This would hint at the B-cells playing a role in disease pathogenesis through autoantibody production[167,168].

FIGURE 1-2

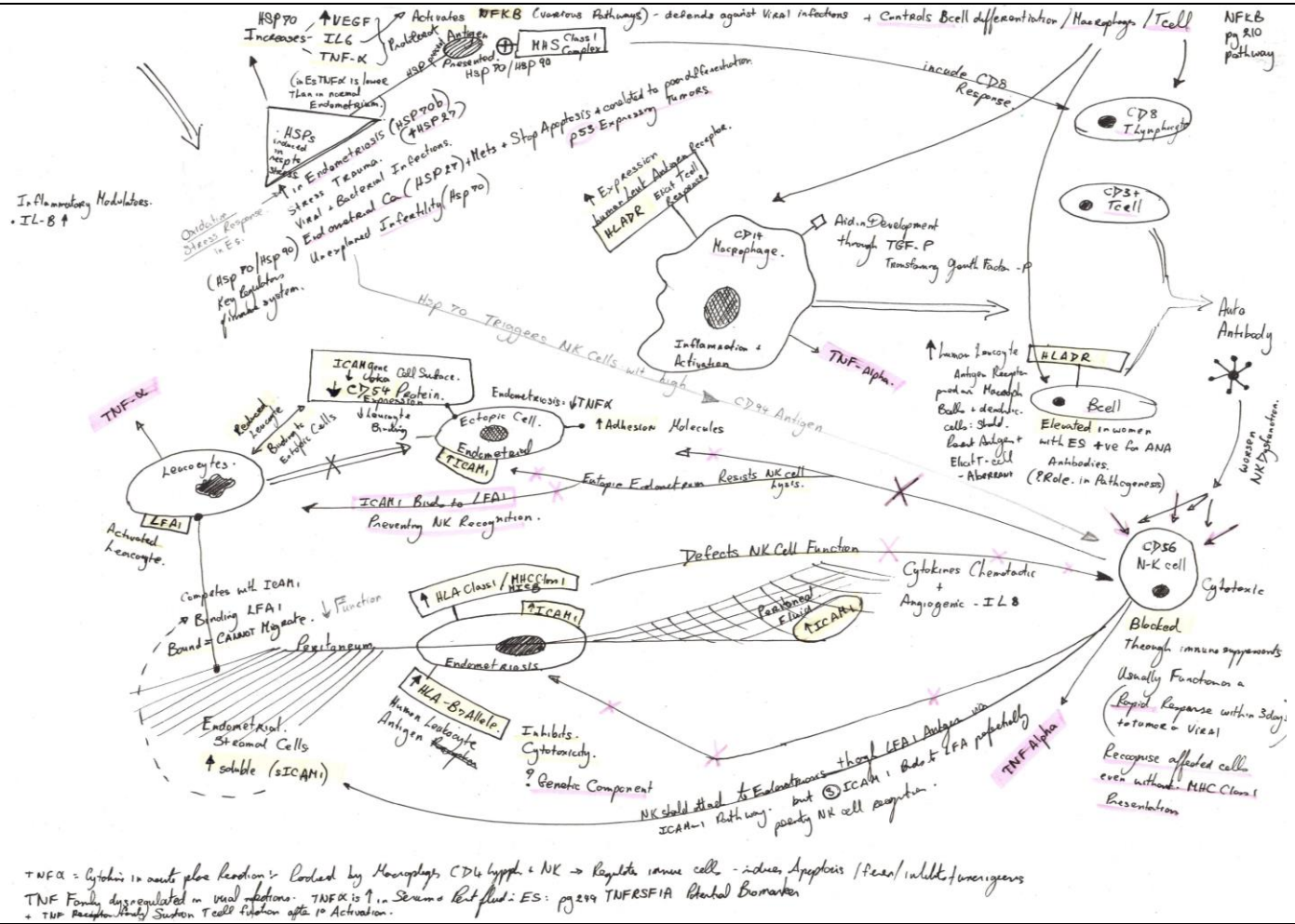

Hand drawn illustration of various immune system deregulations contributing to endometriosis development

1.6.12.1 Major histocompatibility complex class 2 (MHC class 2)

The human leukocyte antigen receptor (HLA-DR) is a αβ heterodimer cell surface receptor found predominately on macrophages, B-cells and dendritic cells. Its purpose is to present antigenic or foreign substances to the body's immune system and elicit a T-cell response. Studies showing aberrant increased expression of HLA-DR antigen in the endometrium of patients with endometriosis indicate immune anomalies contributing to disease formation[169].

1.6.12.2 Major histocompatibility complex class 1 (MHC class 1)

Surface HLA class 1 molecules are known to impair NK-like T lymphocytes lysing cells. Endometriosis is seen to have elevated levels of MHC class 1 expression which is attributed to defective functioning of the NK cells[131]. The HLA-B7 allele inhibits cytotoxic activity[134] and is elevated in endometriosis[131]. This supports the theory of escape from immune surveillance and suggests a genetic component.

1.6.12.3 Intercellular adhesion molecules

The intercellular adhesion molecule 1 gene (ICAM1) codes for the ICAM1 or Cluster of Differentiation 54 (CD54) protein. This is a cell surface glycoprotein expressed within endothelial cells and binds to integrins in turn mediating cell to cell interactions and allows cellular binding of fibronectin, collagen and laminin (Figure 1-2). ICAM is also responsible for binding integrins such as CD11a, CD18, and CD11b.

Endometrial cells of women with endometriosis have shown decreased expression of the CD54 protein[170]. This might explain the reduced binding of leucocytes to these ectopic cells. *In vitro* models show that endometrial stomal cells from women with endometriosis have increased levels of soluble intracellular adhesion molecules (sICAM-1). This competes with ICAM-1 binding the leucocyte functioning antigen-1 (LFA-1) which is expressed on activated leukocytes. Once bound, they are less able to adhere to target cells and transmigrate, preventing further leukocyte activation and function. This failure to recognise and remove pelvic endometrial cells through these mechanisms is believed to attribute to the pathogenesis of the disease[171].

1.6.12.4 Heat shock proteins (HSPs)

HSPs are the most conserved proteins in eukaryotic cells and are induced in response to stress, inflammation or trauma. They function by enabling the correct folding of proteins which would otherwise be disrupted during stress responses[172] causing aberrant activation of cellular pathways. Intracellularly, they protect the cell from lethal insults and interact with cellular apoptosis. Extracellularly they mediate immune responses[173]. Their presence in serum is associated with stress conditions varying from inflammation to viral and bacterial infections[173]. In mammals there are 5 families of HSPs depending on their molecular size. (HSP 100, 90, 70, 60 and the small HSPs such as HSP27). HSP70 and HSP90 are key regulators of the immune system. They present antigens in conjunction with the MHS class-1 complexes[165,174-176] inducing an antigen specific CD8+ T lymphocyte cell response[166,177]. Certain HSPs such as HSP 70 and HSP27 are increased in cellular exposure to stress. HSP27 are at increased levels in cancers such as endometrial, breast and leukaemias[138]. Increased levels of HSP27 are also implicated in increased cellular tumorigenesis[138,178], metastasis[179] and prevent apoptosis[137]. They are elevated in endometriosis[180,181]. Elevated levels of HSP70 have also shown to increase cancer cell tumorigenicity in

experimental mice[178] and are implicated in the endometrium of women with unexplained infertility[181]. HSP70 and HSP90 are correlated with the histology of endometrial carcinomas[182] especially the poorly differentiated tumours which often expresses p53 expression. Elevated HSP70b levels are reported in the serum of women with endometriosis, implicating an oxidative stress response in the pathology[183]. The HSP70 is also seen to increase the production of vascular endothelial growth factor (VEGF), Interleukin-6 (IL-6) and tumour necrosis factor-alpha (TNF-α) in the macrophages of women with endometriosis[184] enabling disease proliferation.

1.6.12.5 Natural killer cells (NK cells)

NK cells are analogous in function to T lymphocytes. In general, cells express antigens via the MHC complexes initiating an immune response. Whereas cytotoxic T cells form part of the body's adaptive immune response, NK cells provide a rapid response to tumour or viral infection within 3 days. They are able to recognise affected cells in the absence of antibodies or MHC[185] class 1 presentation. In endometriosis there is a defect in the function of the NK cells[92] which seems to correlate to disease severity (Figure 1-2). The eutopic endometrium of women with endometriosis is also more resistant to lysis by NK cells[92]. NK cells are activated and can attach to endometrial cells though the LFA-1 antigen via the ICAM-1 dependant pathway. It is postulated that in endometriosis, the eutopic endometrium, peritoneal fluid and endometriotic cells, all secrete soluble forms of ICAM-1. This binds to LFA-1 presenting lymphocytes preventing their recognition by NK cells[171]. Peripheral blood serum analysis has failed to recognise changes in the amounts or functions of NK cells despite variances within the peritoneal fluid[92,186,187]. HSP70 is identified as a triggering factor for NK cells which have a high cell surface density of antigen CD94[188,189].

1.7 Infertility and endometriosis: prevalence figures

Studies assessing the prevalence of infertility and the amounts of couples seeking medical help, provide an insight on the severity and prevalence of the disease. Humans have an estimated monthly fecundity rate of around 20%[190]. Endometriosis has been reported to be prevalent in around 0.5-5% of fertile women and 25-40% of infertile women[191,192]. In one study of over 6,000 randomly selected women, that around 10-15% of couples in the UK alone, experience infertility[190]. In 2009, out of a survey involving 4,466 women, one in 5 women in the North East of Scotland attempting to achieve a pregnancy reported infertility[51] with endometriosis being one of the leading causes, infections (Sexually transmitted infections (STI)), chemotherapy, obesity and other health problems being listed as causative factors. There are other studies debating the quoted numerical validity of the reported current lifetime prevalence of infertility and the true values of those seeking treatment modalities as they recognise limitations in numerical data due to sample size[193]. Another limiting factor to assessing the true prevalence of endometriosis is its definitive method of diagnosis. Laparoscopy is deemed to be the gold standard for definitive diagnosis. It is however an invasive method with associated co-morbidity and only performed in women with symptoms. Its true prevalence rate is therefore masked by its diagnostic limitations. The prevalence is reported as 40% in infertile women[60] and is found in more than 33% of women with chronic pelvic pain[194]. In one study, where laparoscopy was performed for unexplained infertility, it was present in up to 47% of infertile women with regular menstrual cycles having normospermic partners[195,196].

Findings were unchanged between symptomatic and asymptomatic patient groups. These figures make endometriosis the most important cause of infertility in the abovementioned group[197]. Degrees of endometriosis are classified according to the ASRM[58]. Whilst there is evidence supporting the strong link between endometriosis and infertility, controversial issues in this relationship still exist especially in the case of mild or minimal endometriosis[60,198]. Endometriosis is also known to occur in women with male factor infertility[199] and in those with irregular anovulatory cycles[200,201]. These patient groups have not been studied in detail to provide actual prevalence figures. Over the past 25 years, changes and ameliorations in both classification methods and diagnostic optic equipment have led to improved methods of recognition. This might indicate a bias in reported previous prevalence figures of the disease[202]. Today, there is recognition that subtle peritoneal lesions can also manifest as endometriosis, leading to an increase in diagnosed cases as compared to the mid-1980s[203]. Overlapping symptoms of endometriosis, pelvic inflammatory disease (PID) and irritable bowel syndrome (IBS) all contribute to a delay in diagnosis[5,204,205].

1.8 Endometriosis and pregnancy

The effects of pregnancy and endometriosis are largely unexplored. Due to ethical issues, the effects of pregnancy on endometriosis in humans are unknown. Symptoms of disease during pregnancy are subjective and the ability to achieve pregnancy itself can affect the woman's psychological wellbeing and her perception of symptoms. Early studies from the 1960s[206] assessed 24 cases of endometriosis and found that the effects of pregnancy on the disease were variable. Whereas a few cases were seen to have endometriotic lesions which regressed, most lesions progressed. A few case reports have been since published, supporting these findings, however, good quality studies in humans are limited. Animal models have been used in limited studies, to assess for the effects of pregnancy on the development of intraperitoneal disease. Studies performing laparoscopies on pregnant baboons in the first and second trimesters did not show significant effects of pregnancy on the growth of endometriotic lesions[207]. Other earlier conflicting studies showed a regression of endometriosis in pregnant animals[208,209].

It is now well known that diseases which are inflammatory in nature such as Chron's and Rheumatoid arthritis have adverse effects on pregnancy[210,211] such as preterm delivery and its associated risks of neonatal morbidity and death. There are some publications linking subfertility to conditions such as preeclampsia and placental abruption[212]. A link to endometriosis has been postulated in this publication, but studies with improved designs and numbers are advisable. In another published study, the link between endometriosis and preeclampsia has been explored. The theory behind this association lies in the fact that both endometriosis and preeclampsia are associated with defective junctional zone remodelling of placental bed spiral arteries[213]. Other conflicting publications have shown a reduction of preeclampsia in women with endometriosis, attributing this to an increased level of angiogenic factors and increased vascular perfusion[213]. All these studies have limitations due to small sample sizes. In a large study of around 3000 women with endometriosis, there was no link between the presence of disease and preeclampsia[214]. An Australian retrospective cohort study looked at the pregnancy outcome of 630 women with endometriosis undergoing fertility treatment. There results imply that women with endometriomas have a risk of small for gestational age babies and preterm deliveries[215]. It was postulated

that endometrial abnormalities potentially present in endometriosis might be the causative factor of the observations. It was however noted that assisted reproduction itself might attribute to an increased level of pregnancy complications.

A Swedish retrospective birth study analysed data from around 1,400,000 births between 1992 and 2006. Their data shows an association between endometriosis and the risk of preterm delivery, preeclampsia and antepartum haemorrhage as well as pre-labour Caesarean sections[216]. Various confounding factors in this population are recognised. In this study, it was suggested that altered prostaglandin levels in women with endometriosis[217] could partially be the cause for preterm birth and preterm premature rupture of membranes. None of the above theories has been confirmed.

Endometrial fluid analysis has also been utilised to identify possible biomarkers for endometriosis[218]. There is some evidence of differences in this fluid between cases and controls. The endometrium covering the uterine lining is known to secrete proteins which change in response to the menstrual cycle[219]. Proteins and enzymes secreted from the endometrium can be found within the endometrial fluid of the uterine cavity[220,221] and have been suggested as key players in embryonic implantation[222,223]. The analysis of these proteins could provide insights into embryo implantation and deregulation of the process in the presence of pathology[224]. Their dysregulation has been associated with failure of implantation and infertility[225].

1.9 Location of endometriotic lesions

1.9.1 Peritoneal endometriosis

Peritoneal lesions vary in their presentation ranging between macro and microscopic disease. Their appearance varies with early active lesions appearing red, glandular or vesicular, advanced lesions appearing black or puckered and chronic healed lesions which may be white or fibrotic. Peritoneal endometriosis appears to be a dynamic disease[226] with atypical subtle lesions visualised at laparoscopy appearing and disappearing[227] on the peritoneal surface. Their importance has been attributed to the reduced fecundity experienced by women even with clinically mild disease[228]. The clinical significance of mild disease is still a controversial topic[203,229,230]; it is believed that the disease is progressive though further prospective studies without therapeutic interference are required for its verification.

1.9.2 Rectovaginal endometriosis

Deep sited endometriosis often found in extensive disease, has been classified into three different types by Koninckx and Martin[231]. Type 1 has been described as the conical infiltrative type, Type 2 is the retracted type covered by adhesions and Type 3 is the spherical rectovaginal nodule. In rectovaginal disease it is the Type 3 lesion more commonly described. Rectal ultrasound has been used to identify deeply infiltrating bowel lesions during the selection of patients suitable for surgery[232,233].

1.9.3 Ovarian endometriosis

Disease on the ovary can vary from small plaques to enlarged 'chocolate' cysts. Small endometriomas may go unnoticed unless punctured at surgery. Most of the ovarian endometriomas are pseudocysts in nature with the invaginated ovarian cortex comprising the cyst 'wall'. This invaginated cortex is then covered by a superficial endometrium-like tissue. In a paper by Hughesdon[234], a non uniformal invagination of the ovary occurs with the inner cortex being obscured by smooth muscle metaplasia, whereas the outer extended cortex thins out and loss of the original layers occurs. Hughesdon supported the theory or surface implantation or metaplasia. Two different cyst types have been described[235]. Red cysts are lined by surface epithelium and highly vascular stroma without glands covering the whitish or slightly pigmented wall. Black cysts have dark, poorly vascularised and pigmented tissue. Suggestions have been made as to different surgical techniques required for the different cyst types[235] with superficial ablation advocated in the red cysts and excision of the fibrotic wall in the black cysts.

1.10 Diagnosis of endometriosis- techniques

Certain lesions are overtly visible at laparoscopy. In these cases, visual identification of the pathology may be adequate; nevertheless, it is ideal to verify the nature of the lesions by histological assessment, confirming the presence of ectopic endometrium within the biopsied samples. ESHRE advises that in deeply infiltrating endometriosis or of ovarian endometriomas over 3 centimetres, histology serves not only to confirm clinical visualised pathology, but to exclude rare instances of malignancy[31].

1.10.1 Current investigative/diagnostic tools

Surgery, albeit an invasive option, is the only current technique giving a definitive diagnosis and enabling direct treatment, excision and removal of visible endometriosis infiltrated areas. Endometriosis is a multifactorial condition with widespread effects in the body depending on the sites of its implantation, amounts present and its rate of proliferation. Patient symptoms (when present) may aid clinicians in diagnosing and locating endometriosis. The use of magnetic resonance imaging (MRI), ultrasound (transrectal, transvaginal, renal or abdominal), intravenous pyelography (IVP) and even barium enema studies have all been utilised to non-invasively attempt to identify location and severity of disease. Interpretation of radiological techniques is user dependant and, even in the best of hands, is found to be very limited in the mapping of this disease.

1.10.2 Ultrasound and magnetic resonance imaging (MRI)

Ultrasound is the technique whereby cyclic sound waves (in the range above the upper limit of human hearing) are used to penetrate tissues and media, generating a reflection signature. This signature is then translated into an image and used as a non-invasive method of diagnosing intracorporal pathology. The technique has its limitations. It is useful in diagnosing the presence of ovarian endometriomas and in expert hands, can be used to identify rectal or bladder disease infiltration. It however has no role in diagnosing pelvic or peritoneal endometriosis[236,237]. Assessment of adenomyosis has been possible with radiological screening both through the utilisation of ultrasound and MRI[238,239]. The junctional zone

(visible as a low T2 signal layer on MRI) is a region beneath the endometrium representing the inner myometrium. In adenomyosis there is thickening and loss of definition of the junctional zone, making it an important diagnostic feature of disease. One review of 2,312 women showed that for adenomyosis, transvaginal ultrasound retains a sensitivity of 72% and specificity of 81%, whilst MRI had a pooled sensitivity of 77% and a specificity of 89%. This shows that the correct diagnosis was obtainable more often by the latter rather than former method[240]. When comparing MRI to laparoscopy, MRI has limited value as a means of diagnosing endometriosis[237].

1.10.3 Blood tests

Serum cancer antigen 125 (Ca125) is also known as mucin 16 or MUC16. It is a carbohydrate antigen first discovered around 1983 and belongs to the mucin family of glycoproteins[241]. Ca125 is the marker most consistently elevated in ovarian cancer and is used as a prognostic factor in assessing response during primary chemotherapy[241]. It is however expressed in other gynaecological (endometrial and fallopian tube) and non-gynaecological (pancreas, breast, colon and lung) cancers[241] and in some benign conditions such as endometriosis[241]. In endometriosis, it is however not related to disease severity and not necessarily co-related with the presence or absence of the disease. Compared to laparoscopy, it is of no value as a diagnostic tool[242]. Studies looking at Ca125 levels in peritoneal fluid at surgery claim it has better sensitivity in detection rates compared to serum levels[243]. Studies looking for an alternative diagnostic test for endometriosis such as the use of the expression of chemokine receptor (CCR1) mRNA in peripheral blood leukocytes and Monocyte chemotactic protein–1 (MCP-1)[244] have been performed. This study quotes a sensitivity of 92.2%, a specificity of 81.6%, a negative predictive value of 83.3%, a positive predictive value of 92.3%, a likelihood ratio of a positive test result of 5.017, and a likelihood ratio of a negative test result of 0.096[244]. It indicates its potential usage but up to date none of the studies have proven to have adequate sensitivity or specificity for clinical use. Another described technique is to quantify the expression of aromatase cytochrome P450 in eutopic endometrium[245] to distinguish between disease free women and those with endometriosis, adenomyosis or leiomyoma. Again this has not proved applicable to clinical practice.

1.11 Methods of treatment

1.11.1 Historical treatments

In the 1940s the advent of androgenic steroid hormones led to their use as a primary therapy in gynaecological disorders. Published articles at the time reported amelioration on disease both post operatively or as an alternative in women who declined surgery[246,247]. Their use as the mainstream therapeutic for the disease was discontinued due to the androgenic side effects experienced by patients including acne hirisutism and irreversible voice changes. In the late 1940s a non-steroidal synthetic oestrogen Diethylstilbestrol (DES) was developed and was tried for the treatment of endometriosis. With today's medical knowledge it is know that chronic unopposed oestrogen therapy, not only causes endometriosis proliferation but also leads to endometrial hyperplasia and malignant transformation. Despite this knowledge, in 1948 Karnaky *et al.* claimed to achieve good results with high doses of unopposed oestrogens causing amenorrhoea[248]. It was also noted that pregnancy rate increased when

oestrogen treatment was terminated. Today, there is a known association between foetuses exposed in utero to DES and clear cell vaginal carcinoma. At the time this association was unknown. In 1958 a publication by Kistner *et al.* claimed that treatment with unopposed oestrogens was unwise due to the unpredictability of disease response and development of endometrial hyperplasia[249].

It has been reported that endometriotic lesions do not correlate to the eutopic endometrial cycles[250], they still show responses to hormonal treatments or modulators. In 1975, a combined hormonal oestrogen and progestogen treatment regime mimicking a pregnant state, called a "pseudo-pregnancy" was reported to improve symptoms[251]. Today, combination regimens are used to obtain a partially inactive endometrium, amenorrhoea and quiesce disease[252,253].

Current treatment modalities for endometriosis work by suppressing ovarian steroids causing a hypooestrogenic state which in turn causes atrophy of the ectopic endometrium. This suppresses rather than eliminates pathology. In women with pain symptoms and a history suggestive of endometriosis in which a diagnosis has not been confirmed, one can opt to pursue various conservative management or therapeutic strategies. Therapies available are limited not only due to their side effects, but by the fact that they inhibit ovulation and therefore are counterproductive in women wishing to conceive[254]. Current non-surgical treatments for endometriosis are unsatisfactory. There is a clear need for the development of more effective novel therapeutics with improved efficacy, tolerability and safety[255].

Counselling, analgesia, alterations in nutrition and the combined oral contraceptive pill (COCP) are regarded as first line treatment modalities[256]. Progestagens, oestrogen-progestin combinations, danazol, gestrinone, medroxyprogesterone acetate, levonorgestrel intrauterine system (LNG-IUS)[257] or Gonadotropin-releasing hormone (GnRH) agonists are all hormonal therapies currently used to reduce pain and suppress, but not eliminate, the disease. In confirmed moderate or severe disease, suppression of ovarian function for 6 months reduces endometriosis. All hormonal drugs which have been studied show varying side effect profiles but ultimately have an equally effective role. Once these treatments are discontinued, symptoms often recur after a period of time. These therapies are limited in their use duration due to the indirectly induced hypoestrogenic side effects which have long term health implications e.g. osteoporosis with GnRH. Reviews assessing possible future therapeutics have been carried out but there is a large discrepancy between promising pre-clinical trials and the clinical ones[255]. This reflects the poor understanding we have of the mechanisms underlying the disease and further research is in dire need.

In women, who decline surgery and are happy to proceed to treatment without a definite diagnosis, a therapeutic trial of hormonal medications which reduce menstrual flow is an option.

1.11.2 Overview of medical treatments

Medical treatments serve to control pain and repress disease but there is no treatment that currently cures endometriosis. Analgesics including non-steroidal anti-inflammatory drugs (NSAIDS) have been used in the clinical setting. Cyclooxygenase-2 (COX-2) inhibitor rofecoxib was used in trials but has been withdrawn due to cardiovascular side effects. TNFα inhibitor (pentoxifylline) use is being researched but is not routinely used in clinical practice[258].

Hormonal treatments including the combined oral contraceptive pills, progesterone only pills and intrauterine progesterone (LNG-IUS), progestins, gestrinone, danazol (despite its masculinisation side effects) and GnRH analogues are all used. Hormonal therapies have substantial symptomatic side effects including menopausal symptoms and infertility whilst on treatment. Immunomodulators such as human recombinant interferons (IFNα-2b) and members of the immune modulating cytokine family have been used as *in vitro* therapeutics. They suppress the growth of *in vitro* endometriosis in a dose dependant manner[259]. Clinical trials looking at effects of intraperitoneal administration of IFNα-2b has shown improvements in the severity and stage of endometriosis but recurrence results are ambiguous[147,153] necessitating further studies.

1.11.3 Non-steroidal anti-inflammatory drugs (NSAIDS)

There is some evidence that this class of drugs may improve pain symptoms experienced in women with endometriosis[260,261]. They function by blocking the COX-1 and COX-2 pathways. The newer ones are selective for COX-2 and therefore minimise gastric side effects. They therefore reduce aromatase activity, oestrogen production and endometriosis proliferation[180]. This class of drugs is not suitable in women who are asthmatic or have a history of gastric ulceration. When taken at mid cycle, an anti-ovulatory effect is noted. There is insufficient evidence on the use of other classes of analgesics.

1.11.4 Hormonal treatments

1.11.4.1 Levonorgestrel intrauterine system

This coil is a slow release system of 20 micrograms levonorgestrel into the intrauterine cavity per 24 hour period. It thereby suppresses the endometrial proliferation reducing the endometrial thickness, menstrual loss, dysmenorrhoea and progression of endometriosis. The system has proven benefit in producing amenorrhea or hypomenorrhea with good patient satisfaction[262]. Again, hormonal side effects of abdominal bloating, breast tenderness, weight gain have all been reported. It also has a contraceptive effect preventing ovulation thereby reducing the fertility of the patient during its usage.

1.11.4.2 Oral contraceptive pill (OCP) and gonadotropin-releasing hormone (GnRH) analogues

There is a limited amount of studies and data comparing the two methods. So far there is no proven benefit of one treatment modality over the other though it is recognised that the available studies are in small numbers and underpowered[263,264]. GnRH analogues are a group of drugs used in the treatment of endometriosis for the last twenty years[265]. Side effects range from hot flushes to osteopaenia (especially in therapy lasting over 6 months) and may be reversed with hormonal add-back therapy. Even with effectively managed endometriosis 5 year recurrence rates with GnRH agonists range between 33%-75%[266].

1.11.5 Immune modulators

Women suffering from endometriosis have an increased risk of immune system and endocrine diseases such as rheumatoid arthritis[24]. One cross-sectional survey[24] assessing 3680 patients with endometriosis

showed that endometriosis patients had higher levels of hypothyroidism (9.6 versus 1.5%, P < 0.0001), rheumatoid arthritis (1.8 versus 1.2%, P = 0.001), systemic lupus erythematosus (0.8 versus 0.04%, P < 0.0001), Sjögren's syndrome (0.6 versus 0.03%, P < 0.0001) and multiple sclerosis (0.5 versus 0.07%, P < 0.0001)[24], Human recombinant interferons (IFNα-2b) members of the immune modulating cytokine family have been used as *in vitro* therapeutics. They suppress the growth of *in vitro* endometriosis in a dose dependant manner[259]. Clinical trials looking at effects of intraperitoneal administration of IFNα-2b has shown improvements in the severity and stage of endometriosis but recurrence results are ambiguous[147,153] necessitating further studies.

1.11.6 Therapies- surgical

Clinically, endometriosis may manifest as palpable lesions, with certain studies suggesting that it is in this subgroup of women where the maximum benefit of surgical resection lies[267]. Surgical excision is still described as the 'gold standard' in diagnosing and treating endometriosis. The Royal College of Obstetricians and Gynaecologists (RCOG) guideline on endometriosis[268] advises that the reduction of endometriotic lesions by ablation supersedes diagnostic laparoscopy alone in pain reduction and that radical resection of all visible lesions reduces pain. This approach has recognised limitations in identification, treatment and symptom relief of the disease. There has been no demonstrable difference between ablation and excisional treatments as far as postoperative pain levels are concerned[269]. Both treatment modalities have been noted to provide good symptomatic relief and reduction of pelvic tenderness with no difference in morbidity[270].

Laser laparoscopy is quoted as a safe, simple, and effective treatment in alleviating pain symptoms in women with stages I, II, and III endometriosis[271]. Good practice by ESHRE advises that lesion type, extent, adhesions should all be recorded in the patient notes. Ideally findings should be recorded on DVD or video[31]. A prospective study by Sutton *et al.*[271] confirmed a marked improvement in pelvic pain in patients with mild or moderate endometriosis if treated by laparoscopic ablation compared to those receiving placebo. Certain retrospective studies into advanced disease showed improvement in those patients actively managed by laparoscopic CO_2 laser ablation[272] whereas others show conflicting long term results, with success rates falling even over short time intervals[267,273]. Studies have failed to show benefits of uterosacral ligament resection or presacral neurotomy[274,275] over conservative laparoscopy in reducing the medium or long term severity of dysmenorrhea[276,277]. Laparoscopic uterosacral nerve ablation (LUNA) has been employed in some studies to assess the impact of the procedure in the management of endometriosis. In the absence of endometriosis it has been found to be effective for dysmenorrhoea though no evidence has been found for its use in chronic pelvic pain related to endometriosis[278].

With presacral neurotomy, the argument of incomplete nerve resection is debated as a reason for its ineffectiveness[279]. This led to the usage of uterosacral ligament resection as a uterine denervating technique[280]. Its effectiveness and validity in achieving pain relief has been inconsistent[281,282] with some studies being suboptimal[277] with others showing no benefit over direct lesion ablation[281]. Placebo studies have hinted at the presence of a post-operative placebo response which disappears within a few months of treatment[283].

Diagnostic laparoscopies with ablation or excision of the lesions are carried out improving fertility and pregnancy rates[284,285]. Timing of surgery to a particular period within the menstrual cycle has not been proven. Nevertheless guidelines from ESHRE also advise women being off hormonal treatment for 3 months to avoid under diagnosis of patients.

Extensive surgery involving bowel and bladder resection has been shown to improve symptoms from the disease but shows an associated increase in concomitant morbidity.

1.12 Quality of life affected by endometriosis

Women suffering from this disease report mixed feelings when questioned about future outcomes of their management and their quality of life. Those women experiencing the most severe pain are the most pessimistic.

The presentation of endometriosis ranges widely from mild to severe disease. Symptoms experienced by patients vary ranging from those who are asymptomatic to those complaining of severely debilitating, chronic, incapacitating symptoms which adversely affect their quality of life, mental health and social interactions[286]. Patients suffering from endometriosis report a deterioration in their work life productivity at an average of approximately 10 hours per week compared to 7 hours in non-affected women[7]. Increased levels of depression and anxiety also occur[287-289].

There is a poor correlation between findings at laparoscopy and histopathological diagnosis[290]. Symptoms do not necessarily correlate to disease extent or severity[11] and a proportion of women are only diagnosed coincidentally[291]. Thus a proportion of women with minor disease are over investigated, treated and even subjected to surgery, whereas a proportion of severely affected women might go unnoticed or under investigated and treated. It is believed that the location, rather than overall severity is implicated in symptom intensity[292]. Pain recurrence and re-operative rates in conservative surgery for symptomatic endometriosis are high and underestimated[293] with operator dependant outcomes.

Assessing patient quality of life has been performed in a number of studies using standardised validated quality of life questionnaires such as the Short Form questionnaire (SF36 or the SF12)[294,295] and pain questionnaires such as the PIQ6. Other recognised tools include The Hospital anxiety and depression scale[296] as well as the revised Sabbatsberg Sexual Rating Scale[297]. Two studies from the USA by Ballweg and Whitney utilised focused group interviews[298,299] and pictorial forms of expression to describe disease severity and its impact on life. An assessment of differences between patient groups for dyspareunia, non-menstrual pelvic pain, psycho-emotional profile, sexual functioning, relationships and overall satisfaction of treatment[274] have been performed. These assessment tools give us an indication as to the overall outcomes of laparoscopic interventions on disease and patient quality of life.

Current medical treatments include pain relieving and hormonal agents which apart from their side effects (hirisutism, acne and weight gain) may induce amenorrhoea and menopausal symptoms (e.g. GnRH analogues) precluding fertility[300]. In addition to these effects, reduction in pain is only achieved in the short term. Laparoscopic surgery using laser ablative techniques in combination with excision of endometriotic lesions and laparoscopic uterosacral ligament resection are techniques used to minimise

disease and pain. Surgeons aim to maximise the post-operative symptom free period but publications vary in their outcomes.

1.12.1 Pain

An estimated 70%-75% of patients with endometriosis suffer from pelvic pain[301] most of which is chronic in nature. In 24% of cases, reports of 2.5 days of bed rest per month due to pain are documented, 22% of women report sexual dysfunction and 25% report dyspareunia[302]. In a study assessing quality of life in patients with deeply infiltrating endometriosis, complete resection of lesions was associated with significantly improved outcomes in painful functional symptoms including dysmenorrhea, deep dyspareunia, dyschesis during menses, lower urinary tract symptoms and chronic pelvic pain, irrespective of the number and location of lesions or concomitant medical issues or characteristics. Reported pain levels in infertile women did not vary in relation to the success of their fertility outcomes post-surgery[303]. Catastrophising and biopsychosocial variables have been recently implicated in the severity and chronic pain experienced in patients with endometriosis[304]. Where these are present, an average of 37.4% reduction in interval pain has been reported but nulliparity and referral to physical therapy showed worse outcomes in interval pain improvement.

1.12.2 Dysmenorrhoea and dyspareunia

In one study, recurrence of moderate to severe dysmenorrhea within the first postoperative year has been quoted at 29% post uterosacral ligament resection and 27% after conservative surgery[274]. Results 3 years after initial surgery have been published though their validity is debatable as the independent analgesic effect of surgery (irrespective of the nature of surgery undertaken) is seen to reduce over time. Up to 40% of patients express distressing recurrence of symptoms within 3 years of their primary surgery. This highlights the importance of long term follow-up.

1.12.3 General health and quality of life

Pain scores are subjective with exacerbated symptoms reported in patients with concomitant systemic disease or depression. The site and type of pain varies between patients but is commonly associated with those having endometriosis[267,300]. Overall, irrespective of whether or not uterosacral resection is performed, laparoscopic surgery is associated with reported improvements in general health, quality of life, emotional wellbeing and sexual satisfaction[274]. Overall surgical dissatisfaction figures of 25% increasing to 37% at 1 and 3 years post operatively have been quoted. This might be a recognised overestimation as figures have included those patients lost to follow up[274].

1.12.4 Sexual function

Dyspareunia is the commonest reported symptom in sexually active women and is linked to the presence of adhesions, endometriomas, uterine retroversion or affected uterosacral ligaments. Patients in this group report improved outcomes and less side effects with surgical rather than medical treatments manifesting less anxiety about the long term effects of surgery even in sub-groups experiencing multiple procedures[305].

1.12.5 Fertility

The impact of mild endometriosis on fertility is a controversial subject with divided opinions on its significance. The direct incidence of infertility secondary to endometriosis is difficult to quantify but around 30%-50% of women with endometriosis suffer some form of infertility[46]. A large multicentre prospective study by the Canadian Collaborative group on stage 1-2 endometriosis (using the American fertility scoring system) in the 1990's looked at the fertility and treatment outcomes of women with endometriosis versus those with unexplained infertility[306]. This study showed a reduction in fertility in those patients with endometriosis but findings were not statistically significant. The same study did show a statistically significant improvement in fertility rates after the treatment of endometriosis[307] which has been confirmed in other publications[308]. A conflicting Italian study failed to show statistical significance in birth rates between treated and untreated patient groups[309]. Current data indicates that it is reasonable to treat stage 1-2 endometriosis when discovered during laparoscopy for fertility[307]. Surgery itself is shown to be superior in outcomes to medical therapy in achieving increased pregnancy rates although there is no statistically observed benefit in ablation over excisional techniques[310]. Laparoscopy for severe rectovaginal endometriosis is less likely to negatively impact fertility outcomes compared to laparotomy[311], with recent studies showing improved *In vitro* fertilisation (IVF)/intra-cytoplasmic sperm injection (ICSI) outcomes and live birth rates (both for spontaneous and assisted conceptions) in patients treated for stage 1-2 endometriosis[312].

1.12.6 Social interactions

The utilisation of forms such as the Short Form questionnaire (SF36 or the SF12) includes 'visualisation' of the impact disease has on social interactions. Endometriosis has been attributed to reduction in the quality of patient social life. The inability to interact has been attributed to strain on personal relationships resulting in break ups as the patient or her partner were unable to cope with constant strain.

1.13 Socio-economic impact of endometriosis

1.13.1 Direct costs

It is currently estimated that in the UK alone, 2 million women suffer from this condition. Published UK hospital statistics in 2003 show that 0.06% (31,238) of hospital bed days were for endometriosis with the mean age of the women requiring hospitalisation being 35 years[313]. In a US study[314] annual costs related to healthcare and general loss of productivity were estimated respectively at $2,801 and $1,023 per patient. Extrapolation for a US population, assuming a 10% prevalence rate, amounts to $22 billion in estimated costs making it a higher cost than that incurred by other common diseases including Chron's and migraine[314]. Debates as to whether surgical or medical therapies are more cost effective in treating endometriosis exist, with no solid conclusions, especially since the development of chronic pelvic pain results in a lifelong ailment. A recent Canadian study in 2011 estimates the mean annual cost incurred by society due lost productivity as a result of endometriosis at $5,200 per patient (95% CI $3,700 to $7,100)[315]. Extrapolated, an estimate of a total annual cost of $1.8 billion (95% CI $1.3 billion to $2.4 billion) due to surgically confirmed endometriosis is made[315].

The costs of endometriosis related infertility are largely unknown and lacking. With an estimated incidence of 30%-50% in women who are infertile[46], its cost impact should be substantial. Estimated costs in 1998 for diagnosing endometriosis in infertile couples were £363 per couple. Where women were younger than 40 years and required surgical (laparoscopic or open) intervention, costs were estimated to range between £801 and £1,622[316].

In the UK, estimate costs for women with mild, moderate and severe endometriosis requiring IVF ranged between £2,115-£4,475, £2,002- £4,622 and £2,002-£4,899 respectively[317].

1.13.2 Indirect costs

These encompass loss of productivity at work, decrease in social interaction and its psychological effects such as depression. Between 1997 and 2002, 75% of all endometriosis admissions were in patients aged between 18-44 years, with the vast majority being labour-force workers[316]. A survey performed in 1996 suggested a mean loss of 177.6 hours per year (1 month in loss productivity) due to chronic pelvis pain in endometriosis[316] amounting to $1,595 loss for the respective employer. If each woman with chronic pelvic pain lost these hours, an estimated cost of $14.7 billion loss of productivity is suffered annually by the US economy. An estimated additional $1.8 billion was incurred by patients themselves in the management of chronic pelvic pain[318].

Despite the current scarcity of data, results above show the significance of the financial impact this disease has on society. Hospitalisation and medical costs are on the general increase making admissions and treatment of a chronic illness more costly over time.

1.14 The cell cycle and an introduction to basic cellular processes and tumour suppressors- an aid to understanding disease processes

FIGURE 1-3

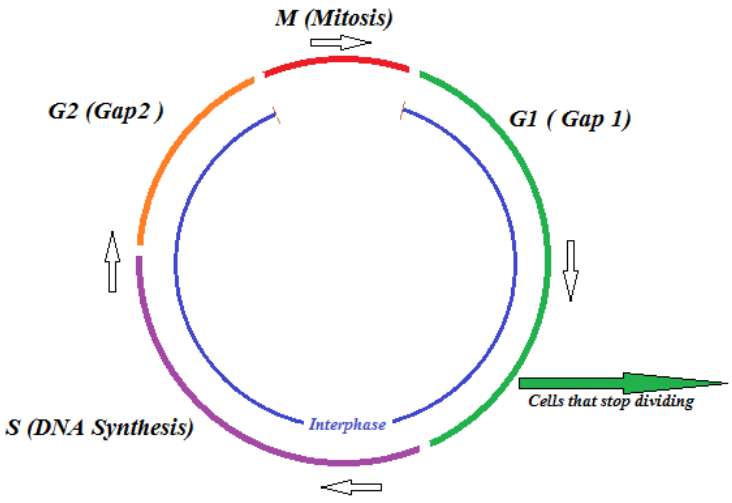

Diagram demonstrating the basic phases of the cell cycle

Cellular division and death is controlled by a series of specific mechanisms which if aberrant can lead to the formation of abnormal pathology. Knowledge of the cell cycle is imperative to understanding the balance between cellular proliferation and death.

Interphase encompasses the G1, S and G2 phase (Figure 1-3). It is a growth phase where cellular metabolic activity occurs in preparation for mitosis. Cellular organelles double, DNA replication and protein synthesis occurs. Chromosomes are not clearly visible in the nucleus, the nucleolus usually is. G1 is the phase where the cell grows, organelles are synthesised and cytoplasmic volume increases, a cell which does not divide again remains in this phase. The S or synthesis phase is also known as the Swanson phase where cellular DNA duplication occurs. G2 phase is the phase in which the cell resumes its growth in preparation for mitosis.

Mitosis (M phase) is subdivided into further components: Prophase, Metaphase, Anaphase, Telophase and Cytokinesis. In prophase, the chromatin condenses becoming visible in the form of chromosomes, centrioles move to opposing ends of the cell, the nucleolus disappears and fibres in the cell form the mitotic spindle. Prometaphase is marked by dissolution of the nuclear membrane and proteins attaching to the centromeres forming kinetochores. Metaphase occurs when spindle fibres cause alignment of the chromosomes forming a metaphase plate. Anaphase is marked by the separation of the paired chromosomes at the kinetochores and their movement towards the opposite poles of the cell along the spindle microtubules. Telophase starts once the chromatids arrive at the cellular opposite poles and new membranes form around the new daughter nuclei. Chromatomes are no longer visible, spindle fibres dissipate and the commencement of cytokinesis occurs. Cytokinesis is the splitting of the original cell into two daughter cells.

1.14.1 Cell cycle regulators and checkpoints

Checkpoints within the cycle assess for DNA damage. Should this be identified, the cell cycle is stalled until repairs are made. Alternatively, should repair be impossible, an effector mechanism causing cellular destruction by apoptosis is initiated. The cell cycle is controlled by proteins called cyclin-dependent kinases (CDKs) which are activated by another group of proteins called cyclins. They enable the movement of the cell between phases, acting as major control mechanisms.

FIGURE 1-1

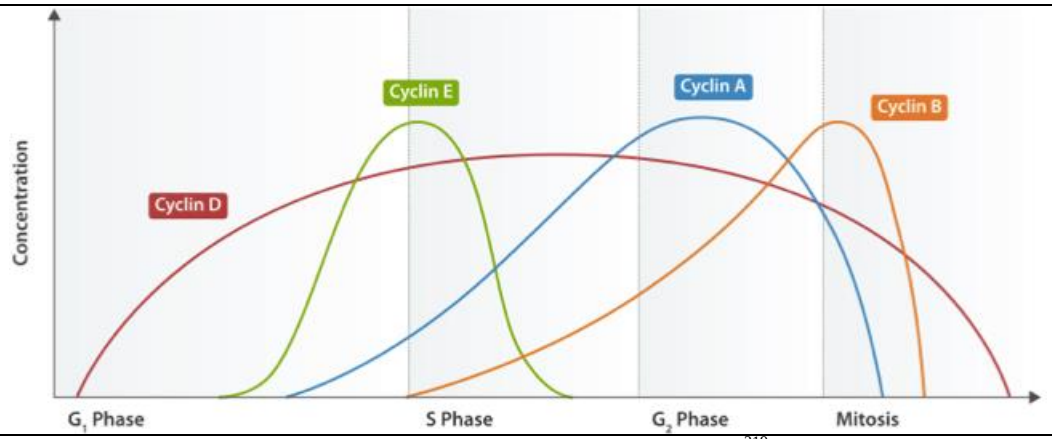

Schematic representation of cyclin alterations within the normal cell cycle phases[319]

The maturation promoting factor or Mitosis promoting factor (MPF) includes the cyclin B and Cdk1 which trigger movement in the cell cycle. In the G1 phase, the main implicated cyclins are the D cyclins together with Cdk4 and Cdk6 , followed by cyclins E and Cdk2 in the S-Phase, Cyclin A and Cdk2 in the G2 phase and B cyclins with Cdk1 (Cdc2) in the Mitotic phase (Figure 1-4).

FIGURE 1-4

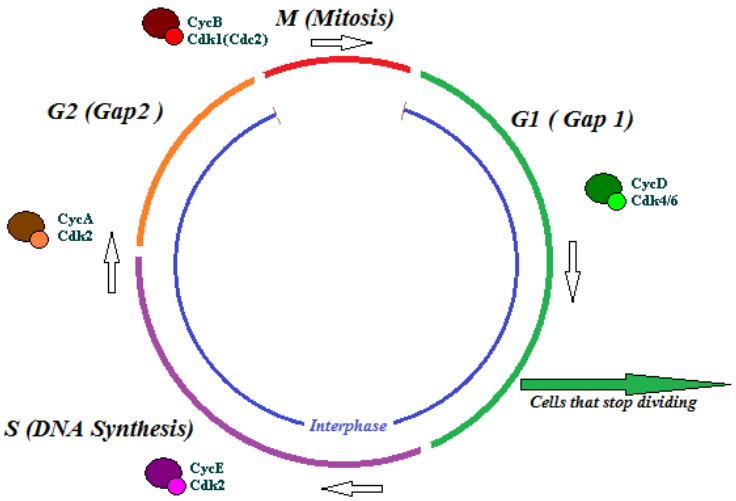

Diagram demonstrating cell cycle regulators and checkpoints

The replication of DNA in the S phase of the cycle is dependent on the expression of required proteins activated by the E2F transcription factor. This transcription factor is regulated by the protein product of the retinoblastoma gene pRB. Between the G0 or early G1 phase, the E2F is inactivated by pRB. In the late G1 phase the CyclnD/Cdk4 complex phosphorylates sites on the pRB releasing the E2F. This then produces proteins for DNA replication to occur. The activated E2F, stimulates in turn the production of further E2F, and Cyclins A and E enabling the formation of the Cyclin E/Cdk2compex. This further phosphorylates pRB moving the cell cycle into the S phase. The formed Cyclin A/Cdk2 complex acts on terminating the DNA replication by phosphorylating the E2F.

1.14.2 Apoptosis

FIGURE 1-5

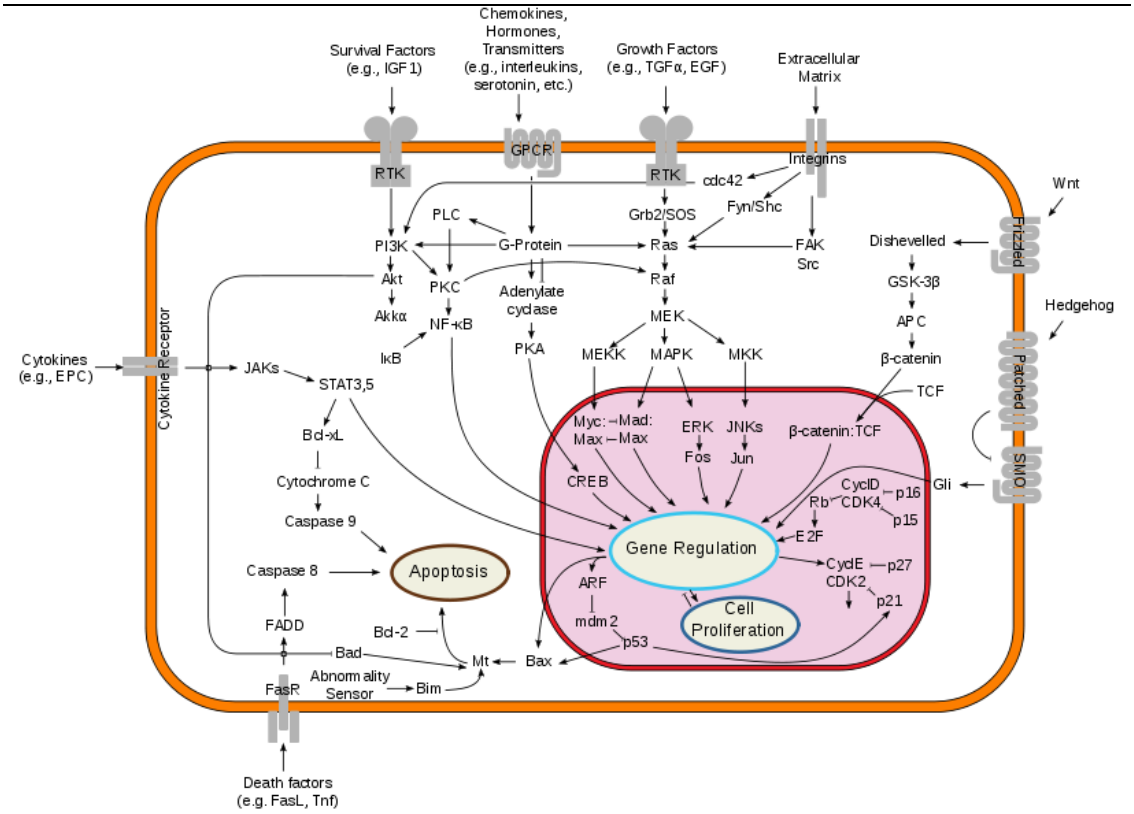

Cellular signal transduction pathways[320]

The caspase class of proteins regulates apoptosis. They control its initiation (e.g. caspase 8 and 10) and execution (caspase 3, 6 and 7) by destroying cellular proteins. Initiating caspases cleave to inactive caspases at specific sites, resulting in the executing caspase degradation of cellular proteins by their proteases. Inducers of apoptosis vary. Some of these include the Fas ligand (FasL/CD95L), a type-II transmembrane protein belonging to the tumour necrosis factor family, TNF-related apoptosis-inducing ligand (TRAIL), the Apo 2 or 3 Ligands (APO-2L, APO-3L) and the tumour necrosis factor (TNF). These bind to apoptosis inducing receptors such as Fas/CD95, TRAIL (TNF-related apoptosis-inducing ligand) death receptors DR4 and DR5 (DR4/DR5), DR3, and the tumour necrosis factor receptor (TNFR). Once the ligands bind to receptors, recruitment of cellular adaptors such as FADD (Fas-associated death domain protein) and TRADD (TNFR-associated death domain protein) occurs and caspases are activated (Figure 1-6).

FIGURE 1-6

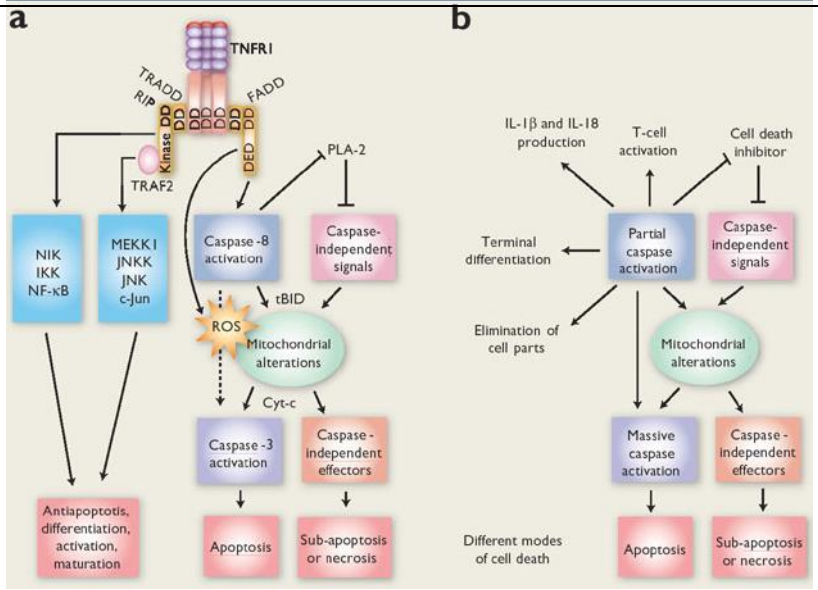

The role of Caspases in cellular signal transduction[321]

1.14.3 P21

P21or WAF1 is also known as cyclin-dependent kinase inhibitor 1 or CDK-interacting protein 1. It is found on chromosome 6 encoded by the CDKN1A gene and binds to and inhibits the activity of CDK1 or CDK2 complexes regulating the cell cycle at G1. It is tightly regulated by p53 and in response to stress stimuli meditates the cell cycle arrest at the G1 phase. It also interacts with a DNA polymerase known as proliferating cell nuclear antigen (PCNA) regulating DNA replication and repair in the S phase of the cell cycle. Unlike p53, mutations in P21 are not associated with increased incidence of malignancy.

1.14.4 P27

P27 is a member of the gene family of Kip/Cip CDK inhibitors (CDKIs) which acts on cyclin-dependent kinases (CDKs) to exert positive and negative regulatory functions at the G1/S phase of the cell cycle[95]. Mutations of the Kip/Cip genes are rare but knock-out mice models of P27 have increased predisposition to tumours. Numerous studies link reduced levels of P27 with worse prognostic tumour outcomes[322,323].

1.14.5 P53

p53 is a tumour suppressor protein encoded by the TP53 gene located on the short arm of chromosome 17 (17p13.1) with an important role in the cell cycle and apoptosis. It is found at low levels in normal cells. Stress signals within the cell or damage to the DNA elevate p53 protein levels. A defect in the protein is linked to abnormal cellular proliferation and malignancy with around 50% of tumours containing p53 mutations. Its role is to arrest the cell cycle in the event of minor DNA damage and to induce apoptosis if the damage is severe. The presence of a genetic defect in p53, also known as Li Fraumeni's syndrome, leads to a high frequency of cancer in affected individuals. Whereas increased levels of p53 induces apoptosis suppressing tumour growth, excess elevation of p53 causes excess apoptosis increasing the

ageing process. The gene Mdm2 via the Ubiquitin system is the major regulator of p53. DNA which is damaged activates protein kinases such as ATM, DNA-PK, or CHK2. Phosphorylated p53 secondary to DNA damage cannot bind to Mdm2 increasing its levels. Once DNA damage is repaired, the kinases are no longer active and p53 dephosphorylation occurs and can be destroyed by the Mdm2. p53 is also known to induce apoptosis via the mitochondrial release of Cytochrome c when it binds to Caspase9. It activates the expression of the Bax gene and Apoptotic protease activating factor 1 (Apaf1). The Bcl-2-associated X protein (Bax) gene stimulates the Cytochrome c release, which on binding to Caspase 9, induces apoptosis. A few studies have looked at the relation between p53 and CDKN1A genotypes in endometriosis. p53 is responsible for the transcriptional induction of the p21 gene (CDKN1A/WAF1/CIP1). These two molecules are known in literature to be associated with pathology sensitivity to cancer. In this study[324], it has been suggested that there are significant differences in the p53 but not the CDKN1A genotype in women with endometriosis. It is postulated that the C (prp) allele of the p53 codon can be associated with development of endometriosis and potentially serve as a marker for this disease.

1.15 Associated pathways- inflammation and angiogenesis

During surgery, increased levels of angiogenesis and vascularity are seen around the sites of implantation of endometriosis. Studies have postulated that the endometrium itself of patients who develop endometriosis has the increased capacity to proliferate, implant and grow predisposing to increased levels of endometrial angiogenesis when compared to normal subjects[325]. Angiogenesis is therefore postulated to be a major pre requisite enabling the development of disease and studies investigating angiogenic repression and its effects on endometriosis have been performed. Once endometrial tissue adheres to other tissues, it induces an inflammatory reaction thereby becoming a chronic process over time[313,326].

Studies have assessed the importance of the angiogenic process in the progression of endometriosis and regression of ectopic endometrium has been noted once angiogenesis is repressed.

The levels of inflammatory modulators such as interleukin-1β (IL-1β) and tumour necrosis factor-alpha (TNF-α) have been found to differ between endometriosis patients and controls. Interleukin-6 (IL-6) is found at higher levels in endometrium and endometriosis tissue of cases compared to controls[327]. Endometriotic tissue was found to have significantly lower levels of TNF-α[327] and significantly higher levels of IL-1β compared to normal endometrium from the cases or controls (Figure 1-2). The endometrium from patient cases was also seen to have a phasic response to levels of IL-1β with their levels increasing in the luteal compared to the follicular phase. The concentrations of IL-1β in endometriosis and in endometrium from controls were positively correlated with IL-6 levels[327]. IL-6 activates nuclear factor kappa beta (NFκB) and is responsible for various pathways within the body. It plays an important role in the body's defence system against pathogens including viral infections. Activities controlled by IL-6 include terminal differentiation and immunoglobulin secretion in B cells, B cell differentiation and growth, haematopoietic stem cell colony formation as well as the differentiation and activation of macrophages and T-cells[328].

1.15.1 Prostaglandin E2 (PGE-2)

The cluster of differentiation 36 (CD36) is an integral cell membrane protein found on the surface of various cell types. It belongs to the class B scavenger receptor family and is involved in inflammation and angiogenesis[329]. Apart from being a receptor for thrombospondin-1 (TSP-1) and forming a complex which mediates cellular interactions between tumour cells, it can act separate to the TSP-1 receptor with other proteins, cytoskeletal proteins, integrins and signalling molecules to exert its effects[329]. Prostaglandins (PGE) are seen to inhibit the expression of CD36 in peritoneal macrophages via the prostaglandin E2 pathway (EP2) reducing their ability to phagocyte cells[330]. In mouse models, endometriotic lesions were seen to increase on treatment with prostaglandins. This growth was reversed when prostaglandins were blocked with cyclooxgenase inhibitors. This indicates an immunological mechanism which may be utilised as a future therapeutic regime[330].

1.15.2 Association with malignancy

The presence of endometriosis has not been attributed to a general increased risk of cancer[331] in the patient population. Chronic sufferers over a 10 year period, have an associated overall increased risk of developing clear cell/endometroid ovarian carcinomas[332] (Table 1-4, Table 1-5, Table 1-6). There are also numerous studies showing a histological transition from benign to malignant endometriotic lesions to malignant ones[333,334] supporting the theories of progressive disease development with chronic worsening of disease. No direct single causative factor has been identified; rather, it is suggested that a cumulative combination of factors is necessary for a chronic progression of disease[332]. Risk factors exist predisposing to the development of endometriosis and associated ovarian carcinomas, some of which include hormonal stimulation, nulliparity, obesity, early menarche and the use of HRT post-menopausally. Studies reporting links with malignancy have limitations leading to misinterpretations of the null hypothesis or overestimations of results. There is however increasing evidence of its links with other malignancies particularly melanomas and Non-Hodgkin's lymphomas where microenvironment and inflammation may play a role. Two large independent cohort studies confirm the link with Non-Hodgkin's lymphoma[335] though statistically significant results were only obtained from a small number of cases and larger studies are required. Humoral immune anomalies, B-cell activation, a common aetiological cause and disease development as a consequence to medication supplied, have all been postulated as theories linking endometriosis to Non-Hodgkin's lymphomas.

TABLE 1-4

Studies on the frequency of endometriosis in patients with ovarian cancers according to the malignant histotype

	Ovarian cancer histotype					
Authors	**Serous**	**Mucinous**	**Endometrioid**	**Clear cell**	**Other**	**Total**
Aure *et al.*	0% (0/357)	1% (1/203)	9% (20/212)	24% (14/59)	…	4% (35/831)
Kurman and Craig	6% (7/118)	4% (2/47)	11% (4/37)	0% (2/28)	…	7% (15/230)
Russel	3% (7/233)	4% (3/69)	28% (20/72)	48% (16/33)	…	11% (46/407)
Vercellini *et al.*	4% (8/220)	6% (6/94)	26% (30/114)	21% (8/38)	12% (11/88)	11% (63/556)
De La Cuesta *et al.*	0% (0/10)	6% (1/18)	39% (9/23)	41% (7/17)	45% (5/11)	28% (22/79)
Toki *et al.*	10% (9/88)	9% (3/33)	30% (16/54)	50% (22/44)	0% (0/16)	21% (50/235)
Jimbo *et al.*	9% (8/92)	3% (1/35)	23% (3/13)	41% (13/32)	…	15% (25/172)
Fukunaga *et al.*	10% (6/63)	6% (2/35)	42% (13/31)	54% (27/50)	67% (2/3)	27% (50/182)
Ogawa *et al.*	7% (4/60)	0% (0/17)	43% (3/7)	70% (30/43)	…	29% (37/127)
Vercellini *et al.*	3% (2/61)	3% (1/30)	20% (13/66)	14% (5/35)	6% (1/17)	10% (22/209)
Oral *et al.*	4% (3/70)	6% (2/35)	22% (4/18)	9% (1/11)	8% (4/49)	8% (14/183)

Frequency of endometriosis in patients with Ovarian cancers[331]

TABLE 1-5

Relationship between endometriosis and ovarian cancer

Studies	Study design	Entity of the association	
		OR, SIR, or RR	95% CI
Brinton *et al.*	Cohort	1.9	1.3-2.8
Ness *et al.*	Case-control	1.7	1.2-2.4
Ness *et al.*	Case-control	1.7	1.1-2.7
Berglund *et al.*	Cohort	1.4	1.2-1.7
Brinton *et al.*	Cohort	1.3	0.6-2.6
Borgfeldt and Andolf	Case-control	1.3	1.0-1.7
Modugno *et al.*	Case-control	1.3	1.1-1.6

OR: odds ratio, SIR: standardized incidence ratio, RR; relative risk, CI: confidence interval

Relationship between endometriosis and Ovarian Cancer[331]

TABLE 1-6

Relationship between endometriosis and non-ovarian gynaecological cancers

Studies	Study design	Entity of the association	
		OR, SIR, or RR	95% CI
Breast cancer			
Moseson *et al.*	Case-control	4.3	0.9-20.4
Schairer *et al.*	Cohort	3.2	1.2-8.0
Schairer *et al.*	Cohort	3.0	0.7-4.1
Brinton *et al.*	Cohort	1.3	1.1-1.4
Weiss *et al.*	Case-control	1.1	0.7-1.8
Venn *et al.*	Cohort	1.0	0.7-1.5
Olson *et al.*	Cohort	1.0	0.8-1.2
Borgfeldt and Andolf	Case-control	1.1	1.0-1.2
Brinton *et al.*	Cohort	0.8	0.6-1.1
Cervical cancer			
Brinton *et al.*	Cohort	0.7	0.4-1.3
Berglund *et al.*	Cohort	0.6	0.5-0.8
Borgfeldt and Andolf	Case-control	0.6	0.4-0.9
Endometrial cancer			
Brinton *et al.*	Cohort	1.1	0.6-1.9
Olson *et al.*	Cohort	1.2	0.6-2.5
Borgfeldt and Andolf	Case-control	0.6	0.4-0.8
Brinton *et al.*	Cohort	0.8	0.3-1.9
Melanoma			
Wyshak *et al.*	Case-control	3.9	1.2- 12.4
Frisch *et al.*	Case-control	1.1	0.5-2.3
Holly *et al.*	Case-control	0.9	0.5-1.4
Brinton *et al.*	Cohort	1.0	0.7-1.5
Olson *et al.*	Cohort	0.7	0.2-1.8
Brinton *et al.*	Cohort	2.1	1.0-4.4
Non-Hodgkin's lymphoma			
Brinton *et al.*	Cohort	1.8	1.2-2.6
Olson *et al.*	Cohort	1.7	1.0-2.9
Berglund *et al.*	Cohort	1.2	1.0-1.5

OR: odds ratio, SIR: standardized incidence ratio, RR; relative risk, CI: confidence interval

The study from Schairer *et al*. focused on two different cohorts: patients who underwent hysterectomy and those who underwent oophorectomy.

Relationship between endometriosis and non-ovarian Gynaecological Cancers[331]

Interestingly, other studies have mentioned a possible reduction in the risk of cervical and endometrial carcinomas. Rather than a direct link to the disease itself, it is believed that possible frequent visits to the general practitioner (GP) might ensure closer checks of the patient with the earlier identification and management of pathology[336]. An Australian study from fertility patients looking at a cohort of 29,700 women failed to show an increased risk in breast cancer[337]. A Swedish study assessing records of around 20,686 women has assessed for types of malignancy in endometriosis patients within this population. Apart from those mentioned above, they reported an increased incidence of breast cancer[336,338]. This has however not been replicated as a finding in other studies and a population bias was thought to be attributed to this finding. The lack of other current databases in multiple populations could also mean that other studies have not shown similar results due to sample size bias. Further research is necessary in this area to enable adequately powered studies.

Links with other types of carcinomas are mostly documented as case reports. Most will describe links with colon and rectal carcinomas, 66% of which were histologically endometroid in nature. Sarcomas were the next most frequent histological type (25%) followed by clear cell (2%)[339].

In ovarian endometriomas where malignancy is suspected, a combination of ultrasound features and Ca125 levels are used in calculating the risk of malignancy (RMI) index. It is however to be noted that Ca125 levels can be elevated in endometriosis without a co-existing malignancy[31]. Case reports of malignant tumours arising from endometriosis both within and external to the gonads have been published and it is believed that the frequency of malignancy arising in endometriosis may be higher than previously believed[340] and the multifactorial aetiology has been implicated in multiple studies (Figure 1-7). In one reported review, 78.7% of malignancies arose in the ovary with 21.3% originating from extraperitoneal locations[340]. Endometroid adenocarcinomas were found in 69% of lesions, clear cell carcinomas in 13.5%, 11.6% were reported as Sarcomas and 6% were rare malignancy cell types[340]. The malignancies reported were predominantly well differentiated and most responded to oestrogenic stimulation[341,342]. Interestingly, just as there tends to be a predominance of left sided ovarian endometriomas, believed to be linked to the left sided stasis of refluxed endometrium, there also seems to be a higher predominance of left sided clear cell carcinoma (54%)[343]. This relationship has not been seen in other histotypes of ovarian carcinoma. The addition of progestin to cases where endometriosis co-exists with unopposed oestrogen therapy has been shown to reduce the incidence of malignant change arising in continually stimulated endometriosis lesions[340]. Young patients with endometriosis tend to have an earlier diagnosis of ovarian cancer with lower grade lesions though survival rate is unclear, this again might be attributed to increased vigilance within this female population[344-346]. Conflicting evidence exists where variations in age and stage of diagnosis are all reported making above observations debatable.

FIGURE 1-7

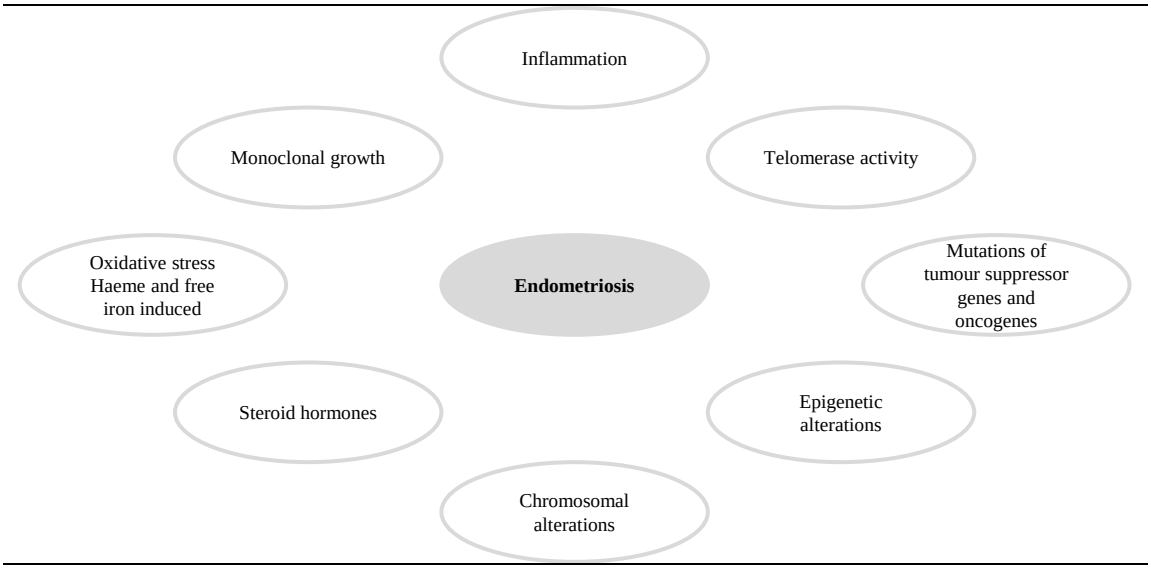

Multifactorial causations of endometriosis

Endometriosis has been subdivided into typical and atypical variants of disease. Atypical endometriosis is classified by the presence of cytological atypia and hyperplastic changes in the invading endometriotic cells and has clinically relevant implications[347]. Atypical endometriosis is often regarded as a lesion that potentially represents a transition from benign to malignant disease with genomic instability and loss of heterozygosity in these atypical tissues[332,348]. Loss of heterozygosity is usually linked to regions where tumour suppressor genes are inactivated which in turn leads to malignant change[349]. Some studies have shown that the loss of heterozygosity in atypical endometriosis is seen to increase in frequency as the disease clinically moves from its moderate to severe forms. This possibly implies a cumulative genetic effect in the progression from endometriosis to malignancy. Certain identified loci of loss of heterozygosity at genetic locus 10q23.3 and PTEN tumour suppressor gene mutations are seen in both endometrial ovarian cysts as well as endometrial and ovarian carcinomas, strengthening the theory that development of pathology is a transitional spectrum of mutations. Studies in mice, demonstrating the inactivation of PTEN tumour suppressor gene through the induced expression of K-RAS oncogene, have shown the development of endometroid ovarian carcinomas. This supports the role of tumour suppressor genes in control of disease[350]. Other mutations in tumour suppressor genes have been linked to endometriosis and malignant potential. Mutations in tumour suppressor gene TP53 encoding for p53 nuclear protein is linked to ovarian malignancy and causes nuclear accumulation of this protein within the cellular nuclei. There are various studies investigating the frequency of p53 mutations in endometriosis and ovarian clear cell carcinomas[351]. Chromosomal loss of TP53 has been seen in late/stage 4 endometriosis[352] with endometriosis adjacent to clear cell carcinomas and endometroid carcinomas showing p53 accumulations[353]. The increase in p53 expression was also noted to be more prevalent in the transition from atypical endometriosis compared to typical lesions[354]. Not all studies have however successfully shown these associations in all endometriotic lesions especially in the absence of malignant development[355,356]. My TMA studies support the findings of an increased prevalence of p53 expression in endometriosis compared to normal endometrium in controls (P=0.0090) and normal endometrium from cases (P=0.0101) (Figure 4-18, Table 4-7, Table 4-8). Other mutations in presumed tumour suppressor

genes such as ARID1A have also been identified in malignancies associated with endometriosis such as ovarian clear cell and endometroid carcinomas. Its associated BAF250a protein lies within the heart of the SW1/SNF chromatin complex which regulates cellular differentiation, suppression and proliferation, avoiding malignant transformation[357].

1.16 Overview of current literature on biomarkers

An early non-invasive test would enable earlier diagnosis and treatment of endometriosis, preventing chronic effects including pain, scarring, psychological trauma and infertility. This test would also serve to reduce surgical patient morbidity and mortality and enable the monitoring of the response of disease to therapeutics and management. The search for biomarkers has as yet not led to a clinically used or validated non-invasive test for endometriosis, but various studies are emerging in the literature with the aim to do so. Biomarkers reported in literature include the following and they range from the use of cytokines, non-cytokines, serum and endometrial biomarkers, the presence of nerve fibres within tissues[358], gene aberrations and miRNAs.

Cytokine panels	**References**
IL-1β, IL-6, IL-8, IL-12, IL-13, TNF-α	359
IL-6, CA125, CA19-9	360
IL-6, CA125	361
IL-6, TNF-α, MIF, MCP-1, IFN-γ, Leptin, CA125	362
IL-2, IL-6, IL-8, IL-15, MCP-1, IFN-γ, VEGF, TNF-α, GM-CSF	363
IL-6, IL-8,TNF-α, CA125, CA-19-9, hs-CRP	364

Non-cytokine panels	**References**
CCR1 mRNA	365
CCR1 mRNA, MCP-1, CA125	244
Neutrophil to Lymphocyte ratio, NLR, CA125,	366
ccf nDNA, ccf mtDNA	367
Urocortin, CA125	368
Follistatin, CA125	369

Other biomarkers	**References**
CA125, CA19-9,IL-6	360
IL-6, CA125	361
Annexin V, CA125,VEGF, sICAM-1, Glycodelin	370

Endometrial biomarkers	**References**
WBC: CD3+, CD16+, CD3-HLADR-, CD3-CD45RA-, CD3+CD16-, CD3+CD56-, CD56-CD16+, CD16b+	371
AromataseP450 (Polymerase Chain Reaction (PCR) and Staining)	372
AromataseP450 mRNA (PCR)	373

Gene aberrations in endometriosis/ adenomyosis	References
HOXA10	[374, 375, 376]
PR-B	[377, 378]
Aromatase	[379, 380]
ER-β	[381]
SF-1	[382]
E-Cadherin	[383]

Upregulated miRNA	Downregulated miRNA	References
	miR-23a, let-7b, **miR-100, miR-125a, miR-143,** miR-195, **miR-199a,** miR-199a-AS, miR-21, miR-214, mi-R22, **miR-221,** miR-222, miR-23b, miR-24, miR-26a, miR-29a, let-7a, let-7c, let-7d, let-7f, let-7i, miR-10b, miR-125b, miR-145, miR-27b, miR-99a, miR-107, miR-146b, miR-191, miR-30a-5p, miR-30b, miR-30c, miR-30d, miR-451, miR-103, miR-126, miR-15b, miR-16, miR-17-5p, miR-193b, miR-19b, miR-29c, miR-30e-5p, miR-342, miR-423, miR-494, miR-92	[384]
miR-145, miR-143, miR-99a, miR-99b, **miR-126, miR-100,** miR-125b, **miR-150,** miR-125a, miR-223, miR-194, **miR-365, miR-29c, miR-1**	**miR-196b, miR-20a,** miR-34c, miR-424, miR-142-3p, **miR-200b,** miR-141, **miR-200a**	[385]
miR-1, miR-100, miR-101, **miR-126,** miR-130a, **miR-143, miR-145,** miR-148a, **miR-150,** miR-186, miR-199a, miR-202, miR-221, miR-28, miR-299-5p, miR-29b, **miR-29c,** miR-30e-3p, miR-30e-5p, miR-34a, **miR-365,** miR-368, miR-376a, miR-379, miR-411, miR-493-5p, **miR-99a**	miR-106a, miR-106b, miR-130b, miR-132, miR-17-5p, miR-182, miR-183, **miR-196b, miR-200a, miR-200b,** miR-200c, **miR-20a,** miR-25, miR-375, miR-425-5p, miR-486, miR-503, miR-638, miR-663, miR-671, miR-768-3p, miR-768-5p, miR-93	[386]
	miR-9, miR-9*, miR-34b, miR-34c-5p, miR-34c-3p, miRPlus_42 780	[387]

The miRNA in bold text are mentioned in one or more of the other studies but do not necessarily correlate in them being up or down regulated

Dysregulated miRNA in eutopic endometrium	References
miR-17-5p, miR-23a, miR-23b, miR-542-3p	[388]
miR-9, miR-34,	[389]
miR-21	[390]

There is the postulated use of proteomic analysis of endometrium and patient blood using 2-DIGE and SELDI-TOF MS technology[391-394]. No biomarker panels have so far been identified from this. Peripheral

blood studies using SELDI TOF MS report proteins altered in endometriosis[395-399]. None of these have maintained sensitivity and specificity to be used in clinical settings.

Plasma Protein/ Peptide peaks using SELDI-TOF MS	References
2058 m/z, 2456 m/z, 3883 m/z, 14694m/z, 42065 m/z	395-399
2189 m/z (Use of MALDI-TOF/TOF MS)	394
5830 m/z	395

Endometrial studies using SELDI-TOF MS	References
90.675kd (T-Plastin protein) (upregulated), 35.956kd (Annexin V protein) (upregulated) 1.9kd, 2.5kd (downregulated)	391
6898 m/z, 5891 m/z, 5385 m/z 6448 m/z, 5425 m/z	400
15334 m/z, 15128 m/z, 16069 m/z	401
2072 m/z, 2973 m/z, 3623 m/z, 3680 m/z, 21133 m/z	402

1.17 MicroRNA (miRNA) studies on endometriosis

MiRNAs are short (approx. 22nt) non-coding RNAs discovered in 1993. They are now regarded to have major translational or repressive effects controlling cellular function, proliferation[403], death[404] and protein production[405]. They regulate around 30% of the human genes[406] and repress over 60% of the protein coding genes[407]. MiRNAs are also believed to be responsible for gene regulation[408] and are now believed to interact with messenger RNA (mRNA) encoding proteins on the ribosomes enhancing their expression[409] (Figure 1-8).

FIGURE 1-8

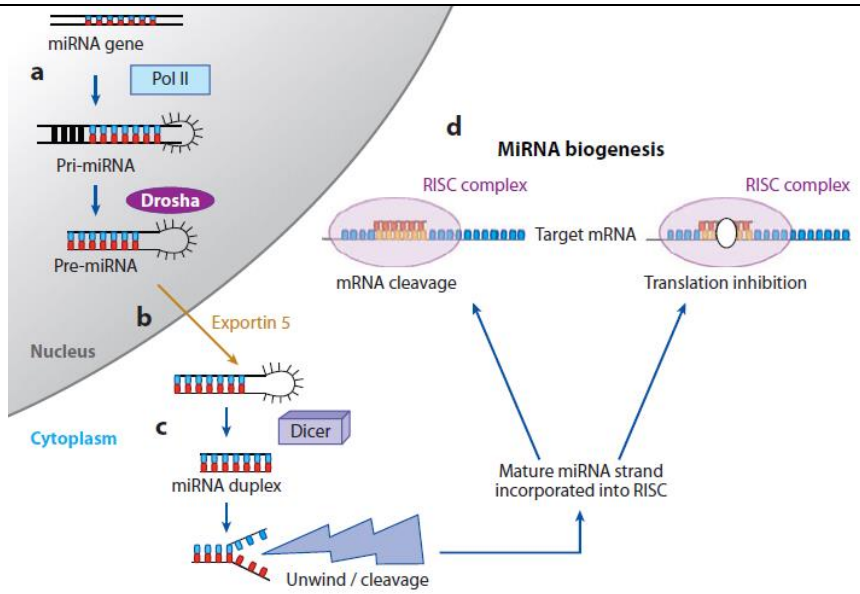

miRNA biogenesis: miRNA are transcribed by RNA polymerase 2 into primary miRNA transcripts of variable size (pri-miRNA) (a). These are cleaved in the nucleus by RNase3 resulting in hairpin pre-miRNA (b). This is moved from nucleus to cytoplasm by exportin 5 and processed by the enzyme dicer (c) giving a transient duplex 19-24 nucleotide length. The strand of the duplex (mature miRNA) is incorporated into RNA-induced silencing complex (RISC) (d) leading RISC to cleave mRNA or cause translational repression depending on the miRNA target complementarity[410]

Currently, there are approximately 700 identified human genome miRNAs. Predictions from genome wide studies indicate that we may be underestimating their numbers by 10-100 fold[411]. A study by Creighton *et al.*[412] assessed 13 different types of gynaecological tissues ranging from normal endometrium to endometriosis and cancer. In this study, looking at 103 tissues or cell line samples, they identified 7 novel miRNAs and 51 predicted novel miRNAs indicating that further novel miRNA information is yet to be discovered from future studies to increase our knowledge of disease.

MiRNAs were discovered after the observation that the gene lin-4, (a gene controlling *c.elegans* larval development) resulted in the production of a pair of small RNAs which, rather than coding for a protein, repressed the gene lin-14[413]. The pair of RNAs resulting from lin-4 were of different lengths, one was around 22nt and the other was around 61nt. The longer of the two was initially believed to fold into stem loops and act as the precursor of the shorter RNA. Further studies indicated that the lin-4 RNA's had antisense complement codes to multiple areas on the 3' UTR of the lin-14 gene[413,414], which were known to repress the lin-14 by lin-4. It was noted that this regulation, caused translational repression of the lin-14 protein without changes in the levels of lin-4 mRNA. This 22nt lin-4 was recognised as the founding member of miRNAs[415-417]. In 2000, another gene let-7 in *C.elegans*, was found to be similar in structure to lin-4[418,419] and it was then discovered in other species including insects, mammals and humans. Since that time, increased numbers of miRNAs have been reported and are now implicated as regulators of the cellular cycle, neuronal patterning and modulation of hematopoietic lineage differentiation in flies, nematodes and mammals respectively. These miRNAs are also found within the plant kingdom regulating growth development and reproduction[420]. The discovery of miRNA in both kingdom *Animalae* and *Plantae* indicate their presence in the common ancestral lineage through evolution[421].

Since their first discovery, hundreds of miRNAs are now known[415,422] and are noted to be evolutionally conserved especially, but not uniquely, in closely related species[423]. They are now regarded as one of the more abundant cellular complexes. Certain miRNAs are extremely abundant within cells (e.g. miR-52 or miR-2 have more than 50,000 molecules per adult worm cell)[424]. There is debate as to whether this reflects molecular stability or slow decay. Other miRNAs are expressed at lower levels, reflecting either a high expression in a few cells or low expression over a larger volume of cells[415]. There is now a registry which is set up to catalogue discovered miRNAs and helps in the naming and identification of newly discovered genes. Most of the human miRNAs are isolated not clustered. Clustered miRNAs are usually, but not always, related to one another and they may have functional relationships[425]. miRNAs are also seen to be conserved through different animal lineages (albeit with differences in size of the respective gene family) with nearly all cloned miRNAs conserved in closely related animals such as mouse and human species[426].

Most of the miRNA genes are believed to originate from separate transcription units[427]. Approximately 25% of miRNAs lie within the introns of pre-mRNAs, suggesting, that like for many small nucleolar RNAs (snoRNAs) their transcription does not occur from independent promoter regions but are processed from the introns themselves. This combination will allow for the combined expression of both proteins and miRNAs and maintains the relationship between miRNA and mRNAs. miRNAs have distinct expression profiles that are seen to vary between different stages of development in-keeping with the

wide variation visible in gene expression. This explains why certain miRNAs, despite being abundant in cells, can be missed in cloning efforts[428,429].

Computational methods[340] such as MiRscan and miRseeker[426] are now being used for the prediction and identification of related miRNAs as well as genetic orthologs and paralogs[423]. Another identification method is to search for the neighbouring stem loops of miRNA genes which might belong to the same cluster[416,429,430]. Mammalian miRNAs can be difficult to clone and are less conserved in some co-related species e.g. fish. This implies that they are less likely to be identified in computational methods thereby reducing confidence of the upper bound estimate of precision on the actual number of human genes[431]. MiRNA transcription processes in mammals vary and are not completely understood. Around two thirds of miRNA are found within introns and are believed to share their transcripts with their host genes (pre-mRNA)[341]. Other miRNAs are not within introns but within coding exons[424,432,433] and are believed to have their own promoters which are as yet unidentified[434,435]. They can regulate gene expression by either inhibiting the translation or degradation of mRNA. Its expression is deregulated in malignancy[436,437] and has been linked to deregulation of oncogenes and tumour suppressor genes[438]. This relationship has led to their use as possible diagnostic or prognostic tools[439].

1.17.1 miRNA and endometriosis-published studies

Endometrial tissue changes throughout the menstrual cycle in response to hormones. Data from sampling of eutopic and ectopic endometrium reflects the particular moment in time when they were collected. Animal mouse modelling has been used to give a longer term visualisation of result fluctuations in an in–vivo model of disease[440,441]; data provided by mouse models is reported to closely reflect human profiles[441]. Various mechanisms controlling inflammation, implantation and neovascularisation are implicated in disease development[442,443]. In small limited pilot studies there is evidence that altered expression of some miRNAs occurs in endometriosis. Expression of these genes is controlled by ovarian hormones and may regulate the development of endometriosis. There are four published studies on miRNA analysis in endometriosis.

Pan *et al.* published a study in 2007 where a total of 16 tissue samples in the early mid secretory phase were assessed[384]. Four samples were of normal endometrium from unaffected women, 8 samples were paired ectopic and eutopic endometrium from 4 women with endometriosis and another 4 samples were from ectopic endometrium from women undergoing hysterectomy for leiomyomas or severe endometriosis. Cells were cultured *in vitro* and RNA was extracted. The quality of RNA and its miRNA fractions were assessed using a bioanalyser. The miRNA was then labelled and hybridised to mirVana miRNA Bioarray Slides. Real time PCR was used to verify seven of the miRNA expressions which targeted genes linked to endometriosis. These included transforming growth factor-β receptor 2 (TGF-βR2), oestrogen receptor-α (Erα), oestrogen receptor-β (Erβ) and progesterone receptor (PR). 65 miRNAs were globally identified above a set threshold with 48 differentially expressed between tissues post ANOVA analysis. Cells were further separated into glandular and stromal endometrial cells and 32 miRNAs were listed as differentially expressed. There were no direct comparisons between eutopic and ectopic endometrial tissues from women with the disease. In this paper, only hsa-miR21, hsa-miR26a,

hsa-miR142-5p were confirmed to be dysregulated between ectopic and eutopic endometrium (Table 1-7).

TABLE 1-7

Pan *et al.*- differentially expressed miRNAs	
hsa-let-7a	miR-19b
hsa-let-7b	miR-21
hsa-let-7c	miR-214
hsa-let-7d	miR-22
hsa-let-7f	miR-221
hsa-let-7i	miR-222
miR-100	miR-23a
miR-103	miR-23b
miR-107	miR-24
miR-10b	miR-26a
miR-125a	miR-27b
miR-125b	miR-29a
miR-126	miR-29c
miR-143	miR-30a-5p
miR-145	miR-30b
miR-146b	miR-30c
miR-15b	miR-30d
miR-16	miR-30e-5p
miR-17-5p	miR-342
miR-191	miR-423
miR-193b	miR-451
miR-195	miR-494
miR-199a	miR-92
miR-199a-AS	miR-99a

In another study by Ohlsson *et al.*, seven patients were recruited to compare paired eutopic and ectopic endometrial samples[385]. Fourteen miRNAs were upregulated and eight miRNAs were downregulated in endometriosis compared to eutopic endometrium from the same patients. PCR was used to confirm six identified transcripts. The program TargetScan was used to assess for predicted mRNAs. The mRNAs identified were then confirmed to pre-published studies looking at mRNA analysis[442,444]. Twelve pathways were identified, and these were associated with cell cycling, proliferation, movement, angiogenesis, death, connective tissue, muscular and nervous system development as well as disorders attributed to the endocrine and reproductive system (Table 1-8).

TABLE 1-8

Ohlsson *et al.*- differentially expressed miRNAs	
Upregulated	**Downregulated**
miR-145	miR-200a
miR-143	miR-141
miR-99a	miR-200b
miR-99b	miR-142-3p
miR-126	miR-424
miR-100	miR-34c

miR-125b	miR-20a
miR-150	miR-196b
miR-125a	
miR-223	
miR-194	
miR-365	
miR-29c	
miR-1	

Filigheddu *et al.* performed a third study looking at follicular phase eutopic and ectopic endometrium (from ovarian endometriomas) from 3 patients[386]. 27 miRNAs were found to be upregulated whilst 23 were downregulated. 5 miRNAs were confirmed by PCR, 3,093 mRNA targets were predicted controlling 49 functional networks (Table 1-9).

TABLE 1-9

Filigheddu *et al.*- differentially expressed miRNAs	
miR-1	miR-25
miR-100	miR-28
miR-101	miR-299-5p
miR-106a	miR-29b
miR-106b	miR-29c
miR-126	miR-30e-3p
miR-130a	miR-30e-5p
miR-130b	miR-34a
miR-132	miR-365
miR-143	miR-368
miR-145	miR-375
miR-148a	miR-376a
miR-150	miR-379
miR-17-5p	miR-411
miR-182	miR-425-5p
miR-183	miR-486
miR-186	miR-493-5p
miR-196b	miR-503
miR-199a	miR-638
miR-200a	miR-663
miR-200b	miR-671
miR-200c	miR-768-3p
miR-202	miR-768-5p
miR-20a	miR-93
miR-221	miR-99a

Six miRNAs are mentioned in all three studies (miR-29c, miR-145, miR-143, miR-99a, miR-126, miR-100). Filigheddu's and Ohlsson's studies show concordance in the direction of regulation (upregulation or downregulation) of the 13 miRNAs commonly expressed in both studies. Pan's study was discordant for the directions of the expressed miRNAs except for miR-17-5p which was also downregulated in Filigheddu's study. Discrepancies in published studies might be attributed to limited data obtained due to

the small number of patients recruited. Some patients were also reported as having surgery for concomitant pathology such as leiomyomas, which has been shown to cause miRNA deregulation irrespective of whether other pathology such as endometriosis co-exists[445]. Their presence in subject samples could therefore distort the presented miRNA profile results.

1.17.2 Differences in miRNA of eutopic endometrium of cases and controls

A study by Burney *et al.* looked at normal endometrium from four cases of endometriosis and three controls (day 15-18 of the menstrual cycle). The controls were women undergoing surgery for leiomyoma. They identified six statistically significant downregulated miRNAs and confirmed three of these miRNAs by PCR (Table 1-10). Software to assess pathway analysis showed networks related to the control of the cell cycle, cell death and links to the molecular mechanisms of cancer[387].

TABLE 1-10

Burney *et al.*- differentially expressed miRNAs
Downregulated
miR-9
miR-9*
miR-34-b*
miR-34c-5p
miR-34c-3p
miRPlus_42 780

1.18 Proteomics and endometriosis

The proteome is the entire protein content of a cell, a tissue or an organism in a defined state under defined conditions, it is the protein equivalent of the genome[446,447]. As there are more proteins than genes, the proteome is larger than the genome itself especially in eukaryotic cells. Proteomics is a science which analyses the proteome. Due to the nature of the human body, fluid proteome has a large dynamic range of protein concentrations resulting in problems with quantitation[448]. Proteomes are studied at two levels i.e. the structure of the proteins and their functional interaction. The common technique of analysis is twofold, the first being two dimensional protein separation by gel electrophoresis and the second being mass spectrometry. Proteomic profiling has been used extensively for tumour marker discovery[449,450]. Identifying biomarkers for a disease has the advantage of their use in the clinical setting. Patients can be diagnosed and stratified according to disease severity. They can then be offered specific treatments. Alternatively, therapies offered can be monitored for tissue response and effectiveness of treatment[448].

FIGURE 1-9

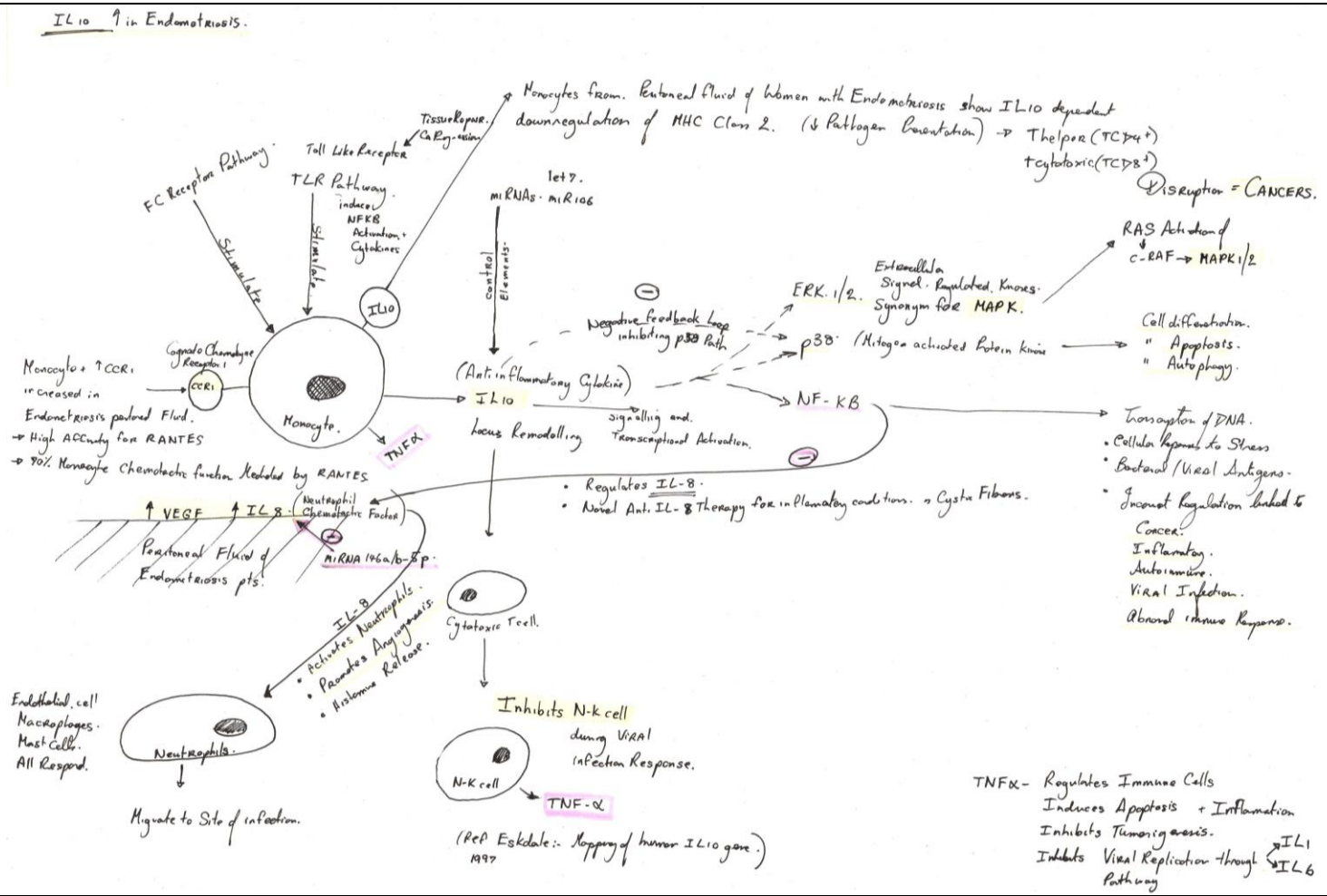

Hand drawn image demonstrating the contribution of various pathways and IL-10, IL-8 and VEGF in the development of endometriosis

There are various studies showing differential protein expression in the peritoneal fluid[451,452] or in endometrium[218,453-455] of women with endometriosis compared to controls (Figure 1-9). Elevated levels of IL-10 in the peritoneal fluid of women with endometriosis has been noted[451]. These studies used two-dimensional gel electrophoresis for protein analysis which limited them in being labour intensive and required intact proteins in large numbers. To date, a non-invasive test for endometriosis does not exist. The majority of attempts by researchers towards producing non-invasive diagnostic tests for endometriosis have looked at levels of growth factors and/or cytokines[456] involved in inflammation, angiogenesis and tissue remodelling[457]. Most of these investigations have looked into single markers of the inflammatory process. This line of thought developed after previous studies noted elevated concentrations of macrophages in the peritoneal fluid of endometriosis sufferers[458]. Studies have suggested increased levels of TNF-alpha and IL-6 levels in endometriosis[459] associating these elevated levels with infertility (Figure 1-2, Figure 1-9). Other conflicting results on reported elevations in inflammatory cytokines interleukin IL-1, IL-6[361] and TNF-α exist [359,460-464]. In one study assessing 119 prospective surgical cases it was reported, that the use of IL-6 in cases of minimal to mild endometriosis with a threshold of 25.75 pg/ml shows a diagnostic sensitivity of 75% and specificity of 83%[361]. Confounding factors, including the presence of non-malignant ovarian pathology and uterine leiomyomas, are noted in the study.

An increase in the number of leukocytes within the peritoneal fluid of women with endometriosis has been identified. Chemokines are responsible for the recruitment of monocytes to inflammatory regions[465]. In the peritoneal fluid of endometriosis patients, 70% of monocyte chemotactic function is mediated by regulated upon activation, normal T cell expressed and secreted (RANTES) gene[365,466]. The cognate chemokine receptor-1 (CCR1) has a high affinity for RANTES and is expressed on the surface of the monocytes[465]. It has been shown to be elevated in its levels in the peritoneal fluid of women with endometriosis[467]. In studies looking at the CCR1 level in peripheral blood leukocytes of women with disease in the follicular phase of the cycle, an increased level of the CCR1 levels has been shown[365]. Again, controls were women who did not suffer from endometriosis but showed non-malignant pathology such as uterine leiomyomas. Elevated expressions of CCR1 were also noted in women who were pregnant or who had inflammatory pelvic pathology[365]. At best, looking at symptomatic women with chronic pelvic pain and with disease, the use of CCR1 as a marker for endometriosis showed a sensitivity of 94%, specificity of 71% and a negative predictive value of 80% with a positive predictive value of 91%[365]. The ability to identify disease in women who did not report chronic pain was reduced with a sensitivity of 90% and specificity of 74%[365].

Angiogenic factors IL-8 and vascular endothelial growth factor (VEGF) are also reported as elevated in peritoneal fluid of women with endometriosis[452,458,468]. Other studies, which are small in number and sample size, have looked for alternate serum markers with less definite results obtained[359,469,470].

Tumour markers such as CA125 and CA19-9 have also been assessed as potential biomarkers[471,472]. In one study looking at CA125 levels in moderate to severe cases of endometriosis, the CA125 with a cut off threshold of 35 IU/ml gave a specificity of 97% and sensitivity of 47% for endometriotic cases[361]. A smaller study looking at 45 women, gave a CA125 sensitivity of 27% and specificity of 97%[360], they attempted to combine the CA125 with CA19-9 and IL-6 but failed to show an increase in the validity of

obtained information over CA125 alone. The resulting sensitivity and specificity was quoted at 42% and 71% respectively[360]. A combination of CA125 levels and analysis of endometrial leukocyte subsets has also been attempted[371]. Using a multiple logistic regression model, combining leukocyte subsets, CA125 levels and risk factors, a specificity of 95% and sensitivity of 61% was obtained. The positive predictive value was calculated around 91% and the negative predictive value was around 75%[371].

Two-dimensional gel electrophoresis (2-DE gels) has been used in one study in combination with peptide mass mapping identifying the following dysregulated proteins possibly having a functional role in endometriosis. The proteins assessed include molecular chaperones (including heat shock protein 90 and annexin A2), proteins involved in cellular redox state (such as peroxiredoxin 2), proteins involved in protein and deoxyribonucleic acid (DNA) formation/breakdown (including ribonucleoside-diphosphate reductase, prohibitin and prolyl 4-hydroxylase) and secreted proteins (such as apolipoprotein A1)[473].

Two studies have been published showing some promising preliminary findings in the serum from women with endometriosis[457,474]. Zhang *et al.* reports thirteen known protein spots from patient serum and eleven known protein spots from endometrium as being differentially expressed between women with and without endometriosis. In particular, vimentin, beta-actin and ATP synthase beta subunit hybridised substantially differently between the sera from controls and cases[474]. Another paper by Liu *et al.* examining plasma from endometriosis patients, reports twenty different protein peaks with a sensitivity of 87.5% and specificity of 80% in the diagnosis of endometriosis[475]. Even as this technology continues evolving, to date, it has not yet led to a single new therapy or tested biomarker partly due to the multifactorial nature of endometriosis itself[476].

A recent 2011 study by Kyama *et al.*[477] looked at protein expression in the endometrium of 29 patients with endometriosis and laparoscopically confirmed controls in the secretory phase of the cycle. In the preliminary study, ProteinChip technology was used to assess the expression of various protein profiles in endometrium of women with and without disease. Transgelin (a smooth muscle actin-binding protein) was identified as being upregulated in endometriosis cases[392]. In the evaluation study, protein profiles from 29 patients were obtained using surface-enhanced laser desorption ionisation time-of-flight mass spectrometry (SELDI-TOF-MS) allowing the identification of proteins and peptides otherwise poorly detected by other methods[477]. Precautions which could cause sample bias were documented[478] and peaks with mass-over-charge <1.6kDa were excluded avoiding interference from matrix ions[477]. 73 mass peaks were seen to be expressed differently in the secretory endometrium of endometriosis patients at all stages compared with controls[477], whilst 30 mass peaks were differentially expressed between controls and patients with minimal to mild disease. Their data using the SELDI-TOF-MS techniques and the use of mass peaks identified by stepwise logistic regression provided clinically relevant biomarkers with high sensitivity (100%) and specificity (100%)[477]. Other studies using similar techniques but analysing plasma samples, report decreased sensitivity of 92% and specificity of 80%[479]. T-plastin (a cytoplasmic protein regulating actin assembly and cellular motility) and Annexin V (a calcium phospholipid-binding protein) were upregulated in endometriosis. Validation studies are pending.

Further studies are required into this new field which has already shown high potential of clear pattern identification for this disease. Additional studies of proteins already identified will assist in developing

diagnostics and treatments for endometriosis. None of these have shown adequate specificity or sensitivity for their current use as a diagnostic marker.

2 Protocols and suppliers

2.1 List of materials and suppliers

Supplier	Material
Agilent Technologies	Feature Extraction Software
Agilent Technologies	Microarray Hybridization Chamber
Agilent Technologies	miRNA Microarray System with miRNA Complete Labelling and Hyb Kit
Agilent Technologies	RNA 6000 Nano Assay
Agilent Technologies	SureScan Microarray Scanner C
Agilent Technologies	SureScan Cassette
Applied Biosystems	TaqMan 2X Universal PCR Master Mix
Applied Biosystems	TaqMan MicroRNA Assays
Beckman Coulter	Vi-Cell XR Cell Viability Analyser
Biogenix	SS-enhanced Polymer detection system
BMG Labtech	FLUORstar OPTIMA
Bristol-Myers Squibb	Etopophos (Etoposide)
Custom Biogenic Systems	Liquid nitrogen Dewar tank Isothermal V-1500 series
Dako	Dako-autostainer system
EBOS Healthcare	BD Vacutainer SST
Genetix	ARIOL imaging system
Hirschmann	Ceramus laboratory dispenser
IKA	Vibramax
IKA	KS501 shaker
Kimtech	Kimwipe
Life Technologies	Invitrogen DMEM (Dulbecco's Modified Eagle Medium)
Life Technologies	mirVana miRNA Isolation Kit
Life Technologies	mirVana PARIS
Life Technologies	MultiScribe Reverse Transcriptase
Life Technologies	RNAlater
Life Technologies	RNaseZap
Medline Scientific	Shaking SI-600 incubator
NanoString Technologies	nCounter miRNA Expression Assay
NorgenBiotek	Total RNA purification kit
Olympus	BX61 microscope
PAA Laboratories	Lymphoprep LSM 1077
Promega Corporation	Maxwell 16 Blood DNA Purification Kit/ Standard Elution Volume Instrument
Promega Corporation	Maxwell 16 SEV Instrument
Qiagen	TissueLyser II
Select Science	TrakMate tubes and rack
Sigma-Aldrich	Ficoll
Sigma-Aldrich	Quadriperm dishes
Techne	Circulating water bath
Thermo Scientific	Nanodrop Spectrophotometer/ Fluorospectrometer
Thermo Scientific	Nalgene Mr Frosty
Thermo Scientific	Nalgene rack
Thermo Scientific	Orbital shaker

Thermo Scientific	Sorvall Legend centrifuge
Thermo Scientific	VisionMate scanner
VWR International	Virkon

2.2 Methods

In this chapter, I describe and critically analyse the optimised techniques of surgically obtained tissue processing and its miRNA extraction. Data obtained for identified tissue miRNA markers of interest was confirmed by real time polymerase chain reaction (PCR) and the downstream effects of the identified miRNA markers were explored through immunohistochemistry of endometriosis and control tissue microarrays. Cells from the tissues obtained at surgery were also processed for storage and cell culture. These cultured cells were used in therapeutic *in vitro* experiments with Galectin inhibitors. Blood taken at surgery was processed, serum and lymphocytes were separated. Proteomic antibody studies and miRNA extractions were performed on the serum samples. RNA extraction with quantitative PCR was performed on the serum lymphocytes to substantiate miRNA serum findings.

2.3 Subject recruitment and sample collection

Research participants for this study were women between 18 and 50 years of age recruited with informed consent (Ethics reference REC 10/H0711/24) who were known (or strongly suspected from current investigations) to suffer from endometriosis (Figure 2-1). Cases (n=17) were defined as women, between 18 and 50 years of age (mean age 30.75 years), in a haematologically confirmed phase of their menstrual cycle at the time of surgery (n=8 follicular, n=9 luteal) (Table 2-1). Hormonal analysis for FSH, LH Oestradiol and progesterone levels were used to define the cycle phase at recruitment. Samples were divided into follicular phase and luteal phase samples respectively. Cases were further subdivided into patients with ovarian (n=3) or peritoneal (n=14) disease.

TABLE 2-1

Cases: ID	Age (yr)	Ethnicity	Cycle stage	Endometriosis	Other pathology	Medications
1	26	Asian	Follicular	Peritoneal	None	None
2	32	Caucasian	Follicular	Peritoneal	None	None
3	33	Caucasian	Follicular	Peritoneal	B thalassaemia trait	None
4	37	Caucasian	Follicular	Peritoneal	Mildly elevated T4	None
5	40	Caucasian	Follicular	Peritoneal	None	None
6	32	Caucasian	Follicular	Peritoneal	None	None
7	31	Asian	Luteal	Peritoneal	None	None
8	40	Asian	Luteal	Peritoneal	None	None
9	30	Asian	Luteal	Peritoneal	None	None
10	30	Caucasian	Luteal	Peritoneal	None	None
11	40	Caucasian	Luteal	Peritoneal	None	None
12	30	Caucasian	Luteal	Peritoneal	None	None
13	32	Caucasian	Luteal	Peritoneal	None	None
14	26	Caucasian	Luteal	Peritoneal	None	None
15	44	Asian	Follicular	Ovarian	None	None
16	32	Asian	Follicular	Ovarian	None	None
17	37	Caucasian	Luteal	Ovarian	None	None

Controls	Age (yr)	Ethnicity	Cycle stage	Endometriosis	Other pathology	Medications
18	27	Caucasian	Follicular	None	None	None
19	30	Caucasian	Follicular	None	None	None
20	24	Caucasian	Follicular	None	None	None
21	42	Caucasian	Follicular	None	None	None

Summary of recruited patients for tissue miRNA analysis

FIGURE 2-1

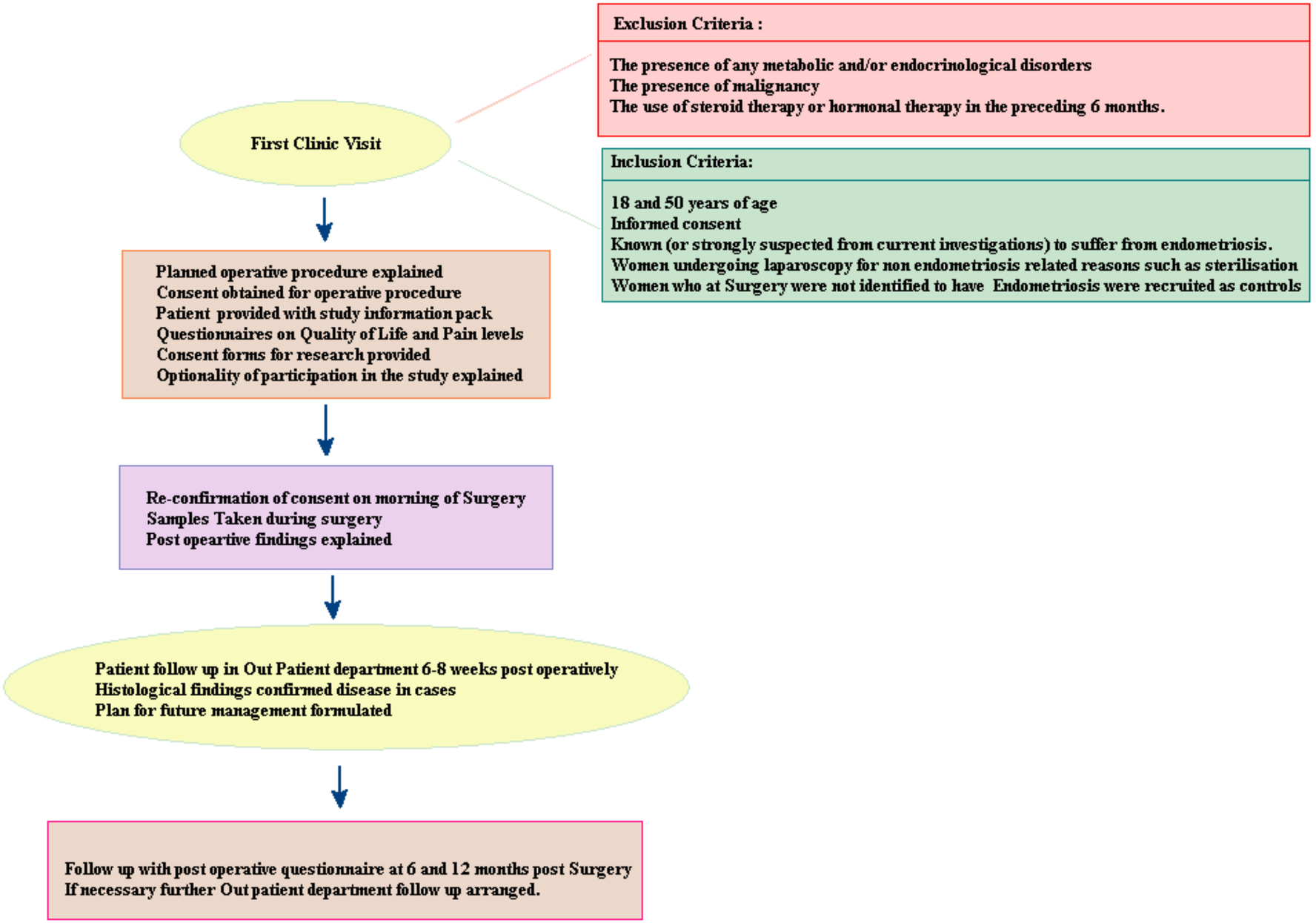

Overview of recuitment criteria and consent processes for study participation

Women undergoing laparoscopy for non-endometriosis related reasons such as sterilisation or women who at surgery were not identified to have endometriosis were recruited as controls. The revised American Fertility Society (rAFS) classification system was used to classify disease at surgery. Exclusion criteria involved the presence of any metabolic and/or endocrinological disorders, malignancy, or the use of steroid therapy or hormonal therapy in the preceding 6 months.

Information about the study was given in the gynaecology out-patient department (GOPD). A patient information pack for the project titled "Gene Protein and miRNA Expression in Women with Endometriosis" REC ref-10/H0711/24 was distributed to all possible candidates. Any questions from the participants were answered and further explanations when requested were given. In the situation where language difficulties existed, qualified hospital interpreters were used for translation and consents at both the preliminary recruitment discussion and later in the consent and follow up meetings. These translated the written forms as well as the verbal discussions. It was emphasised that recruitment was completely optional and would not affect patient care or management. Information leaflets about endometriosis and the study were given to the patients prior to surgery enabling ample time for reflection and decision as to whether to participate or not. Patients taking part in the study were given the option of being provided with the results of the study should they wished to be informed. Women taking part in the study were provided with contact information which enabled them to easily ask questions or gain access to the investigator should they wish to do so.

Consent was obtained on the morning of the surgery together with the routine consent form for her planned surgical procedure. On the day of surgery, candidates for the study had a full medical history taken by the chief investigator to assess and reconfirm eligibility. The date of the last menstrual period was recorded for all candidates to establish the menstrual cycle phase. This was furthermore confirmed by hormonal profile assessments taken on the day. Quality of life questionnaires including SF12 and SF36 together with a pain score questionnaire PIQ-6 were completed by the patient prior to surgery enabling assessment of the impact endometriosis was having on daily life. A pregnancy test was performed to exclude pregnancy.

All samples collected were from recruited and consented patients undergoing surgery with no additional invasive procedures incurred by the patient. To minimise confounding factors, all the cases from whom the samples were collected underwent laparoscopy by the same surgical team, utilising similar operative techniques. In the anaesthetic room, at routine patient cannulation for surgery, blood was taken for the following serum tests: Ca125, CEA, Ca19.9, TFT, serum oestrogen, serum progesterone, follicle stimulating hormone (FSH) and lieutenising hormone (LH). Another blood vial was taken for serum and white blood cell extraction in the research laboratory. All blood and tissue vials were stored at approximately 4^{o}C until the end of the procedure. They were then processed on the same day. All samples were assigned a random coded number ensuring anonymity of patients.

2.3.1 Sample sizes

Initially 17 patients and 4 controls were recruited surgically. These patients were used to obtain primary tissue samples used for tissue miRNA analysis and serum samples which were used for serum miRNA and antibody analysis. This small sample batch was used to perform preliminary miRNA work to

demonstrate whether there were changes between samples and controls for the disease of endometriosis (See section 2.3.2, 4.4.1). These primary samples were also used for tissue cell culture and the therapeutic experimentation (See sections 2.10, 7.3.1, 7).

Once changes were demonstrated from the tissue miRNA studies, an additional 179 tissue samples were obtained from Barts and the London Trust tissue bank (histologically confirmed cases of endometriosis and controls) to perform the tissue microarray studies (See section 2.7, 4.4.3).

An additional 52 patients were recruited for the serum biomarker studies (Total sample size 73). These were either patients with previous surgery confirming endometriosis (Cases) or patients who had previous surgery which was normal (Controls) (See section 2.6.1, 5, 6).

2.3.2 Surgical procedures

2.3.2.1 Hysteroscopy

The patient was cleaned and draped in position. To minimise its risk of injury during laparoscopy, an in and out catheter was used to empty the bladder. Bimanual vaginal examination established uterine size, its position and degree of mobility. At the same time, it assessed for the presence of pelvic masses. Endometrial curettings were taken prior to the insertion of the hysteroscope to minimise the risk of distorting uterine tissue during surgical manipulation or laparoscopic dye insertion. The saline hysteroscopy was performed at the end of the laparoscopy to avoid the dilution of collected intra peritoneal fluid with saline and disrupt the endometrial milieu.

2.3.2.2 Laparoscopy

The abdomen was insufflated using a closed Veress needle technique. The abdomen was insufflated with about 3.5 litres of CO_2 pneumoperitoneum to obtain a port entry pressure of 20mm Hg. All ports were inserted under direct vision to minimise the risk of entry injuries. On entry with the laparoscope, initial assessment of the abdomen, liver and pelvis was performed. Patients with evidence of infection within the pelvis such as Fitz Hugh Curtis syndrome or the presence of hydrosalpinges were excluded. When identified, endometriosis was graded using the AFS classification. Biopsies from cases recruited for the study were excised without the use of concomitant thermo coagulation avoiding thermal damage to the tissues which could have distorted the results. A section of the collected biopsy was sent for histological analysis using formal saline as a transport medium. The tissue samples for RNA extraction were stored in separate vials in an RNA stabilisation medium- RNAlater®. The samples in RNAlater® solution were left at 4ºC for 12 hours to enable adequate tissue permeation. They were then stored at -80ºC till RNA extraction was performed. Where possible, photographic evidence of the lesions were taken and stored in the patient's file together with the documented operative notes.

Postoperatively, surgical findings were explained fully to the patient. Any questions were answered and a routine six week follow up in the general gynaecology clinic was arranged to assess recovery and outcome. Patients were invited to repeat the SF12, SF36 and the PIQ-6 questionnaires at 4 and 12 months post-operatively either in clinic or telephonically. They were given the opportunity to meet with the

principal investigator in the gynaecology outpatient department at St. Bartholomew's Hospital after their procedures.

In a rare circumstance, where unexpected and important clinical information was discovered whilst analysing the samples (e.g. the discovery of a cancer or borderline tumour from the histology of the samples), the participant was contacted and invited to an early hospital consultation where the information was disclosed and appropriate clinical management offered. They were then excluded for the purposes of the study.

2.3.3 In summary

Current diagnosis and management of endometriosis leaves a lot of deficiencies in the understanding of both the mechanisms of disease and its therapeutic options. Surgery and the induction of chemical menopause remain the two options for treatment and are unsatisfactory. It was therefore the aim of this thesis to investigate the mechanisms related to the development of disease and relate these findings to potential future therapeutic and diagnostic options.

2.4 Tissue miRNA extraction

Total RNA from specimens was extracted using the *mir*Vana™ PARIS™ kit (Ambion) as per their supplied protocol. The first step of the *mir*Vana PARIS procedure is to disrupt samples in Cell Disruption Buffer. The samples were all between 10^2–10^7 cultured eukaryotic cells or 0.5–100 mg of tissue. All samples were weighed prior to commencing the extraction. Tissues were blotted on absorbent paper to remove excess RNA Later solution which would interfere with the RNA extraction technique. Extraneous material was manually removed from the samples to ensure that only areas of interest to the study (e.g. endometriosis infiltrated areas) were dissected in the laboratory. Initially pulverisation of the tissues was attempted by using a technique which involved manual lysis of the tissues with a mortar and pestle and liquid nitrogen. It was noted, that whereas the normal endometrium was relatively easy to pulverise giving high RNA yields at good purity, the peritoneal tissue and the tissue infiltrated by endometriosis, gave substantially lower yields of RNA concentration using the same technique. Maximisation of yield from all tissues was obtained by manually dissecting and cutting the tissues into minute pieces and then lysing the tissues mechanically with the aid of the Retsch TissueLyser2 (Qiagen). Dissected samples were placed in 2ml vials together with a 5mm stainless steel bead and 625µl of ice cold cell disruption buffer. The plates of the Lyser had been pre cooled to avoid sample heating and possible material degradation. Tissues were lysed with a program of 30beats/second for a total of 20 minutes.

2.4.1 Organic extraction

The homogenised lysate was mixed with an equal volume of 2X Denaturing Solution (at room temperature). The high concentration of guanidinium thiocyanate in the 2X Denaturing Solution prevents the RNA degradation by cellular ribonucleases. Samples were incubated on ice for 5-10 minutes to ensure complete cell disruption. Acid-Phenol:Chloroform equal to the total volume of the sample lysate plus the 2X Denaturing Solution was then added. Care was taken to withdraw the bottom phase containing Acid-

Phenol:Chloroform and not the aqueous buffer that lay on top of the mixture. Samples were vortexed for 30-60 seconds to ensure good mixing. Samples were then centrifuged for 5 min at 14,000 rpm at room temperature to separate the mixture into its aqueous and organic phases. If a compact interphase was not achieved at initial centrifugation, re-centrifugation was repeated. The upper (aqueous) phase was carefully removed without disturbing the interphase or lower phase and transferred to a fresh labelled tube. The volume recovered was noted.

2.4.2 Final RNA isolation

1.25 volumes of room temperature 100% ethanol were added and thoroughly mixed with the aqueous phase obtained from the abovementioned step. For each sample, a filter cartridge was added into one of the collection tubes. The tubes were labelled according to the sample being processed. Up to 700µl of the lysate/ethanol mixture was pipetted onto the respective filter and 30 seconds of centrifugation (max of 10,000 rpm) were allowed for the sample to pass through the filter. The flow through was discarded and the procedure was repeated until all the lysate/Ethanol mixture was passed through the filter. 700µl of miRNA Wash solution 1 (working solution mixed with ethanol) was applied to the filter cartridge and centrifuged (max of 10,000 rpm) for 15 seconds. The flow through was discarded from the collection tube and filter cartridge was replaced into the same collection tube. 500µl of wash solution was then applied to the filter cartridge respectively and the above process was repeated. After the flow through from the last wash was discarded, the filter cartridge was spun in the same collection tube for 1 min to remove residual fluid from the filter. The filter was then transferred into a new collection tube and 100µl of preheated 95ºC elution solution was slowly added to the centre of the filter and centrifuged for 30 seconds to recover the RNA.

The RNA extracted was assessed using the Nanodrop ND-1000 spectrophotometer (Thermo Fisher Scientific) to determine RNA concentration (ng/µl), minimal contamination from protein (ratio Abs260/Abs280) and from organic compounds (Abs260/Abs230). RNA in the remaining eluate was then stored at -80ºC.

2.4.3 nCounter® miRNA expression assay for tissue samples

RNA quantification and integrity was assessed using the Eukaryote total RNA nano assay by Aligent Technologies™. Following validation, 100ng of total RNA was used in the nCounter® miRNA Expression Assay (NanoString Technologies) enabling an ultrasensitive miRNA detection in total RNA across all biological levels of expression without the use of reverse transcription or amplification. 735 human and human-associated viral miRNAs derived from miRBase were scanned for. Unique multiplexed annealing of specific oligonucleotide tags were ligated onto their target miRNA followed by an enzymatic purification to remove all unligated tags. Excess unbound probes and RNA were washed using a two-step magnetic bead-based purification system on the nCounter Prep Station. Remaining miRNA was attached to a cartridge surface and polarised. The Cartridge was scanned and data collection was performed on the nCounter digital analyser. Digital images were processed and miRNA counts were tabulated.

2.4.4 miRNA real-time PCR

Microarray data was validated by real time PCR using individual TaqMan® MicroRNA assays following supplied protocols by Applied Biosystems®. TaqMan® arrays can detect and quantify miRNA over six logs of dynamic scale and can detect low levels as little as 1-10ng of total RNA allowing conservation of limited samples. Assays detect mature miRNA excluding precursors with a single base discrimination. Complimentary DNA (cDNA) was synthesized from total RNA using a commercially available specific EBV-miR-bart2-5p assay. RNU-44 and hsa-miR-26b were used as the mature miRNA endogenous controls. Each 15µl RT reaction contained 5µl of RNA containing 2.5ng/µl of RNA, 7µl of master mix (0.15µl of 100mM deoxynucleotide solution mix (dNTPs) (with Deoxythymidine triphosphate (dTTP), 1.00µl of MultiScribe™ Reverse transcriptase 50 U/µl, 1.50µl 10X Reverse transcription buffer, 0.19µl of Ribonuclease (RNase) Inhibitor 20U/ µl, 4.16 µl nuclease-free water) and 3µl of the primer (Table 2-2). All reagents were available in the TaqMan® MicroRNA reverse transcription kit. Reverse transcription was performed on a thermal cycler by incubation of the reagents at 16ºC for 30min, 42ºC for 30min,85ºC for 5 minutes and held at 4ºC. The resulting cDNA was diluted in nuclease free water at a 1:15 ratio as advised per protocol.

2.5 Critical analysis of tissue sample collection and RNA extraction

RNA and biomolecule extraction is one of the most fundamental and crucial steps in sample preparation for analysis and downstream processing[480]. Tissues vary in their biological composition making certain samples (e.g. fibrous peritoneal tissues) more difficult to homogenise, process and therefore extract nuclear material compared to others (e.g. endometrial tissue which is cyclically regenerating, proliferative, glandular tissue). To ensure successful nucleic acid extraction in a pure format, four important steps need to be adhered to. First there is the requirement for effective disruption/ homogenisation of the cellular material, followed by denaturation of nucleoprotein complexes, inactivation of nucleases (RNase in my case) and avoidance of contamination. Both the quality and integrity of obtained nuclear material is known to effect results obtained[481].

2.5.1 Patient sample recruitment techniques

This project involves the collection of fresh patient samples during surgery. Samples from case studies included: intrauterine endometrial tissue, pelvic peritoneal tissue infiltrated with endometriosis, pelvic peritoneal tissue clear of endometriosis and in some cases, ovarian tissue infiltrated with disease (ovarian endometriomas). Cases conforming to all inclusion criteria were difficult to recruit. Most women with suspected endometriosis undergoing surgery were on hormonal therapy at time of surgery making them inappropriate for inclusion. Timing of the menstrual cycle was also variable in patients (even in those with a regular cycle) making it difficult to time the surgery within the follicular proliferative phase of their cycles. Adequate biopsy size from peritoneal samples was another limiting factor. Patients with endometriosis, fitting recruitment criteria, were either found to have small localised areas of deep infiltrative disease or extensive nodular areas in the pouch of Douglas, adherent to bowels, making safe excision of large biopsies difficult. Thermal damage to biopsy tissue during surgical excision is reported to cause alterations in gene expression profiles related to tissue stress responses[482]. This was avoided by

performing sample excision without concomitant thermal coagulation. Bipolar or monopolar diathermy to bleeding sites were performed post biopsy if necessary.

2.5.2 Stabilising RNA

Once extracted, RNA is an unstable molecule with a short half-life. Biologically it serves its purpose as a transient message from an activated gene. In the cell, once gene transcription stops, the existing RNA is degraded preventing unwanted translation of proteins[483]. Transport between surgical theatres and laboratories can take up to a few hours and due to time restrictions it was not always possible to extract tissue RNA on the day of sample obtainment. These factors would be responsible for RNA degradation with subsequent molecular profile alteration and erroneous results. To avoid this, samples at time of biopsy were immediately placed into an RNA stabiliser solution called RNA*later*®. This aqueous tissue storage reagent rapidly permeates most tissues to stabilise and protect RNA. Reports have shown that tissues can be stored indefinitely in RNA*later*® solution at -20ºC or below, with RNA*later*® efficiently preventing RNA degradation[484]. Where samples could not be processed on the day of biopsy, RNA*later*® was left to permeate the tissues at 4ºC overnight (data from Ambion® shows that RNA is stable at 4ºC for up to a month in RNA*later*®) and samples where then stored at -80º till RNA extraction was possible. If the tissue stored in RNA*later*® is poorly permeated RNA degradation can still occur. To overcome this, all samples were cut into sections less than 0.5cm in any single dimension. Fresh tissues were also put into 5-10 volumes of RNA*later*® solution as advised by Ambion® guidelines for the use of RNA*later*® solution. RNA*later*® is reported in Ambion® guidelines to be compatible with mirVana™ miRNA isolation kit which was then used in the next step for miRNA extraction.

2.5.3 Effective disruption and homogenisation of cellular material

Disruption and homogenisation are two distinct steps for nucleic acid purification. Complete disruption of cell membranes is required to release nucleic acids within the samples. Incomplete disruption prevents the lysis buffer (which inactivates nucleases (e.g. RNases)) from contacting and protecting nucleic acids stored within the intact cell. Homogenisation reduces the viscosity of the obtained cell lysates. If these steps are not performed efficiently DNA and RNA yields are significantly reduced with resulting biased results. Various techniques were attempted. Normal endometrial tissue was easy to disrupt but substantial problems were encountered with the peritoneal tissue, both normal peritoneum as well as peritoneum infiltrated with endometriosis, due to their connective tissue/fibrous nature. Initially, manual disruption and homogenisation of tissues was attempted. Tissues were placed on a bed of ice in petri-dishes and scalpels were used to shave off fine layers of cellular material from the biopsy samples. This process was lengthy, resulted in unequal thawing of the tissue and did not result in adequate complete tissue lyses with probable ensuing result bias. RNAs obtained from the samples using this method were of good purity but provided low levels of ng/microlitre of RNA per mg of tissue. Small sample size made this process even more difficult and this method was abandoned.

Manual disruption by pulverising tissues using liquid nitrogen and a mortar and pestle was tested. This method improved, but did not complete, sample disruption/pulverisation to the desired level. Small sample size, incomplete sample pulverisation and repeated thawing and re-freezing of tissues during this

manual disruption technique were not ideal for maintaining RNA integrity during extraction. RNA levels of ng/microlitre of RNA per mg of tissue and RNA purity obtained, only marginally improved when compared to the first method.

Manual lysis was shifted to a mechanical one. Mechanical lysis was performed on the samples using the TissueLyser from Qiagen®. With this lyser, disruption and tissue homogenisation is achieved through stainless steel 7mm beads which beat and grind the tissues at speeds from 3 to 30HZ (180-1800 oscillations per minute). RNA*later*® was removed from previously stored samples and these were weighed. 0.5–100 mg of tissue was required per sample for the mirVana™ PARIS™ Kit RNA extraction step. The samples were manually dissected into small sections on ice and immediately placed into a 2ml microcentrifuge tube together with one 7mm stainless steel bead per tube and 625µl of ice cold cell disruption buffer containing a non-ionic detergent (the first step in the RNA extraction protocol of the mirVana™ PARIS™ Kit). 5mm tungsten carbide beads were used in an attempt to maximise sample disruption with smaller beads but these were seen to react with the mirVana™ PARIS™ Kit cell disruption buffer and their use was therefore abandoned. Tissues were mechanically lysed at a rate of 30Hz for a total of 3 minutes or until most of the sample was disrupted and homogenised within the cell disruption buffer. Normal endometrium was seen to disrupt and homogenise more quickly and effectively than the peritoneal samples. Despite rigorous mechanical grinding, some of the peritoneal samples remained intact. Nevertheless it was this method which provided the best level of sample lysis and homogenisation. RNA levels of ng/microlitre of RNA per mg of tissue were substantially higher and good RNA purity was maintained. Due to the rapidity of bead oscillation, heat damage to the tissues during lysis might have occurred, this was reduced by pre cooling the adapter sets holding the 2ml microcentrifuge tubes for a few minutes at -80ºC prior to the start of processing.

2.5.4 Denaturation of nucleoprotein complexes and inactivation of nucleases (RNase)

Once the sample was homogenised as described above, an equal volume of 2X Denaturing solution from the mirVana™ PARIS™ Kit was added. This solution contains a high concentration of guanidium thiocyanate which prevents RNA degradation by cellular ribonucleases. Prior to processing, the sample was incubated on ice for 10 minutes to ensure complete sample disruption. Acid-Phenol:Chloroform equal to the total volume of the sample lysate plus the 2X Denaturing Solution were then added and care taken to withdraw the bottom phase containing Acid-Phenol:Chloroform and not the aqueous buffer that lay on top of the mixture. Samples were vortexed for 30-60 seconds to ensure good mixing. Samples were then centrifuged at room temperature for 5 minutes at 14,000 rpm to separate the mixture into its aqueous and organic phases. If a compact interphase was not achieved at initial centrifugation, re-centrifugation was repeated. The upper (aqueous) phase was carefully removed without disturbing the interphase or lower phase and transferred to a fresh labelled tube. The volume recovered was noted.

2.5.5 Final RNA isolation

1.25 volumes of room temperature 100% Ethanol were added to the aqueous phase from the abovementioned step and thoroughly mixed. For each sample, a filter cartridge was added into one of the collection tubes. The tubes were labelled according to the sample being processed. Up to 700µl of the

lysate/ethanol mixture was pipetted onto the respective filter and 30 seconds of centrifugation at a maximum of 10,000 rpm were used for the sample to pass through the filter. The flow through was discarded and the step above was repeated until all the Lysate/ethanol mixture passed through the filter.

2.5.6 Avoidance of contamination

Contamination by RNases from surfaces such as skin is possible with ensuing sample RNA deterioration. Gloves were used at all times whilst handling samples. Experiments were carried out in a hood which was thoroughly cleaned with RNase Zap® prior to commencing the RNA extraction procedure. RNase Zap® was also used to clean equipment utilised for the above process minimising RNase contamination. Care was taken to ensure appropriate sample contamination even though a level of contamination affecting results may still be possible.

TABLE 2-2

Component	**Master mix volume per 15-µL reaction†**
100mM dNTPs (with dTTP)	0.15µL
MultiScribe™ Reverse Transcriptase,50 U/µL	1.00µL
10✕ Reverse Transcription Buffer	1.50µL
RNase Inhibitor, 20 U/µL	0.19µL
Nuclease-free water	4.16µL
Total volume	**7.00µL**

† Each 15-µL RT reaction consists of 7µL master mix, 3µL of 5X RT primer, and 5µL RNA sample

Real time PCR amplification was performed on triplicates of each sample using the TaqMan 2X Universal PCR Master Mix (Applied Biosystems®). The miRNA 26b is a commonly expressed vertebrate miRNA and was used as a control primer for the reactions. The mir-ebv-BART2-5p miRNA was validated. Each 20µl reaction contained 1µl of the specific TaqMan® MicroRNA assay (20X), 1.33µl of the RT product (diluted 1:15 with nuclease free water), 10µl of TaqMan universal PCR Master Mix no AmpErase® UNG, 7.67µl nuclease-free water. Reactions were incubated in a 96 well plate at 95ºC for 10 minutes, followed by 50 cycles of 95 ºC for 15 seconds and 60ºC for 60 seconds.

2.6 Blood analysis

This section describes the techniques used for isolation of peripheral blood lymphocytes and the extraction of serum from peripheral blood. It proceeds to describe the techniques for serum miRNA extraction and processing.

2.6.1 Peripheral white blood cell extraction

Samples were taken from a cubital vein using a sterile vacutainer and needle. Blood was collected directly into EDTA vials, was inverted 8-10 times and was stored at a temperature of 4°C until processing. 7mls of Lymphoprep™ (LSM1077), a separation solution made with Ficoll™ density gradient media, was placed into a 15ml tube. Ficoll™ is a 400 000 Dalton hydrophobic polymer used for the production of density gradients for cell separation. Sedimentation is achieved via centrifugation due to gravity. 7mls of

blood from the vials was gently trickled down the side of the tube creating a second layer over the 7mls of Lymphoprep™ (Figure 2-2 Step 1).

FIGURE 2-2

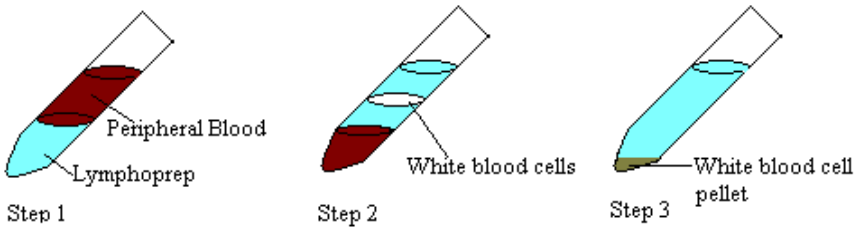

Figure depicting technique of Lymphocyte separation and isolation from peripheral blood

Samples were spun at 1500RPM for 25 minutes and the middle layer of white blood cells was collected and placed into a fresh tube (Figure 2-2 Step 2). Cells were washed with 3mls of Dulbeco phosphate buffered saline (PBS) to maintain cells at a physiological pH range of 7.2-7.6. Cells were then spun down for 7 minutes at 1500RPM. The fluid was poured off and the cellular pellet retained (Figure 2-2 Step 3). Cells were re-suspended in freeze mix medium (Mix of 350mls Roswell Park Memorial Institute medium (RPMI) + 50mls Dimethylsulphoxide (DMSO) + 100mls heat inactivated Foetal Bovine Serum (FBS)) and stored at -80°C for future use.

2.6.2 Peripheral blood serum extraction

Samples were taken from a cubital vein using a sterile vacutainer and needle. Blood was collected directly into a gold topped serum separator vial (SST™ tube), was inverted 5 times and was stored at a temperature of 4°C until processing (Figure 2-3 Step 1) The tubes contain silicone and microionised silica particles to accelerate clotting. An internal gel composed of a polyester-based proprietary formulation separates the serum from red blood cells during centrifugation. The silicone coating reduces red cell adherence to blood tube walls. Samples were spun at 2500RPM for 10 minutes. The top serum layer was removed and stored at -80°C for future use (Figure 2-3 Step 2).

FIGURE 2-3

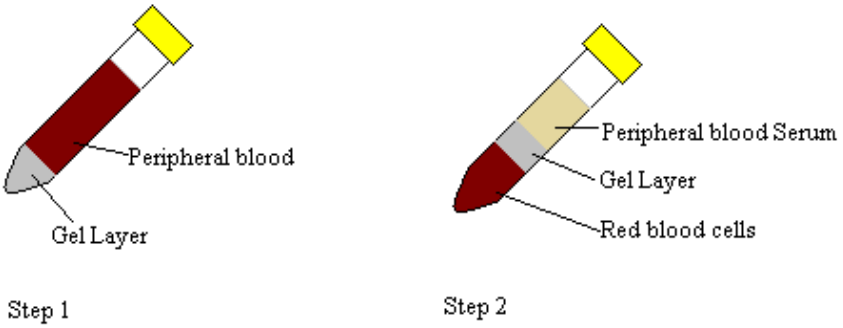

Figure depicting technique of serum isolation from peripheral blood

2.6.3 Extraction and processing of endometriosis serum samples

A set of 51 serum samples were used for the purpose of extracting circulating total RNA, including miRNA, and analysing the miRNA profile of the samples. These samples were taken from individuals with endometriosis, at various stages of the reproductive phase, ('case'; 36 samples) as well as healthy individuals ('control'; 15 samples). The samples were randomised and then sequentially numbered (1-51). Subsequently, an additional 21 control samples, taken from healthy individuals, were also received and processed (see section 2.3 for recruitment criteria).

All the above samples were processed as described below in the "Norgen Biotek total RNA purification kit protocol") for RNA isolation. Serum was collected in blood vials containing EDTA as the anticoagulant. 200µl of serum were used for each sample. The original serum vial was aliqouted into smaller volumes preventing multiple freeze thaw cycles possibly affecting the samples.

2.6.3.1 Lysis

For cell lysis, 200µl of serum was added to an RNase-free microcentrifuge tube. 300µL of lysis solution was added to every 100µL of serum (600µl of Lysis Solution (containing 1% β-mercaptoethanol) was added) and the sample mixture was vortexed for 10 seconds. 400µL of 95 – 100% ethanol was added to every 400µL of the lysate. A total of 800µl of 100% ethanol was added (equivalent to every 100µL plasma or serum used). The sample was vortexed for 10 seconds.

2.6.3.2 Binding RNA to Column

The RNA extracted was then bound to a column. 600µL of the lysate with the ethanol was placed into a column and centrifuged for 1 minute. It was ensured visually that all the lysate volume passed through the tube. Spinning for an additional minute was performed if any lysate volume was still present in the tube. The flowthrough was discarded and the column was reassembled with its collection tube.

2.6.3.3 Column Wash

400µL of 95–100% ethanol was added to the column (for washing) and centrifuged for 1 minute. If the ethanol was not seen to have passed the column, the sample was spun for an additional minute. The flowthrough was discarded. The steps for washing were repeated twice. The third wash was performed by adding another 400µL of 95–100% ethanol and centrifuging for 1 minute. The flowthrough was discarded and the spin column was reassembled with its collection tube. The column was spun for a further 2 minutes to thoroughly dry the resin and the collection tube was discarded.

2.6.3.4 RNA elution

To elute the RNA, the column was placed into a fresh 1.7mL Elution tube. 50µL of Elution Solution was added to the column and centrifuged for 2 minutes at 200xg (~2,000 revolutions per minute (RPM)), followed by 1 minute at 14,000xg (~14,000 RPM). Note the volume eluted from the column. If the entire 50µL was not eluted, the column was spun at 14,000xg (~14,000 RPM) for 1 additional minute. The purified RNA sample was stored at –20°C for a few days or –70°C for long term storage.

Once extracted, the samples were quantified (OD260 units) using the NanoDrop ND8000. All samples (51) had a final yield over 100ng. Each sample was assigned a new random number for further sample randomisation prior to the miRNA labelling. Samples were randomised and the new order for processing can be seen in the attached Excel spreadsheets ***(see 'Extracted samples_HTS' tab on the spreadsheet ["Endometriosis_HTS_working plate_20120423.xlsx"] and "HTS_Endometriosis Ctrl Samples for normalisation.xlsx")***.

2.6.4 Microarray processing

Microarray processing of all endometriosis serum samples (both original and controls) was carried out according to the manufacturer's procedure outlined in the Agilent Technologies miRNA Microarray System with miRNA Complete Labelling and Hyb Kit protocol (Version 2.4).

2.6.4.1 Spike-in solution preparation

FIGURE 2-4

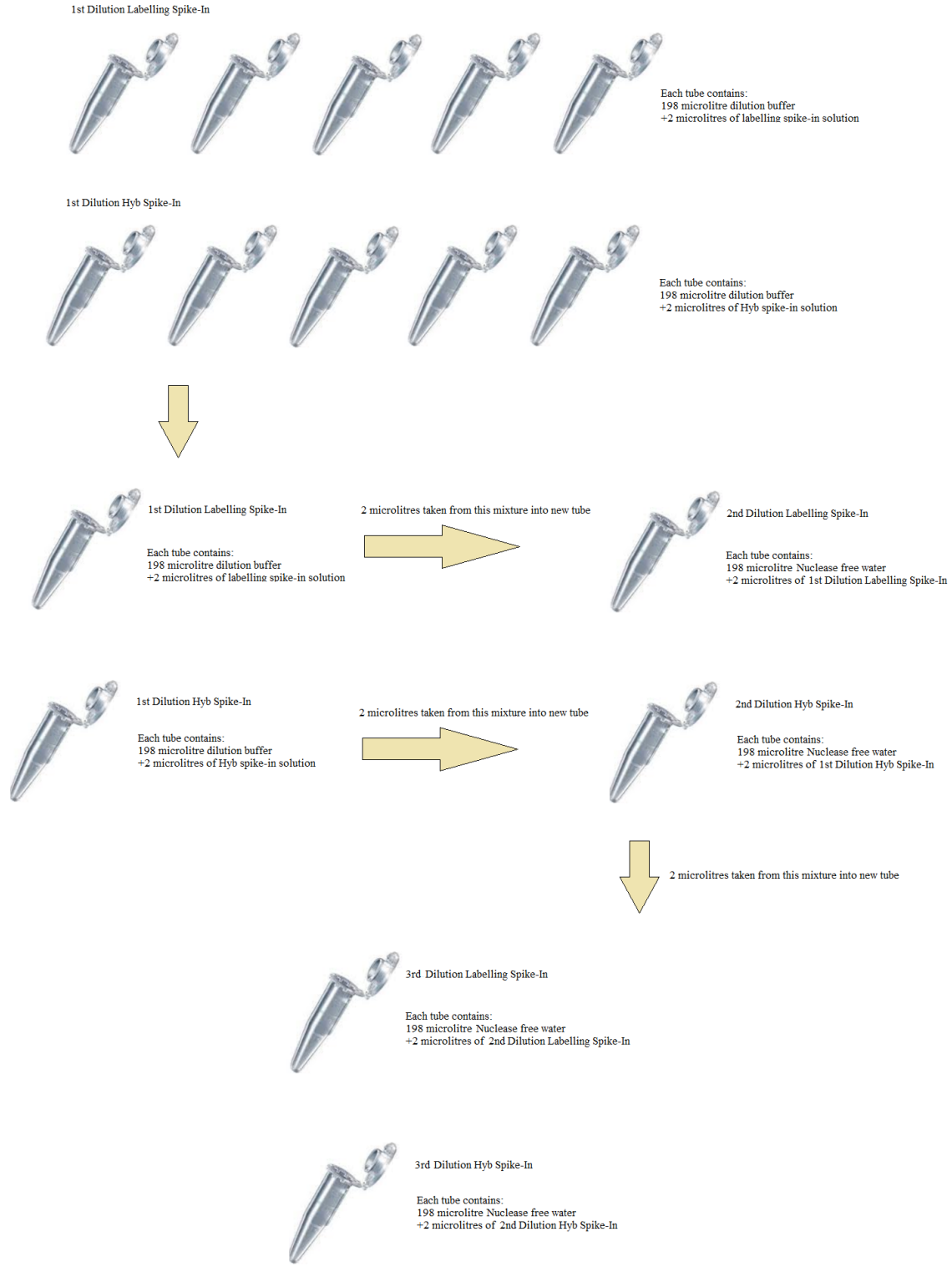

Spike in solution preparation[485]

Agilent's miRNA Spike-In kit (p/n 5190-1934) consists of two miRNA spike-in solutions for process control. Their use is to help distinguish significant biological data from processing issues. The labelling spike-in solution was spiked into the labelling reaction while the Hyb spike-in solution was spiked into the hybridization reaction. Components in the kit were thawed and spun for adequate mixing (Figure 2-4).

Five tubes were labelled as '1st Dilution Labelling Spike-In' and an additional 5 tubes '1st Dilution Hyb Spike-In'. 198µL of the dilution buffer was added to each of the 10 tubes and 2µL of the labelling spike-in solution was added to each of the 5 tubes that were labelled '1st Dilution Labelling Spike-In'. 2µL of the Hyb Spike-In solution were added to each of the 5 tubes that were labelled '1st Dilution Hyb Spike-In' tubes. Tubes were briefly spun and mixed well. One aliquot of the '1st Dilution Labelling Spike-In' and '1st Dilution Hyb Spike-In' were used at a time and the other aliquots were stored in freezers at -80°C.

Four new tubes were labelled as follows: '2nd Dilution Labelling Spike-In', '3rd Dilution Labelling Spike-In', '2nd Dilution Hyb Spike-In', '3rd Dilution Hyb Spike-In' and 198µL of nuclease-free water were added into each of the tubes. To make the second dilution solutions, 2µL from the '1st Dilution Labelling Spike-In' tube were added into the '2nd Dilution Labelling Spike-In' tube. 2µL from the '1st Dilution Hyb Spike-In' tube were added into the '2nd Dilution Hyb Spike-In' tube. Samples were mixed and spun briefly.

To create the third dilution solution 2µL from the '2nd Dilution Labelling Spike-In' tube were added into the '3rd Dilution Labelling Spike-In' tube. 2µL from the '2nd Dilution Hyb Spike-In' tube were added into the '3rd Dilution Hyb Spike-In' tube.

2.6.4.2 Sample labelling and hybridization

Agilent's miRNA Complete Labelling and Hyb Kit (p/n 5190-0456) generates fluorescently-labelled miRNA with a sample input of 100ng of total RNA. This method involves the ligation of one Cyanine 3-pCp molecule to the 3' end of an RNA molecule.

2.6.4.3 Dephosphorylation

The total RNA sample was diluted to 50ng/µL in DNase/RNase-free water. 2µL (100ng) of the diluted total RNA was placed in a 1.5mL microcentrifuge tube and maintained on ice. The calf intestinal alkaline phosphatase (CIP) master mix was prepared from the following protocol (Table 2-3).

TABLE 2-3

CIP Master Mix with labelling spike-in solution

Components	**Volume (µL) per reaction**	**Volume (µL) per 9 reactions**
10X calf intestinal phosphatase buffer	0.4	3.6
Labelling spike-in	1.1	9.9
Calf intestinal phosphatase	0.5	4.5
Total volume	2.0	18.0

Protocol for preparation of calf intestinal alkaline phosphatase (CIP) master mix– Aligent miRNA Microarray system with miRNA complete labelling and hybridisation kit

2µL of CIP master mix was added to each sample tube for a total reaction volume of 4µL. Dephosphorylation was achieved by incubation at 37°C in a circulating water bath. Denaturation of samples was achieved by adding 2.8µL of 100% DMSO to each sample and incubating them at 100°C in a circulating water bath for 10 minutes. Samples were then transferred to an iced water bath after incubation to prevent re-annealing of RNA.

2.6.4.4 Ligation step

Ligation was achieved by the addition of 4.5µL of the ligation master mix to each sample tube for a total reaction volume of 11.3µL. Samples were gently mixed and incubated at 16°C in a circulating water bath for 2 hours. The samples were then dried using a vacuum concentrator at 45 to 55°C. Samples were deemed dry when pellets were seen not to move or spread on tube flicking. Completely drying the sample ensured that there was no residual DMSO which would adversely affect the hybridization results.

2.6.4.5 Hybridisation step

For hybridisation, a water bath was prepared at 100°C. The dried sample was re-suspended in 17µL of nuclease-free water. The 10X blocking agent was reconstituted in 125µL of nuclease-free water and 4.5µL of the 10X blocking agent was added to each sample. 22.5µL of 2X Hi-RPM hybridization buffer was added to each sample for a total of 45µL. The sample was mixed well on a vortex and was incubated at 100ºC for 5 minutes. It was then immediately transferred to a water bath for 5 minutes. Samples were then quickly spun to collect condensation at the base of the tube.

2.6.4.6 Preparation of the hybridization assembly

The slides were successfully scanned (Agilent Scanner C, at 3 microns) and feature extracted (using Agilent Feature Extraction software, version 10.7.3).

For instructions on how to load slides, assembly and disassembly of chambers, the Agilent Microarray Hybridization Chamber User Guide was used (G2534-90002). A clean gasket slide was added into the Agilent SureHyb chamber base with the label facing up and aligned with the rectangular section of the chamber base. It was ensured that the gasket slide was flush with the chamber base and not ajar. For Agilent scanning and feature extraction, the slides were positioned so that the barcode label was on the left and samples were loaded left to right. Slow dispension of all of the volume of the hybridization sample into the central gasket well was performed. Care was taken to avoid bubble trapping. An array 'active side' was slowly placed down onto the SureHyb gasket slide so that the 'Agilent'-labelled barcode was facing down and the numeric barcode was facing up. Verification that the sandwich-pair was properly aligned was ascertained. The SureHyb chamber cover was placed onto the sandwiched slides and the clamp assembly was slid and tightened onto both pieces. The assembled chamber was vertically rotated to wet the gasket and assess the mobility of the bubbles. The assembled slide chamber was placed in rotisserie in a hybridisation oven set to 55°C at 20 rpm for 20 hours.

2.6.4.7 Microarray wash

2mL of the provided 10% Triton X-102 were pipetted into the wash buffer 1 and 2 respectively in the cubitainer. The caps of the cubitainer were replaced and the solutions were mixed. 1000mL of Gene Expression Wash Buffer 2 was added directly into a sterile 1000mL bottle and placed in a 37°C water bath the night before the washing of the arrays. A slide-staining dish (dish 3) was placed into a 1.5L glass dish three-fourths filled with water. This was warmed to 37°C by storing overnight in an incubator set to 37°C. All equipment was washed copiously with Mill-Q water to remove contaminants.

Slide-staining dish 1 was filled with gene expression wash buffer 1 at room temperature. A slide rack was placed into slide-staining dish 2 and a magnetic stir bar was added. Slide-staining dish 2 was filled with enough Gene Expression Wash Buffer 1 at room temperature to cover the slide rack and this dish was placed on a magnetic stir plate. The pre-warmed 1.5L glass dish was filled with water and contained slide-staining dish 3 on a magnetic stir plate with the heating element. Slide-staining dish 3 was filled to approximately three-fourths capacity with gene expression wash buffer 2 warmed to 37°C. A magnetic stir bar was added and the heating element maintained the gene expression wash buffer 2 at 37°C. A thermometer was used to check the temperature. One hybridisation chamber was removed from the incubator. The time and presence of any bubbles was recorded. Any significant loss of hybridisation volume was noted.

2.6.4.8 Hybridisation chamber disassembly

The hybridisation chamber assembly was placed on a flat surface and the thumbscrew was loosened turning counter-clockwise. The clamp assembly was slid off and the chamber cover removed. The array-gasket sandwich was separated from the chamber base by grabbing the slides from their ends. The microarray slide numeric barcode was kept facing up as the sandwich was transferred to slide-staining dish 1 containing Gene Expression Wash Buffer 1. The sandwich was opened from the barcode end whist submerged in Gene Expression Wash Buffer 1 and a forceps was used to release the slide form the gasket. The slide was then placed into the slide rack in slide-staining dish 2 containing Gene Expression Wash Buffer 1 at room temperature. When all slides were placed in the slide rack, the rack was stirred on moderate speed for 5 minutes. The slide rack was transferred to slide-staining dish 3 containing Gene Expression Wash Buffer 2 at 37°C. It was stirred once again at moderate speed for 5 minutes. The slide rack was gently removed to minimise droplets and slides were transferred to a slide holder. The slides were scanned immediately to avoid effects on signal intensity by environmental oxidants.

2.6.4.9 Scanning and feature extraction

FIGURE 2-5

Slide in slide holder for SureScan microarray scanner

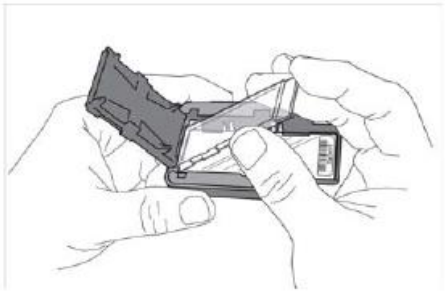

Inserting the ozone-barrier slide cover

Image demonstrating the microarray mount for scanning[485]

The protocol from the Agilent microarray scanner user guide was used. The slide holders were placed into the SureScan cassette and miRNA settings were verified according to manufacturer's recommendations (Figure 2-5). All original serum samples and additional endometriosis control samples were successfully processed. The attached Excel spreadsheets ***(see "Plate3_(1-53)_ExperimentalSummary.xlsx" and "Plate1_(1-21)_ExperimentalSummary.xlsx")*** outlines the sample hybridisation layout scheme for the respective sample sets (i.e. the slide number and array area used for each sample). The slides were successfully scanned (Agilent Scanner C, at 3 microns) and feature extracted (using Agilent Feature Extraction software, version 10.7.3).

2.7 Tissue microarray (TMA)

Tissue microarrays consist of tissue cores from paraffin blocks which are situated in a sequenced fashion to allow multiplex histological analysis. Tissue blocks containing multiple samples were first introduced in 1986 by H. Battifora named 'multitumor (sausage) tissue block'[486]. In 1990 this was modified and improved and renamed 'the checkerboard tissue block'[487]. The current utilised technique was finalised by J. Kononen in 1998 and it involved the production of a block with similarly sized and shaped tissues, enabling a more precise and dense platform to work on[488]. Modern microarrays provide a platform enabling collation of hundreds of patient specimens, at different disease stages and sites. Thousands of genes and proteins can then be analysed in a single experiment. Analysis of various tissue pathologies and their gene or protein expression profiles helps in establishing and understanding the diagnostic, prognostic and therapeutic response outcomes of the pathology in question.

The development of endometriosis has been linked to inflammatory, apoptotic and angiogenic pathways. The genes and signalling pathways involved in the above all hold a key into the development of the disease. It is through identification of these genes that novel understanding and therapies are possible.

Due to the stringent criteria used, the number of patients recruited at surgery was low. To create a microarray with adequate numbers of tissues, 200 tissue blocks were retrospectively recruited from the histology database at Barts and the London NHS Trust. Identification of confirmed histological endometriosis was performed by a consultant histopathologist and samples were subdivided into groups according to the site, type and extent of the pathology identified. Malignancies were excluded and all slides were duly coded.

Tissues of interest were identified and confirmed by histopathologists from a haematoxylin and eosin stained section. Criteria relating to the tissues themselves such as hormonal influences, site of specimen biopsy and areas of pathology were recorded. A hollow needle (1 mm^2) was used to remove tissue cores of interest from the original biopsy and these cores were then inserted in a recipient paraffin bock in a predefined and precisely spaced array pattern. A microtome was then used to cut sections (5-10 micrometres) in thickness to produce between 100-500 arrays which were utilised for immunostaining. Most endometriotic lesions are histologically heterogenous in nature with the possibility of creating a false representation of the pathology. To minimise this discrepancy, triplicate cores were taken from each sample.

2.7.1 Immunohistochemistry protocol

2.7.1.1 Slide preparation

TMAs were mounted onto adhesive coated slides to minimise compromisation of tissue adherence during heat-induced epitope retrieval especially with fatty or bloody tissue. Slides were labelled with the appropriate information and were incubated at 60ºC for 12 hours prior to processing.

2.7.1.2 De-waxing and de-hydration

To de-wax and de-hydrate the slides, these were placed in de-waxing xylene in the fume cupboard for 5 minutes. They were then transferred into IMS solution for two minutes. Endogenous peroxidise activity was blocked by placing the slides into 2% hydrogen peroxide in IMS solution for 5 minutes. Slides were then transferred into final IMS solution for 2 minutes and were afterwards rinsed in running tap water for 5 minutes.

2.7.1.3 Antigen retrieval

Three litres of vector antigen unmasking solution (50mls of Vector unmasking solution 3300 diluted in 5000mls of distilled water) were placed into the pressure cooker and the temperature was set at 450ºC. Once the solution boiled, the slides were inserted and left within it for 10 minutes. The solution was cooled down with the addition of running ambient temperature tap water for approximately 5 minutes. Preparation of 500mls of wash buffer (Tris-buffered saline with tween (TBS-T)) was performed by mixing one part of wash buffer solution with 9 parts distilled water. (i.e. 50mls wash buffer with 450mls distilled water). Slides were removed from the 'cooker' and placed into a trough with wash buffer.

2.7.1.4 Tissue microarray immunohistochemical staining and analysis

For Maspin, E- Cadherin, B-cell lymphoma 2 (Bcl-2)-associated transcription factor (BCLAF) and p53 the SS-enhanced Polymer detection system (Biogenix) was applied using the Dako-autostainer system (Dako). Incubation with optimally diluted primary antibody in BSA and sodium azide (Table 2-4) was performed following antigen retrieval. Staining enhancement was achieved by adding enhancer reagent increasing the antigen location-specific horseradish peroxidase (HRP) activity. Subsequent incubation with chromogen, 3,3'-diaminobenzidine (DAB) produced a brown precipitate at the antigen site. Sections were counterstained with haematoxylin.

The ARIOL imaging system (Genetix, San Jose, CA) was used for TMA antibody staining quantification. Slides were scanned at low resolution (1.25x) followed by high resolution (20x) using the Olympus BX61 microscope with an automated platform (Prior). Training and stain quantification was performed on the high resolution images. Training of the system for detection of stained and unstained cells by the colour intensity and shape of stained regions was performed. Positive staining, as determined by appropriate isotype negative controls, was classified by manually defined hue, saturation and intensity limits. Only epithelial areas were analysed through the use of the manual include/exclude drawing tool (Figure 2-6). The software generated the mean intensity (0-255) of all pixels considered positive, which was subsequently corrected so that the higher the value, the greater the intensity. Results were exported to an Excel sheet and non-parametric statistical analysis was performed on each of the subgroups using a

Mann-Whitney U Test. A P value of <0.05 between the groups was regarded as statistically significant. The resulting data was then plotted graphically.

TABLE 2-4

Antigen	Clone	Dilution	Supplier
Maspin	Clone EAW24	1:100	Novocastra
E Cadherin	Clone 36B5	1:200	Novocastra
BCLAF	Rabbit polyclonal	Dilution 1:100	Sigma Prestige
p53	Clone D07	Dilution 1:3000	Dako

FIGURE 2-6

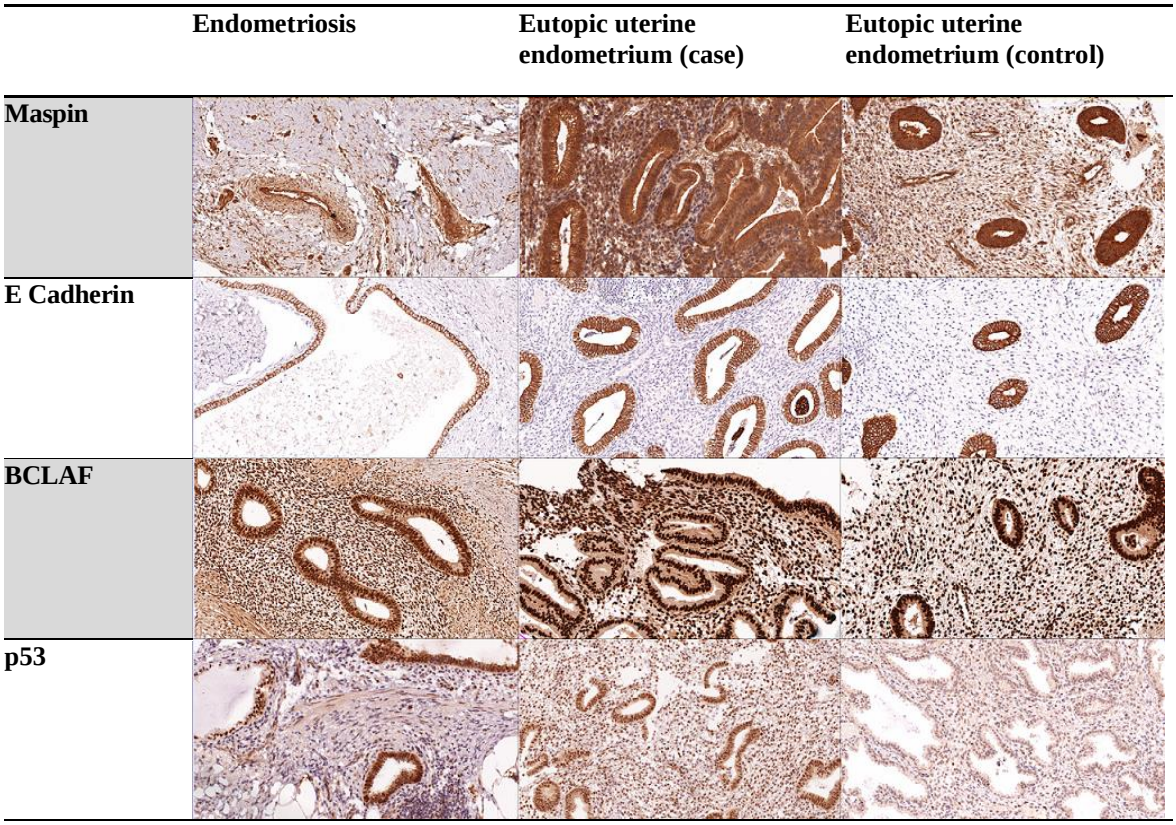

Representative selection of samples from the created TMA's stained by the indicated antibodies

2.8 Protocol for protein biomarker serum study

Below is the protocol used for the assay of binding of human serum antibodies to protein arrays and their detection to determine the binding profile for particular samples.

2.8.1 Assay precaution

Virkon was not used in the vicinity of the assay work as it could cause increased general fluorescence across the array. The work area, assay implements and gloves were all kept scrupulously clean during assay to prevent contamination of the assay solutions and arrays. Slides were not wiped on coloured paper towels as these may contain soluble fluorescent dye. Buffers were prepared and ready for use (0.1% v/v

Triton/0.1% w/v bovine serum albumin (BSA) in phosphate buffered saline (PBS)). Three litres of spiked assay buffer (SAB) buffer were required to assay 24 arrays.

The computer was switched on and the VisionMate scanner software loaded. The workstation and a laminar flow class II cabinet were cleaned. A disinfectant bath was prepared using a 1% solution of Virkon or Trigene for the disinfection of wash, probing solutions and plasticware. To avoid interference with results, Virkon contaminated materials were kept away from the assay work bench. 200 mL cold SAB was poured into a slide processing box and left at 4°C until required. 2 litres of SAB were poured into a 2L Duran bottle and equilibrated to 20ºC for 30 min in a designated Techne circulating water bath. A 50mL laboratory dispenser was fixed to the bottle before use. 1 litre of SAB was poured into a 1L Duran bottle and equilibrated to 20ºC for 30 minutes in a designated Techne circulating water bath. A 10mL laboratory dispenser was fixed to the bottle before use. The required number of 15mL Falcon tubes were numbered from 1 up to 24 and placed in order in a polystyrene tube rack. 4.5mL of SAB (20 ºC) were pipelled into each tube using the designated Hirschmann laboratory dispenser. The Quadriperm dishes were labelled on the bottom below each chamber with consecutive numbers corresponding to the number of samples (up to 24). 24 Pap jars were placed into a suitable rack and labelled with consecutive numbers corresponding to the number of samples (up to 24). The lids for the Pap jars were placed in a box ready for use in the work area. The bowl of the Sorvall Legend centrifuge was cleaned to remove any dust. Samples were checked and numbers confirmed by two independent laboratory personnel to ensure correct labelling. Samples within the assay rack were not allowed to thaw unnecessarily unless ready for processing. These were placed into the scanner rack according to their designated numbers and the VisionMate software was run inputting the relevant sample details for each. Each sample was visually checked to ensure that each of the tubes had sufficient serum (22.5µL) for the assay. The plate was carried in a containment tray and placed in the Medline shaking incubator to thaw at 20°C for 30 minutes. When completely thawed, each sample was vortexed for a count of three at full speed (IKA Vibramax). The tubes were placed in assay order starting at position 1 in a designated Eppendorf microcentrifuge. A plastic Rawplug support was required in each tube to support the TrakMate tubes. The serum samples were centrifuged for 3 minutes at 13000rcf using a designated Eppendorf microcentrifuge.

The tubes were then removed from the centrifuge and replaced in the TrakMate rack in the same order and positions that they were taken i.e. A1 to B24. The serum samples were diluted in SAB buffer to provide the assay solutions. Care was taken not to disturb the vortexed samples with movement. 100µL pipettes were used to pipette 22.5µL of the sample into 4.5mL of SAB Buffer. In case of sediment, care was taken to tilt the tube when aspirating to ensure that the sera were sampled from below the lipid layer at the top but did not touch the bottom of the tube. The samples were gently vortexed.

2.8.2 Assay set up

2.8.3 Washing and probing the arrays

The slide box and rack containing 200mL cold SAB were place in the containment tray. Each array was removed in turn using forceps from its storage buffer. The excess liquid from the array was drained by touching the edge of the array on the rim of the Pap jar. The assay rack was lifted from the slide staining

dish and placed in a slot with the array facing towards the second slot. It was replaced in the staining dish solution. Each slide in the slide box from left to right was in turn added to the slide rack with 200mL cold SAB making sure the slides were all in the same orientation. When all the arrays were added, the rack was gently shaken up and down five times to aid mixing at the slide buffer interface.

The lid was placed on the slide box and shaken at 50 rpm for 5 minutes on an orbital shaker (IKA KS501). 4.0 mL of each diluted sample from the 15mL Falcon tubes was pipetted into their corresponding chambers in the Quadriperm dishes. When the slides finished washing they were removed in order from the rack. Slides were gripped from their labels and the back of the array was wiped using colour free Kimwipe tissue paper. The long edge of the array was blotted three times on a wad of lint free tissue paper.

The array was immediately placed into the probing solution in the correct chamber of the Quadriperm dish. The plate was gently swirled to cover the slide with incubation solution after which the next slide was added. Sample identification was double checked at all stages ensuring no sample errors. To prevent slopping of solutions between chambers, the lids of the Quadriperm dishes were replaced and it was ensured that the dishes were kept horizontal at all times. The dishes were placed in the Medline shaking incubator and shook at 50 rpm during incubation at 20ºC for 120 minutes.

2.8.4 Washing after serum binding

Towards the end of the incubation period the 24 Pap jars were filled with 30mL of SAB using a laboratory dispenser (Eppendorf). An empty Nalgene tube rack was used to hold the Pap jars on the horizontal shaker (IKA KS501). When the incubation time was over, each array was removed from the Quadriperm dishes and washed individually in a Pap jar. The Pap jar was capped and inverted 4 times before placing in the Nalgene rack on the orbital shaker and shook at 50 rpm at 20ºC for 20 minutes.

After the 20 minutes incubation had finished, the first array was taken and the wash solution was poured off into an empty beaker. Another 30 mL of SAB was dispensed into the tube at the back of the array and the Pap jar was inverted four times and again placed in the empty Pap jar rack on the shaker at 50 rpm at room temperature for 20 minutes. The remaining tubes were each processed in turn.

When incubation was complete, a slide staining box and rack were taken and 200mL of SAB was added. The first Pap jar was taken and the buffer was poured off. The array was placed in the second position in the slide rack with the array facing towards slot 1. The rack in the buffer was placed in the slide staining box. The remaining arrays were added sequentially until all slides were transferred. The slide rack was replaced in buffer during the addition of each array. When all the arrays were added, the slide rack was gently moved up and down five times to aid mixing. The lidded box was placed onto a shake (IKA KS501) for the remainder of the incubation time and was shaken at 50 rpm at room temperature. Preparations were made for the secondary antibody probing solution process.

2.8.5 Incubation with Cyanine dye 3 (Cy3)-anti Immunoglobulin G (IgG)

200mL of SAB were measured at 20ºC into a volumetric flask and 200µL of Cy3-antihuman IgG was added. Mixing was performed by repeated inversion. The resulting solution was poured into a fresh slide staining box and covered until required.

The rack of arrays (described above) was removed from the wash solution and placed on a wad of Kimwipe tissues. Then it was gently tapped on the tissues five times to remove excess wash buffer. The arrays were then immediately placed in the Cy3-antihuman IgG solution. The rack was shaken up and down five times to help mixing of the probing solution at the surface of the arrays. The box was then covered and placed in a medline shaking incubator at 50 rpm at 20ºC for 120 minutes incubation time.

2.8.6 Washing after incubation with Cy3-anti IgG

Towards the end of the incubation period a slide staining box was filled with 200mL SAB buffer at 20°C. When the incubation had finished, the slide rack was lifted from its incubation solution and placed into the fresh SAB wash solution. The rack was agitated gently up and down five times. The lid of the container was replaced and shaken for 5 minutes at 50 rpm at room temperature (IKA KS501). After the first wash, the slide rack was lifted out of the dish and the buffer poured off into a beaker and replaced with 200 mL of fresh SAB buffer (20ºC). The rack was gently shaken up and down five times, the lid was replaced and the container shaken for 5 minutes at 50 rpm at room temperature (IKA KS501). This was repeated for the third wash.

When the third wash had finished, the slide rack was lifted out of the dish and the SAB was poured off. The box was filled with high purity water. The slide rack was placed in the water and shaken gently up and down five times. The lidded box was then placed on the shaker at 50 rpm for 10 seconds to ensure that buffer components were washed from the slide rack and arrays.

A wad of Kimwipe tissue was placed in the containment tray and two layers of Kimwipe tissues were placed into the bottom of a dry slide staining box. The slide rack was removed from the dish and placed on the wad of tissues, banging it gently five times to remove any excess water. The slide rack was placed in the fresh staining box on top of the Kimwipe tissues. The box was lidded and moved to the Sorval centrifuge. The staining box lid was removed and the box placed in a microtitre plate holder and a balancing rack was added. The arrays were dried by centrifugation for 2 minutes at 240xg at 20°C. The slide rack was moved to a clean bench and each slide was loaded into an Agilent type 2 slide-holder. Once all slides were transferred the lid of the holder was shut and the slide holder was placed into an Agilent slide carousel. The samples were then transferred from the slide rack into a pre-labelled slide box in preparation for scanning.

2.9 Protocol for DNA extraction from peripheral blood lymphocytes

In the section below I outline the technique used for DNA extraction from peripheral blood lymphocytes.

The Maxwell® 16 SEV Instrument and Maxwell® 16 Blood DNA Purification Kit enabled extraction of DNA from 300µl of patient lymphocytes suspended in elution buffer. The lymphocytes were previously extracted from whole patient blood (see previous protocol for peripheral white blood cell extraction). The manufacturer's protocol for the Maxwell® 16 Blood DNA Purification Kit was followed and the resulting extracted DNA was checked on the Nanodrop® machine for concentration and purity.

2.10 Cell culture from primary patient samples

Primary patient samples were used for *in vitro* therapeutic experiments. Below I describe the techniques employed to create a cell culture from primary patient samples obtained at surgery. I also describe the *in vitro* therapeutic studies performed in 96 well plates to test for Galectin inhibitor effects on primary patient cells. All cell cultures were tested in the laboratory for mycoplasma every three months and remained negative.

2.10.1 Fresh medium preparation

The base medium DMEM with high Glucose and Pyruvate (500mls bottle) was purchased from Invitrogen®. This was left to warm up to room temperature prior to usage. 50mls of heat inactivated fetal calf serum (FCS) (56 ºC for 30 minutes), 5mls of L-Glutamine and 5mls of Penicillin/Streptomycin was added at room temperature into the above solution. The bottle was then labelled, dated and used up to a maximum of four weeks. The medium was heated to 37ºC prior to usage with cells.

2.10.2 Primary patient cellular sample preparation

Primary patient endometriosis samples were taken at laparoscopy. A scalpel was used to scrape endometriosis cells and fragment tissue from the surfaces of endometriotic plaques and endometriomas by manual techniques. This manual fragmentation technique minimised the destruction of cells as happens with automated mechanical methods such as morcellation. The collected tissue samples were also separately sent to histology to confirm the presence of endometriotic cells. Samples were suspended in growth medium between transfers from the operating theatres to the cell culture laboratory minimising cellular death in transport. In the laboratory, cells and tissue debris were filtered through standardised cellular meshes to remove debris. Cells were washed and re-suspended in fresh medium and subsequently placed in 0.1% collagenase for 1 hour. A Vi-Cell® XR Cell Viability analyser was used to assess for cellular concentration and viability. Cells were then centrifuged at 1200rpm for 5 minutes and the pellet was re-suspended in culture medium for tissue culture. The cells were suspended (at a concentration of $1x10^5$ cells per ml) in flasks and allowed to grow in culture incubators at 37ºC at 5% CO_2 for 5 days or until confluence was seen at the base of the flask. Endometriosis cells were seen to be adherent to the base of the culture flasks and were slow growing in nature.

2.10.3 Using the hood in a cell culture room

The hood was wiped clean with 70% IMS. It was ensured that flow and lighting were working correctly. All solution bottles and disposable equipment were opened inside the working hood to minimise

contamination. Disposable instruments were utilised at all stages. To endure optimal growth conditions, the correct media were assigned to the particular cells being cultured.

2.10.4 Cell splitting

At the start of splitting, cells were viewed under the microscope for assessment of their starting density and confluence. The adherent cell lines were grown on the inferior surface (**A**) of the flask (Figure 2-7).

FIGURE 2-7

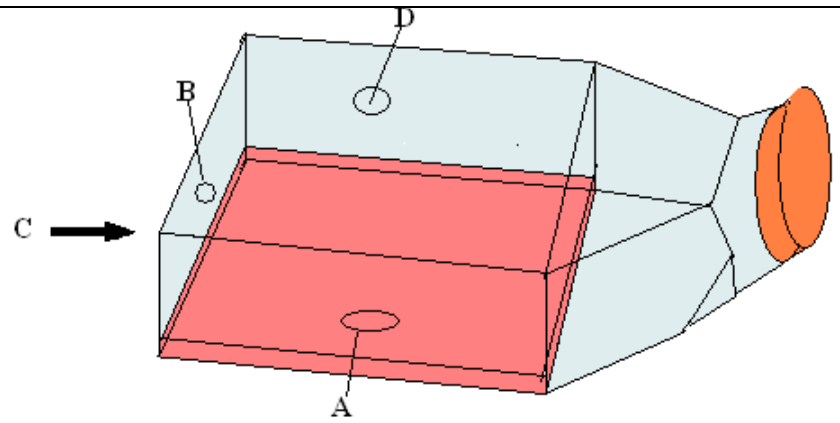

Diagram of a culture flask

The flask was rotated by 90º onto surface (**B**) and a suction pipette was placed at point (**C**) to remove the 'old' medium in which cells were growing. Maintaining the flask in the same position, surface (**A**) was then rinsed with 5mls of sterile PBS. This enabled the removal of any remaining FCS allowing the next trypsinisation step to work effectively. The added PBS was again removed carefully from point (**C**) without disrupting the cellular layer on surface (**A**). The flask was maintained in the upright position whilst 6mls of trypsin were added on to surface (**A**). The flask was sealed and placed gently back onto the incubator at 37º and 5% CO_2 for 10 minutes. This enabled cell trypsinisation and detachment of the adherent cell line from surface (**A**). The cells were assessed under the microscope every 5 minutes to ensure that the amount of time trypsin was in contact with the cells was kept to a minimum.

When the cells were seen to detach, the flask was replaced into the hood onto surface (**B**) and 6mls of warmed medium (at 37º) were added onto the 6mls of previously applied trypsin to dilute the latter's effect. The resulting mixture was gently pipette at point (**C**) to ensure that any clumping of cells was minimised. The mixture was transferred into 15ml tubes and centrifuged at 1500rpm for 5 minutes at 21ºC to obtain a cellular pellet. The supernatant was poured off into a beaker with Virkon® leaving the cellular pellet behind. The pellet was then gently re-suspended into 10mls of fresh medium. Minimisation of cellular clumping and adequate re-suspension was ensured through gentle pipetting.

500microlitres of the new suspension were placed into cell counting containers and the sample was run on the Vi-Cell® XR Cell Viability analyser to assess for cellular concentration and their percentage viability. The Vi-Cell® is an automated haemocytometer which takes up the sample delivering it to a flow cell and camera (Table 2-5). It utilises the trypan blue protocol (1:1 mixture with cellular volume provided). Dead cells are seen to absorb dye whilst live ones do not. The camera elicits grey scale alterations between

viable and non-viable cells which are software predetermined. Fifty images per sample are used to determine the final outcome[489].

TABLE 2-5

System specification	Acceptable ranges
Cell Diameter Range	3 to 70µm
Cell Concentration Range	5 x 104 to 1 x 107 cells/mL
Viability Range	0%-100%
Counting Accuracy	±6%
Sample Volume	0.5mL to 2.0mL
Acquisition Time	2 minutes

2.10.5 Re-suspending cells for new culture flasks

$1x10^5$ healthy cells were transferred into a new flask for growth. Parameters used to calculate this depend on % viability, viability of cells/ml $x10^6$ and cells/ml x 10^6. The following is an example of calculating volume amounts for transfer into new growth flasks (Table 2-6).

TABLE 2-6

Cell type	Viability%	Viability cls/ml x 10^6	Cls/ml x 10^6
Endometriosis Cell line X	97.4	3.99	4.10

This table indicates that there are 3.99 x 10^6 viable cells per ml resulting in an overall 97.4% viability of my culture in this sample. I aimed to re-suspend the cells into 20mls of fresh medium and needed to calculate how many millilitres of the original medium with the re-suspended cells I required.

In 1ml I had 3.99 x 10^6 cells i.e. 39.9 x 10^5 cells. There is a current total of approximately 10mls of this mixture. I needed to calculate how many millilitres of this mixture would enable me to transfer$1x10^5$ cells into a new flask.

Therefore the calculation is as follows:
1/39.9 x 20 mls = 0.5mls of medium with the re-suspended cells

This will be added to 20mls - 0.5mls = 19.5mls of fresh medium into the new flask. The new flask is then labelled, dated and annotated. Any remaining cells were frozen in liquid nitrogen for future use.

2.10.6 Freezing cells in liquid nitrogen- cryopreservation

When culturing cells, cultures can vary from the initial sample due to variations in cell growth and proliferation. There is a tendency for the most rapidly proliferating cells to dominate the culture with slower or less proliferating ones eventually dying out. This gives an altered cellular picture which is not a true reflection of the original or primary culture. Senescence is the natural limitation of normal cells to die out after a fixed number of replications. It is a multifactorial gene occurrence and is thought to be due in part to the terminal DNA sequences situated in the telomeres to replicate at each cellular split. Telomeres will progressively grow shorter until the inability to divide further is reached[490]. Tumour cells are not

limited by this mechanism, being able to replicate terminal DNA sequences in the telomeres. Instability within genes or phenotypes also renders the necessity of cryopreservation. Overall, finite human cell lines are genetically stable[491], but care must be taken to avoid and recognise cellular mutations once they occur. *In vitro* spontaneous rates are noted to be higher than in vivo ones and once mutant cells are present they are not eliminated as would occur in an in vivo scenario. Other factors including the possibility of cell line contamination by microorganisms, cross contamination with other cell lines, misidentification of cells due to carless handling, incubator failure and the future need to possibly distribute to alternate users[491], all make cryopreservation a sensible, time and material sparing step in current laboratory practice. Minimising the intracellular ice crystal formation and cryogenic damage from solutes of high concentration on intracellular freezing is what enables the best recovery and growth of cells after they are thawed. Four steps are advised in cell culture literature[491]: slow freezing to allow water exit from the cell but not slow enough to encourage the formation of ice crystals; using a hydrophilic cryoprotectant to sequester water (called a freeze mix (Table 2-7)); storing cells at the lowest possible temperature to minimise the effect of ice formation within the cell; and ensuring a rapid thaw minimising ice crystal expansion and solute formation on the melting of intracellular ice. The prepared samples are then stored in liquid nitrogen.

TABLE 2-7

Freeze mix composition
20% DMSO
50% FCS
30% Medium- Invitrogen® (Dulbecco's Modified Eagle Medium (DMEM) with high Glucose and Pyruvate 500mls bottle)
50mls of heat inactivated FCS (56ºC for 30min) and 5mls of Penicillin/Streptomycin.

Liquid nitrogen is a colourless liquid with density of 0.807 g/mL. It is produced by fractional distillation of liquid air and has a boiling point of -196°C/-321°F and a freezing point of -210°C/-346°F. It causes rapid freezing of living tissues and is therefore perilous to the user if not handled with care. It is used in laboratories primarily to freeze tissues for storage to minimise cryogenic tissue damage.

2.10.7 Preparing the cells for liquid nitrogen storage

The cellular pellet was re-suspended in 3mls of freeze mix (Table 2-7) and pipetted gently to avoid clumping. 1ml of the cell suspension was then transferred to cryophials and these were labelled recording the cellular concentrations at which they were frozen. The cryophials were then placed into Nalgene® Mr Frosty™ Cryo 1ºC freezing container (Nalgene Cat. No. 5100-0001) enabling slow freezing. The container was left overnight at -80ºC. After 24 hours, the cryophials were transferred from the container into the liquid nitrogen Dewar tank (Custom Biogenic Systems (CBS) Isothermal V-1500 series) for long term storage.

2.10.8 Thawing cells

To minimise ice crystal expansion and solute formation on the melting of intracellular ice, ampules were quickly thawed under hot water or in a water bath. Ampules were then swabbed thoroughly with 70%

alcohol and opened in a laminar-flow hood. Cellular contents were transferred into labelled 15ml centrifuge tubes using a 1ml pipette. 10ml of pre-warmed medium were slowly added dropwise to the cell suspension over 2 minutes. Cells were then centrifuged at 1200 rpm for 5 minutes. The supernatant was discarded and cells were re-suspended in 10ml pre-warmed medium with 20% FCS. Cells were then transferred to labelled culture flask and were counted using Vi-Cell ® XR Cell Viability Analyzer.

3 Clinical perspectives- symptom analysis post-surgery

3.1.1 Methods

Patients were asked pre-operatively and at 6 and 12 months post-operatively to rate their symptoms over the previous month. Their general level of health was compared to that in the previous year. Detailed questions assessed their limitation on daily activities, social activities and work due to physical and emotional problems secondary to disease, levels of bodily pain and its interference with physical, social or emotional activities (Figure 3-1). (*See* section 1.12)

3.1.2 Discussion

FIGURE 3-1

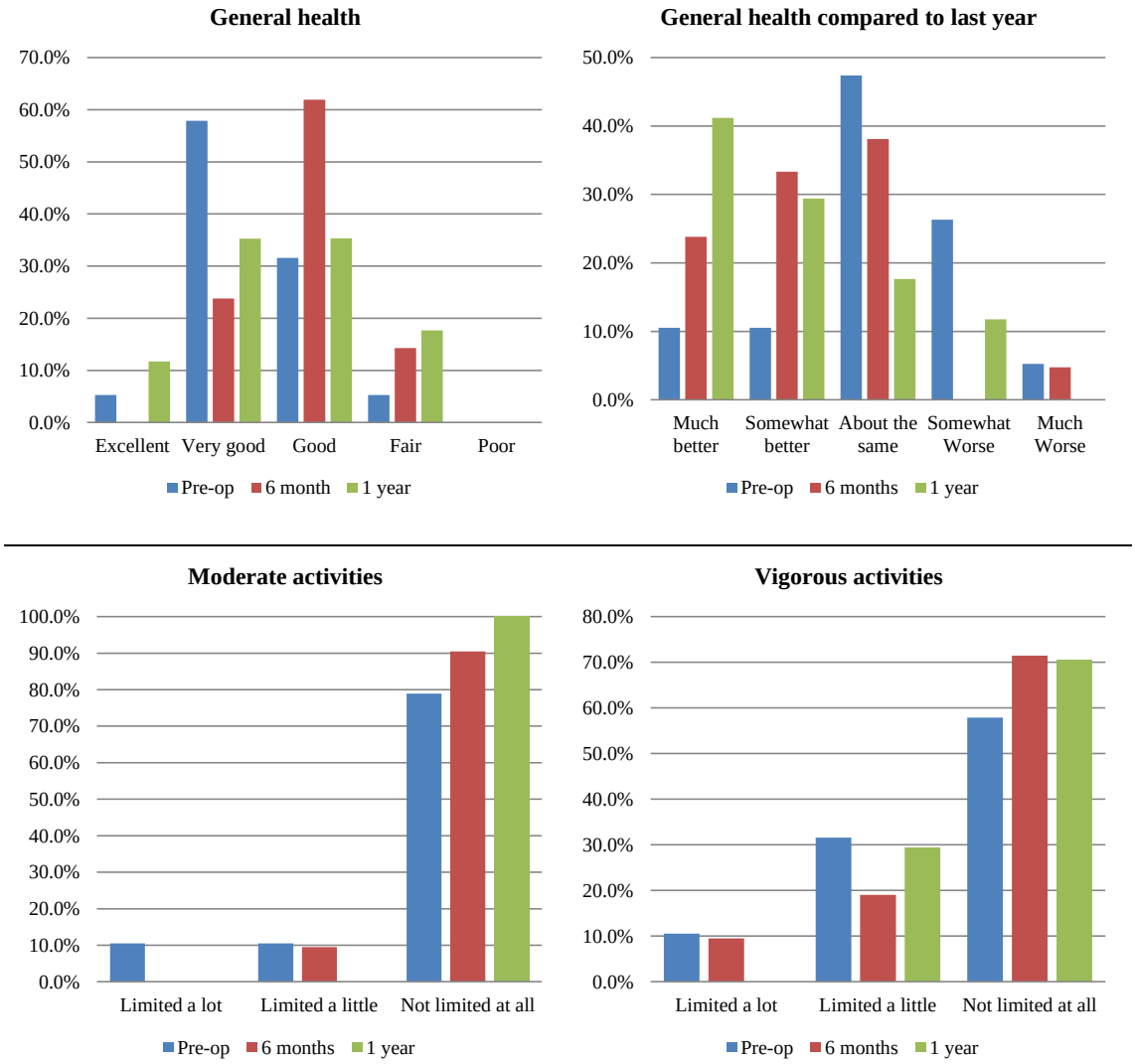

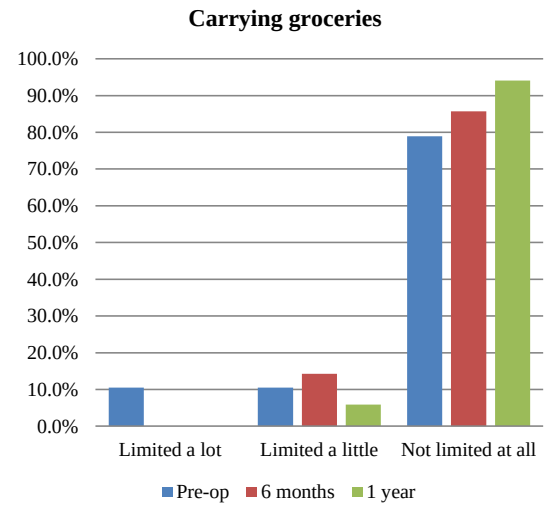
Carrying groceries
100.0%
90.0%
80.0%
70.0%
60.0%
50.0%
40.0%
30.0%
20.0%
10.0%
0.0%
Limited a lot
Limited a little
Not limited at all
Pre-op
6 months
1 year

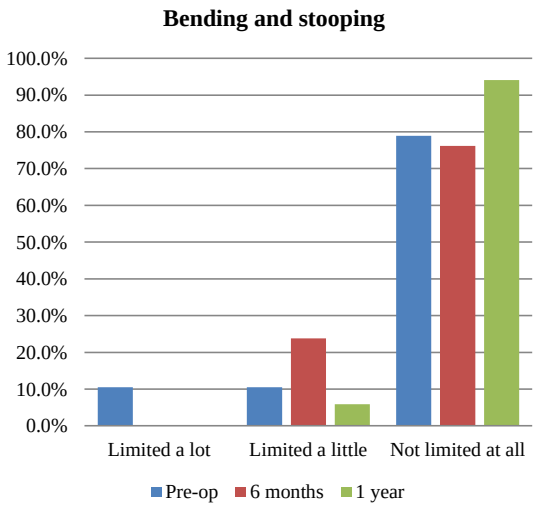
Bending and stooping
100.0%
90.0%
80.0%
70.0%
60.0%
50.0%
40.0%
30.0%
20.0%
10.0%
0.0%
Limited a lot
Limited a little
Not limited at all
Pre-op
6 months
1 year

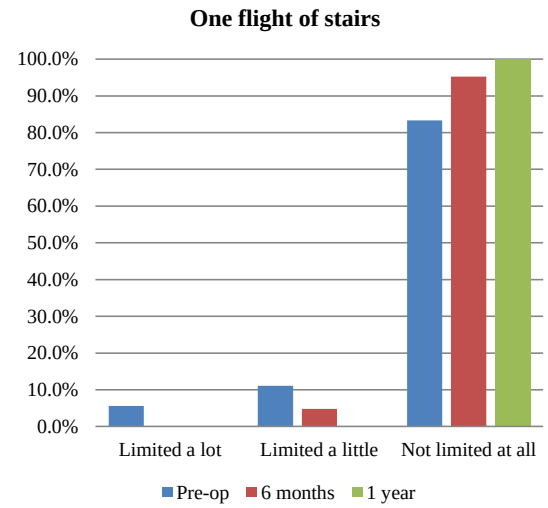
One flight of stairs
100.0%
90.0%
80.0%
70.0%
60.0%
50.0%
40.0%
30.0%
20.0%
10.0%
0.0%
Limited a lot
Limited a little
Not limited at all
Pre-op
6 months
1 year

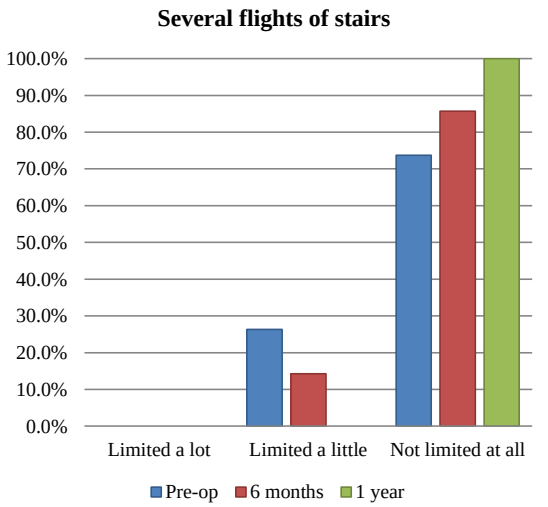
Several flights of stairs
100.0%
90.0%
80.0%
70.0%
60.0%
50.0%
40.0%
30.0%
20.0%
10.0%
0.0%
Limited a lot
Limited a little
Not limited at all
Pre-op
6 months
1 year

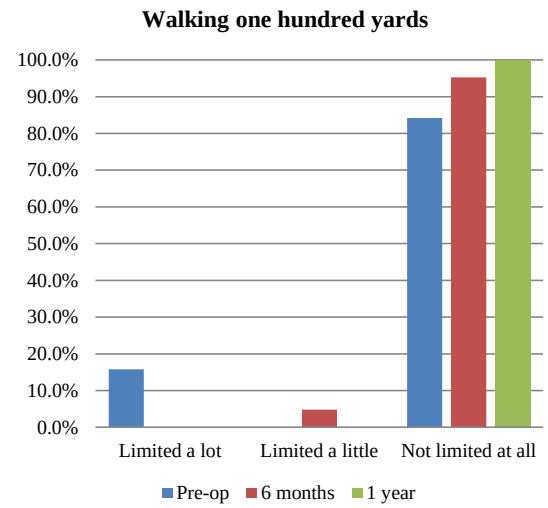
Walking one hundred yards
100.0%
90.0%
80.0%
70.0%
60.0%
50.0%
40.0%
30.0%
20.0%
10.0%
0.0%
Limited a lot
Limited a little
Not limited at all
Pre-op
6 months
1 year

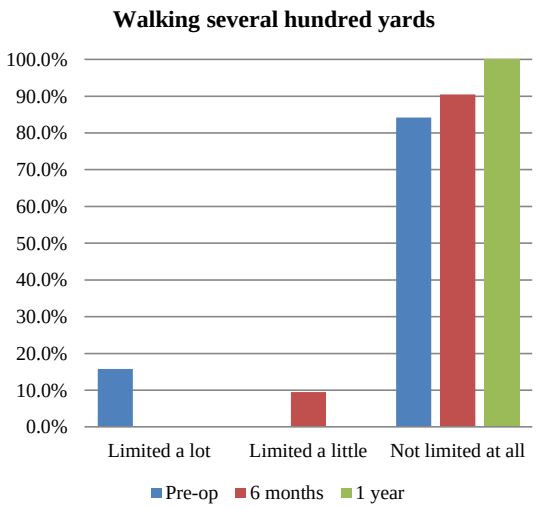
Walking several hundred yards
100.0%
90.0%
80.0%
70.0%
60.0%
50.0%
40.0%
30.0%
20.0%
10.0%
0.0%
Limited a lot
Limited a little
Not limited at all
Pre-op
6 months
1 year

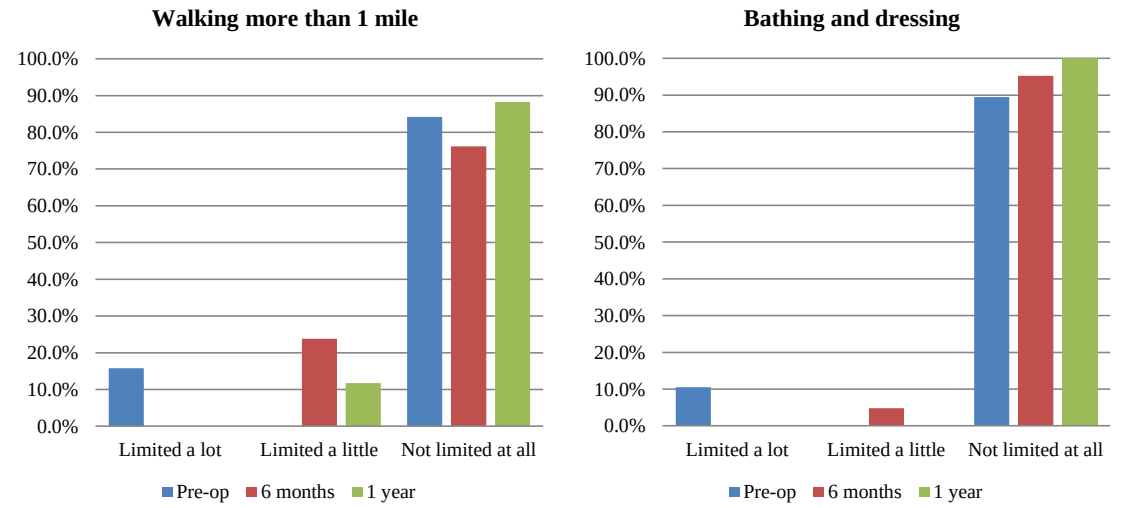

A comparitive graphical rapresentation of limitations experied by endometriosis patients in the pre-opeartive period, six months post operatively and at one year post-operatively.

Within 6 months of surgery, there was an overall improvement in general health of patients with 61.9% of the study patients reporting good overall health levels 6 months post-surgery compared to 31.6% preoperatively (P=0.031). Within a year, reports of the same patients reporting good levels of health fell to 35.3% which is similar to the pre-operative value of 31.6% (P=1). This is in keeping with the short term reported benefits of surgery with high relapse rates necessitating future surgery with increased patient morbidity. There was a small observed increase in the percentage of people reporting excellent levels of health at 1 year post surgery (11.7%) when compared to pre-operative levels of 5.3%. This however did not reach statistical significance (P=0.576). Interestingly within six months of surgery 0% of my study population classified their health as excellent and values were only seen to rise within the 6 month to 1 year post-operative recovery period.

In the pre-operative questionnaires, 5.3% of the study population described their health as fair to poor. Within six months of surgery these reports increased to 14.3% (P=0.329) reaching 17.6% at one year (P=0.329). The reason for this rise is a question of debate. Whilst some might argue that post-operative scarring can contribute to worsening of pain and discomfort, others might attribute perceived increased levels of poor health as a result of the negative psychological impact on patients once a diagnosis of endometriosis has been made.

Interestingly, when patients were asked to compare their post-operative overall health levels, one year following their surgery, to the one year prior to their surgery, the responses was positive. Within 6 months of surgery, 23.8% felt their health had significantly improved when compared to 10.5% pre- operatively (P=0.186). This percentage increased to 41.2% at one year (P=0.096). There was a decrease in the patient groups reporting the worst levels of pre-operative general health, with a reduction from 26.3% to 0% (P=0.021) within 6 months of surgery and a further increase to 11.8% at the one year follow up (P=0.267). From the 5.3% of patients who believed their health was progressively worsening pre-operatively, there was an observed reduction to 4.8% within six months of surgery (P=1) and this fell to 0% at one year post surgery (P=0.329).

The ability to perform moderate activities was reported as limited in a total of 21% of the study patients in the pre-operative period. This percent fell to 9.5% within 6 months and to 0% at their one year follow up (P=0.162). Within 6 months of surgery 71.4% of patients did not report any limitations in performing daily vigorous activities in comparison to the 57.9% in the pre-operative period (P=0.213). This percentage totalled out to 70.6% of the study population at one year post-operatively (P=0.747).

Restrictions in daily functions such as lifting or carrying objects, climbing flights of stairs, bending and kneeling, walking a mile and bathing or dressing showed improvements at the one year post-operative follow up in the patient groups reporting the worst pre-operative symptoms. Respective results were as follows: lifting or carrying objects (10.5% to 0% (P=0.162)), climbing flights of stairs (26.3% to 0% (P=0.021)), bending and kneeling (10.5% to 0% (P=0.162)), walking a mile (15.8% to 0% (P=0.082)) and bathing or dressing (10.5% to 0% (P=0.082)).

FIGURE 3-2

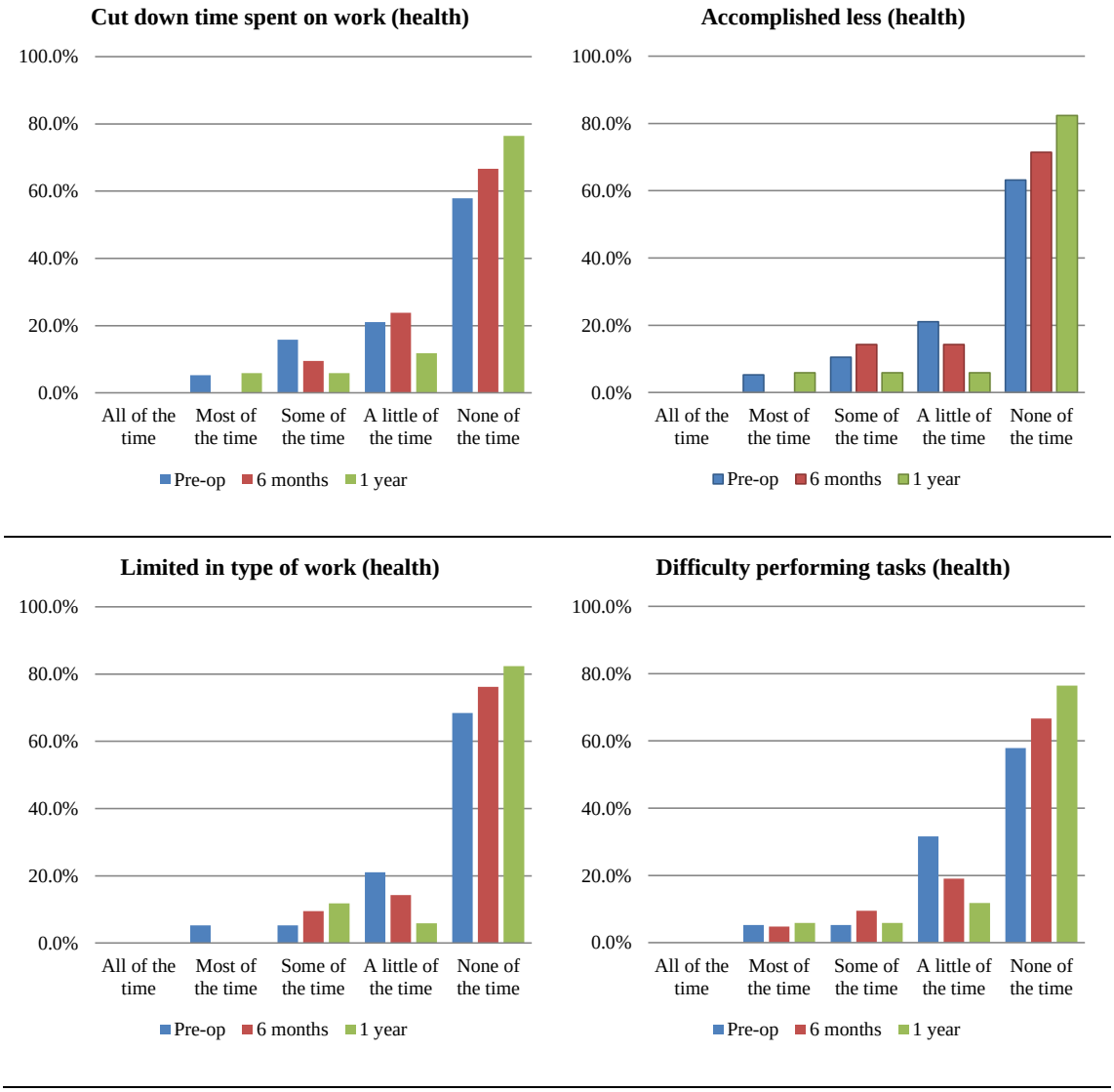

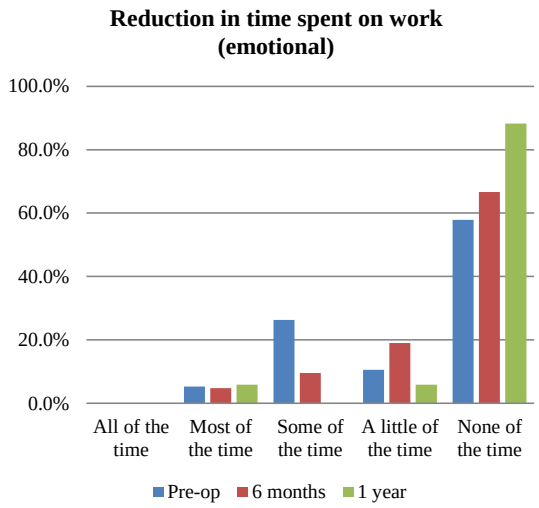
Reduction in time spent on work (emotional)
100.0%
80.0%
60.0%
40.0%
20.0%
0.0%
All of the time
Most of the time
Some of the time
A little of the time
None of the time
Pre-op
6 months
1 year

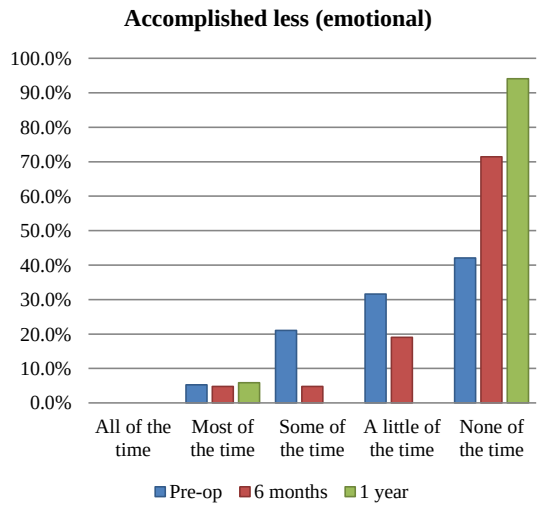
Accomplished less (emotional)
100.0%
90.0%
80.0%
70.0%
60.0%
50.0%
40.0%
30.0%
20.0%
10.0%
0.0%
All of the time
Most of the time
Some of the time
A little of the time
None of the time
Pre-op
6 months
1 year

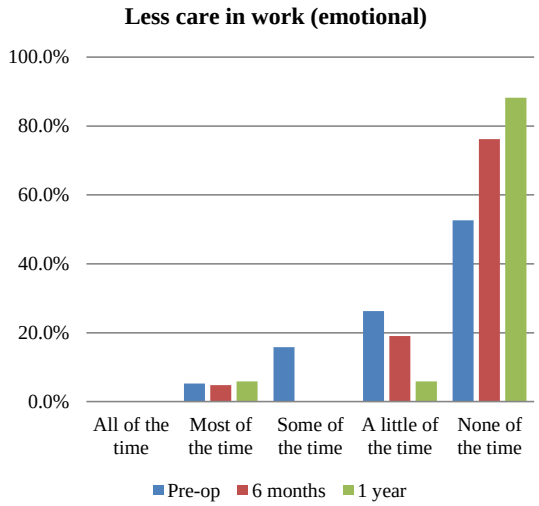
Less care in work (emotional)
100.0%
80.0%
60.0%
40.0%
20.0%
0.0%
All of the time
Most of the time
Some of the time
A little of the time
None of the time
Pre-op
6 months
1 year

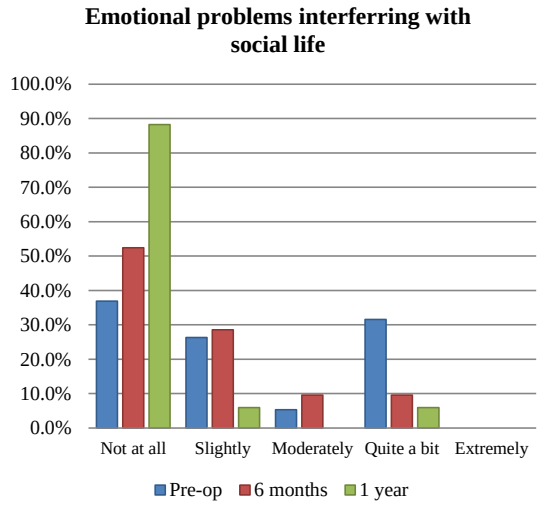
Emotional problems interferring with social life
100.0%
90.0%
80.0%
70.0%
60.0%
50.0%
40.0%
30.0%
20.0%
10.0%
0.0%
Not at all
Slightly
Moderately
Quite a bit
Extremely
Pre-op
6 months
1 year

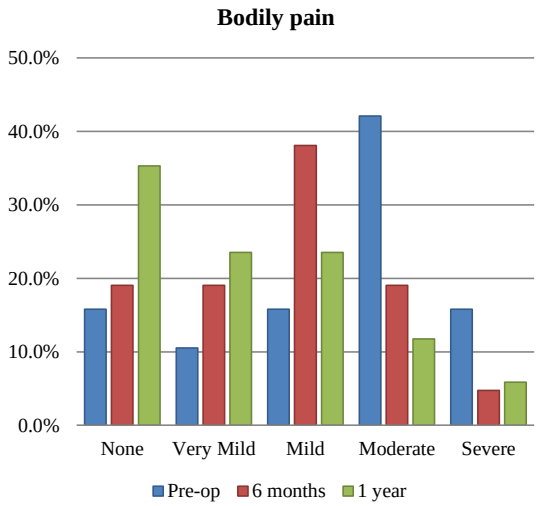
Bodily pain
50.0%
40.0%
30.0%
20.0%
10.0%
0.0%
None
Very Mild
Mild
Moderate
Severe
Pre-op
6 months
1 year

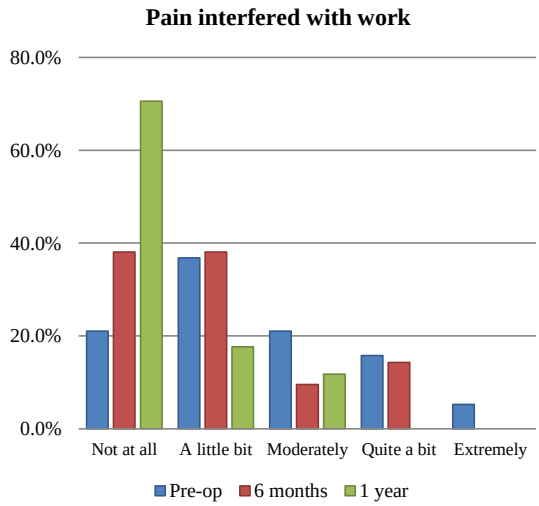
Pain interfered with work
80.0%
60.0%
40.0%
20.0%
0.0%
Not at all
A little bit
Moderately
Quite a bit
Extremely
Pre-op
6 months
1 year

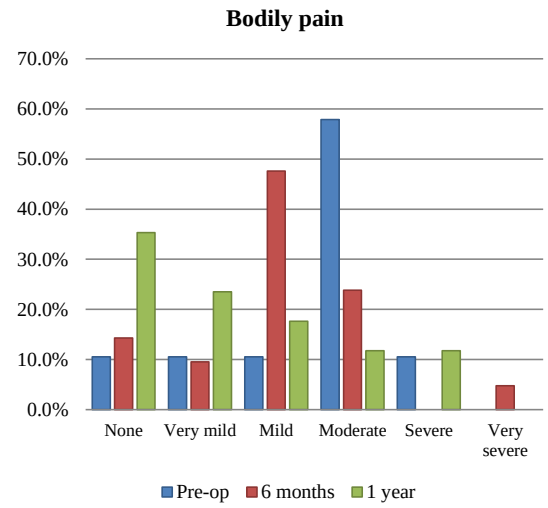
Bodily pain
70.0%
60.0%
50.0%
40.0%
30.0%
20.0%
10.0%
0.0%
None
Very mild
Mild
Moderate
Severe
Very severe
Pre-op
6 months
1 year

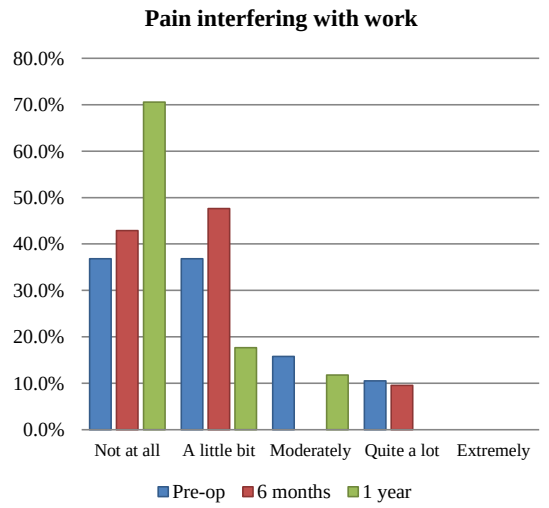
Pain interfering with work
80.0%
70.0%
60.0%
50.0%
40.0%
30.0%
20.0%
10.0%
0.0%
Not at all
A little bit
Moderately
Quite a lot
Extremely
Pre-op
6 months
1 year

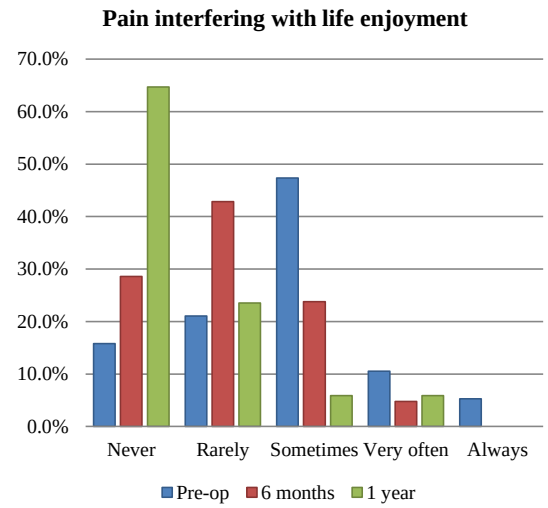
Pain interfering with life enjoyment
70.0%
60.0%
50.0%
40.0%
30.0%
20.0%
10.0%
0.0%
Never
Rarely
Sometimes
Very often
Always
Pre-op
6 months
1 year

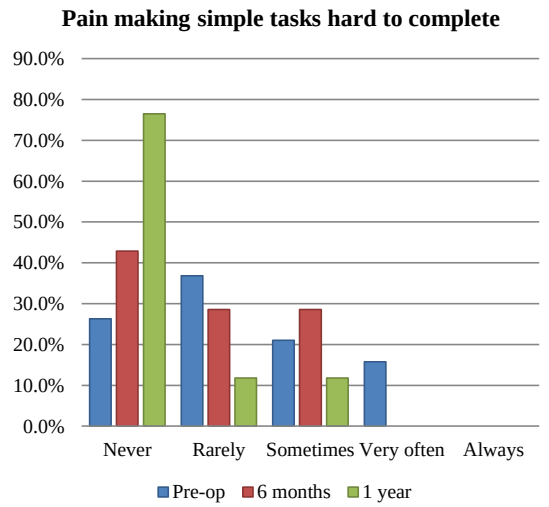
Pain making simple tasks hard to complete
90.0%
80.0%
70.0%
60.0%
50.0%
40.0%
30.0%
20.0%
10.0%
0.0%
Never
Rarely
Sometimes
Very often
Always
Pre-op
6 months
1 year

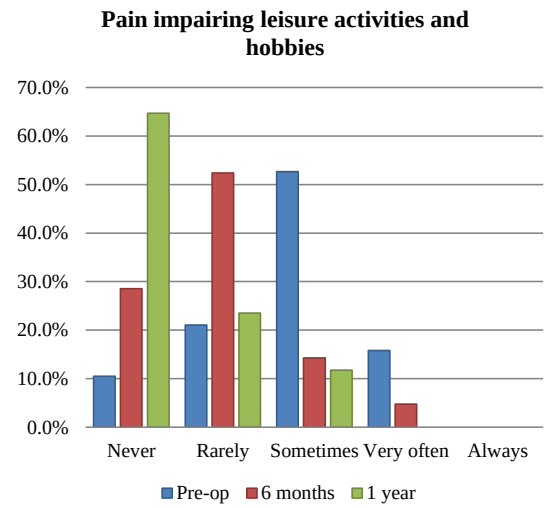
Pain impairing leisure activities and hobbies
70.0%
60.0%
50.0%
40.0%
30.0%
20.0%
10.0%
0.0%
Never
Rarely
Sometimes
Very often
Always
Pre-op
6 months
1 year

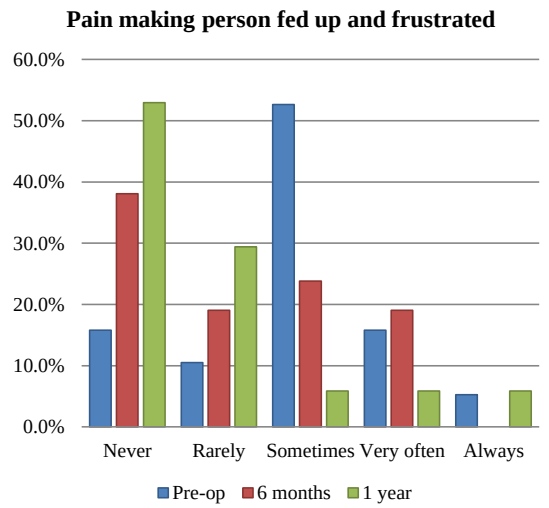
Pain making person fed up and frustrated
60.0%
50.0%
40.0%
30.0%
20.0%
10.0%
0.0%
Never
Rarely
Sometimes
Very often
Always
Pre-op
6 months
1 year

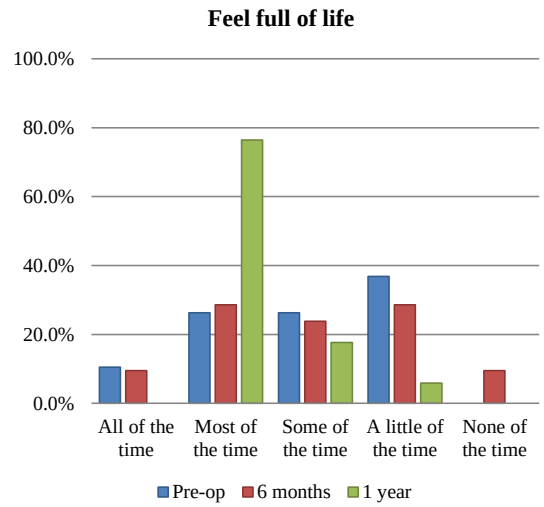
Feel full of life
100.0%
80.0%
60.0%
40.0%
20.0%
0.0%
All of the time
Most of the time
Some of the time
A little of the time
None of the time
Pre-op
6 months
1 year

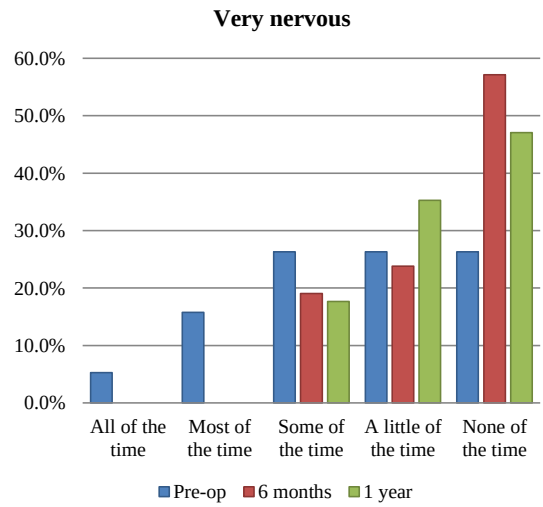
Very nervous
60.0%
50.0%
40.0%
30.0%
20.0%
10.0%
0.0%
All of the time
Most of the time
Some of the time
A little of the time
None of the time
Pre-op
6 months
1 year

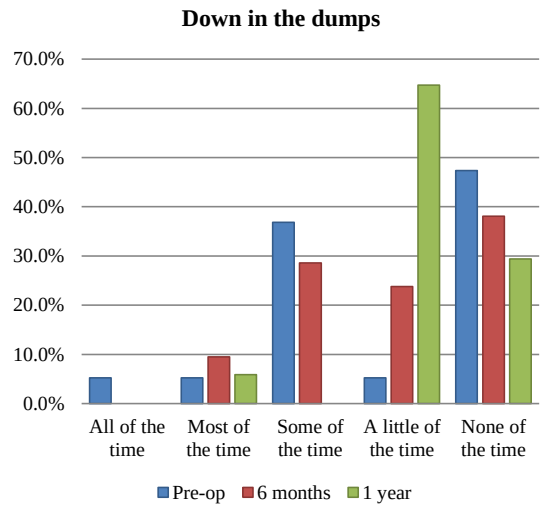
Down in the dumps
70.0%
60.0%
50.0%
40.0%
30.0%
20.0%
10.0%
0.0%
All of the time
Most of the time
Some of the time
A little of the time
None of the time
Pre-op
6 months
1 year

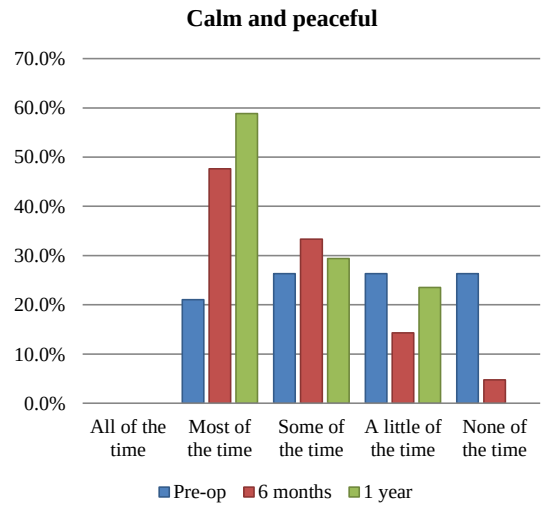
Calm and peaceful
70.0%
60.0%
50.0%
40.0%
30.0%
20.0%
10.0%
0.0%
All of the time
Most of the time
Some of the time
A little of the time
None of the time
Pre-op
6 months
1 year

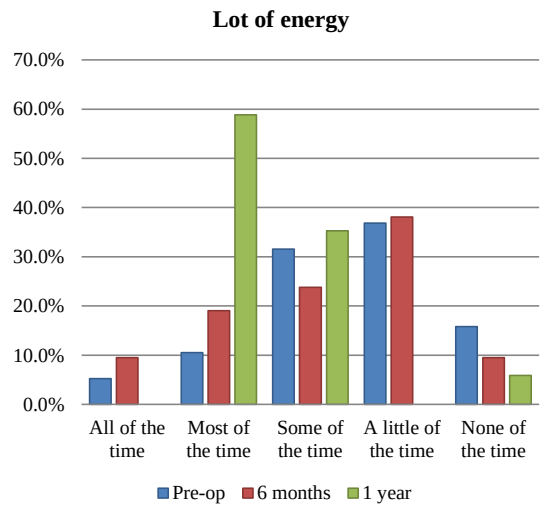
Lot of energy
70.0%
60.0%
50.0%
40.0%
30.0%
20.0%
10.0%
0.0%
All of the time
Most of the time
Some of the time
A little of the time
None of the time
Pre-op
6 months
1 year

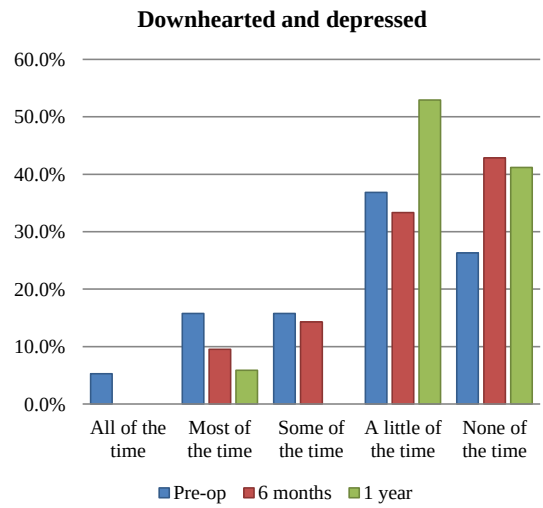
Downhearted and depressed
60.0%
50.0%
40.0%
30.0%
20.0%
10.0%
0.0%
All of the time
Most of the time
Some of the time
A little of the time
None of the time
Pre-op
6 months
1 year

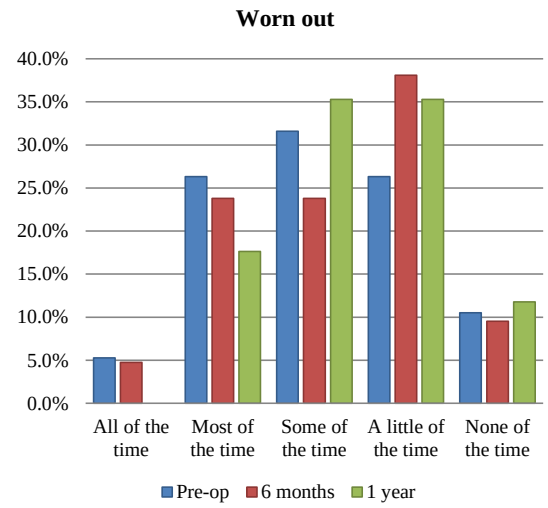
Worn out
40.0%
35.0%
30.0%
25.0%
20.0%
15.0%
10.0%
5.0%
0.0%
All of the time
Most of the time
Some of the time
A little of the time
None of the time
Pre-op
6 months
1 year

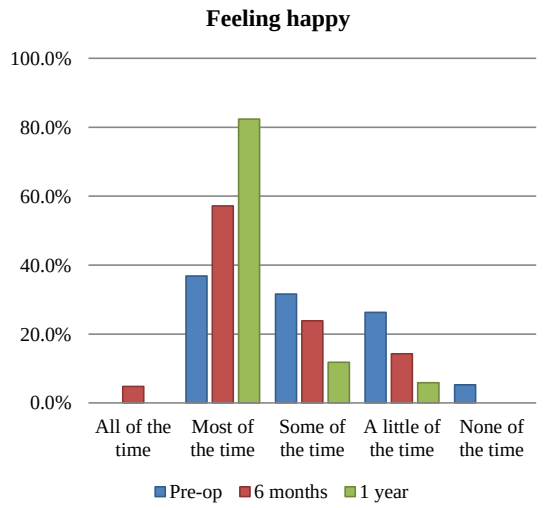
Feeling happy
100.0%
80.0%
60.0%
40.0%
20.0%
0.0%
All of the time
Most of the time
Some of the time
A little of the time
None of the time
Pre-op
6 months
1 year

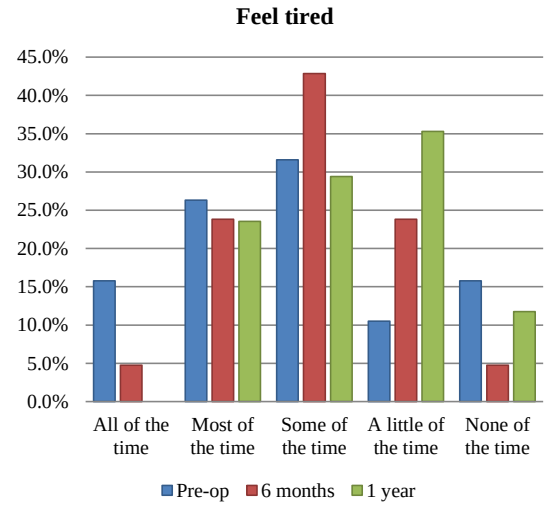
Feel tired
45.0%
40.0%
35.0%
30.0%
25.0%
20.0%
15.0%
10.0%
5.0%
0.0%
All of the time
Most of the time
Some of the time
A little of the time
None of the time
Pre-op
6 months
1 year

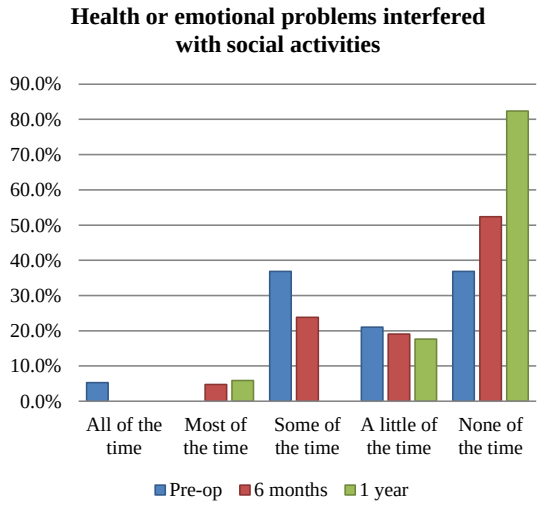
Health or emotional problems interfered with social activities
90.0%
80.0%
70.0%
60.0%
50.0%
40.0%
30.0%
20.0%
10.0%
0.0%
All of the time
Most of the time
Some of the time
A little of the time
None of the time
Pre-op
6 months
1 year

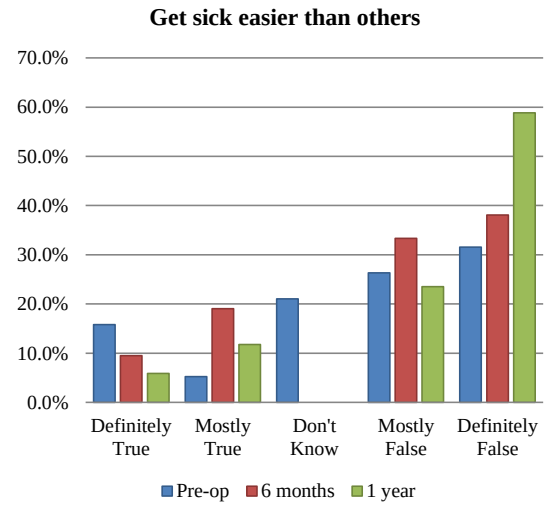
Get sick easier than others
70.0%
60.0%
50.0%
40.0%
30.0%
20.0%
10.0%
0.0%
Definitely True
Mostly True
Don't Know
Mostly False
Definitely False
Pre-op
6 months
1 year

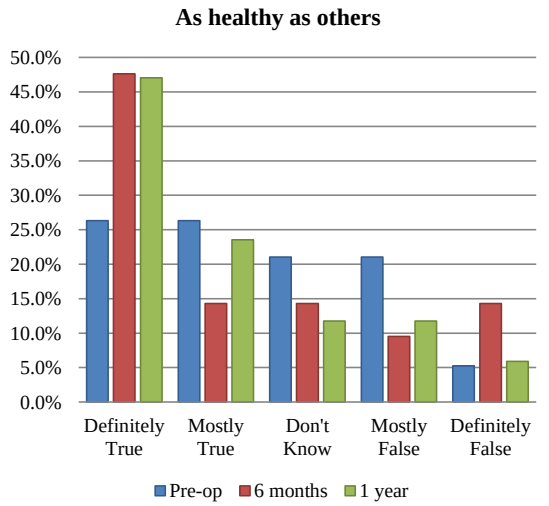
As healthy as others
50.0%
45.0%
40.0%
35.0%
30.0%
25.0%
20.0%
15.0%
10.0%
5.0%
0.0%
Definitely True
Mostly True
Don't Know
Mostly False
Definitely False
Pre-op
6 months
1 year

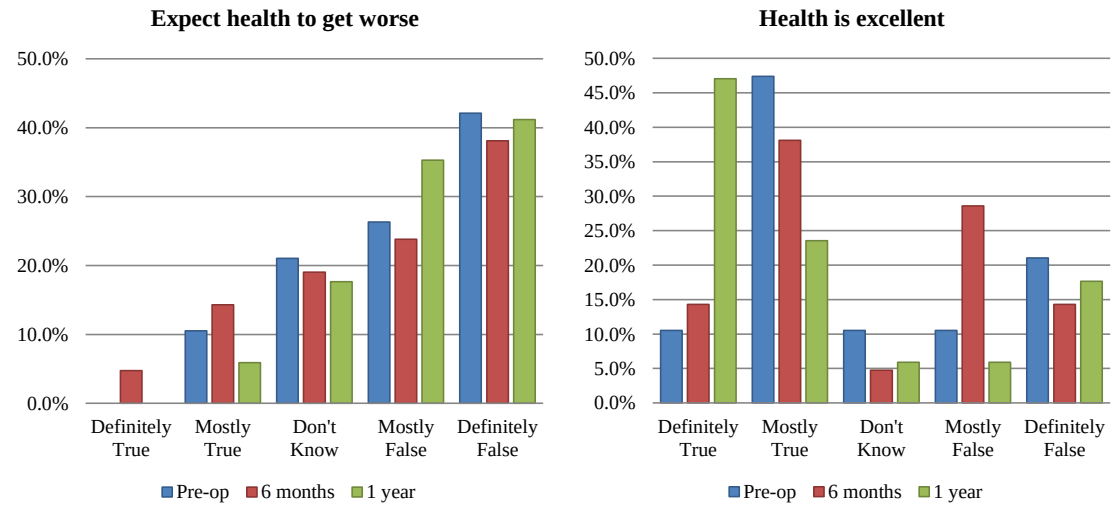

A comparative graphical representation of limitations due to the negative emotional impact experienced by endometriosis patients in the pre-operative period, six months post operatively and at one year post-operatively.

In the questionnaires I also assessed the activities which could be impacted by psychological rather than physical symptoms.

Patients were asked whether they had cut down on time from work (See section 1.13.2). In the pre-operative period, 58% of my patient group had never cut down on work due to symptoms of endometriosis. In the one year after their operation, this number rose to 77% (P= 0.54) potentially indicating a positive impact in patients pain or psyche after diagnosis and treatment (Figure 3-2).

Other studies confirm the deterioration in the work life productivity of patients with endometriosis, at an average of approximately 10 hours per week compared to 7 hours in non-affected women[4]. At one year post laparoscopy, 82% of patients reported that their health no longer restrained or limited their work achievements compared to 68% pre-operatively (P=0.77). The percentage of study patients who felt they required an increased level of effort to perform work tasks and who had difficulty performing their work tasks fell by 19% at one year post-operatively. 77% reported no work impediment in the one year post-operative time period compared to the 58% pre-operatively (P=0.576). (Figure 3-2)

Patients were also asked how they felt emotionally (Figure 3-2) and how this impacted their work. Of my pre-operative patient population 58%, reported no adverse impact on their work. This improved to 67% (P=0.266) within six months of surgery and 88% after a one year (P=0.296). Reduction of accomplishments due to emotional barriers was also assessed. At 6 months 71% (P=0.004) and at one year 94% (P=0.04) of my post-operative patient population felt no reduction in their work of life accomplishments due to disease. This contrasts with the 42% of the study population who had claimed they were not impacted by disease pre-operatively. This confirms an increase in patient accomplishment previously impeded due to the emotional impact of endometriosis on their lives.

Non-specific bodily pain levels interfering with work was assessed (Figure 3-2). Pre-operatively, 21% of my patient population had no issues with bodily pain affecting daily work. At six months post-operatively this increased to 38% (P=0.162) and further increased to 71% at the one year follow up (P=0.042).

In my study I also aimed to identify effects of endometriosis on the general emotional wellbeing of my patients. The reduction of emotional problems after treatment of disease is visible (Figure 3-2). In the one year post-operative follow up, 77% of women felt full of life and were not depressed, this contrasts with the 26% who reported not feeling depressed pre-operatively (P=0.028). Energy levels were elevated in 59% of my patients at the one year visit, this can be compared to the 11% reporting good energy levels pre-operatively (P=0.002).A feeling of nervousness fell from 74% pre-operatively to 53% (P=0.378) at the one year follow up and during the same time period, the percentage of patients reporting feelings of calmness increased from 21% pre-operatively to 47% within six months(P=0.05) and 59% at one year (P=0.03). Depression was seen in 37% of my pre-operative patient population, interestingly no patient (0%) reported feeling depressed at the one year follow up visit (P=0.004) (Figure 3-2).

An improvement in social activities was also seen after surgery (Figure 3-2). 65% reported no impact of pain or disease on their social interactions at the one year post-operative visit. Pre operatively, only 16% had felt that their social life was not being adversely affected by endometriosis (P=0.016). Patient's perception of being less healthy than other people they knew fell by 21%. Pre-operatively, only 26% believed they were as healthy as their acquaintances, this was seen to rise to 47% at the one year follow up (P=0.329). Overall, 11% expected their health to deteriorate before their operation, this value rose slightly to 14% (P=0.576) within six months of their procedure and then fell to 6% at their one year follow up (P=0.576).

FIGURE 3-3

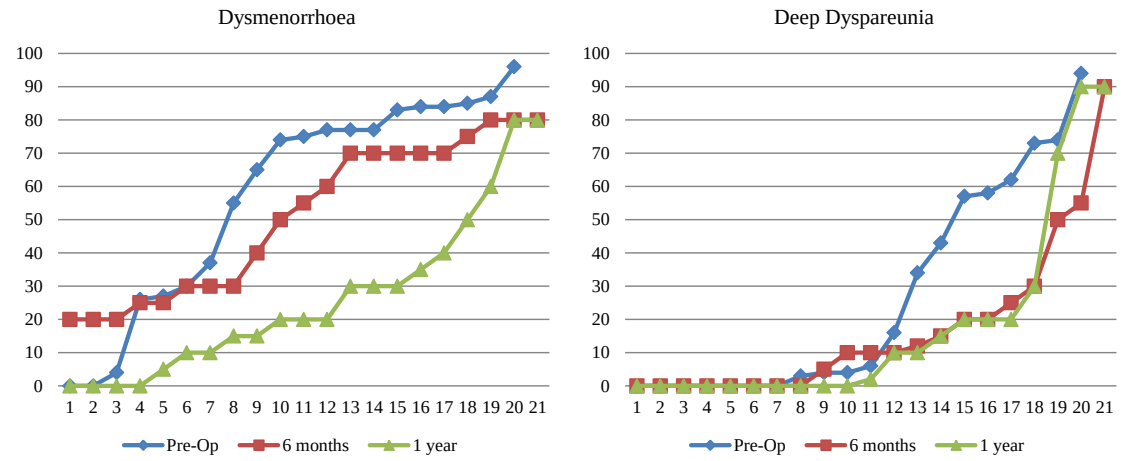

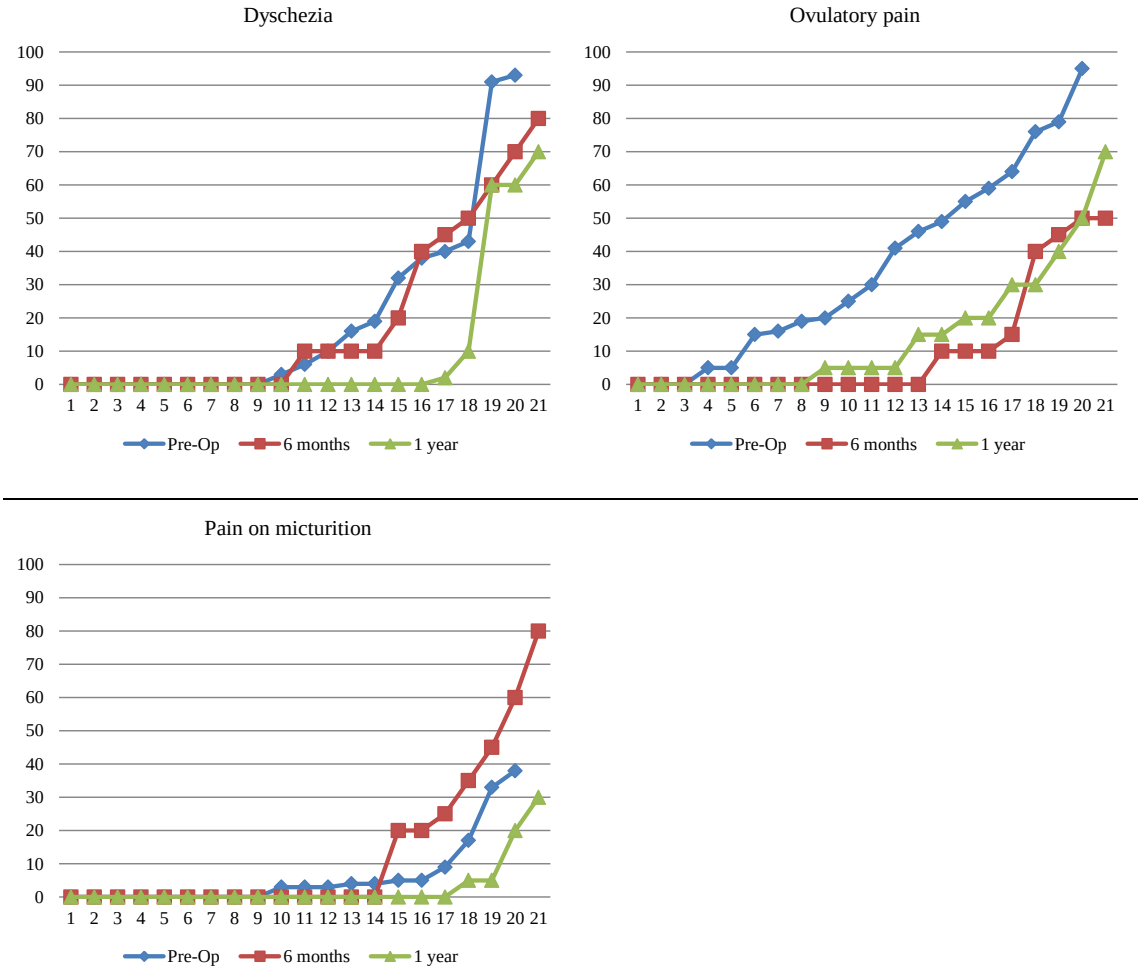

Respective graphical representation of patient subjective pain levels (y-axis pain levels 0-100%) for dysmenorrhoea, deep dyspareunia, dyschesia, ovulatory pain and pain on micturition pre-operatively, at 6 months and one year post operatively.

The perception of pain was also assessed (See section 1.12). I asked patients to rate their pain scores (0% indicating no pain and 100% indicating the highest levels of pain) for dysmenorrhoea, deep dyspareunia, dyschesia, ovulatory pain, chronic pelvic pain and pain on micturition (Figure 3-3). All of these symptoms have been attributed to endometriosis although there is no direct link between severity of disease and pain scores[11]. The patient's perception of pain varies according to the psychology of the individual[304] and therefore pain scores will be subjective rather than objective values. Looking at the graphical results (Figure 3-3) there is a notable decrease in overall experienced pain levels for dysmenorrhoea from the pre-operative time period (Average dysmenorrhoea pain score 59%) when compared to the 6 months (Average dysmenorrhoea pain score 51%) and one year post-operative levels of pain (Average dysmenorrhoea pain score 26%). Overall pain levels for deep dyspareunia also showed an improvement. Deep dyspareunia is not usually experienced by all patients with endometriosis. It is believed to be a result of deeply infiltrating disease in the Pouch of Douglas. Though deep dyspareunia is mostly believed to be due to pathology[268], psychosexual influences of each individual patient will also affect pain scores during intercourse. The average deep dyspareunia pain level pre-operatively stood at 30%, these fell to 17% at 6 months post operatively and 18% at one year post-operatively. Dyschesia is another symptom that is related to endometriosis. This is usually attributed to disease around the rectum

and Pouch of Douglas and changes in bowel habits are also known to be linked to presence of endometriosis[268]. Confounding factors such as irritable bowel syndrome or inflammatory bowel conditions might also deteriorate pre-menstrually so the values of pain are once again patient dependant and subjective. Pre-operatively, pain scores for dyschesia stood at 23%, these fell to 19% within six months of surgery and 10% at one year post-operatively. Pain on micturition was also assessed though this is a clinically rarer reported symptom of endometriosis. This is usually attributed to disease in the vicinity of the bladder on the anterior aspect of the Uterus or the uterovescal fold of peritoneum. Pre-operatively, pain scores were around 8%, they were seen to increase to 14% within 6 months of the operation and fell again to 3% at one year post-operatively (Figure 3-3). This interesting rise in the 6 month follow up could potentially be attributed to an early recovery period or increased pain awareness once a diagnosis of endometriosis has been imparted. Pain perceptions vary with patient psychology which is multifactorial[304]. This makes it difficult to attribute pain levels to the presence of physical disease.

Mid-cycle or ovulatory pain was also assessed in conjunction with chronic pelvic pain. Pain perception varies according to the patient in question and typically patients who complain of chronic pelvic pain will also report mid-cycle ovulatory discomfort[302]. Pain related with ovulation was reported at 38% pre-operatively, falling to 11% at six months and slightly rising to 15% at one year post-surgery. In a similar pattern, chronic pain was reported at 34% pre-operatively, fell to 8% within six months of surgery and there was an increase to 12% at one year (Figure 3-3).

Therapeutic laparoscopic surgery shows benefits in the symptoms and psyche of patients with endometriosis. Surgical risks must be balanced against the benefits which are obtained with symptom resolution. Due to the chronicity of the condition, long term follow up is required in endometriosis, with high recurrence rates reported[274]. A multidisciplinary team follow up will ensure both physical and psychological benefits are achieved in women being treated for this disease[492].

4 Analysis of tissue miRNAs in endometriosis

4.1 Introduction

Micro RNAs were discovered in 1993 and revolutionised the thinking behind the control of RNA expression. There are over 800 currently identified human miRNAs. These are now regarded to have major translational or repressive effects controlling cellular function, proliferation[403], death[404] and protein production[405]. They regulate around 30% of the human genes[406] and repress over 60% of the protein coding genes[407]. MiRNAs are also believed to be responsible for gene regulation[408] and interact with messenger RNA (mRNA) encoding proteins on the ribosomes enhancing their expression[409] (Figure 1-8). As a first step in this project, I aimed to systematically identify miRNAs expressed in patients with histologically proven diagnosis of endometriosis. Previously published data has been poor, being derived from small sample numbers and from patients whose disease phenotype had not necessarily been clearly defined to ensure other pathologies such as fibroids and malignancy had been excluded (Section 1.17.1). This could potentially be a cause of bias in the published results. I was meticulous to identify, document and operated on a set of patients with clearly diagnosed endometriosis without compounding additional pathologies. Following ethical approval and fully informed consent patients were recruited, their disease phenotype annotated, entered into the study were ensured to be free from other pathologies such as infections (e.g. pelvic inflammatory disease, evidence of Fitz Hugh Curtis adhesions on the liver or tubal hysdrosalpinges) and samples from a broad range of associated tissues stored and analysed. The patients were screened to ensure they did not suffer from endocrine disorders, autoimmune disorders, immunocompromisation or benign masses (such as cysts on the ovaries or tubes), uterine polyps or fibroids. Patients on any hormones or taking medication for other diseases were excluded from the study.

4.2 Aims

- To obtain a set of tissue samples at laparoscopy from patients who suffered from endometriosis with no other confounding pathology.
- To assess for differences in miRNA expression between tissue infiltrated with endometriosis and tissue not infiltrated with endometriosis.
- To confirm identified miRNA through a separate confirmatory technique such as quantitative PCR (Section 4.4.2).
- To identify and confirm predicted downstream protein effects of the relevant miRNA on a larger sample of tissues though tissue microarrays (TMAs) (Section 2.7).

4.3 Method

Patients identified were initially screened for eligibility and then offered recruitment into the study. Following fully informed consent, pain score questionnaires and quality of life questionnaires were

performed pre operatively and at 6 and 12 months post operatively (2.3). The tissue for the study was obtained from the consented patients at surgery (Section 2.3). A biopsy of tissue infiltrated with endometriosis and a biopsy from adjacent unaffected tissue not infiltrated by endometriosis were obtained from each recruited case (Section 2.3). MiRNA from the biopsied tissue samples was extracted according to the described protocol (Section 2.4). NCounter® expression assays were performed on the extracted miRNA (Section 2.4.3) and data was obtained. Statistical analysis on the data was performed (Section4.4.1) and subgroup analysis of the results was carried out (4.4.1.2). Results from the tissue subgroups were plotted in Venn diagram format to eliminate overlapping miRNA from the patient sample subsets (Section 4.4.1). Analysis of statistically significant ($P < 0.05$) differentially expressed miRNA and their fold change (FC) between individual groups was calculated (Section 4.4.1.3). Confirmation of the relevant identified miRNAs was carried out through quantitative PCR (Section 4.4.2). Tissue microarrays were performed to identify and confirm downstream effects of the identified relevant miRNAs (Section 4.4.3).

4.4 Results

4.4.1 Tissue miRNA expression in endometriosis-statistical analysis

In this chapter the processing and statistical analysis of the data obtained is described after miRNA extraction from tissue samples (Section 2.4).

4.4.1.1 Differential gene expression analysis

The R project (R version 2.12.1) (http://www.R-project.org) was used for statistical and clustering analysis. Quantified gene expression signal levels derived from the nCounter® miRNA Expression Assay (NanoString Technologies) were logarithmically transformed (base 2) and quantile-normalized prior to further exploration. In order to determine the miRNA expression detectability threshold the log2 signal values were ranked in increasing order and categorised into 0.5 expression levels. Subsequently, the differences in successive expression level frequencies were calculated and the expression value following the most significant signal increase was considered as miRNA expression detectability threshold (Figure 4-1). miRNAs expressed was counted at any level (above log2 expression value of 3.25) in each group and subsequently performed chi-square test to assess if the numbers are significantly different from the expected average. The global expression of miRNAs between all groups was not noted to be significantly different (chi square p-value 0.82664147).

FIGURE 4-1

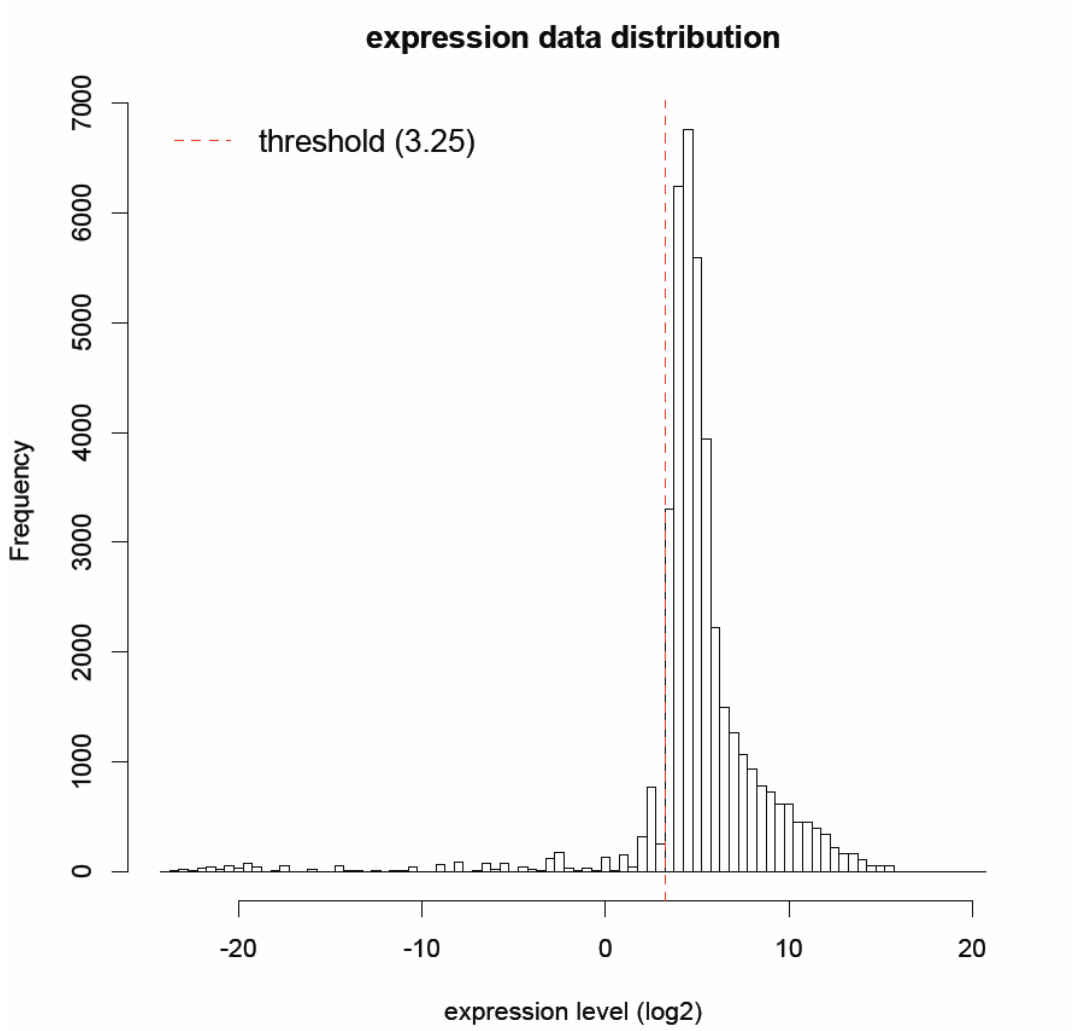

Diagram showing the expression data distribution with selected threshold level of miRNA detectability (dotted red line)

Analysis of variance (ANOVA) was performed per each gene across all samples assigned to appropriate groups in order to identify differentially expressed miRNAs. The Benjamini & Hochberg multiple hypothesis testing correction was applied to control the false discovery rate (FDR). Genes that remained statistically significant (corrected p-value <0.05) were selected for unsupervised hierarchical clustering performed based on distances calculated by means of Spearman correlation coefficient and ward agglomeration method (Figure 4-2, Figure 4-3, Figure 4-4).

FIGURE 4-2

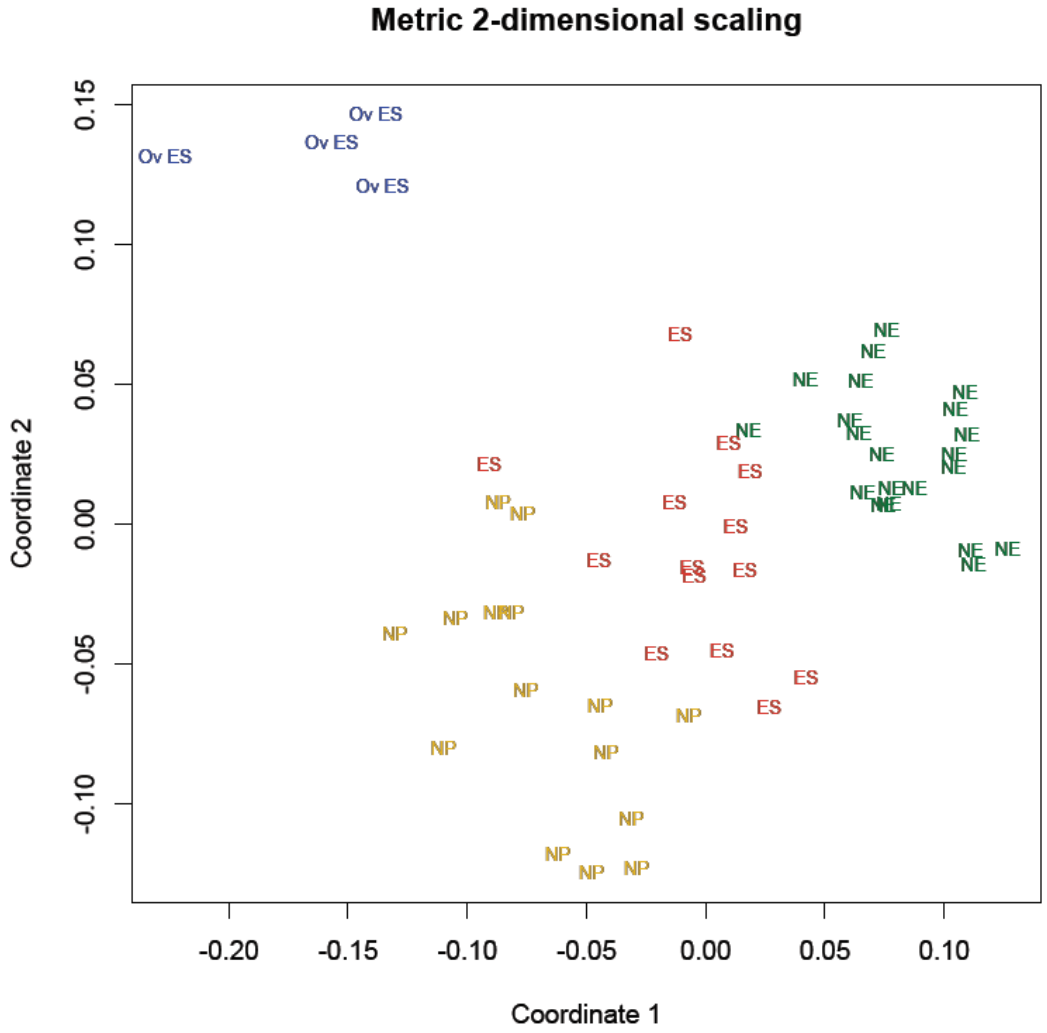
Metric 2-dimensional scaling
Coordinate 2
Coordinate 1
0.15
0.10
0.05
0.00
-0.05
-0.10
-0.20
-0.15
-0.10
-0.05
0.00
0.05
0.10
Ov ES
Ov ES
Ov ES
ES
NE
NE
NE

FIGURE 4-3

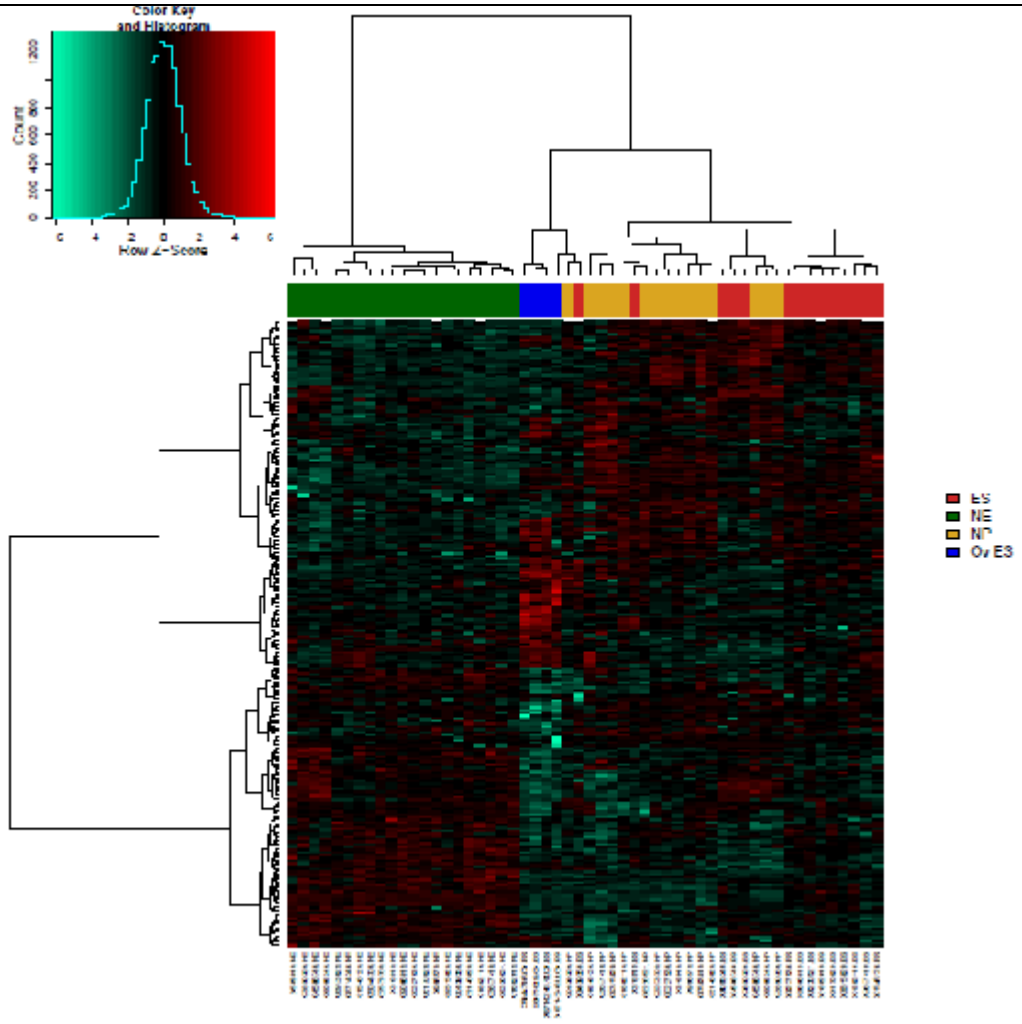

Heat map illustrating unsupervised hierarchical clustering of studies samples. The distances between sample miRNA expression profiles were measured by means of Spearman correlation coefficient technique and clustered using Ward agglomeration method. The colours generated and their intensities reflect miRNAs expression levels. Green and red colours indicate relatively low and high expression levels, respectively.

FIGURE 4-4

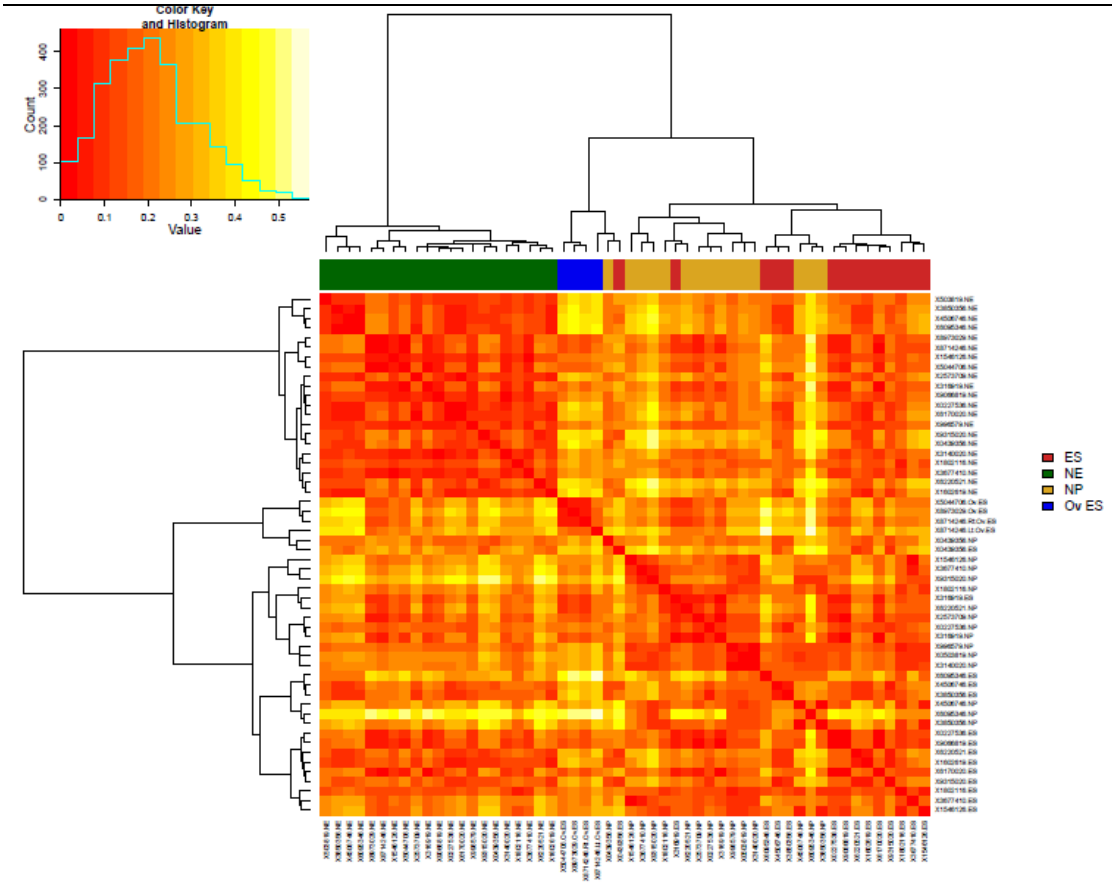

Heat map illustrating similarities and dissimilarities between investigated samples. The distances between sample miRNA expression profiles were measured by means of Spearman correlation coefficient technique and clustered using Ward agglomeration method. The colours generated and their intensities reflect miRNA expression profiles similarities. The red and yellow colours indicate relatively high and low similarity level, respectively.

Subsequently, pairwise t-tests with corrections for multiple testing were applied as a post hoc analysis. Computed t-statistics and signal intensity fold changes were further used to determine significantly up and down regulated miRNAs and to generate Venn diagrams depicting the overlap between miRNAs differentially expressed in investigated groups (Figure 4-5, Figure 4-6, Figure 4-7).

FIGURE 4-5

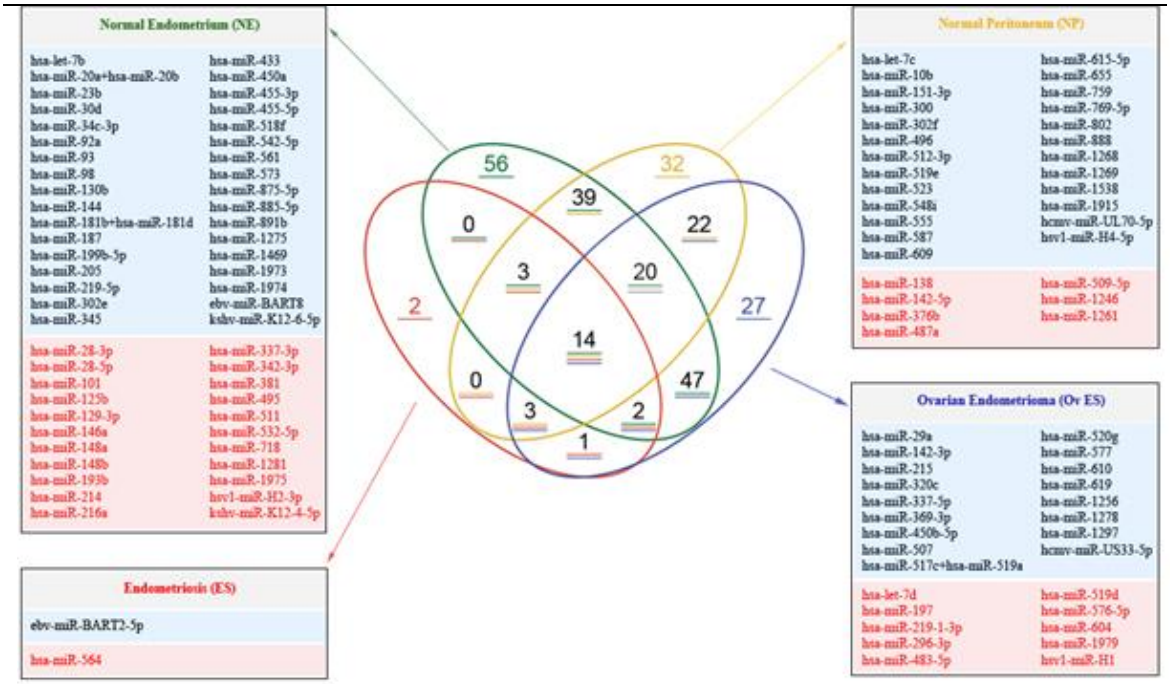

This Venn diagram depicts the miRNA which are statistically significantly differentially expressed (P<0.05) in each of the respective specified subgroups (NE, NP, ES and OvES). Those miRNAs that were statistically significant in any other of the subgroups were indicated in overlapping areas corresponding to appropriate groups (e.g. 39 miRNA expressed in both NE and ES). Those miRNAs upregulated are depicted in black text whilst those miRNA which are downregulated are depicted in red text. miRNAs not significantly differentially expressed in any group were excluded from this Venn Diagram. There were 466 miRNA out of the 734 scanned miRNA for which the P value was not statistically significant.

From the above Venn diagram ebv-miR- BART2-5p and hsa-miR-564 are shown to be the most significantly different in the endometriosis samples compared to all other subsets analysed (Table 9-33). Ebv-miR- BART2-5p is particularly interesting as it has downstream effects on the control of the following proteins; (upregulating Cyclin D1) (Figure 4-22) and (downregulating E-Cadherin, Maspin and BCLAF-1) (Figure 4-11, Figure 4-13 and Figure 4-15). All of these proteins are associated with tumorigenesis seen in head and neck cancer, which is known to be caused by EBV[493].

Ovarian endometriosis samples show miRNAs significantly up or downregulated in this subset when compared to all other subsets analysed (Table 9-34). All the identified miRNAs in the depicted subsets have been listed in Table 9-35 to Table 9-38.

FIGURE 4-6

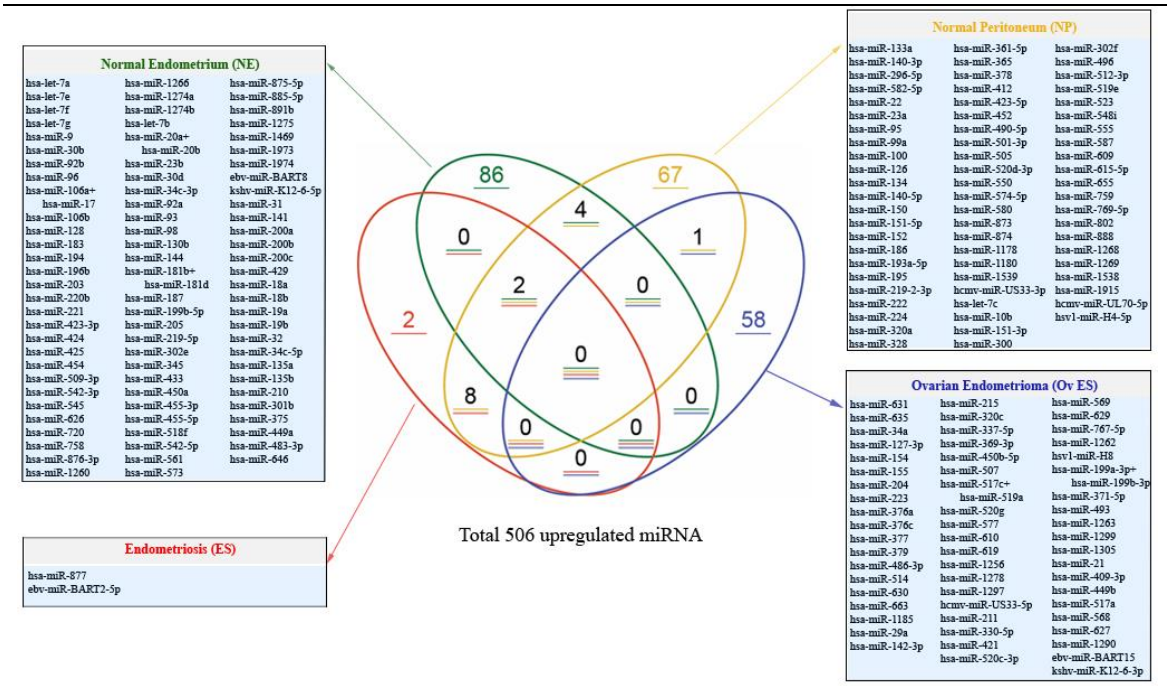

This Venn diagram depicts the miRNA which are statistically significantly differentially upregulated (P<0.05) in each of the respective specified subgroup (NE, NP, ES and OvES) with a positive log fold change. This diagram depicts the miRNA described above irrespective of whether they are concomitantly downregulated in any other group. There were 506 miRNA out of the 734 scanned miRNA for which there was no significant positive log fold change or the fold change was negative.

FIGURE 4-7

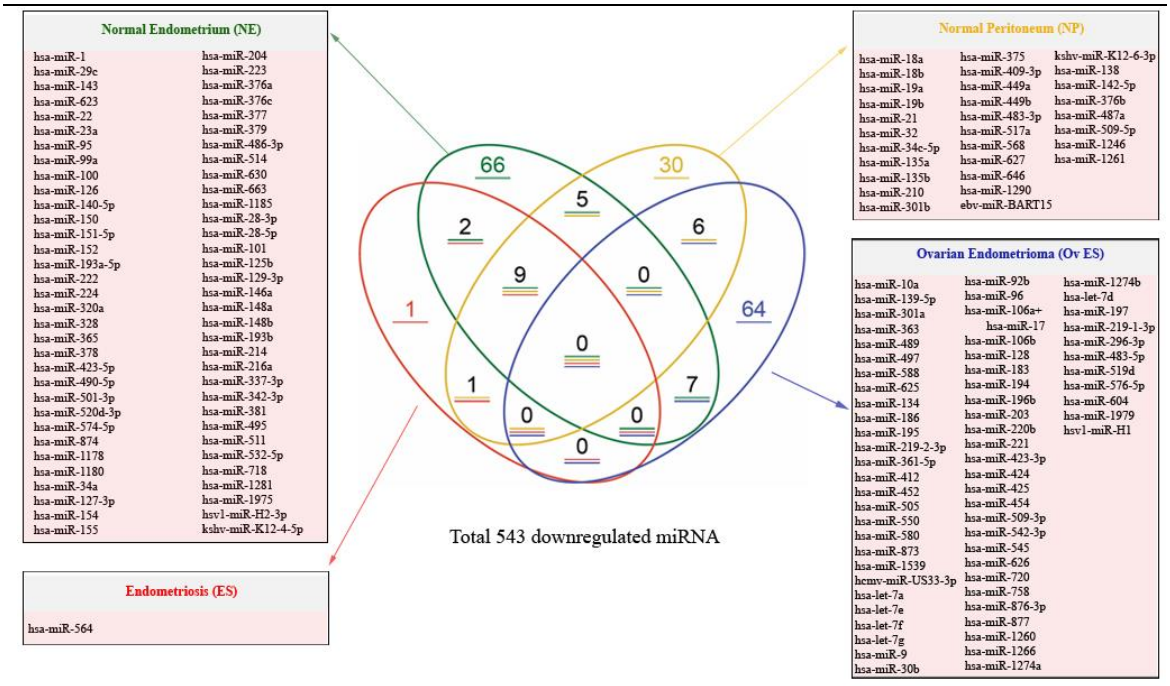

This Venn diagram depicts the miRNA which are statistically significantly differentially downregulated (P<0.05) in each of the respective specified subgroup (NE, NP, ES and OvES) with a negative log fold change. This diagram depicts the miRNA described above irrespective of whether they are concomitantly upregulated in any other group. There were 543 miRNA out of the 734 scanned miRNA for which there was no significant negative log fold change or the fold change was positive.

4.4.1.2 Subgroup analysis

Further subdivision of data analysis was performed on the cases, looking at values obtained in the luteal phase and follicular (proliferative) phase separately. Application of pairwise t-tests between specified groups to identify any significant difference between group means was performed.

4.4.1.2.1 NE from cases and ES cases- follicular phase of the cycle

29 miRNA were significantly differentially expressed between (NE cases) and (ES cases) in the follicular phase of the cycle. Please see Table 9-1 and Table 9-2 in the Appendix.

4.4.1.2.2 NE from controls and NE cases

There were no (0) miRNA significantly differentially expressed between (NE control) and (NE case) in the follicular phase of the cycle.

4.4.1.2.3 NE from cases and ES cases- luteal phase of the cycle

60 miRNA were significantly differentially expressed between (NE cases) and (ES cases) in the luteal phase of the cycle. 30 miRNA were upregulated whist 30 were downregulated. Please see Table 9-3 and Table 9-4 in the Appendix.

4.4.1.2.4 NE from cases and OvES cases- follicular phase of cycle

130 miRNA were significantly differentially expressed between (NE cases) and (OvES cases) in the follicular phase of the cycle. 53 miRNA were upregulated in the ovarian endometriosis samples (OvES). 77 miRNA were downregulated. Please see Table 9-5 and Table 9-6 in the Appendix.

4.4.1.2.5 NE from cases and OvES cases- luteal phase of cycle

54 miRNA were significantly differentially expressed between (NE cases) and (OvES cases) in the luteal phase of the cycle. 28miRNAs were upregulated in ovarian endometriosis in the luteal phase of the cycle. 26 miRNA were downregulated. Please see Table 9-7 and Table 9-8 in the Appendix.

4.4.1.2.6 Normal peritoneum from controls (NP control) and normal peritoneum cases (NP cases)

2 miRNA were significantly differentially expressed between (NP control) and (NP cases) in the follicular phase of the cycle. One was upregulated and the other downregulated. Please see Table 9-9 and Table 9-10 in the Appendix.

4.4.1.3 Analysis of statistically significant (P <0.05) differentially expressed miRNA and their fold change (FC) between individual groups

These values were obtained by performing a T-test between the particular group analysed and all the other groups. The P value for each miRNA is demonstrated as well as its fold change (FC). A negative Log FC indicates a downregulation of the particular miRNA compared to all other groups.

4.4.1.3.1 Normal endometrium

The following miRNA were significantly expressed in normal endometrium (NE) compared to endometriosis (ES), normal peritoneum (NP) and ovarian endometriosis (OvES). A positive log fold change indicates upregulation whereas a negative fold change indicates downregulation. Please see Table 9-11 in the Appendix.

4.4.1.3.2 Normal Peritoneum

The following miRNA were significantly expressed in normal peritoneum (NP) compared to endometriosis (ES), normal endometrium (NE) and ovarian endometriosis (OvES). Please see Table 9-12 in the Appendix.

4.4.1.3.3 Peritoneal endometriosis

The following miRNA were significantly expressed in endometriosis (ES) compared to normal endometrium (NE), normal peritoneum (NP) and ovarian endometriosis (OvES). Please see Table 9-13 in the Appendix.

4.4.1.3.4 Ovarian endometriosis

The following miRNA were significantly expressed in ovarian endometriosis (OvES) compared to normal endometrium (NE), normal peritoneum (NP) and endometriosis (ES). Please see Table 9-14 in the Appendix.

4.4.2 Polymerase chain reaction (PCR) results- confirmation of miRNA findings

PCR was performed to validate the ebv-miR-BART2-5p miRNA results. Three miRNA were quantified using qRT_PCR analysis. In concordance with the miRNA data, the pCR showed significant differential expression of the ebv-miR-BART2-5p miRNA between eutopic endometrium from controls, eutopic endometrium from women with endometriosis and endometriosis samples. Statistically, when comparing ebv-miR-BART2-5p levels between normal endometrium from controls and endometriosis, the p-value is significant (P=0.0067). The p-value is also significant when comparing normal endometrium from cases and endometriosis (P=0.02) (Figure 4-8, Figure 4-9). However, there was no statistical significance between normal endometrial samples from cases and normal endometrial samples from controls.

4.4.2.1 PCR EBV results

Sample with ebv-miR-BART2-5p primer	Ct	Sample with 26B Primer	Average	Delta CT	NE Control Calibration	Delta Delta CT	Fold change	Endometriosis	Normal endometrium Controls	Normal endometrium Cases
51 ES BART	44.77	51 ES 26B	26.13	18.64	13.04	5.60	0.02	0.02		
54 ES BART	40.49	54 ES 26B	26.87	13.62		0.58	0.67	0.67		
57 ES BART	40.94	57 ES 26B	24.58	16.36		3.32	0.10	0.10		
31 ES BART	40.74	31 ES 26B	25.79	14.95		1.91	0.27	0.27		
3 NE Control BART	44.18	3 NE Control 26B	27.38	16.80		3.76	0.07		0.07	
8 NE Control BART	44.63	8 NE Control 26B	26.17	18.46		5.42	0.02		0.02	
10 NE Case BART	41.38	10 NE Case 26B	26.44	14.94		1.90	0.27			0.27
12 NE Case BART	41.72	12 NE Case 26B	26.39	15.33		2.29	0.20			0.20
27 NE Case BART	41.70	27 NE Case 26B	25.06	16.64		3.60	0.08			0.08
30 NE Case BART	42.30	30 NE Case 26B	26.74	15.56		2.52	0.17			0.17
32 NE Case BART	42.75	32 NE Case 26B	26.06	16.69		3.65	0.08			0.08
35 NE Case BART	46.84	35 NE Case 26B	26.93	19.90		6.86	0.01			0.01
38 NE Case BART	45.74	38 NE Case 26B	25.87	19.87		6.83	0.01			0.01
42 NE Case BART	46.73	42 NE Case 26B	26.86	19.87		6.83	0.01			0.01
44 NE Case BART	42.42	44 NE Case 26B	26.02	16.41		3.37	0.10			0.10
46 NE Case BART	43.37	46 NE Case 26B	25.73	17.65		4.61	0.04			0.04
49 NE Case BART	40.43	49 NE Case 26B	26.68	13.75		0.71	0.61			0.61
53 NE Case BART	40.51	53 NE Case 26B	28.00	12.51		-0.53	1.44			1.44
11 ES BART	39.43	11 ES 26B	25.07	14.36		1.32	0.40	0.40		
17 ES BART	41.67	17 ES 26B	24.32	17.35		4.31	0.05	0.05		
14 ES	37.01	14 ES	28.66	8.35		-4.69	25.80	25.80		
29 ES	43.75	29 ES	27.15	16.60		3.56	0.08	0.08		
34 ES	40.58	34 ES	27.62	12.96		-0.08	1.06	1.06		
36 ES	37.58	36 ES	27.48	10.10		-2.94	7.65	7.65		
40 ES	37.54	40 ES	25.53	12.01		-1.03	2.04	2.04		
43 ES	39.96	43 ES	27.79	12.17		-0.87	1.83	1.83		
45 ES	36.52	45 ES	27.36	9.16		-3.88	14.68	14.68		

48 ES	38.72	48 ES	28.55	10.17	-2.87	7.30	7.30			
51 ES BART	41.23	51 ES miR44	27.69	13.54	0.50	0.71	0.71			
54 ES BART	41.63	54 ES miR44	27.70	13.93	0.89	0.54	0.54			
57 ES BART	37.94	57 ES miR44	25.60	12.34	-0.70	1.63	1.63			
31 ES BART	37.33	31 ES miR44	26.57	10.76	-2.28	4.87	4.87			
5 NE Control	42.56	5 NE Control	26.39	16.17	3.13	0.11		0.11		
25 NE Control	43.16	25 NE Control	27.09	16.06	3.02	0.12		0.12		
16 NE Case	43.00	16 NE Case	26.84	16.16	3.12	0.12			0.12	
14 ES BART	38.48	14 ES 26B	27.63	10.85	-2.19	4.56	4.56			
29 ES BART	36.39	29 ES 26B	25.66	10.72	-2.32	4.98	4.98			
34 ES BART	36.33	34 ES 26B	26.90	9.43	-3.61	12.20	12.20			
5 NE Control BART	38.77	5 NE Control 26B	25.73	13.04		1.00		1.00		
16 NE Case BART	35.90	16 NE Case 26B	25.63	10.26	-2.78	6.84			6.84	
25 NE Control BART	40.72	25 NE Control 26B	26.74	13.99	0.95	0.52		0.52		
36 ES BART	41.86	36 ES 26B	25.41	16.45	3.41	0.09	0.09			
40 ES BART	40.83	40 ES 26B	24.94	15.89	2.85	0.14	0.14			
43 ES BART	38.24	43 ES 26B	25.71	12.53	-0.51	1.42	1.42			
45 ES BART	37.07	45 ES 26B	25.47	11.60	-1.44	2.72	2.72			
48 ES BART	38.75	48 ES 26B	26.50	12.24	-0.80	1.74	1.74			
Average							**3.75**	**0.31**	**0.71**	

T-test	**0.01**	**NE Control and ES**
T-test	**0.02**	**NE Case and ES**
T-test	**0.44**	**NE Case and NE Control**

FIGURE 4-8

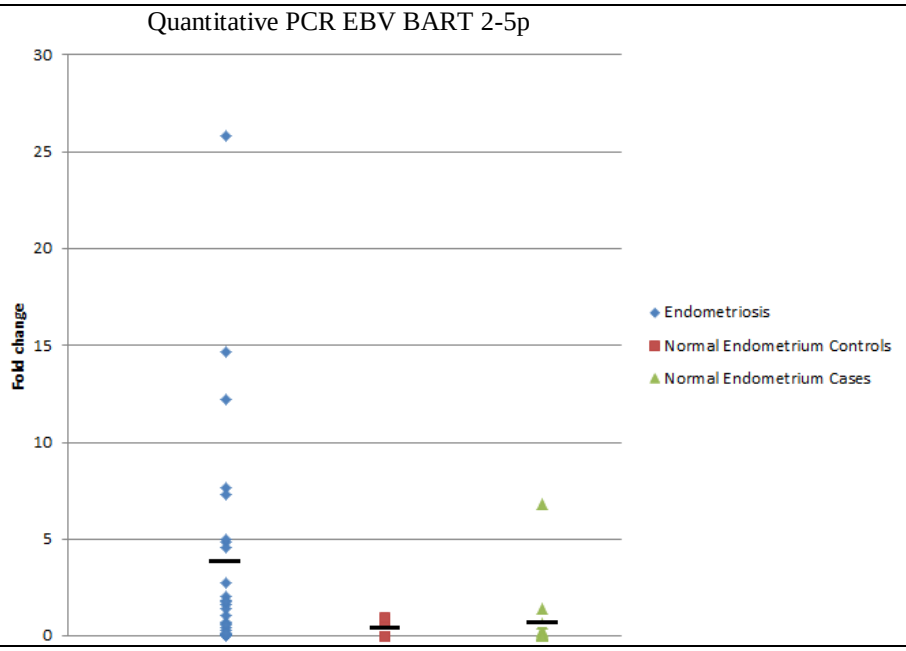

Quantitative PCR results with outliers included

FIGURE 4-9

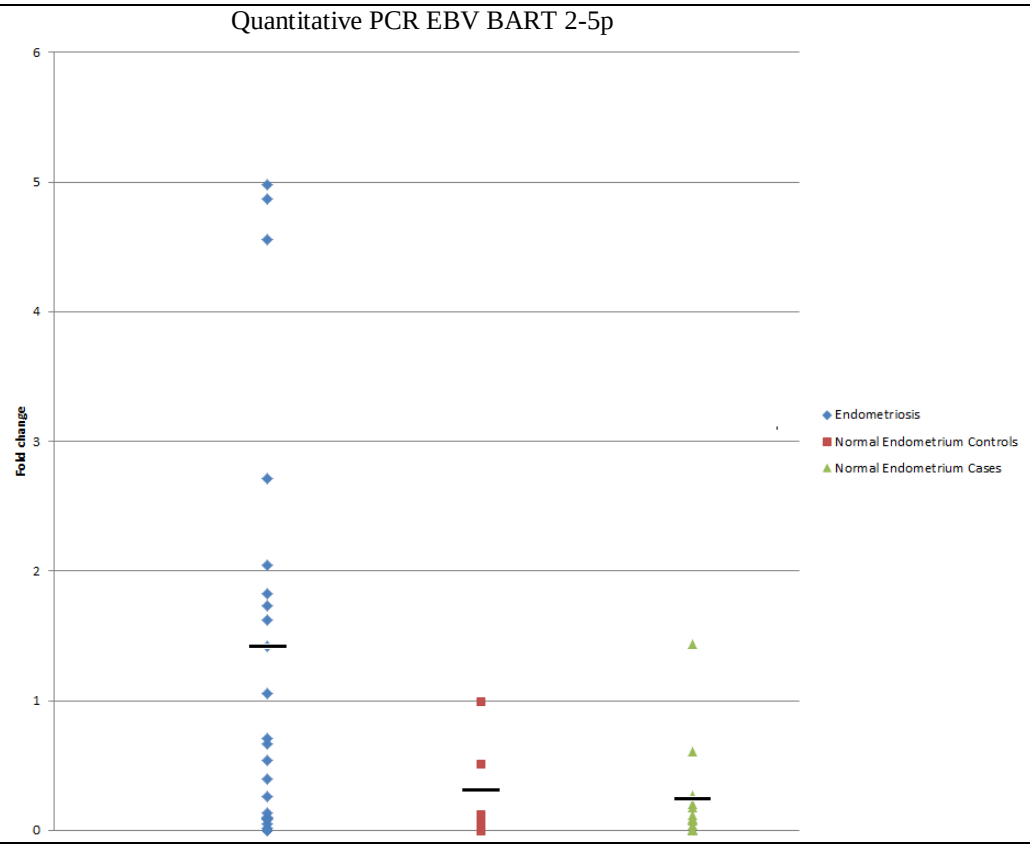

Quantitative PCR results with outliers excluded

4.4.3 Tissue microarray results- downstream effects of EBV presence

Immunohistochemistry was performed on tissue microarrays from endometriosis tissues as described in section 2.7. The downstream effects of EBV on expected protein expression were explored by quantifying expression levels of E-Cadherin, Maspin, BCLAF-1, p53 and cyclin D1 (predicted downstream protein expression patterns under BART 2-5p miRNA control) from the endometriosis tissue microarrays (Figure 4-10). Galectin-3 expression levels already proven to be upregulated in endometriosis were performed with the aim of potentially using Galectin 3 inhibitors as a novel therapeutic for the disease. In-situ hybridisation for the EBV virus within cells was performed with the aim of finding evidence of in vivo viral involvement in endometriosis. Data was analysed by non-parametric statistical analysis performed on each of the subgroups (endometriosis (circles on graphs), normal endometrium from controls (squares on graphs) and normal endometrium from cases (triangles on graphs)) using a Mann-Whitney U Test. A p-value of <0.05 between the groups was regarded as statistically significant. The resulting data was then plotted graphically below (Figure 4-12, Figure 4-14, Figure 4-16 and Figure 4-18).

FIGURE 4-10

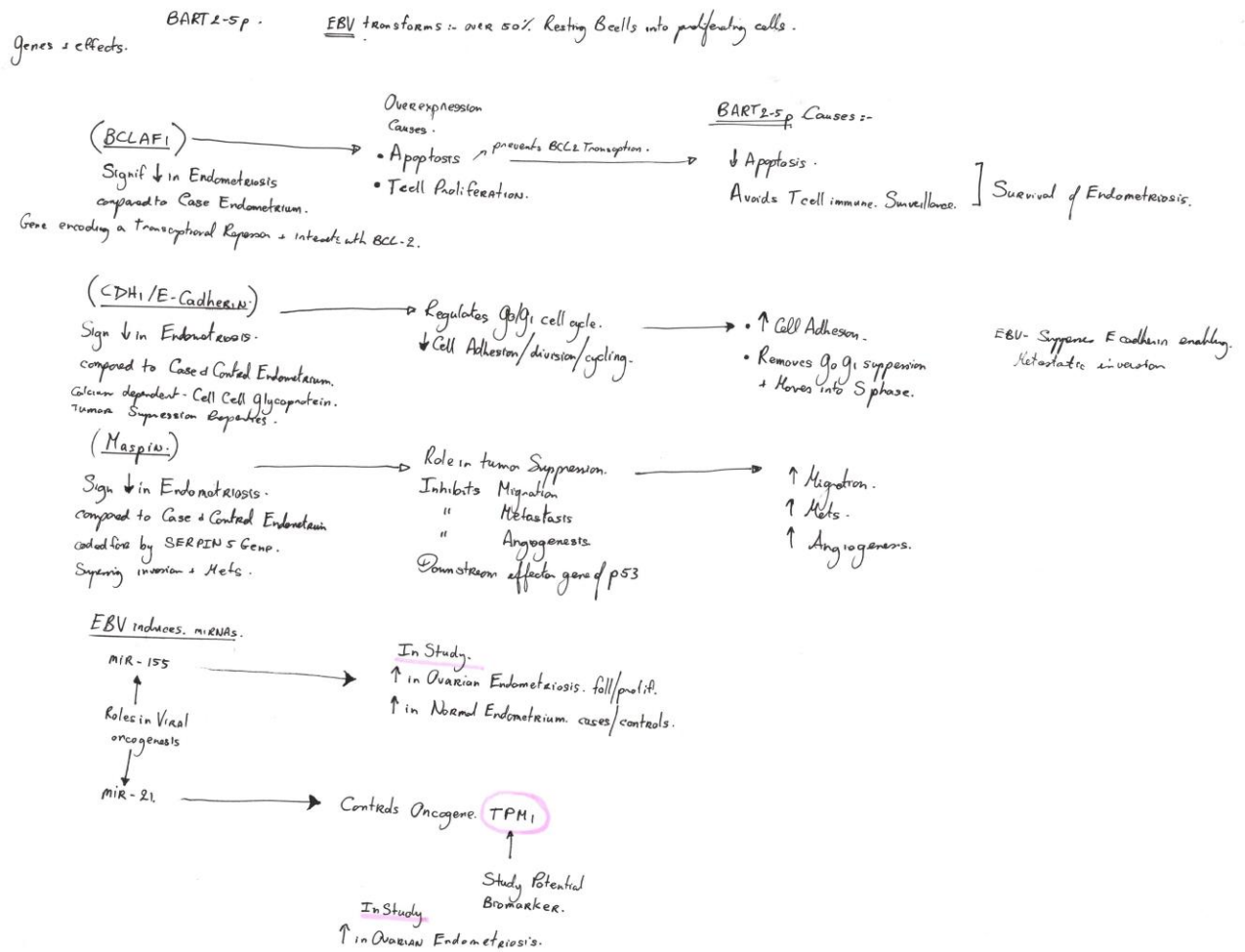

Hand drawn diagram showing the downstream effects of EBV virus on BCLAF1, E-Cadherin and Maspin

4.4.3.1 E-Cadherin

Downregulation of E-Cadherin is demonstrated in endometriosis on tissue microarray (TMA) analysis (Figure 4-11). There is a statistically significant downregulation of E-Cadherin in endometriosis compared to normal endometrium from controls (P<0.0001) and normal endometrium from cases (P=0.0017) (Figure 4-12, Table 4-1, Table 4-2).

FIGURE 4-11

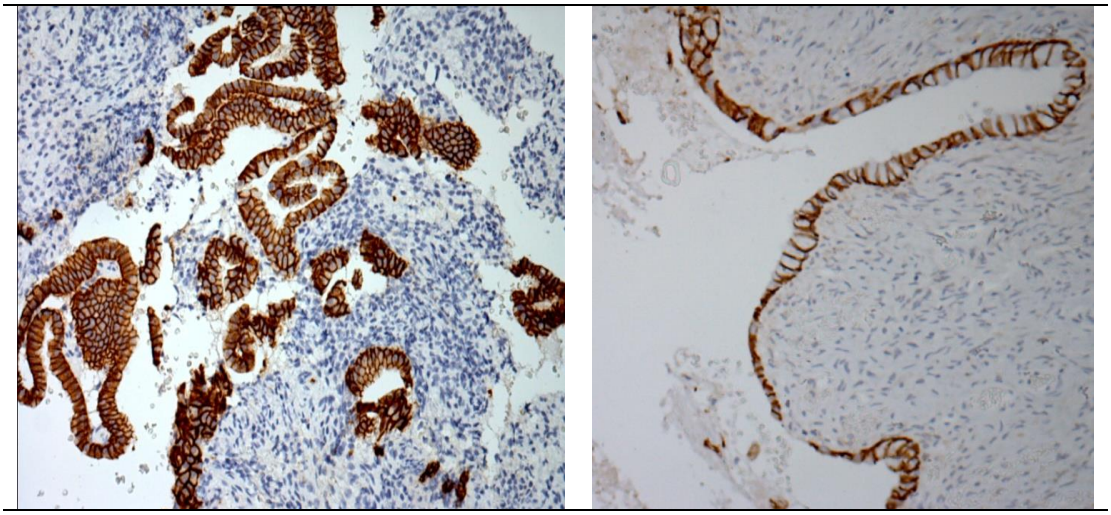

Images showing reduced E-Cadherin levels in endometriosis compared to normal endometrium tissue

FIGURE 4-12

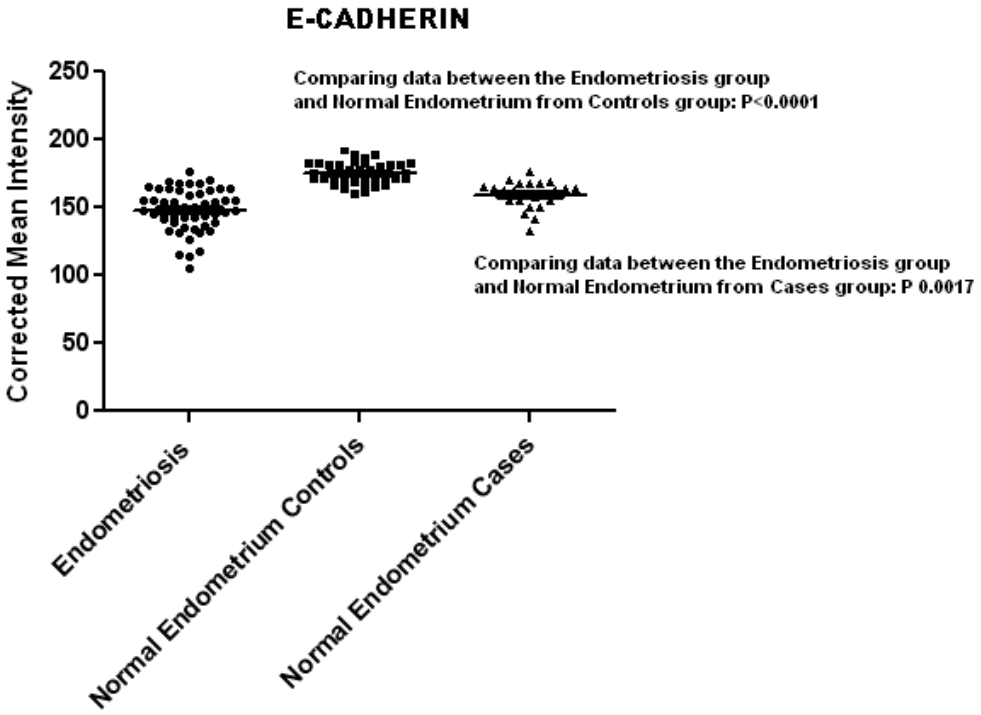

Figure illustrating the levels of E-Cadherin in TMA studies

TABLE 4-1

Table Analyzed	E-Cadherin
Column A vs Column C	**Endometriosis vs Normal endometrium from Cases**
Mann Whitney test	
P value	0.0017
Exact or approximate P value?	Gaussian Approximation
P value summary	**
Are medians signif. different? (P<0.05)	Yes
One- or two-tailed P value?	Two-tailed
Sum of ranks in column A,C	1720, 1206
Mann-Whitney U	342

TABLE 4-2

Table Analyzed	E-Cadherin
Column A vs Column B	**Endometriosis vs Normal endometrium Controls**
Mann Whitney test	
P value	< 0.0001
Exact or approximate P value?	Gaussian Approximation
P value summary	***
Are medians signif. different? (P<0.05)	Yes
One- or two-tailed P value?	Two-tailed
Sum of ranks in column A,B	1461, 3293
Mann-Whitney U	82.5

4.4.3.2 Maspin

Reduction of MASPIN is confirmed on TMA analysis (Figure 4-13). Comparing levels between endometriotic tissue and normal endometrium, there is a statistically significant downregulation of MASPIN in endometriosis compared to normal endometrium from controls (P<0.0001) and normal endometrium from cases (P=0.2760) (Figure 4-14, Table 4-3, Table 4-4).

FIGURE 4-13

Normal endometrium	Endometriosis infiltrating bowel and peritoneum (below)

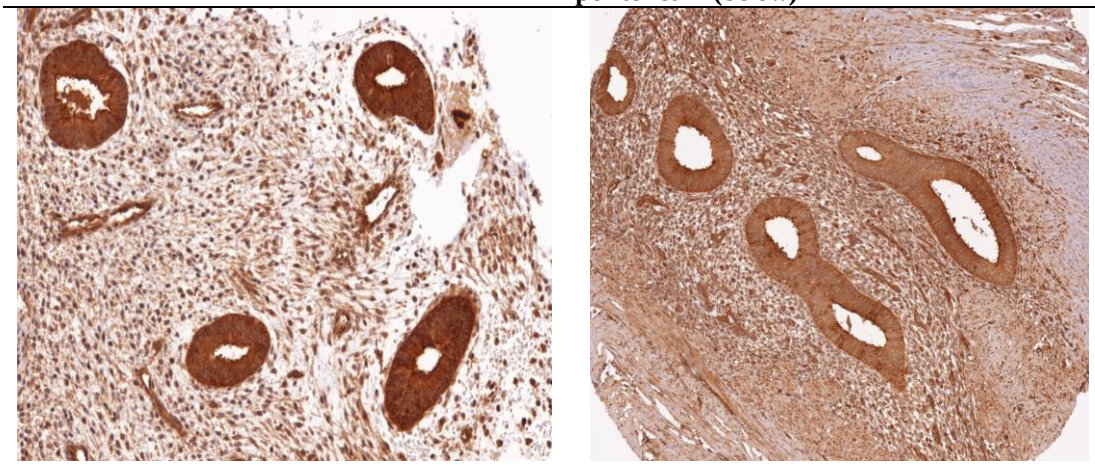

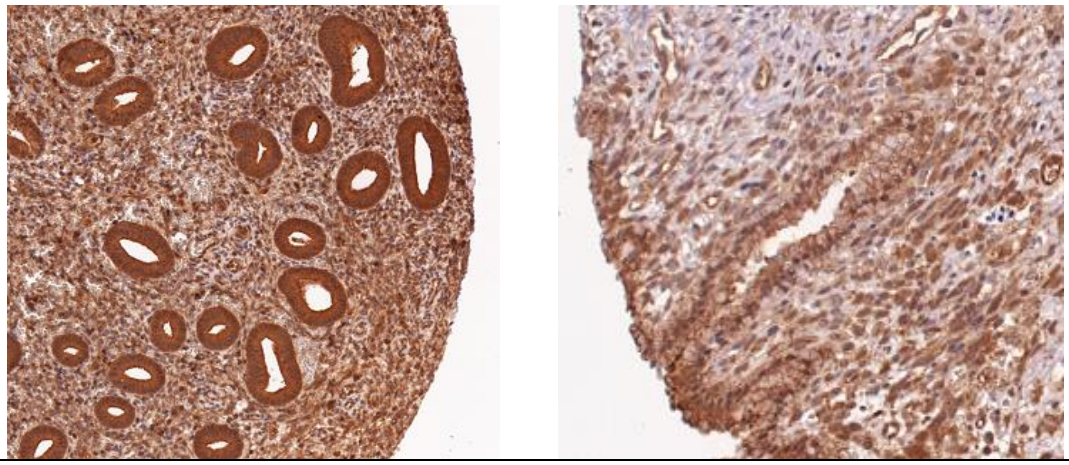

Images showing a reduction in Maspin levels in endometriosis

FIGURE 4-14

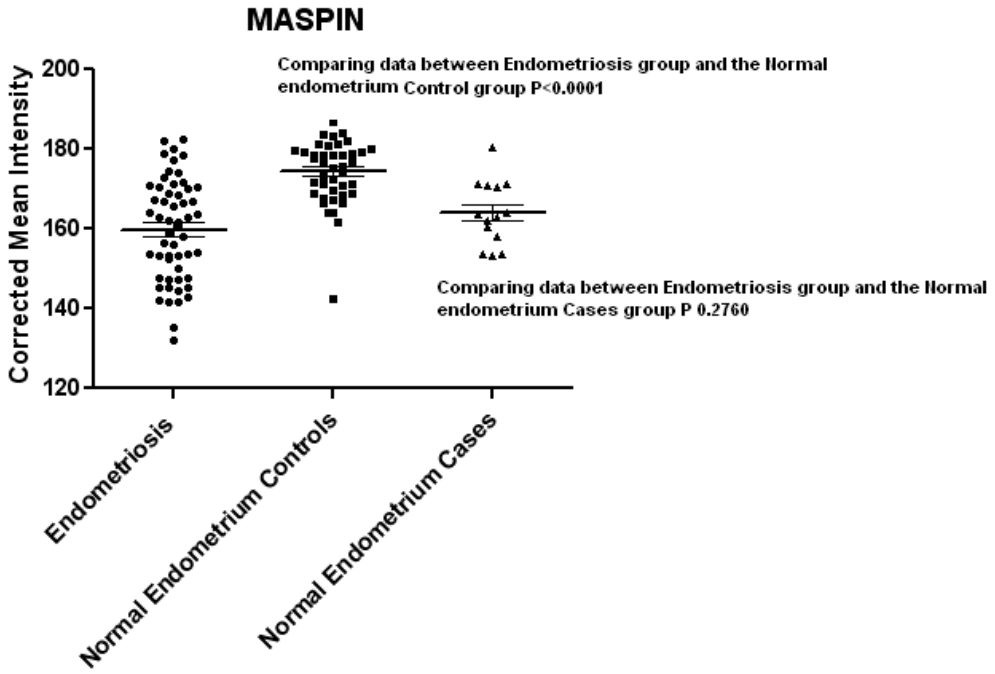

Figure illustrating the levels of Maspin in TMA studies

TABLE 4-3

Table Analyzed	Maspin
Column A vs Column B	**Endometriosis vs Normal endometrium Controls**
Mann Whitney test	
P value	< 0.0001
Exact or approximate P value?	Gaussian Approximation
P value summary	***
Are medians signif. different? (P < 0.05)	Yes
One- or two-tailed P value?	Two-tailed
Sum of ranks in column A,B	1939, 2815
Mann-Whitney U	398.5

TABLE 4-4

Table Analyzed	Maspin
Column A vs Column C	**Endometriosis vs Normal endometrium Cases**
Mann Whitney test	
P value	0.276
Exact or approximate P value?	Gaussian Approximation
P value summary	Ns
Are medians signif. different? (P < 0.05)	No
One- or two-tailed P value?	Two-tailed
Sum of ranks in column A,C	1852 , 563.5
Mann-Whitney U	311.5

4.4.3.3 BCLAF-1

Reduction of BCLAF-1 is confirmed in endometriosis on TMA analysis (Figure 4-15). Comparing levels between endometriotic tissue and normal endometrium, there is a statistically significant downregulation of BCLAF-1 in endometriosis compared to normal endometrium from cases (P<0.0001) (Figure 4-16, Table 4-5, Table 4-6).

FIGURE 4-15

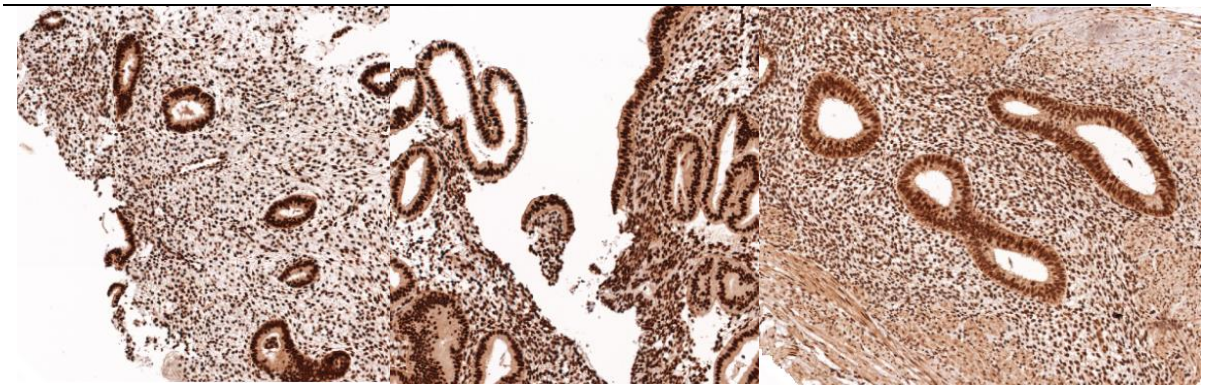

TMA images showing downregulation of BCLAF-1 in endometriosis

FIGURE 4-16

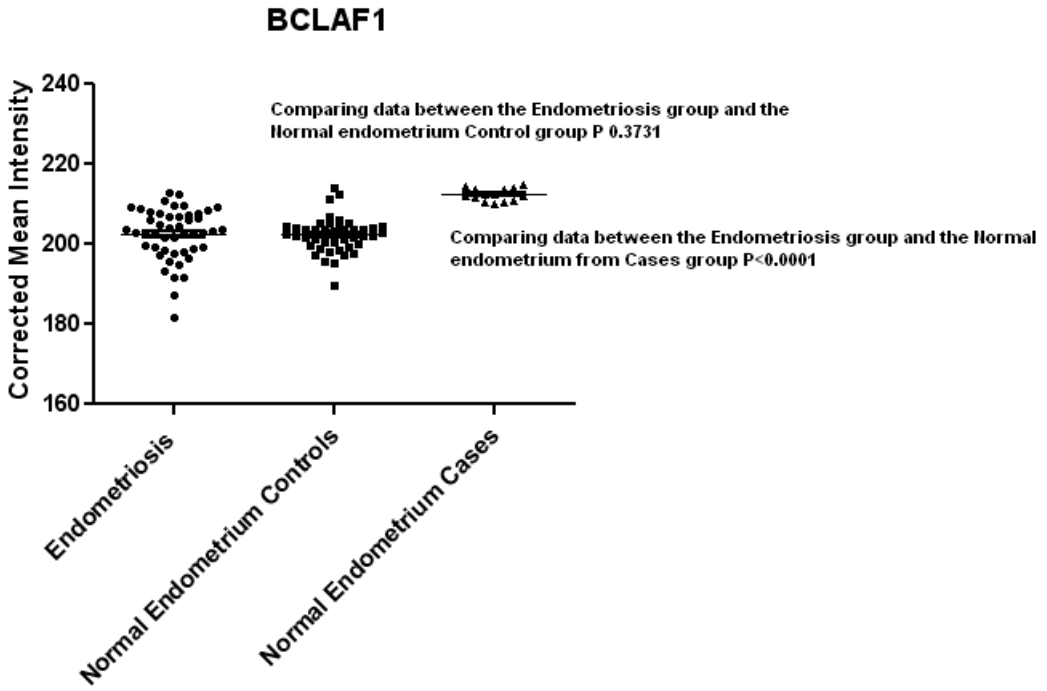

Figure illustrating the levels of BCLAF1 in TMA studies

TABLE 4-5

Table Analyzed	**BCLAF1**
Column A vs Column B	**Endometriosis vs Normal endometrium Controls**
Mann Whitney test	
P value	0.3731
Exact or approximate P value?	Gaussian Approximation
P value summary	ns
Are medians signif. different? (P < 0.05)	No
One- or two-tailed P value?	Two-tailed
Sum of ranks in column A,B	2520 , 2040
Mann-Whitney U	1005

TABLE 4-6

Table Analyzed	**BCLAF1**
Column A vs Column C	**Endometriosis vs Normal endometrium Cases**
Mann Whitney test	
P value	< 0.0001
Exact or approximate P value?	Gaussian Approximation
P value summary	***
Are medians signif. different? (P < 0.05)	Yes
One- or two-tailed P value?	Two-tailed
Sum of ranks in column A,C	1297 , 783
Mann-Whitney U	22

4.4.3.4 p53

TMAs, confirmed an elevated level of p53 in endometriosis compared to normal endometrium in controls (Figure 4-17) (P=0.0090) and normal endometrium from cases (P=0.0101) (Figure 4-18, Table 4-7, Table 4-8).

FIGURE 4-17

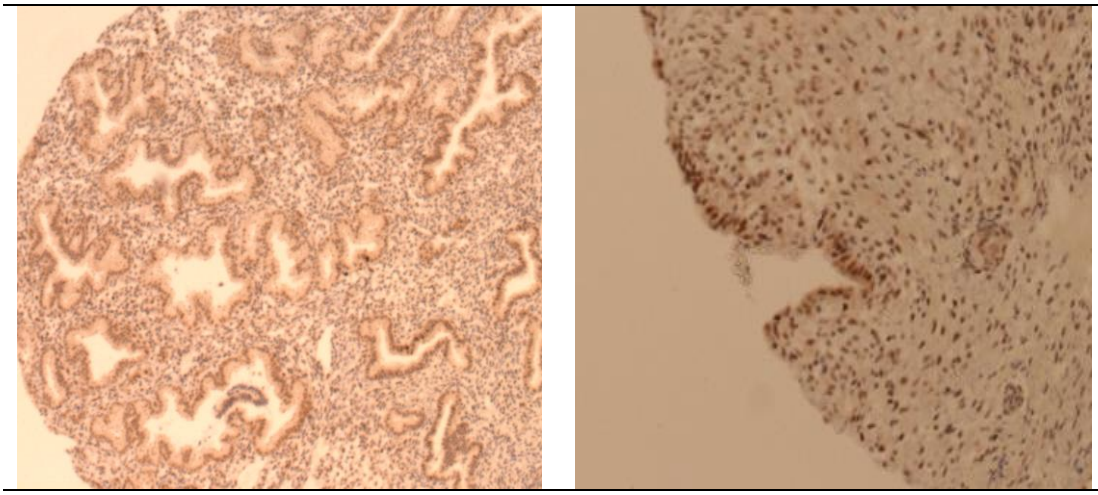

TMA image showing increased levels of p53 in endometriosis

FIGURE 4-18

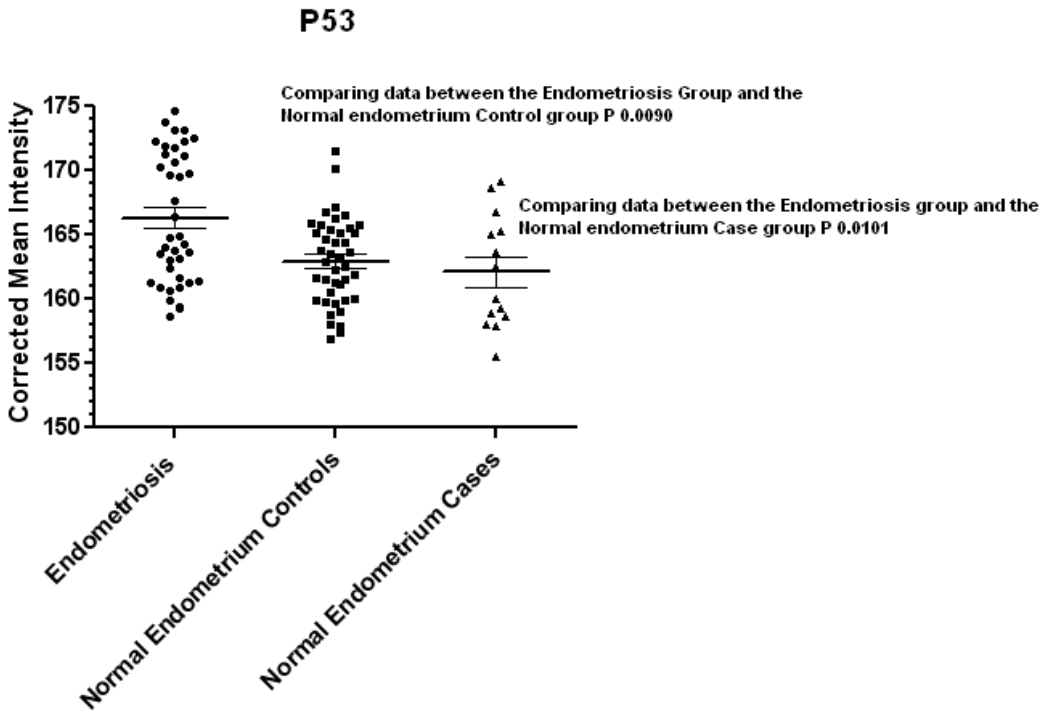

Figure illustrating the levels of P53 in TMA studies

TABLE 4-7

Table Analyzed	p53
Column A vs Column B	**Endometriosis vs Normal endometrium Controls**
Mann Whitney test	
P value	0.009
Exact or approximate P value?	Gaussian Approximation
P value summary	**
Are medians signif. different? (P < 0.05)	Yes
One- or two-tailed P value?	Two-tailed
Sum of ranks in column A,B	1876 , 1445
Mann-Whitney U	542

TABLE 4-8

Table Analyzed	p53
Column A vs Column C	**Endometriosis vs Normal endometrium Cases**
Mann Whitney test	
P value	0.0101
Exact or approximate P value?	Gaussian Approximation
P value summary	*
Are medians signif. different? (P < 0.05)	Yes
One- or two-tailed P value?	Two-tailed
Sum of ranks in column A,C	1181 , 250
Mann-Whitney U	145

4.4.3.5 Ebv-miR-BART2-5p

This MicroRNA was uniquely upregulated in pelvic endometriosis in the proliferative or follicular phase of the cycle (P=0.0163829) (Figure 4-5). It shows a positive fold change (FC) of 1.449 compared to normal endometrium, normal peritoneum and ovarian endometriosis. It was found at higher levels in the endometriosis tissue compared to eutopic endometrium in paired samples. It was identified by the Nanostring expression array which did not require an amplification step. Findings were confirmed with PCR. In situ hybridisation for EBV on tissue microarrays did not confirm the presence of active EBV within the endometriotic epithelial cells (Figure 4-19) but 5 of the 42 endometriotic samples on TMA-A gave a positive reading for EBV presence in some of the lymphocytes.

FIGURE 4-19

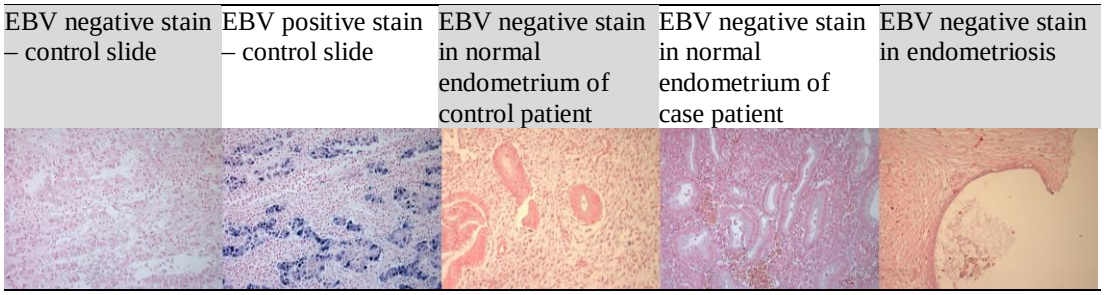

Figure demonstrating stains in various tissues looking for the presence of EBV

This finding is in keeping with previous studies discounting the presence of active viruses within the tissues but might indicate a viral effect on lymphocytes. This does not discount the importance of the influence of the effects EBV has on the development of disease as implicated by my analysis. Potential mechanisms of function may be developed through viral derived endosomes recently shown to play important roles in carcinogenesis, selectively placing EBV miRNAs into the endosome to transfer them to epithelial cells and alter growth characteristics.

4.4.3.6 Cyclin D1

Cyclin D1 is a kinase activator involved in cellular protein binding and cellular mitosis. It has also been implicated as having a role in spermatogenesis and is regulated by oestrogen in the body[494].

It is involved in the cell-cycle (Figure 4-20). The Wnt signalling pathway (Figure 5-14) and the Phosphoinositide 3-kinase pathway (PI 3-kinase pathway) which incorporates a family of enzymes involved in cellular growth, proliferation, survival and the development of malignancy. It is the PI 3-kinase pathway, in conjunction with oncogene phosphoinositide-3-kinase, catalytic, alpha (PIK3CA) and the tumour suppressor Phosphatase and tensin homolog (PTEN), are responsible for cancers which are insensitive to insulin and insulin-like growth factor 1 (IGF-1)[495]in dietary restrictions (Figure 4-21).

FIGURE 4-20

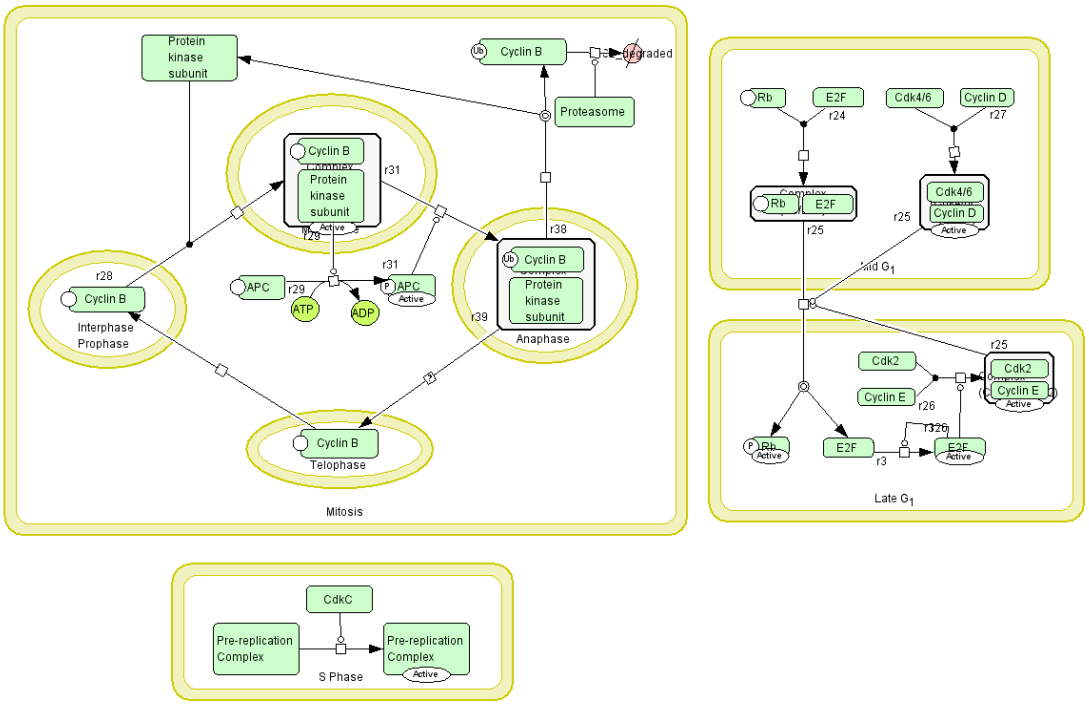

Cell cycle pathway[496]

FIGURE 4-21

Figure split over two continuous parts:

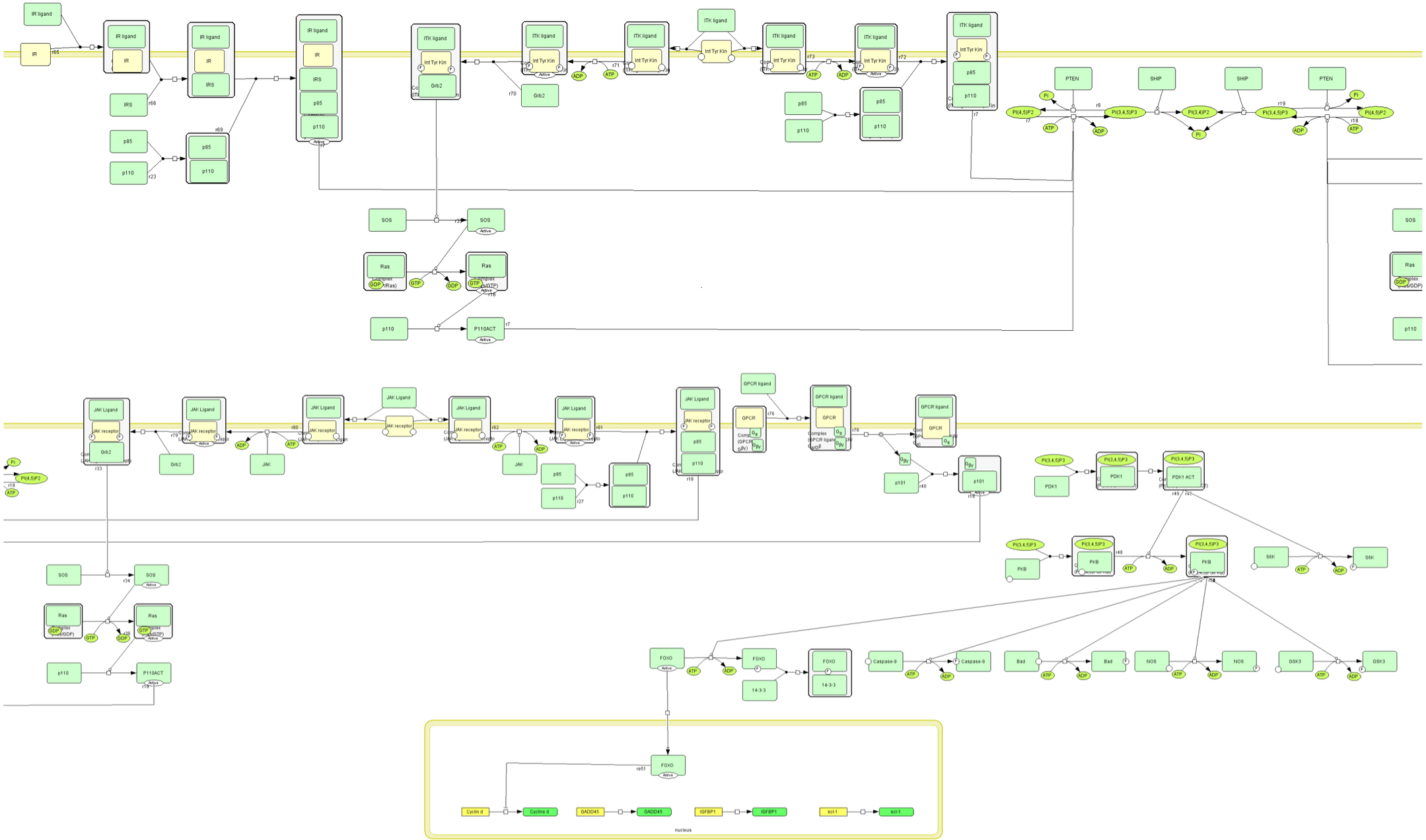

PI 3-kinase pathway in conjunction with cyclin D1[200]

In endometriosis elevated levels of Cyclin D1 as well as c-MYC and growth regulation by oestrogen in breast cancer (GREB1) (all oestrogen regulated genes) have been reported, potentially explaining how cells proliferate survive and invade in this disease[494]. This study also shows an increased level of gene MYCBP responsible for the production of c-MYC. The increased levels of Cyclin D1 in endometriosis has also been attributed to an increased mitogen-activated protein kinase (MAP kinase) in endometrial cells of women with endometriosis in turn decreasing the inhibition of Cyclin D1 by 3,5-cyclin adenosine 5-monophosphate[497]. TMA studies confirm the increased level of Cyclin D1 in endometriosis. Cyclin D1 is also a substrate on which tested therapeutics such as GCS-100 are known to act, increasing evidence of this galectin-3 inhibitor as a potential novel therapeutic medication (Chapter 7). It is also regulated by the gene TOM1 (a potential identified biomarker in my study of endometriosis) and is explored fully in later sections of this thesis (see TOM1).

FIGURE 4-22

Normal endometrium	**Endometriosis**
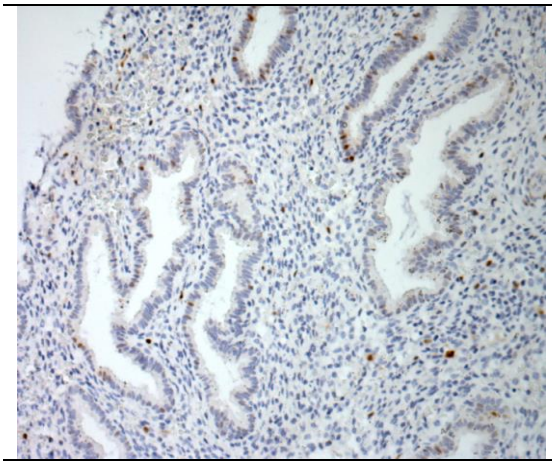	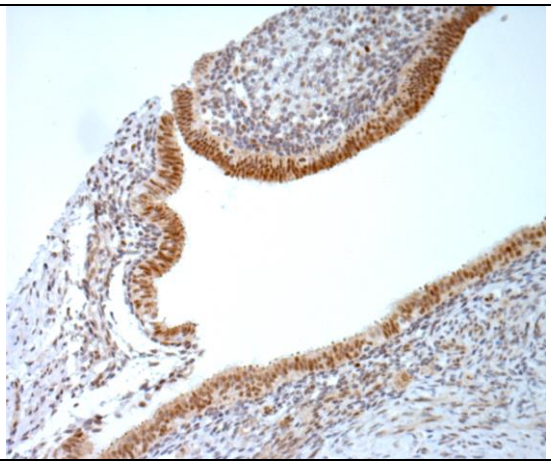

TMA images showing elevated Cyclin D1 levels in endometriosis

4.4.3.7 Galectin-3

FIGURE 4-23

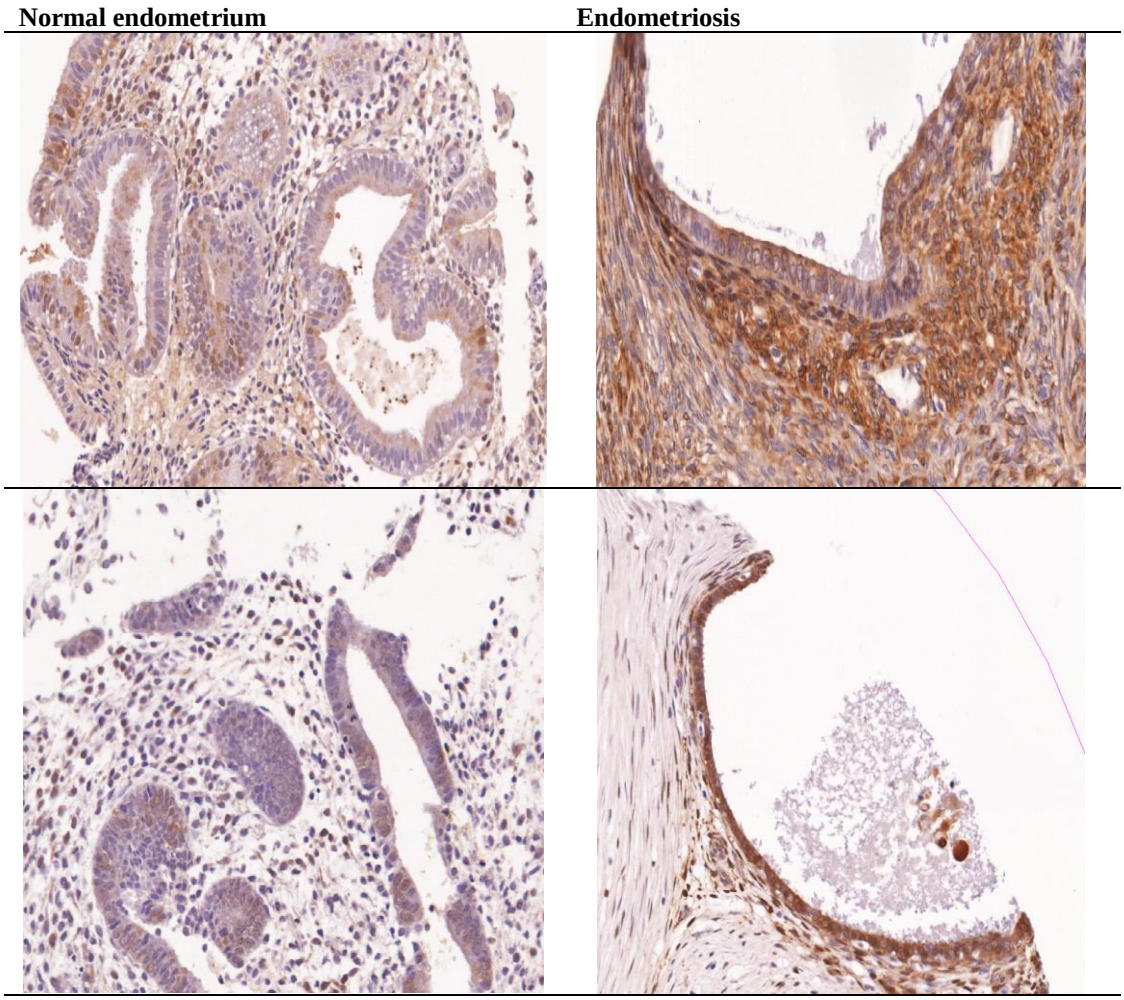

TMA images showing increased levels of Galectin 3 in endometriosis

4.5 Discussion of patient data

4.5.1 Tissue miRNA studies- salient points of note

- The ebv-mir-BART2-5p is detected in endometriosis.
- Endometriosis cells contained higher levels of ebv-mir-BART2-5p compared to eutopic endometrium. This was confirmed by quantitative PCR.
- Ebv-mir-BART2-5p suppresses T-cells and encourages adhesions and angiogenesis in affected tissues.
- Downstream proteins from EBV upregulation are affected. This study demonstrates the upregulation of Cyclin D1) (Figure 4-22) and downregulation of E-Cadherin, Maspin and BCLAF-1) (Figure 4-11, Figure 4-13, Figure 4-15 and Figure 4-10).

- Ebv-mir-BART2-5p may be an initiator for engraftment of endometrial cells to the peritoneum causing the development of endometriosis.
- The presence of ebv-mir-BART2-5p is a permissive event for the development of endometriosis.

4.5.2 A summary of the data

4.5.2.1 Upregulation of Ebv-miR-BART2-5p

In my study I have shown that the Ebv-miR-BART2-5 is uniquely upregulated in pelvic endometriosis in the proliferative or follicular phase of the cycle this was confirmed by quantitative PCR. In situ hybridisation for EBV on tissue microarrays did not confirm the presence of active EBV within the endometriotic epithelial cells (Figure 4-24) but 5 of the 42 endometriotic samples on TMA-A gave a positive reading for EBV presence in some of the lymphocytes. PCR on the peripheral blood monocytes confirms overall higher levels of EBV DNA in the monocytes of people with endometriosis compared to controls (see Table 9-39 in the Appendix). There were no detected EBV levels in the surgically confirmed control patient samples.

FIGURE 4-24

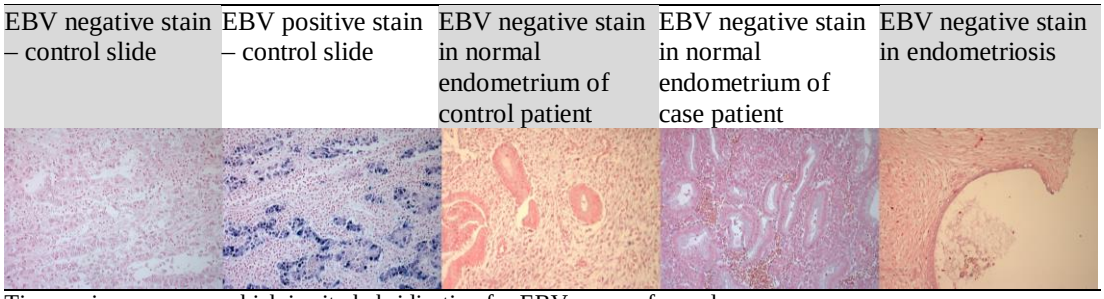

Tissue microarrays on which in situ hybridisation for EBV was performed

This finding is in keeping with previous studies discounting the presence of active viruses within the tissues but might indicate a viral effect on lymphocytes. This does not discount the importance of the influence of the effects EBV has on the development of disease as implicated by my analysis. The presence of these miRNAs in my case tissue samples further helps to substantiate the role of ebv-BART2-5p as a key player in endometriosis. Potential mechanisms of function may be developed through viral derived endosomes recently shown to play important roles in carcinogenesis, selectively placing EBV miRNAs into the endosome to transfer them to epithelial cells and alter growth characteristics.

Metazoan organisms encode miRNAs which regulate gene expression by binding to the 3'UTR terminal of mRNAs. Herpes viruses are known to induce persistent lifelong infections in their latent stage by evading the host's immune system[498]. miRNAs have been identified within DNA viruses of the herpes family[499-501]. Identified tumorigenic viruses associated with latent infections, evasion of the host immune responses[502] and epithelial, endothelial or lymphoid malignancies include Cytomegalovirus (CMV)[503], Kaposi's sarcoma associated herpesvirus (KHSV)[504] and Epstein-Barr Virus (EBV)[505]. Problems with predicting viral miRNA targets with available algorithms exist[506] as both cellular and viral targets can interact and should be analysed[507]. As viral targets are poorly conserved this is not always possible and their experimental validation has been limited[499].

FIGURE 4-25

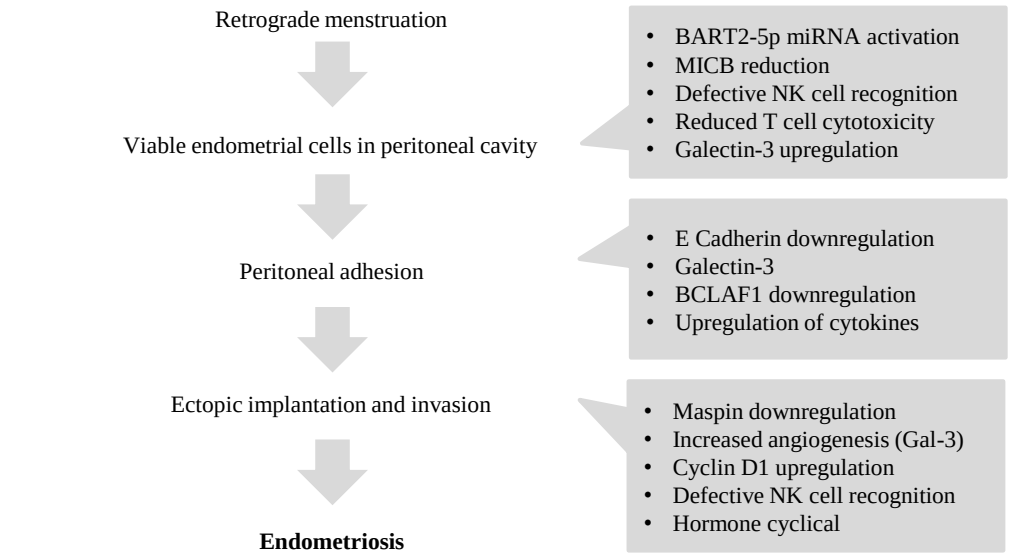

Figure illustrating the various mechanisms involved in development of endometriosis

There are a series of identified mechanisms and pathways which I theorise result in the development of endometriosis (Figure 4-25, Figure 4-10). My findings indicate an EBV viral effect on lymphocytes which potentially plays an important role in development of disease. During latent infection, EBV has been reported to induce certain host miRNAs which play a role in viral oncogenesis such as miR-155 and miR-21[508] (Figure 4-10). miR-21 controls the oncogene Tropomyosin alpha-1 chain (TPM1). TPM1 has been identified in my study as a potential antibody marker from the serum of patients with disease (Section 6.7.3.8). miR-155 has also been identified in this study as being upregulated in Ovarian endometriosis (P=0.00001720) (Table 9-4) specifically in the follicular/proliferative phase of the cycle (P=0.0004878) (Table 9-5). It is also seen to be upregulated in the normal endometrium of cases (average value of expression from all case samples 6.308624) compared to the normal endometrium from controls (average value of expression from all control samples 3.818766) (***see Excel analysis-Thesis excel data (my modified lists of miRNA decideTests_resultsV2).xls***).. MiR-21 is also seen to be dysregulated in my study and is expressed in Ovarian endometriosis (P=0.00140219) (Table 9-14). miR-21 is also seen to be dysregulated in this study. It is expressed in Ovarian endometriosis (P=0.00140219) (Table 9-14). miR-21 was also seen in the normal peritoneum of cases (Table 9-12) (average value of expression from all case samples 12.30429) and in the normal peritoneum of controls (average value of expression from all control samples 12.29785). The data from the normal peritoneum does not necessarily refute the presence of this miRNA in peritoneum of women developing disease. It is recognised that small sample numbers might provide a limitation to their true expressed levels. In addition, the location of a peritoneal biopsy well away from the growth of endometriosis might lessen the incidence of deregulated miRNA in these sampled tissues.

EBV was the first virus to be associated with a human tumour[509] (Figure 4-27) and is seen in lymphomas and epithelial malignancies such as undifferentiated nasopharyngeal carcinoma. *In vitro* studies show the pivotal role of EBV in oncogenesis. It is capable of transforming over 50% of resting B-cells into continuously proliferating cells with latent virus within a few days[510]. Infection of epithelial cells with

EBV is not completely understood. There is the possibility of virus as well as exosomes transferring genetic material. This results in epithelium demonstrating the default program of infection[511,512]. Unlike B-cells, epithelial cells are unable to become memory cells and the LMP proteins cannot "turn off". Thus even in immunocompetent individuals infection can persist. The same theory could be true of endometriosis. Publications show that the presence of healthy, functional NK cells is inversely proportional to the presence of EBV virus and its effects[513]. There are a number of predicted human target genes for EBV BART2-5p which have particular roles enabling ectopic tissue to engraft and survive. The BCLAF1 gene linked to apoptosis, the CDH1/E-Cadherin linked to cell adhesion and the MASPIN linked to p53 signalling are all implicated. Over expression of the BCLAF1 induces apoptosis and T cell proliferation. The expression of BART2-5p provides a survival advantage to ectopic endometrium having reduced apoptosis and avoiding immune surveillance by the t-cells. This study demonstrates the reduction of BCLAF-1 on tissue microarray analysis (TMA). Comparing levels between endometriotic tissue and normal endometrium, there is a statistically significant downregulation of BCLAF-1 in endometriosis compared to normal endometrium from cases ($P<0.0001$) (Figure 4-16, Table 4-5, Table 4-6).

CDH1/E-Cadherin is a master regulator of the G0/G1 stage of the cell cycle and its role is to reduce cell adhesion, division and cycling. Its suppression in ectopic endometrial tissue predicts an increase in cell adhesion (observed in endometriosis) and removes the suppression on the G0/G1 cell cycle stage moving cells into the S phase. This study demonstrates the downregulation of E-Cadherin in endometriosis on tissue microarray (TMA) analysis. There is a statistically significant downregulation of E-Cadherin in endometriosis compared to normal endometrium from controls ($P<0.0001$) and normal endometrium from cases ($P=0.0017$) (Figure 4-12, Table 4-1, Table 4-2). The reduction in E-Cadherin enables the tissues to metastasise and infiltrate causing disease progression and creating an invasive pattern often seen in endometriosis. Maspin is expressed in normal endometrial cells and its suppression by BART2-5p leads to an increase in ability for the endometrium to migrate and survive. An activating p53 binding site was identified and showed Maspin to be the downstream effector gene. My study confirms the reduction of Maspin on tissue microarray (TMA) analysis. Comparing levels between endometriotic tissue and normal endometrium, there is a statistically significant downregulation of MASPIN in endometriosis compared to normal endometrium from controls ($P<0.0001$) and normal endometrium from cases ($P=0.2760$) (Figure 4-14, Table 4-3, Table 4-4).

4.5.2.2 Downregulation of hsa-miR-564

In my study, hsa-miR564 was the miRNA found to be downregulated exclusively in the endometriosis tissue samples. Overall, most cancers show aberrant miRNA expression and an overall level of downregulation of relevant miRNAs when compared to normal tissues. This miRNA has been found to be downregulated in leukocytes of patients with chronic myeloid leukaemia[514] and in papillary thyroid carcinoma with lymph node metastasis[515]. It has been postulated that the downregulation of this miRNA is mediated by the activity of BCR-ABL tyrosine kinase gene and its protein[514] (Figure 4-26). The ABL oncogenes play a role with Cyclin D1 and K-RAS to induce cellular transformation both *in vitro* and in vivo models[514]. The predicted targets of miR-564(Target Scan predictive analysis tool) include E2F transcription factor 3 (E2F3) and Akt2 gene. The E2F family of genes play a role in the cell cycle, DNA replication and the upregulation of E2F3, an oncogene with strong proliferative potential. It is associated

with poor prognosis in hepatocellular carcinomas[516] and in tumour studies it has been proposed as a marker of poor patient prognosis. In studies involving lung cancer patients, the targeting of E2F3 by a tumour suppressive miRNA (mir-449a) induces remission and improved survival of patients[517]. E2F is also a target of transforming proteins and gene products of DNA tumour viruses such as adenovirus E1A, papillomavirus E7, simian virus 40 and poliomavirus large T antigens[518]. The Akt2 gene codes for the enzyme RAC-beta serine/threonine-protein kinase and has been described as an oncogene in ovarian carcinoma[519]. It has been associated with poor prognostic outcomes and increased tumour aggressiveness when upregulated[519]. Ak2 has also been found upregulated in EBV virus immortalised B cells[519].

FIGURE 4-26

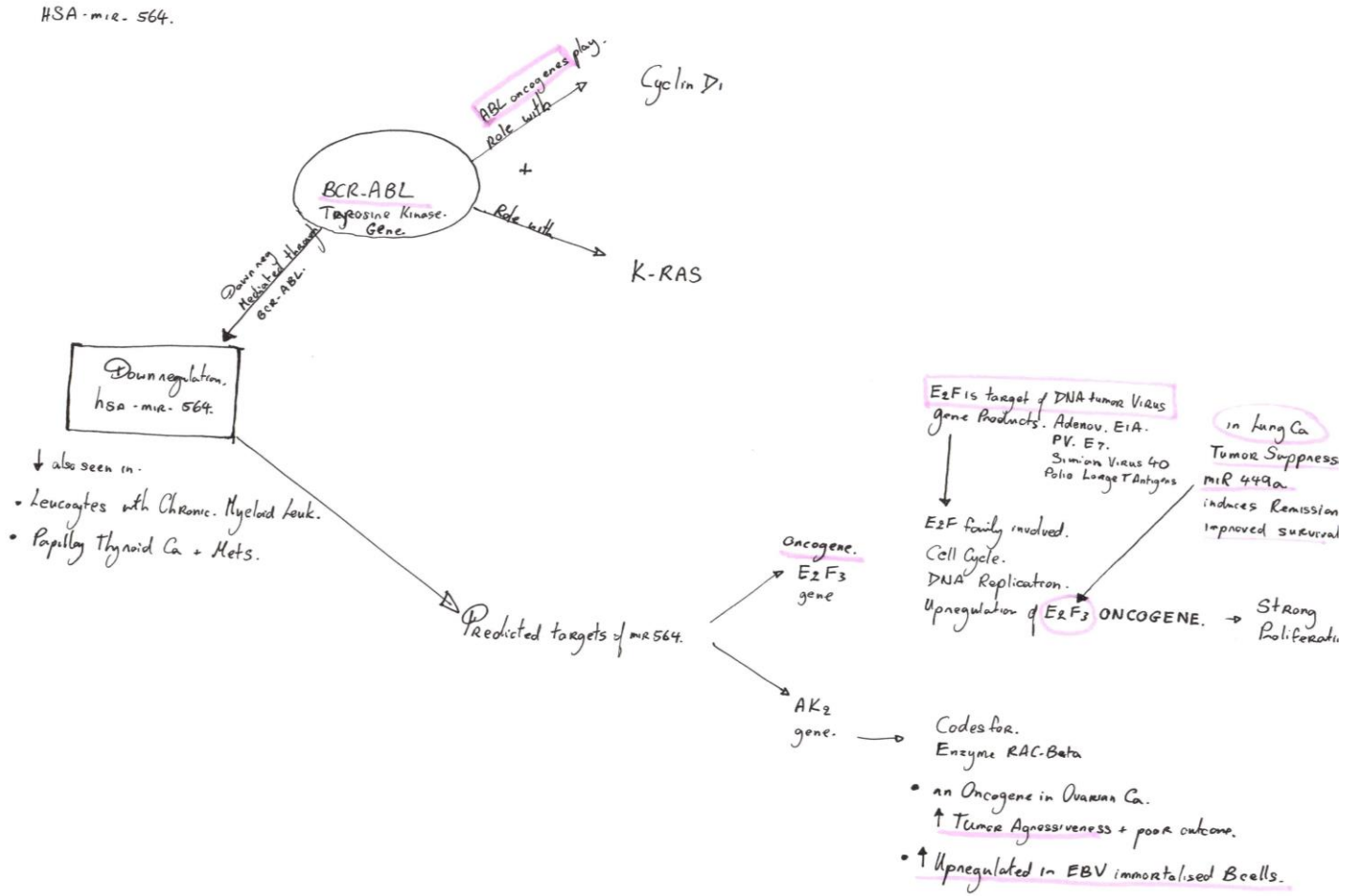

Hand drawn diagram showing the effects of HSA-miR-564

4.6 The EBV virus- its role in the development of disease

4.6.1 EBV associated malignancies

Tumours usually result from multifactorial changes resulting in genetic alterations that enable the immortalisation of the implicated cell[520]. Viruses are amongst the implicated causative factors of these changes. The existence of viral oncogenes created a window of understanding as to how viruses function towards the development of tumours[521]. EBV (Ebstein Barr Virus or Human Herpesvirus 4) of the Genus *Lymphocryptovirus* and subfamily *Gammaherpesvirinae* (gamma 1 subtype) is a lymphotrophic gamma human herpesvirus and infects around 90-95% of the population within the first 40 years of life. It was the first virus to be associated with a human tumour[509] (Figure 4-27). Whereas the infection is prevalent in early life in underdeveloped countries, it tends to present towards adolescence in developed countries, as a benign lymphoproliferative disorder[522]. In the acute and latent phase, EBV is in itself benign but it has a known association with various cancers including Burkitt's lymphoma.

In vitro studies show the pivotal role of EBV in oncogenesis. It is capable of transforming over 50% of resting B-cells into continuously proliferating cells with latent virus within a few days[510]. Interestingly, when B lymphocytes from chronic carriers of the virus are cultured (in the absence of T lymphocytes), it is those affected by EBV that proliferate forming lymphoblastoid cell lines all carrying viral copies and showing the Latency 3 program of infection (Table 4-9). EBNA-2 and LMP-1 are the viral protein essential for this clonal proliferation of *in vitro* cells.

Burkitt's lymphoma is associated with translocations in chromosomes 2, 14 or 22 causing the downregulation of MYC proteins and enabling increased B-cell proliferation[523]. Other lymphomas such as Hodgkin's and Non-Hodgkin's Lymphomas are also associated with EBV infection and latent transcripts in the BAMHI region of the EBV genome are also identified in Hodgkin's Lymphoma[524]. Other associated epithelial malignancies include undifferentiated nasopharyngeal carcinoma demonstrating expression of the EBV LMP2A and LMP 2B genes. Nasopharyngeal carcinoma has also shown the presence of latent transcripts identified in the BAMHI region of the EBV genome in the opposite direction of the conventional mRNAs transcribed in this region[524]. In undifferentiated (non-keratinising) carcinoma of the nasopharynx, there is a visible lymphocytic infiltration near the tumour cells. These tumours have been shown to be monoclonally EBV positive[525] (Figure 4-28).

FIGURE 4-27

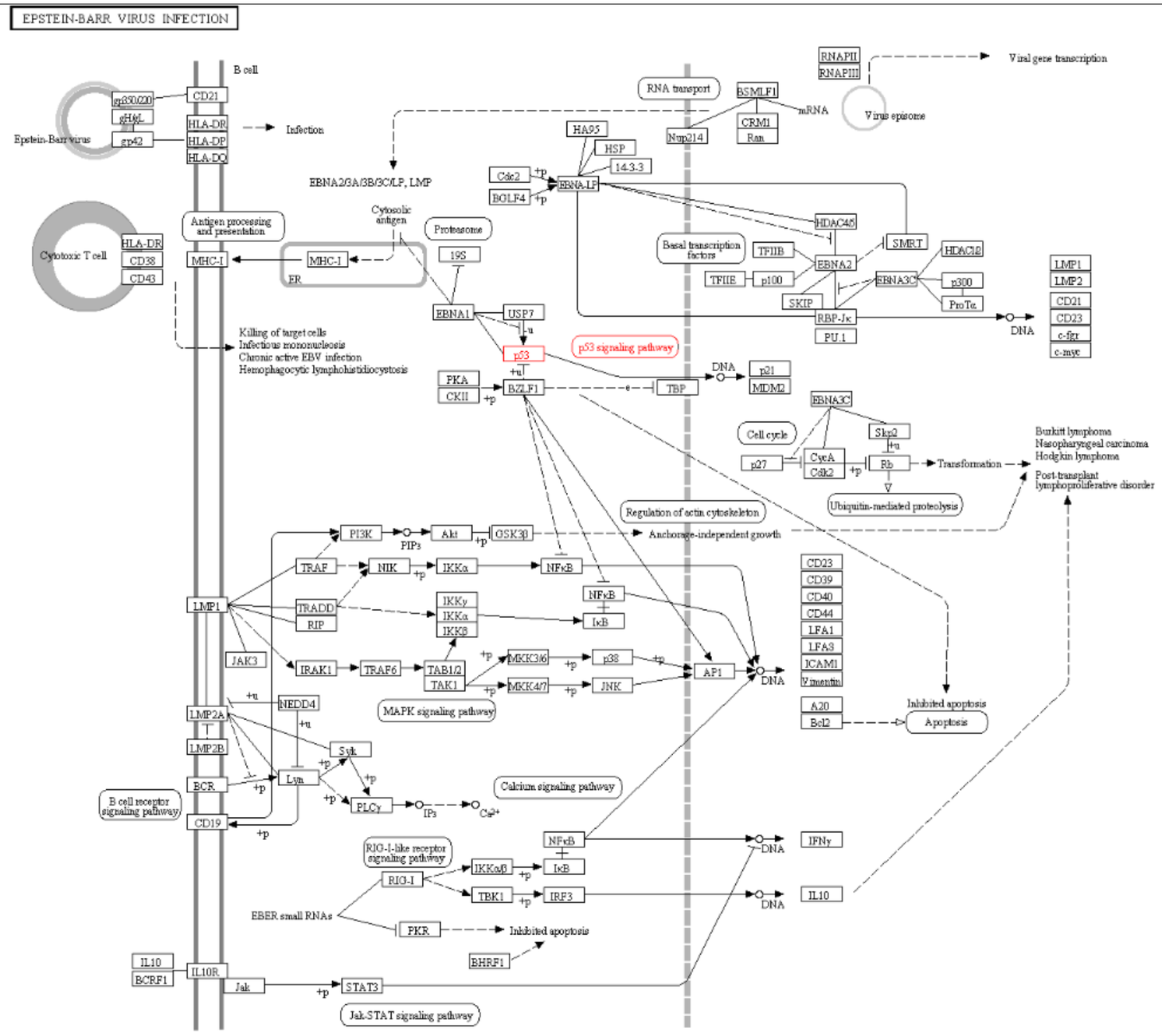

Pathways affected by the Epstein-Barr Virus (EBV)[20]

FIGURE 4-28

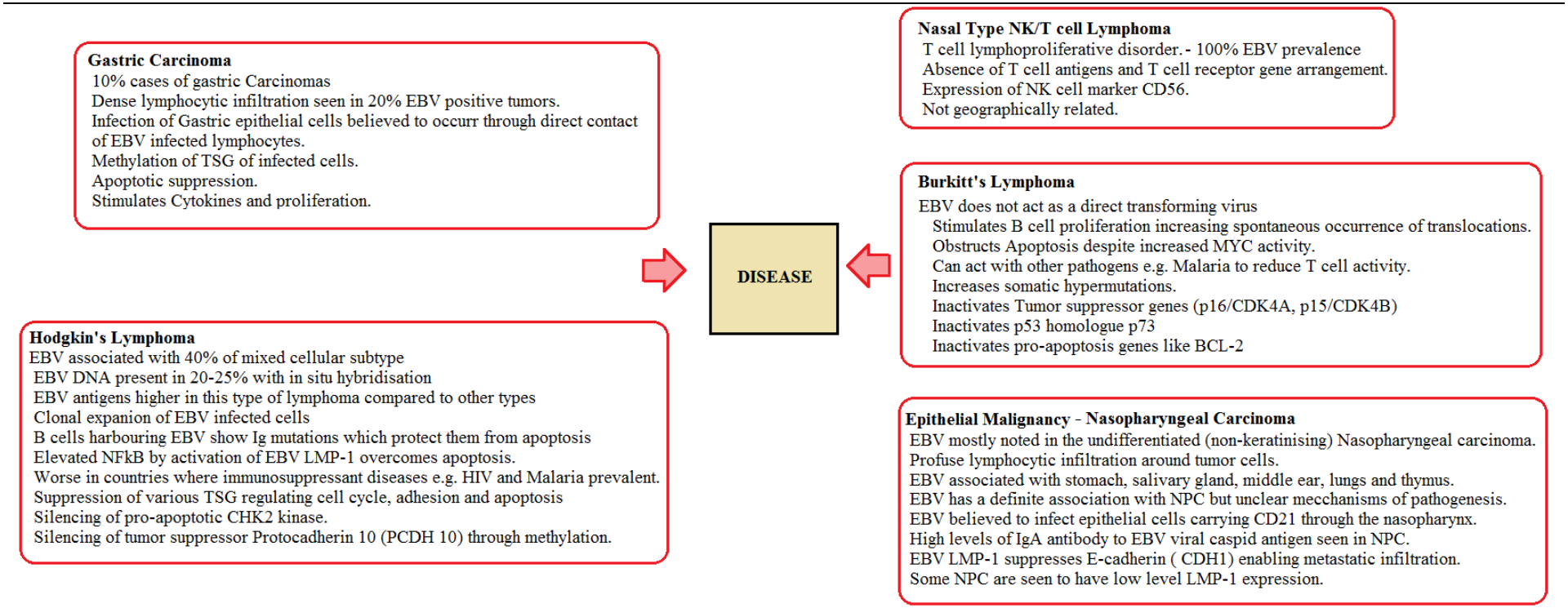

Diagram representing an overview of EBV associated malignancies

It is believed that in all EBV associated tumours, the starting point in malignant development arises with a persistent EBV infection[527]. It is to be noted that though 90-95% of adults have latent EBV, not all develop tumours. This supports the theory of multifactorial agents causing disease. Depending on their location, the effect on infected B-cells by the EBV virus varies. If the B-cells are found in peripheral blood, the virus is often dormant. Conversely, in the lymphoid system of the nasopharynx, the active virus is found. In the nasopharynx, the virus is believed to have been transferred through saliva[528] and crosses the epithelial cells. One of the mechanisms of infection is believed to lie in a primary infection of the oropharyngeal epithelial cells with the EBV virus. The virus is then transferred through direct methods of contact to the subepithelial cells causing them to invade B cells. The affected B cells stimulate a CD8 T cell response which attempts to eliminate all the infected B cells. Most but not all B cells are eliminated resulting in cells harbouring the EBV virus causing a latent infection (Figure 4-29).

FIGURE 4-29

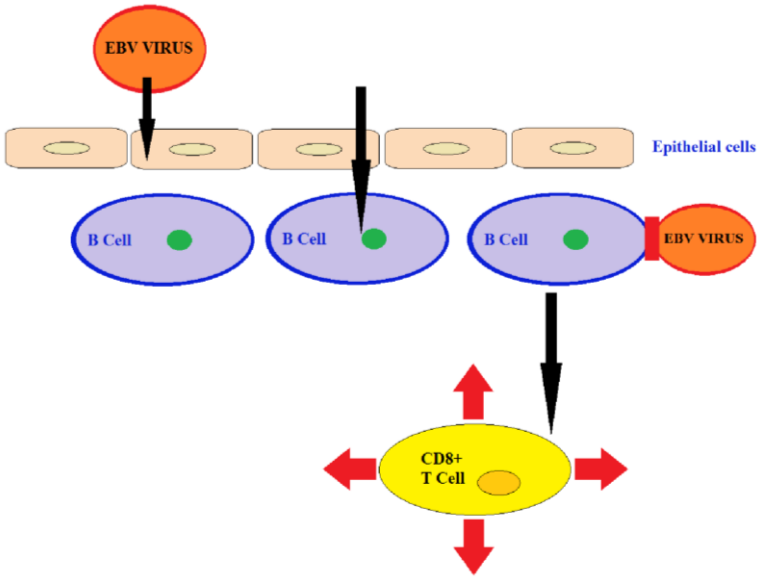

Schematic representation of latent EBV infection in B Cells

4.6.2 Survival of EBV

When a B-cell is activated, it migrates to the germinal centre producing antibody generating plasma cells and memory cells[529]. Studies have shown that infected B cells attain properties enabling them to proliferate into cell lines containing and expressing latency associated viral proteins (Epstein-Barr nuclear antigens (EBNA) 1, 2, 3A, 3B, 3C and LP) and latent membrane proteins (LMP) 1, 2A and 2B[530]. In EBV infected B-cells the activation process occurs but due to undefined signalling in the follicles, the default program of infection occurs where EBNA-1, LMP-1 and LMP-2A provide signalling for differentiation of lymphoblasts into memory cells maintaining persistently infected cells. Apart from being seen in B-cell cellular mutation, the default program of infection is also seen where the virus inappropriately infects non B-cells such as nasopharyngeal epithelial cells. The method of viral transfer is not completely understood with the possibility of virus as well as exosomes transferring genetic material. This results in epithelium demonstrating the default program of infection[511,512]. Unlike B-cells, epithelial cells are unable to become memory cells and the LMP proteins cannot “turn off”. This explains how even in immunocompetent individuals infection can persist. The same theory could be true of endometriosis (Figure 4-30).

FIGURE 4-30

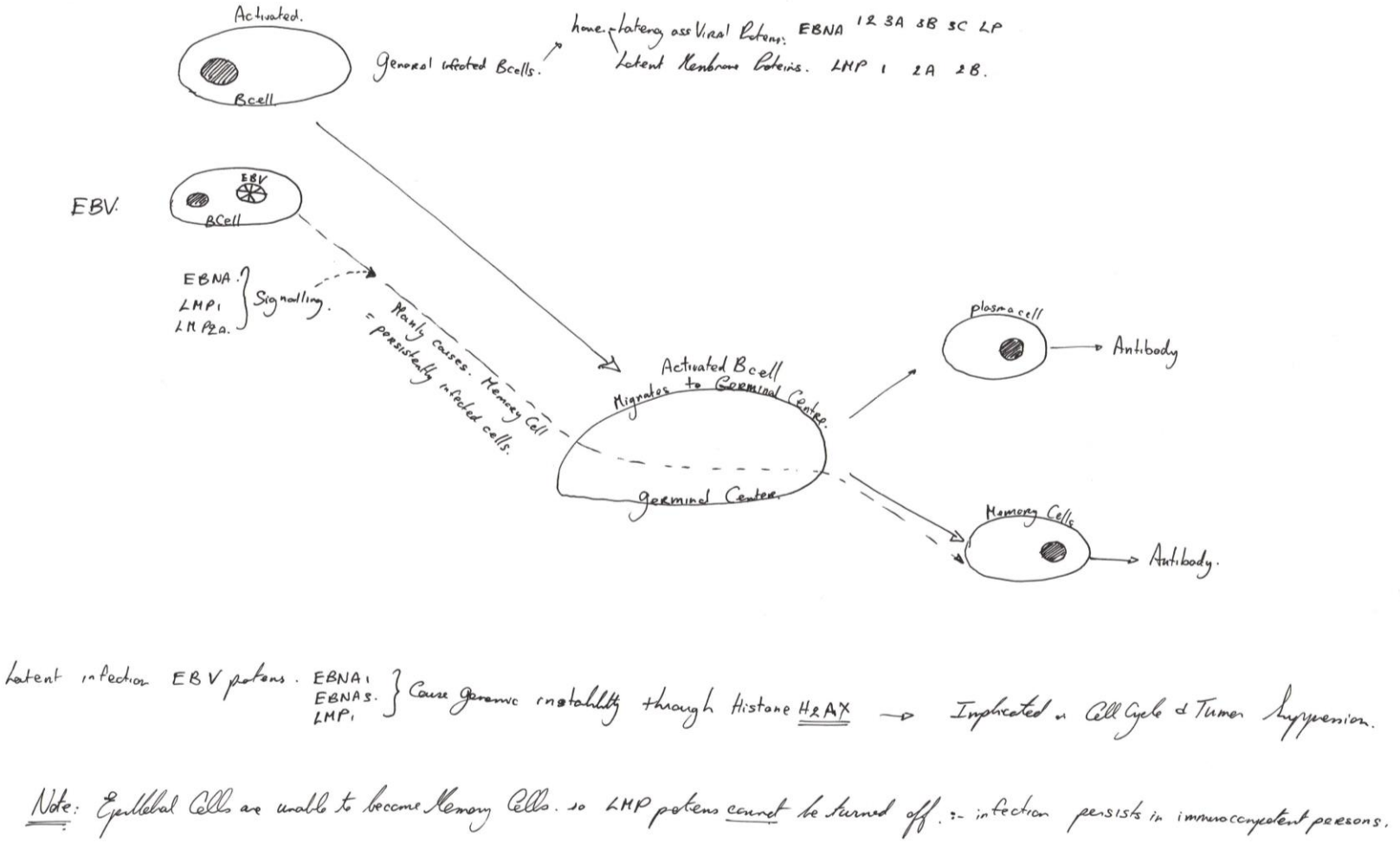

Hand drawn diagram depicting EBV survival techniques

One would therefore expect that malignancies linked with EBV express these proteins too. Interestingly not all EBV associated malignancies express these proteins due to the presence of genetic aberrations and deregulations which will in turn disregulate oncogenes and tumour suppressor genes causing malignancy[531]. An alternate theory explaining the failure of immunohistochemical studies to find significant EBV in germinal centres is due to the fact that infected B cells do not always give rise to a full germinal centre or they alternately differentiate and expand outside of the germinal centre itself[532].

When looking at malignancies associated with EBV, one may look for cell lines which express similar aberrations due to clonal proliferation[533]. These are often used as malignancy markers. Interestingly, tumour development is also associated with errors in DNA repair causing aberrations which are not necessarily clonal. The DNA breaks can and are lethal to cells when they divide so new aberrations will be seen with each new cell cycle.

It is interesting to note that the EBV proteins expressed during latent infection, in themselves cause genomic instability and chromosomal abnormalities[530]. EBNA 1, 3 and LMP 1 cause instability in the genome associated with DNA breaks and phosphorylation of histone H2AX which is implicated in the checkpoints of the cell cycle and tumour suppression (Figure 4-31, Figure 4-30).

FIGURE 4-31

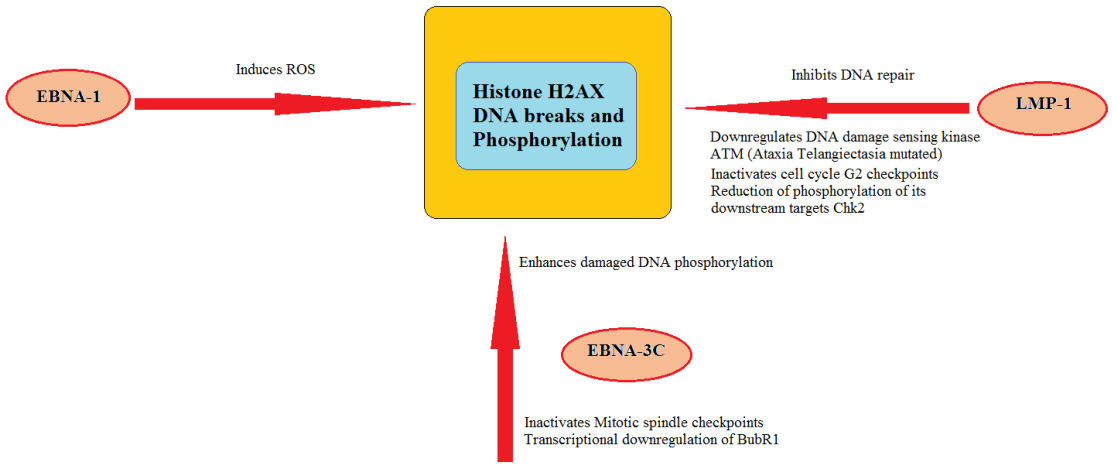

Schematic representation of the functions of EBV proteins expressed during latent infection

As is described above, the targets of EBV associated proteins affect cell cycle checkpoints and therefore destabilise the integrity of the genome. Several types of cancers associated with EBV do not have high expression of viral genes as the viral genome itself is seen to be heavily methylated.

Survival of the virus within the system is attributed to the fact that affected cells do not express growth-promoting genes, surviving in the peripheral circulation as resting memory cells[534]. Apart from the latency programme maintaining the viruses in check, the body's immune system also serves as a controller of virus containing cells. Cytotoxic t-lymphoctes identify and destroy expression of any virally infected cells outside of the memory pool[535]. Any dysregulation within the host's immune system will adversely affect the t-cell function enabling continuing viral existence or active pathology. In immunocompromised hosts, the EBV infected cells are seen to proliferate and give rise to EBV associated tumours which typically regress with cytotoxic t-cell lymphocyte therapy.

4.6.3 Genes expressed in latency and associated pathways affecting the immune system

Latency programme of infection resides in peripheral blood B-cells accounting for lifelong benign infection. Persistence of infection is described as stable numbers of affected B-cells (Table 4-9).

TABLE 4-9

Gene expressed	**EBNA-1**	**EBNA-2**	**EBNA-3A**	**EBNA-3B**	**EBNA-3C**	**EBNA-LP**	**LMP-1**	**LMP-2A**	**LMP-2B**	**EBER**
Product	Protein	Protein	Protein	Protein	Protein	Protein	Protein	Protein	Protein	ncRNAs
Latency I	+	–	–	–	–	–	–	–	–	+
Latency II	+	–	–	–	–	+	+	+	+	+
Latency III	+	+	+	+	+	+	+	+	+	+

Table showing the 3 types of expressed latency programs proteins of EBV[536]

The infectious state is associated with salivary viral shedding. Associated cytotoxic t-cells and antibodies are seen in the presence of viruses and these are usually at stable levels. It is mutations in the virus that lead to the development of oncogenesis, carcinomas and lymphomas. A resting B-lymphocyte, once infected, can rapidly proliferate giving rise to disease[537,538]. The EBV associated proteins affect the cell cycle at various checkpoints and all have a role in destabilisation of the genome and dysregulation of the cell cycle and its pathways (Figure 4-32).

FIGURE 4-32

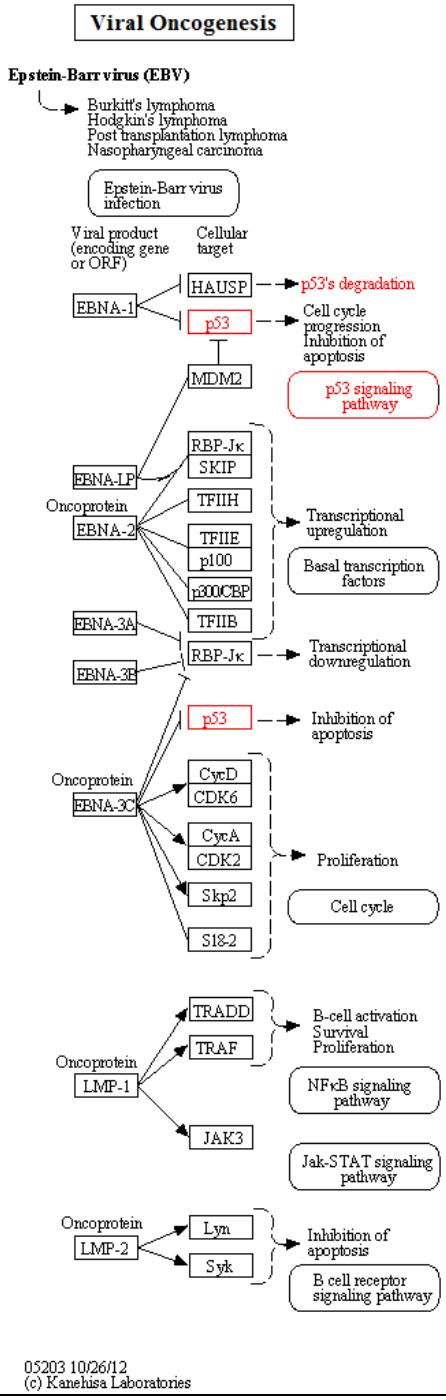

Figure illustrating the genes expressed in latent EBV infection and their associated pathways[526]

EBNA-1 (Epstein-Barr nuclear antigen-1) a nuclear associated viral latency protein ensures the replication of the viral genome in cell division. It enables this by linking the viral nuclear material to the cellular one enabling its replication with cellular division[539].

EBNA-2 acts as a surrogate for the Notch intracellular domain within the Notch signalling system and controls the transcription which halts B cell differentiation in proliferation[540]. It also activates the growth program viral proteins and activates cellular activation through the C-Myc pathway acting as a protoncogene[541].

EBNA-3C has a poorly known mechanism where there is inactivation of the retinoblastoma (Rb) tumour suppressor. This enables cell cycle progression from the G1 to the synthesis phase enhancing proliferation[542].

LMP-1 (latent membrane protein-1) interacts with TRAF (Tumour necrosis factor receptor-associated factor) an intermediary of the TNFR family of cell surface receptors[543] for the delivery of both survival and death signals[544]. Its carboxy terminal domain is a functional homologue of CD40[545,546] (though differs in its signalling pathway) with interchangeable signal domains[547]. This rescues B-cells from apoptosis thereby driving proliferation. There are various pathways which are activated by LMP-1 binding. LMP-1 not only interacts with TRAFs but also interacts with the JaK3 (Janus activating kinase) activating the NFκB pathway, the activator protein 1 through c-Jun N-terminal kinase (JNK) and the pathways for the signal transducers and activators of transcription (STAT) pathways.

LMP-2A (Latent membrane protein-2A) contains the same ITAMs (immunoreceptor tyrosine-based activation motifs) found on the α and β chains of B-cell receptors. This enables them to interact with the tyrosine kinases (Src family) mimicking the signalling of a B-cell receptor which has been engaged by antigens. This promotes signalling for growth through the RAS pathways and alternate mechanisms. Usually in the absence of an antigen signal, the B-cell receptor maintains B-cell survival by controlled signalling levels. LMP-2 mimics this signalling thereby preventing the death of B-cells which lack their surface immunoglobulin[548].

4.6.4 EBV and exosomes

The role of miRNA in the repression of mRNA translation into proteins has been well documented. This regulatory role is a finely balanced process in healthy tissues but is dysregulated in tumours or virally infected cells[549]. miRNAs are not only human in origin but also viral and are actively secreted through vesicles called exosomes which serve as protection from RNases[550]. The vesicles (approximately 50nm diameter) were seen to contain transferrin receptors that enable the process of endocytosis and cell protein recycling. Exosomes of EBV transformed B-cells are known to have plasma membrane lipid domains rich in cholesterol[551]. Functionally the exosome can enable the combination of ligands which would be able to bind simultaneously with different cell-surface receptors which might not happen in a "normal" cellular scenario. The response of activation of multiple ligands can mimic cellular interactions without the need for actual cellular contact. Exosomes can also transport new cell surface molecules to cells enabling them to achieve new properties such as adhesion and they can also enable transfer of cytosol and proteins between various cellular types. This again might alter cellular properties[552] (Figure 4-33). The horizontal transfer of miRNAs which are non-coding is emerging as a possible evolutionary conserved method enabling intercellular communications. In vivo evidence is scarce. *In vitro* studies have indicated that mature functional miRNAs can be secreted through exosomes and have been seen in B cells[553], stem cells, immune cells, placental cells[554] and cancer cells[550,555,556]. Once present in the host cells, the transferred miRNA cause alterations in the cell triggering oncogenic properties. In the study by Raposo[553], the exosomes secreted by EBV transformed B-cells, triggered CD4+ t-cell stimulation, mimicking antigenic activation. The T-cell response was however less potent[553]. Interestingly, exosomes might also have

immune-suppressive effects which are independent of antigens. Certain viral proteins within exosomes such as LMP-1 inhibit anti CD3 and anti-CD28 induced T-cell proliferation[557].

The analysis of microvesicle and nano-exosome carried miRNA is today used in the understanding of cellular processes. Understanding their cellular impacts might provide insights in their potential use as specific disease biomarkers or therapeutic response markers. They are also being looked at as transporters for immunotherapies as novel future treatments. The role of exosomes in B-cell mediated cross talk in humans has also been explored[555,558]. The presence of such vesicles explains how miRNAs can exert functions outside of their producing cells and possibly serve as intercellular communications[559,560]. There are papers exploring (through quantitative RT-PCR) how virally EBV infected B-cells transfer their miRNAs through exosomes[550]. In diseases affected by EBV, the EBV DNA is seen to be present or restricted to peripheral blood lymphocytes but the miRNAs for the EBV have been found to accumulate in non-infected surrounding cells. These transferred miRNAs cause gene repression in neighbouring cells enhancing evidence of their presence and function[550]. Once infected, a B-cell can express four different types of programmes. One of these programmes results in the production of an active virus, whereas the other 3 code for latent infections (Figure 4-34)[541]. In the latency programmes the infectious virus is not produced, but latent proteins are expressed. In the growth programme all nine latent proteins are expressed. The latency programme is what is found in 95% of adults carrying a benign lifelong infection and it enables the in vivo virus to last despite being transcriptionally quiet[541,534].

FIGURE 4-33

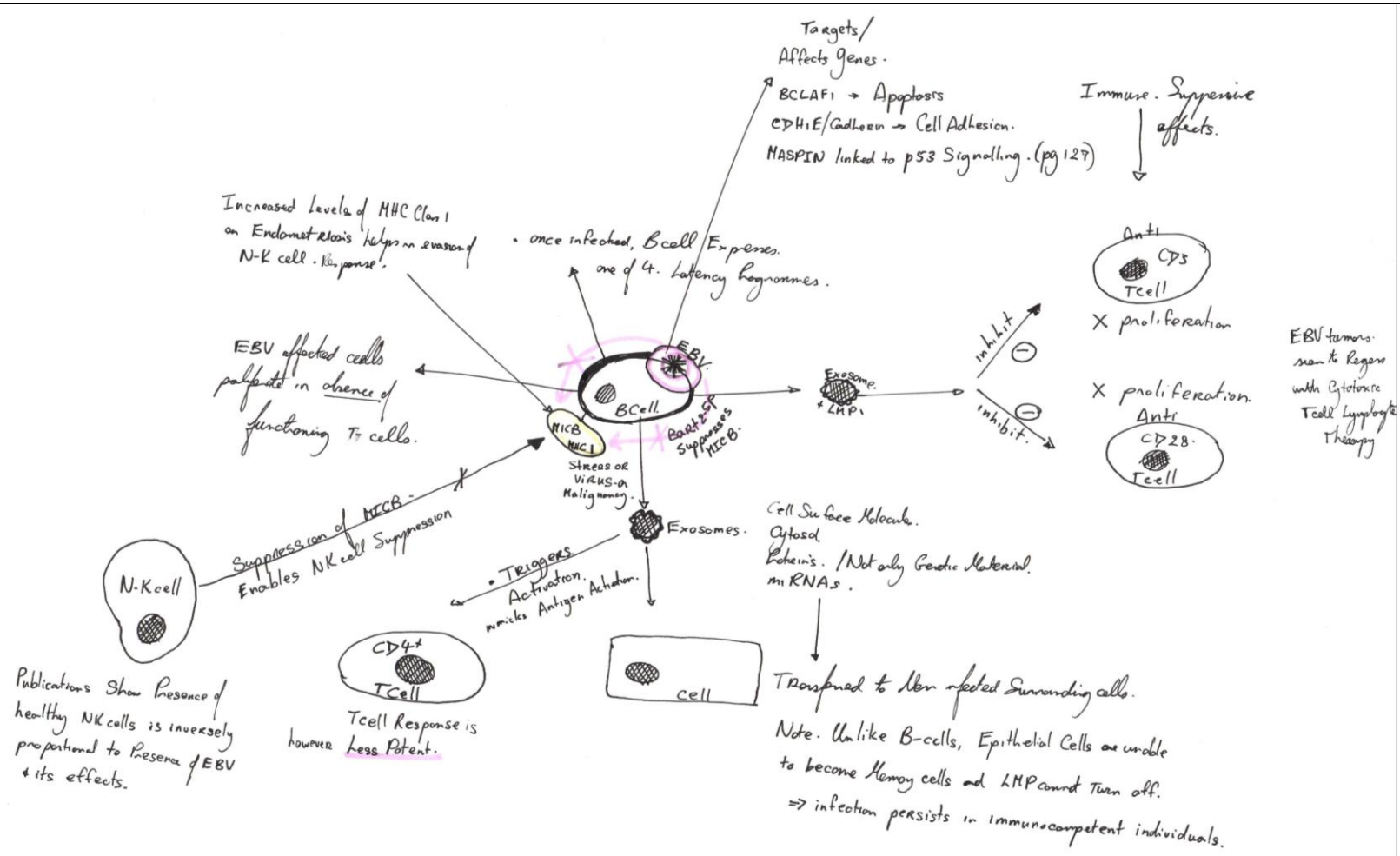

Hand drawn figure depicting the effects of exosomes from EBV-infected B-cells

FIGURE 4-34
Latency transcription programmes

	Genes expressed	Proposed function
Growth programme *	EBNA1-6 LMP1 LMP2A-B	Activates a resting B cell to become a proliferating lymphoblast
Default programme ǂ	EBNA1 LMP1 LMP2A	Provides necessary survival signals (i) infected lymphoblasts to differentiate into memory, and (ii) maintenance of persistently infected memory cells
Latency programme	None (LMP2A§)	Allows persistence of the virus in resting recirculating memory cells in a way that is non-pathogenic and not detectable by the immune system

' Sometimes referred to as Latency III ǂ Sometimes referred to as Latency II. § The transcript for LMP2A is often detected in these cells. EBNA, Epstein-Barr Virus nuclear antigen; LMP, latent membrane proteins

Figure showing three latency transcription programmes. Taken from Nature article by Thorley-Lawson *et al.*[541]

4.6.5 EBV associated with immunocompromisation

Endometrial cells are dynamic tissues that regenerate and differentiate in response to the hormonal stimuli controlling female menstruation. Their function is particularly important in preparing the uterus for embryo implantation during pregnancy[561]. Pregnancy itself is an immunocompromised state, one can theorise that any defect in the immune system potentially caused by viruses such as EBV, will affect the immune interactions within the endometrium causing failure of implantation. Excluding other confounding factors, patients with endometriosis have higher infertility rates when compared to women without endometriosis and the mechanism is not completely understood[34,198,562]. In understanding how EBV acts in immunocompromised patients could potentially allow us to understand the link between endometriosis and infertility.

As mentioned above in the *in vitro* studies, EBV affected B cells proliferate in the absence of functioning t-cells. Clinically this would be replicated in immunocompromised individuals such as in those with immunoblastic lymphomas where the disease is stimulated through EBV affected B cells in the absence of other genetic alterations and regresses with optimisation of the immune system through therapeutics. A classic clinical presentation is the development of tumours in transplant patients who are being immunocompromised to prevent organ rejection. In these patients immunosuppression leads to cytotoxic t-cell loss and the accumulation of EBV infected B cell proliferation[563].

In an immunocompetent person EBV is still associated with tumours. In these cases it is believed to be one of the contributing factors to malignancy rather than the sole causator. Burkitt's Lymphoma, Hodgkin's Lymphoma or nasopharyngeal carcinomas are all linked to earlier EBV infections[527].

Natural Killer cells play an imperative role in the elimination of cells which are either virally infected or transformed[564,565]. In 1992, a published study showed decreased NK cell activity on the peripheral blood and peritoneal fluid of women with endometriosis[566] (Figure 1-2). Tumour cells lacking major histocompatibility complex (MHC) class 1 expression preferentially cause NK cell recruitment and

activation causing lysis of the affected cells[565]. It is reported that increased levels of MHC class 1 on endometrial stromal cells of women with endometriosis helps in the evasion of NK cell response[567] (Figure 1-2). Monocytes from peritoneal fluid from women with endometriosis show an Interleukin- 10 (IL-10) dependant down regulation of expression of MHC class 2[568].

The prime role of this miRNA is to bind the MHC Class I Polypeptide-Related Sequence B (MICB) normally expressed in cells to ligate NK cells leading to death of the cell (Figure 1-2, Figure 4-33). MICB is induced in cells experiencing 'stress' or insults such as viral infections, inflammation or malignancy. If in endometriosis the MICB expression is suppressed by BART2-5p, this leads to the evasion of cell death by NK cells in the ectopic environment permitting ectopic endometrial cellular implantation. Observations of reduced NK cell activity in women with endometriosis supports the role of EBV BART2-5p in the avoidance of immune surveillance in endometriosis. Other publications show that the presence of healthy, functional NK cells is inversely proportional to the presence of EBV virus and its effects[513]. There are a number of predicted human target genes for EBV BART2-5p which have particular roles enabling ectopic tissue to engraft and survive. The BCLAF1 gene linked to apoptosis, the CDH1/E-Cadherin linked to cell adhesion and the MASPIN linked to p53 signalling are all implicated.

BCLAF1 gene encodes for Bcl-2-associated transcription factor 1 which is a Bcl-2 family protein. It does not however share structural similarities with these proteins[569]. Over expression of the BCLAF1 induces apoptosis and T cell proliferation. The expression of BART2-5p provides a survival advantage to ectopic endometrium having reduced apoptosis and avoiding immune surveillance by the t-cells (Figure 4-10). My study demonstrates the reduction of BCLAF-1 on tissue microarray analysis (TMA). Comparing levels between endometriotic tissue and normal endometrium, there is a statistically significant downregulation of BCLAF-1 in endometriosis compared to normal endometrium from cases ($P<0.0001$) (Figure 4-16, Table 4-5, Table 4-6).

CDH1/E-Cadherin is a master regulator of the G0/G1 stage of the cell cycle. It is associated with uterine tissue and the formation of correct placentation between the embryo and maternal circulation. Its role is to reduce cell adhesion, division and cycling. Loss of function or mutations in this gene are seen in gynaecological cancers. Its suppression in ectopic endometrial tissue predicts an increase in cell adhesion (observed in endometriosis) and removes the suppression on the G0/G1 cell cycle stage moving cells into the S phase.

Studies published show a reduction of E-Cadherin in endometriosis cells compared to normal endometrium. *In vitro* studies looking at collagen invasion assays show increased invasive potential with E-Cadherin negative cells. This is not seen in normal endometrial cells. This study confirms the downregulation of E-Cadherin protein in endometriosis as predicted with the BART2-5p up regulation. My study demonstrates the downregulation of E-Cadherin in endometriosis on tissue microarray (TMA) analysis. There is a statistically significant downregulation of E-Cadherin in endometriosis compared to normal endometrium from controls ($P<0.0001$) and normal endometrium from cases ($P=0.0017$) (Figure 4-12, Table 4-1, Table 4-2). The reduction in E-Cadherin enables the tissues to metastasise and infiltrate causing disease progression and creating an invasive pattern often seen in endometriosis.

Maspin gene was first identified in normal mammary cells but not in breast cancer derived epithelial cells, implicating it as having a role in tumour suppression, inhibition of cell migration angiogenesis and metastasis. It is expressed in normal endometrial cells and its suppression by BART2-5p leads to an increase in ability for the endometrium to migrate and survive. An activating p53 binding site was identified and showed Maspin to be the downstream effector gene. My study confirms the reduction of Maspin on tissue microarray (TMA) analysis. Comparing levels between endometriotic tissue and normal endometrium, there is a statistically significant downregulation of MASPIN in endometriosis compared to normal endometrium from controls ($P<0.0001$) and normal endometrium from cases ($P=0.2760$) (Figure 4-14,Table 4-3,Table 4-4).

4.6.6 Diagnosing pathology associated with EBV

Amplification through the polymerase chain reaction (PCR) or Nucleic acid sequence based amplification (NASBA) of viral nucleic acids of EBV is a technique used to identify the presence of virus. It cannot however differentiate between latent or active infection. PCR is however a good method to quantify EBV viral loads, which clinically is important when assessing for patient response to treatments[570].

Serum from patients with EBV associated malignancies can be processed with immunofluorescent assays or enzyme-linked immunosorbant assay (ELISA), both of which are EBV protein specific and are used to distinguish between latent and active infections. Viral antigens as well as immunoglobulins to the antigens can all be targeted in this approach but not all malignancies express these patterns to the same level making the technique unreliable for the identification of all known EBV associated tumours.

Other techniques employed include Southern blotting, the culturing of infected EBV lymphocytes and their study using electron microscopes, gene expression profiles and microarrays.

In my project I used tissue microarrays to analysis the miRNA expression between diseased and control tissues. I then used EBV in-situ hybridisation locating the virus within lymphocytes infiltrating the tissues. Quantitative PCR was then used to assess for the presence and numbers of EBV virus within the peripheral blood lymphocytes of cases versus control patients.

4.6.7 Treatments for EBV related tumours- research and therapeutics

4.6.7.1 Immunotherapies

Cytotoxic t-cells have been successfully used to directly target EBV antigens[571]. In the study by Heslop[571], 114 patients were given EBV specific cytotoxic t-cell infusions to prevent or treat post-transplant lymphoproliferative disorders. Apart from local areas of irritation, the therapies were successful. Out of the 101 patients who received infusions for prophylaxis, none developed disease while 11 of 13 patients who were treated for proven or probable lymphoproliferative disease had complete remission. In a separate study, peripheral blood was collected from allograft recipients prior to starting their immunosuppressive therapy. The t-lymphocytes were then stimulated *in vitro* to function as EBV specific cytotoxic t-lymphocytes. The primed lymphocytes were then transferred back into the patients believed to have high risk of developing post-transplant lymphoproliferative disease due to high initial tissue EBV levels[572]. The treatment was tolerated well by the recipient patients and despite the

immunosuppressive therapy, cytotoxic t-cell levels and functions were maintained. The EBV levels as assessed by their DNA levels were seen to fall in the treated group. Similar cytotoxic T-lymphocytes infusions were studied in patients who received T-cell depleted allogenic bone marrow transplants[573]. Once more, no major toxicity was reported and none of the transfused patients developed post-transplant lymphoproliferative disease compared to 15% of those who were not treated. Caution as to the efficiency of such therapies in advanced or rapidly progressive disease has been mentioned, making these therapies an exciting possibility for chronic slow growing diseases such as endometriosis. Future studies in the use of immunotherapies for endometriosis look promising.

4.6.7.2 Combination therapies for induction of lytic EBV infection

Inducing a lytic EBV infection within tumours through lytic-inducing chemotherapy releases EBV kinases that in turn activate Ganciclovir to its active cytotoxic state. Combined treatments are seen to be more effective than individual ones. The identification of CD70 in certain EBV positive tumours creates another target for anti-CD70 monoclonal antibodies. Monoclonal antibodies to CD20 (Rituximab), another protein expressed in EBV positive cancers, is another form of therapy used to target the EBV positive B cells in post-transplant lymphoproliferative disorders.

Combinations of therapies leading to cell cycle apoptosis (Gangiciclovir) and therapies that would upregulate viral enzymes (Butyrate) seem promising.

4.6.7.3 Cytotoxic therapies

With cytotoxic therapies the balance between the dosage and its resulting morbidity and mortality is vital. Therapies tend to be reduced in strength to prevent extreme morbidity. Unfortunately one sees a higher level of relapse at lower treatment dosages. Certain therapies show increased cytotoxicity in those cells expressing EBV virus which makes them ideal target therapies. Such a compound was Tubacin, which is seen to inhibit histone deacetylase 6 and was toxic to EBV positive cells through a caspase independent-3-pathway[574]. Cytotoxic therapies would not be ideal in women of reproductive age for the treatment of endometriosis. They might however be useful in women with severe endometriosis expressing high EBV levels and who have completed their family.

5 Endometriosis serum miRNA biomarker discovery study (molecular)

5.1 Introduction

Following the tissue miRNA study, other potential miRNA markers were examined for disease presence in the serum of patients compared to that of controls. The ability to predict presence of disease through a non-surgical technique would reduce patient morbidity and enable earlier disease identification and treatment.

5.2 Aims

- To obtain a set of serum samples from clinically well characterised patients who suffered from endometriosis with no other confounding pathology (Disease samples) and samples from surgically confirmed women without endometriosis or confounding pathology (Control samples).
- To assess for differences in serum miRNA expression between the serum of patients with endometriosis and the controls.
- To identify a panel of potential miRNA serum markers that could be used as a non-invasive diagnostic test for endometriosis.

5.3 Method

51 serum samples (endometriosis (n=36) vs control (n=15)) were taken from the patients recruited at surgery. Samples were stored at -80 ºC until required. They were then rapidly aliquoted from thawing to circumvent degradation of the samples during repeated freeze thaw cycles. Polypropylene sample tubes were labelled with sample identities ready for use and serum samples were then thawed at 20ºC for 30 minutes. One 300µL sample was taken from each tube for miRNA analysis and 22.5µLwas taken for autoantibody analysis. The remaining volume was dispensed into 5 x 200µL aliquots in labelled sample tubes (Table 9-16, Table 9-17). Any remaining sample was left in the original sample tube. The tubes were frozen and stored at -80ºC together with the original sample tubes. Due to variation in sample volumes some samples only yielded 2 or 3 aliquots. Samples were thawed directly prior to the assay and were randomised and split into assay racks of 23 samples each. Each assay rack contained both case and control samples and one pooled normal human serum control sample which was used to monitor assay performance. The serum was assayed for the presence of miRNAs using the Discovery Array v2.0 and the standard biomarker discovery protocol (Section 2.6.3 and Section 2.6.4).

5.3.1 Validation of miRNA in serum of subjects suffering from endometriosis using qPCR

For quantitative PCR (“qPCR”) usage, Life Technologies’ (“LifeTech”) TaqMan® miRNA assays were used. These assays are continuously aligned with releases from the miRBase database and they represent

all known miRNAs from human beings, as well as all known human viral miRNAs. The TaqMan® miRNA assays employ a novel target-specific stem-loop reverse transcription primer to address the challenge of the short length of mature miRNA. The primer extends the 3' end of the target to produce a template that can be used in standard TaqMan® assay–based real-time PCR. Also, the stem-loop structure in the tail of the primer confers a key advantage to these assays: that of the specific detection of the mature, biologically active miRNA. Using the significant markers identified in the miRNA microarray experiments, a sub-selection of miRNAs were analysed using the LifeTech TaqMan® miRNA qPCR assays, according to their standard protocol[575].

The TaqMan® miRNA assays were scanned using a ViiA™ 7 Real-Time PCR System using an excitation wavelength suitable for the detection of the labelled miRNAs. The qPCR scans produced traces for each TaqMan® miRNA assay which can be used, to determine the amount of specific miRNA within a given sample, relative to a passive reference dye (for example, but not limited to, ROX). The raw qPCR traces contained raw signal intensity to which an assay threshold was applied after the raw traces have been baseline normalised, which removed aberrant signals. This threshold line intersects the qPCR trace at the point on the qPCR trace where the trace is logarithmic. From this, the qPCR cycle (Ct) was determined. The qPCR traces were analysed using LifeTech's proprietary analysis software. The median Ct and mean quantity was taken across the three sample replicates for each TaqMan® miRNA assay. Testing for statistically significant associations between the two groups (case vs control) was carried out by applying linear models to the normalised sample data to identify general miRNA changes between case samples and control samples. Statistical differences were calculated using a t-test. The data from the microarray and TaqMan® miRNA qPCR assays were analysed for Pearson correlation to assess the cross-platform robustness of the observed results (Figure 5-1). Figure 5-1 demonstrates that there is good correlation between a subset of the miRNA probes used for qPCR compared to those identified on the microarrays.

FIGURE 5-1

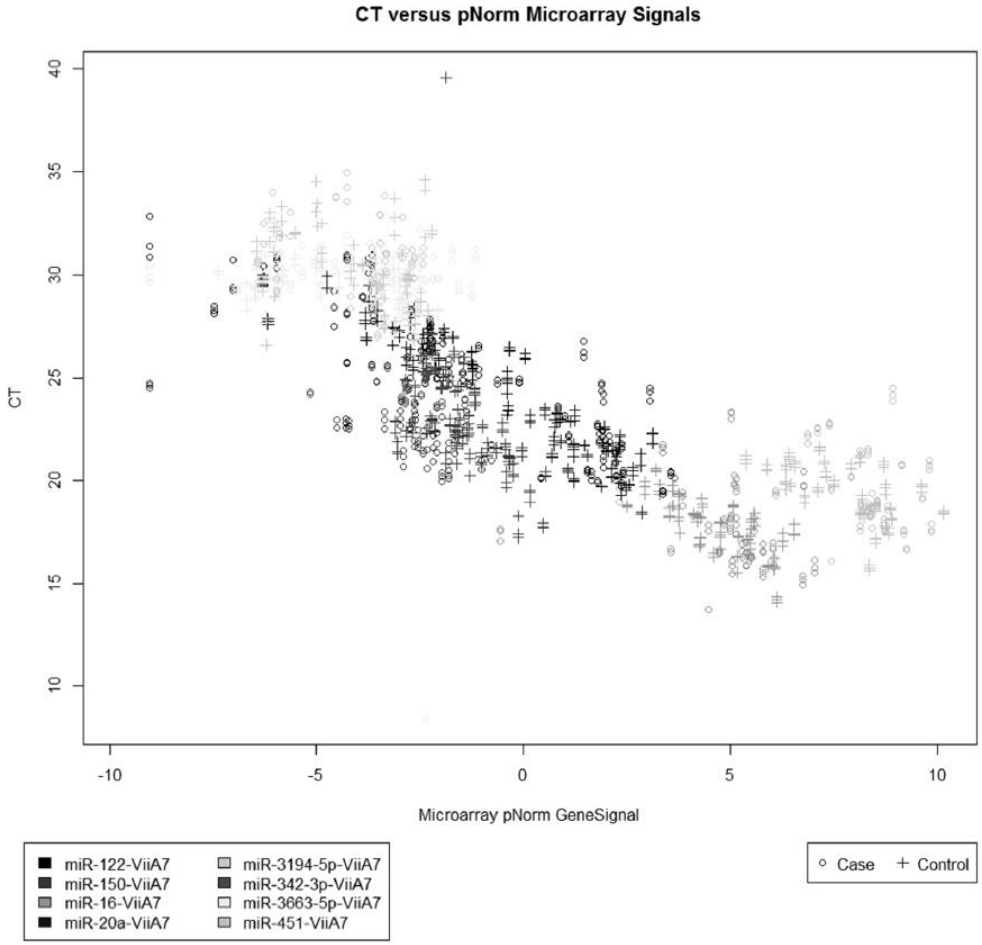

Scatter plot showing CT versus pNorm for microarray signals

5.4 Results

MiRNA microarray assays were carried out to identify putative markers for distinction of endometriosis cases from healthy control samples (Table 5-1). All samples passed quality control- arrays passed all of 584 scanning, labelling and spike-in quality control metrics to a standard of 'good' or 'excellent'. All arrays passed the cut off for the minimum number of miRNAs detected (100). Pooled tissue control samples show good Pearson correlation (0.9) of detected miRNAs with those run in previous array batches.

TABLE 5-1

Cohort	Reproductive cycle stage		Total samples
Endometriosis case	Follicular	21	36
	Mid	3	
	Luteal	12	
Healthy control	Follicular	9	35
	Luteal	26	
Pooled tissue control			2
Total samples			**73**

Table showing the categorisation of samples used for serum miRNA experiments

5.4.1 Data handling

Data was filtered to only include miRNAs detected in at least 75% of either cases or controls (217 miRNAs). Signals below the limit of detection were set to half the value of the minimum observed signal. Signals were normalised to the 95th percentile. Logs of these signals were used for statistical analysis. There was a difference between the 2 batches of arrays, with more miRNAs being consistently detected in the additional batch of controls. This difference causes clear artefacts for many of the miRNAs and the batch data was therefore included in the statistical model to attempt to mitigate the effect of this bias in the analysis. Samples were checked for clustering via Principal Component Analysis (PCA) and hierarchical clustering for all provided annotations to look for general patterns in the data. None of the provided sample annotations appear to be driving large scale effects in the data and so have not been included as factors in the analysis.

5.4.2 Differential expression

The probed and dried arrays were scanned using a microarray scanner using an excitation wavelength suitable for the detection of the labelled miRNAs and to determine the magnitude of miRNA binding to the complementary detection probe. The microarray scans produced images for each array that were used to determine the intensity of fluorescence bound to each oligonucleotide spot which were used to normalise and score array data. The raw microarray scan image contained raw signal intensity (also referred to as the relative fluorescent unit, RFU) for each oligonucleotide spot (also referred to as a feature) on the array. The images were feature extracted using Agilent's proprietary feature extraction software. The resulting average intensities of all oligonucleotide features on each array were then normalised to reduce the influence of technical bias (e.g. laser power variation, surface variation, input miRNA concentration, etc.) by a percentile normalisation procedure. A linear model was fitted to evaluate statistical differences in miRNA expression between cases and controls. In the volcano plot below, the x-axis shows the log2 fold change between case and control and the y-axis shows statistical significance (negative log of the p-value to the base of 10). A selection of significant hits is highlighted (Figure 5-2).

FIGURE 5-2

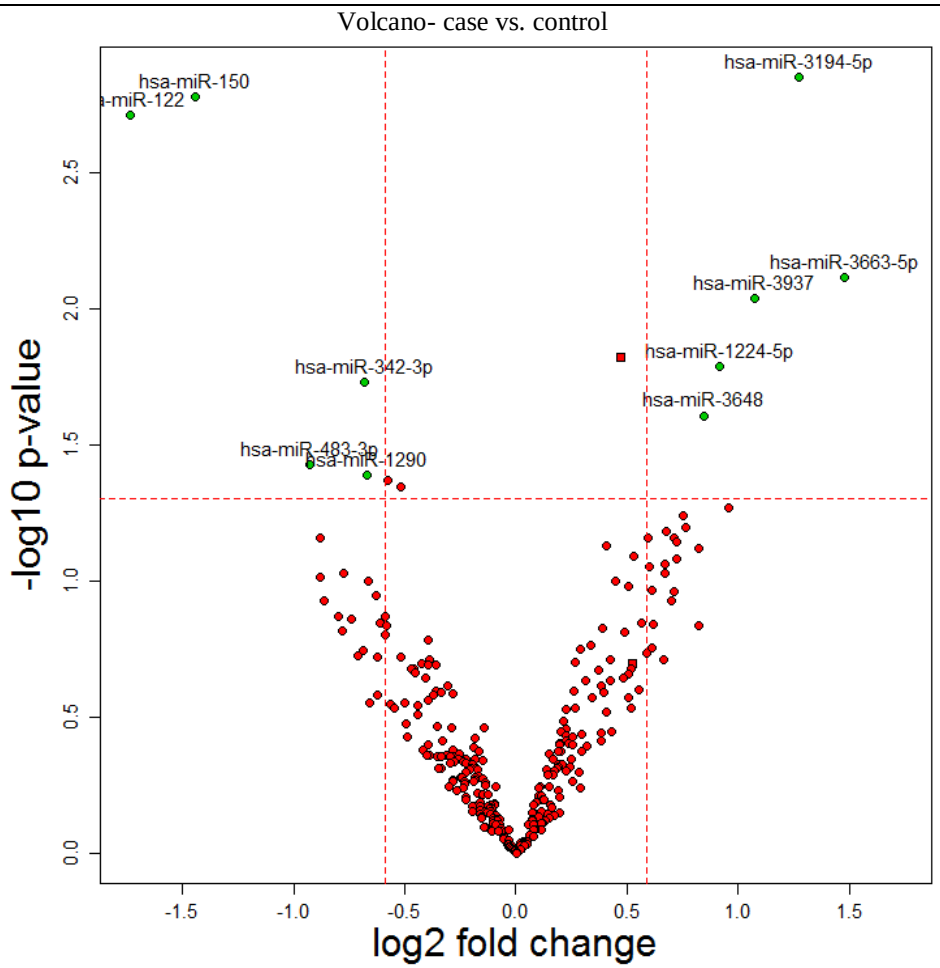

On the volcano plot, the x-axis shows the log2 fold change between case and control and the y-axis shows statistical significance (negative log of the p-value to the base of 10). The volcano plot analysing case vs. controls indicates a selection of significant hits in the serum miRNA experiments seen as dots above the horizontal line.

The hierarchical clustering of the significant miRNAs according to the type of tissue (i.e. case vs. control) is shown in Figure 5-3, where black signifies high expression, white signifies intermediate expression, and grey signifies low expression.

FIGURE 5-3

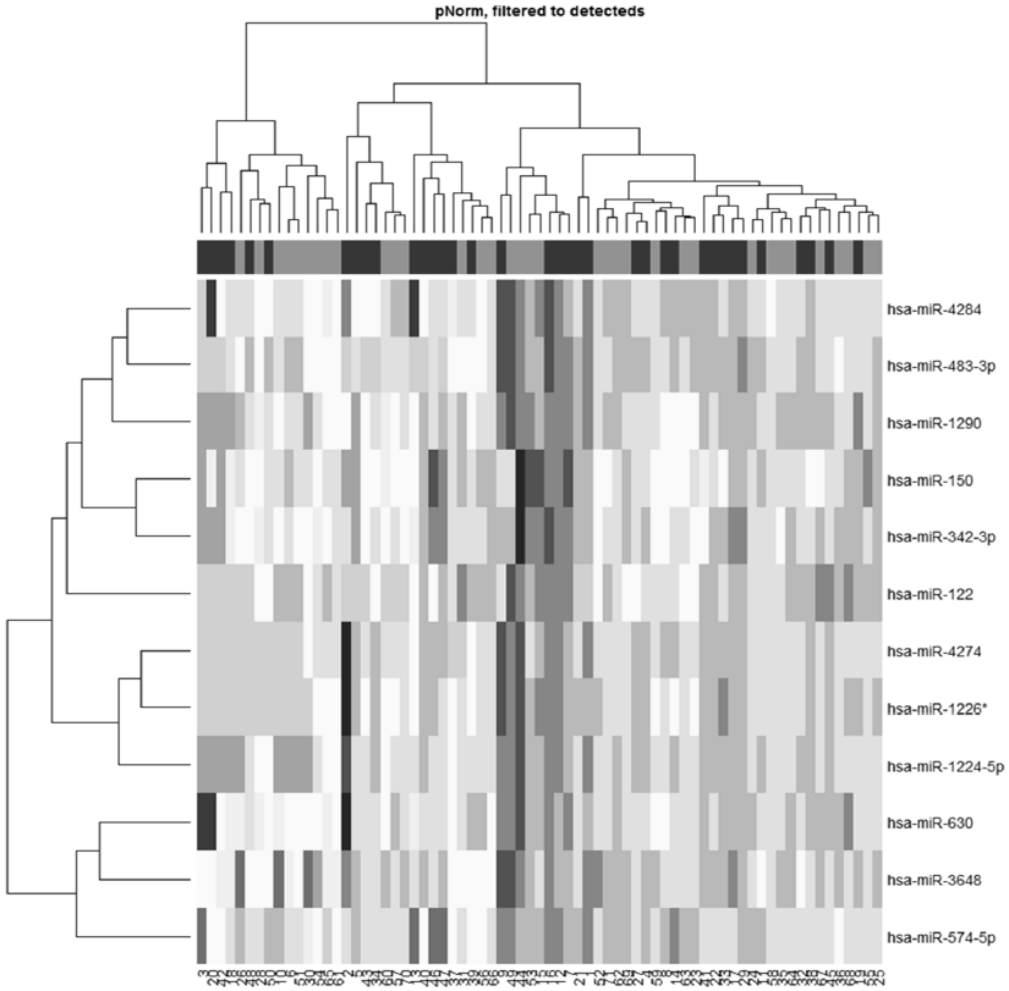

Hierarchical clustering of the significant miRNAs according to the type of tissue case versus control

5.4.3 Differential expression- additional samples

The addition of a further 20 control samples (to balance the numbers of case and control numbers) changed some of the significant hits, generally allowing the removal of probable false-positive hits near the lower limit of detection from the original data set.

The plots below show the results from analysis prior to inclusion of the additional controls (Figure 5-2) to that with their inclusion (Figure 5-4). The most significant hits remain largely unchanged.

FIGURE 5-4

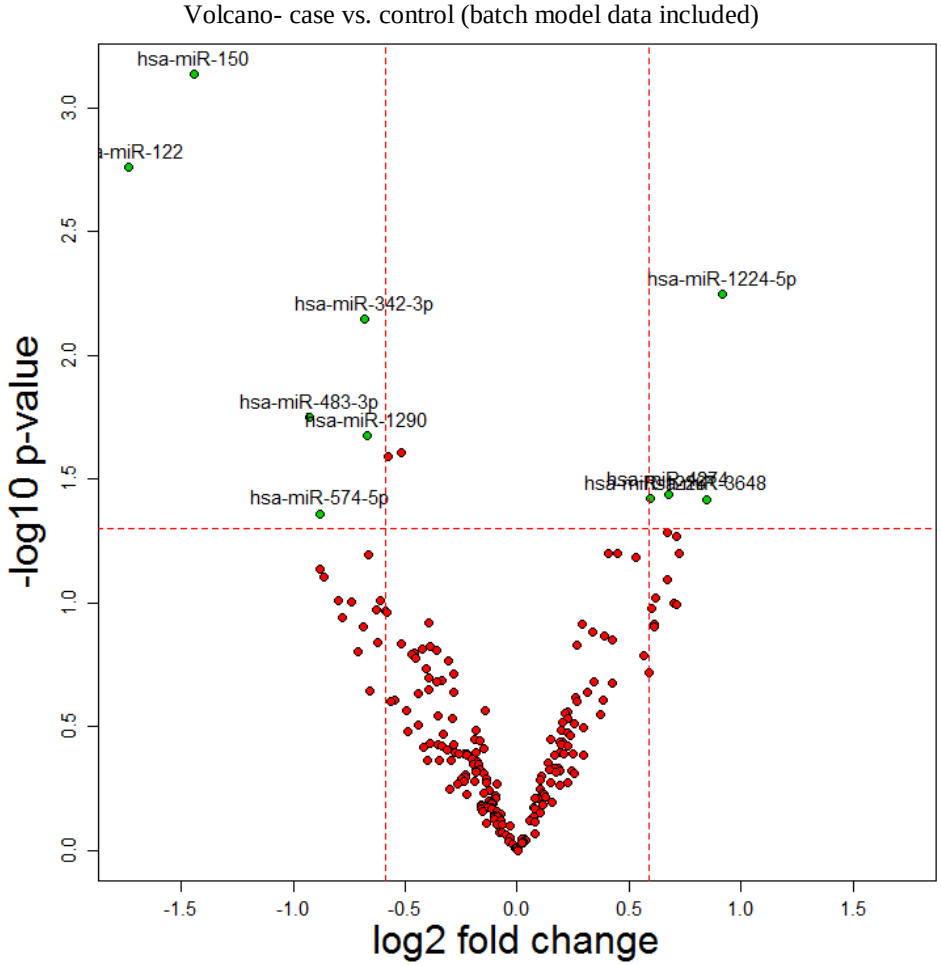

On the volcano plot, the x-axis shows the log2 fold change between case and control and the y-axis shows statistical significance (negative log of the p-value to the base of 10). The volcano plot analysing case vs. controls (batch model data included) indicates a selection of significant hits in the serum miRNA experiments.

5.4.4 Case vs. control top hits- downregulated in disease

8 markers are significantly downregulated in disease ($p < 0.05$, no multiple testing correction). Below are the distributions for the top 2 downregulated miRNAs by p-value i.e. hsa-miR-150 and hsa-miR-122 (Figure 5-5).

FIGURE 5-5

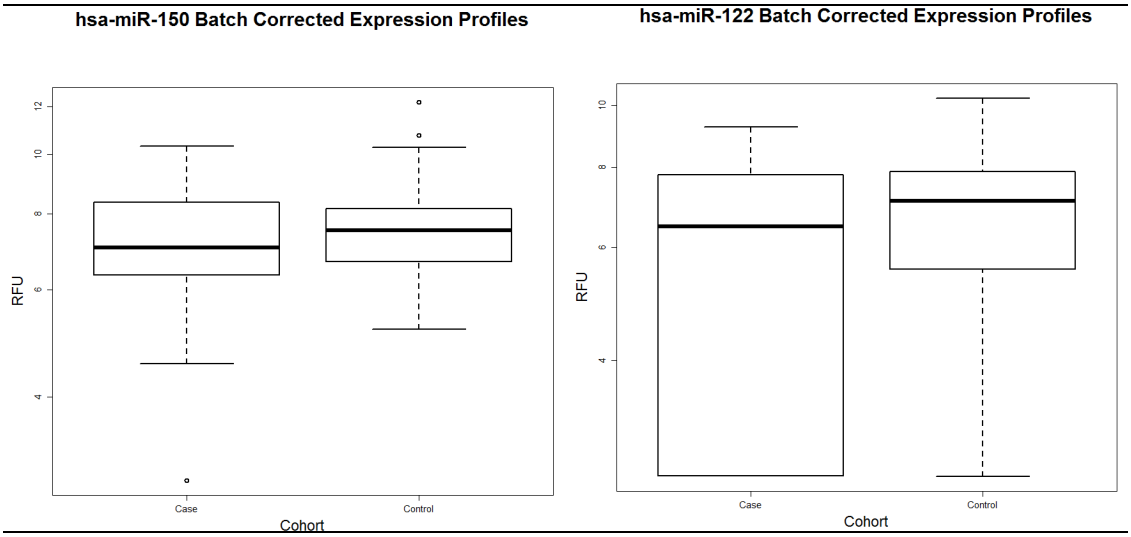

Boxplots showing distribution for the top 2 markers (hsa-miR-150 and hsa-miR-122) downregulated in endometriosis in serum miRNA experiments.

5.4.5 Case vs. control top hits- upregulated in disease

4 miRNAs are significantly up regulated in disease ($p < 0.05$, no multiple testing correction applied). Below are the distributions for the top 2 upregulated miRNAs by p-value i.e. hsa-miR-1224-5p and hsa-miR-4274 (Figure 5-6).

FIGURE 5-6

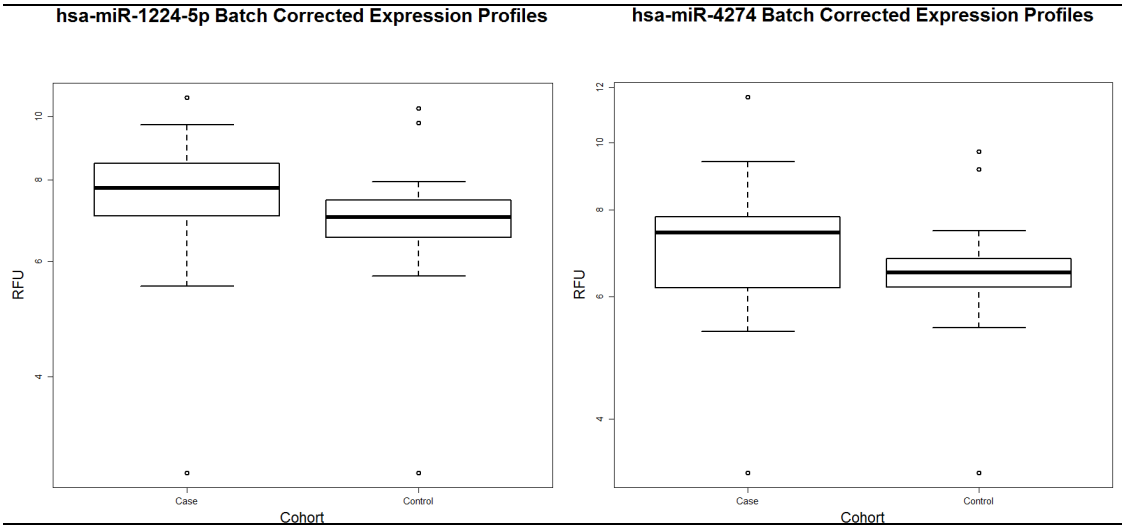

Boxplots showing distribution for the top 2 markers (hsa-miR-1224-5p and hsa-miR-4274) upregulated in endometriosis in serum miRNA experiments.

5.4.6 Expression- all significant hits

The heat map (Figure 5-7) shows the expression in case and control samples of the 12 significant markers (8 downregulated and 4 upregulated). Samples are in columns and are coloured by disease stage, with green indicating controls and red indicating the cases. miRNA data is scaled by row, with red signifying

high miRNA expression, yellow intermediate miRNA expression and blue low miRNA expression (Figure 5-7).

FIGURE 5-7

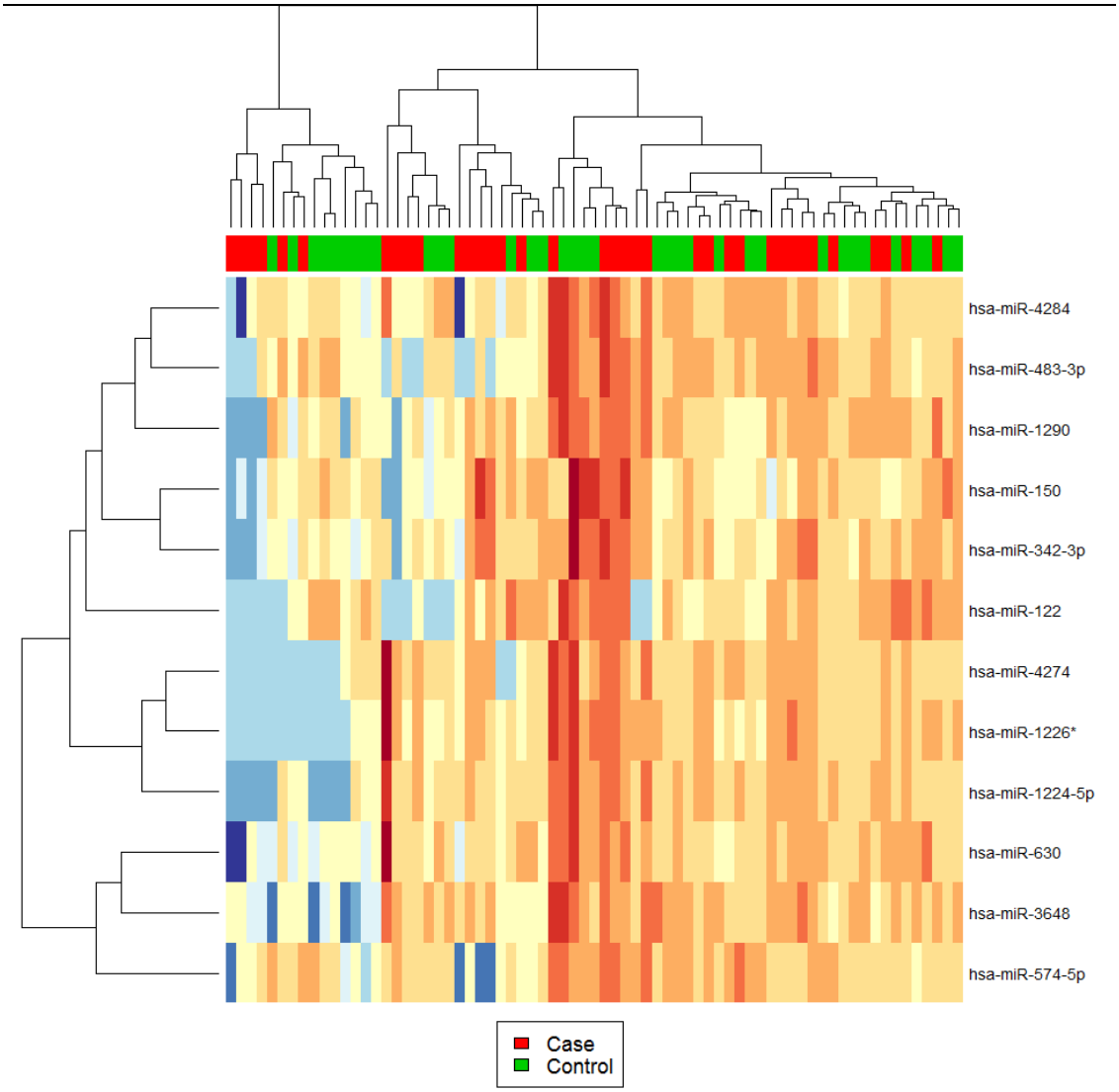

The heat map shows the expression in case and control samples of the 12 significant markers. The x-axis demonstrates control samples in green and case samples in red. The y-axis lists the identified markers, each categorised by miRNA data intensity expressed: red signifying high miRNA expression, yellow intermediate miRNA expression and blue low miRNA expression.

5.4.7 miRNA in serum- qPCR analysis

A set of 5 differentially expressed and 3 control miRNAs (451, 16, 20a) were assayed via qPCR across the full set of endometriosis and healthy volunteer samples. In the qPCR a positive reaction was determined by fluorescent signal levels. The cycle threshold (Ct) was used to define the number of qPCR cycles required for the fluorescent signals to cross the background level threshold. The higher the amount of target miRNA present, the lower the Ct level. Data of Ct results was plotted in a scatter diagram against the normalised values of the gene signals obtained through the microarrays. These assessed for any correlation between the data obtained through these two separate analysis techniques. 2 of the markers show poor correlation between the microarray and qPCR data (Pearson rho less than 0.2). These

are the 2 markers with the lowest levels of detection and were not significantly different on addition of the further controls (miRNAs 3663-5p and 3194-5p).

4 of the selected miRNA markers show good correlation (Pearson rho 0.5 to 0.7). These are miRNAs 150, 122, 342-5p and 451 (control) (Figure 5-8).

FIGURE 5-8

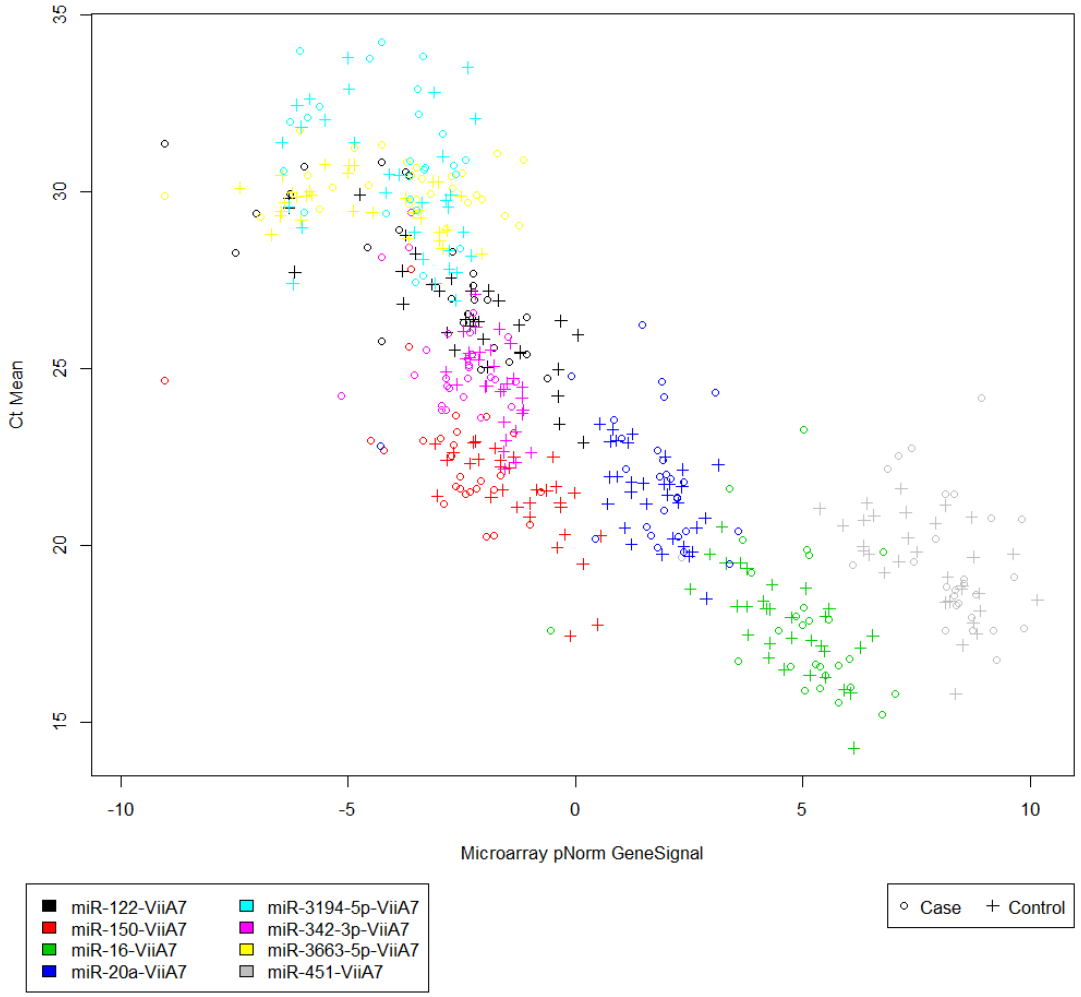

Scatterplot of Ct results (y-axis) against the normalised values of the gene signals obtained through the microarray (x-axis) in cases and controls

There is evidence ($p<0.05$) for batch differences between the control samples from the first and second collection. This has been corrected for in the analysis. T-tests show that miRNAs 150 and 122 are significantly down in disease ($p<0.05$). These markers are also showing good correlation between the platforms. miRNA 342-3p is significant at a less stringent confidence ($p < 0.1$) and is also down-regulated in disease (Figure 5-9).

FIGURE 5-9

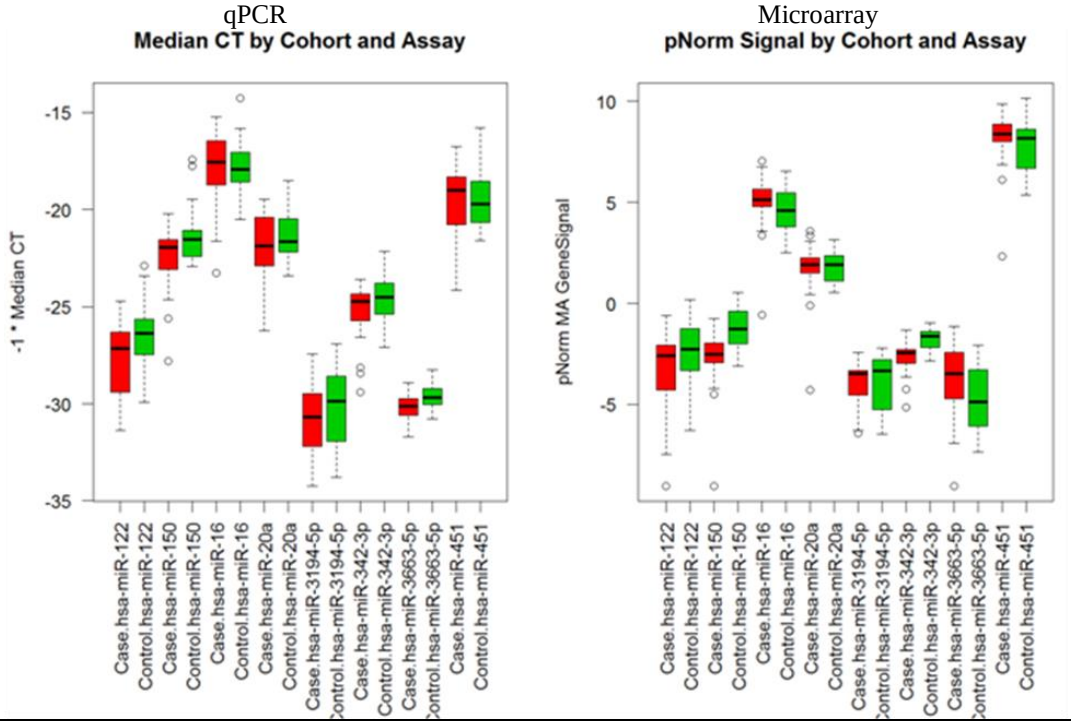

The left boxplot shows results obtained from PCR. It plots on the x-axis each identified miRNA marker against the median Ct value for case (red box) and controls (green box). The right boxplot shows results obtained from microarray. It plots on the x-axis each identified miRNA marker against the pNorm gene signal value for case (red box) and controls (green box).

Some significant markers have been identified in case vs. control samples (uncorrected $p<0.05$). The most significant markers have low signal strength, near the lower limit of detection for the microarray platform. qPCR analysis is supportive of three of the markers that have significant downregulation in disease: miRNAs 150, 122 and 342-3p. There is a significant batch effect correction in this data. Some of the selected markers have been influenced by this and one cannot be sure that the correction is working perfectly. Therefore, some caution is required in interpreting these results.

5.5 Discussion

5.5.1 miRNA serum analysis

A minimum of six on-line prediction databases were accessed for each analysed miRNA (Gene cards, microrna.org, Target Scan, Star Base, Diana Lab, miRDB).Prediction targets for each miRNA were assessed from the databases and hits ran numerically from a thousand to seven thousand in number. The PCT is the probability of conserved targeting for highly conserved miRNA families. Target gene tables were sorted by the highest PCT value (0.8 and higher). The top 100 predicted targets from each database were selected and each predicted target was counter checked for similarity against each database. Targets that gave hits in at least two of the databases were selected as potential targets for the respective miRNA. Results were inserted into gene prediction programs such as STRING™ and a literature search for each assessed miRNA was performed to identify pathways of disease. Panther™ program was used to predict

involved pathways regulated through identified miRNA and an extensive summary of their functions and pathway involvement was performed.

The following section is aimed at analysing the molecular and cellular functions of the proteins which were most highly associated with the respective upregulated and downregulated identified miRNAs. In Section 5.8 I proceeded to look at the overall cellular functions affected by the identified miRNAs and their proteins which could give us a better clinical understanding of how this multifactorial disease develops.

5.5.2 Summary and salient points of identified pathways linked to upregulated hsa-mir-1224-5p, hsa-mir-4274 and downregulated hsa-mir-150, hsa-mir-122

- Pathways affected by miRNAs expressed in endometriosis could potentially contribute to development of disease through the deregulation of their control. Below is a summary and list of all the genes and their associated pathways. It is beyond the scope of this chapter to determine which are the most likely proteins or genes or pathways to cause (or enable to a larger extent) the development of the disease of endometriosis. This would require a separate body of work with functional models to determine important molecular or protein roles (Figure 5-10, Figure 5-11).

- Table 5-2 , Table 5-3, Table 5-4 and Table 5-5 summarise pathways affected by the respective miRNAs, which will been discussed in the following sections of my thesis (see sections 5.5.2, 5.7 and 5.8).

- Identified miRNAs are seen to interact with a number of important pathways listed below. There could potentially be effects on cellular mitosis and meiosis, cellular structure, intra and intercellular signalling, vesicular transport including exo and endocytosis and cellular apoptosis. All of these changes can result in endometriotic cells that replicate at accelerated rates, adhere to ectopic sites, enable angiogenesis and growth, evade normal apoptotic mechanisms and evade immune responses (Figure 5-10, Figure 5-11).

- Certain identified pathways act as tumour suppressors that could potentially explain the non-malignant properties in the majority of cases of endometriosis. These include the p38 MAPK[1] pathway and the p53 tumour suppressor genes[2].

- Other pathways summarised below are known to be associated with tumorigenesis and have pro-oncogenic properties, these include the RAS, WNT, TRK receptors and MAPKKKK pathways.

- It is the fine balance between tumour suppressors and oncogenes that probably control the transition between endometriosis and endometrial carcinomas.

FIGURE 5-10

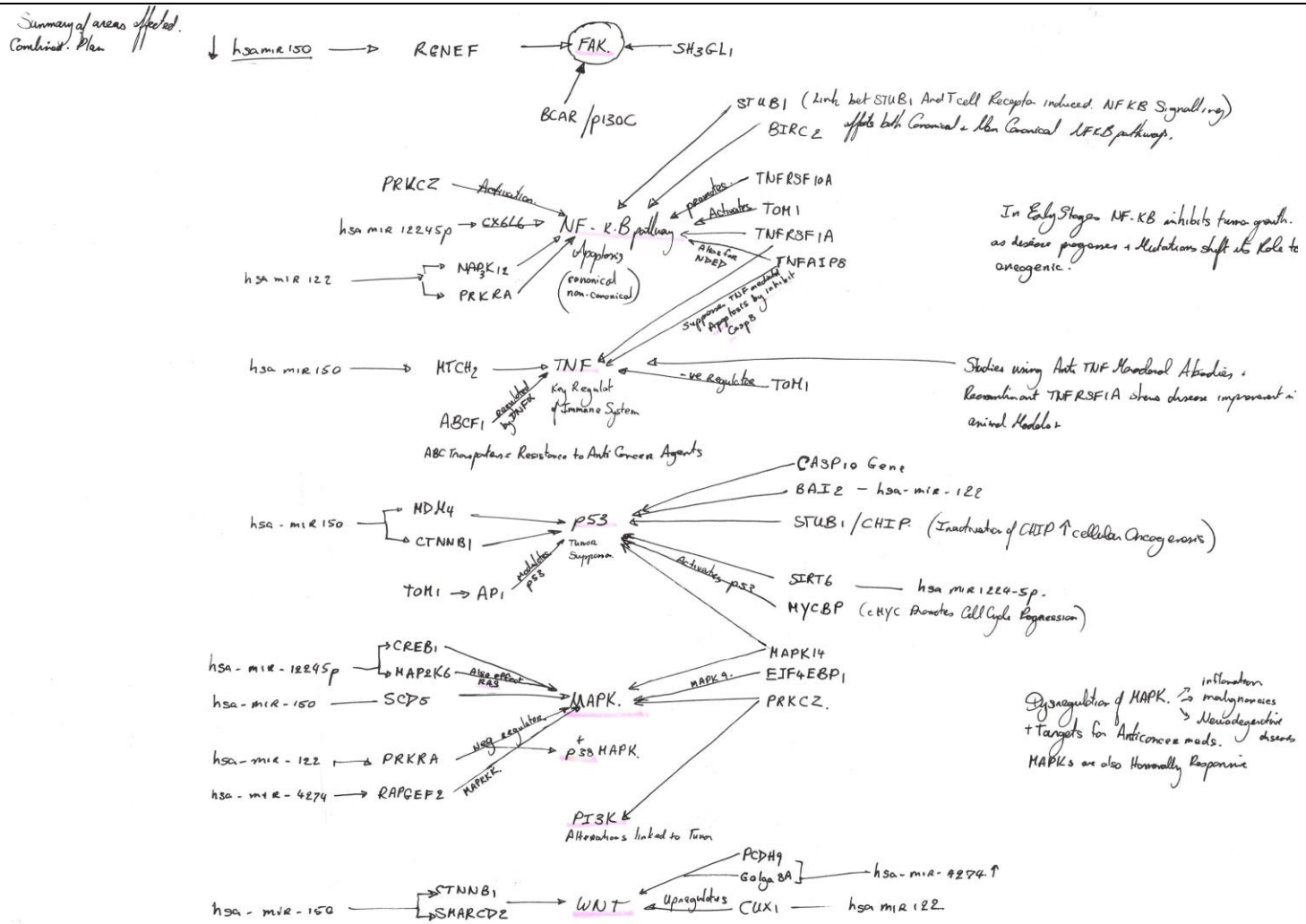

Hand drawn figure summarising the function of identified miRNAs, their associated genes and proteins and the pathways they effect

FIGURE 5-11

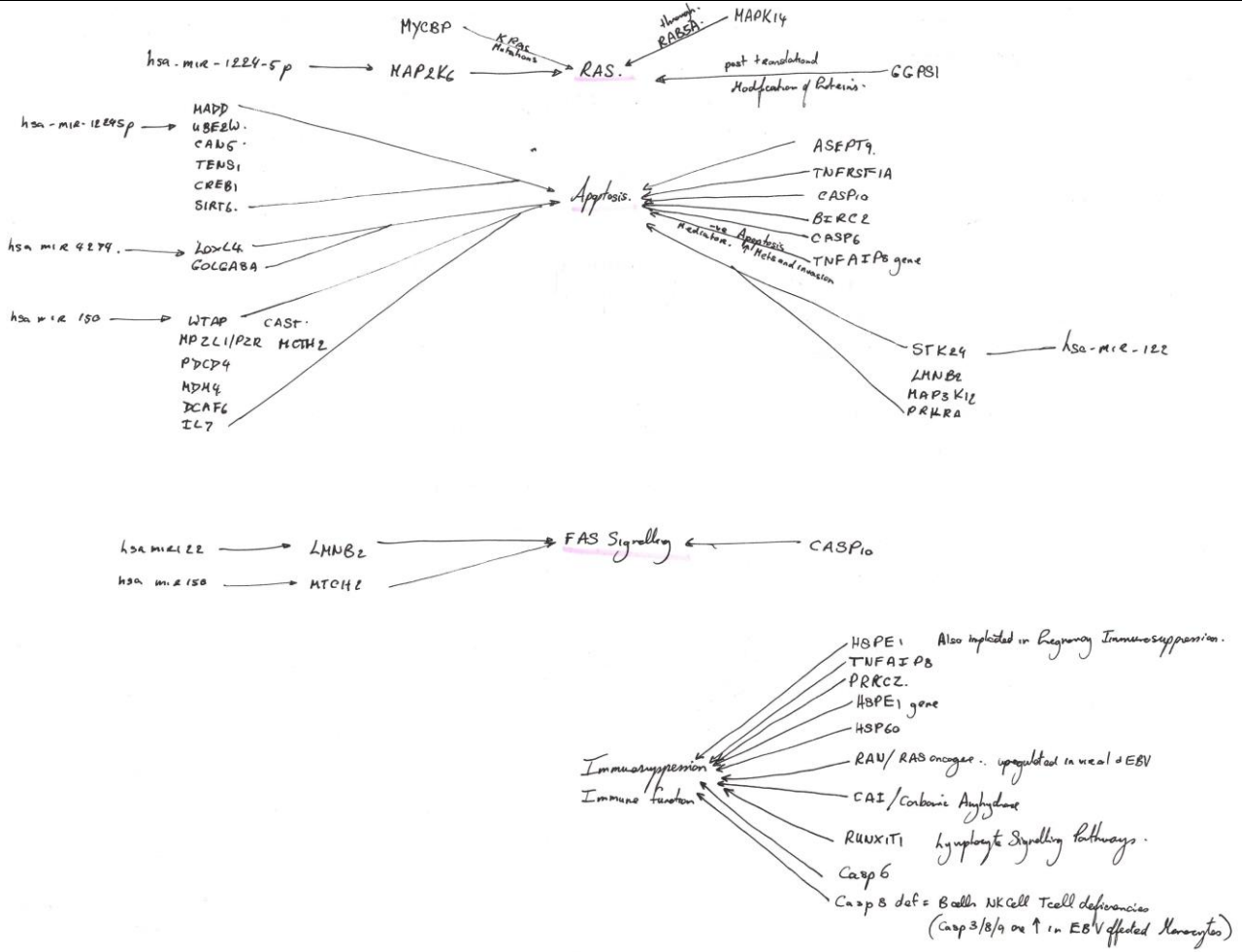

Hand drawn figure summarising the function of identified miRNAs, their associated genes and proteins and the pathways they effect

TABLE 5-2

Pathway	Genes regulated by hsa-miR-1224-5p
Apoptosis signalling pathway	Cyclic AMP-responsive element-binding protein (CREB1)
B Ras pathway	Dual specificity mitogen-activated protein kinase kinase 6 (MAP2K6)
Cytokine-mediated signalling pathway	C-X-C motif chemokine 6 (CXCL6)
EGF receptor signalling pathway	Dual specificity mitogen-activated protein kinase kinase 6 (MAP2K6)
FGF signalling pathway	Fibroblast growth factor receptor 1 (FGFR1)
G-protein coupled receptor protein signalling pathway	SEC14 domain and spectrin repeat-containing protein 1 (SESD1)
Gi alpha and Gs alpha mediated pathway	Cyclic AMP-responsive element-binding protein (CREB1)
Gonadotropin releasing hormone receptor pathway	Cyclic AMP-responsive element-binding protein (CREB1) Transcription factor Sp1 (SP1) Dual specificity mitogen-activated protein kinase kinase 6 (MAP2K6)
Heterotrimeric G-protein signalling pathway	Cyclic AMP-responsive element-binding protein (CREB1)
I-kappaB, kinase/NF-kappaB cascade	C-X-C motif chemokine 6 (CXCL6)
Inflammatory pathway mediated by chemokine and cytokine signalling	Cytohesin-2 (CYTH2)
JNK cascade	SEC14 domain and spectrin repeat-containing protein 1 (SESD1) C-X-C motif chemokine 6 (CXCL6) MAP kinase-activating death domain protein (MADD)
p38 MAPK pathway	Cyclic AMP-responsive element-binding protein (CREB1) Dual specificity mitogen-activated protein kinase kinase 6 (MAP2K6)
P53 pathway	NAD-dependent deacetylase sirtuin-6 (SIRT6)
Rod outer segment phototransduction	Cyclic nucleotide-gated cation channel beta-3 (CNGB3)
Signalling pathway of heterotrimeric G-protein	Cyclic nucleotide-gated cation channel beta-3 (CNGB3)
Tyrosine kinase signalling pathway	Fibroblast growth factor receptor 1 (FGFR1)
Ubiquitin proteasome pathway	Ubiquitin-conjugating enzyme E2 W (UBE2W)

A table summarising pathways affected by miRNA hsa-miR-1224-5p expressed in endometriosis.

TABLE 5-3

Pathway	Gene regulated by hsa-mir-4274.
Alzheimer's disease amyloid secretase pathway	Serine/threonine-protein kinase N2 (PKN2)
Cadherin signalling pathways	Protocadherin-9 (PCDH9)
cGMP dependent pathways	cGMP-dependent protein kinase 2 (PRKG2)
Endothelin signalling pathway	cGMP-dependent protein kinase 2 (PRKG2)
G-protein coupled receptor protein signalling pathway	Rap guanine nucleotide exchange factor 2 (RAPGEF2) Pituitary adenylate cyclase-activating polypeptide type I receptor (ADCYAP1R1)
Gonadotropin releasing hormone receptor pathway	Pituitary adenylate cyclase-activating polypeptide type I receptor (ADCYAP1R1)
Hedgehog signalling pathway	Golgin subfamily A member 8A (GOLGA8A)
Heterotrimeric G-protein signalling pathways (G1/Gs α and Gq/G0 α)	Regulator of G-protein signalling 20 (RGS20)
MAPKKK cascade	Rap guanine nucleotide exchange factor 2

	(RAPGEF2)
Muscarinic acetycholine receptor 1 and 3 signalling pathway	Serine/threonine-protein kinase N2 (PKN2)
PDGF signalling pathway	Serine/threonine-protein kinase N2 (PKN2)
Transmembrane receptor protein tyrosine kinase signalling pathway	Rap guanine nucleotide exchange factor 2 (RAPGEF2)
Wnt signalling pathways	Protocadherin-9 (PCDH9) Golgin subfamily A member 8A (GOLGA8A)

A table summarising pathways affected by miRNA hsa-miR-4274 expressed in endometriosis.

TABLE 5-4

Pathway	**Gene regulated by hsa-miR-150.**
Alzheimer's disease presenilin pathway	Catenin beta-1 (CTNNB1)
Angiogenesis	Catenin beta-1 (CTNNB1)
Cadherin signalling pathways	Catenin beta-1 (CTNNB1)
Cytokine-mediated signalling pathway	Interleukin-7 (IL7)
Erythrocyte membrane protein band 4.1-like protein 5 (EPB41L5)	Erythrocyte membrane protein band 4.1-like protein 5 (EPB41L5)
Insulin/IGF pathway-protein kinase B signalling cascade	Protein Mdm4 (MDM4)
Gonadotropin releasing hormone receptor pathway	Adiponectin receptor protein 2 (ADIPOR2) Catenin beta-1 (CTNNB1)
Interleukin signalling pathway	Interleukin-7 (IL7)
JAK-STAT signalling pathways	Interferon-induced protein with tetratricopeptide repeats 5 (IFIT5)
Janus kinase and signal transducer and activator of transcription (JAK-STAT) cascade	Interleukin-7 (IL7)
Methionine biosynthesis pathway	Cystathionine gamma-lyase (CTH)
Methycitrate cycle	Cytoplasmic aconitate hydratase (ACO1)
Nicotine pharmacodynamics pathway	Erythrocyte membrane protein band 4.1-like protein 5 (EPB41L5)
p53 pathway	Protein Mdm4 (MDM4) Catenin beta-1 (CTNNB1)
Semaphorin mediated axon guided pathway	Semaphorin-3A (SEMA3A)
TNF-α/ FAS death receptor pathways	Mitochondrial carrier homolog 2 (MTCH2)
Trans-sulfuration pathway	Cystathionine gamma-lyase (CTH)
Tricarboxylic acid cycle	Cytoplasmic aconitate hydratase (ACO1)
WNT signalling pathway	SWI/SNF-related matrix-associated actin-dependent regulator of chromatin subfamily D member 2 (SMARCD2) Catenin beta-1 (CTNNB1)

A table summarising pathways affected by miRNA hsa-miR-150 expressed in endometriosis.

TABLE 5-5

Pathway	**Genes regulated by hsa-miR-122**
Apoptosis signalling pathway	Interferon-inducible double stranded RNA-dependent protein kinase activator. A (PRKRA)
Complement activation pathways	Testican-2 (SPOCK2)
Dopamine receptor mediated signalling pathway	Chloride intracellular channel protein 4 (CLIC4)
FAS signalling pathway	Lamin-B2 (LMNB2)
G-protein coupled receptor protein signalling pathway	ARF GTPase-activating protein GIT1 (GIT1) Brain-specific angiogenesis inhibitor 2 (BAI2)
Gonadotropin releasing hormone receptor pathway	Mitogen-activated protein kinase kinase kinase 12 (MAP3K12)
I-kappaB kinase/NF-kappaB cascade	Mitogen-activated protein kinase kinase kinase 12 (MAP3K12)

JNK signalling oxidative stress response pathway	Dual specificity protein phosphatase 4 (DUSP4) Mitogen-activated protein kinase kinase kinase 12 (MAP3K12)
Nicotine pharmacodynamics pathway	Chloride intracellular channel protein 4 (CLIC4)
P53 pathway	Brain-specific angiogenesis inhibitor 2 (BAI2)
Serine/threonine kinase signalling pathway	Mitogen-activated protein kinase kinase kinase 12 (MAP3K12)

A table summarising pathways affected by miRNA hsa-miR-122 expressed in endometriosis.

5.6 Detailed analysis for upregulated miRNAs

4 miRNAs were upregulated in endometriosis with the top two miRNAs identified as hsa-mir-1224-5p and hsa-mir-4274.

5.6.1 Hsa-mir-1224-5p

FIGURE 5-12

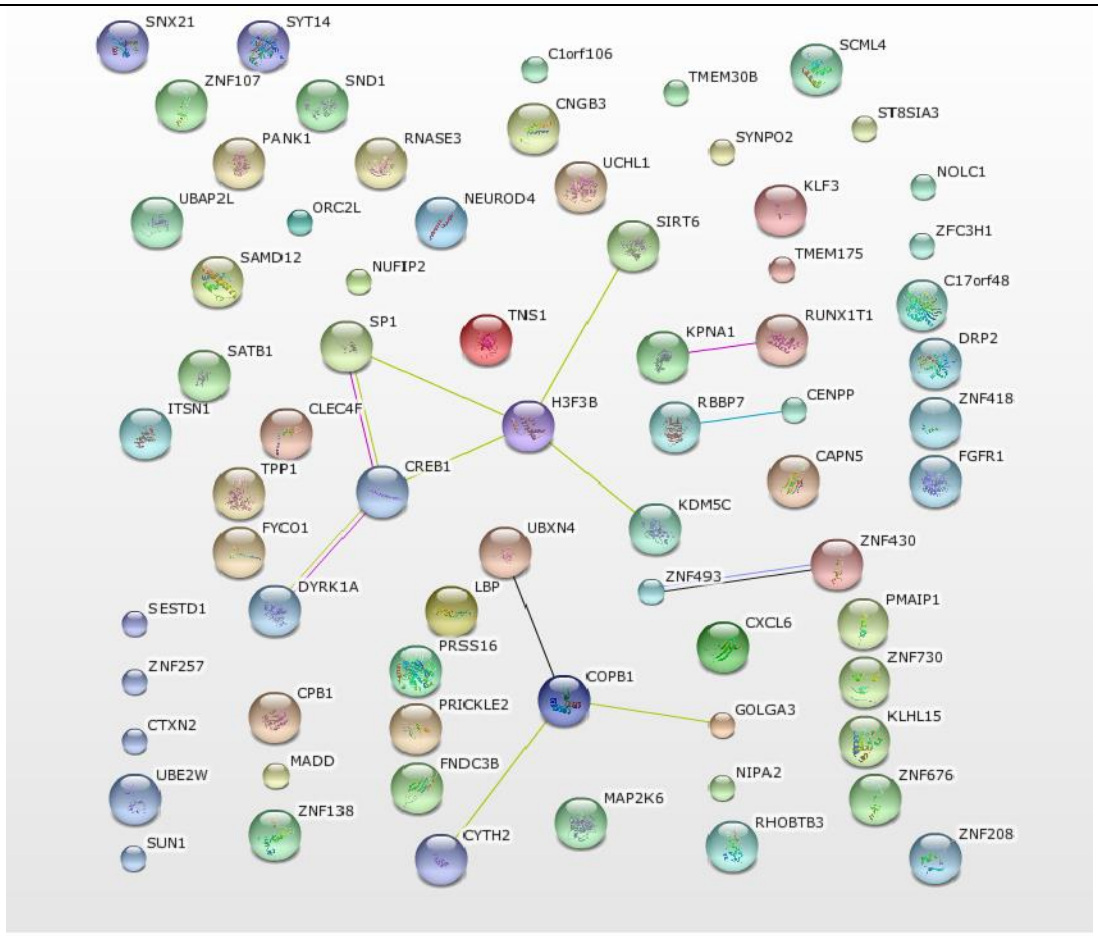

Predicted evidence view of interactions of Hsa-mir-1224-5p[576]

A number of pathways, proteins and genes have been identified associated with development of disease (Figure 5-12).

Ubiquitin-conjugating enzyme E2 W (UBE2W) is a gene with ligase activity involved in various cellular processes, regulating chromosome segregation and dorsal ventral axis specification of nuclear cellular material[496,577,578]. It is implicated in the processes of mitosis and meiosis as well as protein modification and cellular proteolysis. UBE2W is a negative regulator of apoptosis and has been noted as a key role player in embryonic development. It is part of the ubiquitin proteasome pathway[526]. By negatively regulating apoptosis and altering cellular replication processes it could potentially be one of the genes enabling endometrial cell survival and engraftment in ectopic sites, causing endometriosis.

Fibroblast growth factor receptor 1 (FGFR1) is a member of the tyrosine kinase signalling pathway acting as a transmembrane receptor[496,578]. It is a constituent of the FGF signalling pathway and the angiogenic pathway. Promotion of angiogenesis is a key factor enabling survival and implantation of ectopic endometrial cells.

Sorting nexin-21 (SNX21) is involved in intracellular signalling cascade[496].

Origin recognition complex subunit 2 (ORC2) is responsible for DNA replication origin binding within the cell cycle. Cellular effects of genes such as SNX21 and ORC2 are complex as they act on the cell cycle and signalling. Possible dysregulation of finely tuned cellular functions at this level can result in endometriosis cells achieving properties enabling them to proliferate and survive in ectopic body sites.

Sex comb on midleg-like protein 4 (SCML4) has chromatin binding and transcription factor activity[496,578] and is involved in the cell cycle in the regulation of transcription from the RNA polymerase 2 promoter. It is responsible for the establishment and maintenance of chromatin architecture in the cell[577].

SUN domain-containing protein 1 (SUN1) Synaptopodin-2 (SYNP2) and Prickle-like protein 2 (PRIC2), are all structural constituent of the cellular cytoskeleton. They regulate the morphogenesis of the cell and its components and are important in mitosis and cellular motion processes[496,578]. Like UBE2W, PRIC2 is important in the dorso-ventral axis formation of the cell. Cellular chromatin structure does not only control intra and intercellular signalling, it is also involved in cellular growth, adhesion and proliferation. The presence of genes such as SUN1 and SCML4 identified in patients with endometriosis could potentially contribute to disease development by altering cellular structure, adhesiveness, signalling and proliferation.

Calpain-5 (CAN5) is a gene which has cysteine-type peptidase activity and is involved in calcium, calmodulin and calcium-dependant phospholipid binding in the cell. It is involved in the processes of apoptotic induction, processing of the immune system and proteolysis. In humans it has been linked to PCOS (Polycystic ovarian syndrome) and Huntington's disease[496,577,578]. The apoptotic mechanism is vital in controlling cellular growth, proliferation and differentiation. Recognition of abnormal or ectopic cells is a vital constituent of the patient's immune system. If in endometriosis these two systems are dysregulated, they will potentially contribute to formation of endometriotic cells, aid implantation and avoid immune system recognition.

Tensin-1 (TENS1) is again another structural cytoskeleton constituent with a phosphoprotein phosphatase activity and has a role in actin binding[496,578]. It is involved in numerous cellular processes including cell cycle control, signal transduction, cellular adhesion and motion and the induction of apoptosis. It also has

a role in the immune system and mesodermal development. Aberrations in the cellular cycle and abovementioned cellular functions will potentially contribute to altered cellular properties enabling growth of disease such as endometriosis.

Transcription factor Sp1 (SP1) is involved in transcription from RNA polymerase 2 promoter and has a role in the immune system[496]. In humans it is a constituent of the gonadotropin releasing hormone receptor pathway[526]. GnRH analogues are one of the current treatments used for the suppression of endometriosis. They induce a "medical menopause" for a period of usually three to six months depending on their dosage. They do not treat disease, but rather suppress proliferation in preparation for other medical interventions such as surgery or fertility treatments. Mechanisms explaining their exact effect and function on endometriotic cells are not completely understood. The regulation of SP1 could potentially explain part of their clinical action and understanding endometriosis at such a molecular level could potentially give us insights into novel disease therapeutics.

Cyclic AMP-responsive element-binding protein (CREB1) has transcription factor activity and has a role in nucleic acid binding and regulating transcription from RNA polymerase 2 promoter[496,578]. It is found in numerous biological and cellular processes including ectodermal and nervous system development and immune system processes. Within the cell is has the function of signal transduction and is seen in cellular stress responses. It has roles in six major pathways including: Heterotrimeric G-protein signalling pathway-Gi alpha and Gs alpha mediated pathway->CREB binding protein, p38 MAPK pathway->cAMP response element binding protein, transcription regulation by bZIP transcription factor->cAMP response element binding protein, enkephalin release->cAMP response element binding protein, gonadotropin releasing hormone receptor pathway->CREB and the apoptosis signalling pathway->Activating transcription factor[526]. Any dysregulation of the CREB1 protein can potentially impact the cell function at various levels through important pathways as discussed above. This could explain the development of pathology such as endometriosis that requires alterations in cellular adhesion, signalling, function and immune system evasion to proliferate in ectopic sites.

Krueppel-like factor 3 (KLF3) is another gene with transcription factor activity, regulating transcription from RNA polymerase 2 promoter[496,577,578]. It is implicated in B-cell mediated immunity, mesodermal development and haemopoiesis. In my study, I have already identified the EBV virus as being present and potentially a contributing factor to development of endometriosis (See sections 4.5.2.1, 4.5, 4.4.2.1 and 4.4.3.5). Complex interactions between B and T cells of the immune system could also be deregulated by other genetic alterations or aberrations such as those in KLF3. This gene might therefore be yet another contributor to development of endometriosis and is therefore another potential therapeutic target.

SEC14 domain and spectrin repeat-containing protein 1 (SESD1) is a regulator of GTPase activity and is involved in guanyl-nucleotide exchange factor activity. It is implicated in B cell mediated immunity and cellular defence response, calcium mediated signalling and neurological system processes. It is part of the JNK cascade and the G-protein coupled receptor protein signalling pathway.

C-X-C motif chemokine 6 (CXCL6) is a chemokine involved in response to interferon-gamma, macrophage activation and the cellular defence responses. It has a function in cell-cell and calcium mediated signalling and motion. It is a part of the cytokine-mediated signalling pathway, JNK cascade

and I-kappaB, kinase/NF-kappaB cascade. Biologically it is involved in mesoderm development, angiogenesis and blood coagulation. This chemokine is yet another example of a molecule involved in important cellular processes. Endometriosis is a multifactorial disease involving ectopic cells with altered characteristics of adhesion, implantation and growth as well as the ability to evade the immune system. CXCL6 has links to all of these functions making it another potentially interesting molecule attributing to disease development.

Lipopolysaccharide-binding protein (LBP) is involved in the processes of macrophage activation, defence responses to bacteria and lipid transport[496,578]. It is released in response to cellular stresses and is also a constituent of other metabolic processes such as that of cholesterol.

C-type lectin domain family 4 member F (CLC4F) is a member of the c-type lectin superfamily which has receptor activity[496,577,578]. It is involved in macrophage activation, intracellular protein transport, receptor-mediated cellular endocytosis, cell surface receptor linked signal transduction, cell-cell adhesion and cell surface receptor linked signal transduction. Biologically it is involved in the cellular defence response and blood coagulation pathways. Alterations in any of these pathways could contribute to the development of endometriosis though alterations of cellular properties and evasion of the cellular defence response mechanisms.

Pantothenate kinase 1 (PANK1) has kinase activity and is a coenzyme in metabolic processes[496,578]. It is involved in the production of Coenzyme A from panthotenate.

Dual specificity mitogen-activated protein kinase kinase 6 (MAP2K6) is a protein kinase involved in the phosphate metabolic process and amino acid phosphorylation within the cell[496]. It is involved in EGF receptor signalling pathway (Dual specificity mitogen-activated protein kinase kinase 3 and 6), bRas Pathway (Mitogen-activated protein kinase kinase 3 and 6), gonadotropin releasing hormone receptor pathway (MKK3/6) and the p38 MAPK pathway (mitogen-activated protein kinase kinase 6)[526]. Pathways such as the EGF signalling pathways are linked to the development of tumours and have been the targets for therapeutics in the field[579]. The presence of MAP2K6 could affect important tumorigenic pathways such as EGF and RAS enabling the development of endometrial ectopic tissue into endometriosis. An effect on the hormonal GnRH pathways could also affect endometriosis where cells are known to proliferate under hormonal triggers.

Sia-alpha-2,3-Gal-beta-1,4-GlcNAc-R:alpha 2,8-sialyltransferase (ST8SIA3) has transferase activity for glycosyl groups and is involved in polysaccharide and lipid metabolic processes and protein amino acid glycosylation[496,578].

Eosinophil cationic protein ribonuclease, RNase A Family, 3 (RNASE3) has endoribonuclease activity and is involved in nucleic acid and protein binding as well as inhibits enzyme activity[496,577,578]. Biologically it is involved in RNA catabolic processes, mesodermal development and angiogenesis. Any molecule supporting angiogenesis is vital for implantation and growth of tissue at ectopic sites. Endometriosis tissues are seen to implant ectopically within the pelvis proliferating once angiogenesis has occurred.

Staphylococcal nuclease domain-containing protein 1 (SND1) has transcription factor and co-factor activity. It enables transcription from RNA polymerase 2 promoter and binds to nucleic acid[496,578].

Zinc finger protein 208 (ZNF208), DNA-binding protein SATB1 (SATB1), Putative zinc finger protein 730 (ZNF730), Zinc finger protein 107 (ZNF107) Zinc finger protein 418 (ZNF418), Zinc finger protein 676 (ZNF676), Protein core-binding factor, runt domain, alpha subunit 2; translocated to 1 (CBFA2T1) (RUNX1T1) all have transcription factor activity and regulate transcription for RNA polymerase 2 promoter[496,577,578]. These genes (apart from special AT-rich sequence binding protein 1 (SATB1) and RUNX1T1) are Krüppel associated (KRAB) box transcription factors. RUNX1T1 also maintains cellular chromatin architecture.

NAD-dependent deacetylase sirtuin-6 (SIRT6) is involved in chromatin and nucleic acid binding and has deacetylase activity. It regulates transcription from RNA polymerase 2 promoter and maintains cellular chromatin architecture[496]. It forms part of the p53 pathway[526]. The p53 pathway is usually activated by stress signal such as oncogenes, cellular damage, DNA damage or abnormal adhesion molecules[580]. It then is involved in response to the stressors through regulation of growth or cellular arrest, apoptosis or repair of damaged DNA. Changes in this pathway through molecules such as SIRT6 could create an environment where ectopic cells such as endometriotic cells can proliferate and grow. Studies looking at gynaecological cancers in the presence of endometriosis, have shown common alterations in p53, PTEN and ARID1A[581]. Endometriosis has not been classified as a malignant tumour, though it does have properties of proliferation, dissemination, implantation at ectopic sites, angiogenesis, growth and evasion of the body's immune system, all of which are seen in malignancies. Disruption of certain pathways such as the p53 pathway in addition to other multifactorial influences ranging from environmental oxidative stressors to viral infections, growth factors, hormonal influences, diet and an altered patient immune system[581] may all play a fine balance in enabling endometriosis growth but preventing overt development of malignancy.

Dual specificity tyrosine-phosphorylation-regulated kinase 1A (DYRK1A) has protein tyrosine kinase activity and is a non-membrane spanning protein[496,578].

Thymus-specific serine protease (PRSS16), Carboxypeptidase A6 (CPA6), Ubiquitin carboxyl-terminal hydrolase isozyme L1 (UCHL1), Tripeptidyl-peptidase 1 (TPP1) are all involved in proteolysis[496,577,578]. PRSS16 and TPP1 are serine proteases. CPA6 is a mettaloprotease and UCHL1 is a cysteine protease. UCHL1 has been implicated in disease such as Parkinson's.

Lysine-specific demethylase 5C (KDM5C) has zinc finger transcription factor activity and causes transcription from an RNA polymerase 2 promoter. It has been implicated in spermatogenesis[496].

Dystrophin-related protein 2 (DRP2) is a structural constituent of the cytoskeleton and causes binding of both Actin and Calcium. Biologically it is involved in a multitude of cellular processes including muscle contraction, neurological system processes and nervous system development, neuromuscular synaptic transmission and nitric oxide mediated signal transduction[496,578]. Cellularly it is involved in cellular adhesion, motion, morphogenesis of its components and the cell cycle, it is also involved in ectodermal and mesodermal development.

MAP kinase-activating death domain protein (MADD) has multiple cellular functions[496,577,578]. It binds proteins, is a regulator for GTPase activity and acts in guanyl-nucleotide exchange. It is implicated in the neurological system process and synaptic transmission, induction of apoptosis and the JNK cascade. It is involved in ectoderm and nervous system development.

Neurogenic differentiation factor 4 (NEUROD4) has transcription factor and nuclease activity regulating transcription from RNA polymerase 2 promoter[496,577,578]. It acts in neurological system processes and nervous system development. It has a role in ectoderm development.

Kelch-like protein 15 (KLH15) has serine-type peptidase activity and transcription factor and cofactor activity[496,578]. It is involved in the regulation of transcription from the RNA polymerase 2 promoter forming a structural constituent of cytoskeleton involved in actin binding; it is therefore responsible for the morphogenesis within cellular components. Cellular morphogenesis enables vesicular transfer with and between cells, enabling transmission of cell signals or components. The vesicular system is also used by viruses such as EBV (See section 4.6.4) enabling the transfer of viral genetic material[553,554,560] through endo and exocytosis. Proteins affecting cellular vesicles such as KLH15, ITSN1 (below) and SYT14 (below) may therefore contribute directly or indirectly to enabling disease development of endometriosis.

Intersectin-1 (ITSN1) functions as a small GTPase regulator. It is involved in cellular calcium and G-protein binding and is responsible for transmembrane protein trafficking in the cell and controls endocytosis[496,577,578]. Other cellular functions involve signal cellular transduction and synaptic transmission through neurotransmitter secretion.

Synaptotagmin-14 (SYT14) is a membrane trafficking regulatory protein[496,578]. It has a role in endocytosis and exocytosis of synaptic vesicles and intracellular protein transport. It too therefore has a function in cellular signal transduction and synaptic transmission.

Cytohesin-2 (CYTH2) is a guanyl-nucleotide exchange factor[496,578]. It forms part of the inflammatory pathway mediated by chemokine and cytokine signalling involved in the process of exocytosis and cataboloic cellular processes with amino acids.

Cyclic nucleotide-gated cation channel beta-3 (CNGB3) has voltage gated potassium channel activity as well as cation channel and cyclic nucleotide-gated ion channel activity[496,578]. It has a role in signal transduction and cation transport and is involved in the signalling pathway of heterotrimeric G-protein and the rod outer segment phototransduction.

Histone-binding protein RBBP7 (RBBP7) has receptor activity and is seen in various biological processes including: intracellular protein transport, peroxisomal transport, intracellular signalling cascades, DNA repair and nuclear mRNA splicing, via spliceosome[496,577,578]. It is also involved in the establishment or maintenance of chromatin architecture.

Rho-related BTB domain-containing protein 3 (RHOBTB3) is a member of the small GTPase class of proteins[496,578]. It is involved in the process of protein binding, intracellular protein transport and the intracellular signalling cascade and has a role in receptor-mediated endocytosis and the G-protein coupled receptor protein signalling pathway. As discussed previously, proteins such as KLH15, ITSN1, SYT14

and COPB1 (See below) all have a role in vesicular cellular transfer. Vesicles are an important means of inter and intracellular transfer of information and have been used by viruses to escape immune system recognition and invade new cells. EBV utilises the same vesicular transport mechanisms for transfer of its exosomes (See section 4.6.4) to and between cells, molecules such as the ones above will therefore enable the transmission of the EBV virus aiding the formation and growth of diseased endometriosis cells.

Coatomer subunit beta (COPB1) is a vesicle coat protein and enables intracellular protein transport and exocytosis[496,578].

Importin subunit alpha-1 (KPNA1) is a transfer/carrier protein which targets proteins and enables nuclear transport[496].

The following genes and proteins have been identified as downstream targets of hsa-mir-1224-5p[496,576,578]. Their roles and functions in literature are not currently clearly defined: *Zinc finger protein 138 (ZNF138), Zinc finger protein 493 (ZNF493), UBX domain-containing protein 4 (UBXN4), Uncharacterized protein C1orf106 (C1orf106), Centromere protein P (CENPP), Magnesium transporter NIPA2 (NIPA2), FYVE and coiled-coil domain-containing protein 1 (FYCO1), Cortexin-2 (CTXN2), Transmembrane protein 175 (TMEM175), Cell cycle control protein 50B (TMEM30B), Fibronectin type III domain-containing protein 3B (FNDC3B), Sterile alpha motif domain-containing protein 12 (SAMD12), Zinc Finger protein 430 (ZNF430), Golgin subfamily A member 3 (GOLGA3), Zinc finger C3H1 domain-containing protein (ZFC3H1), Ubiquitin-associated protein 2-like (UBAP2L), Manganese-dependent ADP-ribose/CDP-alcohol diphosphatase (C17orf48), Phorbol-12-myristate-13-acetate-induced protein 1 (PMAIP1), Zinc finger protein 257 (ZNF257), Nucleolar and coiled-body phosphoprotein 1 (NOLC1).*

5.6.1.1 Summary of important identified points

- From the above list of genes and proteins controlled by Hsa-mir-1224-5p, one can see effects on the cellular functions of apoptosis, cell adhesion, cellular migration, cytoskeletal structure, cellular signal transductions and vesicular formation. Various proteins are also seen to potentially affect the immune system, altering ectopic cellular recognition, facilitating evasion and enabling implantation and growth.

- Relating back to the information above, there are varied roles which each protein or gene is known to carry out though it is difficult to determine which of these pertains a leading role, or which of these follow on as a secondary response to alternate cellular processes.

- It is beyond the scope of this chapter to determine which are the most likely proteins or genes to cause (or enable to a larger extent) the development of the disease of endometriosis. This would require a separate body of work with functional models to determine important molecular or protein roles.

- Using the identified proteins and genes, to perform functional modelling studies, to establish which molecules have more pertinent roles, could serve as an interesting body for future work.

5.6.2 Hsa-mir-4274

FIGURE 5-13

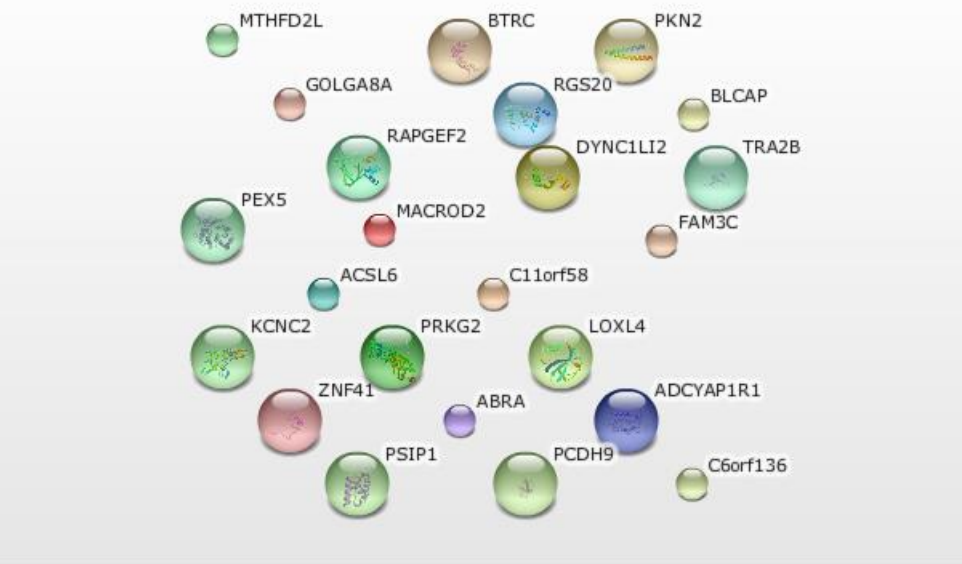

String™ prediction protein analysis diagram[576]

The following are predicted targets for Hsa-mir-4274 (Figure 5-13):

PC4 and SFRS1-interacting protein (PSIP1) has growth factor, transcription factor and cofactor activity[496,578]. Biologically it is involved in the immune system processes. At a cellular level it is involved in cell-cell signalling, signal transduction and regulates transcription from the RNA polymerase 2 promoter. The immune system in a normally functional state identifies aberrant or ectopic cells and causes apoptosis and elimination of these cells. Alterations at various levels in the immune system may aid in survival of ectopic cells that progress towards endometriosis.

Zinc finger protein 41 (ZNF41) is a protein with KRAB box transcription factor activity and is involved in spermatogenesis[496,578]. This protein is also seen to regulate transcription from RNA polymerase 2 promoter affecting the cellular cycle.

Regulator of G-protein signalling 20 (RGS20) binds proteins and has small GTPase regulator activity[496,578]. Biologically it contributes to cellular dorso-ventral axis specification and is involved in heterotrimeric G-protein signalling pathways (G1/Gs α and Gq/G0 α) regulators of G protein signalling.

Rap guanine nucleotide exchange factor 2 (RAPGEF2) is a member of the PDZ domain containing guanine nucleotide exchange factor family[496,578]. They stimulate the exchange of guanyl nucleotides through the use of a GTPase. It has functions of protein binding, small GTPase regulator activity and guanyl-nucleotide exchange factor activity involved in mitosis, the transmembrane receptor protein tyrosine kinase signalling pathway, G-protein coupled receptor protein signalling pathway and the MAPKKK cascade[526]. Receptor tyrosine kinases serve as cell surface receptors for molecules such as growth factors and cytokines[582] and are associated with regulation of cellular processes. Alterations in the functioning of tyrosine kinases are associated with malignancy development[583] and have been used as potential targets for cancer prevention. Subtle effects of RAPGEF2 on the transmembrane receptor

protein tyrosine kinase signalling pathway could potentially contribute to the development and formation of a disease such as endometriosis. If through functional studies, it appears to be an important component in endometriosis development, it could be used as a therapeutic target for this disease too. The G-protein coupled receptor protein signalling pathway is related to various important cellular functions. Pertinent to my study is its regulation of inflammation and the immune system as well as being linked to tumour growth and metastasis[584]. In recent years this is another family of receptors that are targeted for novel therapeutics[585]. Once again we can see a pathway which when disrupted, is responsible for ectopic tumorigenic growth and metastatic potential. Extrapolated to endometriosis, a disease where ectopic tissue implants grows and can even "metastasise" to organs outside of the pelvis, one can potentially see the importance of the roles of such pathways. Again functional studies are necessary with the potential of novel targeted therapeutics for endometriosis. The MAPKKK cascade is linked to the antiapoptotic RAS cascade and protein which in my study has been identified as one of the upregulated markers in the serum of women with endometriosis (See Table 6-4 Section 6.4.7). Mutations in the RAS/MAPK cascades have been linked to endometrial cancers[586], it is therefore not difficult to postulate that milder aberrations in the pathways caused by Hsa-mir-4274 could be linked to development of endometriosis which is itself not classified as a malignancy but has properties of cell implantation, growth survival and dissemination.

Long-chain-fatty-acid-CoA ligase 6 (ACSL6) is a protein with ligase and transporter activity[496,578]. It too is involved in the immune system and fatty acid metabolism processes.

Methenyltetrahydrofolate cyclohydrolase (MTHFD2L) has oxidoreductase and hydrolase activity[496,578]. It is involved in metabolic processes which are purine and pyrimidine based and has a role in the amino acid biosynthetic processes within the cell.

Lysyl oxidase homolog 4 (LOXL4) has oxidoreductase, serine-type peptidase and receptor activity[578]. Biologically it is implicated in macrophage activation and the cellular defence response and has a role in proteolysis, cell-cell adhesion, signal transduction and extracellular transport[496]. It is observed in the processes involving the neurological system as a negative regulator of apoptosis. LOXL4 loss of expression has been seen in the development of bladder tumours, with its re-introduction decreasing the ability of the tumour to form colonies[587]. They can therefore function as tumour suppressor genes and inhibit the Ras/ERK (extracellular signal-regulated kinase) pathway in cancers. If LOXL4 acts in a similar way in endometriosis, it could be one of the contributing factors which could prevent endometriosis from developing into endometrial cancer.

Transformer-2 protein homolog beta (TRAB2B) is an mRNA splicing factor and functions in mRNA splicing and in transesterification in mRA binding[496].

Serine/threonine-protein kinase N2 (PKN2) is a serine-threonine protein kinase family member[496]. It is an annexin and calmodulin protein class member. It has protein-kinase activity and is involved in calcium iron and calmodulin binding as well as calcium dependant phospholipid binding[496,578]. It is involved in calcium mediated signalling processes as well as protein amino acid phosphorylationas as well as involvement in the following three pathways: PDGF signalling pathway, Alzheimer's disease amyloid secretase pathway and the muscarinic acetycholine receptor 1 and 3 signalling pathway[526]. The platlet-derived growth factor is one of the machrophage derived growth factors[588] and the pathway is involved in

cellular growth and the process of angiogenesis. Studies showing the elevation of PDGF in the peritoneal fluid of endometriosis have partly attributed the proliferative properties of ectopic endometrial tissue forming endometriosis to this growth factor[589]. It too is being investigated as a potential novel therapeutic target[589].

cGMP-dependent protein kinase 2 (PRKG2) is a non-receptor serine-threonine protein kinase member[496,578]. It binds proteins and has protein kinase and kinase regulator activity biologically involved in muscle contraction, intracellular signalling cascades, cellular mitosis and phosphorylation of amino acids. It is also involved in neurological system processes forming part of the cGMP dependent pathways and endothelin signalling pathway[526].

Peroxisomal targeting signal 1 receptor (PEX5) targets proteins and is involved in peroxisomal transport as another membrane trafficking regulatory protein[578].

Pituitary adenylate cyclase-activating polypeptide type I receptor (ADCYAP1R1) has G-protein coupled receptor activity and is seen in cellular stress responses[496,578]. It is a member of the antibacterial response proteins and is implicated in the cellular immune response. Modifications in this response might all contribute to the development of endometriosis in preventing aberrant cell elimination. Within the cell it has roles in cellular glucose homeostasis, synaptic and non-synaptic vesicle exocytosis enabling synaptic cellular transmission. It is also responsible for intracellular protein transport. Biologically it is involved in spermatogenesis, mesodermal and heart development and is involved in the G-protein coupled receptor protein signalling pathway and gonadotropin releasing hormone receptor pathway[526]. GnRH analogues are used for the enhancement of apoptosis in endometriotic cells[590] and are one of the medical treatments used to suppress endometriosis pre-operatively or pre-fertility treatment. Understanding the effects of receptors such as *ADCYAP1R1* on GnRH pathways could potentially provide another window to understanding this multifactorial disease.

Protocadherin-9 (PCDH9) binds calcium ion and has G-protein coupled receptor activity[496,578]. Biologically it has been linked to visual perception and the sensory perception of sound. At a cellular level, it is involved in cell-cell adhesion, cell motion and morphogenesis of the cellular components. Embryonically it is involved in ectoderm and mesoderm development, nervous system development, heart and muscle organ development as well as the Wnt signalling pathways (Figure 5-14) and cadherin signalling pathways[526] (Figure 5-15). The Wnt signalling pathway regulates cell growth motility and survival[591] and molecular defects or alterations in this pathway have been associated with the development of multiple types of tumours[591]. Molecules such as PCDH9 might be responsible for minor changes within the function of this pathway which in endometriosis could result in ectopic cell survival or growth. Genes or proteins that are involved in cellular modification, signalling, motion and morphogenesis, all have a fine balance in controlling and ensuring correct cellular function and viability. Any derangement or alteration in these molecules could potentially disrupt the normal cellular properties enabling a cell to grow, proliferate uncontrollably and potentially avoid or repress apoptosis. All these properties are seen in endometriotic cells and it is possible that it is through the understanding of the importance of molecules such as PCDH9 that we might obtain a better insight into development of the disease process of endometriosis and its associated pathways.

FIGURE 5-14

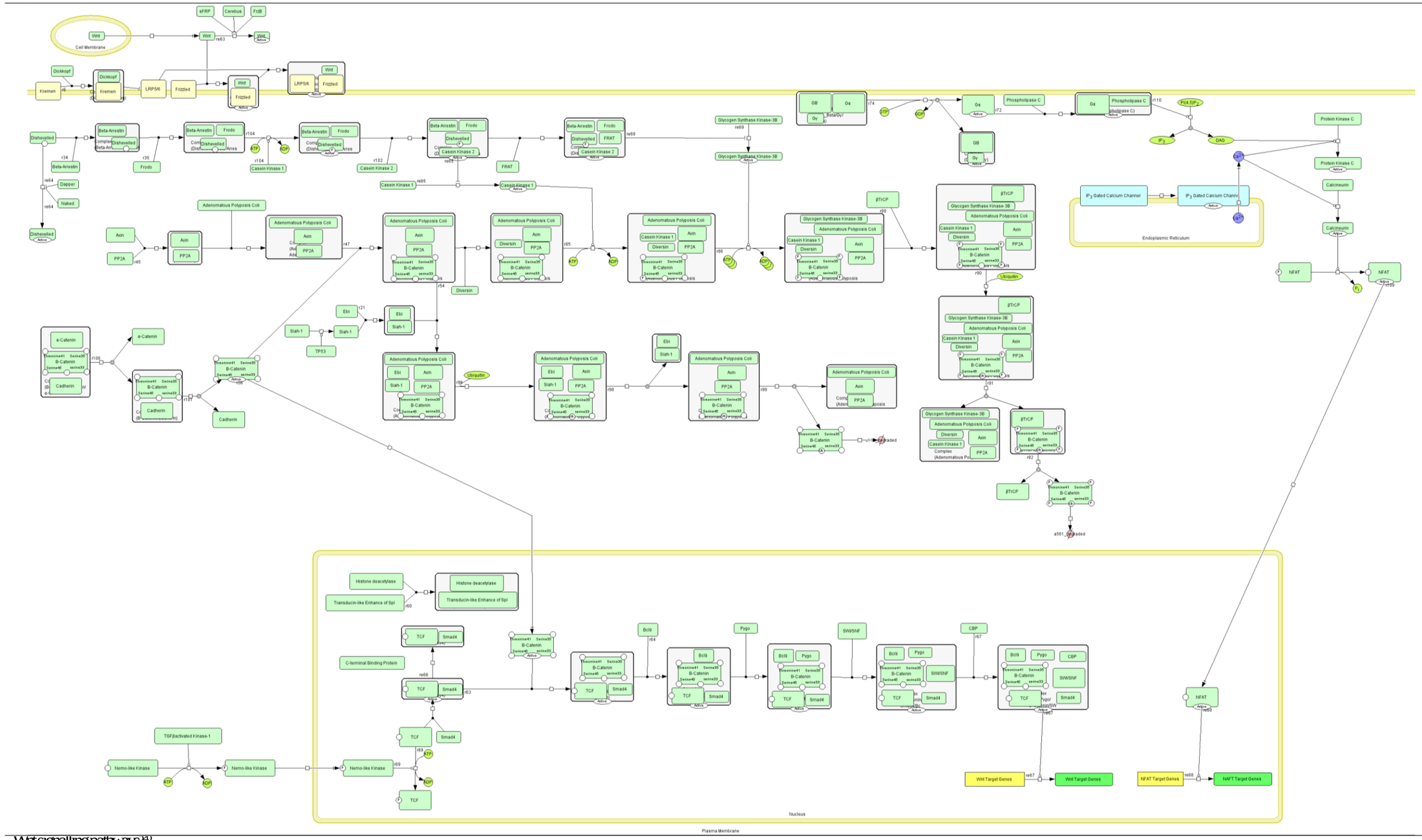

Wnt signalling pathways[20]

FIGURE 5-15

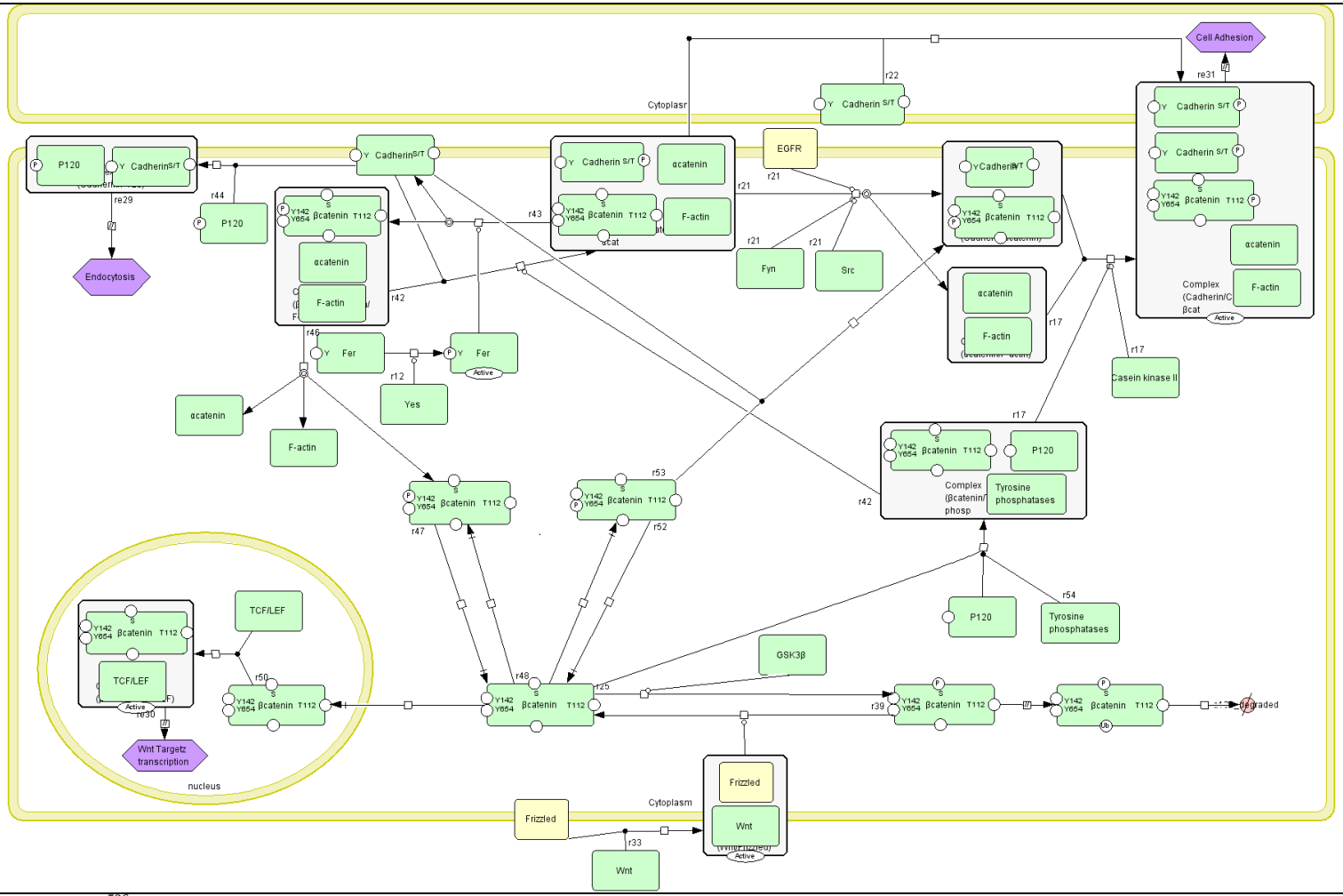

Cadherin signalling pathway[526]

Cytoplasmic dynein 1 light intermediate chain 2 (DYNC1LI2) binds proteins and is a structural component of the cytoskeleton[496]. Intracellularly, it is found within microtubule and acts as an enzyme modulator and has a role in the morphogenesis of cellular components and intracellular protein transport, RNA localisation and vesicle mediated transport. It has a role in the cell cycle and the intracellular signalling cascades. DYNC1LI2 is implicated in Huntington's disease involving the dynein complex[496,578].

Potassium voltage-gated channel subfamily C member 2 (KCNC2) also contains cation channel activity and is involved in cation transport. It is involved in cellular signal transduction and synaptic transmission. Biologically it is involved in muscle contraction and neuronal action potential propagation[496,578].

Golgin subfamily A member 8A (GOLGA8A) is another membrane trafficking protein. F-box/WD repeat-containing protein 1A (BTRC) is involved in Parkinson's disease and three separate pathways: hedgehog signalling pathway, Wnt signalling pathway and the toll pathway in drospophila[526]. The importance of the effects of the Wnt signalling pathway in tumorigenesis, cellular survival and proliferation has already been suggested previously[591] with other molecules such as PCDH9 affecting the same pathway. Interestingly if multiple molecules affect this major pathway at different levels, this might further encourage cellular changes and endometriotic disease growth. There will be potential expressed counteracting or stabilising tumour suppressor genes such as LOXL1 which can explain the prevention of development of overt malignancy.

The following genes and proteins have been identified as downstream targets of hsa-mir-4274. Their roles and functions in literature are not currently clearly defined[496,526,577,578]: Protein family with sequence similarity 3, member C1 (FAM3C), actin-binding rho-activating protein (ABRA), uncharacterized protein C6orf136 (C6orf136), MACRO domain-containing protein 2 (MACROD2). Bladder cancer-associated protein (BLCAP) may regulate cellular apoptosis and cell cycle proliferation by a mechanism independent from TP53/p53.

5.6.2.1 Summary of important identified points

- From the above list of genes and proteins controlled by Hsa-mir-4274, one can see still see effects on the cellular functions of apoptosis, cell adhesion, migration, cytoskeletal structure, cellular signal transductions and vesicular formation. Various proteins controlled by this miRNA are also seen to potentially affect the immune system, altering ectopic cellular recognition, facilitating cellular evasion and enabling implantation and growth.

- *SP1* has a role in the immune system and in humans it is a constituent of the gonadotropin releasing hormone receptor pathway. Other identified molecules such as MAP2K6 and *ADCYAP1R1* are also associated with effects on the gonadotropin releasing hormone receptor pathway. This is one of the targeted pathways by medical GnRH analogues that aim to promote apoptosis in endometriosis.

- Other genes such as KLF3 are also know to affect B-cell mediated immunity which can be used by viruses such as EBV to invade proliferating cells which can evade immune recognition.

- Molecules such as CREB1, MAP2K6 affect the RAS and MAPK pathways have been linked to hsa-mir-4274, all of which are associated with potential tumorigenesis, providing cells with the ability to proliferate, invade and grow. PCDH9 affects Wnt signalling pathways which also mediate cell survival and growth. These are all characteristics which are shared by endometriosis cells enabling ectopic growth.

- Relating back to the information above, there are varied roles which each protein or gene is known to carry out though it is difficult to determine which of these pertains a leading role, or which of these follow on as a secondary response to alternate cellular processes.

- It is beyond the scope of this chapter to determine which are the most likely proteins or genes or pathways to cause (or enable to a larger extent) the development of the disease of endometriosis. This would require a separate body of work with functional models to determine important molecular or protein roles.

- Using the identified proteins, pathways and genes to perform functional modelling studies to establish which molecules have more pertinent roles that could serve as an interesting body for future work.

5.7 Detailed analysis for downregulated miRNAs

8 miRNAs were downregulated in endometriosis with the top two identified miRNAs being hsa-miR-150 and hsa-miR-122. Hsa-miR-342-3p is significant at a less stringent confidence. qPCR analysis is supportive of 3 of the markers that have significant down-regulation in disease: miRs 150, 122 and 342-3p.

5.7.1 hsa-miR-150

FIGURE 5-16

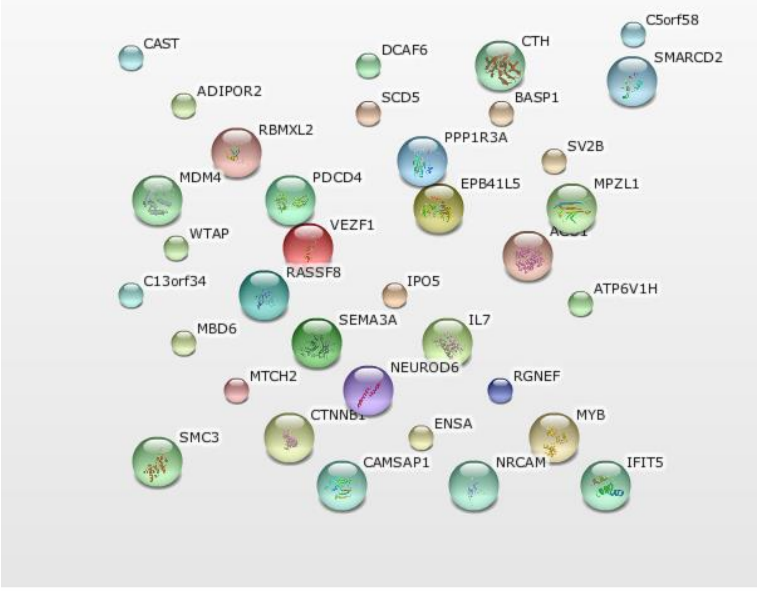

String™ prediction protein analysis diagram[576]

There are a number of predicted targets for hsa-miR-150 (Figure 5-16):

DDB1- and CUL4-associated factor 6 (DCAF6) is a member of the nuclear receptor interaction protein family[496]. It has GTPase activity and is involved in apoptosis and signal transduction pathways. Through signal transduction it regulates the nucleotide and nucleic acid metabolic processes regulating the nucleobase. The control of cellular nucleic acid processes is vital for correct cellular division and function.

Programmed cell death protein 4 (PDCD4) is a translation elongation factor protein involved in translation and nucleic acid binding as well as induction of apoptosis[496,576]. Aberrations in any of the finely tuned cellular processes can potentially lead to abnormal cellular phenotypes and can result in aberrant control of apoptosis and cellular proliferation enabling a disease such as endometriosis to grow and disseminate.

Protein Mdm4 (MDM4) is a p53 binding protein and has a ubiquitin-protein ligase activity shifting ATP to AMP[496,578]. It is a negative regulator of apoptosis and is implicated in a number of cellular pathways including the p53 pathway, its feedback loops and the insulin/IGF pathway-protein kinase B signalling cascade (Figure 5-17, Figure 5-18). P53 is a crucial tumour suppressor that responds to cellular stressors by arresting the cell cycle, causing senescence and inducing apoptosis[2]. MDM4 counteracts the action of p53, potentially enabling cells to proliferate in situations where their growth would have otherwise been arrested or apoptosis induced. This could explain how ectopic endometrial cells progress towards growth and implantation in sites such as the pelvis, where they would have otherwise perished.

FIGURE 5-17

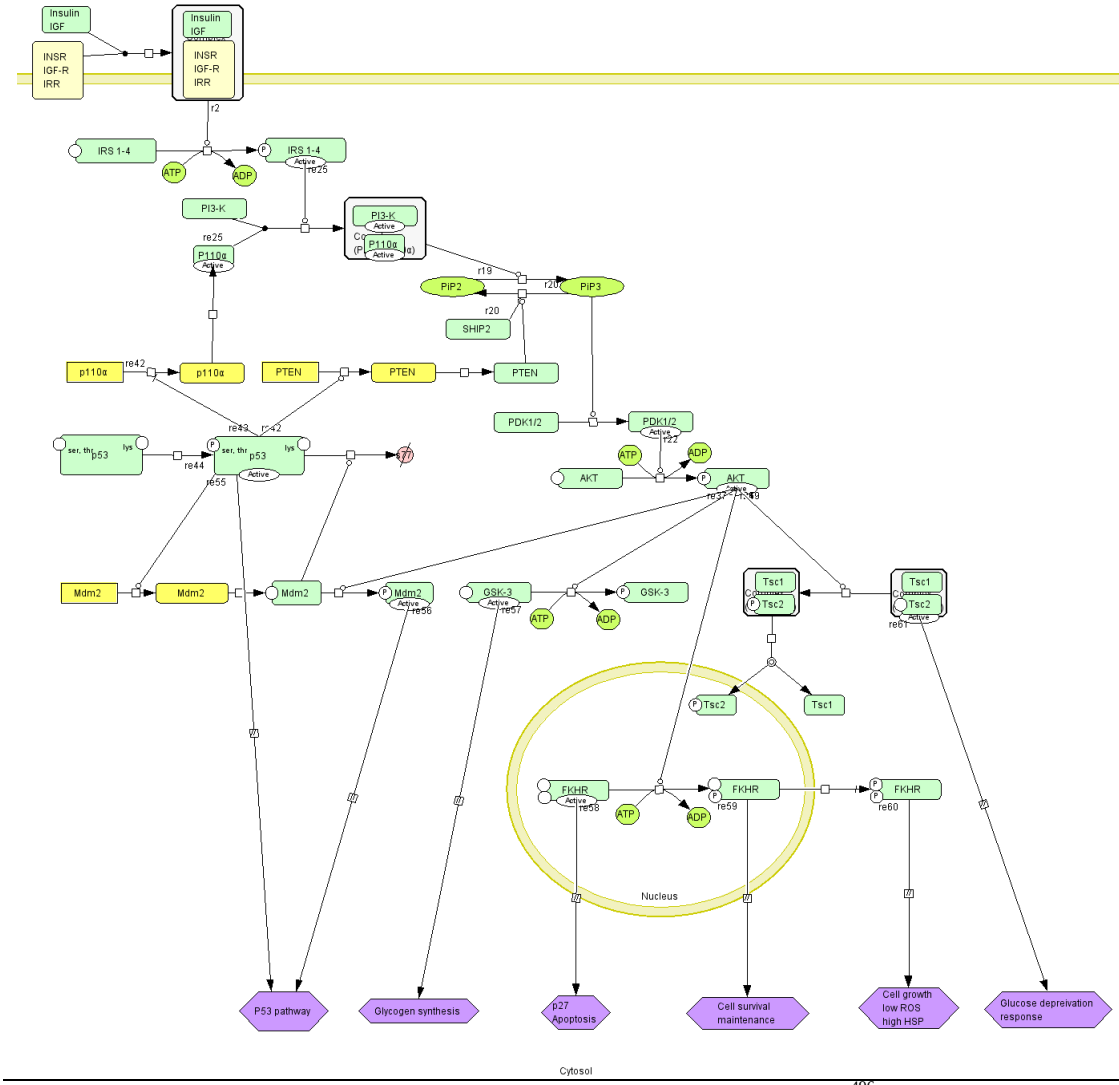

Panther™ pathway showing Insulin IGF pathway- protein Kinase B signalling cascade[496]

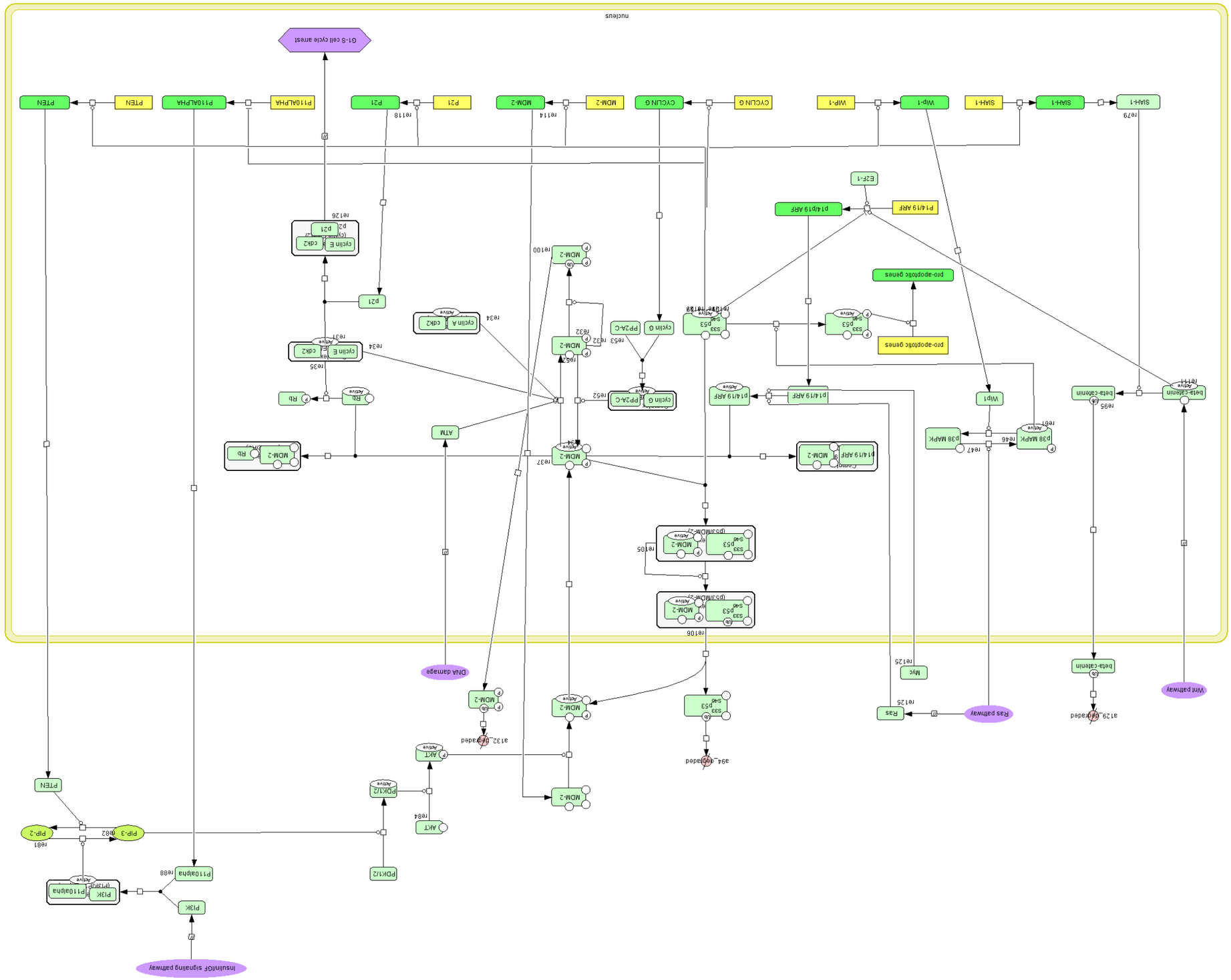
nucleus
G1-S cell cycle arrest
SIAH-1
Wip-1
CYCLIN G
MDM-2
P21
P110ALPHA
PTEN
E2F-1
p14/p19 ARF
pro-apoptotic genes
beta-catenin
WIP1
p38 MAPK
ATM
Rb
cyclin E
cdk2
cyclin A
PP2A-C
PDK1/2
AKT
PI3K
P110alpha
PIP-3
PIP-2
Wnt pathway
Ras pathway
DNA damage
Insulin/IGF signaling pathway

FIGURE 5-18

Transcriptional activator Myb (MYB) is a DNA binding protein which has transcription factor activity and is involved in the cell cycle as a negative regulator of apoptosis[496,578]. It is also involved in a number of cellular biosynthetic processes including the purine base metabolic process, the rRNA metabolic processes, fatty acid metabolic processes and the cellular amino acid biosynthetic process, regulation of transcription from RNA polymerase 2 promoter and the termination of this transcription process, as well as signal transduction through cell surface receptor linked transduction. The negative regulation of apoptosis and aberrations in cellular control mechanisms, as discussed earlier, can potentially be a cause for prolonged cellular survival aiding in endometriosis growth and development.

Adiponectin receptor protein 2 (ADIPOR2) has receptor functions in cell surface receptor linked signal transduction and the fatty acid metabolic processes[496,578]. It is involved in the gonadotropin releasing hormone receptor (GnRH) pathway (Figure 5-19)[526]. Current medical therapies for endometriosis, include temporary medical suppression of disease through the use of GnRH analogues. Obtaining an insight as to which components of the GnRH pathway are particularly elevated or altered in endometriosis, might serve in the identification of more specific targeted therapeutics for the disease.

FIGURE 5-19

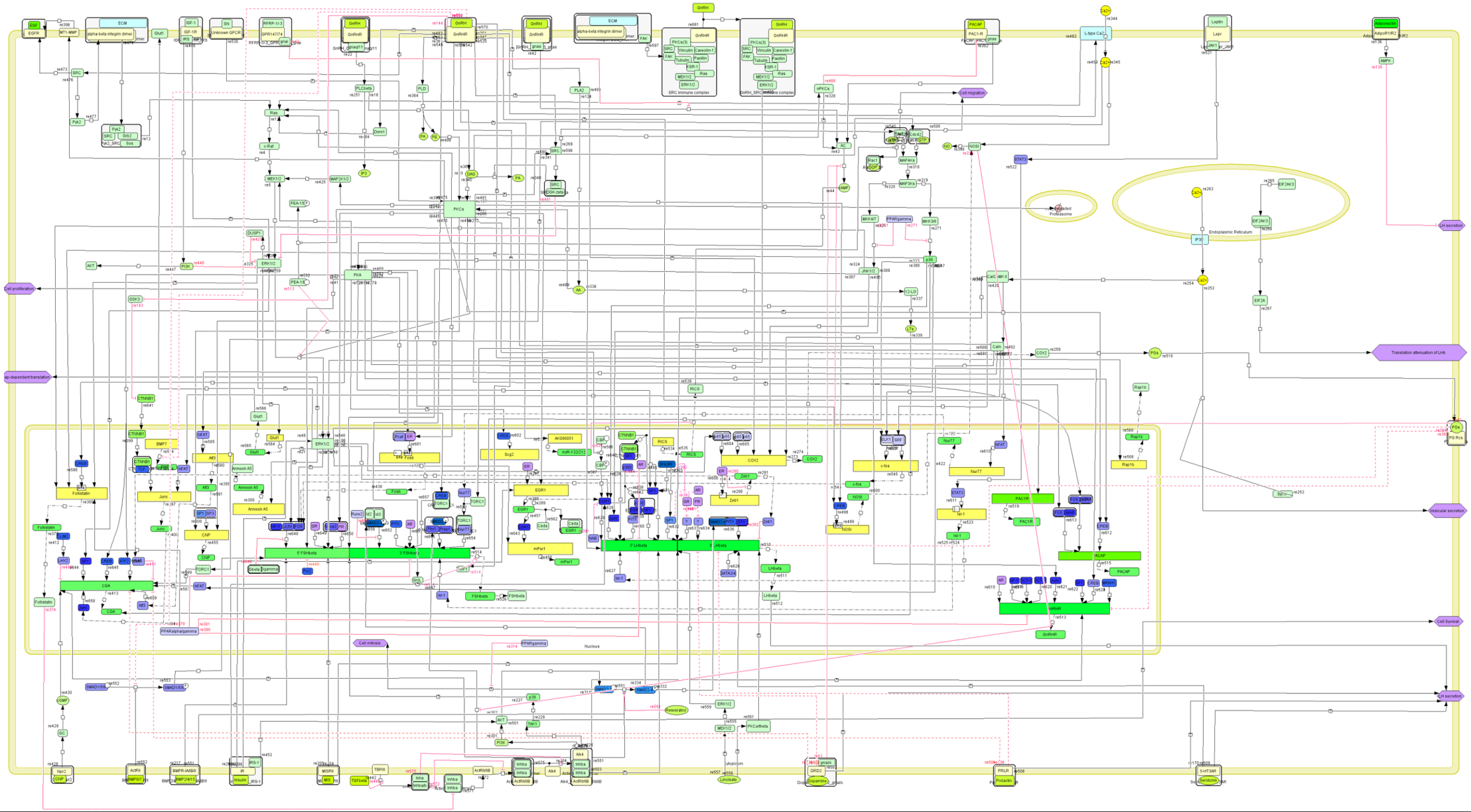

Panther™ gonadotropin releasing hormone receptor pathway[86]

Structural maintenance of chromosomes protein 3 (SMC3) is a protein which has hydrolase activity and binds nucleic acid and chromatin[496]. It acts as a chromatin- chromatin binding protein establishing and maintaining chromatin architecture and segregation. Cellularly, it is involved in mitosis, meiosis, DNA replication and repair[578].

Cytoplasmic aconitate hydratase (ACO1) is located within mitochondria and cellular cytosol and is involved in hydrolase processes within the tricarboxylic acid cycle as well as carbohydrate metabolic processes and cellular amino acid biosynthetic processes[496,578]. It is a component of the methycitrate cycle[526] (Figure 5-20) and a master regulator of cellular iron metabolism during cellular proliferation[592].

FIGURE 5-20

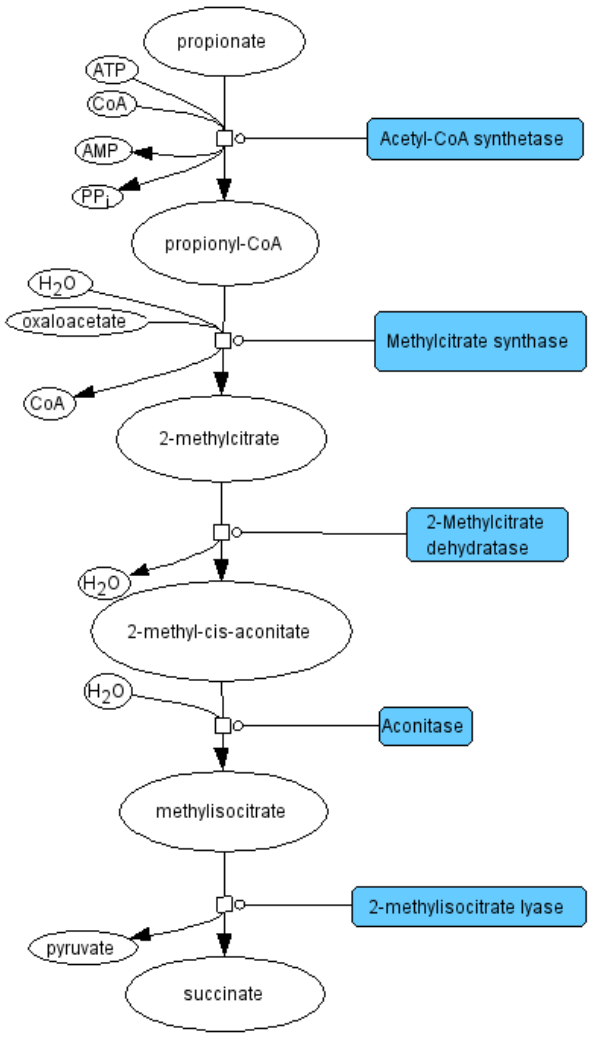

Panther™ Methycitrate pathway[496]

Interleukin-7 (IL7) is a member of the cytokine family of signalling molecules which are seen to be expressed by leukocytes[496,578,592]. They negatively regulate apoptosis and are vital in the processes of the immune system. In my study, I have already identified the EBV hsa-mir-BART2-5p miRNA being elevated in the leukocytes of women with endometriosis when compared to controls (See section 4.5.2.1). In theory, leukocytes that negatively regulate apoptosis containing higher levels of EBV miRNA might, not be able to function optimally and identify and eliminate ectopic endometrial cells. This would enable

the ectopic cellular survival, implantation and growth into endometriosis. IL7 are also constituents of the cytokine-mediated signalling pathway, janus kinase and signal transducer and activator of transcription (JAK-STAT) cascade, the Interleukin signalling pathway (Figure 5-21) and have a role in cell-cell signalling[526].

FIGURE 5-21

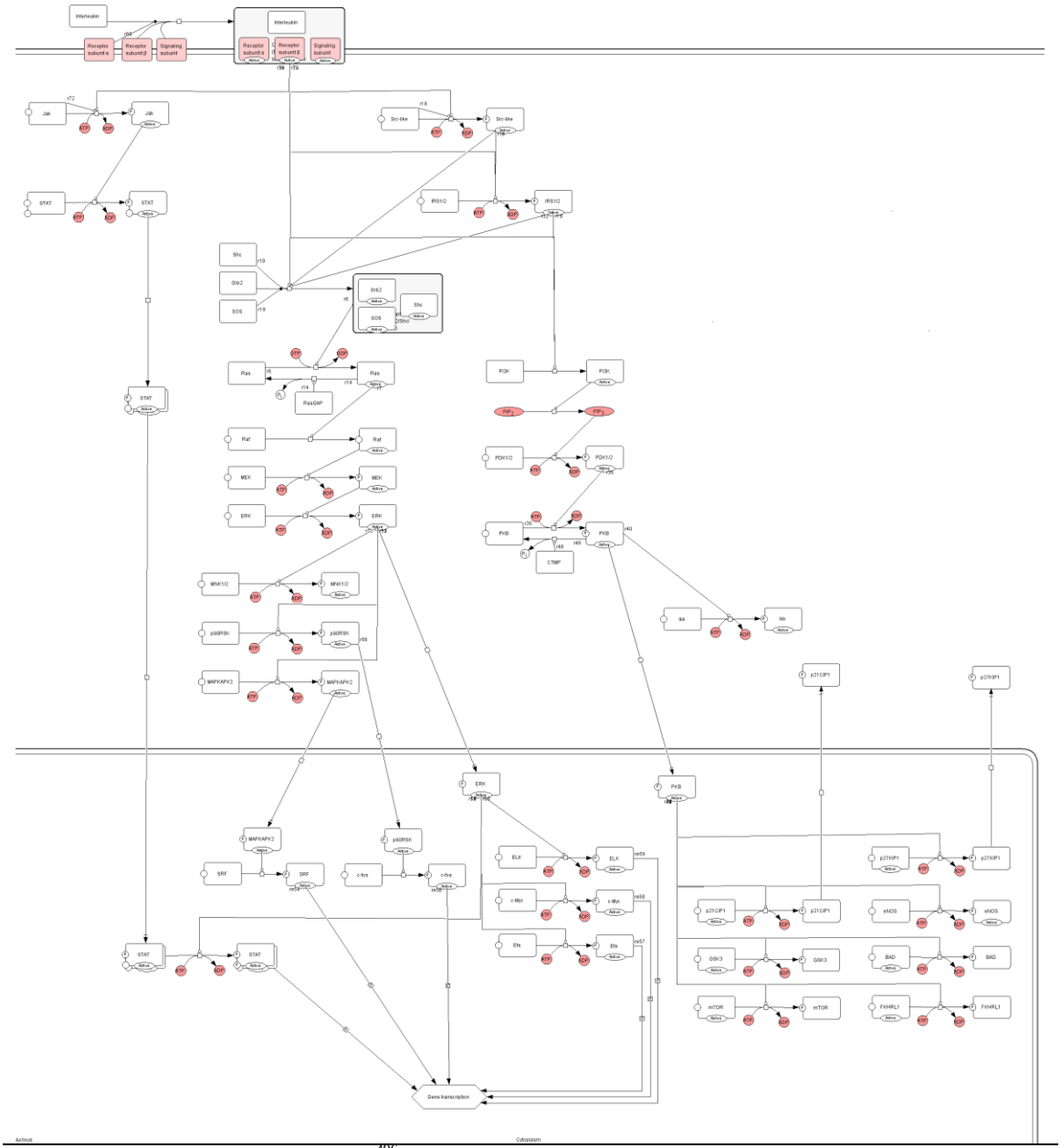

Panther™ interleukin signalling pathway[496]

Neuronal cell adhesion molecule (NRCAM) is a linker protein within the extracellular matrix and acts as a cell surface receptor controlling signal transduction, protein modification and cell-to-cell interaction[496]. It is a member of the immunoglobulin superfamily of cell adhesion and receptor molecules and involved in the processes of cell matrix adhesion, intercellular adhesion and motion[578,592]. It has phosphoprotein phosphatase activity and is located within the extracellular matrix of the cell and involving various cellular processes, the immune system, neurological and nervous system processes and muscle

contraction. Embryologically, there is a role in the development of ectoderm and mesoderm, angiogenesis and the development of muscle organs and the nervous system[496].

Semaphorin-3A (SEMA3A) is a membrane bound signalling molecule with receptor binding properties and involved in the neurological and immune system processes and the development of the heart[496,578,592]. It forms part of the transmembrane receptor protein signalling pathways and the intracellular signalling cascades and has a role in cell-cell adhesion. Embryologically, there are roles in ectodermal and mesodermal development and a component of angiogenesis. It is directly involved as a component of the semaphorin mediated axon guided pathway (Figure 5-22) [526]. Genes controlling or affecting angiogenesis are vital for the survival of any ectopically implanted cell. Without a novel vascular supply, an ectopic cell is not able to grow and disseminate, making the angiogenic properties of SEMA3A and NRCAM potentially important components of endometriotic cell survival and growth.

FIGURE 5-22

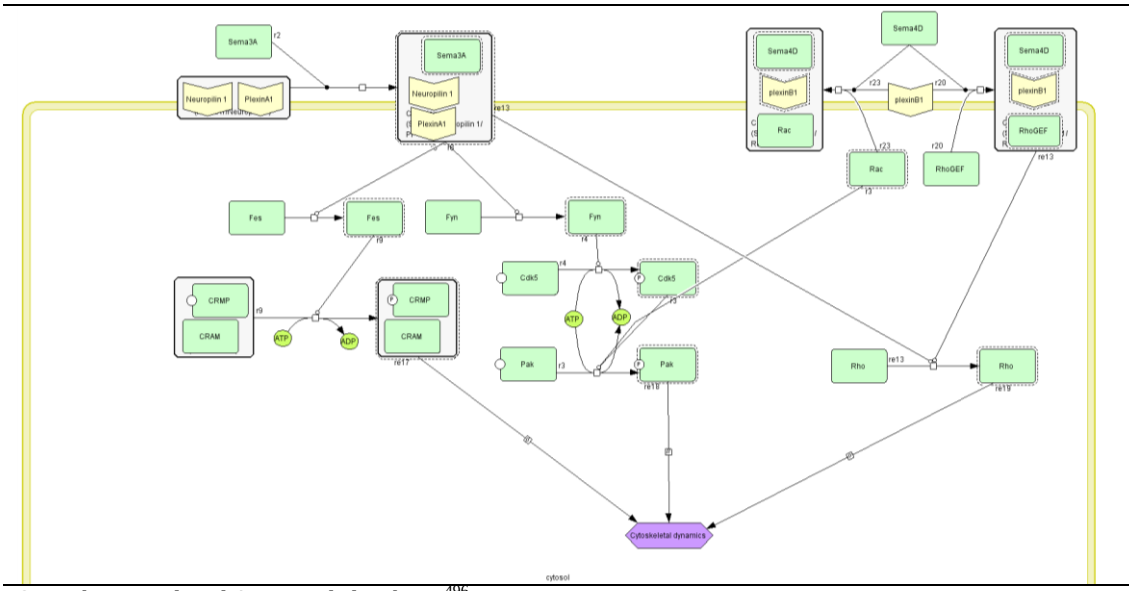

Semaphorin mediated Axon guided pathway[496]

Interferon-induced protein with tetratricopeptide repeats 5 (IFIT5) is a protein released in response to interferon gamma or cellular stimuli induced by recombinant human IFN-alpha in NB4 cells[496,592]. This gene has been found in elevated levels in retinoic acid treated acute promyelocytic leukaemia cell lines (NB4 cells) and was seen to increase with myeloid differentiation[593]. It is also expressed in untreated hematopoietic and non-hematopoietic cell lines. The interferon induced (IFIT) gene family has also been recently implicated in host organism antiviral defences (Figure 5-23). Intereferon secretion indicates host antiviral immunity. Interferons exert their anti-viral functions through the induction of antiviral proteins and the IFIT gene family is one of hundreds which are stimulated. The primary interferons responsible for the IFIT gene family induction are interferons type 1 and 3. These are regulated by the JAK-STAT signalling pathways. The genetic suppression of IFIT genes or methylation by viral molecules are mechanisms employed by viruses to escape host antiviral defences[594]. Their presence enables the restriction of viral replication, stimulates apoptosis in virally infected cells and regulates immune responses. IFIT family members are today believed to be imperative in the production of novel vaccines and viral restriction mechanisms. In my study, EBV virus is believed to be an important component of

development of the ectopic endometrial cells into endometriosis (See section 4.5.2.1). In endometriosis, potential malfunctions in the IFIT5 cellular mechanisms might allow EBV infected cells to proliferate, evade immune detection and apoptosis and enable ectopic tissue implantation and growth.

FIGURE 5-23

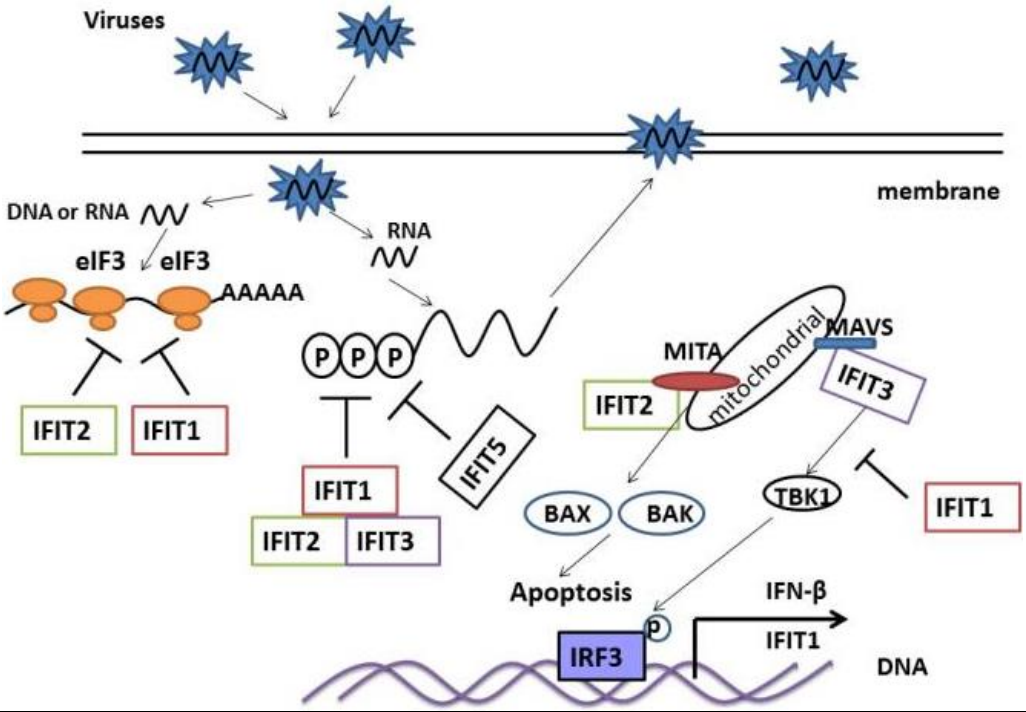

Antiviral and immune regulated function of IFIT family genes[594]

Protein phosphatase 1 regulatory subunit 3A (PPP1R3A) is a protein that directly interacts with phosphatase affecting and modulating its activity[496,578]. Inactivation of phosphatase proteins has been shown to cause anomalies in cell growth and division. Mutations in the PP1R3 gene has been shown in colorectal cancers, haematological malignancies, lung, ovarian and gastric cancers[595]. It is also directly related to lymph node and liver metastasis[596]. Interestingly, association of (AU)AT- rich element polymorphisms in PPP1R3 demonstrates metabolic features of PCOS which include insulin resistance, type 2 diabetes mellitus and hyperandrogenaemia irrespective of patient BMI[597]. The presence of the mutated form of this gene in various malignancies has led to PPP1R3 being identified as a candidate tumour suppressor gene[598]. Potentially, it carries a tumour suppressive function in the disease of endometriosis, preventing malignant cellular transition. Further functional studies would be required to ascertain the importance of its tumour suppressive effect in endometriosis.

Cystathionine gamma-lyase (CTH) is an enzyme within the cellular amino acid metabolic process and is involved in the methionine biosynthesis pathway (Figure 5-24)[526]. It is also a key enzyme in the trans-sulfuration pathway using L-cysteine to produce hydrogen sulphide (H2S)[496,578]. The CSE (CTH)/H2S system has effects on cellular growth and proliferation and overexpression of CSE inhibits cell proliferation and DNA synthesis[599]. Poymorphisms in the CTH gene have been linked to bladder malignancies[600].

FIGURE 5-24

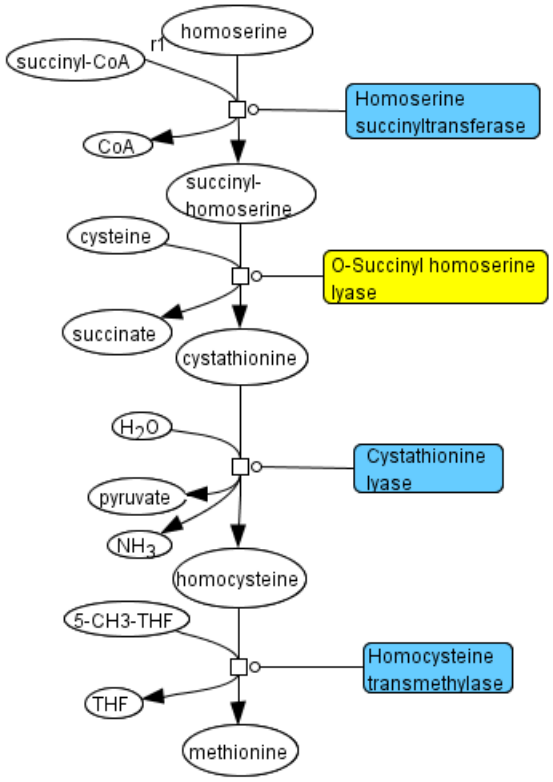

Methionine biosynthesis pathway[496]

Stearoyl-CoA desaturase 5 (SCD5) is involved in fatty acid/ lipid metabolism and has oxidoreductase activity[496,578,592]. In rat experimentations IGF-1 and FSH are seen to increase SCD2 (SCD5 synonym) expression in the ovary. IGF-1 and FSH are involved respectively with the MAPK3/MAP1 and PIK3R1/AKT pathways. SCD2 is believed to have a role in the follicular growth and oocyte maturation in the rat ovary[601]. SCD2 was also shown to be expressed in rodent testes and epididymis as well as other tissues such as human brain, pancreas and the nervous system. It is seen to be elevated in certain malignancies such as Burkitt's lymphoma[602]. SCD5 is also reported to have a role in the control of cellular endocytosis[603] and might play a role in viral infections such as EBV. It is considered as one if the molecules which could potentially be altered to treat viral infections[604] making it another potential target in the treatment of endometriosis, through the inhibition of the EBV effects on ectopically implanted endometriosis cells.

SWI/SNF-related matrix-associated actin-dependent regulator of chromatin subfamily D member 2 (SMARCD2) is a nucleic acid and chromatin binding protein. It has a role in the establishment of chromatin architecture, nucleic acid and nucleotide metabolic processes[496,578]. It is involved in the WNT signalling pathway (Figure 5-14)[526] which has been associated with cellular malignant development[591]. Potentially alterations in this pathway contribute to the development of endometriosis within patients.

Vascular endothelial zinc finger 1 (VEZF1) is a DNA binding protein and a zinc finger transcription factor which is a regulator of transcription from the RNA polymerase 2 promoter[496,578]. It is seen expressed in endothelial cells where it plays an important role in angiogenic regulation[605] and the maintenance of vascular haemostasis in the adult[606] and is also thought to be involved in both normal and

pathological processes of cellular proliferation and differentiation[577]. As discussed in earlier sections of this thesis, angiogenesis is a vital requirement for development of ectopic or disseminated cells such as endometriosis[29].

Calpastatin (CAST) is a cysteine protease inhibitor involved in proteolysis. The calpain-calpatatin system is involved in membranous fusion events such as exocytosis of neural vesicles and aggregation of platlets and red blood cells[577]. It has a role in metastatic tumour progression which depends on cell-cell and cell-matrix adhesions[496]. Proteolytic degradation of cadherin and focal adhesion complexes though calpain mediation enables disassembly of cell-cell and cell-matrix adhesions which are able to invade surrounding tissues due to enhanced motility. Members of the calpain family have been implicated in integrin-mediated cell migration, cytoskeletal remodelling, cell differentiation and apoptosis (Figure 5-25, Figure 5-26)[496,578,592]. CAST demonstrates its involvement in a number of processes associated with the development of tumorigenic and metastatic potential within cells. It is not unreasonable to postulate that similar changes occur in endometriotic cells which have the ability to disseminate, implant and grow in ectopic sites.

FIGURE 5-25

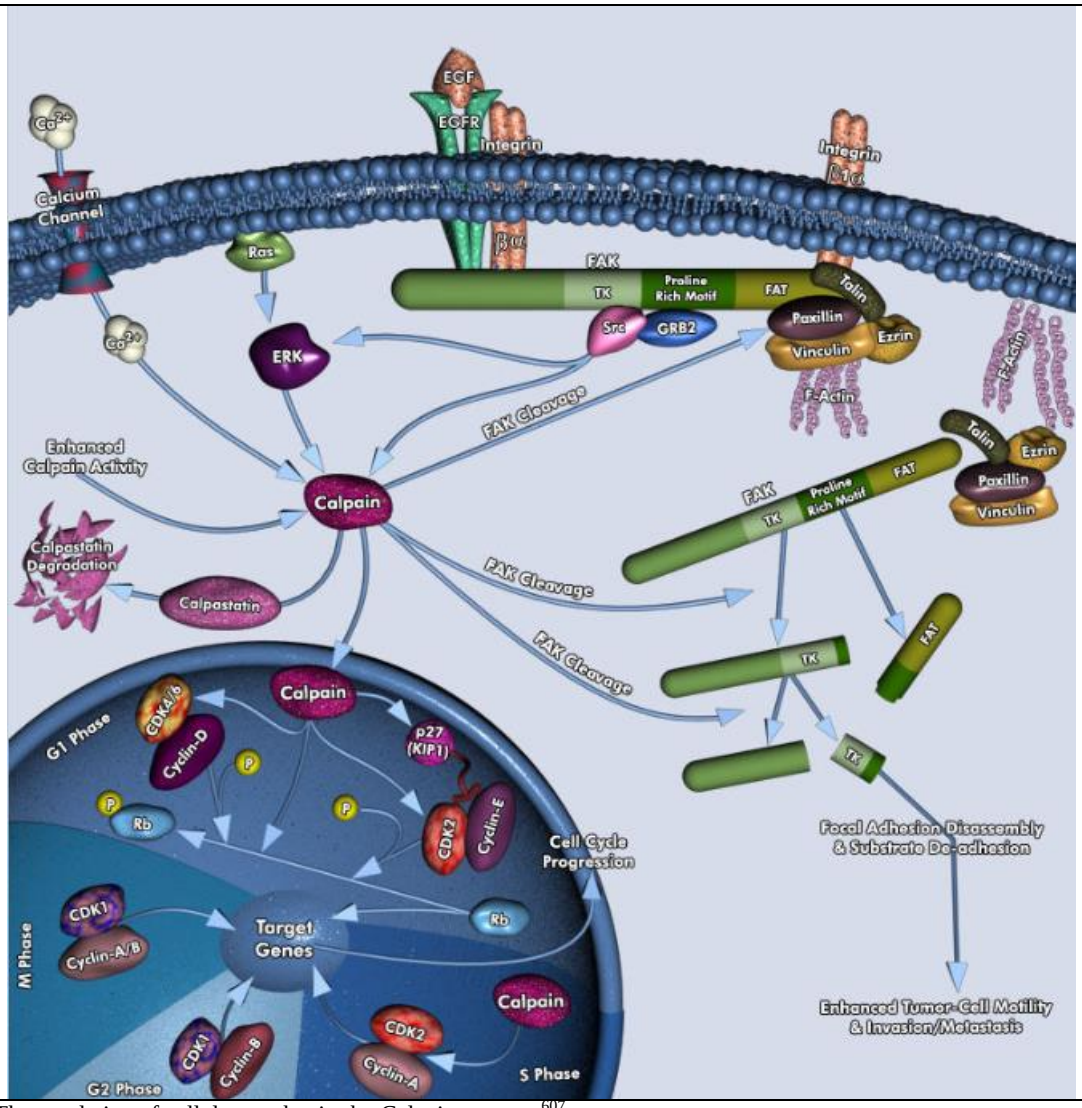

The regulation of cellular mechanics by Calpain protease[607]

FIGURE 5-26

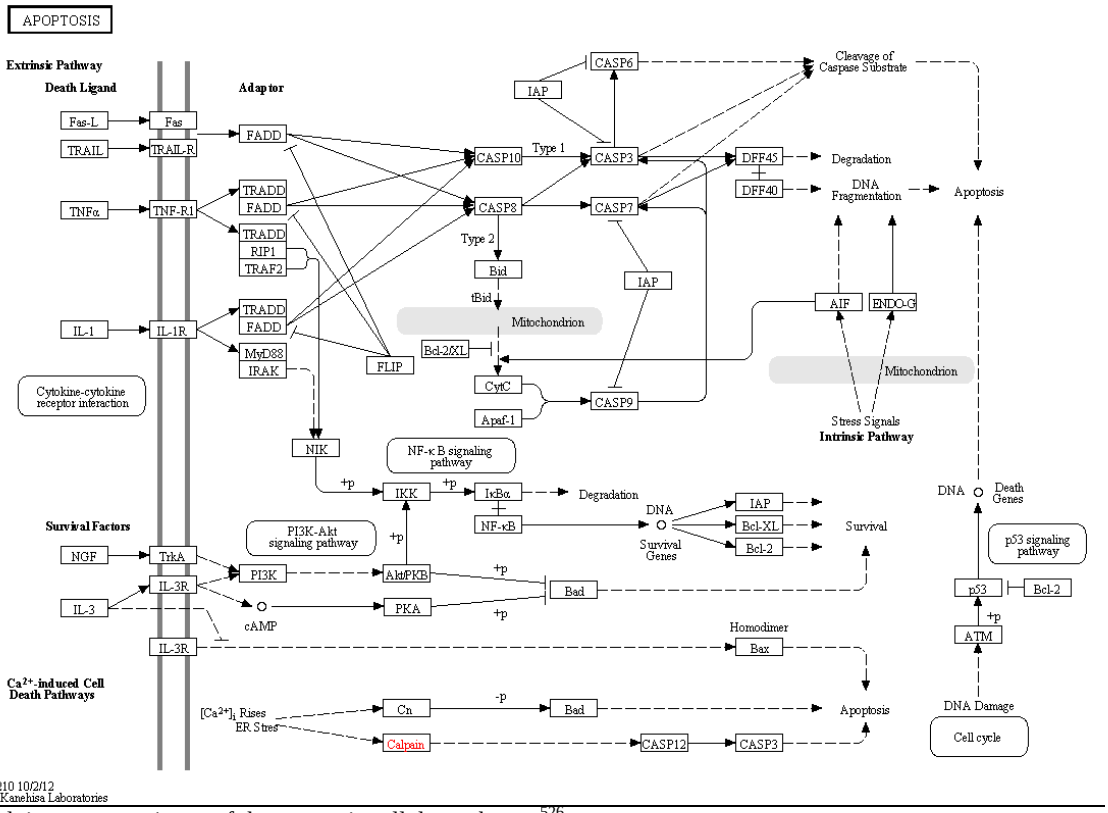

Calpian as a constituent of the apoptotic cellular pathways[526]

RNA-binding motif protein, X-linked-like-2 (RBMXL2) is a subfamily of nuclear ribonucleoprotein complex (hnRNPs) and a structural constituent of the ribosome which acts as an mRNA splicing and polyadenylaton factor[496,578,592]. The proteins influence pre-mRNA processing in the nucleus as well as mRNA metabolism and transport. It is important in the functioning of the cell cycle, DNA replication and nuclear mRNA splicing via the spliceosome. It has a role in rRNA and protein metabolism and is involved in ectoderm and nervous system development. RBMXL2 is a germ cell nuclear protein which is seen to be a testis-specific splicing regulator protein[608]. It primarily localises to the nucleus of meiotic spermatocytes. Genetic defects resulting in reduced levels of this protein could potentially be a cause of male infertility in humans[609].

Neurogenic differentiation factor 6 (NEUROD6) is a basic helix-loop-helix transcription factor nuclease. The protein may be involved in the development and maintenance of the nervous system (Figure 5-27). It regulates transcription from RNA polymerase 2 promoter and is also involved in ectodermal development[496,578].

FIGURE 5-27

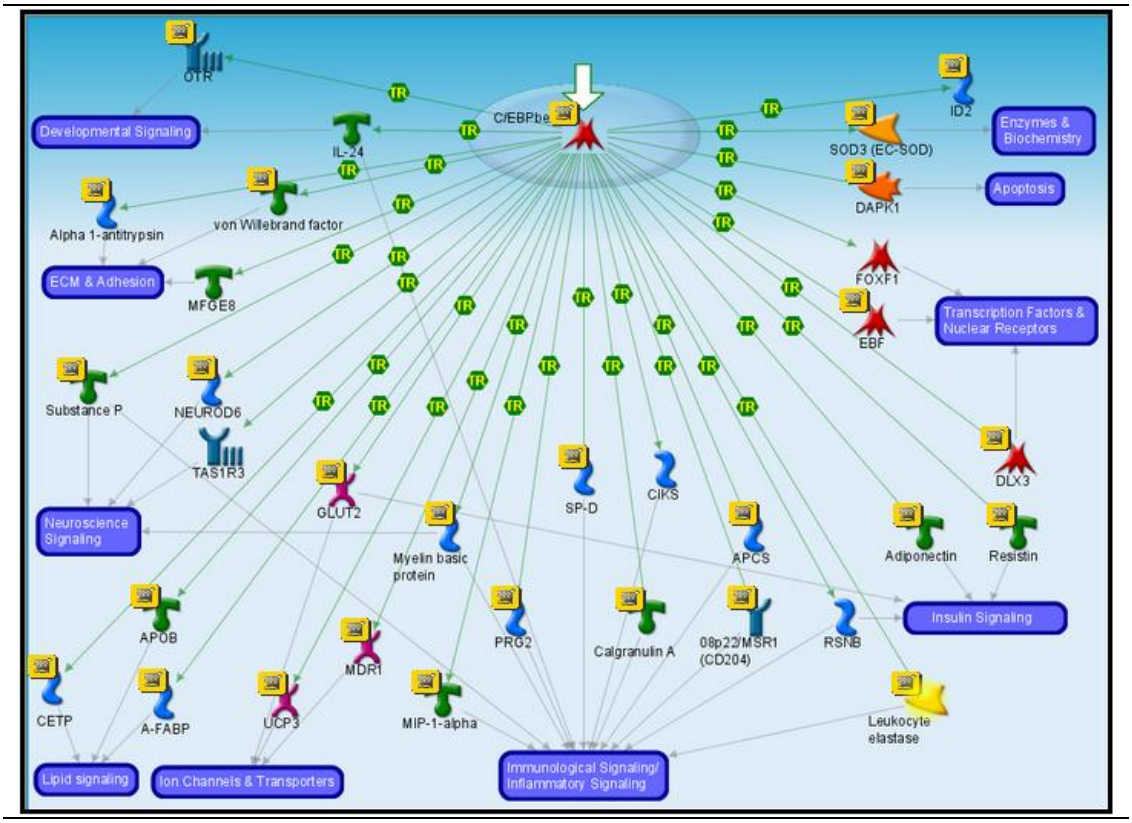

Pathway depicting the targets of CCAAT/enhancer-binding protein beta (C/EBPbeta). It regulates immunological, apoptotic and inflammatory processes and is linked to Insulin signalling pathways[610]

Brain acid soluble protein 1 (BASP1) is a neuronal axonal membrane bound protein involved in intracellular protein transport and exocytosis[496,578]. Embryologically, it is involved in ectodermal and nervous system development and in the development of the neurological systems. This calcium calmodulin dependant binding protein was found to be differentially expressed in a number of human cancer cell lines including endometrial cancers. The highest expression is seen in cervical adenocarcinoma cell lines[611]. Studies have shown that the BASP1 causes inhibition of Myc-induced cell transformations and it has been identified as a potential tumour suppressor[612]. Its presence in endometriosis could potentially prevent malignant change in this chronic condition.

Synaptic vesicle glycoprotein 2B (SV2B) is a transfer/carrier protein involved in neurotransmitter secretion and has a role in synaptic transmission[496,578].

Mitochondrial carrier homolog 2 (MTCH2) is a mitochondrial transport/carrier protein found on the surface of mitochondria[496,578,592]. The MTCH2 complex is seen to participate in the mitochondrion apoptotic process in response to the TNF-α/ FAS death receptor pathways[613]. It is also potentially associated with the BCL-2 apoptotic program[614]. A study on solid cancers has shown MTCH2 to be one of five genes expressed in multiple cancers which may play a role in enhancing invasive properties of tumour cells and their metastatic potential thereby affecting clinical outcomes[615]. Obesity has been linked to insulin resistance, diabetes and higher levels of oestrogen and non-oestrogen dependant malignancies such as endometrial and colorectal cancer respectively. MTCH2 is one of the identified genetic markers of obesity which potentially could be used to aid in identifying an increased risk for endometrial

cancer[616]. In endometriosis, which is hormonally responsive, the control of MTCH2 through hsa-mir-150 could potentially enable growth and dissemination of ectopic cells causing proliferation of disease.

Rho-guanine nucleotide exchange factor (RGNEF) is a gene encoding a protein which acts as a Guanine nucleotide exchange factor regulating integrin and growth factor related pathways[496,578,592]. It is implicated in various cellular processes including cellular adhesion, synapses, motility and activation of B-lymphocytes. It may also have a role in cellular apoptosis. In colon tumours, RGNEF has been seen in higher levels and promotes the progression, invasion and motility of tumours through the interaction with focal adhesion kinase. It binds to focal adhesion kinase (FAK) and this linkage facilitates fibroblast focal adhesion formation on fibronectin[617]. It might have a similar role in the migration of endometriotic cells and their invasion[442].

Myelin protein zero-like protein 1 (MPZL1) (PZR) is a protein with voltage gated sodium channel activity and cation channel activity with a role in cation transport, cellular adhesion and morphogenesis of the cell components[496,578]. MPZL1 is involved in the regulation of Ca(2+)-activated K(+) (BK) channel protein interactions controlling cellular death and survival[618]. PZR is a member of the immunoglobulin superfamily and enables cell signalling through an interaction with tyrosine phosphatase SHP-2[619]. It enables fibronectin-dependant migration of cells which express the SHP-2 molecule and regulates cellular motility[620]. It is also seen in early embryonic formation[621]. Ectopic endometrial cells with the ability to adhere, migrate and grow could potentially explain their development into endometriosis.

V-type proton ATPase subunit H (ATP6V1H) is also known as Nef[496,578,592]. It has been reported as one of the genes which is upregulated in endometrial tissue biopsies[622]. In viral infections such as HIV1 Nef (an accessory protein of HIV) and a vacuolar ATPase facilitate CD4 internalisation reducing CD4 expression on infected cells, enabling vial survival and infection[623].

Catenin beta-1 (CTNNB1) is a structural constituent of the cellular cytoskeleton with receptor binding properties. It can act as a storage protein and aids in intracellular transport as a signalling molecule[496,578]. It also functions in cellular signal transduction and Cell-cell adhesion. This gene is involved in various pathways including those controlling angiogenesis (Figure 5-28), Gonadotropin releasing hormone receptor pathway (Figure 5-29), Alzheimer's disease presenilin pathway, cadherin signalling pathways (Figure 5-15), p53 pathway feedback loops (Figure 5-30) and the Wnt signalling pathway (Figure 5-14)[526].

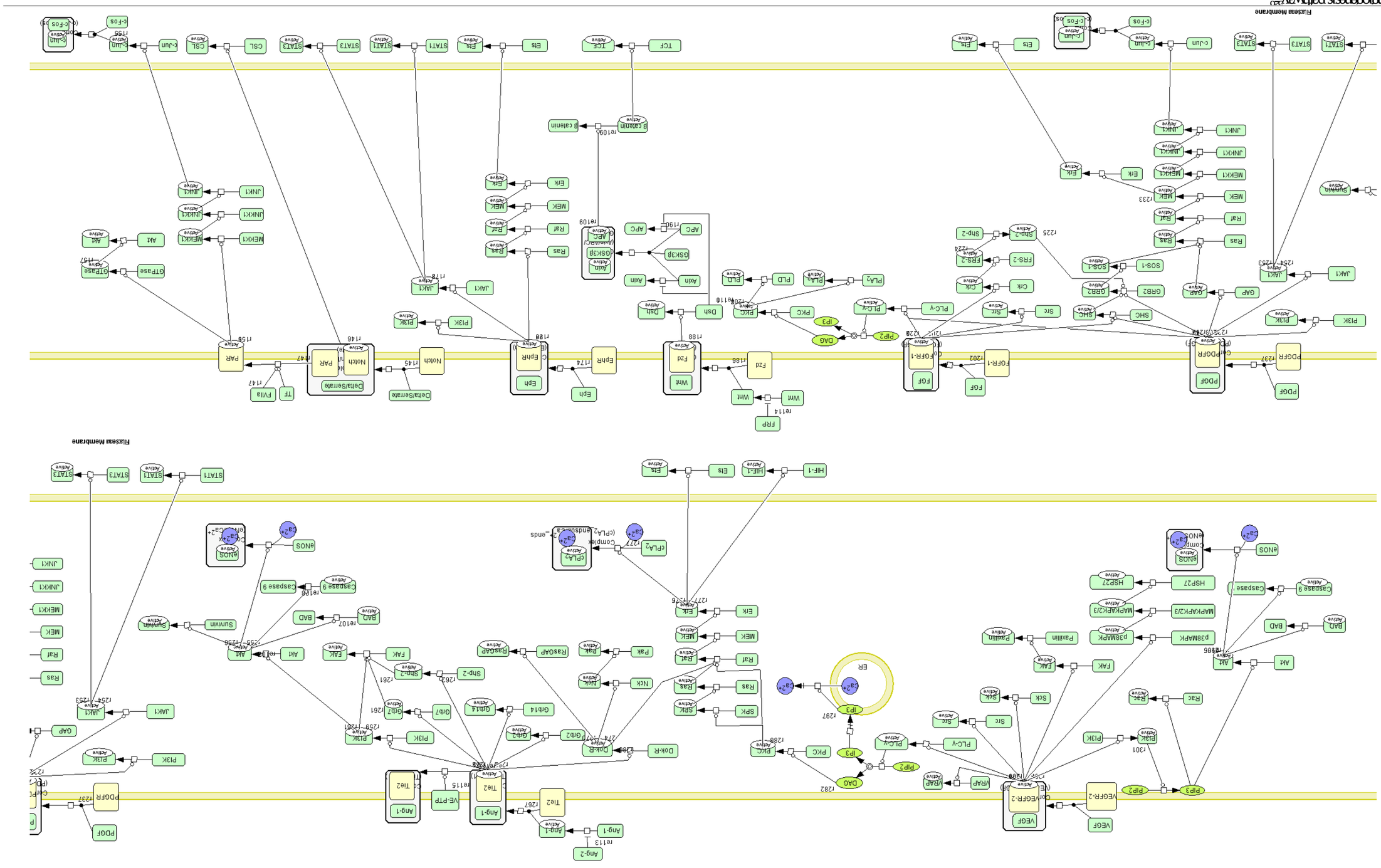

FIGURE 5-28
Figure split over two continuous parts:

FIGURE 5-29

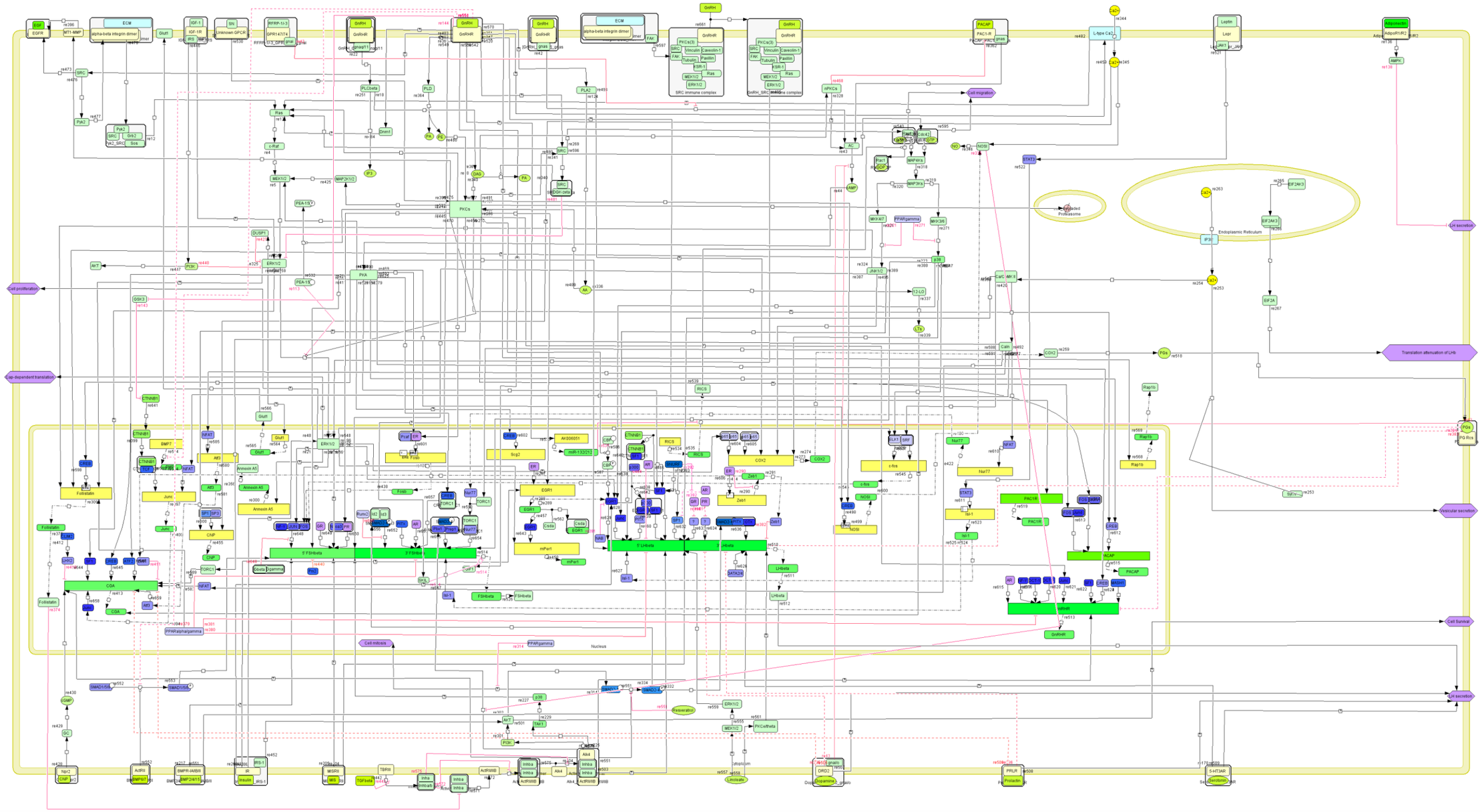
Cell proliferation
Cap-dependent translation
Cell migration
Endoplasmic Reticulum
Translation attenuation of LHb
Vesicular secretion
LH secretion
Cell Survival
Nucleus
Cell mitosis
Ca2+
cAMP
PKA
PKCs
MAPK1/2
ERK1/2
PI3K
AKT
JNK1/2
p38
COX2
PGs
PG Rcs
NOS
NO
STAT1
STAT3
Ca2+ L-type
Leptin
Adiponectin
AMPK
Gi/o
Gq/11
Gs
PACAP
GnRH
GnRHR
SRC
FAK
Vinculin
Caveolin-1
Paxillin
Tubulin
Talin-1
Ras
MEK1/2
ERK1/2
PKCs(3)
SRC immune complex
GnRH_SRC_FAK complex
Ca2+ L-type Ca2+
Leptin
Lepr
JAK2
Jak
Adiponectin
AdipoR1/R2
Ca2+
Ca2+
Ca2+

FIGURE 5-30

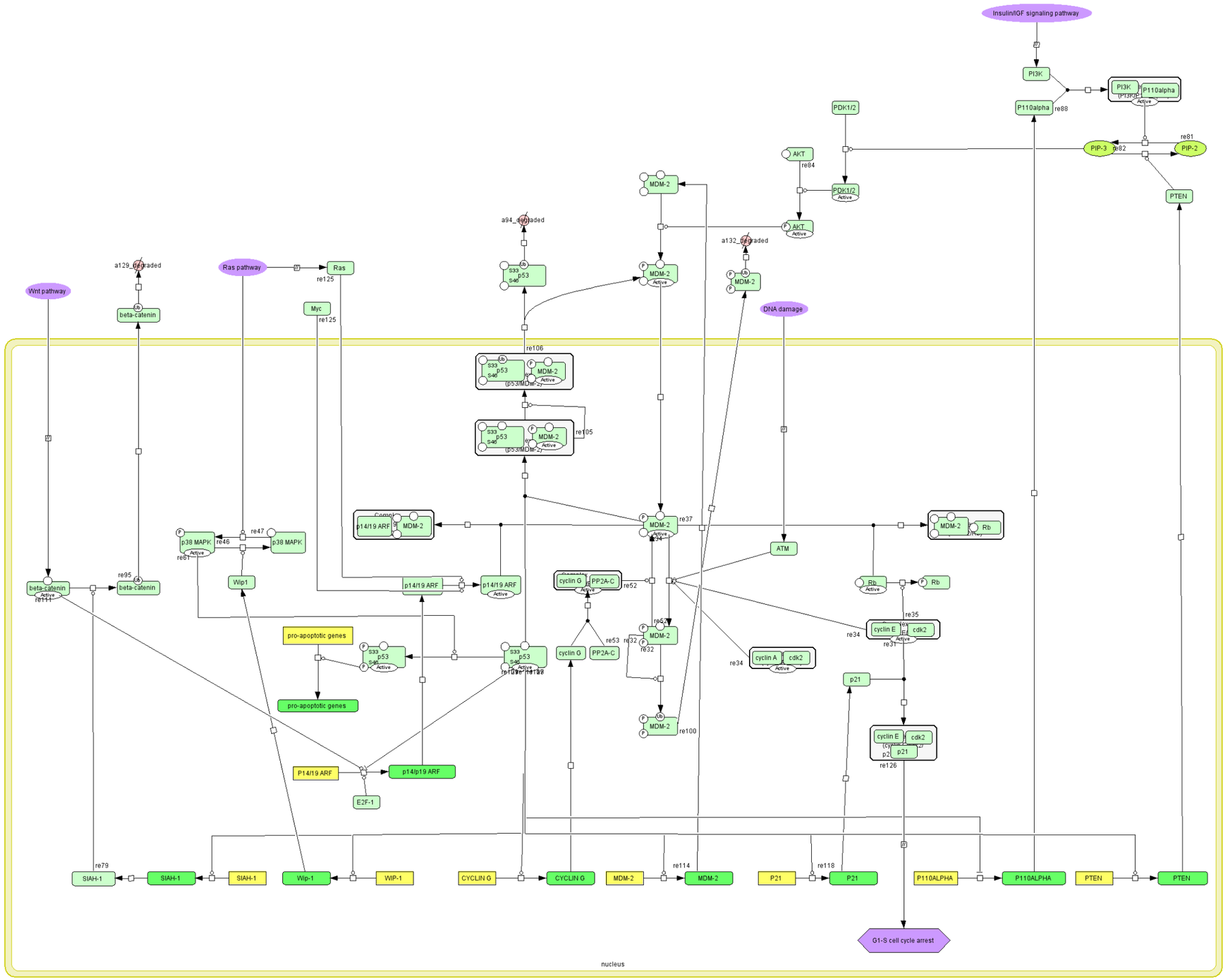

p53 pathway feedback loops [26]

Importin-5 (IPO5) is a transmembrane transporter protein of the importin Beta family. It acts as a G-protein modulator, binds proteins and has small GTPase regulator activity[496,578]. It has a role in cellular protein targeting, nucleocytoplasmic transport, transporting nucleic acid metabolic processes and RNA cellular localisation. Certain viruses such as influenza[624] and EBV[625] amongst others have been shown to use these importing molecules to infiltrate cellular structures and evade host immune systems. This could therefore be a molecule potentially used by EBV in the infiltration of lymphocytes in women with endometriosis.

Erythrocyte membrane protein band 4.1-like protein 5 (EPB41L5) is a member of the CRB-MPP5 polarity complex in mammals[626]. It regulates cellular tight junctions to maintain correct cellular polarity. Changes in the cytoskeletal genes are associated with influences in cell polarity, adhesion and invasive properties and have been shown in cancer progression[627]. EPB41L5 is involved in the Dopamine receptor mediated pathway (Figure 5-31) as well as the nicotine pharmacodynamics pathway (Figure 5-32)[526].

FIGURE 5-31

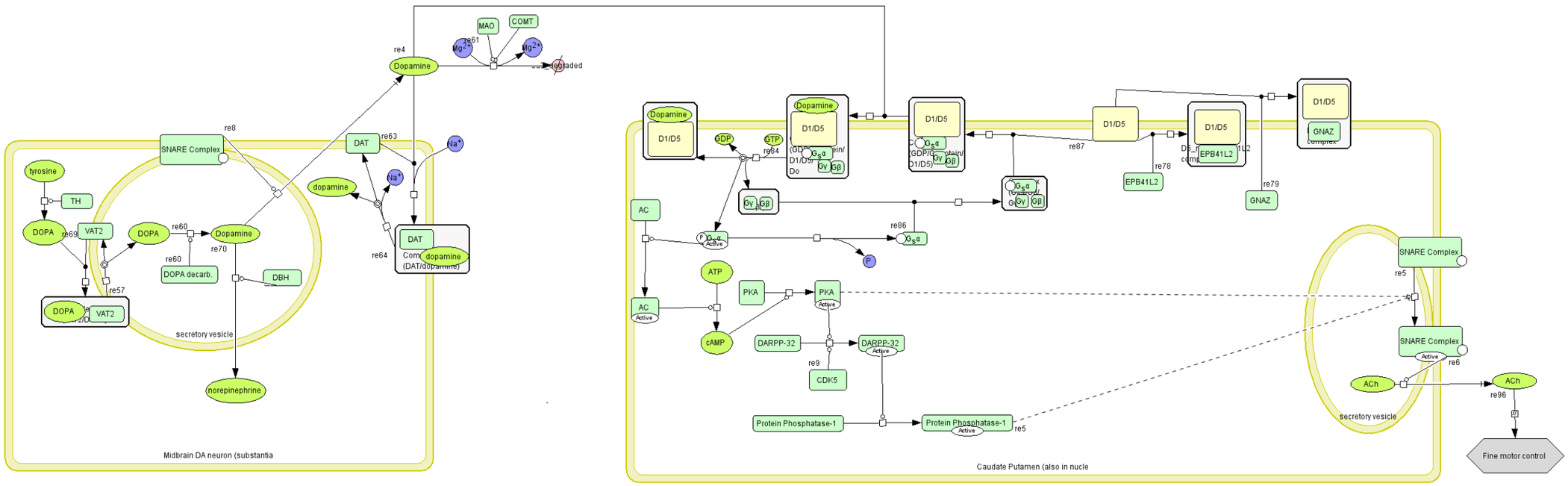

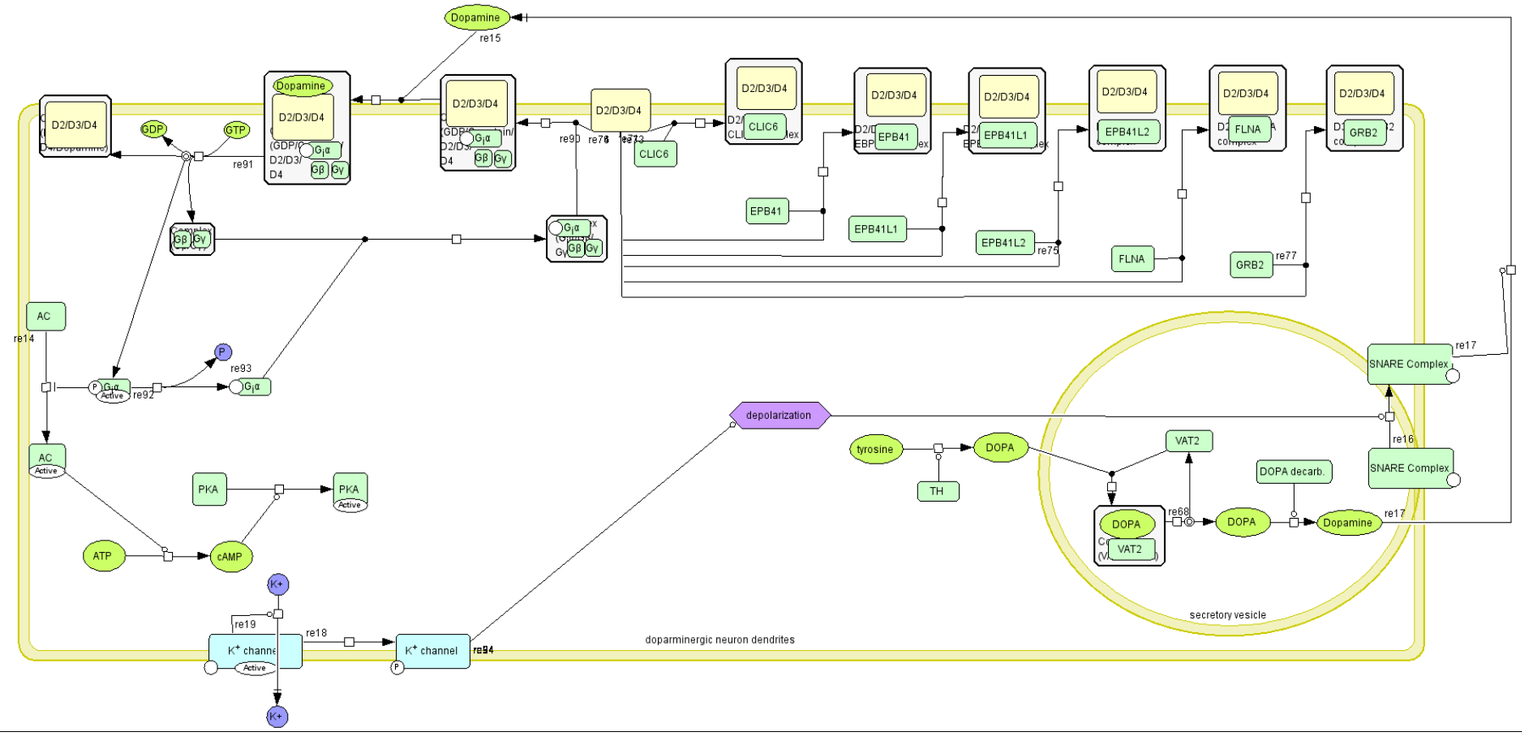

Dopamine receptor mediated pathway[20]

FIGURE 5-32

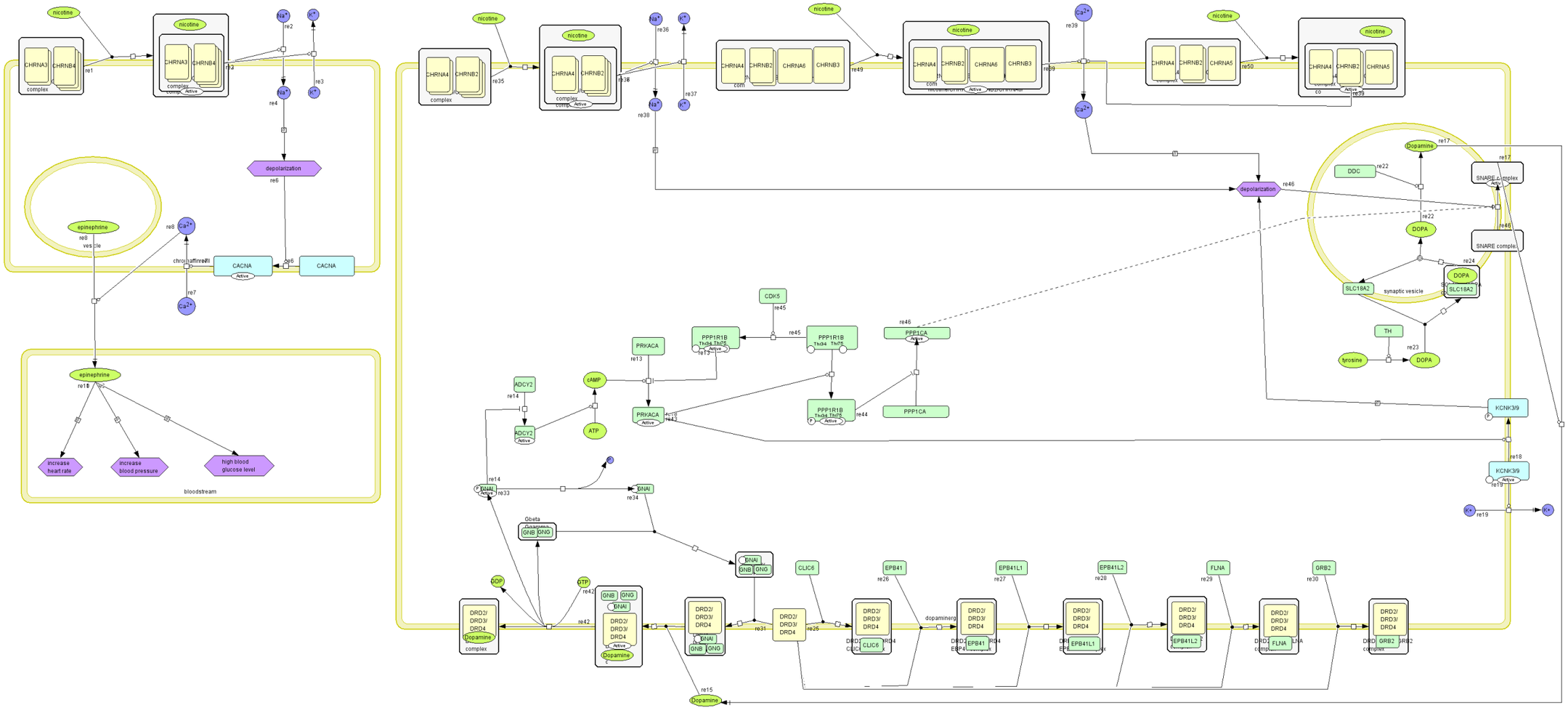

Nicotine pharmacodynamics pathway[20]

Wilms tumour 1 associated protein (WTAP) is a nuclear protein which is a pre-mRNA-splicing regulator[496,578]. In mice it is essential for embryonic development. In mammals its role is not completely understood though IGF-1 (Insulin Growth factor-1) is directly seen to reduce its abundance in the cell. It is postulated that the reduction in cellular WTAP is necessary for the antiapoptotic roles of IGF-1. It is believed to be a binding partner of Wilms tumour suppressor gene (WT1) which is essential in the development of the genitourinary system[628]. WTAP1 degradation is seen to reduce pro-apoptotic Survivin-2B and increase anti-apoptotic Survivin[629], this could explain in role enabling the growth of endometriotic cells.

Alpha-endosulfine (ENSA) is expressed in a wide range of tissues including brain and endocrine tissues[496,578,592]. It can block potassium channels which are ATP sensitive and stimulates insulin release from Beta cells[630]. The role it exerts on potassium channels in the brain can affect neurotransmitter release and cognitive function. Decreased levels of ENSA are seen in Down's and Alzheimer's disease. In endocrine tissues ENSA SNP17 may reduce the ability of Beta cells to compensate for reduced insulin sensitivity which increases the patient's chance of developing type 2 diabetes mellitus[631].

5.7.1.1 Summary of important identified points

- From the above list of genes and proteins controlled by Hsa-mir-150, one can see effects on the cellular functions and mechanisms at multiple levels. *DCAF6, MYB and SMC3* have roles in cellular nucleic acid division and function whilst MPZL1 affects cellular motility and potential of migration. Aberrations in these processes will potentially result in cellular mutations and abnormal cellular properties, enhancing the potential of disease development such as endometriosis.

- Apoptotic inducers such as *PDCD47 and* WTAP1 are identified and these balance out against anti-apoptotic molecules such as *MDM4 and MYB IL7* which promote cellular survival and growth. Alterations in any of these genes or molecules could be responsible in part for the development of endometriosis whilst concomitantly preventing progression to malignancy.

- Angiogenesis is a vital requirement for the survival of ectopically implanted tissue such as endometriosis and *NRCAM, SEMA3A, VEZF1 and CNNB1* are all identified angiogenic promoters.

- Molecules such as *CAST, MTCH2, RGNEF*, and EPB41L5 are all linked to metastatic tumour progression, and from my literature search, a pathway associated with carcinogenesis (e.g. WNT) is linked to hsa-mir-150. MDM4 is an anti-tumour suppressor, counteracting the action of p53. The presence of these molecules, genes and pathways can to an extent explain why endometriotic cells grow, disseminate, implant and avoid undergoing apotosis like eutopic endometrial cells.

- CTNNB1 is also linked to hsa-mir-150. In its non- mutated state it functions as a tumour suppressor, other tumour suppressors linked to hsa-mir-150 include *PPP1R3A and* BASP1. These molecules could be responsible for preventing overt malignant changes in endometriotic implants.

- Endometriosis is a hormonally responsive disease. Unsurprisingly, therefore, identified *ADIPOR2 and CTNNB1* are linked to the GnRH pathway which is a medical target of GnRH analogues used to suppress endometriosis.

- Relating back to the information above, there are varied roles which each protein or gene is known to carry out though it is difficult to determine which of these pertains a leading role, or which of these follow on as a secondary response to alternate cellular processes.

- In this study EBV within the leukocytes of patients with endometriosis, could be a potentially important mechanism in disease development. IFIT5 is one of the molecules identified as interacting with hsa-mir-150 which restricts viral replication and stimulates apoptosis in virally infected cells. Other molecules such as *ATP6V1H and* IPO5 counteract the function of IFIT5 enabling viral survival and cellular infection.

- It is beyond the scope of this chapter to determine which are the most likely proteins or genes to cause (or enable to a larger extent) the development of the disease of endometriosis. This would require a separate body of work with functional models to determine important molecular or protein roles. Identification of the most pertinent associated disease molecules or genes could enable future targeted approaches to disease.

- Using the identified proteins and genes, to perform functional modelling studies, to establish which molecules have more pertinent roles, could serve as an interesting body for future work.

5.7.2 hsa-miR-122

FIGURE 5-33

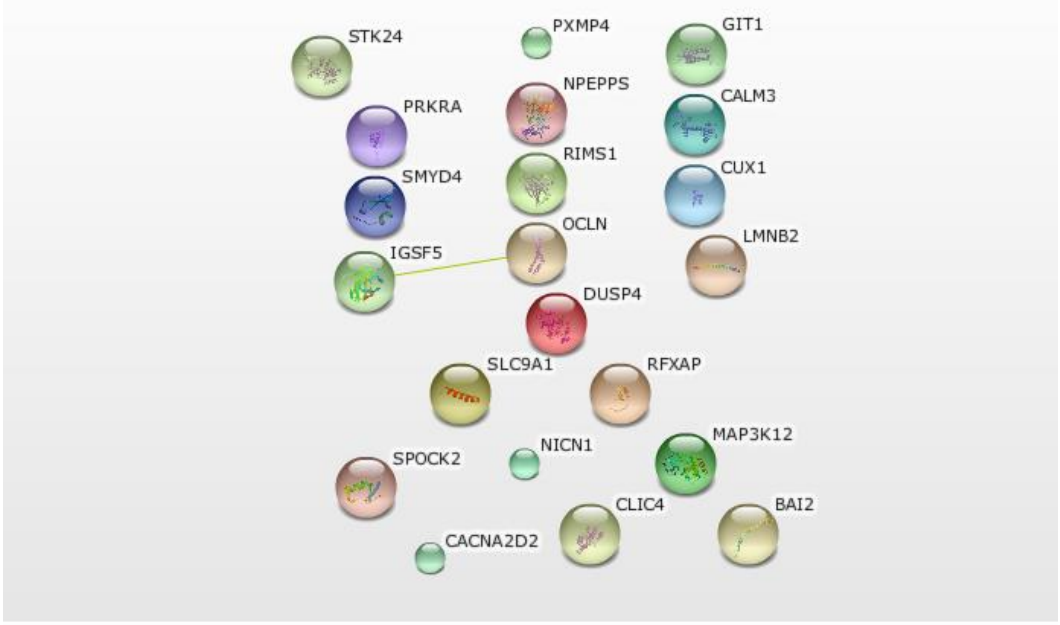

String™ prediction protein analysis diagram[576]

There are a number of predicted targets for hsa-miR-122 (Figure 5-33):

Immunoglobulin superfamily member 5 (IGSF5) is an immunoglobulin superfamily junctional cell adhesion molecule involved in cell adhesion, ectodermal and nervous system development[496,578]. JAM4 is a synonym of IGSF5 and is a cell adhesion molecule which interacts with tight junction proteins. JAM4 is

involved in cellular endocytosis in conjunction with an endocytic scaffold Ligand-of-Numb protein X1 (LNX1). This redistributes transforming growth factor beta in mammary epithelial cells[632]. The immunoglobulin superfamily has recently gained interest as a contributing cell adhesion molecule in metastasis[633] enabling cell-cell adhesion which is a key process in the survival of ectopic cells. Its similar function in ectopic endometrial cells could explain its role in the development of endometriosis.

Occludin (OCLN) is a cellular transcription cofactor involved in cellular tight junctions, cell adhesion and RNA elongation from RNA polymerase 2 promoter[496,578,634]. Studies from normal human vaginal and cervical cells have shown that OCLN can be remodelled through oestrogen receptor alpha mediation, thereby altering tight junction resistance. Normal cells are seen to secrete matrix-metalloproteinase-7 (MMP-7) into the luminal solution, enabling the decrease of tight junctional resistance through oestrogen and estrogen is also seen to act on the cellular golgi system increasing cellular luminal exocytosis processes controlling in –vivo cellular permeability[635]. Oxidative stress responses within the cell are also known to affect cellular distribution levels through its tyrosine- kinase dependant phosphorylation[636]. In endometrial carcinoma, occludin expression levels are seen to decrease resulting in loss of tight junction control. This loss of junctional regulation shows a close relationship with the progression and metastatic ability of the tumour and the formation of cellular atypia[637]. Similar mechanisms could be occurring in endometriosis enabling cellular dissemination and proliferation.

ARF GTPase-activating protein GIT1 (GIT1) is a nucleic acid binding and G-protein modulator[496]. It is part of the G-protein coupled receptor protein signalling pathway and is involved in cell adhesion, control of cellular permeability and cellular endocytosis[578]. It forms complexes with phospholipase C gamma 1 (PLC gamma1) and guanine exchange factor beta-Pix, activates Calpains and calcium-dependant proteases and has a vital role in cellular integrin mediated spreading and motility[638]. A recently identified member of the myosin superfamily, (MYO18A) is seen to interact with other GIT1 complexes (PAK2/betaPIX/GIT1) affecting epithelial cellular mobility and migratory properties[639] playing a role in disease and malignancy. This could be yet another molecule which explains the disseminative properties in endometriosis tissues.

Lamin-B2 (LMNB2) is a structural component of the cytoskeleton which alters the morphology of the cellular components and chromatin architecture of the cytoskeleton[496,578,634]. It is a component of the FAS signalling pathway (Figure 5-34) and it has a role in cellular apoptosis[640]. Lamin proteins are involved in nuclear stability and mutations and are associated with lipodystrophies. Higher levels of LMNB2 expression in tissues are associated with increased metastatic potential in tumours such as lung adenocarcinomas[641], it could also have a similar role in enabling the disseminative properties of endometriosis.

FIGURE 5-34

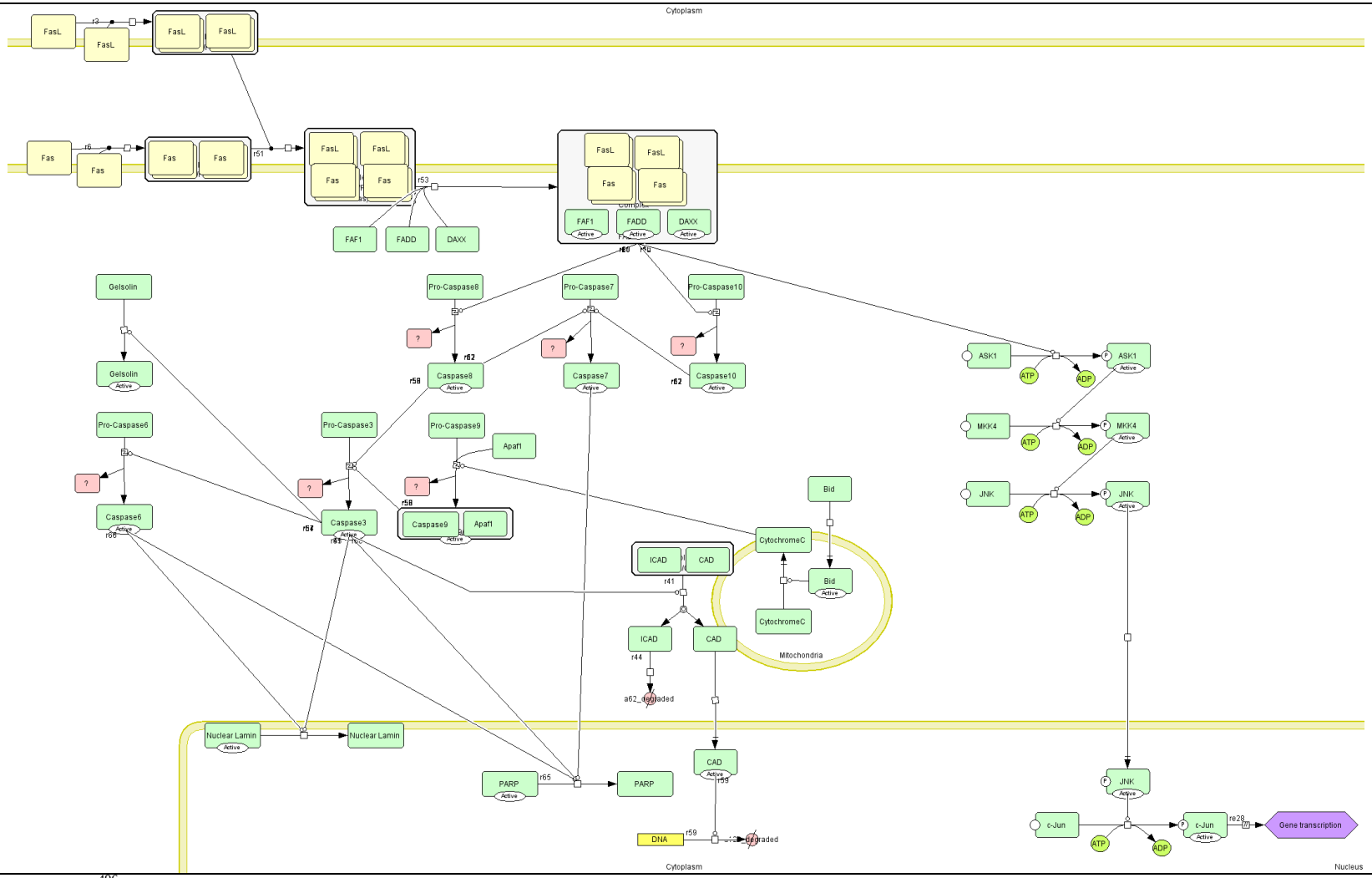

FAS signalling pathway[496]

Dual specificity protein phosphatase 4 (DUSP4) is a mitogen activated protein kinase (MAPK) phosphatase as well as a kinase inhibitor and regulator[496,578]. The DUSP4 proteins serve as negative regulators of the MAP kinase superfamily (MAPK/ERK, SAPK/JNK and p38) which are linked to cellular differentiation and proliferation[577]. It is therefore involved in numerous cellular processes, is a constituent of the cell cycle and has a role in DNA replication, glycolysis and protein and amino acid phosphorylation. DUSP4 also has a role in the immune system, forms part of the JNK cascade, is involved in mesodermal and muscle development and is also involved in the JNK signalling oxidative stress response pathway[642] (Figure 5-35)[526]. Abnormal MAPK signalling is believed to be implicated in the development and progression in human cancers. MAPK regulation in normal tissues shows that deregulation of this tightly controlled process can initiate or develop cancer, determine cellular responses to cancer therapies and alter patient prognosis[643]. As a negative regulator of the MAPK superfamily, the DUSP4 could play a role in preventing endometriosis from transforming itself into more aggressive disease serving as a regulator for disease dissemination.

FIGURE 5-35

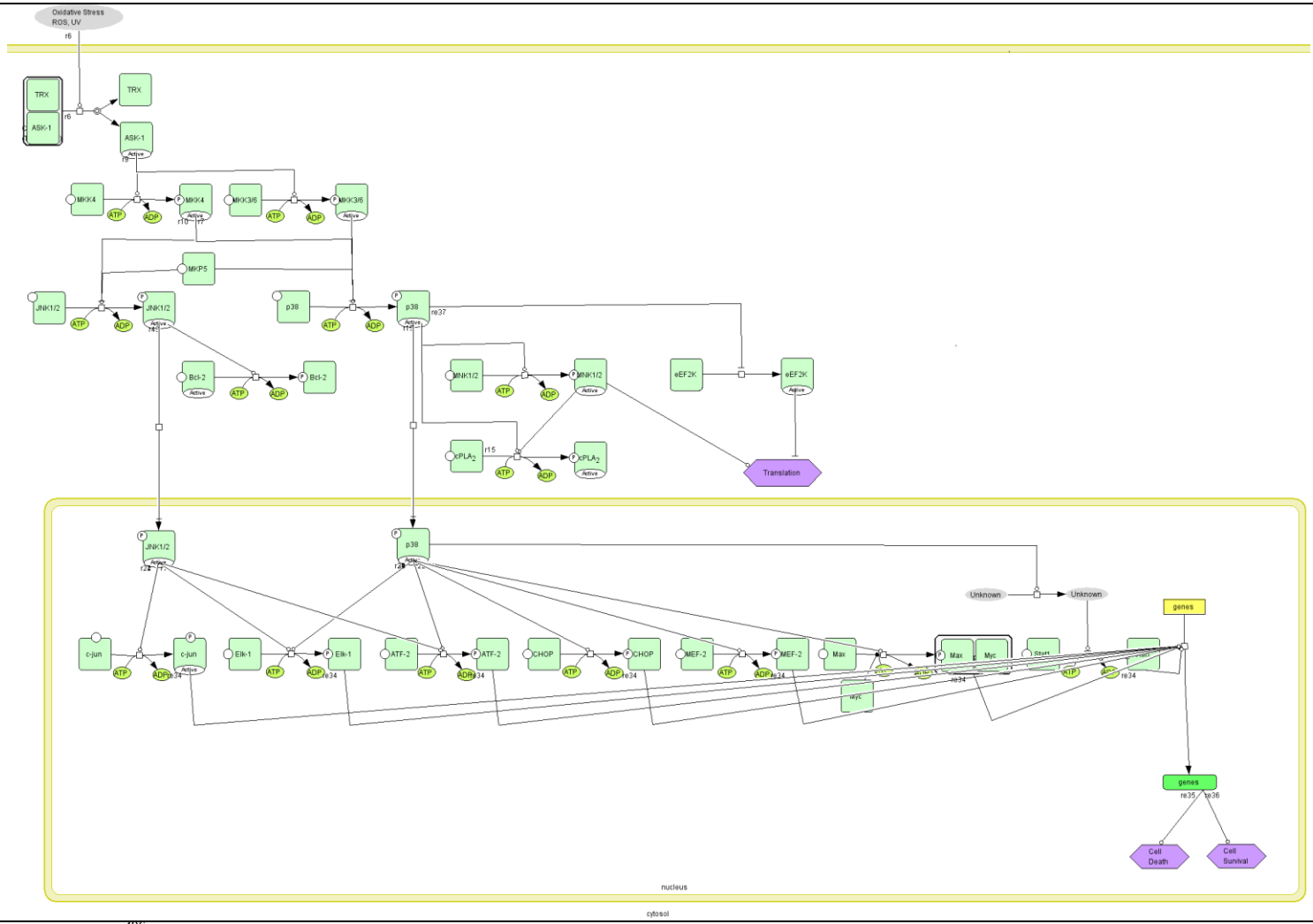

Oxidative stress response pathway[496]

Chloride intracellular channel protein 4 (CLIC4) is an intracellular chloride channel involved in most cellular processes. It is a structural constituent of the cytoskeleton and acts as a protein, an anion channel, a transferase, a signalling molecule, a reductase, a translation-elongation factor and an epimerase[496,577,578,592]. It is a constituent of the nicotine pharmacodynamics pathway (Figure 5-32)[526] and the dopamine receptor mediated signalling pathway (Figure 5-36). CLIC4 plays a role in the immune system process and response to cellular toxins, anion transport and intracellular signalling cascades, the metabolic processes of oxygen reactive species and cellular translation. In ovarian cancer, upregulation of CLIC4 by reactive oxygen species causes TGF-beta1 differentiation of fibroblasts to myofibroblasts which is a mark of active tumour stroma. It is therefore postulated that inhibition of CLIC4 night be a potential therapeutic option for stromal tumour targeting in ovarian tumours[644,645]. Potentially, changes within CLIC4 levels can be attributed to changes in the properties of ectopic endometrial cells of women, with endometriosis. If this link were to be established, it could be utilised as a therapeutic target for the treatment of endometriosis.

FIGURE 5-36

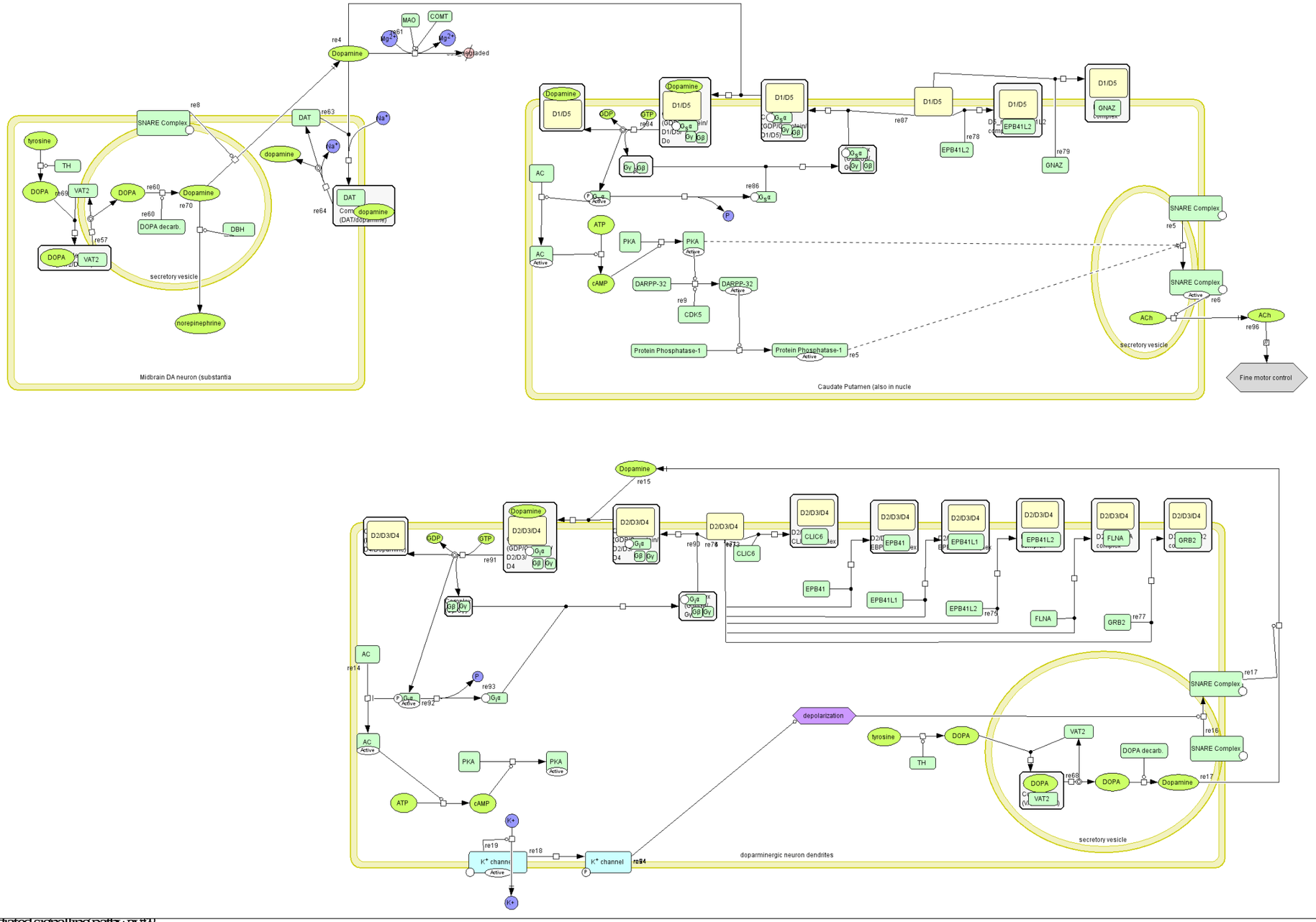

Dopamine receptor mediated signalling pathway[35]

Serine/threonine-protein kinase 24 (STK24) is involved in phosphate metabolic process and protein amino acid phosphorylation[496,578]. Mammalian sterile 20-like kinase 3 (MST3) is a synonym of STK24 and mediates cell death by suppressing JNK survival pathway and upregulating haemoxygenase 1 expression in the cell[646]. These anti tumorigenic and anti-cellular migratory properties[592,647] serve to control disease proliferation and spread, potentially preventing a condition such as endometriosis from disseminating further or developing overt malignant features.

Homeobox protein cut-like 1 (CUX1) regulates transcription from RNA polymerase 2 promoter and has a role in nucleic acid binding[496,578]. CUX1 is an important mediator in tumour invasion and a target for tumour growth factor beta (TGF beta). Wingless-type MMTV integration site family, member 5A (WNT5A) (A member of the Wnt multigene family) is seen to be upregulated by CUX1 increasing cellular potential for survival, proliferation and invasion in pancreatic tumours[648]. miRNA-122 targets CUX1 (CUTL1) and represses it. This might play a role in the suppression of cellular proliferation[649] and a similar effect could potentially be occurring in endometriosis, moderating disease proliferation, invasion and growth.

SET and MYND domain-containing protein 4 (SMYD4) regulates transcription from RNA polymerase 2 promoter and acts as a transcription cofactor[496,578]. It has been identified as a tumour suppressor gene in breast cancer. It inhibits the expression of platelet-derived growth factor receptor alpha polypeptide (Pdgfr-alpha) which is highly expressed in malignant cells and could potentially be a target for treatment of disease[650]. In endometriosis, its tumour suppressive properties could be important in the prevention of disease progression to an overt malignant state.

Puromycin-sensitive aminopeptidase (NPEPPS) has metallopeptidase activity and is involved in proteolysis[496,578]. It exhibits neuroprotective roles over neurodegenerative disease though proteolysis of the neurotoxic hyperphosphorylated TAU protein[651].

Mitogen-activated protein kinase kinase kinase 12 (MAP3K12) is involved in female gamete generation[496]. It is released in response to stress and has a role in a multitude of cellular processes, cell morphogenesis and the cell cycle. It is involved in apoptotic induction, cell adhesion, protein amino acid phosphorylation and is part of the immune system process[578,592]. It has also been involved in the gonadotropin releasing hormone receptor pathway (Figure 5-19), transmembrane receptor protein serine/threonine kinase signalling pathway, the JNK cascade (Figure 5-35) and I-kappaB kinase/NF-kappaB cascade (Figure 5-37)[526]. Recent advances in genomic technologies can give us an improved insight into the central pathways involved in cellular pathogenesis and their survival[652]. The MAP3K12 locus has been identified as an important locus in tumorigenesis[652]. In endometriosis, similar effects of MAP3K12 enabling ectopic cellular growth and apoptotic evasion can be postulated, it could potentially serve as a future target for directed therapeutics in disease.

FIGURE 5-37

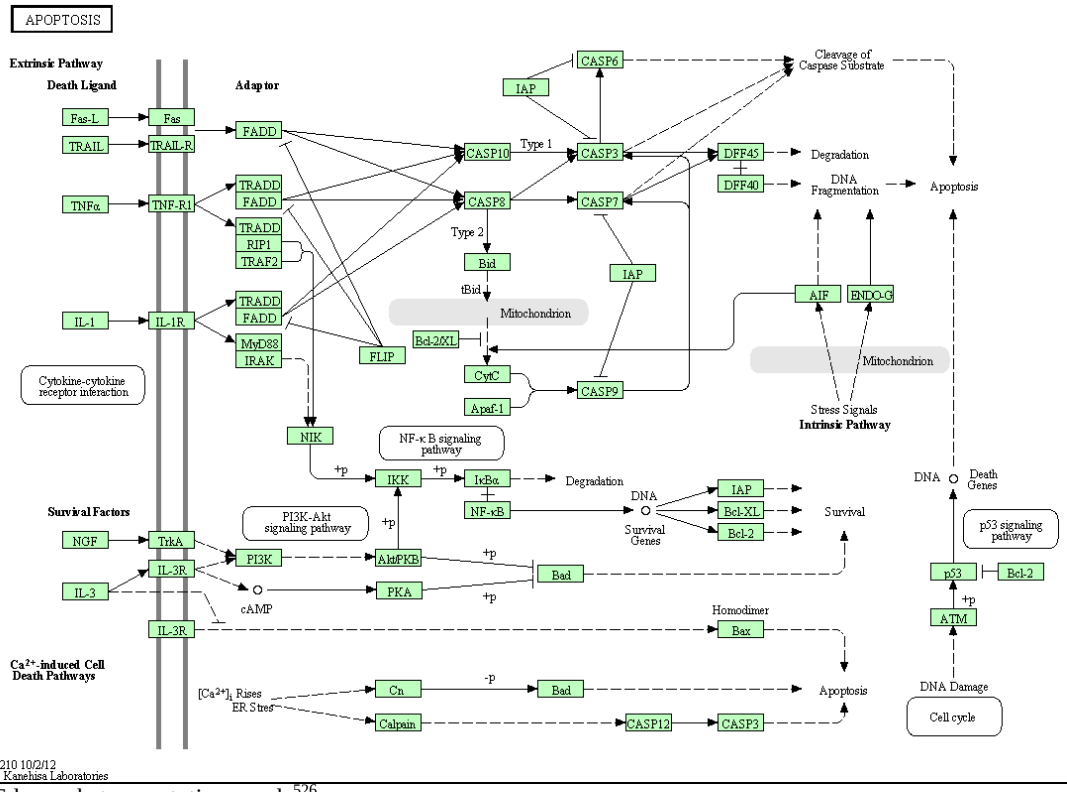

NF-kappa beta apoptotic cascade[526]

Brain-specific angiogenesis inhibitor 2 (BAI2) is a G-protein coupled receptor and acts as an antibacterial defence response protein and a stress response protein[496,578]. It has a role in cellular immune response and regulates intracellular protein transport, cell adhesion, synaptic vesicle exocytosis and transmission and is implicated in spermatogenesis, angiogenesis, cardiac and mesodermal development via involvement in the p53 pathway (Figure 5-38)[526] and the G-protein coupled receptor protein signalling pathway[526]. Analysis of BAI2 in in vivo cerebral ischemia models and *in vitro* hypoxic models showed that its angiostatic properties relate to decreased neovascularisation in the adult brain. In hypoxia, it is responsible for the neovascularisation in the adult brain in combination with elevated levels of vascular endothelial growth factor (VEGF) which is itself angiogenic[653]. In endometriosis, potential effects of BAI2 in the presence of external stressors or hypoxic milieu can account for neovascularisation developing around ectopic implants enabling their growth within the body.

FIGURE 5-38

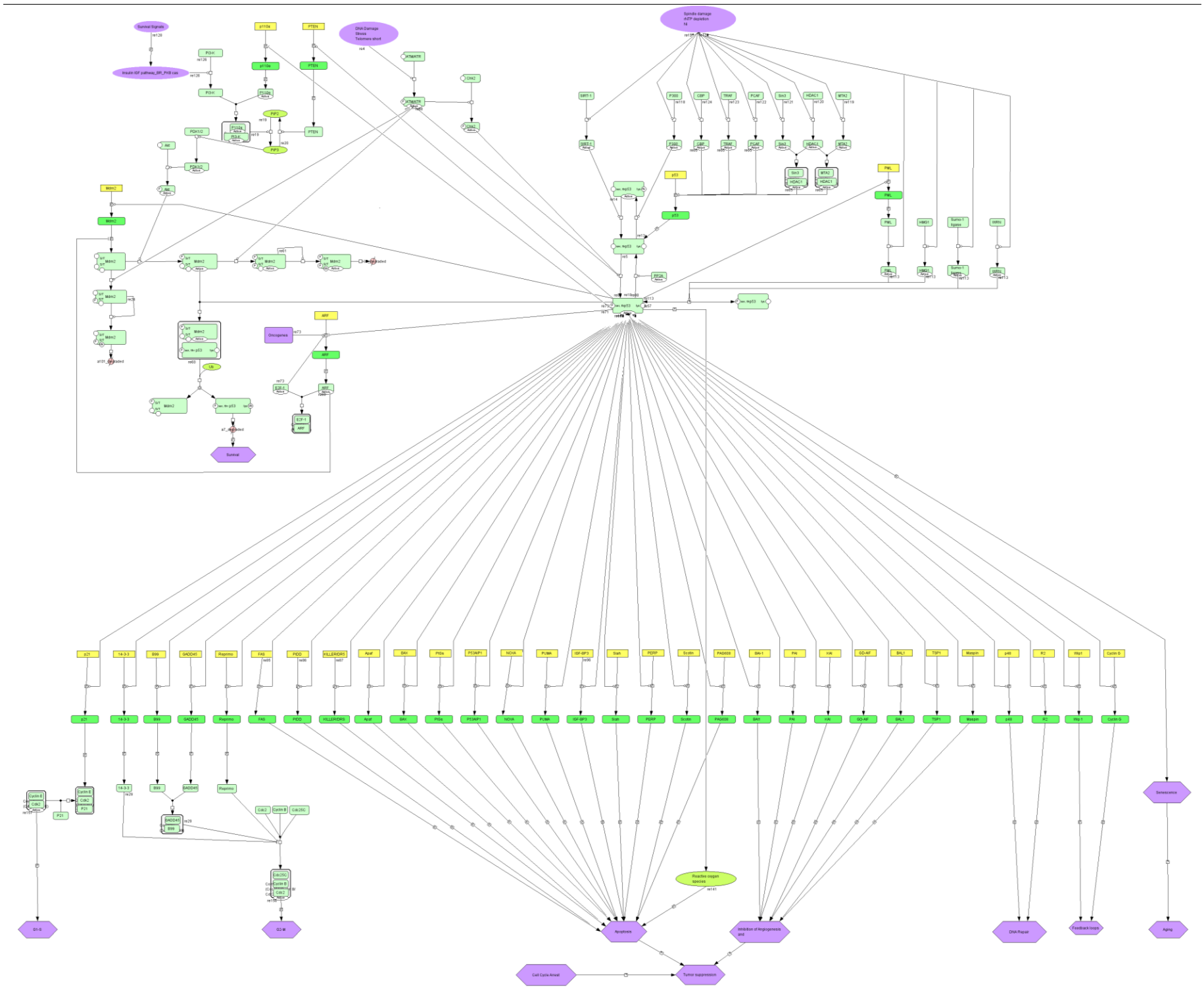

p53 Pathway[56]

Interferon-inducible double stranded RNA-dependent protein kinase activator. A (PRKRA) is a DNA and RNA binding protein[496]. It also acts as an immunity protein, a deaminase and a kinase activator within the cell. Cellularly it is involved in cell cycle control, anterior/posterior cell axis specification and RNA localisation[578,592]. It has a role in purine base and protein metabolic processes and in response to interferon gamma, regulates and forms part of the apoptosis signalling pathway (Figure 5-39)[526] as well as being implicated in spermatogenesis and neurological system processes. The activation of the PKR family is not completely understood. It is believed that activating stimuli such as cytotoxins, stresses, viral infections or even chemotherapy cause the PKR activator RAX to initiate reactions and cause TNF-alpha activation[654] of apoptosis. Similar mechanisms might be occurring within endometriosis altering cellular and apoptotic controls. The PRKRA protein is therefore seen to have important effects on cell modulation and growth through multiple pathways including the TNF-induced activation of nuclear factor-kappaB (NF-kappaB) and mitogen-activated protein kinases (MAPKs)[655]. It is seen overall to positively regulate NF-kappaB (IkappaB) alpha kinase (IKK) and c-Jun N-terminal kinase (JNK) whilst negatively regulating mitogen-activated protein kinases (MAPKs) (p44/p42 MAPK and p38MAPK)[655]. MAPKs could potentially play an important role in the disease of endometriosis[656] so PRKRA regulation might make this an important target in this disease.

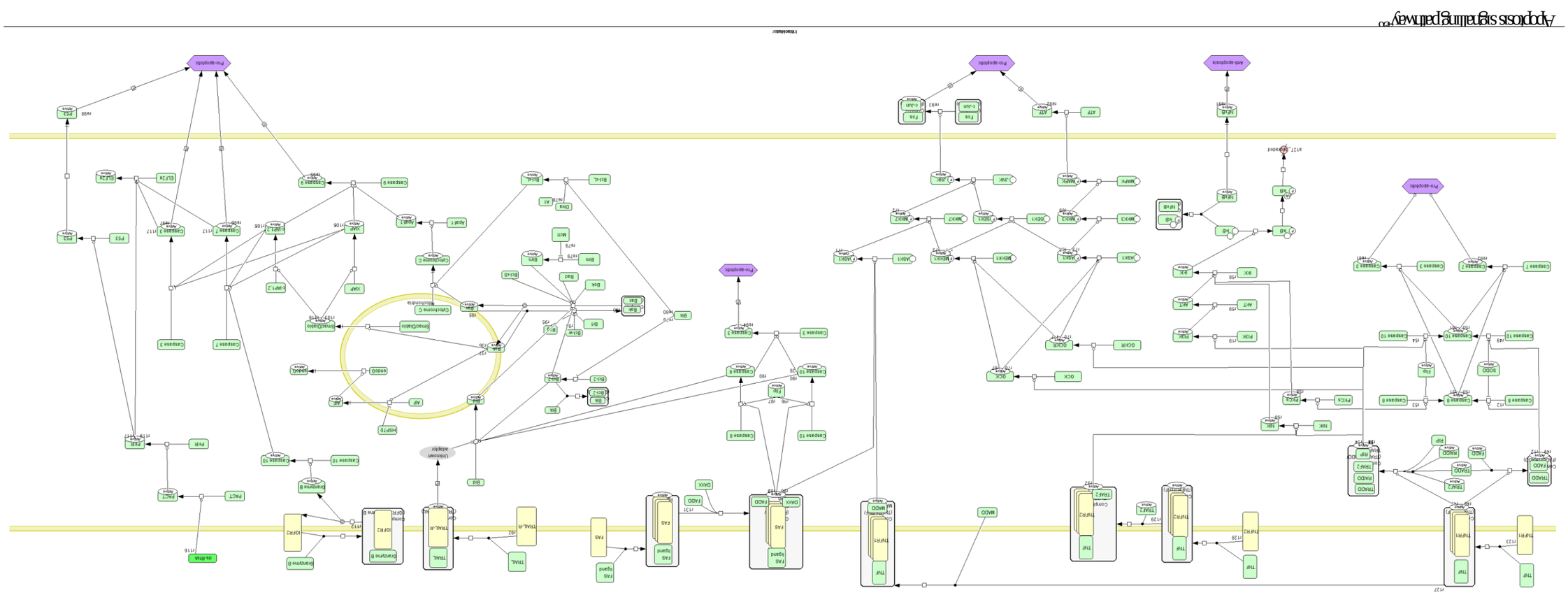

FIGURE 5.39

Apoptosis signaling pathway[30]

Voltage-dependent calcium channel subunit alpha-2/delta-2 (CACNA2D2) has voltage gated and cation channel activity. It is involved in cation and protein cellular transport and signalling as well as neurological system processes and muscle contractions[496,578,592]. CACNA2D2 has tumour suppressor gene properties which when altered is seen in the development of certain moderate dysplastic lesions in head and neck squamous cell carcinomas[657]. CACNA2D2 is part of a tumour suppressor gene cluster flanking isoform A of the Ras-association domain family member 1 (RASSF1A) gene. RASSF1A is one of the most frequently silenced genes in human tumours. Genetic repression is seen in CACNA2D2 in breast cancer cell lines, providing further evidence of its involvement in development of malignancy[658]. A recently published study has also looked at alterations in RASSF1A and CACNA2D2 in cervical carcinomas and it is postulated that they could be used to diagnose early disease and improve prognosis[659]. In endometriosis, *CACNA2D2* could potentially serve as a tumour suppressor preventing overt changes to malignancy.

Regulating synaptic membrane exocytosis protein 1 (RIMS1) has protein binding and small GTPase regulator activity involved in cellular synaptic transmission (Figure 5-40), intracellular protein transport and exocytosis of synaptic vesicles and cellular constituents[496,578,592]. It is also responsible for visual and sensory perception and defects in its function are associated with pathology such as retinal dystrophies.

FIGURE 5-40

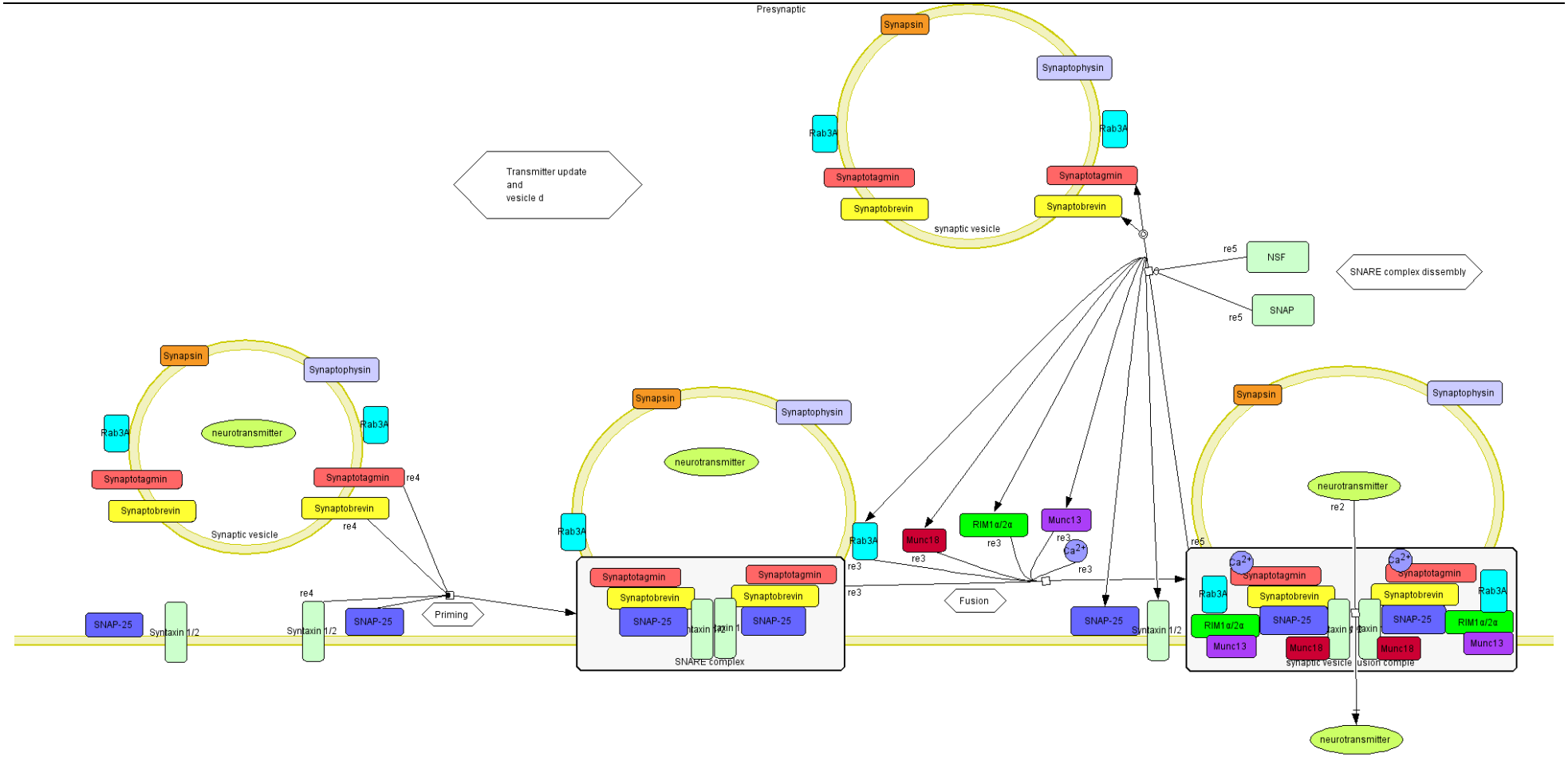

Synaptic vesicle trafficking[496]

Solute Carrier family 9 Sodium/hydrogen exchanger 1 (SLC9A1) is a cation transmembrane transporter involved in cell migration but its pathways are not yet completely understood[496,578,592]. Studies with cervical cancer have shown that NHE1 (Synonym for SLC9A1) is upregulated with epidermal growth factor (EGF) promoting cellular volume regulation, cytoskeletal remodelling, migration and invasiveness[660]. This has clinical implications in the early stages of malignancy. In a similar way, it potentially could have an effect on ectopic endometriosis and its dissemination. NHE's are also important in inflammation and in the maintenance of the body's immune responses. Monocytes and neutrophils generate cytokines and reactive oxygen species as a first defence in response to stimuli. It is the NHE in the system that maintains the correct pH levels for optimal functioning of these immune cells[661]. If in endometriosis, the NHE system is altered, a change in cellular environmental pH could be another causative factor preventing immune cells recognising and eliminating ectopic disseminative cells.

Peroxisomal membrane protein 4 (PXMP4) is described as an anti-tumour gene which is silenced through DNA methylation in prostatic carcinoma cells[662]. In the immune system this peroxisome membrane protein is known to bind to Pex19 which is an intracellular chaperone and is a component of the glycolipid membrane endocytic process[496,578,592]. This process is encoded for by yet another gene controlling Natural killer t-cells (Nkt1). T cells can recognise glycolipids presented on CD1 proteins. It is possible that if peroxisomes alter glycolipid availability for the CD1D presentation, they can influence NKT cell functions[663]. In endometriosis this could be another window enabling survival and development of disease.

Regulatory factor X-associated protein (RFXAP) is one of three proteins (RFXB/ RFX5/RFXAP) comprising the RFX complex. This complex regulates expression of major histocompatibility complex class 2 genes[496,578]. Mutations in the RFX complex have been shown to result in severe immunodeficiency within the organism[664]. If in endometriosis, this protein has the same effects of causing a level of immunodeficiency within the patient, it could (in conjunction with other alterations in cellular properties) explain the ability of ectopic tissue to evade apoptosis and elimination. In combination with another gene, brahma related gene 1 (BRG1), RFXAP is also associated with cellular chromatin remodelling[665] and with the nuclear translocation and expression of MHC class 2 genes[666].

Nicolin-1 (NICN1) is a mammalian gene encoding a 213 amino acid nuclear protein not attributed to a known family[496,578,592]. High levels are found in brain, testes, liver and kidneys. It is low in leukocytes, colon, spleen and small intestine. It is also expressed during development[667]. Not much is known about the gene's function.

Testican-2 (SPOCK2) is a member of the testican group of extracellular proteoglycans[668]. It has a modular structure indicating the potential to participate in various interactions. It has four main domains (follistatin-like, calcium binding domain, thyroglobulin type-1 domain and an acid C-terminal domain with attachment sites for glycosaminoglycans) and is seen to interact with the subcomponent of complement component C1 (C1q) activating complement activation pathways[496,526,578,592]. This indicates its importance in inflammatory or immune processes. Interestingly, epigenetic inactivation of SPOCK2 is seen in the malignant transformation of ovarian endometriosis[669].

5.7.2.1 Summary of important identified points.

- From the above list of genes and proteins controlled by Hsa-mir-122, one can see effects on various cellular processes, properties and pathways. Internally, endocytic processes are altered by IGSF5 and GIT1, potentially disrupting the normally balance cellular milieu. GIT1 is also seen to affect cellular motility whereas CLIC4 and *SLC9A1* increase the adhesive cellular potential enabling implantation of ectopic tissue such as endometriosis.

- Apoptotic mediators such as MAP3K12 are also seen to interact with hsa-mir-122 altering cellular survival potential. LMNB2 and PRKRA are also associated with the apoptotis and FAS signalling pathways, they too can effect cellular survival and growth in endometriosis.

- Neovascularisation is an essential process to maintain survival in growing tissue, including ectopic implants in endometriosis. BAI2 has been linked to hsa-mir-122 and potentially enables survival of ectopic tissue through its effects on neovascularisation.

- IGSF5, LMNB2 and OCLN are all linked to metastatic tumour progression, potentially contributing to the properties of dissemination, proliferation and growth seen in endometriosis. DUSP4, STK24 and CUX1 have counteracting effects causing metastaic repression. Potentially it is a fine balance between these genes and proteins that prevent overt malignant transformation in endometriosis.

- Tumour suppressor properties in SMYD4, *CACNA2D2 and PXMP4* have also been explored. BAI2 is also seen to interact with tumour suppressor p53. The effects of tumour suppressors on a multifactorial disease such as endometriosis might be imperative in preventing malignant transformation within the majority of my patient population.

- Endometriosis is a hormonally responsive disease. MAP3K12 is also seen to affect the GnRH pathway. Current suppressive medical therapies aim to target the GnRH pathway through the use of GnRH analogues to promote cellular apoptosis.

- A correctly functioning immune system is imperative in the recognition and elimination of diseased and/or ectopic cells. Genes and proteins (such as *MAP3K12 and RFXAP) a*ffecting the immune system have been linked to hsa-mir-122. Other proteins and genes such as SLC9A1 affect the milieu in which immune cells function potentially altering their effectiveness. PXMP4 is another gene which affects Natural killer cell function potentially enabling progression of disease.

- Relating back to the information above, there are varied roles which each protein or gene is known to carry out though it is difficult to determine which of these pertains a leading role, or which of these follow on as a secondary response to alternate cellular processes.

- It is once again beyond the scope of this chapter to determine which are the most likely proteins or genes to cause (or enable to a larger extent) the development of the disease of endometriosis. A separate body of work with functional models to determine important molecular or protein roles together with identification of the most pertinent associated disease molecules or genes could enable future targeted approaches to disease.

5.8 Detailed cellular function analysis of upregulated and downregulated serum miRNAs

In this section of my thesis I aim to look at the functional changes that are induced by the proteins and genes explored above. Rather than their analysis on an individual basis I believe it will be clinically relevant to see how their impact on human embryology the cell cycle, cellular architecture, cell signalling, proteolysis and endocytosis as well as their contribution to angiogenesis and their impact on the immune system all conforms to facilitate development of endometriosis.

In my study, miRNAs hsa-mir-1224-5p and hsa-mir-4274 are upregulated in serum of women with endometriosis whilst hsa-miR-150 and hsa-miR-122 are downregulated. These miRNAs control a number of proteins and genes associated with the development of angiogenesis, cell cycle control and inter and intra cellular interactions. Other genes controlled by these miRNAs are involved in cell motion and adhesion, vesicular endo/exocytosis and cell survival through the evasion of the apoptosis and the alteration of the immune system processes of the body. All these effects are tightly controlled in normally functioning cells. Cellular derangement at micro RNA levels can give rise to aberration of control and lead to the development and progression of a disease such as endometriosis.

5.8.1 Embryology

In the theory of Mullerianosis (See section 1.6.3), endometriosis is believed to originate from aberrant or displaced mullerian tissues during embryological development. Publications supporting the embryonic orogin of endometriosis arise from evidence of ectopic endometrium in human female foetuses at different gestations[670]. The reason for the presence of ectopic endometrium could potentially arise from aberrations in genes controlling embryology and organogenesis. The genes linked to ectodermal, mesodermal and embryonic development could potentially be involved in the formation of endometriosis through the function and interactions of the upregulated hsa-mir-1224-5p and/or hsa-mir-4274 or downregulated hsa-mir-150 and/or hsa-mir-122. Each respective miRNA identified in my study has been linked to various other proteins and genes with which they potentially interact.

Hsa-mir-1224-5p (See section 5.6.1) is linked to Ubiquitin-conjugating enzyme E2 W (UBE2W) a key role player in embryonic development. Other associations include Tensin-1 (TENS1), Krueppel-like factor 3 (KLF3), C-X-C motif chemokine 6 (CXCL6), Eosinophil cationic protein ribonuclease, RNase A Family, 3 (RNASE3) and Dystrophin-related protein 2 (DRP2). These are all linked to embryonic mesodermal development. It is the intermediate mesoderm that develops into the urogenital system in adults[671]. Dystrophin-related protein 2 (DRP2), MAP kinase-activating death domain protein (MADD) and Neurogenic differentiation factor 4 (NEUROD4) are linked to embryonic ectodermal development which gives rise in adults to the nervous system, enamel and epidermis[671].

Hsa-mir-4274 (See section 5.6.2) controls and interacts with other molecules including: pituitary adenylate cyclase-activating polypeptide type I receptor (ADCYAP1R1), embryologically involved in mesodermal and heart muscle development and protocadherin-9 (PCDH9). The latter is involved in ectodermal, muscle and heart development.

Hsa-miR-150 (See section 5.7.1) is seen to control a number of genes that have an embryonic role in the development of tissues. Myelin protein zero-like protein 1 (MPZL1) (PZR) is involved in early embryonic tissue formation, neurogenic differentiation factor 6 (NEUROD6) is involved in ectodermal development, neuronal cell adhesion molecule (NRCAM) and semaphorin-3A (SEMA3A) regulate ectoderm and mesoderm development, whilst brain acid soluble protein 1 (BASP1) and RNA-binding motif protein, X-linked-like-2 (RBMXL2) are involved in ectodermal and nervous system development.

Hsa-mir-122 (See section 5.7.2) controls other genes with a role in embryological development. Immunoglobulin superfamily member 5 (IGSF5) is linked to ectodermal and nervous system development. Dual specificity protein phosphatase 4 (DUSP4) controls mesodermal and muscle development, whilst interferon-inducible double stranded RNA-dependent protein kinase activator A (PRKRA) is involved in spermatogenesis and neurological system processes. Mitogen-activated protein kinase kinase kinase 12 (MAP3K12) is associated with female gamete formation and brain-specific angiogenesis inhibitor 2 (BAI2) is linked to mesodermal development and spermatogenesis.

5.8.2 The cell cycle and DNA replication

Cellular mitosis and meiosis are imperative for correct DNA synthesis, progression and replication of a cell through the cell cycle. Aberrations in replication of nuclear material results in cellular mutations, which accumulate as the mutated cells replicate. Multiple cellular mutations are linked to cancer[672] where cells replicate at an increased rate eventually infiltrating surrounding tissues. The development of endometriosis could potentially be attributed to alterations in molecules controlling cellular division, resulting in cells with the potential to disseminate, implant and invade.

Cellular mitosis and meiosis are regulated by the following genes that are influenced by hsa-mir-1224-5p (See Section 5.6.1): ubiquitin-conjugating enzyme E2 W (UBE2W), SUN domain-containing protein 1 (SUN1), synaptopodin-2 (SYNP2), prickle-like protein 2 (PRIC2) and dual specificity tyrosine-phosphorylation-regulated kinase 1A (DYRK1A). Ubiquitin-conjugating enzyme E2 W (UBE2W) and prickle-like protein 2 (PRIC2) control chromosome segregation and dorsal ventral axis specification of the nuclear cellular material[496,578]. Sex comb on midleg-like protein 4 (SCML4) is another molecule that interacts with hsa-mir-1224-5p, binds chromatin and has transcription factor activity.

Hsa-mir-4274 (see Section 5.6.2) controls the regulator of G-protein signalling 20 (RGS20) which enables dorso ventral axis specification and allows for the correct segregation of nuclear material. Aberrations in any of these processes can be responsible for cell cycle dysregulation which can give rise to the formation of pathology. Hsa-mir-4274 is also involved in the mitotic process through the regulation of cGMP-dependent protein kinase 2 (PRKG2) and rap guanine nucleotide exchange factor 2 (RAPGEF2) which has GTPase regulator activity. This miRNA also controls transformer-2 protein homolog beta (TRAB2B) which splices mRNA in mitosis.

In endometriosis, miRNA hsa-mir-1224-5p is seen to control various genes affecting the cell cycle at various points. RNA polymerase 2 is an enzyme within cells that catalyses the transcription of DNA to precursors of mRNA and most snRNAs and miRNAs. Various genes controlled through miRNA hsa-mir-1224-5p regulate the transcription process from the RNA polymerase 2 promoter affecting the cell cycle.

These include sex comb on midleg-like protein 4 (SCML4), transcription factor Sp1 (SP1), cyclic AMP-responsive element-binding protein (CREB1), Krueppel-like factor 3 (KLF3), Staphylococcal nuclease domain-containing protein 1 (SND1), NAD-dependent deacetylase sirtuin-6 (SIRT6), neurogenic differentiation factor 4 (NEUROD4), Kelch-like protein 15 (KLH15), zinc finger protein 208 (ZNF208), DNA-binding protein SATB1 (SATB1), putative zinc finger protein 730 (ZNF730), zinc finger protein 107 (ZNF107) zinc finger protein 418 (ZNF418), zinc finger protein 676 (ZNF676), protein core-binding factor, runt domain, alpha subunit 2; translocated to 1 (CBFA2T1) (RUNX1T1), lysine-specific demethylase 5C (KDM5C). Origin recognition complex subunit 2 (ORC2) is a gene essential for the start of DNA replication in eukaryotic cells, eosinophil cationic protein ribonuclease, RNase A Family 3 (RNASE3) is implicated in the RNA catabolic process, whilst histone-binding protein RBBP7 (RBBP7) is involved in DNA repair. Ubiquitin-conjugating enzyme E2 W (UBE2W) has ligase activity which is implicated in DNA repair and replication whilst MAP kinase-activating death domain protein (MADD) is a GTPase controlling protein biosynthesis at the ribosome.

Hsa-mir-4274 effects and interacts with other molecules within the cell cycle. It regulates PC4 and SFRS1-interacting protein (PSIP1) and zinc finger protein 41 (ZNF41), which are transcription factors from RNA polymerase 2 promoter. Cytoplasmic dynein 1 light intermediate chain 2 (DYNC1LI2) controls RNA localisation and methenyltetrahydrofolate cyclohydrolase (MTHFD2L) is involved in purine and pyrimidine cellular processes. Bladder cancer-associated protein (BLCAP) regulates cell cycle proliferation independent from TP53/p53 pathways.

Under the influence of hsa-miR-150 (See section 5.7.1), erythrocyte membrane protein band 4.1-like protein 5 (EPB41L5) maintains cell polarity during nuclear segregation in preparation for cell splitting whilst DDB1- and CUL4-associated factor 6 (DCAF6) have a role in the nucleotide metabolic process. RNA-binding motif protein, X-linked-like-2 (RBMXL2) affects pre-mRNA processing and mRNA metabolism. Importin-5 (IPO5) has GTPase regulator activity whilst transcriptional activator Myb (MYB), neurogenic differentiation factor 6 (NEUROD6) and vascular endothelial zinc finger 1 (VEZF1) all regulate transcription from RNA polymerase. Programmed cell death protein 4 (PDCD4) is involved in cellular translation whilst structural maintenance of chromosomes protein 3 (SMC3) ensures stabilisation of DNA replication and its repair enabling regulation of the mitotic and meiotic processes. Anomalies in cellular growth and division are seen in mutations in the protein phosphatase 1 regulatory subunit 3A (PPP1R3A) gene. These mutations are seen in various cancers (including ovarian cancers)[595] and are also directly related to organ and lymph node metastasis[596]. Another gene controlled by hsa-miR-150 is cystathionine gamma-lyase (CTH) with effects on cellular growth and proliferation.

Hsa-mir-122 (See section 5.7.2) is also seen to affect the cell cycle through gene modification. Interferon-inducible double stranded RNA-dependent protein kinase activator A (PRKRA) maintains anterior posterior cell axis specification enabling correct nuclear segregation and lamin-B2 (LMNB2) controls nuclear stability and mutations. Occludin (OCLN), homeobox protein cut-like 1 (CUX1) and SET/MYND domain-containing protein 4 (SMYD4), all regulate transcription from RNA polymerase 2 promoter and bind nucleic acids. Cell cycle control is maintained through DNA and RNA binding proteins such as interferon-inducible double stranded RNA-dependent protein kinase activator A (PRKRA). DNA replication is linked to the dual specificity protein phosphatase 4 (DUSP4) which is a

MAPK family member. Abnormal MAPK signalling is believed to be implicated in the development and progression in human cancers. MAPK regulation in normal tissues shows that deregulation of this tightly controlled process can initiate or develop cancer, determine cellular responses to cancer therapies and alter patient prognosis[643].

5.8.3 Chromatin cellular architecture

The establishment and maintenance of chromatin cellular architecture is important for cellular replication, function and growth. Aberrations in the architecture and cytoskeletal structure of cells, lead to the development of disease by altering gene expression, deregulating interactions between cellular components and affecting cellular signalling and cellular processes. Similar aberrations in cellular structure might contribute to the formation of endometriosis.

The hsa-mir-1224-5p (See section 5.6.1), is seen in my study to be upregulated in endometriosis and controls the following genes and proteins responsible for maintenance of the cellular maintenance of chromatin architecture: sex comb on midleg-like protein 4 (SCML4), SUN domain-containing protein 1 (SUN1), synaptopodin-2 (SYNP2), prickle-like protein 2 (PRIC2), RUNX1T1, NAD-dependent deacetylase sirtuin-6 (SIRT6), dystrophin-related protein 2 (DRP2), kelch-like protein 15 (KLH15) and histone-binding protein RBBP7 (RBBP7).

Hsa-mir-4274 (See section 5.6.2) is also involved in the morphogenesis of cellular components and the cellular cytoskeleton through protocadherin-9 (PCDH9) and cytoplasmic dynein 1 light intermediate chain 2 (DYNC1LI2). The expression or aberration of any of the abovementioned genes could possibly contribute to disease formation and development of endometriosis.

Hsa-miR-150 (See section 5.7.1) is seen in my study to be downregulated in endometriosis. It regulates various components affecting cellular chromatin architecture. Catenin beta-1 (CTNNB1), structural maintenance of chromosomes protein 3 (SMC3) and calpastatin (CAST) all have a role in chromatin architecture, segregation and remodelling of the cytoskeleton. SWI/SNF-related matrix-associated actin-dependent regulator of chromatin subfamily D member 2 (SMARCD2) is a chromatin binding protein and myelin protein zero-like protein 1 (MPZL1) (PZR) has a role in morphogenesis of the cellular components. Changes in cytoskeletal genes can cause increased cellular adhesion and enable tumour infiltration and metastasis. A similar effect could potentially occur with ectopic endometrial cells enabling their invasion and growth.

Hsa-miR-122 (See section 5.7.2), also downregulated in endometriosis, controls other structural cytoskeletal components such as chloride intracellular channel protein 4 (CLIC4). The regulatory factor X-associated protein (RFXAP) with brahma related gene 1 (BRG1) is associated with chromatin remodelling and mitogen-activated protein kinase kinase kinase 12 (MAP3K12) regulates cellular morphogenesis. Certain cytoskeletal components regulated by hsa-miR-122 are involved in tumorigenesis. Higher levels of lamin-B2 (LMNB2) expression in tissues are associated with increased tumour metastatic potential[641]. Solute carrier family 9 Sodium/hydrogen exchanger 1 (SLC9A1) further enhances cytoskeletal remodelling with implications for early malignant transformation.

5.8.4 Intracellular signalling

The maintenance of a correct intracellular environment enables for the correct functioning of its pathways. Changes in cellular pathways secondary to stressors or mutations can alter cellular properties. This can lead to mutations and aberrations in a multitude of cellular functions ranging from immune responses to programmed cell death, replication and inflammation[673]. As cellular functions are often interdependent, the effect of one altered pathway can have a substantial impact on numerous cellular functions. Sorting nexin-21 (SNX21), tensin-1 (TENS1), dual specificity tyrosine-phosphorylation-regulated kinase 1A (DYRK1A), MAP kinase-activating death domain protein (MADD) and Rho-related BTB domain-containing protein 3 (RHOBTB3) are all involved in intracellular signalling and the intracellular signalling cascades. These are all regulated by hsa-mir-1224-5p (See section 5.6.1). Any dysregulation in their processes can be attributed to formation and development of endometriosis.

Hsa-mir-4274 (See section 5.6.2) is also associated with intracellular processes. It regulates Calcium mediated signalling through serine/threonine-protein kinase N2 (PKN2). Other signal transduction controlling elements include lysyl oxidase homolog 4 (LOXL4) and cGMP-dependent protein kinase 2 (PRKG2). Intracellular protein transport is modulated through cytoplasmic dynein 1 light intermediate chain 2 (DYNC1LI2) and pituitary adenylate cyclase-activating polypeptide type I receptor (ADCYAP1R1). The regulation of synaptic transmission for cellular signal transduction is through the potassium voltage-gated channel subfamily C member 2 (KCNC2).

5.8.5 Cellular proteolysis

Growth regulators and control of cells through various stages of the cell cycle are controlled by proteolysis[674]. Aberrations in the cell cycle or cellular division can give rise to mutations which are further replicated. Any changes in the tight control of the cell cycle through effects on proteolysis can potentially give rise to aberrant cellular characteristics such as those seen in ectopic endometrial tissue developing into endometriosis. A number of genes controlling proteolysis are seen to be regulated by hsa-mir-1224-5p (See section 5.6.1) and can therefore be implicated as having roles in cellular disease. These genes include: thymus-specific serine protease (PRSS16), carboxypeptidase A6 (CPA6), ubiquitin carboxyl-terminal hydrolase isozyme L1 (UCHL1), tripeptidyl-peptidase 1 (TPP1) and ubiquitin-conjugating enzyme E2 W (UBE2W). Hsa-mir-4274 (See section 5.6.2) controls proteolysis through lysyl oxidase homolog 4 (LOXL4).

Hsa-miR-150 (See section 5.7.1) regulates calpastatin (CAST) which is a cysteine protease inhibitor and a regulator of cellular proteolysis. Hsa-miR-122 (See sectionhsa-miR-122) is involved in the regulation and modulation of puromycin-sensitive aminopeptidase (NPEPPS) controlling proteolysis of neurotoxic proteins inhibiting development of neuropathies.

5.8.6 Cellular endocytosis and exocytosis

In cellular endocytosis or exocytosis, the cell incorporates or releases vesicles containing proteins, enzymes or transmitters (synaptic vesicles) enabling incorporation of materials or their transport between cells. As described earlier in this thesis, viral infections use the formation of vesicles with endocytosis

and exocytosis to transfer and incorporate their own RNA or DNA into the cellular genome. EBV is a virus known to act in this way, (EBV hsa-mir-BART2-5p was identified as being elevated in the lymphocytes of patents with endometriosis- section 4.5.2.1) and the control of these processes trough a miRNA which is elevated in disease might indicate another facet of disease pathogenesis in endometriosis.

Hsa-mir-1224-5p (See section 5.6.1) affects the exocytic or endocytic cellular processes in the following way: C-type lectin domain family 4 member F (CLC4F) is involved in receptor mediated endocytosis whilst intersectin-1 (ITSN1), Rho-related BTB domain-containing protein 3 (RHOBTB3) and Synaptotagmin-14 (SYT14) have roles in cellular endocytosis, exocytosis, synaptic vesicle and transmembrane protein trafficking. Importin subunit alpha-1 (KPNA1) has a role in nuclear transport. Cytohesin-2 (CYTH2) and coatomer subunit beta (COPB1) control intracellular protein transport and exocytosis.

Hsa-mir-4274 (See section 5.6.2) regulates extracellular transport through lysyl oxidase homolog 4 (LOXL4). Golgin subfamily A member 8A (GOLGA8A), peroxisomal targeting signal 1 receptor (PEX5) are membrane trafficking proteins. Cytoplasmic dynein 1 light intermediate chain 2 (DYNC1LI2) is involved in vesicle mediated transport and the exocytic process for synaptic and non-synaptic vesicles is controlled through pituitary adenylate cyclase-activating polypeptide type I receptor (ADCYAP1R1).

Importing molecules such as importin-5 (IPO5) have been used by viruses such as influenza[624] and EBV[625] amongst others, to infiltrate cellular structures and evade host immune systems. Calpastatin (CAST) is an example of a gene controlled by hsa-mir-150 (See section 5.7.1) which regulates exocytosis of neural vesicles. Brain acid soluble protein 1 (BASP1) regulates exocytosis and intracellular protein transport.

5.8.7 Cellular adhesion and motion

In endometriosis, the proliferation of cells and their dissemination to nearby pelvic sites or distant areas is possibly enabled through changes in the properties of cellular adhesion and motion. Tensin-1 (TENS1), C-type lectin domain family 4 member F (CLC4F) and dystrophin-related protein 2 (DRP2) are the genes affecting cellular adhesion properties which are controlled by hsa-mir-1224-5p (See section 5.6.1). Cellular motion is affected through SUN domain-containing protein 1 (SUN1), Synaptopodin-2 (SYNP2), prickle-like protein 2 (PRIC2), tensin-1 (TENS1), C-type lectin domain family 4 member F (CLC4F) and dystrophin-related protein 2 (DRP2).

Hsa-mir-4274 (See section 5.6.2) controls cellular adhesion through lysyl oxidase homolog 4 (LOXL4) and protocadherin-9 (PCDH9). PCDH9 is also involved in cell motion.

Neuronal cell adhesion molecule (NRCAM) is a component of the immunoglobulin superfamily of cell adhesion and receptor molecules. Catenin beta-1 (CTNNB1), semaphorin-3A (SEMA3A), rho-guanine nucleotide exchange factor (RGNEF) and myelin protein zero-like protein 1 (MPZL1) (PZR) have roles in cell-cell adhesion and are regulated by hsa-mir-150 (See section 5.7.1). Myelin protein zero-like protein 1 (MPZL1) (PZR) enables fibronectin dependant migration of cells and erythrocyte membrane

protein band 4.1-like protein 5 (EPB41L5) causes changes in cytoskeletal genes causing adhesion and invasiveness of the affected cells. Other genes which affect cellular adhesive properties enabling invasion and metastasis include calpastatin (CAST), mitochondrial carrier homolog 2 (MTCH2) and rho-guanine nucleotide exchange factor (RGNEF).

5.8.8 Intercellular cell-cell signalling

Intercellular signalling is controlled through various processes and multiple genes. Hsa-miR-1224-5p (See section 5.6.1) controls some of the genes involved in cellular signalling. It has a role in synaptic transmission through Synaptotagmin-14 (SYT14) and a role in signal transduction and cation transport through cyclic nucleotide-gated cation channel beta-3 (CNGB3). Intracellular signalling cascades are also controlled through the histone-binding protein RBBP7 (RBBP7), C-X-C motif chemokine 6 (CXCL6) and C-type lectin domain family 4 member F (CLC4F) all affected by hsa-mir-1224-5p. Any disseminative disease will usually survive through various body processes. In general, the evasion of apoptosis, the formation of angiogenesis and alteration or escape from detection by the host's immune system enables unregulated proliferation, dissemination and implantation of diseased tissues at peripheral sites. Negative regulators of apoptosis such as ubiquitin-conjugating enzyme E2 W (UBE2W) is controlled by the hsa-miR-1224-5p which is elevated in endometriosis. Apoptotic inducers are also regulated by the same miRNA. These include Calpain-5 (CAN5), tensin-1 (TENS1) the GTPase MAP kinase-activating death domain protein (MADD) and transcription factor Sp1 (SP1) through the apoptosis signalling pathway.

Hsa-mir-4274 (See section 5.6.2) has a role in cell signalling through the PC4 and SFRS1-interacting protein (PSIP1) and regulates calcium mediated signalling through the serine/threonine-protein kinase N2 (PKN2). Bladder cancer-associated protein (BLCAP) is another regulator of apoptosis and is modulated through hsa-mir-4274. The same miRNA controls a negative regulator of apoptosis called lysyl oxidase homolog 4 (LOXL4).

Hsa-mir-150 (See section 5.7.1) has a role in regulating interleukin-7 (IL7), with a role in cell signalling. and regulates transcriptional activator Myb (MYB) and adiponectin receptor protein 2 (ADIPOR2). Both these genes have a role in cell surface receptor linked transduction. Rho-guanine nucleotide exchange factor (RGNEF) is involved in cellular synapses and synaptic vesicle glycoprotein 2B (SV2B) in neurotransmitter secretion. Intracellular signalling is regulated by neuronal cell adhesion molecule (NRCAM) and catenin beta-1 (CTNNB1) both of which are also controlled by hsa-miR-150.

Hsa-miR-122 (See section 5.7.2) regulates different genes involved in intracellular signalling processes. Brain-specific angiogenesis inhibitor 2 (BAI2) has a role in intracellular protein transport and regulating synaptic membrane exocytosis protein 1 (RIMS1) regulates cellular synaptic transmission. The voltage-dependent calcium channel subunit alpha-2/delta-2 (CACNA2D2) is involved in protein cellular transport and signalling and has tumour suppressor gene properties. Its genetic repression is seen in cancer lines including breast and cervical carcinomas (Section 5.7.2).

5.8.9 Angiogenesis

Angiogenesis supports the survival of abnormal cellular growth or dissemination by providing these cells with nutrients required for survival. Similar requirements are necessary for ectopically implanted endometriosis cells to grow and proliferate. Fibroblast growth factor receptor 1 (FGFR1), C-X-C motif chemokine 6 (CXCL6) and the eosinophil cationic protein ribonuclease, RNase A Family, 3 (RNASE3) are all regulated through hsa-miR-1224-5p (See section 5.6.1). This can explain how endometriosis is supported in its proliferation and survival within the pelvis.

Hsa-miR-150 (See section 5.7.1) is involved in angiogenic regulation through control of neuronal cell adhesion molecule (NRCAM), semaphorin-3A (SEMA3A) and vascular endothelial zinc finger 1 (VEZF1).

Hsa-miR-122 (See section5.7.2) has effects on brain-specific angiogenesis inhibitor 2 (BAI2). In hypoxia, it is responsible for the neovascularisation in the adult brain in combination with elevated levels of vascular endothelial growth factor (VEGF), which is itself angiogenic[653].

5.8.10 Apoptosis

In a multicellular organism, the regulation of cellular numbers results from tight regulation of cellular division and cell death. Apoptosis, or programmed cell death is important in the maintenance of correct embryonic development, organogenesis and the elimination of abnormal, damaged or infected cells in the adult organism[675]. Aberrations or mutations in any of the apoptotic regulator genes can lead to development of diseased tissue such as endometriosis.

Hsa-miR-150 controls apoptotic regulation via DDB1- and CUL4-associated factor 6 (DCAF6), calpastatin (CAST) and rho-guanine nucleotide exchange factor (RGNEF). Negative regulators of apoptosis under control by the same miRNA include protein Mdm4 (MDM4), interleukin-7 (IL7) and transcriptional activator Myb (MYB). Apoptosis inducers include programmed cell death protein 4 (PDCD4). Mitochondrial apoptotic regulators include the mitochondrial carrier homolog 2 (MTCH2). The Wilms tumour 1 associated protein (WTAP) in combination with IGF-1 serves as an antiapoptotic gene under control of the same miRNA.

Hsa-miR-122 regulates apoptosis through lamin-B2 (LMNB2) and interferon-inducible double stranded RNA-dependent protein kinase activator A (PRKRA). The serine/threonine-protein kinase 24 (STK24) mediates cell death by suppressing the JNK survival pathway and upregulating haemoxygenase 1 expression in the cell[646].

5.8.11 Immune system

Various components of the immune system are involved in maintaining cellular regulation within an organism. Genes and proteins involving the host's mediated immune responses are implicated in development of endometriosis through their control by identified up and downregulated miRNAs such as hsa-miR-1224-5p, hsa-mir-4274, hsa-mir-150 and hsa-mir 122. Hsa-mir-1224-5p is associated with the following genes and proteins which I proceeded to analyse (See section 5.6.1). Calpain-5 (CAN5) is

linked to PCOS disease and the processing of the immune system. Tensin-1 (TENS1) and transcription factor Sp1 (SP1) are other cytoskeleton constituents involved in the immune system. B-cell immunity is affected by krueppel-like factor 3 (KLF3) and SEC14 domain and spectrin repeat-containing protein 1 (SESD1). Cyclic AMP-responsive element-binding protein (CREB1) is involved in the maintenance of regulatory T cells and C-type lectin domain family 4 member F (CLC4F), lipopolysaccharide-binding protein (LBP) and C-X-C motif chemokine 6 (CXCL6) are involved in macrophage activation and the cellular defence response.

The control of the immune system through hsa-mir-4274 (See section 5.6.2) occurs via the PC4 and SFRS1-interacting protein (PSIP1), the ligase and transporter activity of long-chain-fatty-acid-CoA ligase 6 (ACSL6) and macrophage activation through lysyl oxidase homolog 4 (LOXL4).Antibacterial response proteins released in the cellular stress response include pituitary adenylate cyclase-activating polypeptide type I receptor (ADCYAP1R1). This protein is also modulated through hsa-mir-4274 stimulating the immune system processes within the organism.

Hsa-mir-150 (See section 5.7.1) affects the immune system through the regulation of the following associated genes: Interleukin-7 (IL7) is expressed by leukocytes, rho-guanine nucleotide exchange factor (RGNEF) and activates B lymphocytes and semaphorin-3A (SEMA3A). It is a membrane bound signalling molecule with receptor binding properties. Interferon-induced protein with tetratricopeptide repeats 5 (IFIT5) is another gene associated with hsa-mir-140. It is a component of the host organism antiviral defences and their presence enables the restriction of viral replication, stimulates apoptosis in virally infected cells and regulates immune responses. The genetic suppression of IFIT genes or their methylation by viral molecules, are mechanisms employed by viruses to escape host antiviral defences[594]. IFIT family members are today believed to be imperative in the production of novel vaccines and viral restriction mechanisms. A similar mechanism could be potentially responsible for the development of the immune evading properties of endometriotic cells. In my study, I have already identified the EBV miRNA (EBV-BART2-5p) as being present in the leukocytes of endometriotic patients (See section 4.4.3.5 and 4.5.2.1) The V-type proton ATPase subunit H (ATP6V1H) (NEF) upregulated in endometrial tissue biopsies facilitates CD4 internalisation reducing the CD4 expression on infected cells thereby enabling vial survival and infection.

Hsa-miR-122 (See section 5.7.2) has a role in the immune system through the role of various genes. Dual specificity protein phosphatase 4 (DUSP4) and mitogen-activated protein kinase kinase kinase 12 (MAP3K12) are part of immune system process and brain-specific angiogenesis inhibitor 2 (BAI2) is an antibacterial defence response protein. Testican-2 (SPOCK2) has a role in the activation of complement activation pathway and its epigenetic inactivation is seen in the malignant transformation of ovarian endometriosis[669]. The solute carrier family 9 Sodium/hydrogen exchanger 1 (SLC9A1) enables maintenance of the body's immune response by stabilisation of a normal pH for monocytes and neutrophils to work. Mutations of certain genes like regulatory factor X-associated protein (RFXAP) are seen to induce host immunocompromisation and make the host organism more susceptible to viral and bacterial infections which can further destabilise cellular control. Peroxisomal membrane protein 4 (PXMP4) is an anti-tumour gene which can influence NKT cell function through the alteration of glygolipid availability for CD1D presentation[663].

Interferon-inducible double stranded RNA-dependent protein kinase activator A (PRKRA) is activated by viral infections or stressor cell through RAX. PRKRA proceeds to induce TNF-alpha activation. Upregulation of chloride intracellular channel protein 4 (CLIC4) by reactive oxygen species causes TGF-beta1 differentiation of fibroblasts to myofibroblasts a mark of active tumour stroma in ovarian cancer. It is therefore postulated that inhibition of CLIC4 night be a potential therapeutic option for stromal tumour targeting in ovarian tumours[644,645]. As discussed in an earlier section of my thesis, similar cellular changes might be potentially linked to ectopic pelvic cells evading immune elimination, implanting and giving rise to endometriosis. If a link (through future studies) shows a direct effect of CLIC4 and development of endometriosis, this could be used as a future therapeutic target for preventing or treating disease.

6 Serum analysis in endometriosis (proteomics)

6.1 Introduction

Following the tissue miRNA study, potential markers for disease presence were examined in the serum. The ability to predict presence of disease through a non-surgical technique would reduce patient morbidity and enable earlier disease identification and treatment.

6.2 Aims

- To obtain a set of serum samples from patients who suffered from endometriosis with no other confounding pathology and samples from surgically confirmed women without endometriosis or confounding pathology (Control samples).
- To assess for differences in serum protein and antibody expression between the serum of patients with endometriosis and the controls.
- To identify a panel of potential miRNA and/or antibody biomarkers that could be used as a non-invasive diagnostic test for endometriosis.

6.3 Method

73 serum samples (endometriosis (n=36) vs. matched controls (n=35)) were taken from the recruited and consented patients. Samples were stored at -80ºC until required. They were then aliquoted when thawed to circumvent degradation of the samples during repeated freeze thaw cycles. Polypropylene sample tubes were labelled with sample identities ready for use and serum samples were then thawed at 20ºC for 30 minutes. One 300µL sample was taken from each tube for miRNA analysis and 22.5µLwas taken for autoantibody analysis. The remaining volume was dispensed into 5 x 200µL aliquots in labelled sample tubes (Table 9-16, Table 9-17). Any remaining sample was left in the original sample tube. The tubes were frozen and stored at -80ºC together with the original sample tubes. Due to variation in sample volumes some samples only yielded 2 or 3 aliquots. Samples were thawed directly prior to the assay and were randomised and split into assay racks of 23 samples each. Each assay rack contained both case and control samples and one pooled normal human serum control sample which was used to monitor assay performance. The serum was assayed for the presence of antibodies using the Discovery Array v2.0 and the standard biomarker discovery protocol (Section 2.6.4 and Section 2.8).

6.4 Results

The use of a “functional protein” array technology has the ability to display native, discontinuous epitopes[676]. Proteins are full-length, expressed with a folding tag in insect cells and screened for correct folding before being arrayed in a specific, oriented manner designed to conserve native epitopes. Each array contains approximately 1550 human proteins representing ~1500 distinct genes chosen from

multiple functional and disease pathways printed in quadruplicate together with control proteins. In addition to the proteins on each array, four control proteins for the BCCP-myc tag (BCCP, BCCP-myc, β-galactosidase-BCCP-myc and β-galactosidase-BCCP) were arrayed, along with additional controls including Cy3-labeled biotin-BSA, dilution series of biotinylated-IgG and biotinylated-IgM and buffer-only spots. Incubation of the arrays with serum samples allowed detection of binding of serum immunoglobulins to specific proteins on the arrays, enabling the identification of both autoantibodies and their cognate antigens[677].

6.4.1 Assay summary

Assays all performed well with no operational issues identified. One pooled control sample and one repeat sample was included in each assay. Of the 57 arrays assayed, only 55 were included in the analysis due to sample problems. Proteins TFPT, RPL22, POU2AF1 and TCL1A are missing from these arrays. In Assay 1, Arrays 13781 (sample 9673929) and 13765 (sample 227536) had high backgrounds and were not included in the analyses. These samples were not repeated as after discussion, experience suggested that these problems were sample related and would not be improved by repetition. In Assay 2 and Assay 3, all arrays were generally good and therefore were all included in the data analysis.

6.4.2 Data analysis from serum protein and antibody study- normalization of raw data

Once the probed and dried arrays were scaned using the Agilent microarray scanner, the scans produced images for each array that would determine the intensity of fluoresence bound to each protein. These were used to normalise and score array data. Raw median signal intensity (also referred to as the relative fluorescent unit, RFU) of each protein feature (also referred to as a spot or antigen) on the array was subtracted from the local median background intensity. Alternative analysis included the use of other measures of spot intensity such as the mean fluorescence and total fluorescence. The results of QC analyses showed that the platform performed well within expected parameters with relatively low technical variation. Tools such as volcano plots (Figure 6-1), scatter plots (Figure 6-2) and boxplots were used to identify candidate biomarkers with combinations of strong p-values and robust fold-changes when comparing case and control cohorts. Several proteins previously associated with endometriosis were identified examples of which include CDC42, EGFR, KIT, PPARG and WT1, thus validating this approach.

FIGURE 6-1

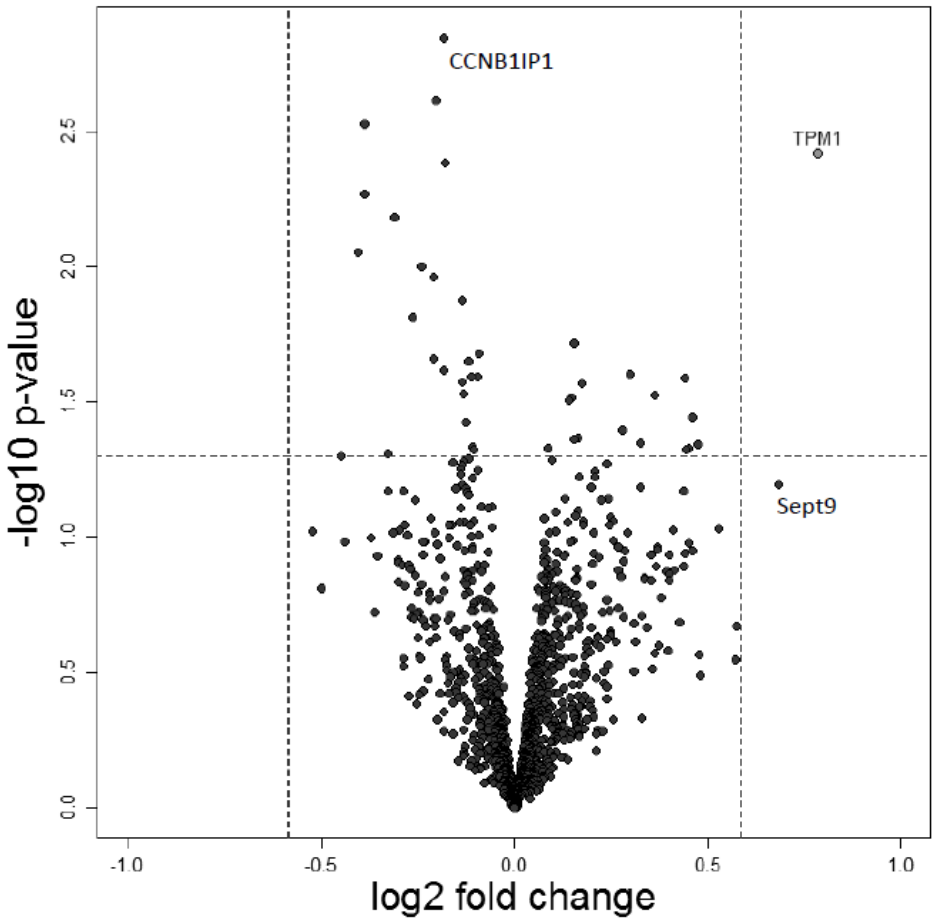

This figure shows a volcano plot displaying the p-value of a microarray t-test on the y-axis versus the fold change in antibody levels between case and controls on the x-axis. The most interesting features can be found in the top left and top right area of the volcano plot. A dotted line is plotted in the graph to differentiate between potential markers and insignificant events. These cut-offs can be varied but a typical minimum selection criteria of a p-value less than 0.05 and a fold change of greater than log2 of 0.585 (1.5-fold) was used to identify candidate biomarkers. Global median normalised data and not raw data is used to derive the fold-change values. Large differences in raw RFUs translate to small changes in this value following normalisation. Several of the best-performing markers (CCNB1IP1, TPM1 and Sept9) in this analysis are indicated.

FIGURE 6-2

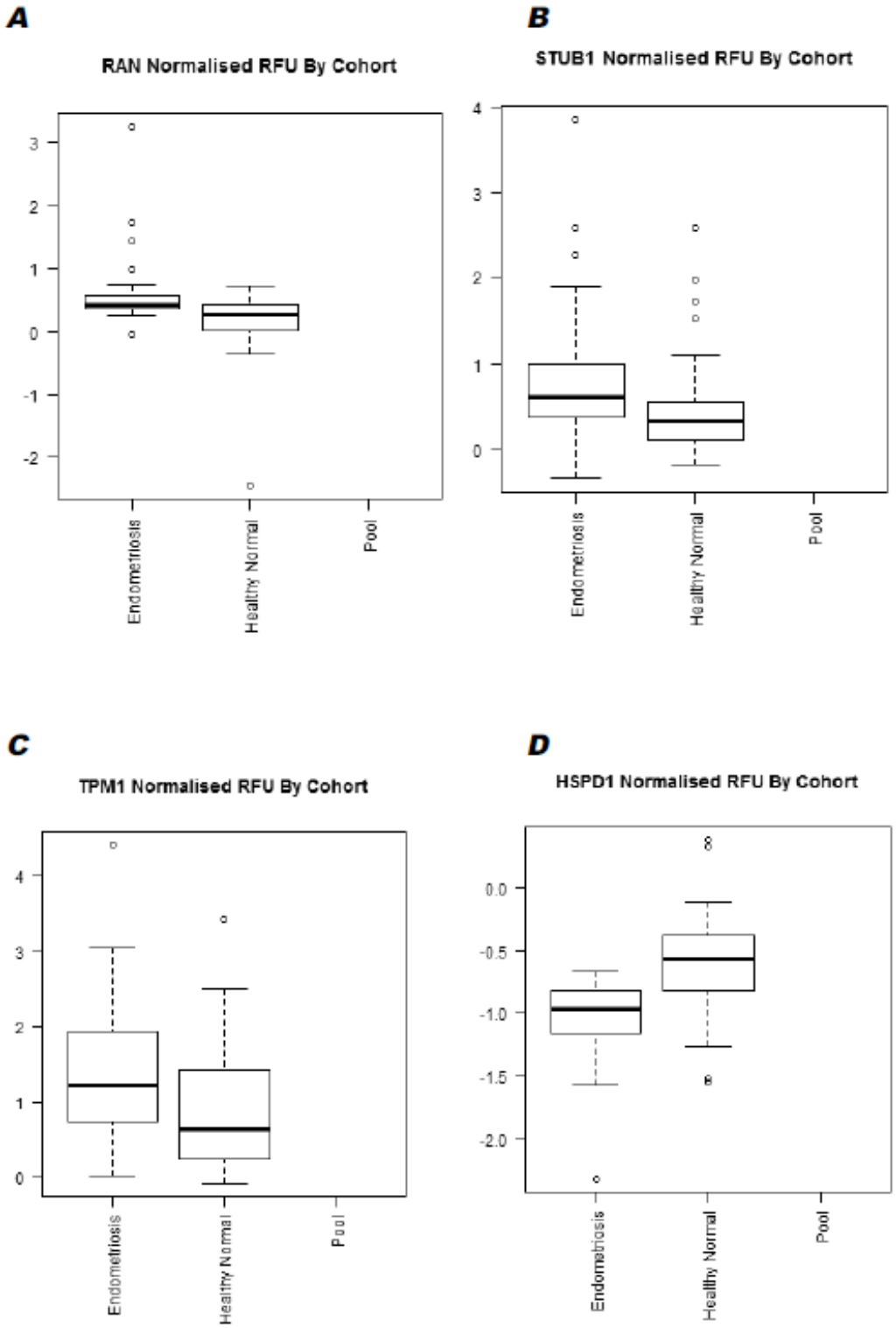

A boxplot is used to graphically depict the data obtained through their quartiles. They are non-parametric and useful in displaying differences between populations without making assumptions of the population distribution. The boxplot whiskers indicate the variability between the upper and lower quartiles within the data, with larger spacings indicating a wider dispersion or skewing of results. This figure shows box plots for normalised data for: (A) RAN, (B) STUB1, (C) TPM1 and (D) HSPD1.

6.4.3 Addition of control samples for autoantibody study

Some significant markers for case vs. control (uncorrected $p<0.05$) have been identified, with small effect size or penetrance. There was however a significant batch effect correction in this data with the addition of more serum controls. Some of the significant markers will have been influenced by this effect and caution is therefore required in interpreting these results. A table of t-test results sorted by p-value order is in the Appendix (Table 9-15).

TABLE 6-1

Cohort	Reproductive cycle stage		Total samples
Endometriosis case	Follicular	21	36
	Mid	3	
	Luteal	12	
Healthy control	Follicular		35
	Luteal		
Pooled tissue control			2
Total samples			**73**

Table showing the categorisation of samples used for serum miRNA experiments

6.4.4 Raw data analysis

The raw data included the original background subtracted data for all replicates for each spot on the arrays. The data was sorted alphabetically by protein symbol and by disease cohort. Any outliers (very high or very low values for one replicate out of four) were removed manually and annotated. A median and mean of the replicates for each protein was created from the sorted raw data. Normalisation for each protein (global median normalised data for each protein) was performed. This was achieved by performing a T-test for each protein (controls with low BCCP values versus endometriosis samples with low BCCP values). P-values for all t-tests were included with a corrected p-value (p-value multiplied by the number of proteins on the array (1344) to a maximum of $p = 1$).

Data was edited and samples with high BCCP values were moved to the extreme right hand side to allow comparison of controls and endometriosis subjects with low BCCP values. Graphs for a number of proteins which may be potential biomarkers were included. The fold-change of each protein on each array was calculated by dividing the median value for each data point by the mean median value for that protein across all of the included arrays. Those data exhibiting a fold change greater than 2 were then selected and the number of samples showing a fold change greater than 2 for the control and endometriosis samples were then calculated and placed into separate columns. The difference in fold change between the case and controls was then performed and the sorting of data by the fold change difference between case and controls demonstrated the proteins which exhibited the biggest difference between case and controls. These proteins were graphed (Median_BCCPminus worksheet). Quality control steps were performed before the data were mined for potential biomarkers. The QC analysis gave no significant cause for concern (Table 6-2). The reproducibility of the raw data was within the expected performance.

TABLE 6-2

QC metrics	
Average within array CV% for all content =	4.5
Within array CV% for Cy3 markers =	5.8
Within Array CV% for IgHG1 =	2.9
Between array CV% for Cy3 markers =	16.6
Between array CV% for IgHG1 =	20.5*

*This higher value for the IgHG1 CV% is due to some samples being highly reactive against BCCP. If these are removed from this calculation the CV% is then reduced to 6.6% which is in line with expectations. Data for this table can be found in ***BMD012_Endometriosis_Excel_analysis_v1.2.xlsx*.

Array performance: QC parameters

6.4.5 Normalisation

The raw autoantibody array data was normalized by consolidating the replicates (median consolidation), followed by normal transformation and then global median normalisation. Outliers were identified and removed. There is no method of normalisation universally appropriate and factors such as study design and sample properties must be considered. For normalization, raw data was processed in 3 steps: median consolidation, transformation to Gaussian (normal) distribution and median normalization. This normalised data was used for the identification of individual candidate biomarkers and for the development of combinations of biomarkers ("panels"). Boxplots show 'raw' relative fluorescence units (RFU) using a log scale (Figure 6-3) and the normalised data (Figure 6-4). Boxes are coloured by cohort. No arrays were excluded from the analysis due to quality control (QC) failures.

FIGURE 6-3

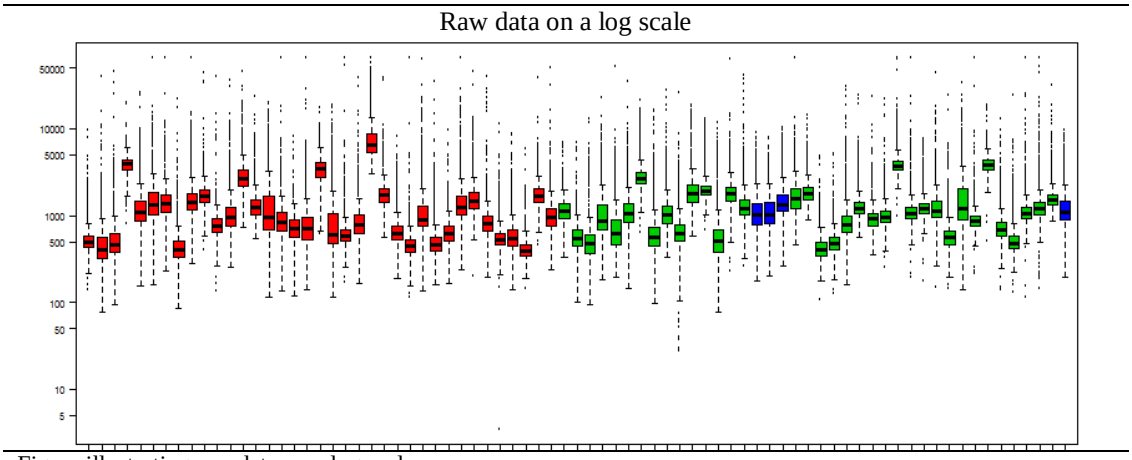

Figure illustrating raw data on a log scale

FIGURE 6-4

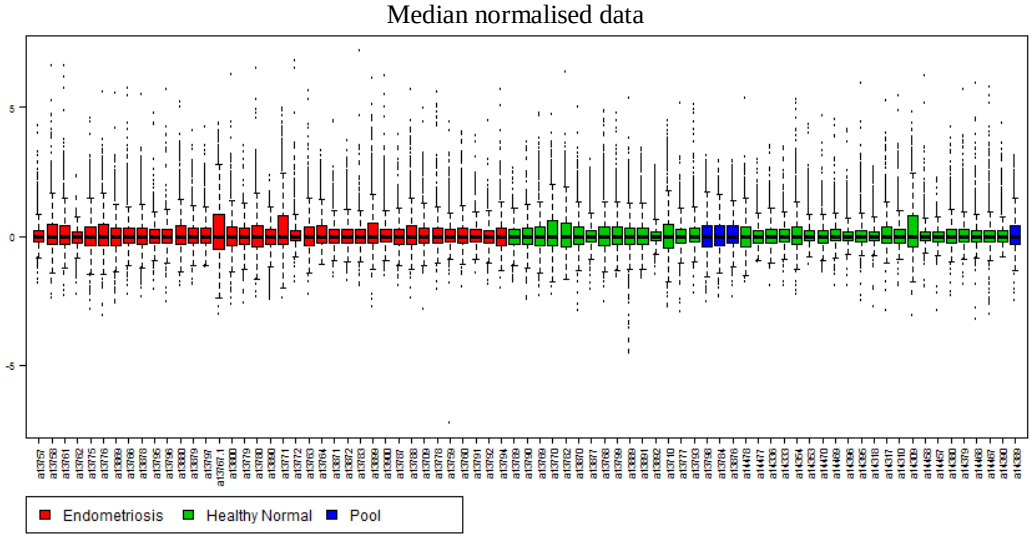

Figure illustrating median normalised data

6.4.6 Volcano plot of data

The volcano plot is a convenient way to visualize statistical significance (p-value from a t-test, without multiple testing correction applied) and magnitude of difference between case and controls. Each point relates to an individual protein. The y axis is the inverse of the p-value on a logarithm base 10 scale i.e. higher values correspond to greater significance. The x axis is the logarithm in base 2 of the ratio of the mean expression in the case to the mean expression in the control. Vertical lines correspond to a 2-fold difference. The horizontal line denotes a significance threshold of 95% confidence. Any proteins found to exhibit significant p-values and a 2-fold difference between case and control were assessed (Figure 6-5). The volcano plot did not find any significant hits for the endometriosis data set which could be of use as a standalone test in a clinical setting.

FIGURE 6-5

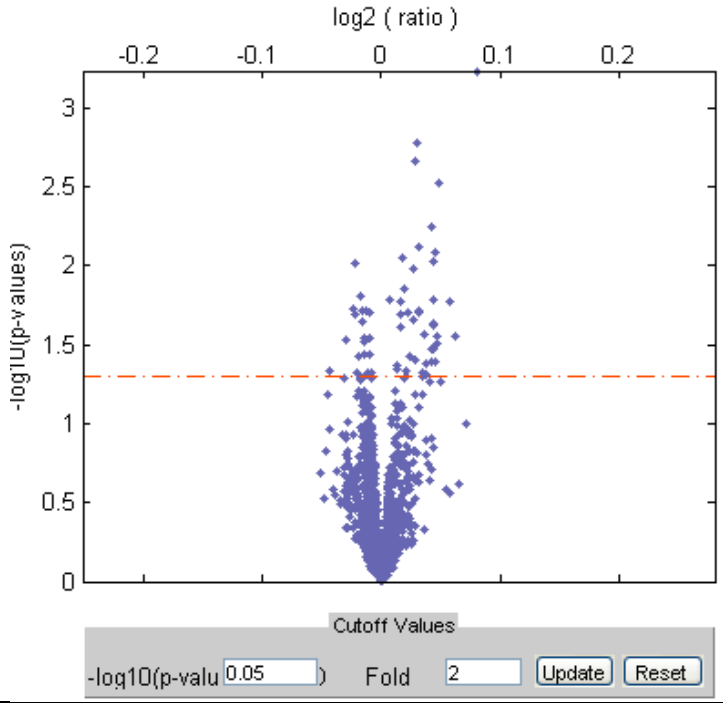

On the volcano plot, the x-axis shows the log2 fold change between case and control and the y-axis shows statistical significance (negative log of the p-value to the base of 10). The horizontal line denotes a significant threshold of 95% confidence. The plot did not identify significant protein hits for the endometriosis data which could be used in the clinical setting as a diagnostic standalone test.

A linear model was fitted to look for differentially expressed markers between the disease and healthy samples. This model also used the batch as a factor to correct for batch effects. Little change was observed in the most significant hits, with 8 of the 10 most significant hits prior to the further controls being added, remaining in the top 10 (Figure 6-6).

FIGURE 6-6

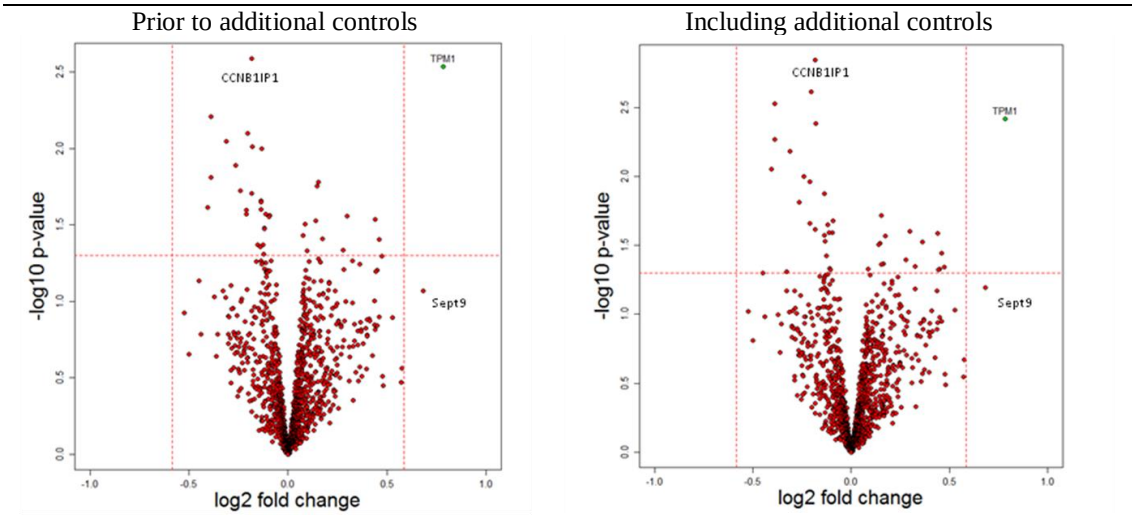

On both the volcano plots, the x-axis shows the log2 fold change between case and control and the y-axis shows statistical significance (negative log of the p-value to the base of 10). The horizontal line denotes a significant threshold of 95% confidence. These plots demonstrate the data resulting when the batch data was used to correct for batch effects. The volcano plot on the right demonstrates that an increase in the amount of control data did not alter significant hits.

6.4.6.1 Frequency selection of biomarkers

In frequency selection, the number of samples above a set threshold was compared between the case and control samples. Those proteins showing the largest difference between case and controls for the frequency of responses above the threshold were used to rank the proteins. Those showing the largest positive or negative responses were identified as potential biomarkers. In this analysis the threshold was set to 2x the mean median response of the 'low_BCCP' controls. On this basis a number of proteins showed clear differences in response between case and controls as shown in (Table 6-3).

TABLE 6-3

Gene symbol	Frequency of fold change in controls	Frequency of fold change in endometriosis	Difference
SH3GL1	1	11	10
LDHB	0	9	9
RUNX1T1	0	9	9
ALDOA	0	8	8
C19orf50	0	8	8
ILF2	1	9	8
IMPA1	0	8	8
MY CBP	0	8	8
PCBD1	0	8	8
PY CR1	1	9	8
SORD	0	8	8
TFG	0	8	8
TOM1	1	0	-1
TPD52	1	0	-1
ZKSCAN4	1	0	-1
ZNF496	1	0	-1
APEX1	2	0	-2
MAPK9	2	0	-2
STAP1	2	0	-2
ZC4H2	2	0	-2

Some of the proteins showing the greatest positive and negative changes as ranked using frequency selection

The antibody binding profiles of a number of these proteins have been graphed in the ***Median_BCCPminus worksheet***. Since a number of control samples were excluded from the analysis on the basis of their high BCCP responses, the selection of these putative biomarkers must be treated with caution. However, the limited data suggest that there are differences in antibody binding to a number of proteins between case and control samples. Amongst these, the binding to Caspase 10, Apoptosis-Related Cysteine Peptidase (CASP10) (Figure 6-7), SH3-Domain GRB2-Like 1 (SH3GL1) (Figure 6-8) and aSEPT9 are good examples. These three putative markers could potentially differentiate 13 of the 29 endometriosis samples from the control samples.

FIGURE 6-7

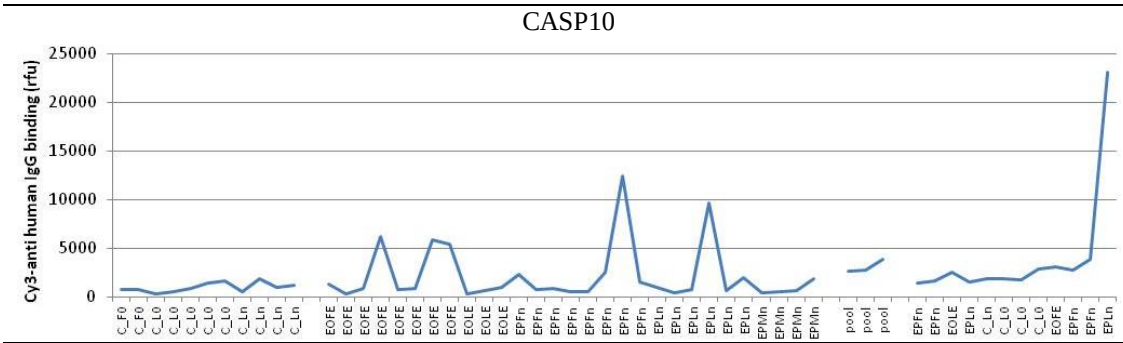

Figure illustrating IgG binding to CASP10 in samples

FIGURE 6-8

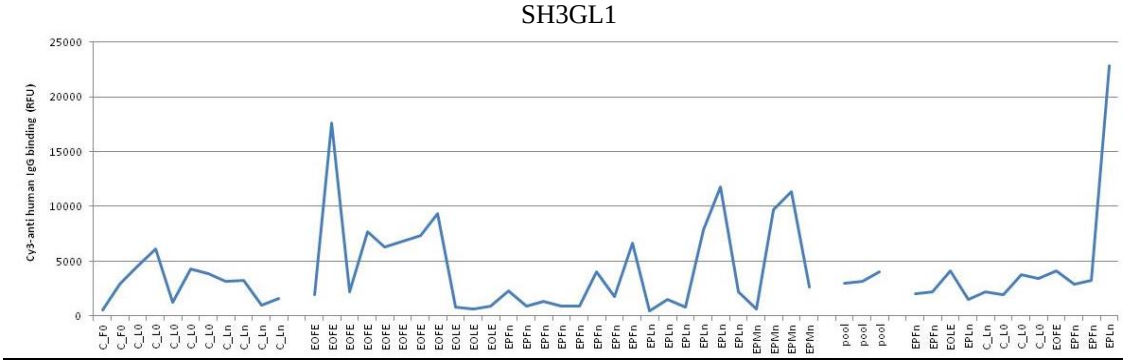

Figure illustrating IgG binding to SH3GL1 in samples

6.4.7 T-test results for proteins upregulated in endometriosis

The table below (Table 6-4) demonstrates all the proteins that are upregulated in endometriosis. It lists the first 10 antibody signals with the lowest p-value for the t-test. The density plots of the ten upregulated protein signals shown demonstrate the non-parametric fit of the endometriosis signals (in red) as compared to the control samples (in blue) (Figure 6-9). The normalized median Relative Fluorescence Units (RFU) value is shown in the figure legend for each protein.

TABLE 6-4

Protein name	p-value	Corrected p-value	Fold change	Log fold change
TPM1	0.003941	1.00	1.08	**0.07**
ADSL	0.013800	1.00	1.03	**0.03**
CKB	0.021877	1.00	1.02	**0.02**
HRSP12	0.024406	1.00	1.03	**0.03**
AIFM2	0.025824	1.00	1.01	**0.01**
NRAS	0.026865	1.00	1.01	**0.01**
SOD2	0.027801	1.00	1.04	**0.04**
ALDOA	0.032673	1.00	1.05	**0.05**
UCK2	0.039842	1.00	1.03	**0.03**
TRIM37	0.041163	1.00	1.02	**0.02**
SEPT9	0.102420	1.00	1.06	**0.06**

6.4.7.1 Density plots for proteins upregulated in endometriosis

Density plots were used to illustrate the distribution of variation of the proteins identified as being upregulated in endometriosis. The red line shows a non-parametric fit of the signals of the endometriosis samples versus the control samples in blue. The normalised median Relative Fluorescence Units was depicted for each protein.

FIGURE 6-9

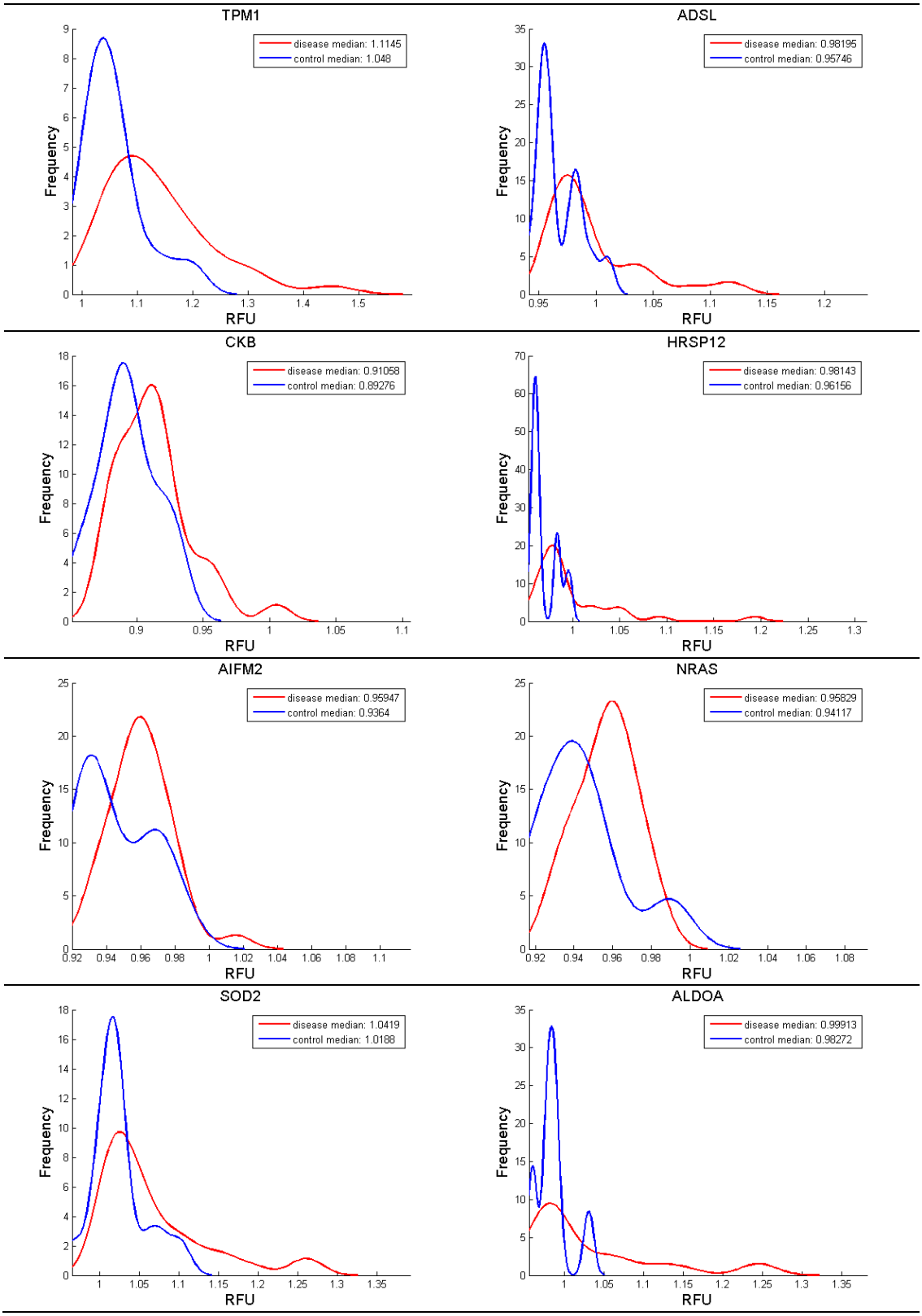

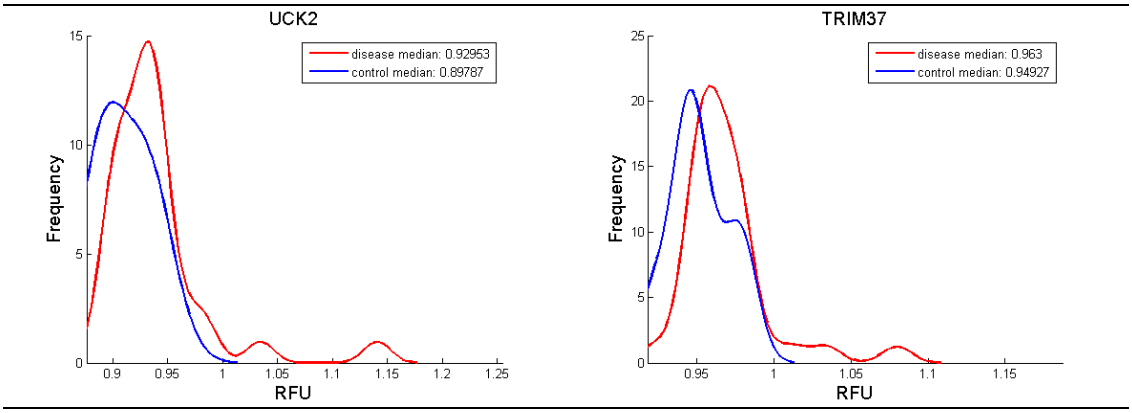

The density plots of ten protein signals which are up regulated are shown. The red line shows a non-parametric fit of the signals of the endometriosis samples versus the control samples in blue. The normalized median Relative Fluorescence Units (RFU) value is shown in the figure legend for each protein

6.4.7.2 Upregulated marker distributions

As for the strongest downregulated markers, a similar boxplot analysis was performed for the strongest upregulated markers ((Tropomyosin 1 (Alpha) (TPM1) and Septin 9 (Sept9)). These markers showed some differences between the cohorts, although without very high statistical confidence (Figure 6-10).

FIGURE 6-10

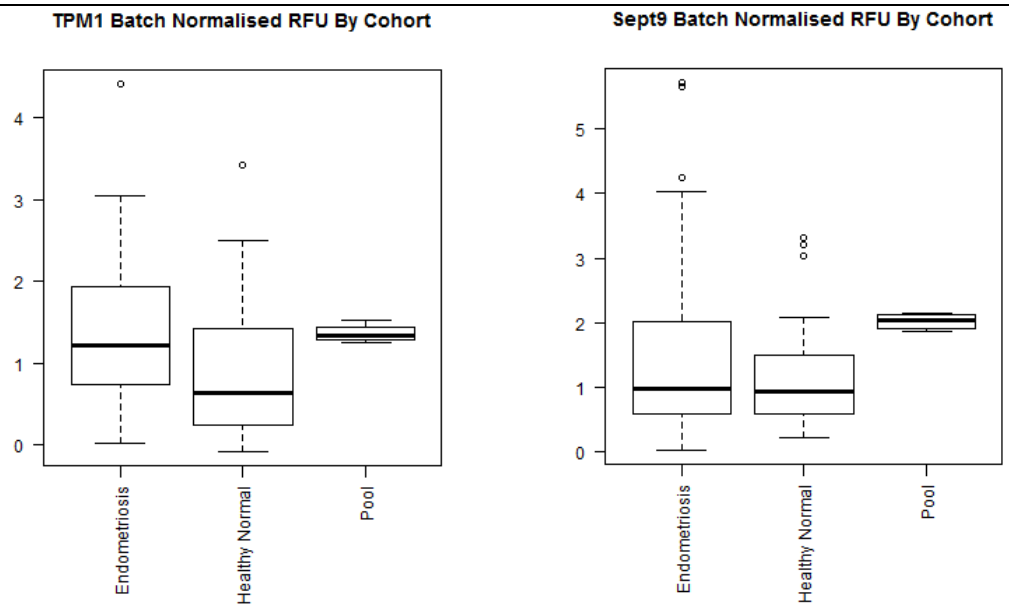

Boxplots showing distributions of upregulated markers

6.4.8 T-test results for proteins downregulated in endometriosis

A t-test is a fast and simple method to test for differences between case and control samples. The table below (Table 6-5) demonstrates all the proteins that are downregulated in endometriosis. It lists the first 10 antibody signals with the lowest p-value for the t-test. The density plots of the ten downregulated protein signals shown demonstrate the non-parametric fit of the endometriosis signals (in red) as compared to the control samples (in blue) (Figure 6-11). The normalized median Relative Fluorescence Units (RFU) value is shown in the figure legend for each protein.

TABLE 6-5

Protein name	p-value	Corrected p-value	Fold change	Log fold change
CCNB1IP1	0.002807	1.00	0.98	**-0.02**
RORC	0.005463	1.00	0.96	**-0.04**
TAOK3	0.006992	1.00	0.98	**-0.02**
HSPD1	0.010996	1.00	0.97	**-0.03**
PAX8	0.011430	1.00	0.97	**-0.03**
NFYA	0.011460	1.00	0.98	**-0.02**
TRAF4	0.013886	1.00	0.98	**-0.02**
GTF2H2	0.014579	1.00	0.98	**-0.02**
USP10	0.016934	1.00	0.97	**-0.03**
SRPK1	0.017187	1.00	0.96	**-0.04**

6.4.8.1 Density plots for proteins downregulated in endometriosis

Density plots were used to illustrate the distribution of variation of the proteins identified as being downregulated in endometriosis. The red line shows a non-parametric fit of the signals of the endometriosis samples versus the control samples in blue. The normalised median Relative Fluorescence Units was depicted for each protein.

FIGURE 6-11

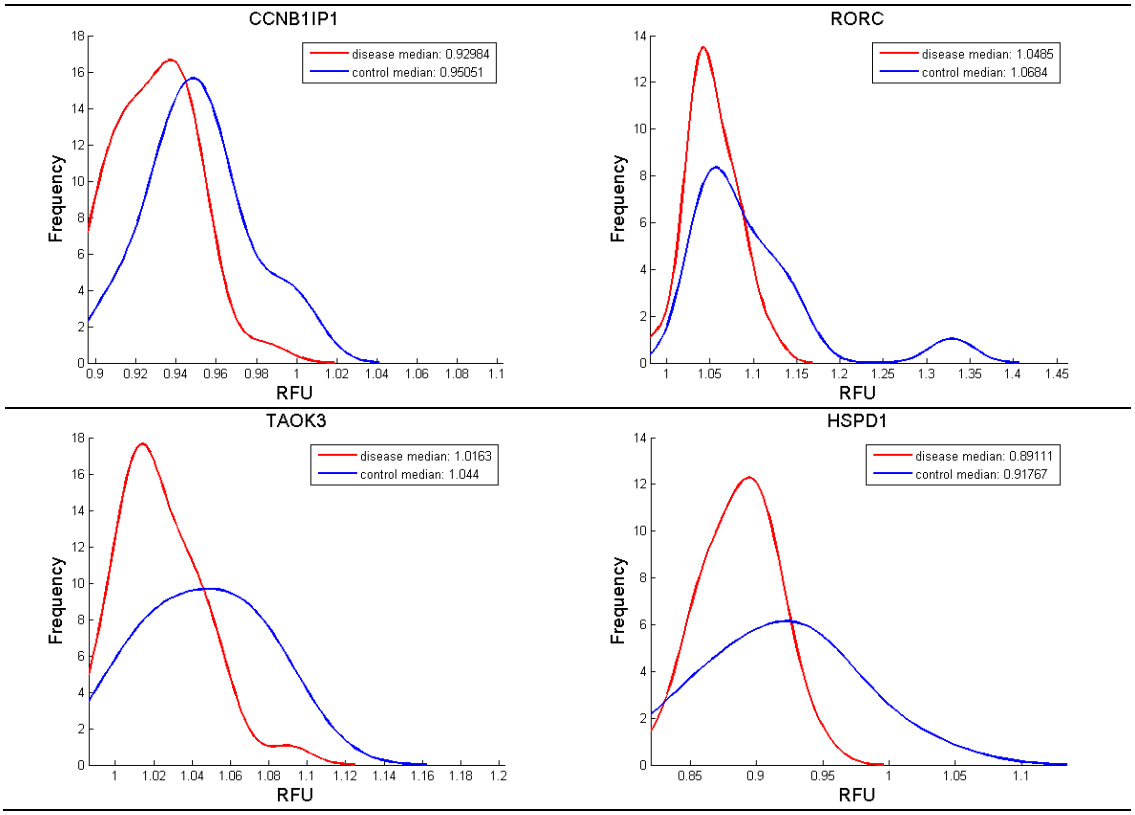

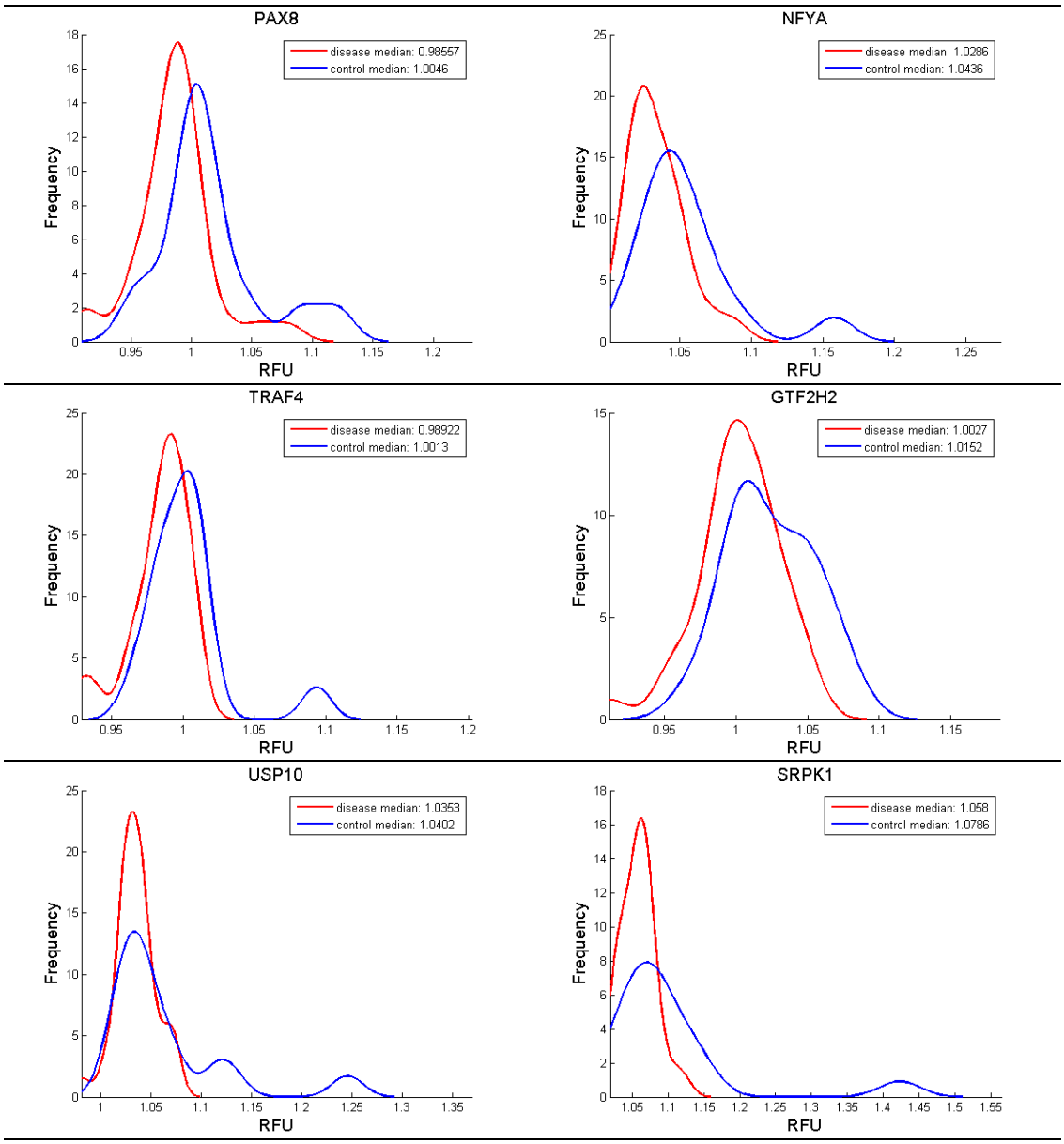

The density plots of ten protein signals which are downregulated are shown. The red line shows a non-parametric fit of the signals of the endometriosis samples versus the control samples in blue. The normalized median Relative Fluorescence Units (RFU) value is shown in the figure legend for each protein

6.4.8.2 Downregulated marker distributions

In order to assess the difference between the two strongest identified downregulated markers (Cyclin B1 Interacting Protein 1, E3 Ubiquitin Protein Ligase (CCNB1IP1) and Heat Shock 60kDa Protein 1 (HSPD1)), data for the cohorts of endometriosis and healthy controls was compiled. A batch of normalised RFU for each cohort was created and the data was then plotted in a boxplot enabling the median of each boxplot to be compared and assessed for fold change. These markers showed some differences between the cohorts but not with high fold change. Of note HSPD1 had a sizable batch effect ($p = 0.06$), with higher expression in the additional controls (Figure 6-12).

FIGURE 6-12

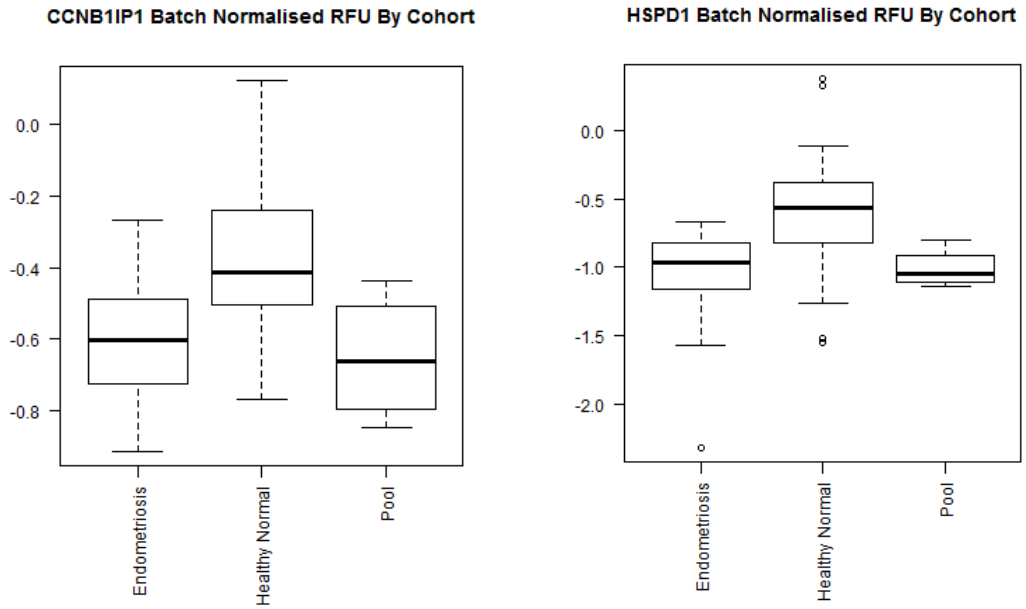

Boxplots comparing data between cohorts for the two strongest downregulated markers, CCNB1IP1 and HSPD1

6.5 The creation of a biomarker panel- combining miRNA and protein data

6.5.1 Multivariate analysis: combination of miRNA and autoantibody biomarkers in serum of subjects suffering from endometriosis

Panels of putative biomarkers were developed consisting of autoantibodies alone, miRNAs alone or combinations containing both autoantibodies and miRNA species. Multivariate analysis was also performed incorporating data for galectin-3 and CA125 as variables however their inclusion did not improve on the performance of the miRNA and autoantibodies identified here. It is not possible to predict a priori which classifier will perform best with a given dataset, therefore data analysis was performed with 5 different feature ranking methods (entropy, Bhattacharyya, T-test, Wilcoxon, ROC) plus forward and backward feature selection. Classifiers were then assessed for performance by referring to the combined sensitivity and specificity (S+S score) and area under the curve (AUC). Data were repeatedly split and analysis cycles repeated until a stable set of classifiers ("panels") was identified. Nested cross validation was applied to the classification procedures in order to avoid overfitting of the study data. The performance of the classification was compared to a randomized set of case-control status samples (permutation assay) which should give no predictive performance and provides an indication of the background in the analysis. A figure close to 1.0 is expected for the null assay (equivalent to a sensitivity + specificity (S+S) score of 0.5 + 0.5, respectively) whereas an S+S score of 2.0 would indicate 100% sensitivity and 100% specificity. The difference between the values for the permutation analysis and the classifier performance indicates the relative strength of the classifier. The antigens and miRNAs identified from this study are provided in Table 9-19 and Table 9-20.

Table 9-23 shows the protein biomarkers that provided good performance, as judged by p value, fold-change, sensitivity, specificity, AUC. The best performing protein biomarkers are shown in Table 9-24.

Table 9-25 shows the miRNA biomarkers that provided good performance, as judged by p value, fold-change, sensitivity, specificity, AUC. The best performing miRNA biomarkers are shown in Table 9-26. The ROC curves for some of the best performing miRNA biomarkers (hsa-miR-150, hsa-miR-574-5p and hsa-miR-342-3p) are shown in Figure 6-13.

FIGURE 6-13

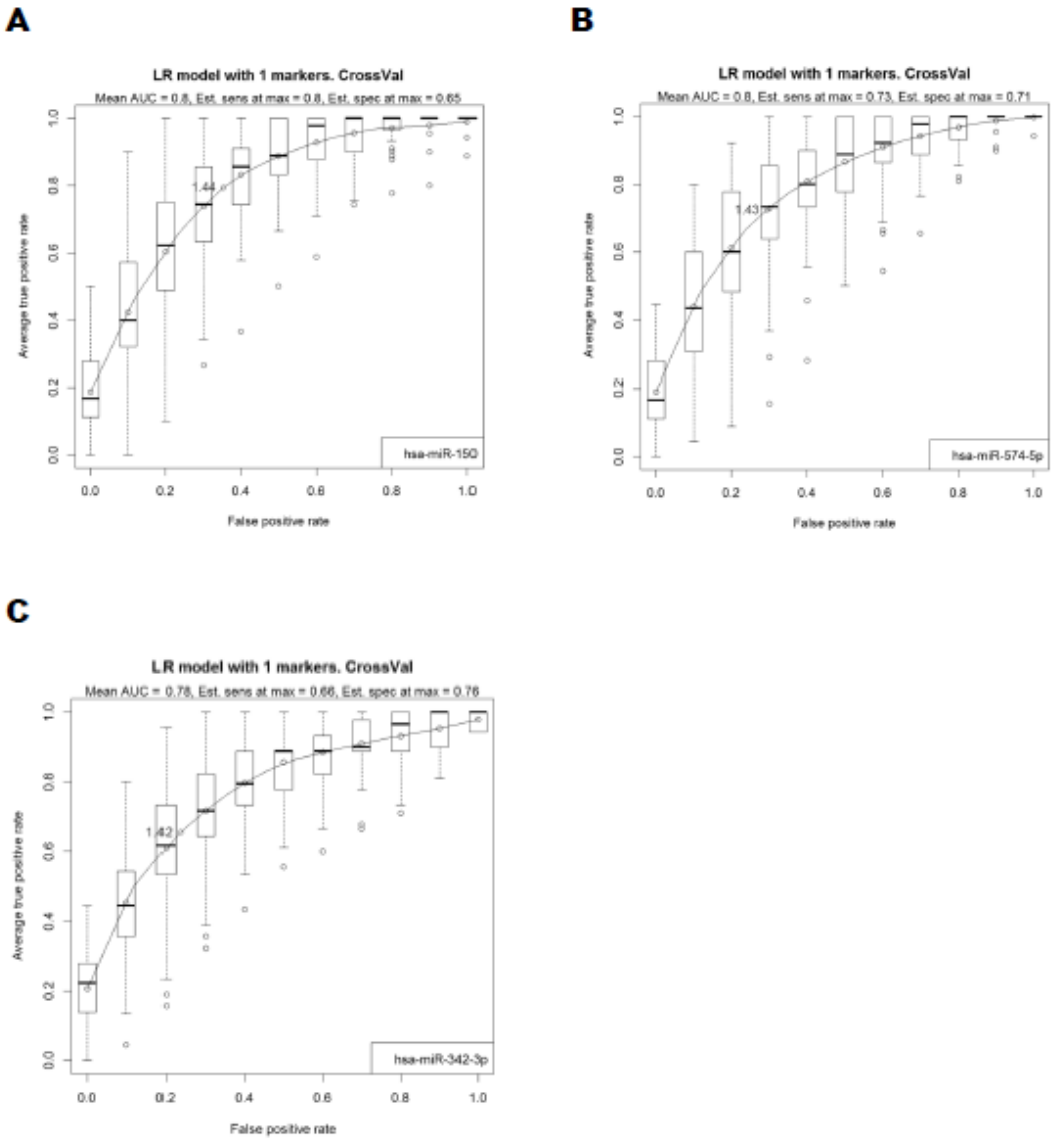

Receiver operating characteristic (ROC) curves for individual miRNAs from the microarray data: (A) hsa-miR-150; sensitivity=0.8, specificity=0.65, AUC=0.8; (B) hsa-miR-574-5p; sensitivity=0.73, specificity=0.71, AUC=0.8; (C) hsa-miR-342-3p; sensitivity=0.66, specificity=0.76, AUC=0.78.

The best performing protein and 30 miRNA biomarkers are shown in Table 9-27. These represent biomarkers of particular interest as they correspond to the subset of biomarkers with the greatest predictive properties. The analysis methods described above were used to build, test and identify combinations of biomarkers with greater sensitivity, specificity or AUC than the individual biomarkers disclosed in Table 1. For each analysis, multiple combinations of putative biomarkers were derived and the performance of the derived panels was then ranked (Table 9-28-Table 9-32). Table 9-28-Table 9-32 show 2-mer, 3-mer, 4-mer, 5-mer and 6-mer panels that provide good performance. The ROC curves for

some of the best performing combinations are shown in Figure 6-18 (A=2-mer panel of hsa-miR-150 and hsa-miR-574-5p; B=2-mer panel of hsa-miR-342-3p and hsa-miR-574-5p; C=2-mer panel of hsa-miR-150 and hsa-miR-342-3p; D=3-mer panel of hsa-miR-150, hsa-miR-122 and hsa-miR-574-5 5p).

The biomarkers with the greatest diagnostic power, as judged by p value, fold-change, sensitivity, specificity, AUC and / or frequency of appearance in the panels derived were identified and combined into a single list of antigens and miRNAs. Figure 6-14 show the ROC curve for a 3-mer panel of TPM1, hsa-miR-150 and hsa-miR-574-5p, which is one of the best performing 10 combinations. Thus, panels containing a mixture of protein and miRNA biomarkers also provide good diagnostic performance.

FIGURE 6-14

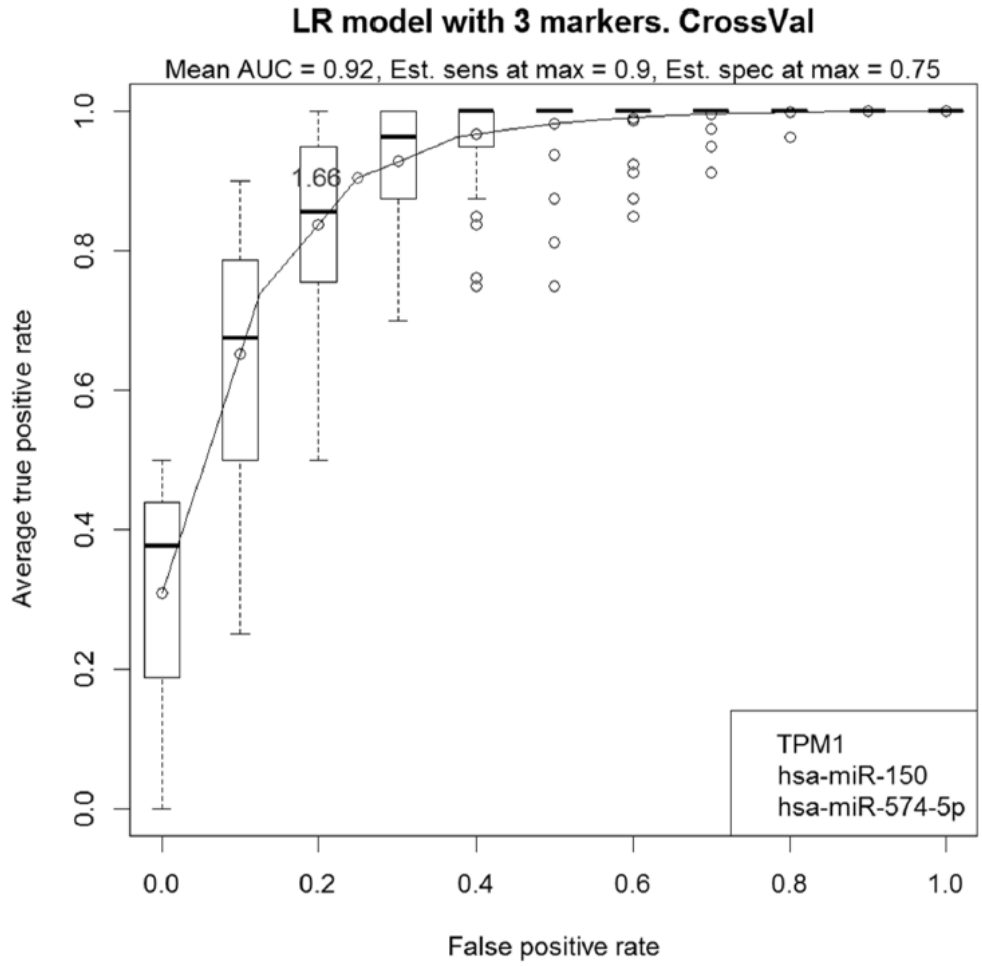

Receiver operating characteristic (ROC) curve for a combination of TPM1, hsamiR-150 and hsa-miR-574-5p; sensitivity=0.9, specificity=0.75, AUC=0.92.

6.5.2 Mixed Auto Antibody (Ab) and miRNA panel performance

The ROC curve for best 3 marker model from mixed miRNA and Ab data can be seen below (Figure 6-14). It is good to note that as these markers were selected from two independent experiments and are being tested against the same sets of data, the problem of over fitting is compounded. Monte Carlo cross-validation alone does not necessarily correct for this so estimates of performance are far from conservative and not truly comparable to the other model classes. They should therefore be considered as absolute best case.

6.5.3 Model performance summary- potential panel of markers for endometriosis

The area under curve (AUC) summary table for the maximum performance (by AUC) from all tested model types can be seen below (Table 6-6).

TABLE 6-6

Panel size	Microarray miR	qPCR	Autoantibody	Mixed: microarray miR + autoantibody
1	0.80	0.70	0.67	
2	0.91	0.76	0.69	0.81
3	0.90	0.74	0.68	0.92
4	0.90	0.73	0.69	0.93
5	0.90	0.71		
6	0.89			

The final data generated can be seen in the Excel sheet titled ***endometriosis_allModels_allPlatforms_V01***, which includes the data for the combined miRNA/autoantibody panels. The panels can be sorted according to whether they have been cross-validated and the AUC or sensitivity/specificity enabled us to identify the best panels. Most of the performance of the combined panels seems to result from a combination of miR-150 and miR-574 and the addition of TPM-1 or RAN has a marginal improvement. Data will have to be verified on a large number of clinical cases to minimise errors resulting from possible batch effects, performance of individual markers, performance of microarray vs qPCR etc. These factors may all influence the selection of the combined panel (TPM-1, mir-150, mir-574) as the best 3 marker model in his slide deck. An example of the best panel combinations can be seen below (Table 6-7).

TABLE 6-7

Model Check Output File	Set Size	Ref	Markers	Auc	Max SplusS	Sensate Max SplusS	SpecAt Max SplusS	Prefix	ROC	Suffix
combiAbMir_allModels_CrossVal.txt	3	75	RAN, hsa-miR-150, hsa-miR-574-5p	0.923594	1.657500	0.782500	0.875	combiAbMir	ROC	CrossVal
combiAbMir_allModels_CrossVal.txt	3	26	TPM1, hsa-miR-150, hsa-miR-574-5p	0.923594	1.655000	0.905000	0.750	combiAbMir	ROC	CrossVal
combiAbMir_allModels_CrossVal.txt	4	73	TPM1, hsa-miR-150, hsa-miR-342-3p, hsa-miR-574-5p	0.928594	1.652500	0.902500	0.750	combiAbMir	ROC	CrossVal
combiAbMir_allModels_CrossVal.txt	4	68	TPM1, hsa-miR-150, hsa-miR-122, hsa-miR-574-5p	0.928125	1.649375	0.899375	0.750	combiAbMir	ROC	CrossVal
combiAbMir_allModels_CrossVal.txt	4	39	TPM1, RAN, hsa-miR-150, hsa-miR-574-5p	0.923125	1.646875	0.896875	0.750	combiAbMir	ROC	CrossVal
combiAbMir_allModels_CrossVal.txt	4	165	RAN, hsa-miR-150, hsa-miR-3648, hsa-miR-574-5p	0.925469	1.646250	0.771250	0.875	combiAbMir	ROC	CrossVal
combiAbMir_allModels_CrossVal.txt	4	145	RAN, STUB1, hsa-miR-150, hsa-miR-574-5p	0.913438	1.635625	0.760625	0.875	combiAbMir	ROC	CrossVal
combiAbMir_allModels_CrossVal.txt	4	54	TPM1, STUB1, hsa-miR-150, hsa-miR-574-5p	0.919844	1.635000	0.760000	0.875	combiAbMir	ROC	CrossVal
combiAbMir_allModels_CrossVal.txt	4	159	RAN, hsa-miR-150, hsa-miR-122, hsa-miR-574-5p	0.914375	1.635000	0.760000	0.875	combiAbMir	ROC	CrossVal
combiAbMir_allModels_CrossVal.txt	4	71	TPM1, hsa-miR-150, hsa-miR-1224-5p, hsa-miR-574-5p	0.913438	1.631875	0.881875	0.750	combiAbMir	ROC	CrossVal
microArray_allModels_CrossVal.txt	2	5	hsa-miR-150, hsa-miR-574-5p	0.910000	1.630000	0.860000	0.760	microArray	ROC	CrossVal

Panel demonstrating the output profiles of the best panel combinations

6.5.4 Estimation of classification performance: miRNA panels

Logistic regression models were used for all combinations of the most interesting markers. 100 fold Monte Carlo cross validation was used to reduce over fitting of model coefficients. Since the selection of markers was carried out using the same data set, the validation is not truly independent and should be considered a 'best case' estimate for predictive power (Table 6-8).

TABLE 6-8

Marker	AUC	Max S+S	Sensitivity at max S+S	Specificity at max S+S	Type	Comment
hsa-miR-150	0.80	1.44	0.80	0.65	microArray	
hsa-miR-574-5p	0.80	1.43	0.73	0.71	microArray	
hsa-miR-342-3p	0.78	1.42	0.66	0.76	microArray	
hsa-miR-3663-5p	0.70	1.26	0.41	0.85	qPCR	Poor correlation with microarray
hsa-miR-150	0.69	1.31	0.47	0.85	qPCR	
TPM1	0.67	1.25	0.69	0.56	autoAb	
STUB1	0.66	1.21	0.65	0.56	autoAb	
hsa-miR-122	0.66	1.25	0.40	0.85	qPCR	
hsa-miR-122	0.65	1.19	0.55	0.65	microArray	
hsa-miR-3648	0.63	1.21	0.85	0.35	microArray	
hsa-miR-3194-5p	0.62	1.14	0.68	0.46	qPCR	Poor correlation with microarray
hsa-miR-342-3p	0.62	1.14	0.76	0.38	qPCR	
HSPD1	0.62	1.15	0.81	0.33	autoAb	
RAN	0.54	1.10	0.87	0.22	autoAb	
hsa-miR-1224-5p	0.48	1.06	0.06	1.00	microArray	

Table of cross validated endometriosis/healthy classification performance for individual markers

A dataset obtained from any population results in a distribution of data that can be graphically plotted as a bell curve. Ideally, when comparing two sets of miRNA results from groups within the population (e.g. endometriosis patients and control patients), there should be two completely separate sets of data from the affected or non-affected patients. In reality, as a disease is multifactorial and has numerous variables, there will be an inevitable area of overlap of data between the two separate groups. As is depicted in the figure below (Figure 6-15, Table 6-9), the overlapping data will result in false positives (Type 1 error) and false negatives (Type 2 error). Depending on the threshold one chooses for the data, the true positives (sensitivity) and the true negatives (specificity) are altered.

FIGURE 6-15

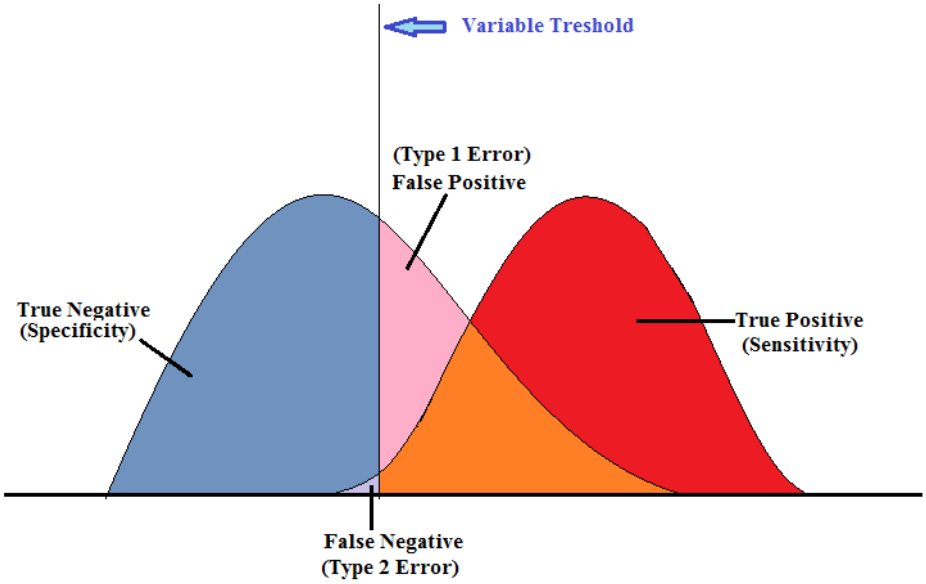

The bell curve indicates the range of results obtained in a population

TABLE 6-9

		Condition	
		Positive	*Negative*
Test outcome	*Test outcome positive*	True positive	False positive
	Test outcome negative	False negative	True negative
		Sensitivity = True positives/ (True positives+ false negatives)	Specificity = True negatives/ (True negatives+ false positives)

In the ideal situation, a marker for a disease should be 100% sensitive and specific. In the absence of this due to multiple disease variables, one must formulate techniques to choose the optimal markers for disease. In order to estimate the performance of chosen markers, data from the miRNA markers was plotted in Receiver Operator Characteristic (ROC) curves. An ROC curve enables the illustration within a graphical plot of the performance of a marker as its discrimination threshold varies. The ideal marker on an ROC curve is seen at the topmost left corner, which indicates 100% sensitivity and 100% specificity. Therefore, the optimal miRNA markers are the ones with the ROC curves closest to the topmost left corner.

FIGURE 6-16

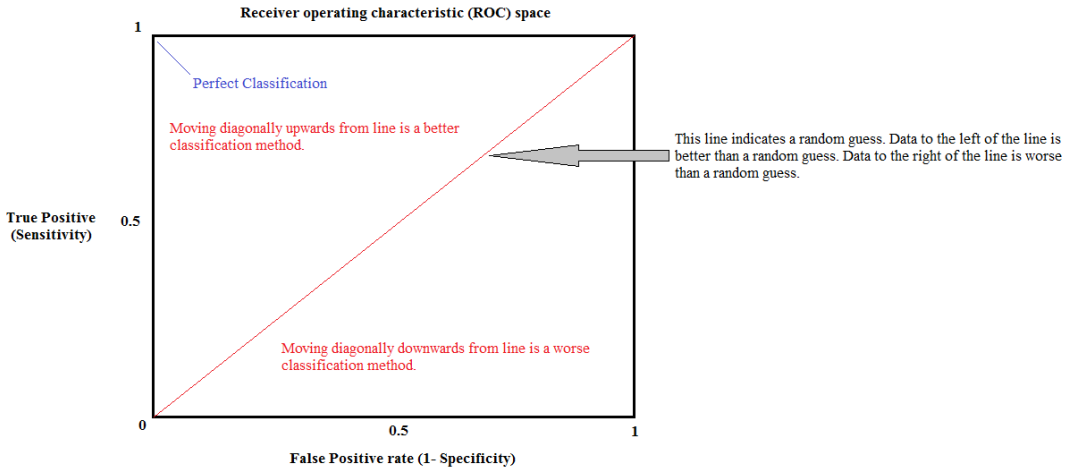

A perfect classification would give 100% sensitivity (No false negatives) and 100% specificity no false positives. Translated into an ROC curve, the best predicition method would be found in the upper left corner or coordinate (0.1)

This figure explains the principles of an ROC space

6.5.5 ROC curves for individual markers from microarray data

For each of the previously identified potential miRNA markers from the microarray panels, an ROC curve has been plotted to assess for the suitability of the identified miRNAs as potential diagnostic markers for the disease of endometriosis. As no single marker showed enough individual promise to identify endometriosis, ROC curves were created not only for individual miRNAs but for pairs of triplicates of these miRNAs in an attempt to create a panel of multiple miRNAs that would be specific and sensitive enough to use in the clinical setting as a non-invasive marker for disease.

From the single miRNA data, hsa-miR-150, hsa-miR-574-5p and hsa-miR-342-3p showed promise (Figure 6-17). However, as can be seen, none of these individually show enough sensitivity and specificity to be valid as a clinical marker.

FIGURE 6-17

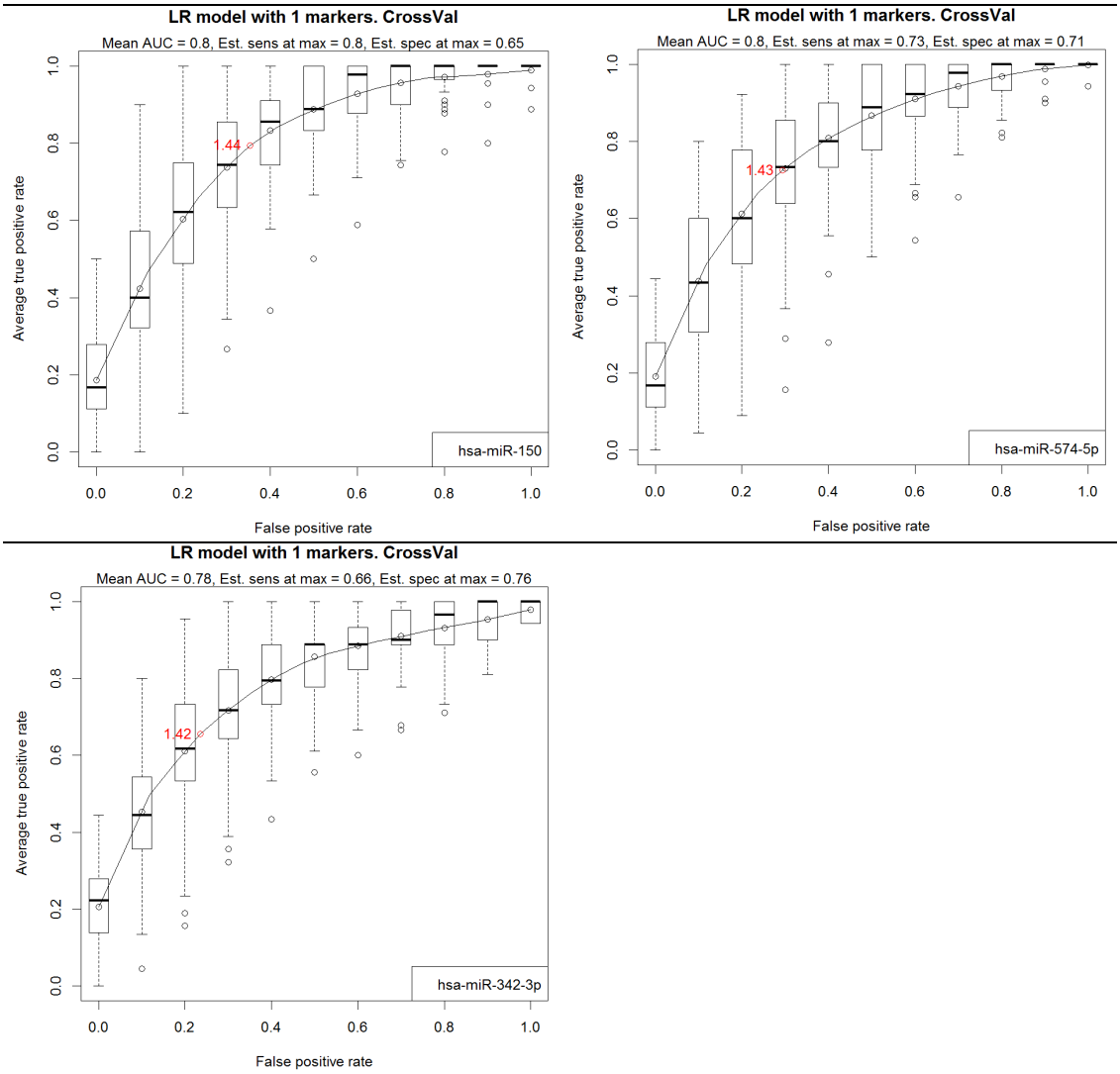

ROC curves showing optimal individual miRNAs that potentially could be used for non-invasive identification of endometriosis.

6.5.6 ROC curves for two marker panels from microarray data

ROC curves were then created for combinations of two of the optimum markers (Figure 6-18). As can be seen from the curves below, the sensitivity and specificity was marginally improved in each case. The combination of miRNA markers showing the greatest promise was hsa-miR-150 and hsa-miR-574-5p, with a sensitivity of 86% and specificity of 76%.

FIGURE 6-18

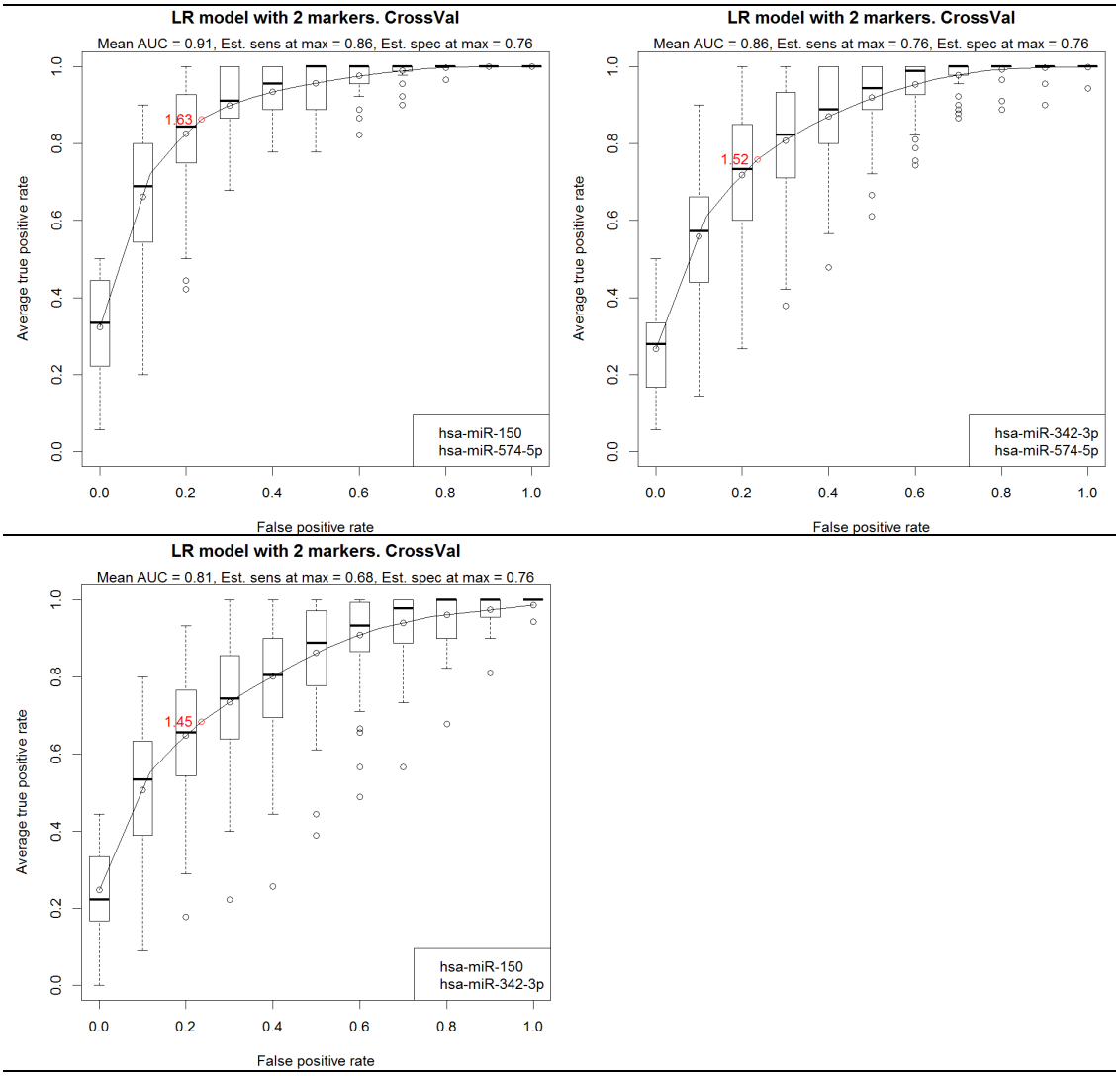

ROC curves showing optimal combinations of two miRNAs that potentially could be used for non-invasive identification of endometriosis.

6.5.7 ROC curves for three marker panels from microarray data

An automated combination of three markers from the original identified miRNAs of interest was performed to identify a potential combination with increased specificity and sensitivity to the one identified above. The addition of hsa-miR-122 to hsa-miR-150 and hsa-miR-574-5p (Figure 6-19) was seen to give a maximum sensitivity of 83% and a specificity of 76%. Although this does not appear to be an improvement over the previous combination of hsa-miR-150 and hsa-miR-574-5p, it is recognised that the limited sample size and batch data might skew results so hsa-miR-122 was maintained as a marker of interest.

FIGURE 6-19

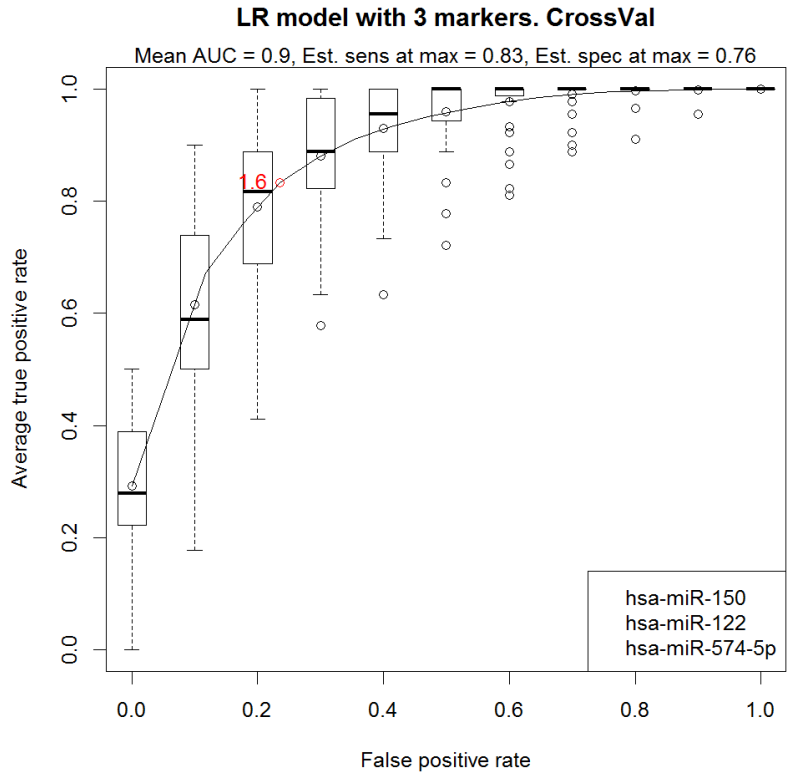

ROC curves showing optimal combinations of three miRNAs that potentially could be used for non-invasive identification of endometriosis.

6.5.8 Estimation of classification performance: qPCR

6.5.9 ROC curves for individual markers from qPCR data

For markers identified through qPCR showing good correlation with microarray data, ROC curves were also plotted. As can be seen below (Figure 6-20), the data obtained from qPCR gives less ideal ROC curves. This indicates that miRNA panels are potentially more optimal ways of identifying the markers.

FIGURE 6-20

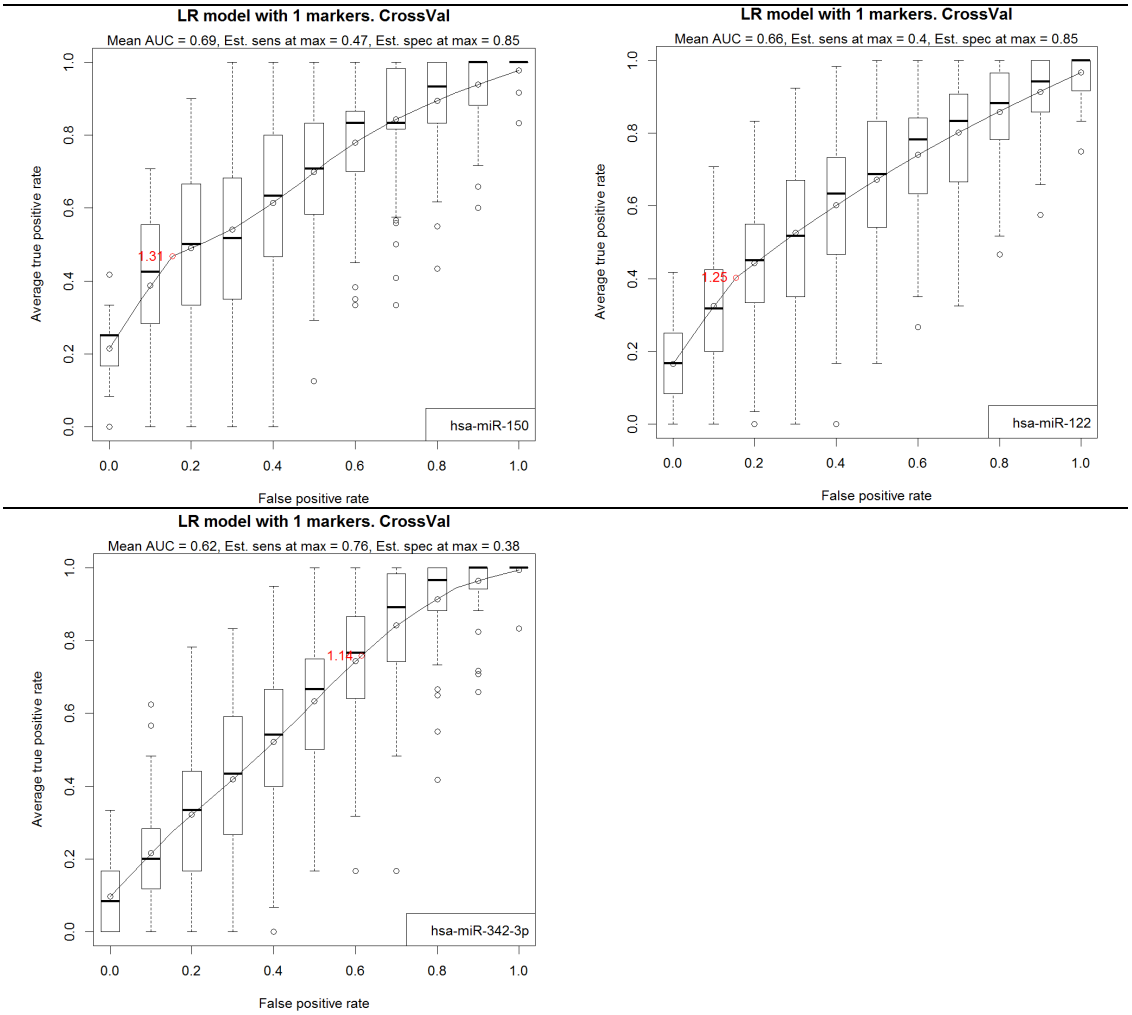

ROC curves from qPCR results assessing the optimal individual miRNAs that potentially could be used for non-invasive identification of endometriosis.

An ROC curve was then plotted from qPCR data for the combined marker set but this did not show improvement over individual markers. Cross-validation was used to test the miRNA identified from the entire dataset. However, when the size of the dataset is small, overfitting might occur in the model, potentially skewing results. A technique to assess for the presence of this skew is to look at the data without cross-validation. Without cross-validation being used, a similar result was observed: the panel of hsa-miR-150, hsa-miR-122 and hsa-miR-342-3p having an area under curve (AUC) of 0.7 and hsa-miR-150 alone having AUC of 0.69 (Figure 6-21). In the qPCR validation, the hsa-miR-451 control miRNA and the hsa-miR-342-3p show good correlation with qPCR, supporting their use. Individually, miRNA markers show significant difference between endometriosis and healthy bloods. Combining these markers into panels indicates the potential for reasonable classification performance on an independent platform (e.g. sensitivity ~35% at specificity ~85% for panel of hsa-miR-150 and hsa-miR-122 from qPCR data), although this requires validation in an independent sample set.

FIGURE 6-21

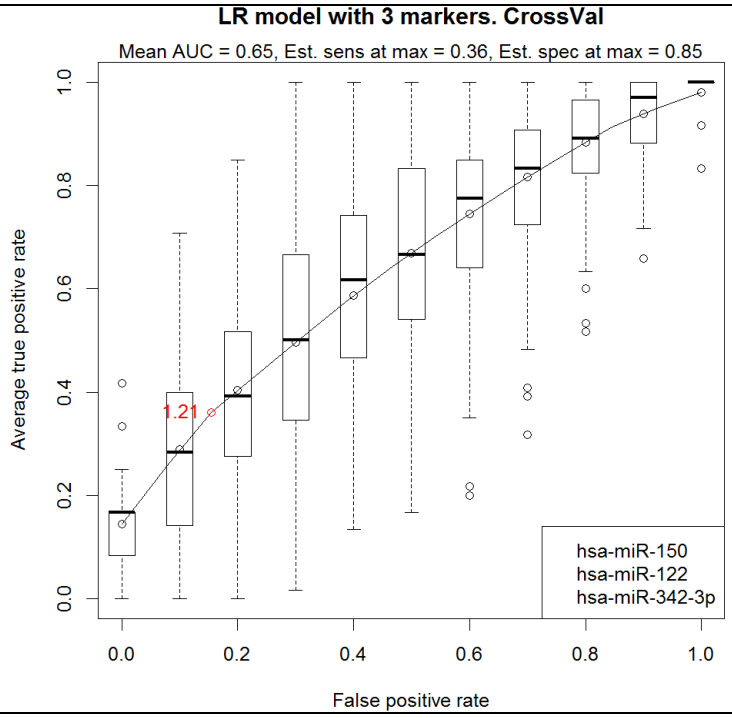

ROC curves from qPCR results assessing the optimal combined miRNAs that potentially could be used for non-invasive identification of endometriosis.

6.6 Summary of identified biomarker panels

The aim of creating a biomarker panel is based on the identification of correlations between endometriosis and the increased or decreased levels of certain proteins and small non-coding miRNAs. This thesis identified a set of miRNAs for which the expression profiles can be used to indicate whether or not a subject has endometriosis. These miRNAs are present at significantly different levels in 10 of the patients with endometriosis and without endometriosis. Detection of the presence or absence of these miRNAs, and/or of changes in their levels over time can potentially be used to indicate that a subject has endometriosis, or has the potential to develop endometriosis in the future. These miRNAs are therefore functioning as biomarkers of endometriosis.

Antigens have also been identified for which the level of auto-antibodies can be used to indicate that a subject has endometriosis. Auto-antibodies against these antigens are present at significantly different levels in subjects with endometriosis and without endometriosis. Detection of the presence or absence of these auto-antibodies, and/or of changes in their levels over time, can also be used to indicate that a subject has endometriosis. The auto-antibodies and their antigens also function as potential biomarkers of endometriosis. The detection of these biomarkers in a subject sample can be used to improve the diagnosis, prognosis and monitoring of endometriosis or the differentiation between the presence of endometriosis and other forms of intra-abdominal inflammation. 343 biomarkers have been identified (Table 9-18) and in the creation of a biomarker panel at least one of these assisted in the diagnosis of endometriosis by measuring the level(s) of the biomarker(s).

Biomarkers, as discussed can be either a protein or a miRNA. A protein biomarker can be either an auto-antibody which binds to an antigen in Table 9-18 and/or (ii) an antigen in Table 9-18. The analysis of patient samples included the determination of the level of Table 9-18 biomarker in the sample, and their levels. The levels provide a diagnostic indicator of whether or not the subject has endometriosis. Analysis of a single Table 9-18 biomarker can be performed, and detection of the autoantibody/antigen or miRNA can provide a useful diagnostic indicator for endometriosis even without considering any of the other Table 9-18 biomarkers but the sensitivity and specificity of diagnosis can be improved, by combining data for multiple biomarkers. It was therefore preferred to analyse more than one Table 9-18 biomarker. Analysis of two or more different biomarkers (a "panel") enhanced the sensitivity and/or specificity of diagnosis compared to the analysis of a single biomarker. Each different biomarker is demonstrated in a panel in a different row in Table 9-18, e.g. measuring both auto-antibody binding to an antigen listed in Table 9-18 and the antigen itself measured as a single biomarker rather than of a panel.

It was found that the combination of the information from protein and miRNA biomarkers as an algorithm provided an enhancement in diagnostic utility, as measured by sensitivity, specificity and/or area under the Receiver Operating Characteristic (ROC) curve. It was decided that the new biomarker panel preferably used at least one protein biomarker from Table 9-18 and at least one miRNA biomarker from Table 9-18 to assist in the diagnosis of endometriosis.

The panel was created after multiple combinations for proteomic and miRNA biomarker were tested. The panel aims to provide a method for analysing a subject sample, comprising a step of determining the levels of x different biomarkers of Table 9-18 (The value of x is 2 or more e.g. 2, 3, 4, 5, 6, 7, 8, 9, 10, 11, 12, 13, 14, 15 or more (e.g. up to 343)). The panels may include (i) any specific one of the 343 biomarkers in Table 9-18 in combination with (ii) any of the other 342 biomarkers in Table 9-18 with a preference the panel includes at least one protein biomarker (e.g. auto-antibodies or an antigen) from Table 9-18 and at least one miRNA biomarker from Table 9-18. Suitable panels are described below and panels of particular interest include those listed in Table 9-28 to Table 9-32. Preferred panels have from 2 to 6 biomarkers, as using >6 of them added little to sensitivity and specificity.

To increase the sensitivity and/or specificity of diagnosis, the Table 9-18 biomarkers could also potentially be used in combination with one or more of: (a) known biomarkers for endometriosis, which may be auto-antibodies, antigens or miRNAs; and/or (b) other information about the subject from whom a sample was taken e.g. age, genotype (genetic variations can affect auto-antibody profiles[678] and considerable progress on the elucidation of the genetics of endometriosis has been made), weight, other clinically-relevant data or phenotypic information; and/or (c) other diagnostic tests or clinical indicators for endometriosis. Known endometriosis biomarkers of particular interest include, but are not limited to, autoantibodies against CA125, CA19-9 and/or any of the antigens listed in Table 9-22.

6.7 Discussion

6.7.1 Overview of results

The results of the quality control (QC) assays and the low CVs provided a high degree of confidence in these results for further reliable analysis. There were clear indications of antibody reactivity in many of the samples. The identification of such autoantibodies and their cognate antigens may potentially form the basis of an exploration of the biology (Figure 6-22).

FIGURE 6-22

Cy3-anti-human IgG binding in several sera to a selection of different proteins

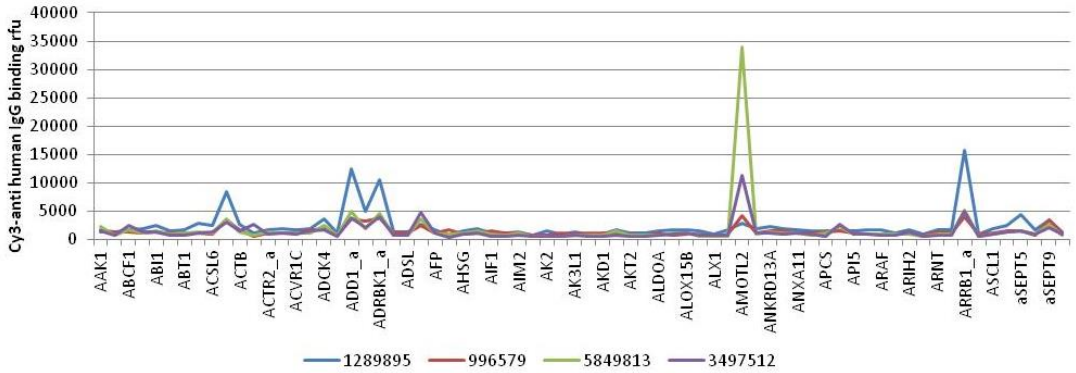

Antibody binding profiles for four different sera to a selection of proteins on the arrays

6.7.1.1 An initial overview of the Cellular cytoskeleton and structure

The cellular cytoskeleton is composed of microtubules composed of both α- and β- tubulins. These tubulins are organised within the centrosome organising areas which control and recruit α- and β- tubulins enabling microtubule formation at the centrioles. These microtubules have a role in cellular division, transport and the maintenance of the cellular architecture[679]. To enable the linkage of α- and β- tubulins, five tubulin cofactors (TBC A-E) are involved[353,680]. They support correct protein folding and recruitment pathways enabling appropriate in vivo tubulin dynamics and cellular function[354]. They are multidynamic molecules with a wide range of functions encompassing roles in tubulin association, storage and even degeneration. It is believed that their control of the amount of tubulin available for polymerisation enables the regulation of the multitude of functions mentioned above. Tubulin cofactors are known to regulate the cell cycle through its various stages. Aberrations in the system have been associated with development of tumorigenesis and ciliary syndromes[679].

FIGURE 6-23

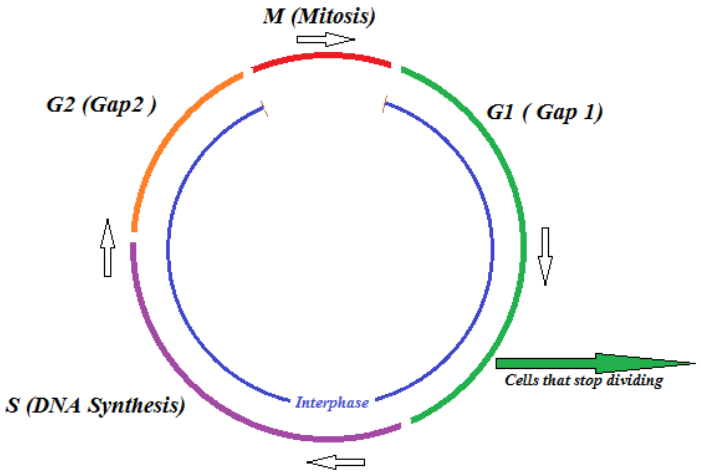

Figure illustrating the basis phases of the cell cycle

Tubulin folding cofactor C or TBCC Tubulin-folding protein is involved in the final stages of the tubulin. It is an important major protein ensuring the correct development of α and β-tubulins into microtubules[681]. Cofactor C is one of the four cofactor proteins A, D and E responsible for the correct folding of beta tubulin. Cofactors A and D are responsible for stabilising β-tubulin intermediates whilst E binds to the formed D/ β-tubulin complex. This complex interacts with cofactor C releasing further β-tubulin polypeptides.

TBCD is mainly found at the centrosome and midbody imperative in its role for centriologenesis, spindle organisation and cellular splitting[679]. It varies in amounts through different cell cycle phases and in the G1 phase is localised on the daughter centriole. In the S phase it localises in the procentriole and in the telophase it is seen to disappear as the protein is recruited into the mid-body[679]. Its overexpression causes G1 arrest of the cell cyle whereas its reduction causes incomplete microtubule retraction and mitotic aberrations during the cell cyle. It is seen to take part in both canonical and non-canonical centriolar pathways. Mutations in TBCD have been studied in various yeast[682] and plant species and are seen to cause aberrations in chromosomal numbers[683] and blockage of the cells in the G1/S phase of the cycle in turn causing problems with cytokinesis. Studies manipulating TBCD levels have been shown to produce centrosomal anomalies which cause defects in cellular spindle formation, anaphase, G1 blockage and cellular abscission failure[679]. Interestingly, defects in abscission are associated with malignant cellular transformation. Defects in cytokinesis are culprits in the development of cancer altering cellular properties and therefore functions[684].

TBCE (Tubulin Folding Cofactor E) is one of the four proteins enabling the correct folding of beta-tubulin. It binds to the cofactor D beta-tubulin complex and interacts with the C cofactor releasing beta-tubulin proteins. It maintains the cellular neuronal microtubule network and controls the dissociation of cellular tubulin heterodimers[578].

6.7.2 Summary of autoantibody analysis

The SH3GL1 gene encodes the Endophilin-A2 protein which is a cystolic protein implicated in cellular synaptic endocytosis. Mutations in the Endophilin A2 protein have been seen to prevent in vivo models of endocytosis[685]. Focal adhesion kinase (FAK) is associated with endophilin A2 interactions causing its

tyrosine phosphorylation with the formation of a focal adhesion steroid receptor coactive complex (FAK/Src complex)[686]. The complex inhibits the interactions between endophilin and dynamin causing attenuation of the endocytosis of the membrane type 1 metalloprotease complex (MT1-MMP)[686]. This in turn causes increase in levels of cellular degradation. Elevated levels of this complex have been associated with increased angiogenesis and tumour growth, identifying it as yet another possible therapeutic target in disease[687]

The aSEPT9 gene codes for Septin 9. This has been linked to tumour migration and invasion as well as apoptosis and pseudopod formation[688]. In eukaryotic cells, septins are a family of GTPases with roles in cytokinesis and neoplasia[689]. SEPT9 is expressed in a large number of human tumours including breast[690], epithelial ovarian[691] and endometrial[689] tumours. Abnormalities of expression are linked to tumour development and a number of genes including SEPT9 are involved in the chromosomal translocations in acute myeloid leukaemia[692]. Metastatic lesions are seen to have higher SEPT9 levels[689] and its presence on cell borders and secretory epithelia indicate a role in membrane vesicle formation[689]. This is itself is associated with roles in neoplastic development[693]. In theory, as discussed previously (See section 6.7.3.2), aSEPT9 can have similar effects on endometriotic tissues. Ectopic endometrial cells are seen to migrate and invade similar to tumours. As endometriosis is not a malignancy, one could potentially theorise that aSEPT9 levels are kept in check though multifactorial effects of tumour suppressor pathways affected by miRNAs which have been discussed in earlier sections of this thesis (See section 5.5.1).

Breast Cancer Anti-Oestrogen Resistance 1 (BCAR1), is associated with an increase in epithelial cellular hyperplasia in mammary tumorigenesis[694]. It is involved in the integrins signalling cellular system and plays a role in cellular motility, migration, proliferation and phagocytosis (Figure 6-28).

Tumour necrosis factor receptor superfamily, member 1A (TNFRSF1A) is a key regulator of the immune system and is a key component activating the NF-κB pathway which controls cellular apoptosis. An increase adherence of endometriotic cells has been postulated as a contributing factor to the development of endometriosis. TNF-α is also known to increase adherence of stromal uterine cells to *in vitro* mesothelium[695] by its activation of fibroblastic proliferation, collagen deposition[162] and an increase in their prostaglandin production[696] The TNF family is interestingly dysregulated in viral infections and is an essential component in the development of infectious disease[697]. The regulation of the TNFRSF1A gene enables protection against virally induced pathology. Diseases can be stimulated or repressed by co-stimulating or regulating TNF factors making the regulators of the TNFR therapeutic targets for controlling disease. Tumour necrosis factor receptor superfamily, member 10a (TNFRSF10A) is another apoptosis mediator and promotes the NF-κB pathway. Studies looking at peritoneal endometriosis, have found evidence for the activation of NF-κB with higher levels demonstrated in active red lesions compared to necrotic black ones[698], making it a potential interesting therapeutic target for disease. In early stages, NF-κB inhibits tumour growth[699] and in endometriosis it might act as a tumour suppressor preventing overt malignant changes. As a disease progresses, mutations in NF-κB shift its role to an oncogenic one, enabling contribution to malignancy[699]. NF-κB is also seen to decrease stabilisation of other tumour suppressors such as p53 increasing the potential for malignant change[700]. In theory this could explain why some cases of severe endometriosis are abutting ovarian and/or endometrial

malignancy[701]. A non-malignant disease such as endometriosis could potentially transform into malignant disease if tumour suppressing mechanisms are lost or pathways altered.

Oestrogen receptor 1 (ESR1) is a transcription factor activated by oestrogen[702] (Figure 6-29); endometriosis is a disease responsive to oestrogen and its signalling. There are elevated levels of ER-α receptors in active red endometriotic lesions compared to black necrotic ones[703]. Increase in ER-α levels also activate other pathways such as insulin-like growth factor-1 (IGF-1) which send powerful mitogenic stimuli causing cellular proliferation and growth. In severe endometriosis, plasma levels of IGF-1 are elevated. This elevation is however not maintained in the endometrium itself[704]. These findings are almost certainly related to the hormonally responsive tissue that endometriosis derives from.

Baculoviral inhibitor of apoptosis proteins (IAP) repeat-containing 2 (BIRC2) plays a major role in cellular control of apoptosis by creating positive or negative feedback signalling on the NF-κB pathway. IAP exerts its function through protein-protein interaction of the proteins involved in apoptosis or cell signalling[705]. Through their ring domain, cIAPs also cause ubiquitination of the tumour necrosis factor receptor complex (TNFR) thereby affecting the Nuclear factor Kappa Beta (NF-κB) complex and its pathways[706] promoting cellular survival, proliferation and inhibition of apoptosis[707]. In an opposite effect, cIAPs can also repress the NF-κB pathway limiting both the canonical and non-canonical signalling of the NF-κB pathway[708]. Biologically, this anti apoptotic mechanism serves to enable cellular survival in stressful conditions such as when cells are detached from their matrix[709] or ER stressors[710]. These mechanisms can explain the increased cell survival capacity of intraperitoneal endometrial cells in endometriosis which can invade and develop disease.

Tropomyosin alpha-1 chain (TPM1) has been identified as a tumour suppressor gene which has the ability to regulate cellular migration and invasion. It is regulated by miR-21 and has recently been identified as a potential serum marker in cancer[711]. At the time of writing this thesis, there is no publication linking TPM1 to endometriosis. In theory, and from this study, it could however act as a potential serum biomarker for this disease. TPM1 is potentially another important tumour suppressor preventing overt malignant change in a disease like endometriosis.

Heat shock protein 60 (HSP60), also known as mitochondrial HSPD1, has immunogenic and inflammatory roles with immune and malignant conditions showing T-cell antibody responses to it. Activated T cells result in proliferation and cytokine expression[712] causing the release of macrophage pro-inflammatory adhesion molecules (Figure 6-31)[713]. HSPs function towards allowing tumour survival either through the inhibition of apoptosis or through the regulation of autoimmunity. Various studies show HSP60 activates the EGFR, Map kinases and TNF-α. The HSPE1 gene has been identified as a potential endometriosis gene marker.

GTP-binding nuclear protein Ran (RAN) is a member of the RAS oncogene family and has a role in cellular transport enabling vesicle fusion at the nuclear envelopes of daughter cell nuclei[714]. In viral infections it has a role in regulating phagocytosis and immunity to the invading virus and is upregulated in virally infected cells[715]. It is upregulated in EBV associated nasopharyngeal carcinoma and has been identified as a candidate for Myc-mediated cancer progression and metastatic potential. Potentially the same mechanisms can be attributed to disease progression in endometriosis.

E3 ubiquitin-protein ligase CHIP (STUB1) is essential for T cell activation and T-cell receptor induced NF-κB signalling[716]. It has a tumour suppressor role and is downregulated in proliferative tumours[717]. It affects the function of p53 causing aberrant stabilisation of mutant p53 in human cancers[718] when inactivated by Hsp90. Potentially this is another mechanism by which malignant change is prevented in endometriosis.

A number of potential protein markers have been identified above, some of which may be bi products of hormonally responsive disease whereas others appear to potentially play a role in the process of endometriosis development and sustainability. The Figure 5-10 and Figure 5-11 provide an overview of interactions between identified miRNAs, associated genes, proteins, antibodies and the pathways they affect.

6.7.3 Detailed analysis of the associations and interactions of identified significant protein in patients with endometriosis.

Below is a summary from the predictive program STRING™ showing the evidence based interactions of all the above-mentioned biomarkers (Figure 6-24).

FIGURE 6-24

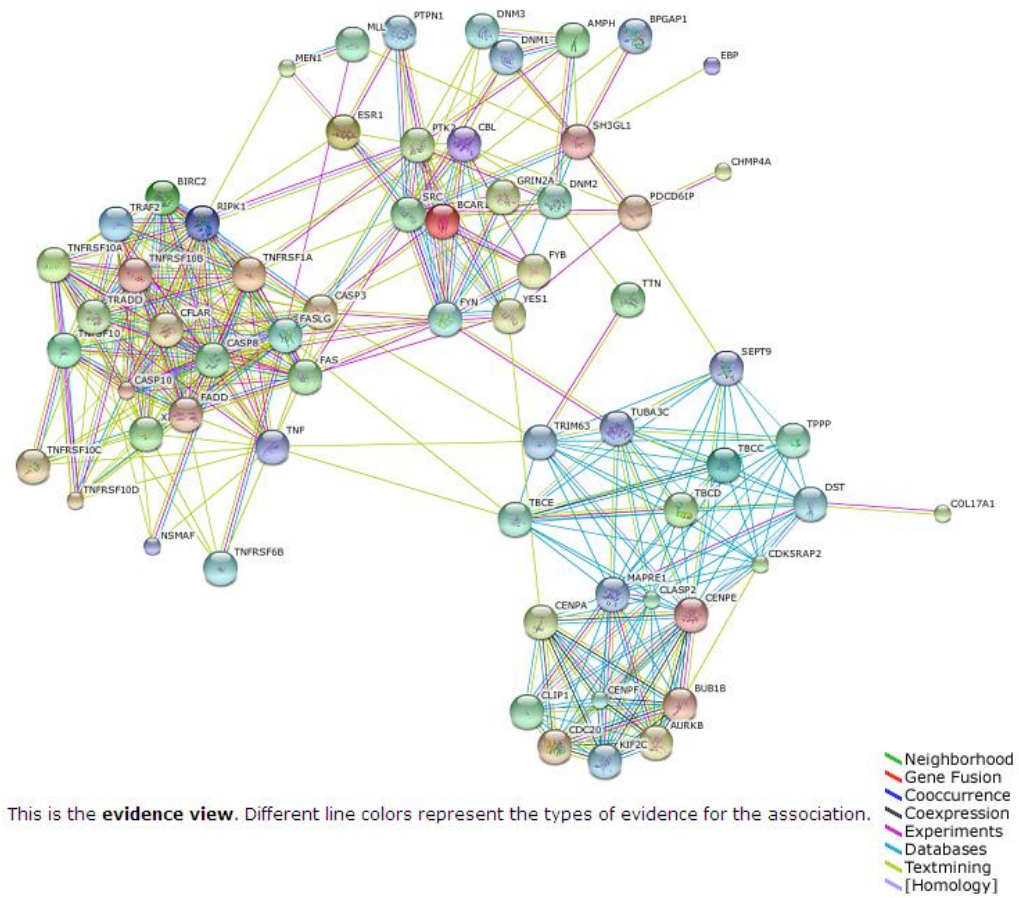

Evidence view of predicted interactions of biomarkers[576]

6.7.3.1 SH3GL1

FIGURE 6-25

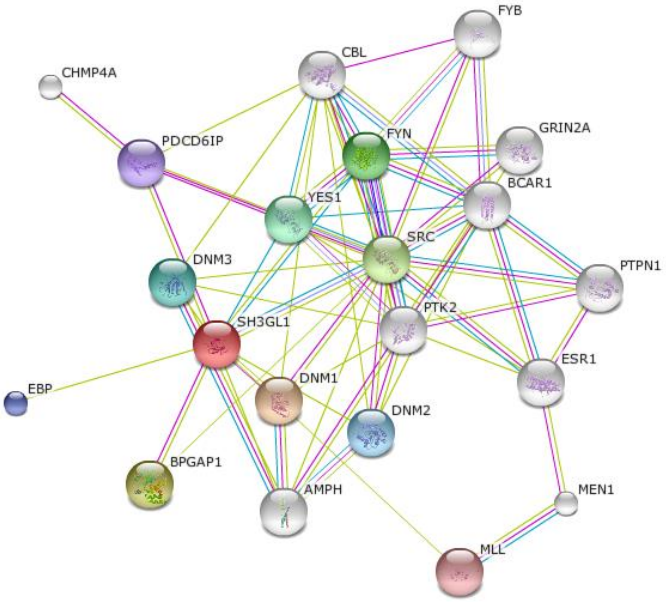

This is the **evidence view**. Different line colors represent the types of evidence for the association

SH3GL1 SH3-domain GRB2-like 1; Implicated in endocytosis. May recruit other proteins to membranes with high curvature (By similarity) (368 aa)
(Homo sapiens)

Predicted Functional Partners:

		Neighborhood	Gene Fusion	Cooccurrence	Coexpression	Experiments	Databases	Textmining	[Homology]	Score
DNM1	dynamin 1; Microtubule-associated force-producing protein involved in producing microtubule bun [...] (864 aa)					•		•		0.980
BPGAP1	Rho GTPase activating protein 8; GTPase activator for the Rho-type GTPases by converting them t [...] (464 aa)					•		•		0.968
SRC	v-src sarcoma (Schmidt-Ruppin A-2) viral oncogene homolog (avian) (536 aa)						•	•	•	0.937
FYN	FYN oncogene related to SRC, FGR, YES; Implicated in the control of cell growth. Plays a role i [...] (537 aa)						•			0.919
YES1	v-yes-1 Yamaguchi sarcoma viral oncogene homolog 1; Promotes infectivity of Neisseria gonorrhoe [...] (543 aa)						•			0.899
DNM3	dynamin 3; Microtubule-associated force-producing protein involved in producing microtubule bun [...] (859 aa)							•		0.899
DNM2	dynamin 2; Microtubule-associated force-producing protein involved in producing microtubule bun [...] (870 aa)							•		0.899
EBP	emopamil binding protein (sterol isomerase); Catalyzes the conversion of Delta(8)-sterols to th [...] (230 aa)							•		0.890
PDCD6IP	programmed cell death 6 interacting protein; Class E VPS protein involved in concentration and [...] (868 aa)					•				0.868
MLL	myeloid/lymphoid or mixed-lineage leukemia (trithorax homolog, Drosophila); Histone methyltrans [...] (3969 aa)							•		0.857

Evidence view of predicted interactions of SH3GL1[576]

Membrane trafficking of cellular compounds occurs by varied processes, one of which is vesicular transport. Vesicular transport involves the detachment of a vesicle from a donor membrane, its transport and identification from the receptor membrane and ultimately its fusion with the receptor membrane whereby it releases its contents. Studies looking at endocytosis at the synaptic interphases between neuronal cells have given an insight to this process[719]. The SH3GL1 gene encodes the Endophilin-A2 protein which is a cystolic protein implicated in cellular synaptic endocytosis. Endophilins are divided into two families, A and B respectively. Endophilin A1 is mainly restricted to neuronal function. Endophilin A2 is ubiquitous in its expression, while Endophilin A3 is mainly within neurons and testes. They have an N-terminal domain called the BAR domain and the C terminal domain called the SH3 domain. Endophilins are regulated by Ca^{2+} ıklux into the neurons[720] and demonstrate binding to the voltage gated calcium channels at the centre of the endophilin SRC Homology 3 Domain (SH3). Calcium binding to the domain disrupts the interaction of the SH3 domain to the nearby prolene rich area adjacent to the calcium binding region. This allows its interaction with the voltage-gated calcium channels thereby permitting endocytosis through the association with dynamin and synaptojanin-1[686]. Mutations in the Endophilin A2 protein have been seen to prevent in vivo models of endocytosis[685]. Focal adhesion kinase

(FAK) is associated with endophilin A2 interactions causing its tyrosine phosphorylation with the formation of a focal adhesion steroid receptor coactive complex (FAK/Src complex)[686]. The complex inhibits the interactions between endophilin and dynamin causing attenuation of the endocytosis of the membrane type 1 metalloprotease complex (MT1-MMP)[686]. This in turn causes increase in levels of cellular degradation. Elevated levels of this complex have been associated with increased angiogenesis and tumour growth, identifying it as yet another possible therapeutic target in disease[687]. The overexpression of FAK is seen in a variety of cancers[721] and is associated with increased potential to invade and metastasise[722,723] (Figure 6-26). In my study SH3GL1 is identified as a potentially significant protein in endometriosis and as seen above, it codes for Endophilin A2 responsible for endocytic cellular processes and interactions with FAK and the FAK/Src complex. This in turn attenuates the endocytosis of (MT1-MMP)[686] leading to increased levels of this complex resulting in angiogenesis and growth[687]. Potentially a similar mechanism occurs in endometriosis aiding the growth and metastasis of ectopically implanted cells.

FIGURE 6-26

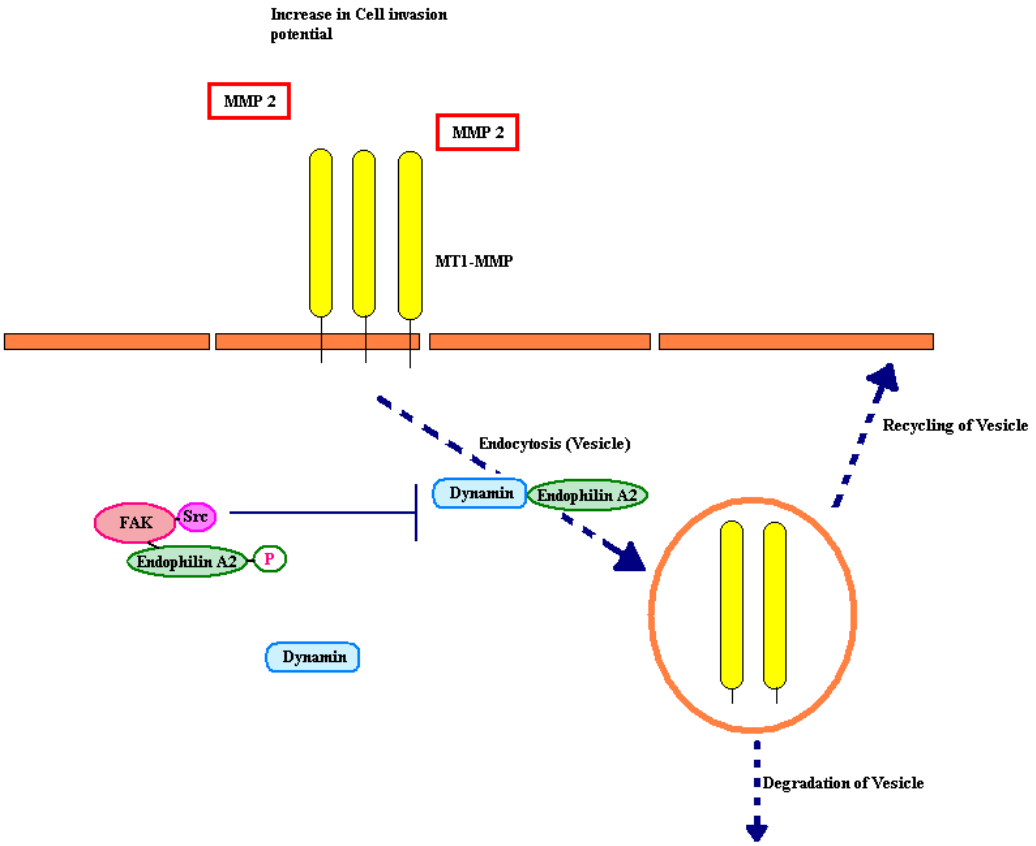

Demonstrating interactions in Cellular endocytosis

6.7.3.2 aSEPT9

FIGURE 6-27

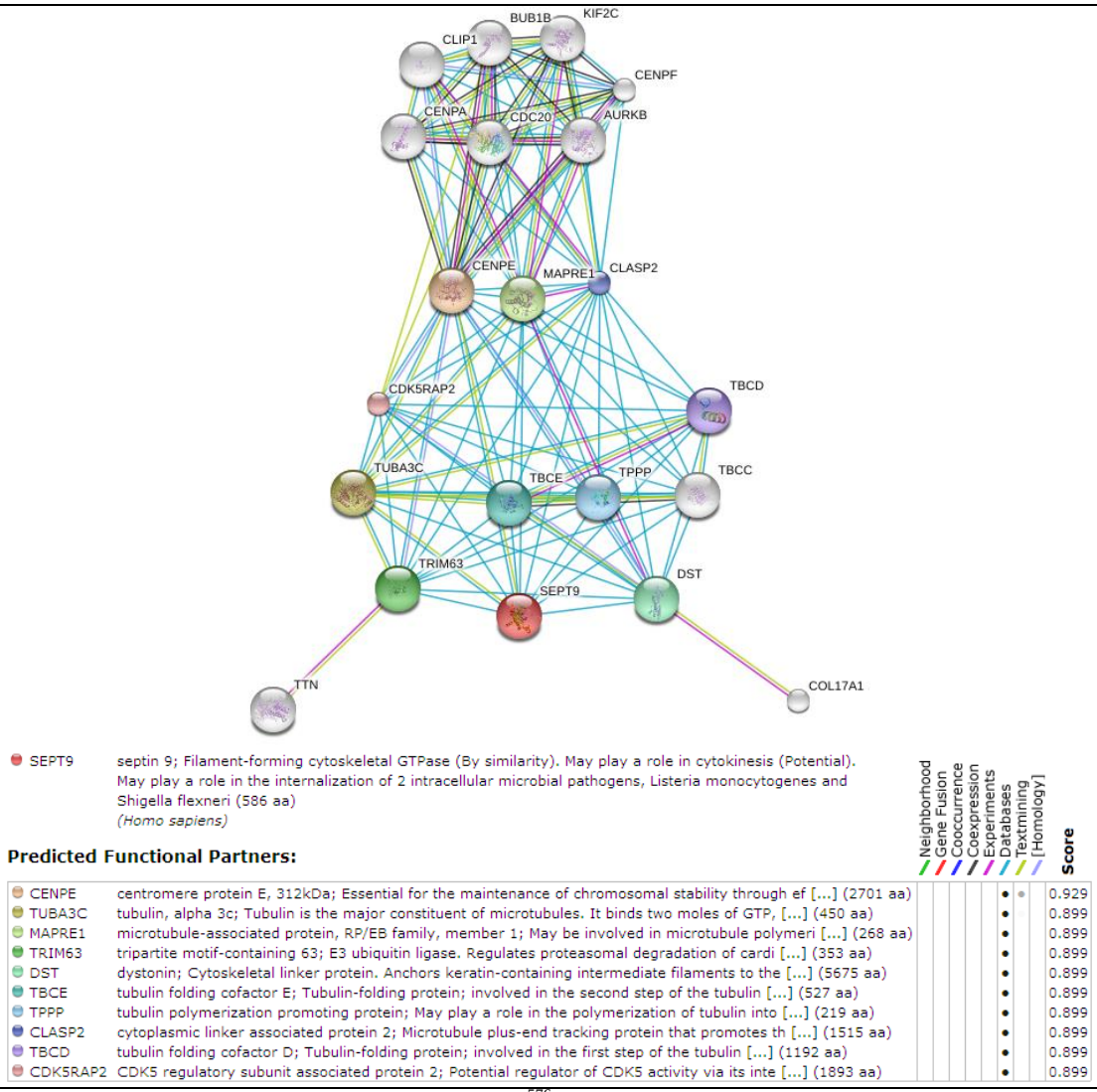

Evidence view of predicted SEPT9 protein interactions[576]

The aSEPT9 gene codes for Septin 9. This has been linked to tumour migration and invasion as well as apoptosis and pseudopod formation[688]. The 12 human septins known to exist are homologous in their core GTP-binding region[724] but vary in the N and C terminals[725]. In eukaryotic cells, septins are a family of GTPases with roles in cytokinesis and neoplasia[689]. They aid in the formation of filamentous complexes with the hydrolysis and binding of cytoplasmic proteins[725]. SEPT9 is expressed in a large number of human tumours including breast[690], epithelial ovarian[691] and endometrial[689] tumours. Abnormalities of expression are linked to tumour development and a number of genes including SEPT9 are involved in the chromosomal translocations in acute myeloid leukaemia[692]. Metastatic lesions are seen to have higher SEPT9 levels[689] and its presence on cell borders and secretory epithelia indicate a role in membrane vesicle formation[689]. This is itself is associated with roles in neoplastic development[693]. In theory, aSEPT9 can have similar effects on endometriotic tissues. Ectopic endometrial cells are seen to migrate and invade similar to tumours. As endometriosis is not a malignancy, one could potentially theorise that

aSEPT9 levels are kept in check though multifactorial effects of tumour suppressor pathways affected by miRNAs which have been discussed in earlier sections of this thesis (See section 5.5.1).

6.7.3.3 BCAR1

Breast Cancer Anti-Oestrogen Resistance 1 (BCAR1), also known as scaffolding protein p130C, is a scaffolding multiadaptor molecule, empirical in the role of intracellular signalling[689]. Its presence is associated with an increase in epithelial cellular hyperplasia in mammary tumorigenesis[694]. Its function derives from the ability to form molecular complexes with effector proteins. P130C is involved in the integrins signalling cellular system and plays a role in cellular motility, migration, proliferation and phagocytosis (Figure 6-28). In theory, BCAR1 could have similar effects in endometriosis, potentially causing ectopic endometrial cellular hyperplasia, proliferation and migration. The cytoplasmic FAK (Figure 6-28) activates integrin mediated cell adhesion and has been shown in experimental mice models to have vital angiogenic and oncologic roles. Its presence in severe ovarian endometriosis correlating with clinical severity and metastatic potential has been explored[726]. Interestingly, in women who suffer from endometriosis, FAK levels were seen to be higher in their eutopic endometrium in the secretory phase of the cycle[727] making it a potential contributory factor to development of disease. Increased FAK expression is seen in a number of cancers and promising therapeutics are targeted towards its inhibition.

FIGURE 6-28

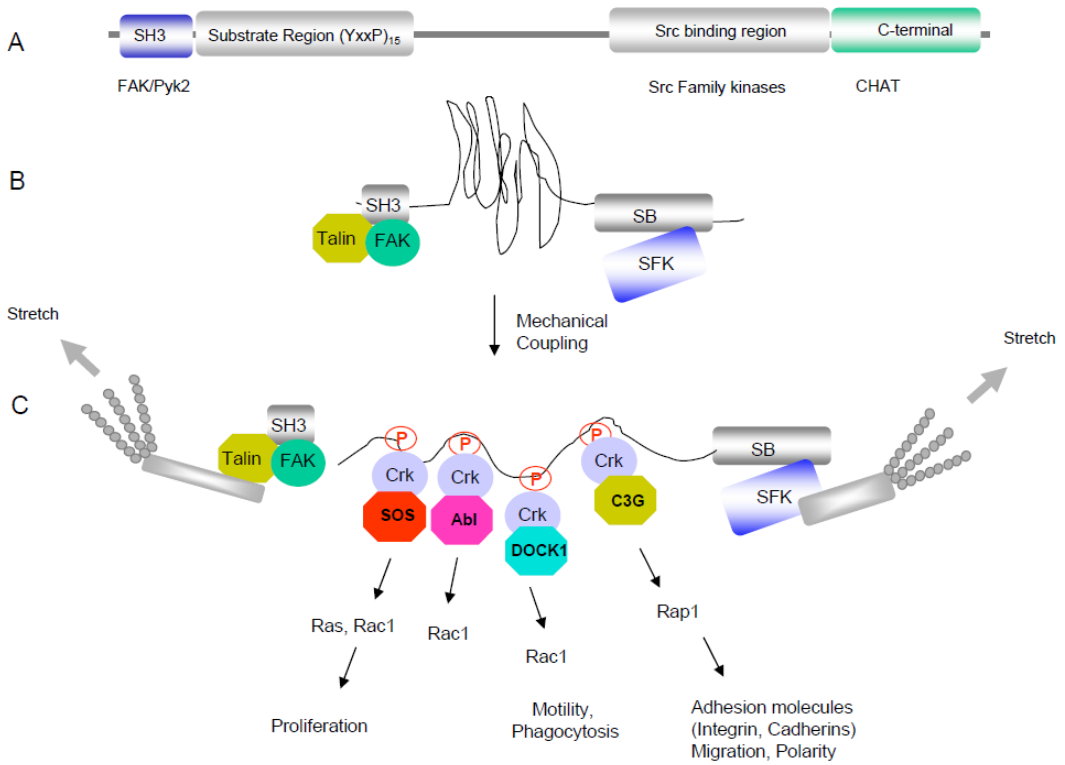

(**A**) P130C contains, an N-terminal SH3 domain, a serine-rich motif that binds Src kinases, and a conserved C-terminal region that binds members of the Chat family of proteins[728]. (**B**). Activation of the compressed central substrate region of p130C occurs with its (**C**). Activation induces Src, tyrosine phosphorylation and recruitment of Crk through its SH2 domain[728]

6.7.3.4 TNFRSF1A

Tumour necrosis factor receptor superfamily, member 1A (TNFRSF1A) is a protein encoded for by the TNFRSF1A gene. It is a key regulator of the immune system and is a receptor for TNFSF2/TNF-alpha and homotrimeric TNFSF1/lymphotoxin-alpha. TNF binds to the ligands of TNFRSF1A and is a key component activating the NF-κB pathway which controls cellular apoptosis. TNF-α is mainly produced by non-haematopoietic cells including activated lymphocytes, macrophages, NK cells and neutrophils whereas TNF-β is produced by lymphocytes.

TNF proteins activate the cytokine cascades, inflammatory responses and cellular apoptosis. It is also implicated in endometrial shedding with epithelial uterine cells showing high expression of its mRNA and associated proteins in its secretory phase[729]. TNF-α serum levels in patients suffering from endometriosis tend to be higher than those of control patients even in the early stages of disease[359]. The levels of TNF in the peritoneal fluid of patients with endometriosis are elevated and correlate to the stage of disease[730]. In the stomal uterine cells, the proliferative phase of the menstrual cycle is associated with elevations in the levels of TNF-α indicating an altered cytokine response[731]. Elevated TNF-α levels also serve in proliferating the endometriotic stromal cells through activation of the IL-8 gene.

An increase adherence of endometriotic cells has been postulated as a contributing factor to the development of endometriosis. TNF-α is also known to increase adherence of stromal uterine cells to *in vitro* mesothelium[695] by its activation of fibroblastic proliferation, collagen deposition[162] and an increase in their prostaglandin production[696] indicating yet another facet to its contribution in endometriotic disease development. Cellular IL-1, endometrial placental proteins and progesterone levels are all known to interact and alter TNF-α expression levels within the cell.

The TNF family is interestingly dysregulated in viral infections and is an essential component in the development of infectious disease[697]. In this study I have already identified EBV virus as being elevated in the leukocytes of women with endometriosis (See section 4.4.3.5 and 4.5.2.1), it is possible that even minor dysregulation of TNFRSF1A can aid in potentiating the EBV effects in development of endometriosis. The regulation of the TNFRSF1A gene enables protection against virally induced pathology. Several members of the TNF/TNF Receptor family are noted to sustain T-cell function in the cell after primary T-cell activation[732]. It therefore follows that any system dysregulation could be mirrored in alterations of T-cell survival and function[733]. Diseases can be stimulated or repressed by co-stimulating or regulating TNF factors making the regulators of the TNFR therapeutic targets for controlling disease.

Experimental intestinal endometriosis in rats has been associated with downregulation of TNFRSF1A and TNFRSF1B gene expression. This is believed to be a protecting mechanism against TNF cytotoxicity. Conversely, over expression of genes encoding for TNF receptor associated factors was increased with overexpressions of ICAM1, Sele, Vegfa, Flt and Kdr[734]. Increased protein levels of TNF and the soluble TNFRSF1B were confirmed in the studied rat peritoneal fluid. The mRNA for TNF was also elevated in diseased rat intestinal segments and their peritoneal leukocytes. This provides evidence of the direct impact of the TNF system in the pathogenesis of endometriosis[734]. Studies using anti TNF monoclonal

antibodies[735] and recombinant human TNFRSF1A (r-hTBP1)[736] show a decrease in disease development in the animal models used.

6.7.3.5 TNFRSF10A

Tumour necrosis factor receptor superfamily, member 10a (TNFRSF10A) is another apoptosis mediator. It promotes the NF-κB pathway by acting as a receptor for the cytotoxic cytokine ligand tumour necrosis factor (ligand) superfamily, member 10 TNFSF10/TRAI. Fas (TNFRSF6)-Associated Via Death Domain (FADD) recruits caspase-8 to the activated TNFRSF10A receptor and the caspase-8 undergoes activation by the death-inducing signalling complex (DISC). A cascade of various caspases is activated and this mediates the apoptotic mechanism. In peritoneal endometriosis, there is evidence for the activation of NF-κB[698] with higher levels demonstrated in active red lesions compared to necrotic black ones, making it a potential interesting therapeutic target for disease. In early stages, NF-κB inhibits tumour growth[699] and in endometriosis it might act as a tumour suppressor preventing overt malignant changes. As disease progresses, mutations in NF-κB shift its role to an oncogenic one, enabling contribution to malignancy[699]. In theory this could explain why some cases of severe endometriosis are abutting ovarian and/or endometrial malignancy[701]. A non-malignant disease such as endometriosis could potentially transform into malignant disease if tumour suppressing mechanisms are lost.

6.7.3.6 Oestrogen receptor 1 (ESR1)

FIGURE 6-29

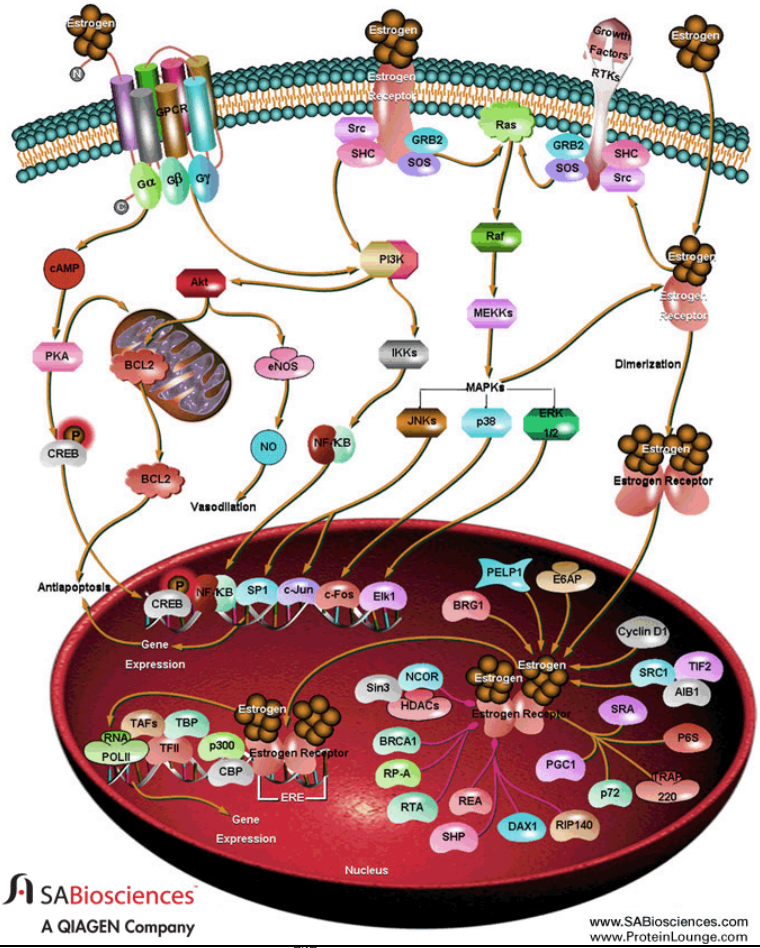

Oestrogen cellular pathways and its interactions[737]

Oestrogen receptor 1 (ESR1) is a gene encoding oestrogen receptor-α (ER-α) also known as nuclear receptor subfamily 3, group A, member 1 (NR3A1). It is a transcription factor activated by oestrogen[702] (Figure 6-29); endometriosis is a disease responsive to oestrogen and its signalling. There are elevated levels of ER-α receptors in active red endometriotic lesions compared to black necrotic ones[703]. The oestrogen (and progesterone) receptors themselves are reported to express polymorphisms increasing the predisposition to disease development[738,739]. Endometriosis also shows an elevated cytochrome P450 and decreased 17β-hydroxysteroid dehydrogenase type 2 expression[740] preventing the change from the more potent oestradiol to oestrone. This results in increased local oestrogen production further enabling endometriosis proliferation.

Genetic polymorphisms are also seen in endometriosis in enzymes from the Cytochrome P450 family such as CYP1A1[741], CYp19[742] and Glutathione S-transferase Mu 1 (GSTM1)[743]. Increase in CYP1A1 levels causes elevations in P459 and oestrogen production[744]. Increase in ER-α levels also activate other pathways such as insulin-like growth factor-1 (IGF-1) sending powerful mitogenic stimuli causing cellular proliferation and growth. The IGF-1 has been associated with malignant development and metastatic potential. There is an increase in its levels in other female cancers such as cervical, ovarian and endometrial[745] and these levels remain constant even post-menopausally. In severe endometriosis, plasma levels of IGF-1 are elevated. This elevation is however not maintained in the endometrium itself[704].

6.7.3.7 BIRC2

Baculoviral inhibitor of apoptosis proteins (IAP) repeat-containing 2 (BIRC2) is also known as cIAP1. It is one of 8 family IAP members and plays a major role in cellular control of apoptosis by creating positive or negative feedback signalling on the NF-κB pathway. The cIAP1 exerts its function through protein-protein interaction of the proteins involved in apoptosis or cell signalling[705]. Apoptosis is inhibited when the cIAPs bind to and sequester Smac from X-Linked Inhibitor Of Apoptosis (XIAP). The latter, in turn, suppresses apoptosis[746]. Through their ring domain, cIAPs also cause ubiquitination of the tumour necrosis factor receptor complex (TNFR) thereby affecting the Nuclear factor Kappa Beta (NF-κB) complex and its pathways[706]. Once the NF-κB is activated or altered, effects on cyto and chemokines occur, which in turn promote cellular survival, proliferation and inhibit apoptosis[707]. Both the NF-κB canonical and non-canonical pathways are affected through the action of cIAPs.

Cellular complexes formed from TNFRSF1A-Associated Via Death Domain (TRADD), receptor-interacting protein 1 (RIP1) and tumour necrosis factor receptor-associated factor 2 (TRAF2) domains are induced when TNF-α binds to tumour necrosis factor receptor (TNFR). cIAPs are recruited to this complex by TRAF2 and this in turn induces the NF-κB pathway through the TNFR. The ring domain of cIAPs activates the K63 polyubiquitination of the RIP1 which itself activates the transforming growth factor-β-activated kinase 1 complex. IKK is phosphorylated activating the NF-κB pathway. K63 polyubiquitination of RIP1 suppresses caspase-8 preventing apoptosis[747]. Once the TNF-α is stimulated and activates the NF-κB pathway, stimulation of genes suppressing the apoptoic signal occurs and the cell survival increases[748]. Interestingly, the NF-κB signalling induced by the anti-apoptotic signalling itself induces further cIAPs. NF-κB is a negative regulator of p53[700] and a reduction of cellular cIAP2 may result in decreased p53 function[749].

In an opposite effect, cIAPs can also repress the NF-κB pathway. When the complex of cIAP, TRAF2 and TRAF3 interact and ubiquitinate NIK, it exerts a repressive effect limiting both the canonical and non-canonical signalling of the NF-κB pathway[708]. Biologically, this anti apoptotic mechanism serves to enable cellular survival in stressful conditions such as when cells are detached from their matrix[709] or ER stressors[710]. These mechanisms can explain the increased cell survival capacity of intraperitoneal endometrial cells which can invade and develop disease. The RAS and E6 oncogenes[750], induce the cIAP expression and the cancers showing high levels usually demonstrate a poorer patient outcome. cIAP themselves have been described as oncogenes with genetic studies showing amplification of the chromosomal locus 11q21-23 region manifested in a range of cancers including renal cell and gastric carcinomas as well as non-small cell lung cancers[751]. IAP antagonists are under development as therapeutic options for a large number of malignancies. B-lymphocytes utilise NF-κB signalling to promote cellular survival and function in the presence of antigenic stimuli.

Baculoviral IAP repeat-containing 2 (BIRC2) is an apoptotic suppressor (also known as cIAP1). It interacts with TRAF1 and TRAF2 forming a complex which is recruited to the tumour necrosis factor receptor 2 (TNFR2) and interferes with caspase activation. BIRC2 has opposing roles in the regulation of the NF-κB pathways. By recruitment of a TNF receptor they activate the NF-κB through RIP1 ubiquitination. Conversely the BIRC2 represses NF-κB by the ubiquitination of NIK resulting in degradation[752]. Once the NF-κB is activated, it promotes cellular growth and survival including the production of IL-6, B-cell activating factors, cell inhibition of apoptosis, I kappa B kinase (IKK), tumour necrosis factors, TNFR, TRAF TRADD, TNFR- associated death domains and multiple pathways associated with increased cellular survival in malignant patterns[752] (Figure 6-30).

FIGURE 6-30

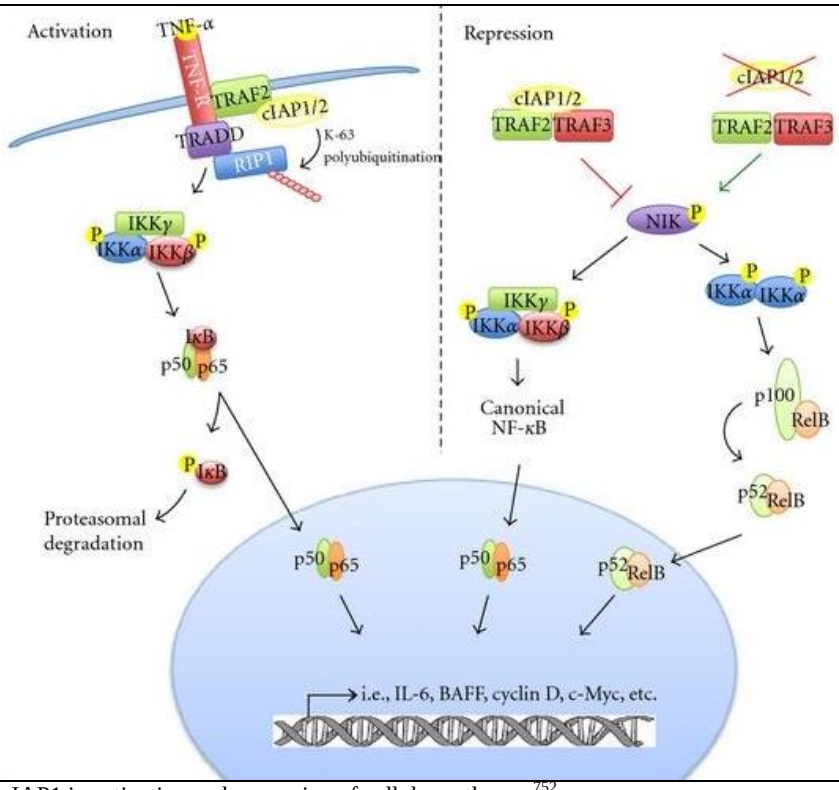

The role of cIAP1 in activation and repression of cellular pathways[752]

6.7.3.8 TPM1

Tropomyosin alpha-1 chain (TPM1) is an alpha tropomyosin actin-binding motor protein which has roles in cellular motor activity and is a structural constituent of the actin cytoskeleton. It is involved in cell motion and cell component morphogenesis as well as muscle contraction and muscle organ development. Embryologically it plays a role in development of ectoderm and mesoderm. TPM1 has been identified as a tumour suppressor gene which has the ability to regulate cellular migration and invasion. MicroRNA-21 (miR-21), also noted as part of my expression profile studies, is a miRNA which functions as an oncogene altering the regulation of TPM1[753] and targets multiple tumour suppressor genes. Epigenetic suppression of TPM1 alters TGF beta tumour suppressor function causing further enhancement of the invasive potential of tumour cells[754]. A recent publication has identified TPM1 as a potential biomarker in the serum of women with ovarian cancer[711]. At the time of writing this thesis, there is no publication linking TPM1 to endometriosis. In theory, and from this study, it could however act as a potential serum biomarker for this disease. TPM1 is potentially another important tumour suppressor preventing overt malignant change in a disease like endometriosis.

6.7.3.9 HSPD1 (HSP60)

FIGURE 6-31

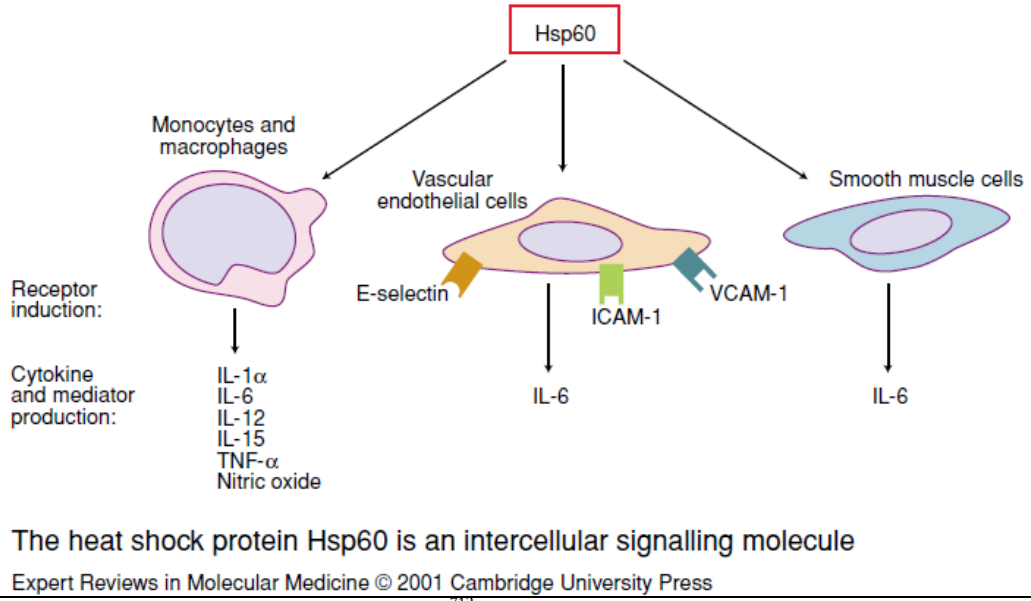

The HSP60 as an intercellular signalling molecule[713]

Heat shock protein 60 (HSP60) is also known as mitochondrial HSPD1. It is a mitochondrial chaperonin that has roles in protein folding and protein complex assembly. It has immunogenic and inflammatory roles. Immune and malignant conditions show t-cell and antibody responses to it. HSP60 causes the release of pro-inflammatory cytokine secretion and adhesion molecule expression on monocytes and macrophages, endothelial and smooth muscle cells respectively (Figure 6-31)[713]. T-cells, which are reactive to HSP60, are present in humans at birth and are capable of responding to stimulation, resulting in proliferation and cytokine expression[712]. They are believed to form part of the neonatal immune response mechanisms and are also seen to play essential roles in malignant cell survival with higher levels prognostic of decreased patient survival in advanced serous ovarian carcinoma[755]. Conversely, patients

with low levels of HSP60 responded to first line chemotherapy. Other immunohistochemistry studies show that in the initial stages of epithelial ovarian carcinomas, the frequency of expression of HSP60 is significantly higher. In these tumours, increased levels[756] are associated with improved disease prognosis. In tumours of the breast, colon, prostate and liver, HSPs are vital for tumour cell survival inhibiting apoptosis and preventing cell death, whereas in tumours of the ovary, bone (osteosarcoma), and skin (melanoma), the HSP's also have a role in immune regulation and autoimmunity[757]. *In vitro* studies looking at the effect of bacterial invasion on epithelial cells show that exogenous HS60, which is released from the invading bacteria or inflammatory cells, promotes epithelial cell migration through EGFR activation and MAP kinases[758]. In studies exploring the relation between endometriosis and HSP60, there seems to be the increased production of Tumour Necrosis factor-α by the mononuclear cells in the peritoneal fluid. This release is due to the induction by HSP60 which is postulated to have a role in peritoneal induced immunity in patients with endometriosis[759]. In women with endometriosis, and tubal factor infertility post Chlamydia infection, HSP60 has been attributed various roles as a causator of infertility by affecting tubal function and endometrial milieu affecting implantation. In my study, HSPE1 gene coding for the HSP family was also flagged up as a potential identified gene marker for endometriosis.

6.7.3.10 RAN

GTP-binding nuclear protein Ran (RAN) is a small GTPase with GTPase and protein binding roles. It is a member of the RAS oncogene family, has roles in cellular nuclear transport during interphase and plays a role in mitosis. During the telophase mitotic component, it is the RanGTP hydrolysis and exchange of nucleotides which enables vesicle fusion at the nuclear envelopes of daughter cell nuclei[714]. Mutations in RAN disrupt the synthesis of DNA. In the nucleotide, Ran exists as GDP-bound and GTP-bound. RCC1 is a nucleotide exchange factor for RAN which is bound to nuclear chromatin in the nucleus. It is the role of RCC1, also known as RanGEF (Ran Guanine nucleotide exchange factor) that converts RanGDP to RanGTP. This GTPase activity of RCC1 occurs through the interaction of Ran GTPase activating protein (RanGAP) and through complex formation with Ran binding protein (RanBP) (Figure 6-32).

FIGURE 6-32

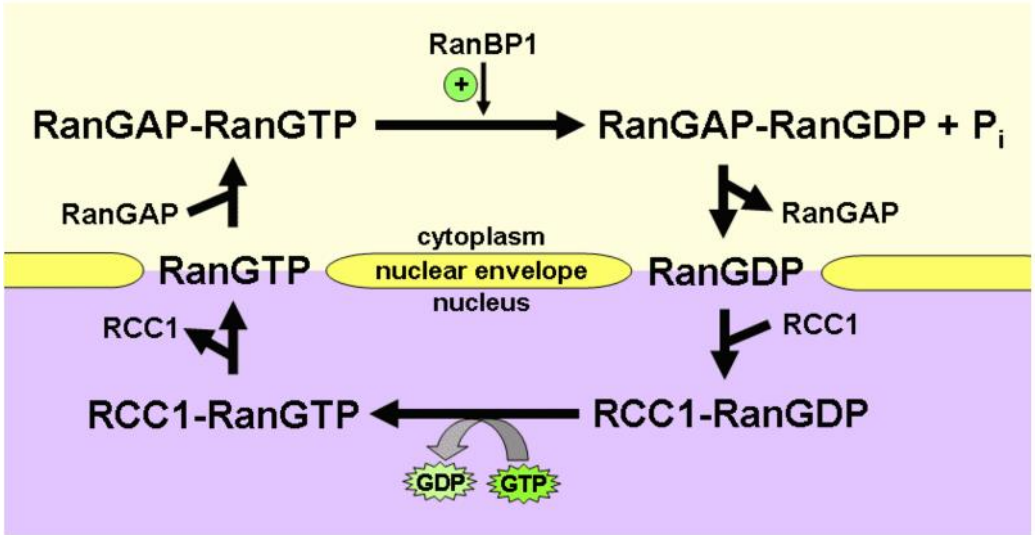

RAN cycle within the cell[714]

Another role of RAN is that of a coactivator for the androgen receptor (ARA24). The increased polyglutamine expansions seen in disease such as Kennedy's disease (an X-linked spinal and bulbar muscular atrophy) cause reduction of RAN coactivation with the Androgen receptors, leading to androgen insensitivity during development of disease[760].

In viral infections, Ran has a role in regulating phagocytosis and immunity to the invading virus. Antiviral phagocytosis can be mediated by Ran in Schneider 2 cell lines with Ran being upregulated in Schneider 2 cells infected with a viral agent[715].

Ran has been identified as one of the genes related to nasopharyngeal carcinoma which is itself linked to EBV infection which I have already identified as linked to the disease of endometriosis (See section 4.4.3.5, 4.5.2.1). In microarray studies confirmed by PCR, Ran was found to be upregulated in more than 80% of nasopharyngeal carcinoma tissues[761]. Ran has also been identified as a candidate for Myc-mediated cancer progression. Myc binds to Ran's upstream sequence and activates the activity of Ran promoter. The over expression of Myc increases Ran expression and higher levels of these proteins are linked to increased metastatic potential and progression of breast and lung cancers[762]. A similar mechanism could be activated in endometriosis supporting metastasis and progression of disease. Potentially we could look at RAN as a therapeutic agent in endometriosis as well as cancers.

6.7.3.11 STUB1

E3 ubiquitin-protein ligase CHIP (STUB1) is a member of the carboxy terminus of hsp70-interacting protein and is a chaperone protein. It is released in response to cellular stress signals and has a role in the immune system and protein folding. It plays a role in the development of pathology such as Parkinson's disease (Figure 6-33).

FIGURE 6-33

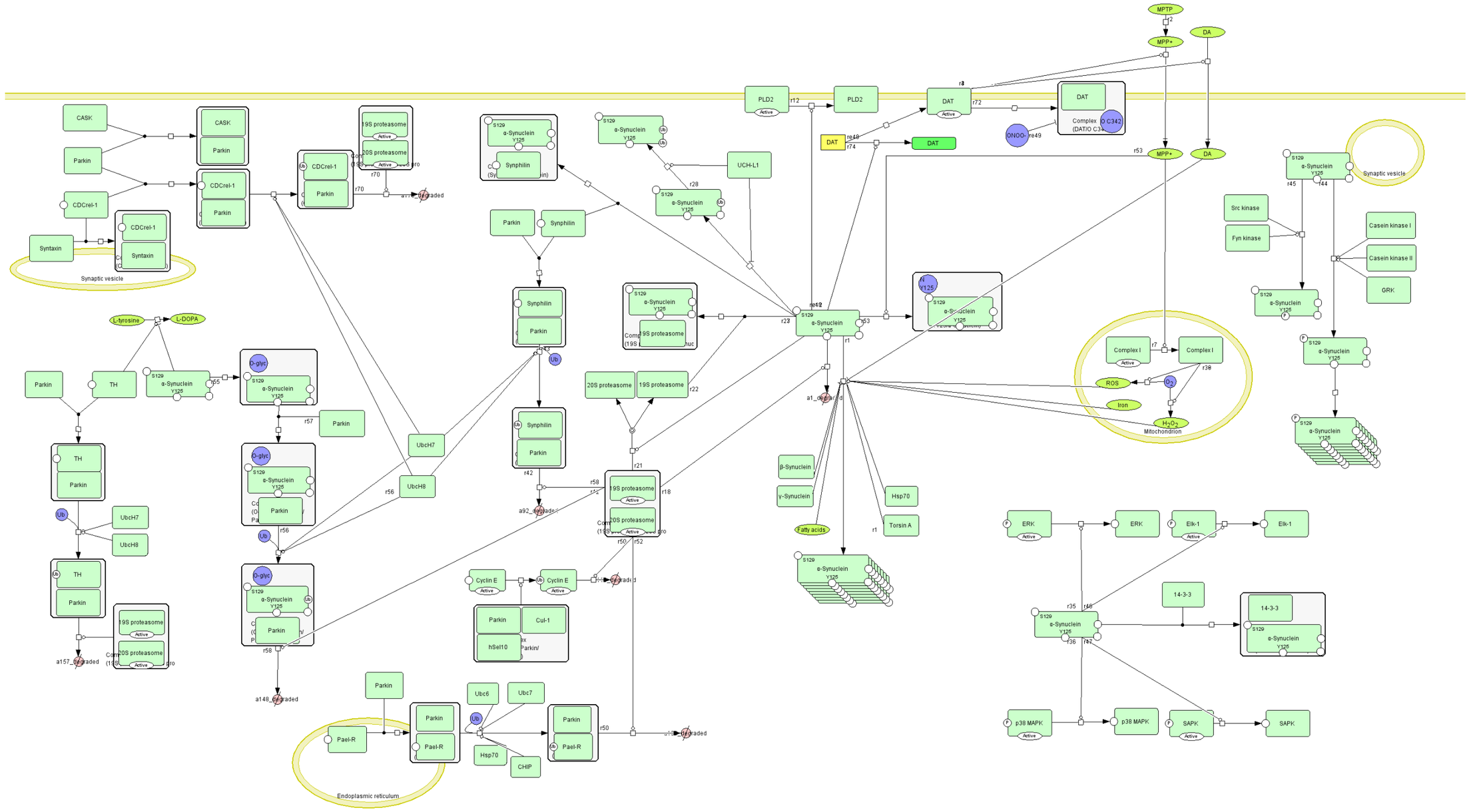

Pathway of involvement in Parkinson's disease[60]

STUB1 (also known as CHIP) has been shown to be essential in the activation of T-cells. This role results from the ubiquitination of Caspase recruitment domain (CARD) containing membrane-associated guanylate kinase (MAGUK) protein 1 (CARMA1) by STUB1 when it is expressed. This ubiquitination enables CARMA1-mediated NF-κB activation. This shows a link between STUB1 and T-cell receptor induced NF-κB signalling[716].

Cancer cells show deregulation of the Hsp70/90 chaperones and their HOP/CHIP co-chaperones. In cancer cells one can see an activation of Hsp 90 chaperone but decreased expression of CHIP. The decreased CHIP expression in proliferating tumour cells supports its tumour suppressor function[717]. In breast cancers CHIP is also seen to have a tumour suppressive role. 30% or breast cancers overexpress the erbB2 (also known as HER2 or neu) gene. This is associated with a poor patient prognosis. *In vitro* and tissue block studies have shown that CHIP downregulates ErbB2 and higher levels of CHIP increase the disease free interval and prolong survival rates in patients. From these studies, CHIP has been postulated as a prognostic marker for breast cancer[763].

CHIP is also seen to affect p53 function. The inactivation of CHIP by Hsp90 causes the aberrant stabilisation of mutant p53 in human cancers[718], increasing cellular ongogenesis. There are two studies that have attempted to link endometriosis with aberrant p53. Of note, in one study, there was an observed increased level of p53 expression in 82.4% of cancers associated with endometriosis and 100% increase of p53 expression in atypical endometriosis. Mutant p53 expression was seen in 11.8% of atypical endometriosis or those endometriosis cases which were associated with cancers. Potentially, this link to p53 expression could serve as an indicative prognostic factor of oncogenic potential in atypical endometriosis[354].

6.8 Potential pathways interacting and disrupted in endometriosis

6.8.1 Summary of data

From the analysis of the antibody profiles, Caspase 10, Apoptosis-Related Cysteine Peptidase (CASP10) (Figure 6-7), SH3-Domain GRB2-Like 1 (SH3GL1) (Figure 6-8) and aSEPT9 are good putative markers. They could potentially differentiate 13 of the 29 endometriosis samples from the control samples. The SH3GL1 gene encodes the Endophilin-A2 protein which is a cystolic protein implicated in cellular synaptic endocytosis. Mutations in the Endophilin A2 protein have been seen to prevent in vivo models of endocytosis[685]. Focal adhesion kinase (FAK) is associated with endophilin A2 interactions causing its tyrosine phosphorylation with the formation of a focal adhesion steroid receptor coactive complex (FAK/Src complex)[686]. In elevated levels, this complex causes attenuation of the endocytosis of the membrane type 1 metalloprotease complex (MT1-MMP)[686]. This in turn causes increase in levels of cellular degradation. Elevated levels of this complex have been associated with increased angiogenesis and tumour growth, all of which occur in endometriosis, identifying it as yet another possible therapeutic target in disease[687]. The overexpression of FAK is seen in a variety of cancers[721] and is associated with increased potential to invade and metastasise[722,723] (Figure 6-26).

The aSEPT9 has been linked to tumour migration and invasion as well as apoptosis and pseudopod formation[688]. It is expressed in a large number of human tumours including breast[690], epithelial ovarian[691] and endometrial[689] tumours. Metastatic lesions are seen to have higher SEPT9 levels[689] and its presence on cell borders and secretory epithelia indicate a role in membrane vesicle formation[689]. This gene may potentially play a role in development and dissemination of endometriotic cells enabling its growth and proliferation. BCAR is a scaffolding multiadaptor molecule, empirical in the role of intracellular signalling[689]. Its presence is associated with an increase in epithelial cellular hyperplasia in mammary tumorigenesis[694]. It forms molecular complexes with effector proteins such as P130C and is involved in the integrins signalling cellular system and plays a role in cellular motility, migration, proliferation and phagocytosis (Figure 6-28). Cytoplasmic FAK activates integrin mediated cell adhesion and has roles in angiogenesis and oncogenesis. It is elevated in severe endometriosis[727]. Increased FAK expression is seen in a number of cancers and promising therapeutics are targeted towards its inhibition.

Tumour necrosis factor receptor superfamily, member 1A (TNFRSF1A) is a key regulator of the immune system. TNF binds to the ligands of TNFRSF1A and is a key component activating the NF-κB pathway which controls cellular apoptosis. The TNF proteins also activate inflammatory and apoptotic responses. TNF-α is mainly produced by non-haematopoietic cells including activated lymphocytes, macrophages, NK cells and neutrophils whereas TNF-β is produced by lymphocytes. The levels of TNF in the peritoneal fluid of patients with endometriosis are elevated and correlate to the stage of disease[730]. TNF-α is also known to increase adherence of stromal uterine cells to *in vitro* mesothelium[695]. The TNF family is interestingly dysregulated in viral infections and is an essential component in the development of infectious disease[697]. Any system dysregulation could be mirrored in alterations of T-cell survival and function[733]. Diseases can be stimulated or repressed by co- stimulating or regulating TNF factors this makes the regulators of the TNFR therapeutic targets for controlling disease. Studies using anti TNF monoclonal antibodies[735] and recombinant human TNFRSF1A (r-hTBP1)[736] show a decrease in disease development in the animal models used. Tumour necrosis factor receptor superfamily, member 10a (TNFRSF10A) promotes the NF-κB pathway and is another apoptosis mediator.

Oestrogen receptor 1 (ESR1) is a transcription factor activated by oestrogen[702] (Figure 6-29). There are elevated levels of ER-α receptors in active red endometriotic lesions compared to black necrotic ones[703]. Increase in ER-α levels also activate other pathways such as insulin-like growth factor-1 (IGF-1) which send powerful mitogenic stimuli causing cellular proliferation and growth. In severe endometriosis, plasma levels of IGF-1 are elevated, this elevation is however not maintained in the endometrium itself[704]. The IGF-1 has also been associated with malignant development and metastatic potential and there is a reported increase in its levels in other female cancers such as cervical, ovarian and endometrial cancers[745].

Baculoviral inhibitor of apoptosis proteins (IAP) repeat-containing 2 (BIRC2) plays a major role in cellular control of apoptosis by creating positive or negative feedback signalling on the NF-κB pathway. Once the NF-κB is activated or altered, effects on cyto and chemokines occur, which in turn promote cellular survival, proliferation and inhibit apoptosis[707]. It promotes cellular growth and survival including the production of IL-6, B-cell activating factors, cell inhibition of apoptosis, I kappa B kinase (IKK), tumour necrosis factors, TNFR, TRAF TRADD, TNFR- associated death domains and multiple pathways

associated with increased cellular survival in malignant patterns[752] (Figure 6-30). A similar function in endometriosis might explain the intraperitoneal cell survival and its proliferation into disease.

The results of the quality control (QC) assays and the low CVs provided a high degree of confidence in the data obtained. There were clear indications of antibody reactivity in many of the samples. A set of putative biomarkers was identified. Further analysis of this data is warranted and the generation of additional data should be considered. The inclusion of data generated from additional samples would provide greater statistical power. Data from other sources could also be integrated into this dataset to increase the potential for discovering biomarkers.The identification of such autoantibodies and their cognate antigens may possibly form the basis of an exploration of the biology as well as serve as potential serum biomarkers. The Figure 5-10 and Figure 5-11 provide an overview of interactions between identified miRNAs, associated genes, proteins, antibodies and the pathways they affect.

6.9 Detailed analysis of potential identified serum gene markers

A total of 21 potential serum gene markers were identified for endometriosis (Table 6-10). In this section, each gene is explored together with its associated protein and genetic interactions. This enables the in-depth analysis of the genetic function and its contribution to disease pathogenesis.

TABLE 6-10

Gene Symbol	Frequency in controls (36)	Frequency in endometriosis (34)	Difference in frequency endometriosis minus controls	% in controls	% in endometriosis	% difference endometriosis minus controls
C19orf50	1	7	6	2.9412	19.4444	16.5033
CA1	1	6	5	2.9412	16.6667	13.7255
RUNX1T1	2	7	5	5.8824	19.4444	13.5621
PRKCZ	2	7	5	5.8824	19.4444	13.5621
PCBD1	2	5	3	5.8824	13.8889	8.0065
ALDOA	3	11	8	8.8235	30.5556	21.7320
CASP10	1	7	6	2.9412	19.4444	16.5033
PYCR1	1	7	6	2.9412	19.4444	16.5033
GGPS1	2	8	6	5.8824	22.2222	16.3399
MYCBP	2	8	6	5.8824	22.2222	16.3399
CASP6	2	8	6	5.8824	22.2222	16.3399
GMEB1	0	5	5	0.0000	13.8889	13.8889
TNFAIP8	0	5	5	0.0000	13.8889	13.8889
HSPE1	3	8	5	8.8235	22.2222	13.3987
EIF4EBP1	0	4	4	0.0000	11.1111	11.1111
MAPK14	0	4	4	0.0000	11.1111	11.1111
ABCF1	1	5	4	2.9412	13.8889	10.9477
IMPA1	1	5	4	2.9412	13.8889	10.9477
LDHB	1	5	4	2.9412	13.8889	10.9477
ATXN3	6	2	-4	17.6471	5.5556	-12.0915
TOM1	5	0	-5	14.7059	0.0000	-14.7059

The 21 potential gene markers were identified for endometriosis

6.9.1 C19orf50

FIGURE 6-34

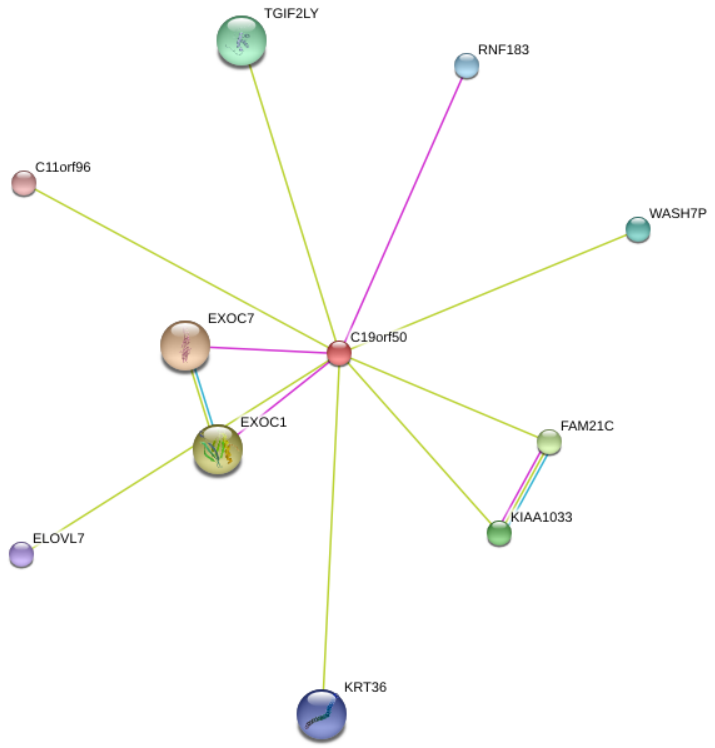

This is the **evidence view**. Different line colors represent the types of evidence for the association.

C19orf50 UPF0459 protein C19orf50 (176 aa) *(Homo sapiens)*

Predicted Functional Partners:

		Neighborhood	Gene Fusion	Cooccurrence	Coexpression	Experiments	Databases	Textmining	[Homology]	Score
EXOC7	exocyst complex component 7; Component of the exocyst complex involved in the docking of exocys [...] (735 aa)					•				0.524
EXOC1	exocyst complex component 1; Component of the exocyst complex involved in the docking of exocys [...] (894 aa)					•				0.524
FAM21C	family with sequence similarity 21, member C (1318 aa)							•		0.515
KIAA1033	KIAA1033 (1173 aa)							•		0.502
TGIF2LY	TGFB-induced factor homeobox 2-like, Y-linked; May have a transcription role in testis. May act [...] (185 aa)							•		0.462
WASH7P	WAS protein family homolog 5 pseudogene (409 aa)							•		0.462
RNF183	ring finger protein 183 (192 aa)					•				0.447
KRT36	keratin 36 (467 aa)							•		0.430
ELOVL7	ELOVL family member 7, elongation of long chain fatty acids (yeast); Could be implicated in syn [...] (281 aa)							•		0.427
C11orf96	Protein Ag2 homolog (435 aa)							•		0.425

Predicted evidence view of interactions of C10orf50[576]

Chromosome 19 open reading frame 50 (C19orf50) (Figure 6-34) is a length of DNA which has an initiation and stop codon. Unlike genes, which code for proteins of known function, an ORF is a genetic region which may or may not be transcribed/translated depending on the presence of promoters and ribosome binding sites. It usually has an unknown function. Projects attempting to map systematically new protein-protein links and networks[764], also known as 'interactome' mapping, try to link features of these networks to biological functions and attempt to provide an insight to disease at a systems level. Over 8000 ORFs have been tested, with pairwise interactions revealing 2800 binary interactions.

6.9.2 CA1- carbonic anhydrase

FIGURE 6-35

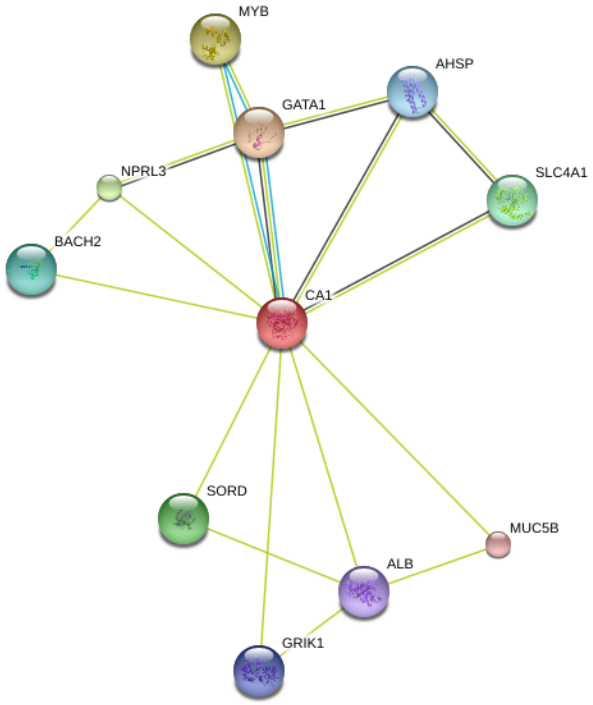

This is the **evidence view**. Different line colors represent the types of evidence for the association.

CA1 carbonic anhydrase I; Reversible hydration of carbon dioxide (261 aa) *(Homo sapiens)*

Predicted Functional Partners:

		Neighborhood	Gene Fusion	Cooccurrence	Coexpression	Experiments	Databases	Textmining	[Homology]	Score
GATA1	GATA binding protein 1 (globin transcription factor 1); Transcriptional activator which probabl [...] (413 aa)						●			0.917
MYB	v-myb myeloblastosis viral oncogene homolog (avian); Transcriptional activator; DNA-binding pro [...] (761 aa)						●			0.902
NPRL3	UPF0171 protein C16orf35 (Alpha-globin regulatory element-containing gene protein)(Protein CGTH [...] (568 aa)							●		0.623
SORD	sorbitol dehydrogenase (357 aa)							●		0.569
SLC4A1	solute carrier family 4, anion exchanger, member 1 (erythrocyte membrane protein band 3, Diego [...] (911 aa)				●					0.529
BACH2	BTB and CNC homology 1, basic leucine zipper transcription factor 2; Transcriptional regulator [...] (841 aa)							●		0.502
AHSP	alpha hemoglobin stabilizing protein; Act as a chaperone to prevent the harmful aggregation of [...] (102 aa)				●					0.500
GRIK1	glutamate receptor, ionotropic, kainate 1; Ionotropic glutamate receptor. L-glutamate acts as a [...] (918 aa)							●		0.469
ALB	albumin; Serum albumin, the main protein of plasma, has a good binding capacity for water, Ca(2 [...] (609 aa)							●		0.469
MUC5B	mucin 5B, oligomeric mucus/gel-forming; Gel-forming mucin that is thought to contribute to the [...] (5765 aa)							●		0.466

Predicted evidence view of interactions of CA1[576]

Carbonic anhydrase is a family of catalysts (enzymes) that maintain cellular pH by regulating the reversible hydration of carbonic acid to bicarbonate and protons (Figure 6-36). The subfamily of carbonic anhydrase present in mammals is the alpha family (α-CA). The α-CA family is divided into 4 groups comprising of cytosolic CA (CA1-3, CA7 and CA13), mitochondrial (CA-VA/VB), secreted CA (CA-6) and membrane associated CAs (CA4/9/12/14/15)[765]. Since their discovery in red blood cells around 80 years ago, their role has expanded from red blood cells catalysis of CO_2 hydration (CO_2+H20⇌HCO_3+H^+) to the involvement in cellular growth, implying links with cellular oncogenesis and malignancy.

FIGURE 6-36

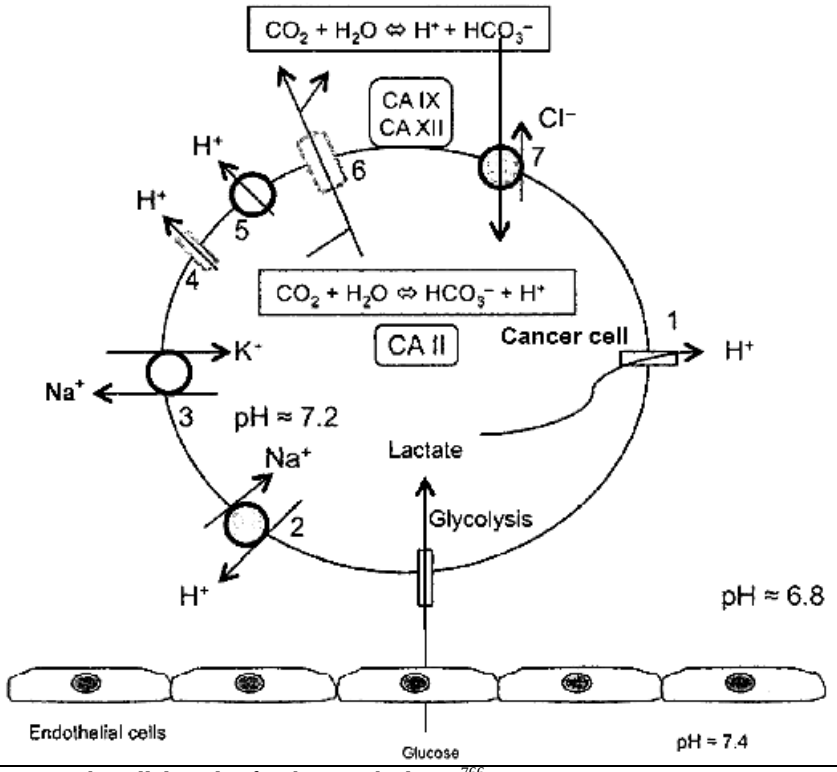

Figure demonstrating the cellular role of carbonic anhydrases[766]

CA2/9 and 12 have both been implicated in malignancy and have been utilised to potentially act as tumorigenic prognostic markers[767]. Their high prevalence in hypoxic tumour tissues, creating an acidic extracellular environment, has been implicated in the cellular invasion process[768].

Carbonic anhydrase 1 (Figure 6-35) codes for carbonic anhydrase, an enzyme with hydro-lase activity. It causes cleavage of an oxygen-carbon bond through water elimination. Metabolically, carbonic anhydrase is involved in anabolic and catabolic cellular processes and has a role in DNA replication and repair as well as protein synthesis and degradation[496].

Research has explored the roles of autoantigens in endometriosis. Candidate autoantigens include carbonic anhydrases[769-771], alpha enolase[772], endometrial transferrin and alpha 2-HS Glycoprotein[562].

In 1996, Brinton[769] described elevated levels of autoantibodies to carbonic anhydrase-2 in the serum of women with unexplained infertility undergoing laparoscopy[769]. CA1 is closely linked to CA2 and CA3 on chromosome 8. Other studies have described similar antibodies against carbonic anhydrase in women with infertility suffering from endometriosis[773]. Increased levels of anti-CA antibodies have been reported in other autoimmune and inflammatory diseases such as primary biliary cirrhosis or Sjogren's, further strengthening the link of its increased levels in autoimmune disorders.

Other members of the carbonic anhydrase family such as CA9 have been implicated in hypoxic tumour survival and proliferation in head and neck tumours. Elevated levels are associated with tumour aggressiveness and poor disease free survival rates[774]. In this study, the presence of CA9 and the uptake

of a proliferative marker (IdUrd) were linked to the identification of a cellular subpopulation which might be the cause of disease progression and cellular repopulation.

6.9.3 RUNX1T1

FIGURE 6-37

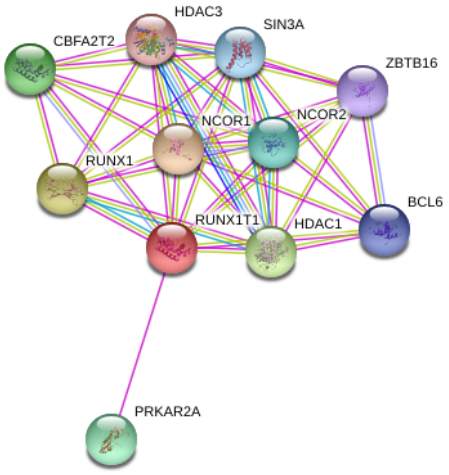

This is the **evidence view**. Different line colors represent the types of evidence for the association.

RUNX1T1 runt-related transcription factor 1; translocated to, 1 (cyclin D-related); Transcription regulator that excerts its function by binding to histone deacetylases and transcription factors. Can repress transactivation mediated by TCF12 (604 aa)
(Homo sapiens)

Predicted Functional Partners:

		Neighborhood	Gene Fusion	Cooccurrence	Coexpression	Experiments	Databases	Textmining	[Homology]	Score
NCOR1	nuclear receptor co-repressor 1; Mediates transcriptional repression by certain nuclear recepto [...] (2440 aa)					•		•		0.999
RUNX1	runt-related transcription factor 1; CBF binds to the core site, 5'-PYGPYGGT-3', of a number of [...] (480 aa)					•	•	•		0.988
HDAC1	histone deacetylase 1; Responsible for the deacetylation of lysine residues on the N-terminal p [...] (482 aa)					•				0.979
CBFA2T2	core-binding factor, runt domain, alpha subunit 2; translocated to, 2; May function as a comple [...] (604 aa)					•		•	•	0.964
PRKAR2A	protein kinase, cAMP-dependent, regulatory, type II, alpha; Type II regulatory chains mediate m [...] (404 aa)					•				0.959
NCOR2	nuclear receptor co-repressor 2; Mediates the transcriptional repression activity of some nucle [...] (2521 aa)					•		•		0.959
SIN3A	SIN3 homolog A, transcription regulator (yeast); Acts as a transcriptional repressor. Interacts [...] (1273 aa)					•				0.949
BCL6	B-cell CLL/lymphoma 6; Transcriptional repressor which is required for germinal center formatio [...] (706 aa)					•		•		0.928
ZBTB16	zinc finger and BTB domain containing 16; Probable transcription factor. May play a role in mye [...] (673 aa)					•		•		0.886
HDAC3	histone deacetylase 3; Responsible for the deacetylation of lysine residues on the N-terminal p [...] (428 aa)					•		•		0.879

Predicted evidence view of interactions of RUNX1T1[576]

Runt-related transcription factor 1 translocated to 1 (cyclin D-related) (RUNX1T1) codes for the protein CBFA2T1 (Figure 6-37). This protein is a zinc-finger transcription factor and an oncoprotein[775] (Figure 6-40). The translocation (8;21)(q22;q22) is seen in 12-15% of AML patients making it one of the most frequent translocations (Figure 6-38, Figure 6-39). The gene RUNX1 on chromosome 21 is rearranged with the RUNX1T1 on chromosome 8 leading to the expression of a fusion gene RUNX1-RUNX1t1 (AML1-ETO) enabling haematopoietic cell renewal whilst inhibiting differentiation[775]. The resulting chimeric gene composed of the 5'region of RUNX1 with the 3'region of the translocation t(8;21)(q22;q22) creates a protein which is believed to link to the nuclear co-repressor/histone deacetylase complex blocking haematopoietic differentiation[776] and repressing transactivation mediated by TCF12.

This myeloid translocation gene on 8q22 codes for a member of the myeloid translocation gene family, interacting with DNA-bound transcription factors which recruit co-repressors and enable transcriptional repression of target genes[578]. The RUNX1t1 is implicated in lymphocyte signalling pathways.

RUNX1T1 has transcription factor and transcription co-factor activity. It modulates the transcription frequency from an RNA polymerase 2 promoter and it has a role in the eukaryotic chromatin structure. In ovarian cancer, the expression of RUNX1T1 is seen to suppress *in vitro* tumour growth[777]. These experiments suggest a tumour suppressor role of RUNX1T1 in ovarian cancer. Aberrations in the TGFbeta/SMAD4 signalling pathways cause silencing of the tumour suppressor RUNX1T1 causing ovarian cancer. Interestingly RUNX1T1 is also responsive to estradiol levels[778]. In the follicular phase of endometriosis, its elevation in levels might act as a tumour suppressor role similar to what occurs in epithelial ovarian cancer.

FIGURE 6-38

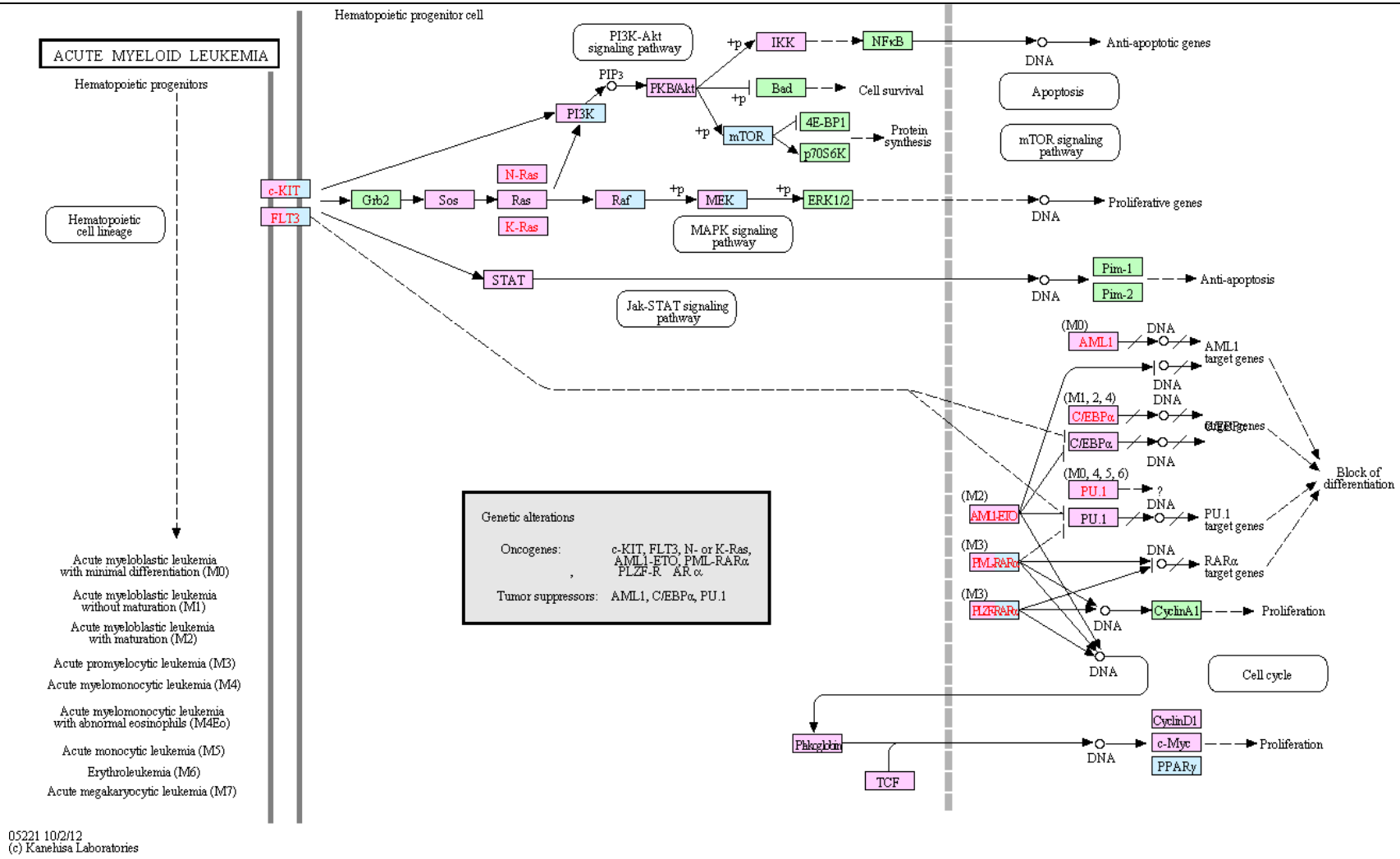

Kegg pathway analysis- acute myeloid leukaemia[526]

FIGURE 6-39

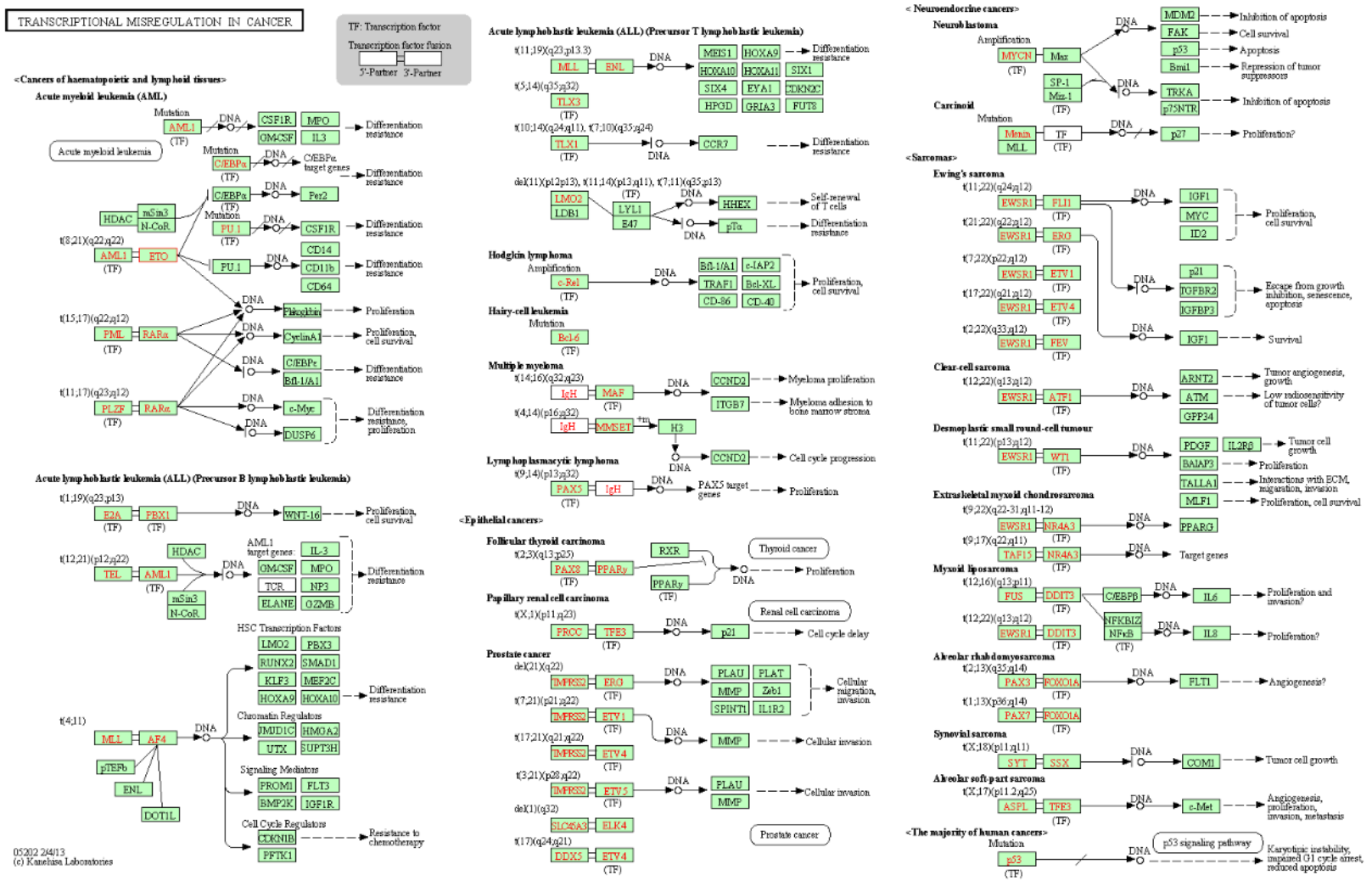

Kegg pathway analysis- transcriptional misregulation in cancer[526]

FIGURE 6-40

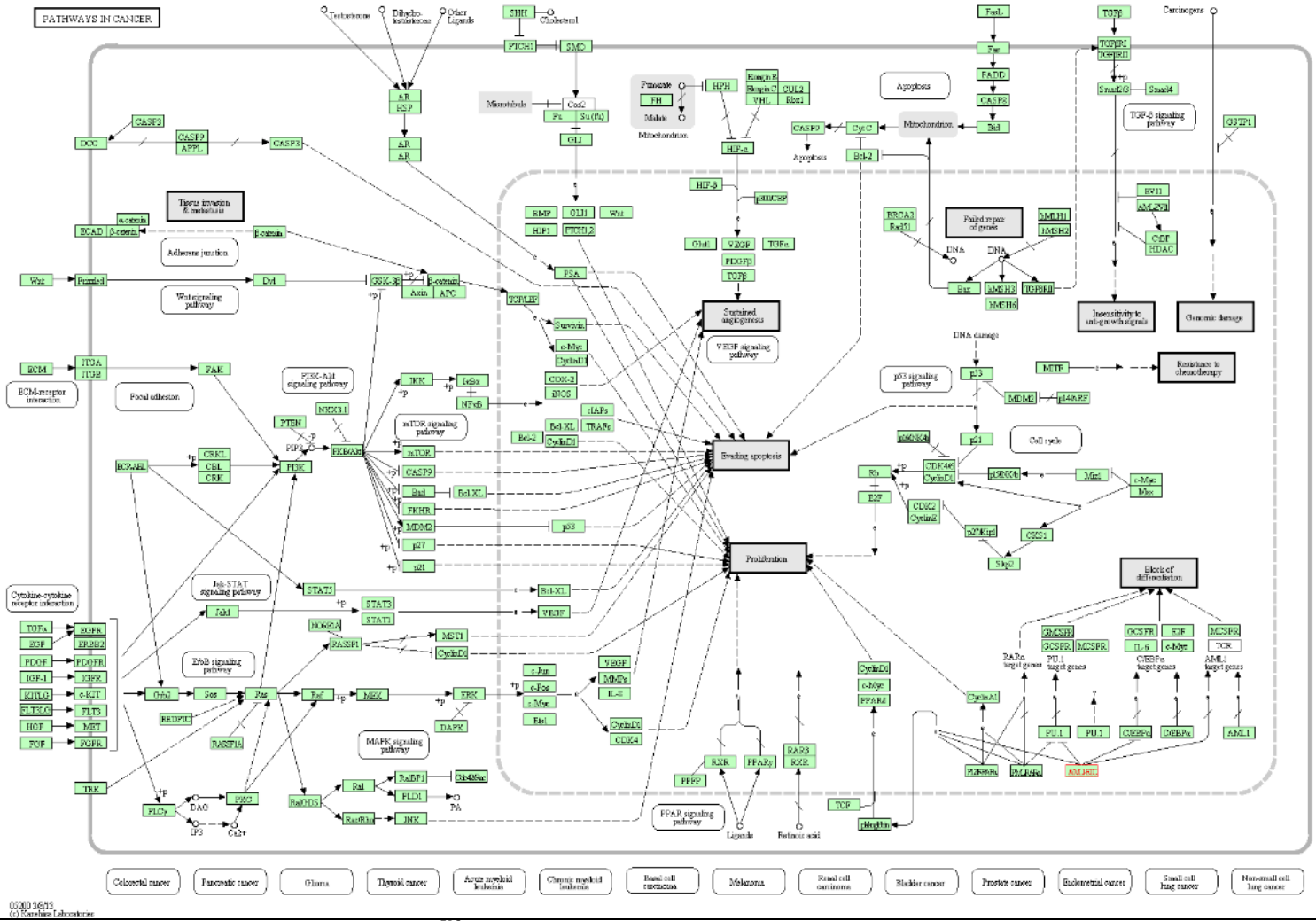

Kegg pathway analysis showing various pathways implicated in cancer[526]

6.9.4 PRKCZ

FIGURE 6-41

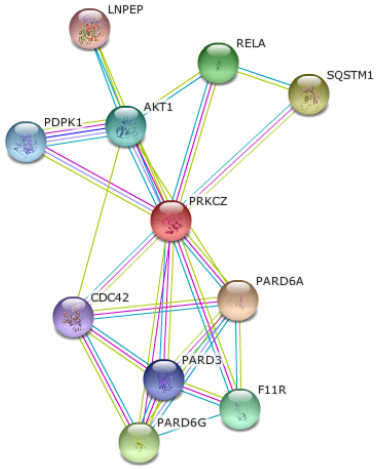

This is the **evidence view**. Different line colors represent the types of evidence for the association.

		Neighborhood	Gene Fusion	Cooccurrence	Coexpression	Experiments	Databases	Textmining	[Homology]	Score
PRKCZ	protein kinase C, zeta; This is a calcium-independent, phospholipid-dependent, serine- and threonine-specific enzyme (592 aa) *(Homo sapiens)*									
Predicted Functional Partners:										
PARD6A	par-6 partitioning defective 6 homolog alpha (C. elegans); Adapter protein involved in asymmetr [...] (346 aa)					●	●	●		0.999
SQSTM1	sequestosome 1; Adapter protein which binds ubiquitin and may regulate the activation of NFKB1 [...] (440 aa)					●	●	●		0.997
PARD6G	par-6 partitioning defective 6 homolog gamma (C. elegans); Adapter protein involved in asymmetr [...] (376 aa)					●		●		0.996
RELA	v-rel reticuloendotheliosis viral oncogene homolog A (avian); NF-kappa-B is a pleiotropic trans [...] (551 aa)					●	●	●		0.994
F11R	F11 receptor; Seems to plays a role in epithelial tight junction formation. Appears early in pr [...] (299 aa)					●	●	●		0.993
AKT1	v-akt murine thymoma viral oncogene homolog 1; General protein kinase capable of phosphorylatin [...] (480 aa)					●	●	●	●	0.993
PDPK1	3-phosphoinositide dependent protein kinase-1; Phosphorylates and activates not only PKB/AKT, b [...] (556 aa)					●		●	●	0.990
PARD3	par-3 partitioning defective 3 homolog (C. elegans); Adapter protein involved in asymmetrical c [...] (1356 aa)					●	●	●		0.985
CDC42	cell division cycle 42 (GTP binding protein, 25kDa); Plasma membrane-associated small GTPase wh [...] (191 aa)					●	●	●		0.981
LNPEP	leucyl/cystinyl aminopeptidase; Release of an N-terminal amino acid, cleaves before cysteine, l [...] (1025 aa)						●	●		0.980

Predicted evidence view of interactions of PRKCZ[576]

Protein kinase C Zeta (PRKCZ) (Figure 6-41) is a kinase belonging to the family of seine/threonine kinases involved in cellular proliferation, differentiation and secretion. This has a kinase activity which unlike other family members is not Calcium dependent in its function. It does not respond to the typical PKC inhibitors and similarly does not respond to the usual activation of this family by phorbol esters[578]. It is involved in various pathways including the activation of NF-kappa beta activation, maintenance of cellular potentiation and mitogenic signalling, cellular proliferation and polarity and the inflammatory response. It also has a function phosphatidylinositol 3-kinase (PI3K) pathway and mitogen-activated protein (MAP) kinase cascade[779,780]. The protein kinase C, zeta (PRKCZ) will activate the MAPK signalling pathway independently of the RAF- 1 activation signals. Its physiological roles are extensive. Multiple target proteins control receptor alterations, alterations of events within membranes and regulation of cellular growth, differentiation, angiogenesis and immune responses (Figure 6-42). Alterations in the PI3K pathway including the PRKCZ component of the pathway, have been linked to tumours[781]. In theory, aberrations in any segment of the complex pathways can impart cellular changes, promoting invasiveness, growth and dissemination. These same cellular characteristics might be attributed to the development of a disease like endometriosis.

FIGURE 6-42

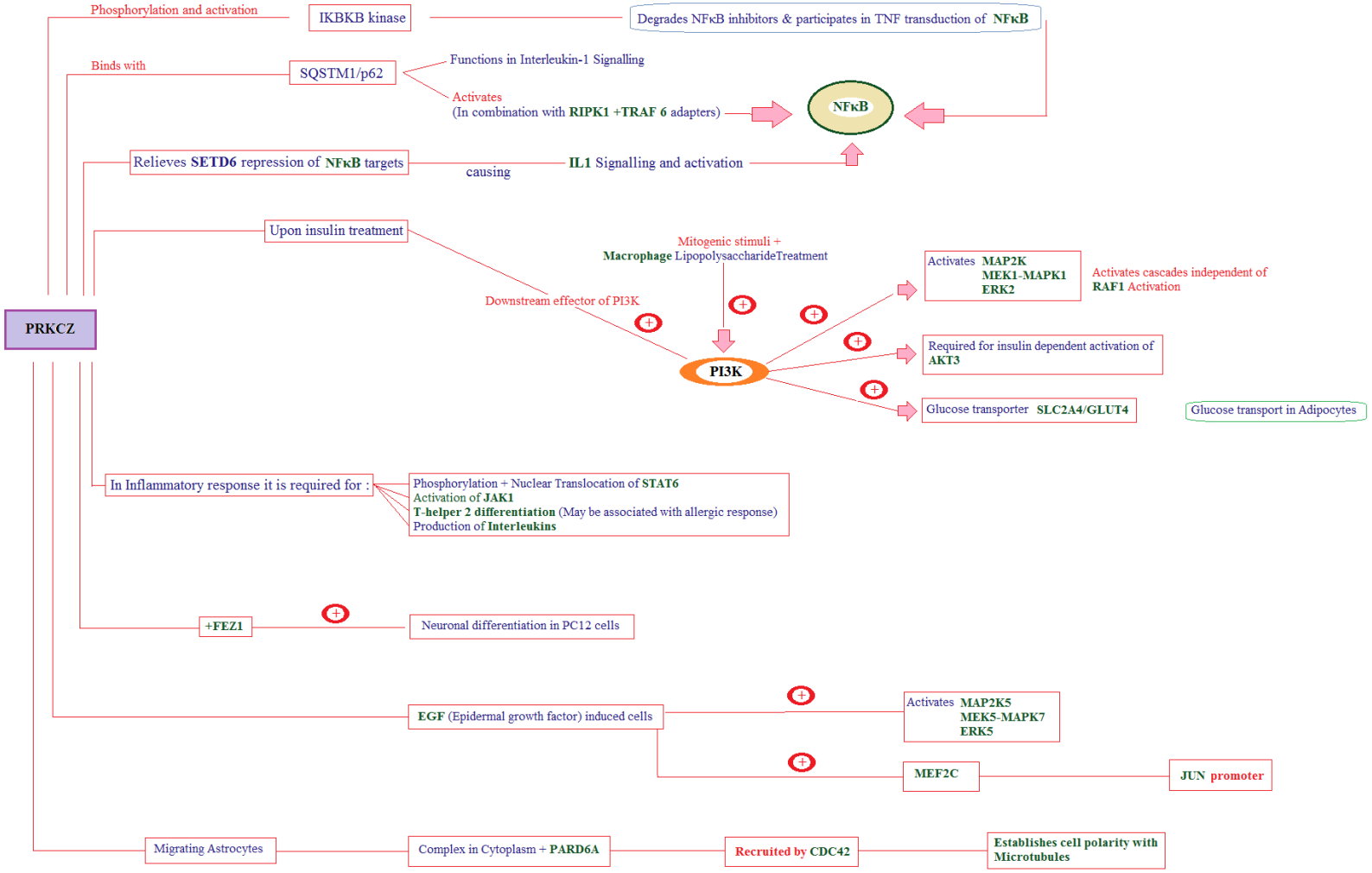

Figure demonstrating the effects of PRKCZ on various cellular functions and pathways

6.9.5 PCBD1

FIGURE 6-43

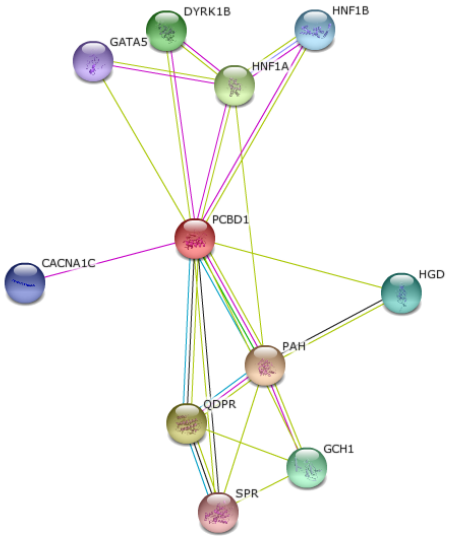

This is the **evidence view**. Different line colors represent the types of evidence for the association.

PCBD1 pterin-4 alpha-carbinolamine dehydratase/dimerization cofactor of hepatocyte nuclear factor 1 alpha; Involved in tetrahydrobiopterin biosynthesis. Seems to both prevent the formation of 7-pterins and accelerate the formation of quinonoid-BH2. Regulates the dimerization of homeodomain protein HNF-1-alpha and enhances its transcriptional activity (104 aa) *(Homo sapiens)*

Predicted Functional Partners:

		Neighborhood	Gene Fusion	Cooccurrence	Coexpression	Experiments	Databases	Textmining	[Homology]	Score
PAH	phenylalanine hydroxylase (452 aa)									0.988
QDPR	quinoid dihydropteridine reductase; The product of this enzyme, tetrahydrobiopterin (BH-4), is [...] (244 aa)									0.972
HNF1A	HNF1 homeobox A; Required for the expression of several liver specific genes. Binds to the inve [...] (631 aa)									0.966
DYRK1B	dual-specificity tyrosine-(Y)-phosphorylation regulated kinase 1B; Dual-specificity kinase whic [...] (629 aa)									0.868
GCH1	GTP cyclohydrolase 1; Positively regulates nitric oxide synthesis in umbilical vein endothelial [...] (250 aa)									0.722
HGD	homogentisate 1,2-dioxygenase (homogentisate oxidase) (445 aa)									0.675
HNF1B	HNF1 homeobox B; Transcription factor, probably binds to the inverted palindrome 5'-GTTAATNATTA [...] (557 aa)									0.641
CACNA1C	calcium channel, voltage-dependent, L type, alpha 1C subunit; Voltage-sensitive calcium channel [...] (2186 aa)									0.621
GATA5	GATA binding protein 5; Binds to the functionally important CEF-1 nuclear protein binding site [...] (397 aa)									0.621
SPR	sepiapterin reductase (7,8-dihydrobiopterin-NADP+ oxidoreductase); Catalyzes the final one or t [...] (261 aa)									0.593

Predicted evidence view of interactions of PCBD1[576]

Pterin-4 alpha-carbinolamine dehydratase/dimerization cofactor of hepatocyte nuclear factor 1 alpha (PCBD1) (Figure 6-43) is localised on the 10q22 chromosome. The gene encodes the pterin-4 alpha-carbinolamine dehydratase enzyme which is involved in phenylalanine hydroxylation. Its deficiency causes hyperphenylalaninemia. The enzyme is also responsible for the homodimerization of the transcription factor hepatocyte nuclear factor 1 (HNF1)[578]. It is reported in various cellular compartments ranging from the nucleolus, nucleus, cytoplasm and cytosol. It has functions in cellular metabolism and is also mentioned to contribute to the DNA dependant regulator of transcription. Antibody staining of various malignant tissues has shown moderate staining to the antibody pertaining to the gene in around 30% of cancers including endometrial and ovarian cancers[634].

6.9.6 ALDOA

FIGURE 6-44

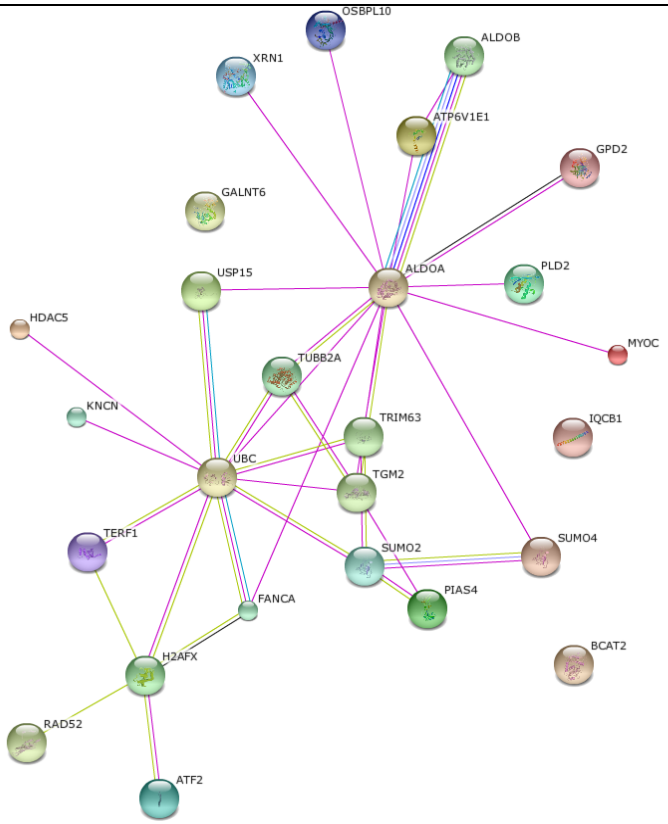

MYOC	myocilin, trabecular meshwork inducible glucocorticoid response; May participate in the obstruction of fluid outflow in the trabecular meshwork (504 aa)
HDAC5	histone deacetylase 5; Responsible for the deacetylation of lysine residues on the N-terminal part of the core histones (H2A, H2B, H3 and H4). Histone deacetylation gives a tag for epigenetic repression and plays an important role in transcriptional regulation, cell cycle progression and developmental events. Histone deacetylases act via the formation of large multiprotein complexes. Involved in muscle maturation by repressing transcription of myocyte enhancer MEF2C. During muscle differentiation, it shuttles into the cytoplasm, allowing the expression of myocyte enhancer factors (1123 aa)
ATP6V1E1	ATPase, H+ transporting, lysosomal 31kDa, V1 subunit E1; Subunit of the peripheral V1 complex of vacuolar ATPase essential for assembly or catalytic function. V-ATPase is responsible for acidifying a variety of intracellular compartments in eukaryotic cells (226 aa)
USP15	ubiquitin specific peptidase 15 (952 aa)
PIAS4	protein inhibitor of activated STAT, 4; Functions as an E3-type small ubiquitin-like modifier (SUMO) ligase, stabilizing the interaction between UBE2I and the substrate, and as a SUMO-tethering factor. Plays a crucial role as a transcriptional coregulation in various cellular pathways, including the STAT pathway, the p53 pathway, the Wnt pathway and the steroid hormone signaling pathway. Involved in gene silencing. Promotes PARK7 sumoylation. In Wnt signaling, represses LEF1 and enhances TCF4 transcriptional activities through promoting their sumoylations (510 aa)
PLD2	phospholipase D2; May have a role in signal-induced cytoskeletal regulation and/or endocytosis (By similarity) (933 aa)
ATF2	activating transcription factor 2; Transcriptional activator, probably constitutive, which binds to the cAMP-responsive element (CRE) (consensus- 5'- GTGACGT[AC][AG]-3'), a sequence present in many viral and cellular promoters. Interaction with JUN redirects JUN to bind to CRES preferentially over the 12-O-tetradecanoylphorbol-13-acetate response elements (TRES) as part of an ATF2-c-Jun complex (505 aa)
XRN1	5'-3' exoribonuclease 1; Major 5'-3' exoribonuclease involved in mRNA decay. Required for the 5'-3'processing of the G4 tetraplex-containing DNA and RNA substrates. The kinetic of hydrolysis is faster for G4 RNA tetraplex than for G4 DNA tetraplex and monomeric RNA tetraplex. Binds to RNA and DNA (By similarity). Plays a role in replication-dependent histone mRNA degradation. May act as a tumor suppressor protein in osteogenic sarcoma (OGS) (1706 aa)
OSBPL10	oxysterol binding protein-like 10 (764 aa)
TERF1	telomeric repeat binding factor (NIMA-interacting) 1; Binds the telomeric double-stranded TTAGGG repeat and negatively regulates telomere length. Involved in the regulation of the mitotic spindle. Component of the shelterin complex (telosome) that is involved in the regulation of telomere length and protection. Shelterin associates with arrays of double- stranded TTAGGG repeats added by telomerase and protects chromosome ends; without its protective activity, telomeres are no longer hidden from the DNA damage surveillance and chromosome ends are inappropriately processed by DNA repair [...] (439 aa)
GPD2	glycerol-3-phosphate dehydrogenase 2 (mitochondrial) (727 aa)
IQCB1	IQ motif containing B1 (598 aa)
SUMO4	SMT3 suppressor of mif two 3 homolog 4 (S. cerevisiae); Ubiquitin-like protein which can be covalently attached to target lysines as a monomer. Does not seem to be involved in protein degradation and may modulate protein subcellular localization, stability or activity. Upon oxidative stress, conjugates to various anti-oxidant enzymes, chaperones, and stress defense proteins. May also conjugate to NFKBIA, TFAP2A and FOS, negatively regulating their transcriptional activity, and to NR3C1, positively regulating its transcriptional activity. Covalent attachment to its substrates requires p [...] (95 aa)
BCAT2	branched chain aminotransferase 2, mitochondrial; Catalyzes the first reaction in the catabolism of the essential branched chain amino acids leucine, isoleucine, and valine. May also function as a transporter of branched chain alpha-keto acids (392 aa)
ALDOA	aldolase A, fructose-bisphosphate (364 aa)
UBC	ubiquitin C (685 aa)

Predicted evidence view of interactions of ALDOA[576]

Aldolase A, Fructose-Bisphosphate (ALDOA) gene (Figure 6-44) is located on chromosome 16 and codes for protein Aldolase A. Aldolase A (fructose-biphosphate aldolase) is an enzyme that catalyses the conversion of fructose-1,6-biphosphate into glyceraldehyde 3-phospate and dihydroxyacetone phosphate in a reversible manner (Figure 6-45). It may also play a role as a scaffolding protein. Aldolase A is found in embryogenesis and in adult muscle tissue and its deficiency is linked to myopathy with rhabdoyosis and haemolytic anaemia. Aldolase A is seen in elevated levels in lung cancer[782]. It has also been implicated in the development of malignant pleural cell effusions which demonstrate aberrant glucose metabolism gene expression[783]. The aberrant expression of ALDOA in tumour cells leads to changes in glucose metabolism which is associated with cellular metastatic potential and poorer prognosis in malignancies. It is repressed in the liver, kidney, intestine, brain and other nerve tissues. Elevated levels identified in my study with endometriotic patients might explain changes in endometriotic cells including their potential to metastasise and grow.

FIGURE 6-45

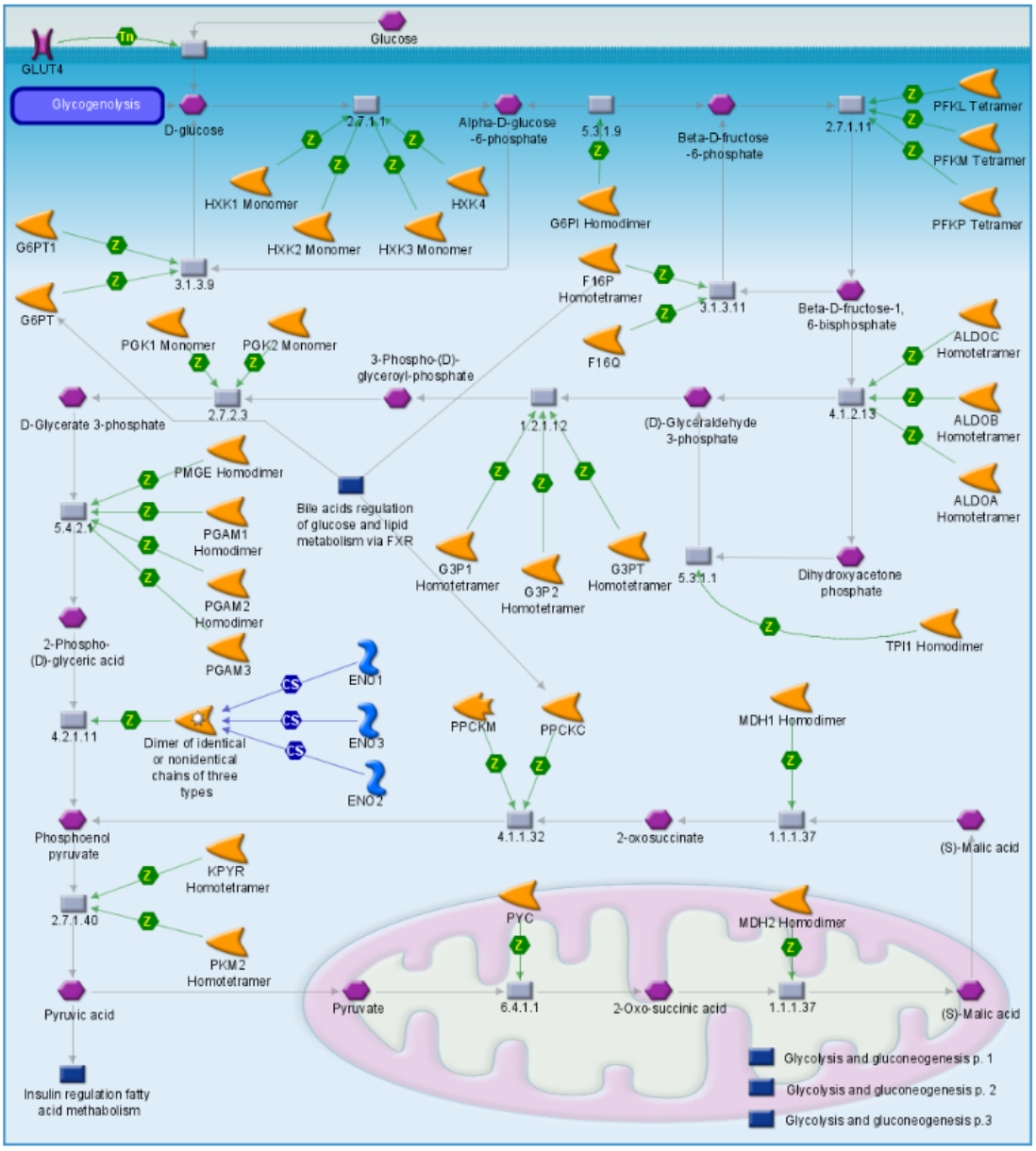

Pathway analysis of glycogenolysis[784]

6.9.7 CASP10

FIGURE 6-46

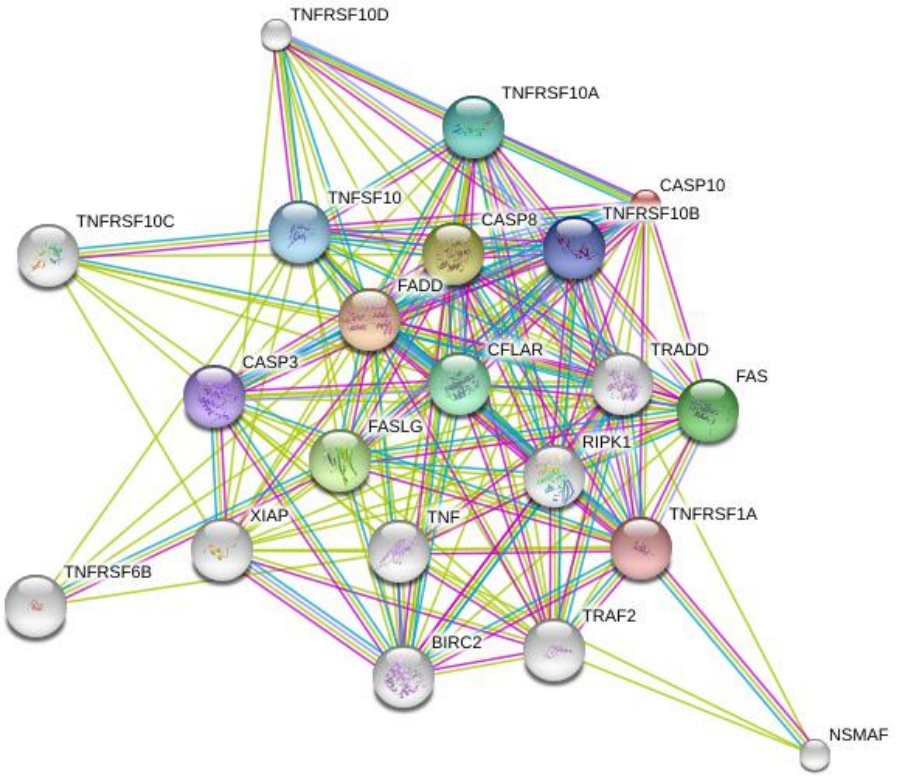

This is the **evidence view**. Different line colors represent the types of evidence for the association.

CASP10 caspase 10, apoptosis-related cysteine peptidase; Involved in the activation cascade of caspases responsible for apoptosis execution. Recruited to both Fas- and TNFR-1 receptors in a FADD dependent manner. May participate in the granzyme B apoptotic pathways. Cleaves and activates caspase- 3, -4, -6, -7, -8, and -9. Hydrolyzes the small- molecule substrates, Tyr-Val-Ala-Asp-|-AMC and Asp-Glu-Val-Asp-|-AMC (522 aa)
(Homo sapiens)

Predicted Functional Partners:

		Neighborhood	Gene Fusion	Cooccurrence	Coexpression	Experiments	Databases	Textmining	[Homology]	Score
FADD	Fas (TNFRSF6)-associated via death domain; Apoptotic adaptor molecule that recruits caspase-8 o [...] (208 aa)					●	●	●		0.999
CASP8	caspase 8, apoptosis-related cysteine peptidase; Most upstream protease of the activation casca [...] (538 aa)					●	●	●	●	0.999
FASLG	Fas ligand (TNF superfamily, member 6); Cytokine that binds to TNFRSF6/FAS, a receptor that tra [...] (281 aa)					●	●	●		0.999
FAS	Fas (TNF receptor superfamily, member 6); Receptor for TNFSF6/FASLG. The adapter molecule FADD [...] (335 aa)					●		●		0.998
CFLAR	CASP8 and FADD-like apoptosis regulator; Apoptosis regulator protein which may function as a cr [...] (480 aa)					●	●	●	●	0.998
TNFRSF10A	tumor necrosis factor receptor superfamily, member 10a; Receptor for the cytotoxic ligand TNFSF [...] (468 aa)					●	●	●		0.992
TNFSF10	tumor necrosis factor (ligand) superfamily, member 10; Cytokine that binds to TNFRSF10A/TRAILR1 [...] (281 aa)					●	●	●		0.988
TNFRSF10B	tumor necrosis factor receptor superfamily, member 10b; Receptor for the cytotoxic ligand TNFSF [...] (440 aa)					●	●	●		0.987
CASP3	caspase 3, apoptosis-related cysteine peptidase; Involved in the activation cascade of caspases [...] (277 aa)					●	●	●	●	0.984
TNFRSF1A	tumor necrosis factor receptor superfamily, member 1A; Receptor for TNFSF2/TNF-alpha and homotr [...] (455 aa)					●		●		0.968

Predicted evidence view of interactions of CASP10[576]

Mutations in the CASP 10 gene (Figure 6-46) cause defects in the apoptosis pathways. Caspase-10 acts as a homologue to the cystene protease Caspase-8 which executes the apoptotic pathway (Figure 6-47).

FIGURE 6-47

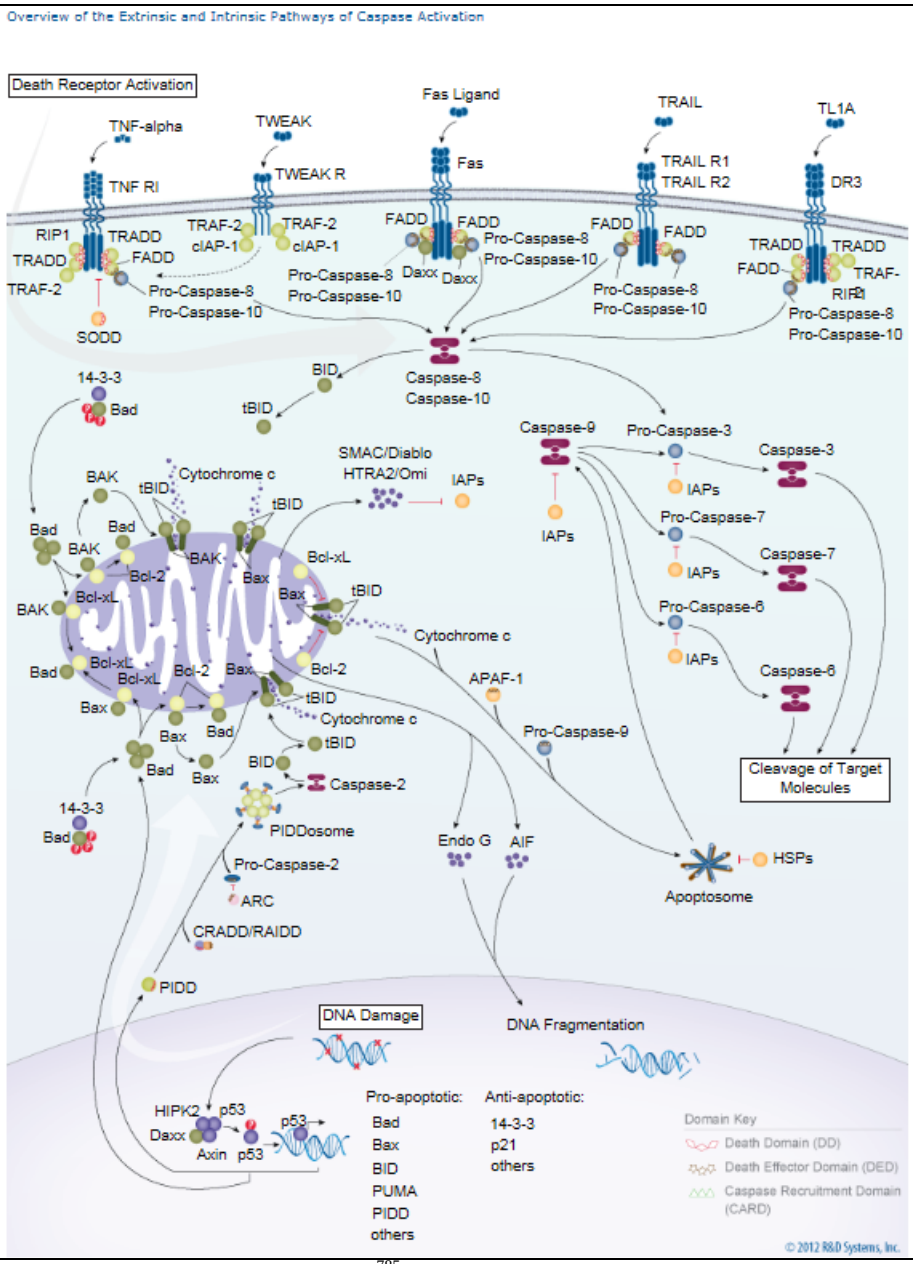

Pathway demonstrating death receptor activation[785]

The CASP10 gene codes for the Caspase 10 enzyme[786]. Its activation causes the transformation and proteolysis of the inactive proenzyme into two subunits dimerising into the active form. The Caspase 10 protein activates Caspases 3 and 7 and is processed by Caspase 8. Biologically, it is involved in the caspase pathway responsible for the execution of apoptosis and the FAS signalling pathway[787]. It is recruited to the TNFR-1 receptors and Fas receptors in a Fas-Associated protein Death effector Domain (FADD) in apoptosis[788] (encoded for by the CFLAR gene[789]). It is linked to the RING1 and YY1-binding protein (RYBP)[790], Tumour necrosis factor receptors 1A and 10B (TNFRSF1A and TNFRSF10B)[787].

There are various isoforms of caspase-10 which perform a different pro or anti-apoptosis function enabling fine regulation of the apoptotic cycle initiation[791]. It has been described as an initiator caspase in death receptor signalling and functions independently of Caspase-8 causing apoptosis mediated by the FAS and Tumour necrosis factor systems[788]. Both Caspase-10 and Caspase-8 interact with the Fas-

Associated protein Death effector Domain (FADD) which serves to bridge the FAS receptor and form the death-inducing signalling complex (DISC) in apoptosis[792] (Figure 6-48). Caspase levels are increased in a p53 dependant manner in the presence of DNA damage. Studies showing in vivo binding of p53 to multiple p53-specific binding sites located within the gene locus of Caspase 10[793] suggest that Caspase 10 is a direct transcription target of p53. Endometriosis has shown increased levels of p53 in my TMA studies. p53, a tumour suppressor, has been shown to be elevated in a proportion of endometriotic lesions with no obvious genetic aberrations[792].

FIGURE 6-48

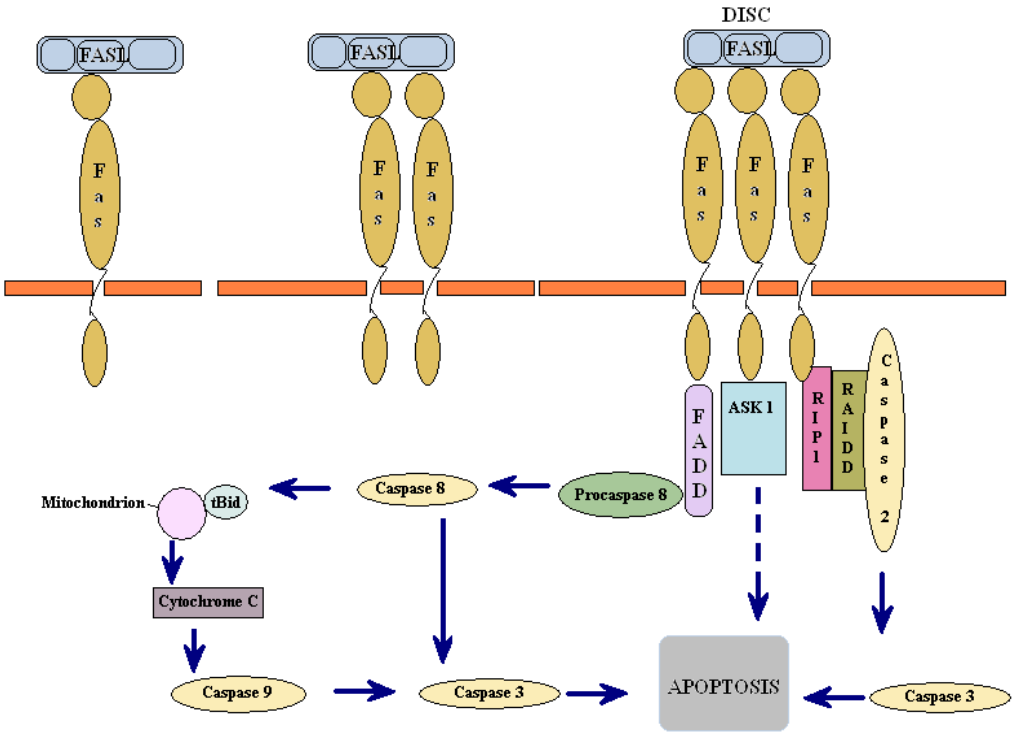

Demonstrating the activation of the apoptotic pathway

6.9.8 PYCR1

FIGURE 6-49

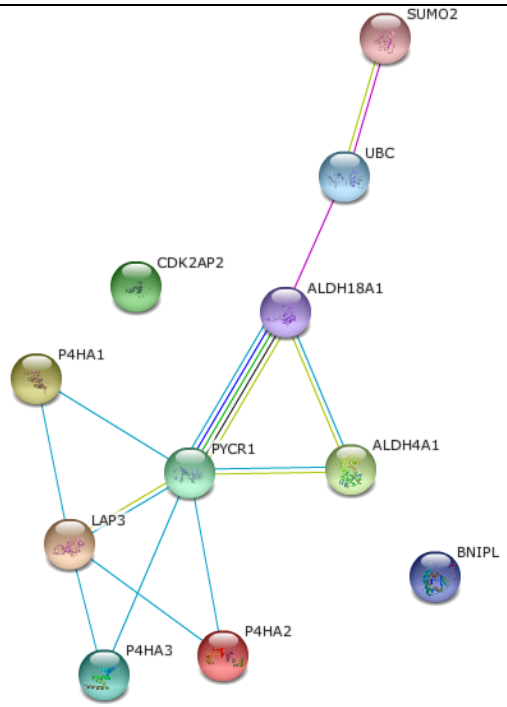

This is the **evidence view**. Different line colors represent the types of evidence for the association.

P4HA2	prolyl 4-hydroxylase, alpha polypeptide II; Catalyzes the post-translational formation of 4- hydroxyproline in -Xaa-Pro-Gly- sequences in collagens and other proteins (535 aa)
LAP3	leucine aminopeptidase 3; Presumably involved in the processing and regular turnover of intracellular proteins. Catalyzes the removal of unsubstituted N-terminal amino acids from various peptides (519 aa)
P4HA1	prolyl 4-hydroxylase, alpha polypeptide I; Catalyzes the post-translational formation of 4- hydroxyproline in -Xaa-Pro-Gly- sequences in collagens and other proteins (534 aa)
ALDH4A1	aldehyde dehydrogenase 4 family, member A1; Irreversible conversion of delta-1-pyrroline-5- carboxylate (P5C), derived either from proline or ornithine, to glutamate. This is a necessary step in the pathway interconnecting the urea and tricarboxylic acid cycles. The preferred substrate is glutamic gamma-semialdehyde, other substrates include succinic, glutaric and adipic semialdehydes (563 aa)
CDK2AP2	cyclin-dependent kinase 2 associated protein 2 (126 aa)
PYCR1	pyrroline-5-carboxylate reductase 1; Involved in the cellular response to oxidative stress (319 aa)
P4HA3	prolyl 4-hydroxylase, alpha polypeptide III; Catalyzes the post-translational formation of 4- hydroxyproline in -Xaa-Pro-Gly- sequences in collagens and other proteins (544 aa)
UBC	ubiquitin C (685 aa)
BNIPL	BCL2/adenovirus E1B 19kD interacting protein like; May be a bridge molecule between BCL2 and ARHGAP1/CDC42 in promoting cell death (357 aa)
ALDH18A1	aldehyde dehydrogenase 18 family, member A1 (795 aa)
SUMO2	SMT3 suppressor of mif two 3 homolog 2 (S. cerevisiae); Ubiquitin-like protein which can be covalently attached to target lysines either as a monomer or as a lysine-linked polymer. Does not seem to be involved in protein degradation and may function as an antagonist of ubiquitin in the degradation process. Plays a role in a number of cellular processes such as nuclear transport, DNA replication and repair, mitosis and signal transduction. Covalent attachment to its substrates requires prior activation by the E1 complex SAE1-SAE2 and linkage to the E2 enzyme UBE2I, and can be promoted b [...] (95 aa) *(Homo sapiens)*

Predicted evidence view of interactions of PYCR1[576]

PYCR1 gene (Figure 6-49) is on chromosome location 17q25.3 and codes for the protein Pyrroline-5-carboxylate reductase 1, mitochondrial. This enzyme converts pyrroline-5-carboxylate to prolene in an NAD(P)H dependant manner[578]. In certain cells it is also responsible for the production of NADP(+). The

protein forms a homopolymer and localises to the mitochondrion. Its defect would cause an autosomal recessive type 2B connective tissue disorder known as cutis laxa.

6.9.9 GGPS1

FIGURE 6-50

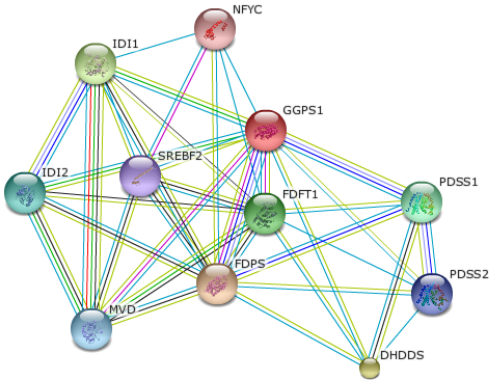

This is the **evidence view**. Different line colors represent the types of evidence for the association.

Your Input:

		Neighborhood	Gene Fusion	Cooccurrence	Coexpression	Experiments	Databases	Textmining	[Homology]	Score
GGPS1	geranylgeranyl diphosphate synthase 1; Catalyzes the trans-addition of the three molecules of IPP onto DMAPP to form geranylgeranyl pyrophosphate, an important precursor of carotenoids and geranylated proteins (300 aa) *(Homo sapiens)*									
Predicted Functional Partners:										
FDPS	farnesyl diphosphate synthase (farnesyl pyrophosphate synthetase, dimethylallyltranstransferase [...] (419 aa)			•		•	•	•	•	0.973
DHDDS	dehydrodolichyl diphosphate synthase; Catalyzes cis-prenyl chain elongation to produce the poly [...] (334 aa)						•	•		0.972
IDI1	isopentenyl-diphosphate delta isomerase 1; Catalyzes the 1,3-allylic rearrangement of the homoa [...] (284 aa)						•	•		0.948
FDFT1	farnesyl-diphosphate farnesyltransferase 1 (417 aa)						•	•		0.939
PDSS1	prenyl (decaprenyl) diphosphate synthase, subunit 1; Supplies decaprenyl diphosphate, the precu [...] (415 aa)			•			•	•	•	0.927
IDI2	isopentenyl-diphosphate delta isomerase 2; Catalyzes the 1,3-allylic rearrangement of the homoa [...] (227 aa)						•			0.924
MVD	mevalonate (diphospho) decarboxylase; Performs the first committed step in the biosynthesis of [...] (400 aa)						•	•		0.922
PDSS2	prenyl (decaprenyl) diphosphate synthase, subunit 2; Supplies decaprenyl diphosphate, the precu [...] (399 aa)						•			0.907
SREBF2	sterol regulatory element binding transcription factor 2; Transcriptional activator required fo [...] (1141 aa)						•			0.902
NFYC	nuclear transcription factor Y, gamma; Stimulates the transcription of various genes by recogni [...] (354 aa)						•			0.899

Predicted evidence view of interactions of GGPS1[576]

Geranylgeranyl Diphosphate Synthase 1 (GGPS1) (Figure 6-50) is a member of the prenyltransferase family which catalyses GGPP synthesis from farnesyl diphosphate and isopentenyl diphosphate. GGPP is a molecule which regulates a nuclear hormone receptor and is responsible for the C20-prenylation of proteins[578].

FIGURE 6-51

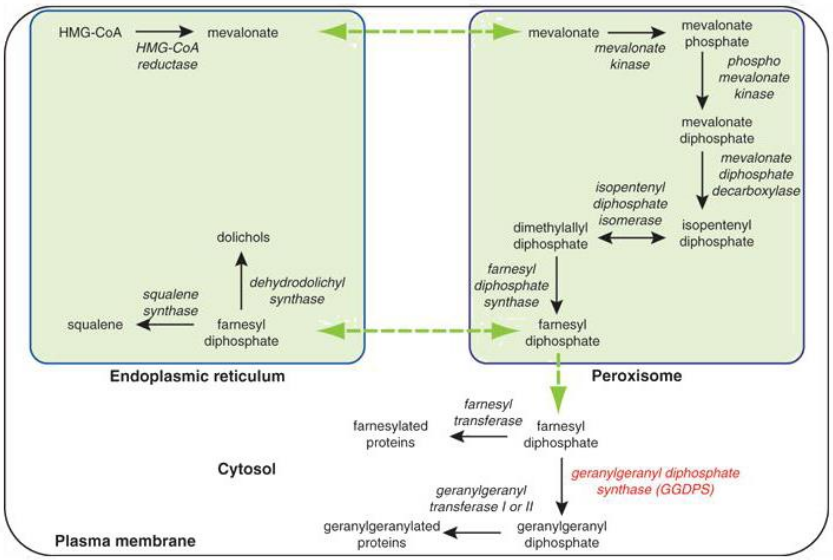

The biosynthesis of geranylgeranyl diphosphate and other isoprenoids from HMG-CoA. Synthesis of mevalonate from HMG-CoA occurs primarily in the endoplasmic reticulum; however, some mevalonate synthesis may occur in peroxisomes. The synthesis of farnesyl diphosphate from mevalonate is peroxisomal. Farnesyl diphosphate is a major branch point of the pathway. Farnesyl diphosphate is utilized in the endoplasmic reticulum for synthesis of sterols and dolichols, and is utilized in the cytosol for synthesis of geranylgeranyl diphosphate and farnesylation. Geranylgeranylation by either geranylgeranyl transferase I or II occurs in the cytosol. HMG-CoA, hydroxymethylglutaryl coenzyme A.

Pathway demonstrating the biosynthesis of genanylgeranyl diphosphate[794]

The isoprenoid biosynthetic pathway is a frequently targeted pathway in the treatment of disease. The isoprenoid inhibitors are of two main classes: the statins and the nitrogenous bisphosphonates which are used in osteoporosis and metastatic bone disease[794]. Statins have the ability to block modification of several oncogenes and are being explored as anticancer agents[795]. GGDPS inhibitors could be used as alternate disease therapeutics where geranylgeranylation has been implicated in the disease process, potentially even for endometriosis. The primary function of geranylgeranyl diphosphate is the post translational modification of proteins of the RAS family of small GTPases. The RHO members of this family are vital in the determination of malignant migration and metastasis. Geranylgeranyl diphosphate has been identified as an important metabolite in growth and metastasis in several human cancers (Figure 6-51). Protein geranylgeranylation is also important in the activation of the signalling pathways of epidermal growth factor receptors which is upregulated in malignancies[796]. In breast cancer the increased expression of RAB27B, a member of the Rab subfamily of GTPases, is associated with a poor prognosis[797]. Rab27 geranylgeranylation has been seen to be necessary for the formation of xenograft tumours in breast cancer cell lines. Overall geranylgeranyl diphosphate is emerging as an important metabolite in the development and metastatic potential of human malignancies. It has also been implicated in animal models looking at infectious diseases such as cryptoosporidosis[798] and Plasmodium in liver disease[799].

6.9.10 MYCBP

FIGURE 6-52

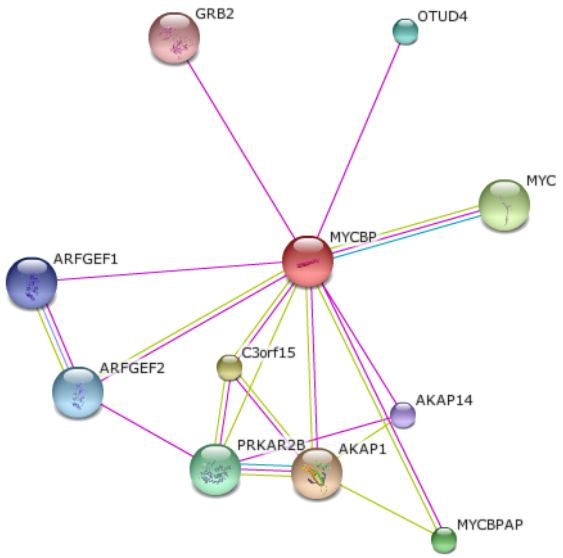

This is the **evidence view**. Different line colors represent the types of evidence for the association.

Your Input:

		Neighborhood	Gene Fusion	Cooccurrence	Coexpression	Experiments	Databases	Textmining	[Homology]	Score
MYCBP	c-myc binding protein; May control the transcriptional activity of MYC. Stimulates the activation of E box-dependent transcription by MYC (103 aa) *(Homo sapiens)*									

Predicted Functional Partners:

AKAP1	A kinase (PRKA) anchor protein 1; Binds to type I and II regulatory subunits of protein kinase [...] (903 aa)					•		•		0.992
C3orf15	AMY-1-associating protein expressed in testis 1 (AAT-1); Isoform 4 may play a role in spermatog [...] (767 aa)					•		•		0.990
MYC	v-myc myelocytomatosis viral oncogene homolog (avian); Participates in the regulation of gene t [...] (454 aa)					•	•	•		0.987
MYCBPAP	MYCBP associated protein; May play a role in spermatogenesis. May be involved in synaptic proce [...] (984 aa)					•		•		0.982
PRKAR2B	protein kinase, cAMP-dependent, regulatory, type II, beta; Type II regulatory chains mediate me [...] (418 aa)							•		0.730
OTUD4	OTU domain containing 4 (1049 aa)					•				0.641
ARFGEF2	ADP-ribosylation factor guanine nucleotide-exchange factor 2 (brefeldin A-inhibited); Promotes [...] (1785 aa)					•				0.636
ARFGEF1	ADP-ribosylation factor guanine nucleotide-exchange factor 1(brefeldin A-inhibited); Promotes g [...] (1849 aa)					•				0.621
AKAP14	A kinase (PRKA) anchor protein 14; Binds to type II regulatory subunits of protein kinase A and [...] (197 aa)					•				0.619
GRB2	growth factor receptor-bound protein 2; Adapter protein that provides a critical link between c [...] (217 aa)					•				0.593

Predicted evidence view of interactions of MYCBP[576]

The MYC binding protein (MYCBP) gene (Figure 6-52) also known as V-Myc Avian Myelocytomatosis Viral Oncogene Homolog, codes for the C-myc binding protein which is a cytoplasmic protein translocating to the nucleus in the S phase of the cell cycle. The protein binds to the C-MYC oncogene protein at its N-terminus[578]. It was originally identified as the retroviral oncogene homologue within the human cell[800]. This protein has been linked to spermatogenesis and is silenced with miRNA-22. It is instrumental in the development of Burkitt's Lymphoma and is elevated in aggressive tumours which are poorly differentiated and carry a poor prognosis[801]. Publications linking endometriosis to the presence of C-MYC are documented in the literature together with other oncogenes and tumour suppressor genes such as p53[802]. The c-MYC oncogene is overexpressed in certain cancers. It is also present with other oncogenes such as HER-2lneu, K-RAS mutations and p53 tumour suppressor gene mutations resulting in overexpression of p53 mutant proteins (Figure 6-53).

FIGURE 6-53

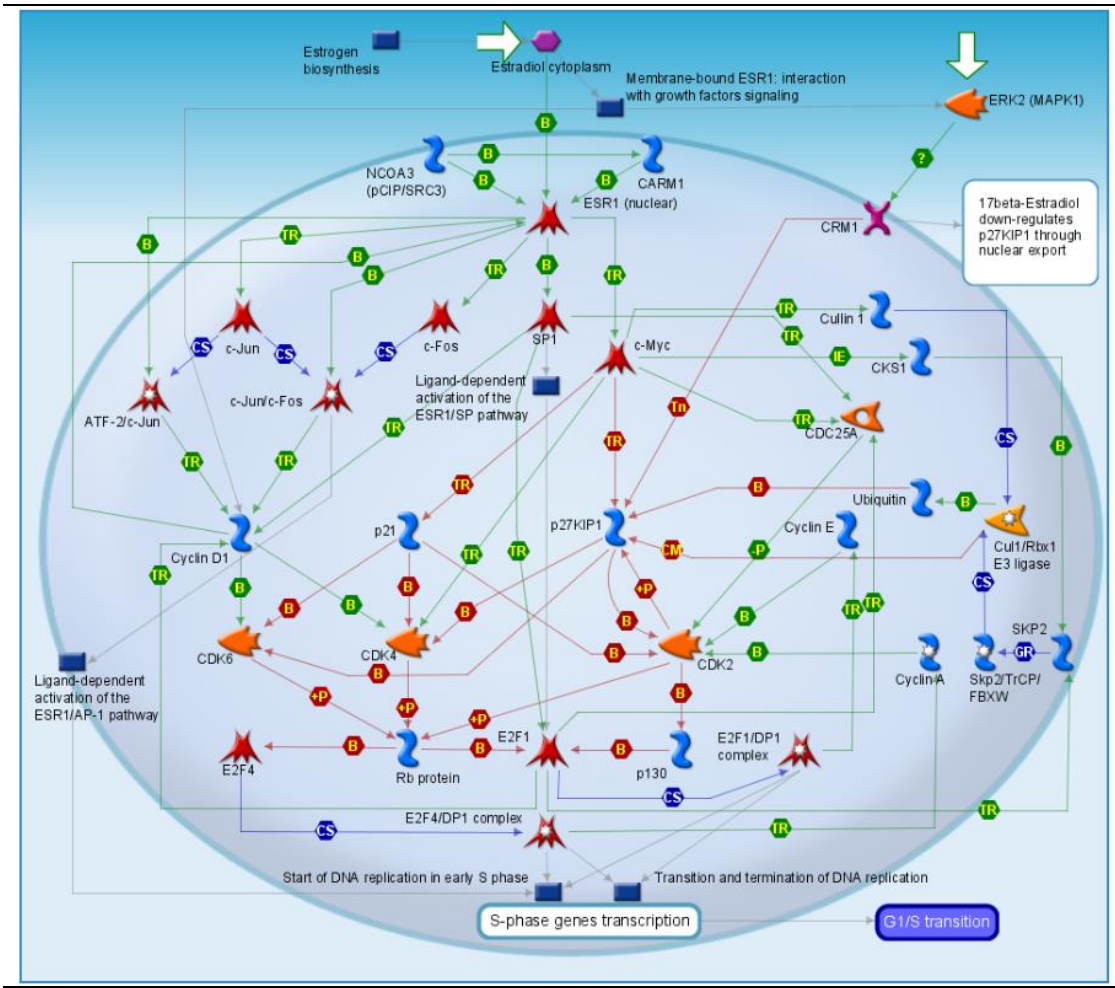

Pathway analysis of C-MYC oncogene[784]

One of the main functions of c-MYC is to promote progression through the cell cycle[803] with *in vitro* experiments showing a rise in c-MYC expression at the onset of G1 phase in the cell cycle[804]. The c-MYC sensitises cells pro-apoptotically and then causes the release of cytochrome C from the mitochondria into the cellular cytosol. It does this through the activation of BAX which is a pro-apoptotic molecule. The release of Cytochome C activates apoptotic protease-activating factor inducing apoptosis (Figure 6-54). The activation of BAX causes the change of mitochondrial membrane porosity and the presence of ATP activates the caspase cascade leading to cell death. The c-MYC also links to ADP-ribosylation factor (ARF) and activates the p53 tumour suppressor. The c-MYC induced apoptosis can be blocked through the promotion of MOMP by the pro-apoptotic protein BID which is in turn activated by Caspase8 through the FADD receptor (Figure 6-54).

FIGURE 6-54

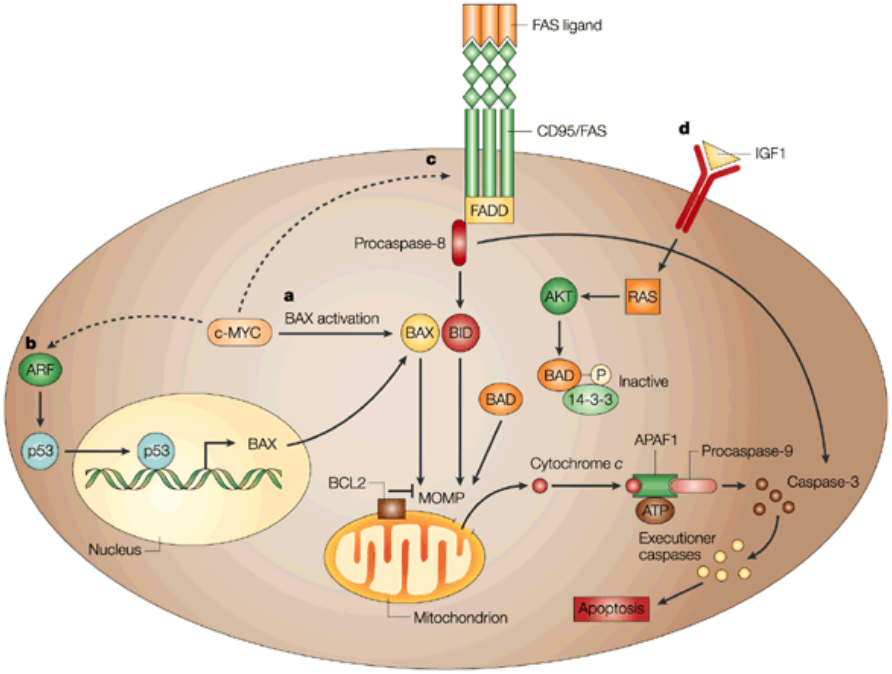

Apoptotic activation mechanisms[805]

6.9.11 CASP6

FIGURE 6-55

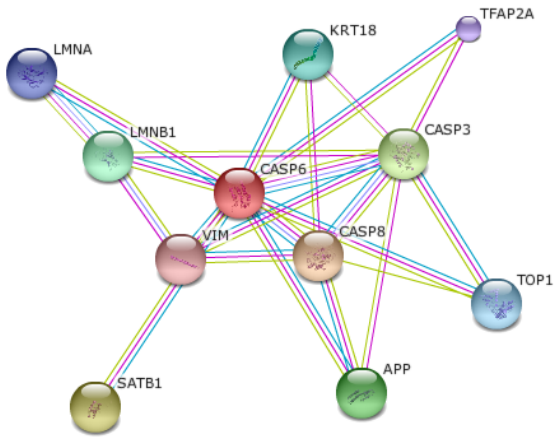

This is the **evidence view**. Different line colors represent the types of evidence for the association.

Your Input:

		Neighborhood	Gene Fusion	Cooccurrence	Coexpression	Experiments	Databases	Textmining	[Homology]	Score
CASP6	caspase 6, apoptosis-related cysteine peptidase; Involved in the activation cascade of caspases responsible for apoptosis execution. Cleaves poly(ADP-ribose) polymerase in vitro, as well as lamins. Overexpression promotes programmed cell death (293 aa) *(Homo sapiens)*									

Predicted Functional Partners:

CASP8	caspase 8, apoptosis-related cysteine peptidase; Most upstream protease of the activation casca [...] (538 aa)					•	•	•	•	0.994
SATB1	SATB homeobox 1; Crucial silencing factor contributing to the initiation of X inactivation medi [...] (763 aa)					•	•			0.989
CASP3	caspase 3, apoptosis-related cysteine peptidase; Involved in the activation cascade of caspases [...] (277 aa)					•	•	•	•	0.984
APP	amyloid beta (A4) precursor protein; N-APP binds TNFRSF21 triggering caspase activation and deg [...] (770 aa)					•	•			0.972
LMNB1	lamin B1; Lamins are components of the nuclear lamina, a fibrous layer on the nucleoplasmic sid [...] (586 aa)					•	•			0.971
KRT18	keratin 18; Involved in the uptake of thrombin-antithrombin complexes by hepatic cells (By simi [...] (430 aa)					•	•			0.970
TOP1	topoisomerase (DNA) I; The reaction catalyzed by topoisomerases leads to the conversion of one [...] (765 aa)					•	•			0.970
LMNA	lamin A/C; Lamins are components of the nuclear lamina, a fibrous layer on the nucleoplasmic si [...] (664 aa)					•	•			0.968
TFAP2A	transcription factor AP-2 alpha (activating enhancer binding protein 2 alpha); Sequence-specifi [...] (437 aa)					•	•			0.967
VIM	vimentin; Vimentins are class-III intermediate filaments found in various non-epithelial cells, [...] (466 aa)					•	•			0.966

Predicted evidence view of interactions of CASP6[576]

The enzyme Caspase 6 (Cysteine-aspartic acid protease family) is coded for by the CASP6 gene[806] (Figure 6-55). Caspases are components of the apoptotic, inflammatory and necrotic pathways and can be divided into roles of initiators and effectors (Figure 6-56). They are crucial in inflammation and cell death and their disruption has been linked to disorders ranging from myocardial infarction to malignancies. More than 400 caspase substrates have been identified so far. Whereas initially they were believed to play a role solely in apoptosis, they are now also known to effect immune cell function, development and differentiation. They can even protect from certain forms of cell death[807].

FIGURE 6-56

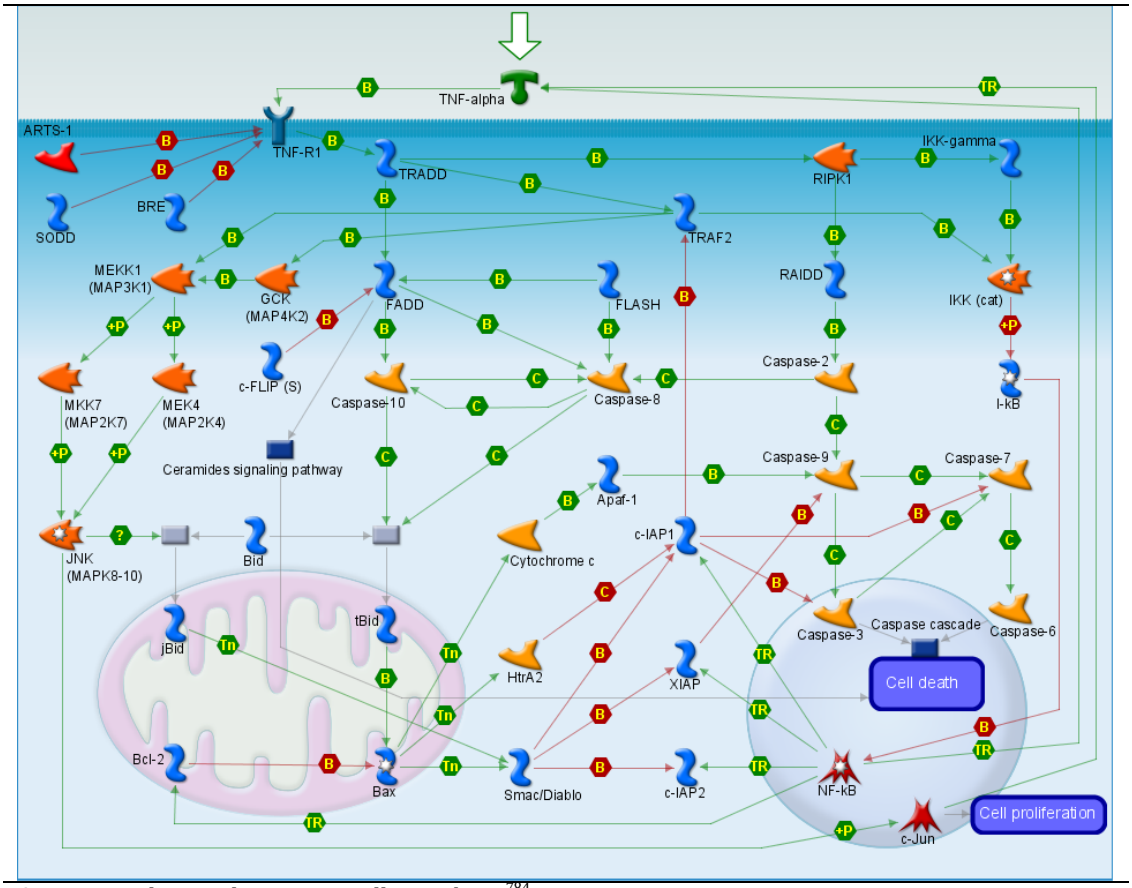

Apoptosis and survival TNFR1 signalling pathway[784]

The caspase proteases are broadly divided into pro- apoptotic or pro-inflammatory. Caspase 6 is an apoptosis effector caspase which has the ability to self-activate independently of other caspase family members[808]. It acts through the extrinsic and intrinsic apoptotic pathways[809] (Figure 6-57) and is induced by varied stimuli. It is known to interact with Caspase 8. Caspase 6 also has a role of B cell entry into the cell cycle. It has a negative regulatory effect on CD-40 and Toll-like receptor (TLR)-dependent G1 entry and conversely promotes S-phase entry later on in the cellular cycle[810]. Caspases are believed to have a role in activation of types of immune cells. The caspases involved in the development of haematopoietic cells and their activation include caspases- 6 and 8. Experimentally a caspase-8 deficiency has shown B cell, NK cell and T cell deficiencies[811]. Deficiency of Caspase 6 leads B-cells to differentiate rather than proliferate and its role in B-cell proliferation following activation with IgM or CD40 antibodies has also been shown in certain studies[812]. EBV is believed to induce apoptosis in a caspase dependant manner with the involvement of the mitochondrial pathway. Certain caspases including Caspase-3,8 and 9 are elevated

in EBV infected monocytes[813] and in my study, I have already identified increased levels of EBV in the lymphocytes of patients with endometriosis (See section 4.4.3.5 and 4.5.2.1). Caspase-6 is a known co-effector and activator of Caspase-8[814] so it too might have a role in cells affected by viral EBV.

FIGURE 6-57

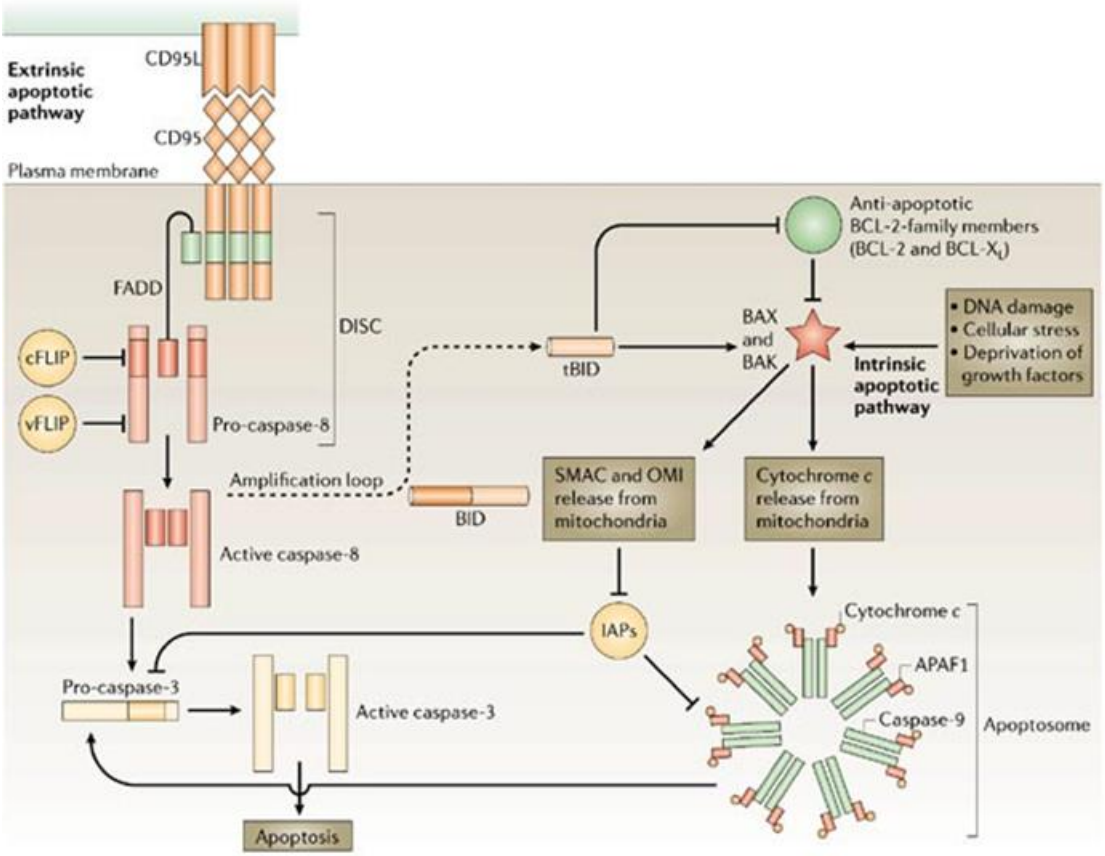

Extrinsic apoptotic pathway[807]

6.9.12 GMEB1

FIGURE 6-58

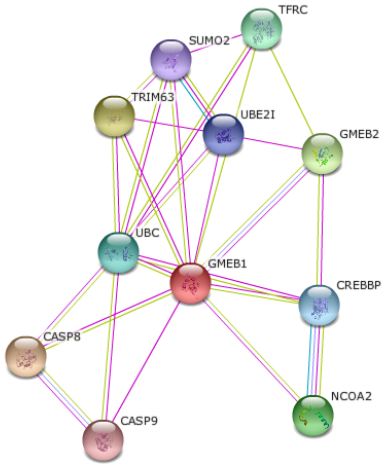

This is the **evidence view**. Different line colors represent the types of evidence for the association.

Your Input:

		Neighborhood	Gene Fusion	Cooccurrence	Coexpression	Experiments	Databases	Textmining	[Homology]	Score
GMEB1	glucocorticoid modulatory element binding protein 1; Trans-acting factor that binds to glucocorticoid modulatory elements (GME) present in the TAT (tyrosine aminotransferase) promoter and increases sensitivity to low concentrations of glucocorticoids. Binds also to the transferrin receptor promoter. Essential auxiliary factor for the replication of parvoviruses (573 aa) *(Homo sapiens)*									

Predicted Functional Partners:

CASP8	caspase 8, apoptosis-related cysteine peptidase; Most upstream protease of the activation casca [...] (538 aa)					•		•		0.919
TRIM63	tripartite motif-containing 63; E3 ubiquitin ligase. Regulates proteasomal degradation of cardi [...] (353 aa)					•		•		0.874
GMEB2	glucocorticoid modulatory element binding protein 2; Trans-acting factor that binds to glucocor [...] (530 aa)					•		•	•	0.698
NCOA2	nuclear receptor coactivator 2; Transcriptional coactivator for steroid receptors and nuclear r [...] (1464 aa)					•				0.684
TFRC	transferrin receptor (p90, CD71); Cellular uptake of iron occurs via receptor-mediated endocyto [...] (760 aa)							•		0.675
UBC	ubiquitin C (685 aa)					•				0.665
CREBBP	CREB binding protein; Acetylates histones, giving a specific tag for transcriptional activation [...] (2442 aa)					•				0.659
UBE2I	ubiquitin-conjugating enzyme E2I (UBC9 homolog, yeast); Accepts the ubiquitin-like proteins SUM [...] (158 aa)					•				0.657
SUMO2	SMT3 suppressor of mif two 3 homolog 2 (S. cerevisiae); Ubiquitin-like protein which can be cov [...] (95 aa)					•				0.642
CASP9	caspase 9, apoptosis-related cysteine peptidase; Involved in the activation cascade of caspases [...] (416 aa)					•				0.621

Predicted evidence view of interactions of GMEB1[576]

The GMEB1 gene (glucocorticoid modulatory element binding protein 1) (Figure 6-58) encodes for the KDWK gene family member which links to the GMEB2 protein. The resulting complex is essential for DNA replications in parvovirus. Animal studies indicate that this gene modulates the activation of glucocorticoid receptors which links to glucocorticoid responses[578]. Functionally, it is linked to Caspase 8, an apoptosis related member of the Caspase family. Caspase 8 is responsible for the cell death through binding of the FADD adapter molecule and activation of the TNFRSF6/FAS and TNFRSF1A pathways (Figure 6-56). The death inducing signalling complex (DISC) is what activates proteolysis by CASP8 and its downstream apoptosis. GMEB1 is also related functionally to Caspase 9, another apoptotic Caspase family member. In neurons, its presence has been seen to counteract and prevent apoptosis induced by oxidative stresses. It is also seen as a Caspase activation inhibitor[815].

6.9.13 TNFAIP8

FIGURE 6-59

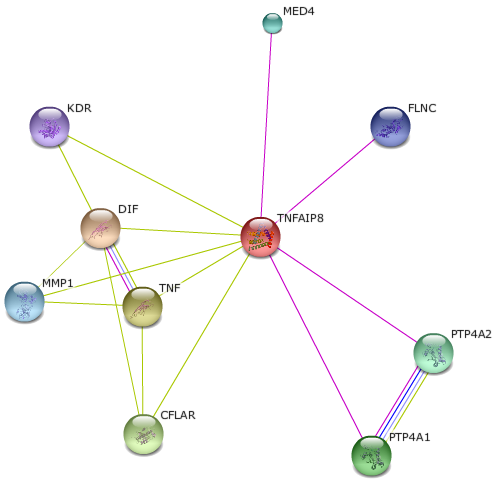

This is the **evidence view**. Different line colors represent the types of evidence for the association.

TNFAIP8 tumor necrosis factor, alpha-induced protein 8; Acts as a negative mediator of apoptosis and may play a role in tumor progression. Suppresses the TNF-mediated apoptosis by inhibiting caspase-8 activity but not the processing of procaspase-8, subsequently resulting in inhibition of BID cleavage and caspase-3 activation (198 aa)
(Homo sapiens)

Predicted Functional Partners:

		Neighborhood	Gene Fusion	Cooccurrence	Coexpression	Experiments	Databases	Textmining	[Homology]	Score
DIF	Tumor necrosis factor Precursor (TNF-alpha)(Tumor necrosis factor ligand superfamily member 2)([...] (233 aa)							●		0.864
TNF	tumor necrosis factor (TNF superfamily, member 2); Cytokine that binds to TNFRSF1A/TNFR1 and TN [...] (233 aa)							●		0.808
CFLAR	CASP8 and FADD-like apoptosis regulator; Apoptosis regulator protein which may function as a cr [...] (480 aa)							●		0.659
PTP4A1	protein tyrosine phosphatase type IVA, member 1; Protein tyrosine phosphatase which stimulates [...] (173 aa)					●				0.657
PTP4A2	protein tyrosine phosphatase type IVA, member 2; Protein tyrosine phosphatase which stimulates [...] (167 aa)					●				0.657
MED4	mediator complex subunit 4; Component of the Mediator complex, a coactivator involved in the re [...] (270 aa)					●				0.467
MMP1	matrix metallopeptidase 1 (interstitial collagenase); Cleaves collagens of types I, II, and III [...] (469 aa)							●		0.462
FLNC	filamin C, gamma; Muscle-specific filamin, which plays a central role in muscle cells, probably [...] (2725 aa)					●				0.429
KDR	kinase insert domain receptor (a type III receptor tyrosine kinase); Receptor for VEGF or VEGFC [...] (1356 aa)							●		0.428

Predicted evidence view of interactions of TNFAIP8[576]

The tumour necrosis factor alpha-induced protein 8 (TNFAIP8) is a member of a family of proteins which regulate cellular and immune control[816] (Figure 6-59). It is also known as the head and neck tumour and metastasis-related protein MDC-3.13. Its role is that of a negative apoptosis mediator and is linked to the ability of a tumour to invade, metastasis and proliferate[817]. It inhibits Caspase-8 resulting in the inhibition of BID cleavage and activation of Caspase 3. It does not affect the processing of procaspase-8[818-820]. Overexpression of TNFAIP8 is implicated in breast cancer, with its expression enhancing cellular invasion and proliferation[818,820,821]. It has also been linked to a poor prognosis and lymph node metastasis in non-small-cell lung cancer[822]. NDED (NF-kappa B-inducible death effector domain containing protein) is an alias for TNFAIP8. This has been shown experimentally to play an essential role in the suppression of TNF mediated apoptosis by the inhibition of Caspase-8[819]. In endometrial cancer, TNFAIP8 is linked to increased metastatic potential and reduced overall patient survival or disease recurrence rates[817] and it has been proposed as a prognostic marker in the recurrence of endometrial cancer. In endometriosis, this protein might also contribute to increased cellular growth and metastatic potentials. I have identified this protein as a potential serum marker in endometriosis and it could potentially be used to predict relapse, aggressiveness or recurrence of disease.

6.9.14 HSPE1

FIGURE 6-60

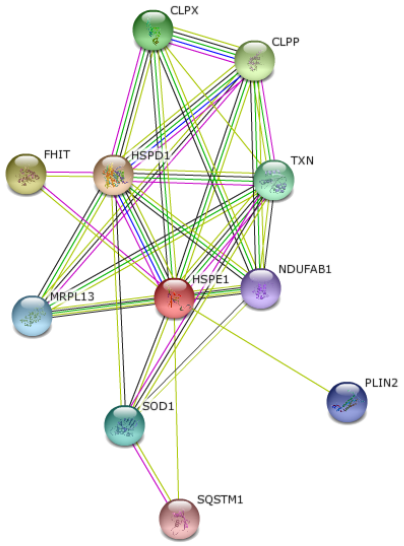

This is the **evidence view**. Different line colors represent the types of evidence for the association.

HSPE1 heat shock 10kDa protein 1 (chaperonin 10); Eukaryotic CPN10 homolog which is essential for mitochondrial protein biogenesis, together with CPN60. Binds to CPN60 in the presence of Mg-ATP and suppresses the ATPase activity of the latter (102 aa)
(Homo sapiens)

Predicted Functional Partners:

		Neighborhood	Gene Fusion	Cooccurrence	Coexpression	Experiments	Databases	Textmining	[Homology]	Score
HSPD1	heat shock 60kDa protein 1 (chaperonin); Implicated in mitochondrial protein import and macromo [...] (573 aa)	•		•	•	•	•	•		0.999
FHIT	fragile histidine triad gene; Cleaves A-5'-PPP-5'A to yield AMP and ADP. Possible tumor suppres [...] (147 aa)					•		•		0.926
CLPP	ClpP caseinolytic peptidase, ATP-dependent, proteolytic subunit homolog (E. coli); Clp cleaves [...] (277 aa)							•		0.877
CLPX	ClpX caseinolytic peptidase X homolog (E. coli); ATP-dependent specificity component of the Clp [...] (633 aa)							•		0.866
TXN	thioredoxin; Participates in various redox reactions through the reversible oxidation of its ac [...] (105 aa)				•			•		0.838
SOD1	superoxide dismutase 1, soluble; Destroys radicals which are normally produced within the cells [...] (154 aa)				•					0.818
MRPL13	mitochondrial ribosomal protein L13 (178 aa)				•					0.816
PLIN2	perilipin 2; May be involved in development and maintenance of adipose tissue (By similarity) (437 aa)							•		0.804
NDUFAB1	NADH dehydrogenase (ubiquinone) 1, alpha/beta subcomplex, 1, 8kDa; Carrier of the growing fatty [...] (156 aa)				•					0.801
SQSTM1	sequestosome 1; Adapter protein which binds ubiquitin and may regulate the activation of NFKB1 [...] (440 aa)							•		0.801

Predicted evidence view of interactions of HSPE1[576]

This gene encodes for heat shock 10 kDa protein 1 (Hsp10) also known as chaperonin 10 (cpn10) or early-pregnancy factor (EPF) (Figure 6-60). The heat shock protein encoded for by this gene is a major HSP functioning as a mitochondrial chaperonin. It enhances protein folding in an ATP dependant manner on binding to a second HSP (HSP60) forming a dimeric complex. It is not only limited to the mitochondrion, but can also be found in the cytosol, cell surfaces and peripheral blood[823]. Its dysregulation is related to pregnancy, cancer[824] and autoimmune inhibition and diseases[825,826]. It has a role in cellular stress[827] protection, immunomodulation and controls cellular proliferation and differentiation. Hsp10 is found in high levels in malignant cells and release into the extracellular space has tumour promoting effects[825]. In endometriosis the effects might potentially enable disease progression and dissemination As Hsp10 does not have an N-terminal peptide as a secretion signal, its transport is believed to occur through independent pathways, not the classic Golgi- dependant pathways. As the secretory pathway of Hsp60 is through exosome mediation[828], it is not unreasonable to infer that a similar pathway might be used by HSPE1.

EPF is the homolog of Hsp10. It is seen in the maternal circulation 24 hours post fertilisation and plays a vital role in maternal immunosuppression, enabling embryonic implantation[829]. Another role of Hsp10 is that of anti-autoimmunity. In rheumatoid arthritis it inhibits cytokine production improving clinical symptoms[830]. In multiple sclerosis it inhibits effector T-cell infiltration and downregulates adhesion molecules[831]. Potentially, Hsp10 may be used as a therapeutic agent in autoimmune disease treatment though the affected pathways are not entirely understood. If further studies can identify Hsp 10 as being particularly relevant to endometriosis in the clinical setting, it too might be used as therapeutic target for disease.

6.9.15 EIF4EBP1

FIGURE 6-61

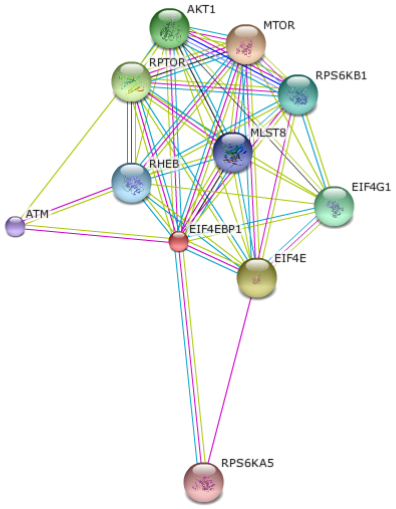

This is the **evidence view**. Different line colors represent the types of evidence for the association.

EIF4EBP1 eukaryotic translation initiation factor 4E binding protein 1; Regulates eIF4E activity by preventing its assembly into the eIF4F complex. Mediates the regulation of protein translation by hormones, growth factors and other stimuli that signal through the MAP kinase and mTORC1 pathways (118 aa) *(Homo sapiens)*

Predicted Functional Partners:

		Neighborhood	Gene Fusion	Cooccurrence	Coexpression	Experiments	Databases	Textmining	[Homology]	Score
MTOR	mechanistic target of rapamycin (serine/threonine kinase); Kinase subunit of both mTORC1 and mT [...] (2549 aa)					●	●	●		0.999
EIF4E	eukaryotic translation initiation factor 4E; Recognizes and binds the 7-methylguanosine-contain [...] (237 aa)					●	●	●		0.999
RPTOR	regulatory associated protein of MTOR, complex 1; Involved in the control of the mammalian targ [...] (1335 aa)					●	●	●		0.999
AKT1	v-akt murine thymoma viral oncogene homolog 1; General protein kinase capable of phosphorylatin [...] (480 aa)					●	●	●		0.998
EIF4G1	eukaryotic translation initiation factor 4 gamma, 1; Component of the protein complex eIF4F, wh [...] (1599 aa)						●	●		0.996
RPS6KB1	ribosomal protein S6 kinase, 70kDa, polypeptide 1; Phosphorylates specifically ribosomal protei [...] (525 aa)					●		●		0.987
RHEB	Ras homolog enriched in brain; Stimulates the phosphorylation of S6K1 and EIF4EBP1 through acti [...] (184 aa)						●	●		0.973
MLST8	MTOR associated protein, LST8 homolog (S. cerevisiae); Subunit of both mTORC1 and mTORC2, which [...] (326 aa)						●	●		0.968
ATM	ataxia telangiectasia mutated; Serine/threonine protein kinase which activates checkpoint signa [...] (3056 aa)					●		●		0.965
RPS6KA5	ribosomal protein S6 kinase, 90kDa, polypeptide 5; Serine/threonine kinase required for the mit [...] (802 aa)					●	●			0.961

Predicted evidence view of interactions of EIF4EBP1[576]

Human EIF4EBP1 (eukaryotic translation initiation factor 4E binding protein 1) is a translation repressor protein which interacts with translation initiation factor 4E in eukaryotes (Figure 6-61). This complex is responsible for the recruitment of the five end of mRNA to the 40S ribosomal subunits. Once EIF4EBP1 interacts with elF4E cellular translation is repressed. Conversely, factors such as insulin signalling and irradiation causes phosphorylation of the complex resulting in mRNA translation[577]. Another role of EIF4EBP1 is that of mediation of protein translation regulation in response to hormonal and growth factor stimuli. The pathways involve include the MAP kinase 9 (Figure 6-63) [526]and mTORC1 pathways (Figure

6-67)[526]. In an ovarian cancer study, 12% of patients exhibited aberrant expression of EIF4EBP1[832] showing worse outcomes in disease if the EIF4EBP1 was up or downregulated compared to normal levels. Elevated levels in the serum of women with endometriosis might also imply a worse outcome for patients with the disease, and it too could be potentially considered as a biomarker for endometriotic disease presence, response and prognosis.

6.9.16 MAPK14

FIGURE 6-62

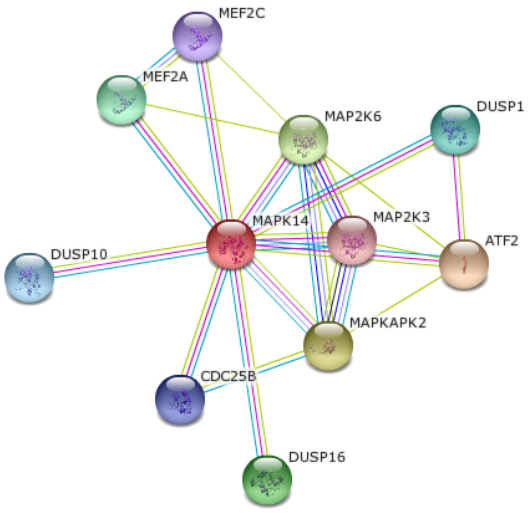

This is the **evidence view**. Different line colors represent the types of evidence for the association.

MAPK14 mitogen-activated protein kinase 14; Responds to activation by environmental stress, pro- inflammatory cytokines and lipopolysaccharide (LPS) by phosphorylating a number of transcription factors, such as ELK1 and ATF2 and several downstream kinases, such as MAPKAPK2 and MAPKAPK5. Plays a critical role in the production of some cytokines, for example IL-6. May play a role in stabilization of EPO mRNA during hypoxic stress. Isoform Mxi2 activation is stimulated by mitogens and oxidative stress and only poorly phosphorylates ELK1 and ATF2. Isoform Exip may play a role in the early onset o [...] (360 aa)
(Homo sapiens)

Predicted Functional Partners:

		Neighborhood	Gene Fusion	Cooccurrence	Coexpression	Experiments	Databases	Textmining	[Homology]	Score
ATF2	activating transcription factor 2; Transcriptional activator, probably constitutive, which bind [...] (505 aa)					●	●	●		0.999
MAPKAPK2	mitogen-activated protein kinase-activated protein kinase 2; Its physiological substrate seems [...] (400 aa)					●	●	●	●	0.999
MAP2K6	mitogen-activated protein kinase kinase 6; Catalyzes the concomitant phosphorylation of a threo [...] (334 aa)					●	●	●	●	0.999
DUSP16	dual specificity phosphatase 16; Involved in the inactivation of MAP kinases. Dephosphorylates [...] (665 aa)					●	●	●		0.999
MEF2A	myocyte enhancer factor 2A; Transcriptional activator which binds specifically to the MEF2 elem [...] (499 aa)					●	●	●		0.998
DUSP1	dual specificity phosphatase 1; Dual specificity phosphatase that dephosphorylates MAP kinase E [...] (367 aa)					●	●	●		0.998
DUSP10	dual specificity phosphatase 10; Involved in the inactivation of MAP kinases. Has a specificity [...] (482 aa)					●	●	●		0.998
CDC25B	cell division cycle 25 homolog B (S. pombe); Tyrosine protein phosphatase which functions as a [...] (580 aa)					●	●	●		0.997
MEF2C	myocyte enhancer factor 2C; Transcription activator which binds specifically to the MEF2 elemen [...] (473 aa)					●	●	●		0.995
MAP2K3	mitogen-activated protein kinase kinase 3; Dual specificity kinase. Is activated by cytokines a [...] (347 aa)					●	●	●	●	0.995

Predicted evidence view of interactions of MAPK14[576]

This gene encodes for Mitogen-Activated Protein Kinase 14. It is a serine- threonine kinase which is a vital component for the signal transduction pathway (Figure 6-62). It is one of four p38 MAP kinases that have a role in cellular responses. MAP kinases are involved in cellular development, proliferation, transcription and differentiation.

Environmental stresses or cytokines which are pro-inflammatory are the activating agents for the MAP kinase family. Activation also occurs through the MAPK14 protein phosphorylation by map kinase kinases, resulting in substrates such as transcription regulators activating transcription factor 2 (ATF2), Myocyte-specific enhancer factor 2C (MEF2C), MYC Associated Factor X (MAX), cell cycle regulators

cell division cycle 25B (CDC25B) and the tumour suppressor p53. Autophosphorylation also occurs through interaction with the protein TGF-Beta Activated Kinase 1/MAP3K7 Binding Protein 1 (MAP3K7IP1/TAB1)[577].

FIGURE 6-63

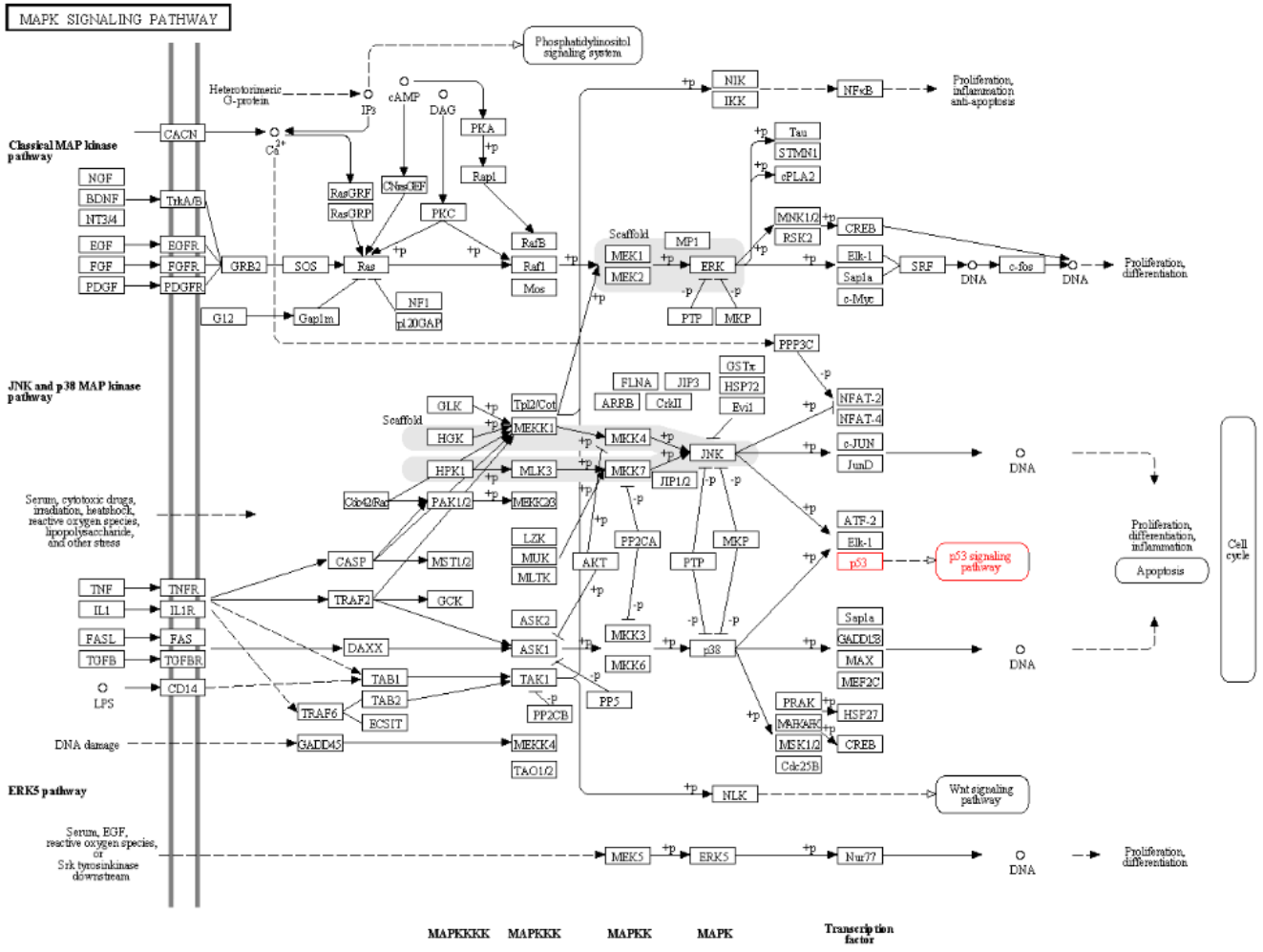

MAPK signalling pathway[526]

MAPK14 interacts with a number of substrates causing various intercellular responses. Its interaction with casein kinase 2 and the autophosphorylation of TP53/p53 results in MAPK14 activation within the cellular MAPK pathways regulating protein turnover[577]. MAPK14 acts on ubiquitin ligases and can interfere with the movement of transmembrane protein ATG9 thereby inhibiting the lysosome degradation pathway of autophagy. It is also responsible through its action on GTPase Ras-Related Protein Rab-5A (RAB5A) for the endocytosis of cellular membrane receptors. MAPK14, is also responsible for the phosphorylation of epidermal growth factor receptors resulting in their cellular internalisation in the presence of inflammatory stresses or irradiation. MAPKs are seen to regulate chromatin modification thereby affecting cellular gene expression and nuclear transcription. There seems to be a direct functional relationship between the gene O-Linked N-Acetylglucosamine (GlcNAc) Transferase (OGT) and MAPK14. Studies have demonstrated that activation of MAPK14 through glucose deprivation increases the OGT interaction and the stimulation of o-Glc-N-acylation. This process is seen to be vital in the embryonically derived placental vessels. Dysregulation of the MAPkinase pathways are linked with inflammation, neurodegenerative diseases[833] and malignancies[834]. They have been identified as a target for anti-cancer medications with various pathway targets being explored. It is interesting to note that MAP kinase pathways are also hormonally responsive. Estrogen-dependant disorders such as Polycystic Ovarian syndrome, leiomyomas and endometriosis have all been linked to the MAPK pathways[835].

6.9.17 ABCF1

FIGURE 6-64

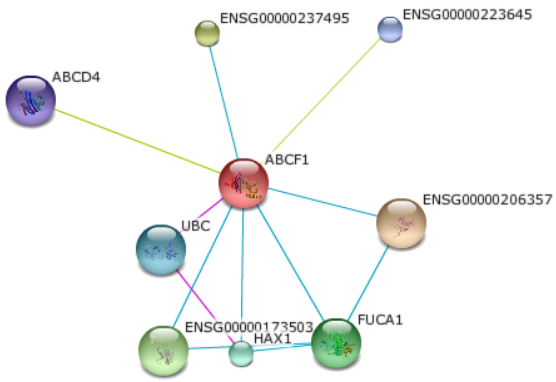

This is the **evidence view**. Different line colors represent the types of evidence for the association.

ABCF1 — ATP-binding cassette, sub-family F (GCN20), member 1; May function in mRNA translation (By similarity) (845 aa) *(Homo sapiens)*

Predicted Functional Partners:

		Neighborhood	Gene Fusion	Cooccurrence	Coexpression	Experiments	Databases	Textmining	[Homology]	Score
ENSG00000206357	microRNA 1236 (387 aa)						•			0.899
ENSG00000237495	Lymphocyte antigen 6 complex locus protein G5c Precursor (225 aa)						•			0.899
ENSG00000173503	Putative uncharacterized protein ENSP00000398430 (205 aa)						•			0.899
FUCA1	fucosidase, alpha-L- 1, tissue; Alpha-L-fucosidase is responsible for hydrolyzing the alpha-1,6 [...] (466 aa)						•			0.899
HAX1	HCLS1 associated protein X-1; Promotes cell survival. Potentiates GNA13-mediated cell migration [...] (279 aa)						•			0.899
UBC	ubiquitin C (685 aa)					•				0.604
ENSG00000223645	annotation not avaliable (295 aa)							•		0.430
ABCD4	ATP-binding cassette, sub-family D (ALD), member 4 (606 aa)							•		0.424

Predicted evidence view of interactions of ABCF1[576]

ABC transporters are proteins responsible for the transmission of membrane molecules between the intra and extracellular domains. There are seven ABC gene subfamilies and ATP-Binding Cassette (Figure 6-64), Sub-Family F (GCN20), Member 1 (also known as TNFalpha-Inducible ATP-Binding Protein) is a member of the GCN20 ABC transporter family[496,578,592]. It is regulated by TNFα[836] and has a role in inflammation and protein synthesis within the cell[577]. It is expressed in ribosomal proteins and has a role in mRNA translation. Unlike other members of its family, this protein lacks the transmembrane domains. Clinically ABC transporters, are linked to resistance to anti-cancer agents by the efflux of these agents outside of the tumour cells[837]. Transcript levels if ABCF1 were lower in non-responders. In endometriosis, the implications of elevated levels of ABCF1 are unexplored. Potentially it could be used to predict responses in patients to varied therapeutics in the future.

6.9.18 IMPA1

FIGURE 6-65

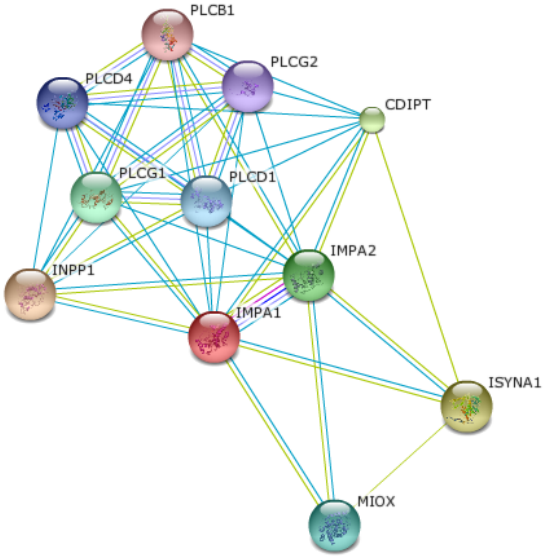

This is the **evidence view**. Different line colors represent the types of evidence for the association.

IMPA1 inositol(myo)-1(or 4)-monophosphatase 1; Responsible for the provision of inositol required for synthesis of phosphatidylinositol and polyphosphoinositides and has been implicated as the pharmacological target for lithium action in brain. Can use myo-inositol monophosphates, myo- inositol-1,3-diphosphate, myo-inositol-1,4-diphosphate, scyllo- inositol-phosphate, glucose-1-phosphate, glucose-6-phosphate, fructose-1-phosphate, beta-glycerophosphate, and 2'-AMP as substrates (336 aa)
(Homo sapiens)

Predicted Functional Partners:

		Neighborhood	Gene Fusion	Cooccurrence	Coexpression	Experiments	Databases	Textmining	[Homology]	Score
INPP1	inositol polyphosphate-1-phosphatase (399 aa)						●	●		0.977
ISYNA1	inositol-3-phosphate synthase 1; Key enzyme in myo-inositol biosynthesis pathway that catalyzes [...] (558 aa)						●	●		0.938
CDIPT	CDP-diacylglycerol--inositol 3-phosphatidyltransferase (phosphatidylinositol synthase); Catalyz [...] (213 aa)						●	●		0.915
IMPA2	inositol(myo)-1(or 4)-monophosphatase 2; Can use myo-inositol monophosphates, scylloinositol 1, [...] (288 aa)				●		●	●	●	0.911
PLCG1	phospholipase C, gamma 1; PLC-gamma is a major substrate for heparin-binding growth factor 1 (a [...] (1291 aa)						●			0.910
MIOX	myo-inositol oxygenase (285 aa)						●	●		0.909
PLCD1	phospholipase C, delta 1; The production of the second messenger molecules diacylglycerol (DAG) [...] (777 aa)						●			0.899
PLCD4	phospholipase C, delta 4; Hydrolyzes the phosphatidylinositol 4,5-bisphosphate (PIP2) to genera [...] (762 aa)						●			0.899
PLCG2	phospholipase C, gamma 2 (phosphatidylinositol-specific); The production of the second messenge [...] (1265 aa)						●			0.899
PLCB1	phospholipase C, beta 1 (phosphoinositide-specific); The production of the second messenger mol [...] (1216 aa)						●			0.899

Predicted evidence view of interactions of IMPA1[576]

Inositol(Myo)-1(Or 4)-Monophosphatase 1 gene encodes an enzyme which demonstrates phosphatase activity which is magnesium dependant (Figure 6-65). It is inhibited by therapeutic lithium concentrations and is used as the pharmacological target for lithium in the brain[577]. Lithium is used to treat bipolar

disorders and their associated manic and depressive episodes. This can be explained when one looks at the inhibition lithium exerts on inositol monophosphate hydroylosis and the resulting depletion of inositol for phosphatidylinositol synthesis. One of the interactions of IMPA1 is the gene Phospholipase C delta 1 which encodes a member of the phospholipase C family. This family of compounds acts in intracellular signalling and function as a tumour suppressor. It has been shown to have an essential role in trophoblastic and placental development. In a study which assessed autoantibodies against tumour associated antigens in women with endometriosis versus controls, IMP1 together with Cyclin B1 were postulated as potential clinical biomarkers of endometriomas[838]. It has not been used in the clinical setting so far.

6.9.19 LDHB

FIGURE 6-66

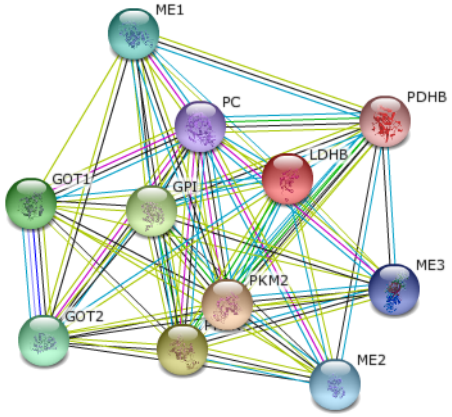

This is the **evidence view**. Different line colors represent the types of evidence for the association.

Your Input:

LDHB lactate dehydrogenase B (334 aa) *(Homo sapiens)*

Predicted Functional Partners:

		Neighborhood	Gene Fusion	Cooccurrence	Coexpression	Experiments	Databases	Textmining	[Homology]	Score
PKM2	pyruvate kinase, muscle; Glycolytic enzyme that catalyzes the transfer of a phosphoryl group fr [...] (531 aa)						•	•		0.987
PKLR	pyruvate kinase, liver and RBC; Plays a key role in glycolysis (By similarity) (574 aa)						•	•		0.984
GPI	glucose phosphate isomerase; Besides it's role as a glycolytic enzyme, mammalian GPI can functi [...] (558 aa)						•	•		0.970
GOT1	glutamic-oxaloacetic transaminase 1, soluble (aspartate aminotransferase 1) (413 aa)						•	•		0.963
GOT2	glutamic-oxaloacetic transaminase 2, mitochondrial (aspartate aminotransferase 2); Facilitates [...] (430 aa)						•	•		0.958
ME1	malic enzyme 1, NADP(+)-dependent, cytosolic (572 aa)						•	•		0.942
ME2	malic enzyme 2, NAD(+)-dependent, mitochondrial (584 aa)						•	•		0.941
ME3	malic enzyme 3, NADP(+)-dependent, mitochondrial (604 aa)						•	•		0.940
PC	pyruvate carboxylase; Pyruvate carboxylase catalyzes a 2-step reaction, involving the ATP-depen [...] (1178 aa)						•	•		0.940
PDHB	pyruvate dehydrogenase (lipoamide) beta; The pyruvate dehydrogenase complex catalyzes the overa [...] (359 aa)						•	•		0.936

Predicted evidence view of interactions of LDHB[576]

Lactate dehydrogenase B is an enzyme in the glycolytic pathway which is a catalyst for the reversible reactions of nicotinamide adenine dinucleotide (NAD and NADH) and the conversions of lactate and pyruvate[577] (Figure 6-66). Lactate dehydrogenase deficiency arises from gene mutations and gives rise to glycogen storage diseases with possible associated renal failure secondary to myoglobinuria. It has been reported in other studies to be elevated in women suffering from endometriosis, in benign and malignant ovarian tumours[839] and in endometrial carcinomas. In endometrial cancer the mammalian target of rapamycin (mTOR) tumour pathway has been identified as a vital pathway in disease development[840] (Figure 6-67). Lactate Dehydrogenase B is critical for hyperactive mTOR-mediated tumorigenesis[841]. In

medulloblastomas with high LDBH levels prognosis of the disease was found to be poor with an increased possibility of metastasis[842].

FIGURE 6-67

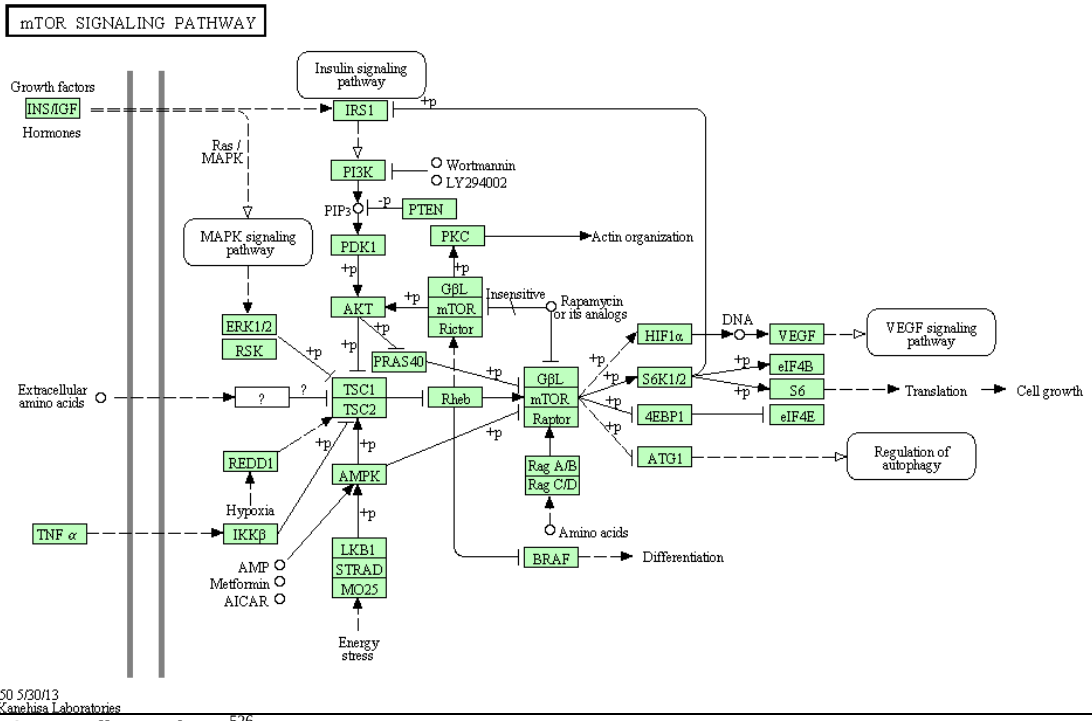

mTOR signalling pathway[526]

6.9.20 ATXN3

FIGURE 6-68

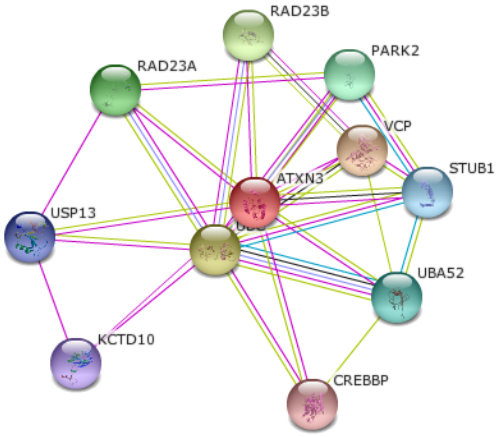

This is the **evidence view**. Different line colors represent the types of evidence for the association.

ATXN3 ataxin 3; Interacts with key regulators (CBP, p300 and PCAF) of transcription and represses transcription. Acts as a histone- binding protein that regulates transcription. Acts as a deubiquitinating enzyme (361 aa) *(Homo sapiens)*

Predicted Functional Partners:

		Neighborhood	Gene Fusion	Cooccurrence	Coexpression	Experiments	Databases	Textmining	[Homology]	Score
VCP	valosin-containing protein; Necessary for the fragmentation of Golgi stacks during mitosis and [...] (806 aa)					•	•			0.999
UBC	ubiquitin C (685 aa)					•				0.999
RAD23B	RAD23 homolog B (S. cerevisiae); Plays a central role both in proteosomal degradation of misfol [...] (409 aa)					•	•			0.997
RAD23A	RAD23 homolog A (S. cerevisiae); Involved in postreplication repair of UV-damaged DNA. Postrepl [...] (363 aa)					•	•			0.991
PARK2	Parkinson disease (autosomal recessive, juvenile) 2, parkin; Functions within a multiprotein E3 [...] (465 aa)					•	•			0.976
UBA52	ubiquitin A-52 residue ribosomal protein fusion product 1; Protein modifier which can be covale [...] (128 aa)					•	•			0.958
STUB1	STIP1 homology and U-box containing protein 1; Modulates the activity of several chaperone comp [...] (303 aa)					•				0.955
USP13	ubiquitin specific peptidase 13 (isopeptidase T-3) (863 aa)					•				0.935
KCTD10	potassium channel tetramerisation domain containing 10 (313 aa)					•				0.925
CREBBP	CREB binding protein; Acetylates histones, giving a specific tag for transcriptional activation [...] (2442 aa)					•				0.893

Predicted evidence view of interactions of ATXN3[576]

Ataxin3 is a deubiquinating enzyme which cleaves Ubiquitin from proteins (Figure 6-68). It has various cellular functions ranging between homeostasis protein maintenance, cytoplasmic trafficking, protein guiding through endocytic pathways, degradation of chaperone substrates which are misfolded, regulation of the cytoskeleton and myogenesis[843]. It has a role in the inhibition of transcription acting as a histone binding protein. Its precise biological function remains incompletely understood. A mutation in the ATXN3 gene causes a trinucleotide repeat expansion and leads to the disease of spinocerebellar ataxia type 3. The accumulation of incorrectly folded proteins affects brain cells and neurons giving rise to neurodegenerative disease such as the autosomal dominant Machado-Joseph disease. ATXN3 has been identified as an autonomous complimentary therapeutic target in cancers with downregulation of phosphatase and tensin homolog (PTEN)[844]. Silencing of PTEN is associated with a hyper-activation of the phosphatidylinositol-3-kinase (PI3K) pathway in cancer[844]. As yet there is no link to endometriosis. One could theorise that its presence may alter cellular characteristics potentially encouraging disease progression. If confirmed as a highly relevant protein in the disease of endometriosis, it might also be considered in the future as a main or complimentary therapeutic target for disease.

6.9.21 TOM1

FIGURE 6-69

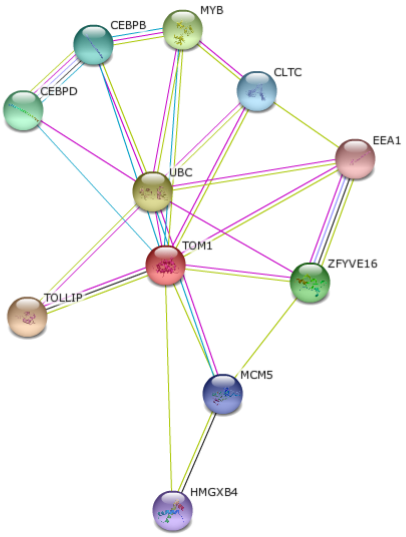

This is the **evidence view**. Different line colors represent the types of evidence for the association.

TOM1 target of myb1 (chicken); May be involved in intracellular trafficking. Probable association with membranes (493 aa) *(Homo sapiens)*

Predicted Functional Partners:

		Neighborhood	Gene Fusion	Cooccurrence	Coexpression	Experiments	Databases	Textmining	[Homology]	Score
TOLLIP	toll interacting protein; Component of the signaling pathway of IL-1 and Toll-like receptors. I [...] (274 aa)					●		●		0.996
UBC	ubiquitin C (685 aa)					●				0.940
MYB	v-myb myeloblastosis viral oncogene homolog (avian); Transcriptional activator; DNA-binding pro [...] (761 aa)						●	●		0.926
ZFYVE16	zinc finger, FYVE domain containing 16; May be involved in regulating membrane trafficking in t [...] (1539 aa)					●		●		0.917
CEBPD	CCAAT/enhancer binding protein (C/EBP), delta; C/EBP is a DNA-binding protein that recognizes t [...] (269 aa)						●			0.899
CEBPB	CCAAT/enhancer binding protein (C/EBP), beta; Important transcriptional activator in the regula [...] (345 aa)						●			0.899
CLTC	clathrin, heavy chain (Hc); Clathrin is the major protein of the polyhedral coat of coated pits [...] (1675 aa)					●				0.848
MCM5	minichromosome maintenance complex component 5 (734 aa)							●		0.819
HMGXB4	HMG box domain containing 4; Negatively regulates Wnt/beta-catenin signaling during development [...] (601 aa)							●		0.794
EEA1	early endosome antigen 1; Binds phospholipid vesicles containing phosphatidylinositol 3-phospha [...] (1411 aa)					●				0.764

Predicted evidence view of interactions of TOM1[576]

Target of Myb1 (Chicken) is a gene which is a target of the viral myeloblastosis oncogene (Figure 6-69). The protein of this gene is associated with intracellular membrane and vesicular trafficking at the endosome as it shares an N-terminal in common with endosomal proteins[577]. It is recruited to the endomsomes through its interaction with endosomal protein endolfin[845]. Another function of this gene is the translocation of growth factor receptor complexes to the lysosome for degradation thereby affecting cellular growth. Studies looking at its antibody expression in various diseases show high levels in endometrial cancers[634]. TOM1 has also been described as a negative regulator of pathways such as IL-1 and TNF[846]. When TOM1 is overexpressed it suppresses, through its VHS domain, the activation of pro inflammatory cytokines NF-κβ and Activating protein-1 (AP-1) (Figure 6-70) through the induction of Interleukin-1β (IL-1β) or Tumour necrosis factor-α (TNF-α)[846] (Figure 6-71). AP-1 proteins control cellular cycle through the regulation of Cyclin D1, p53, p21, p19 and p16. The tumour suppressor p53, found in elevated levels in diseases such as endometriosis, is modulated by AP-1[847].

FIGURE 6-70

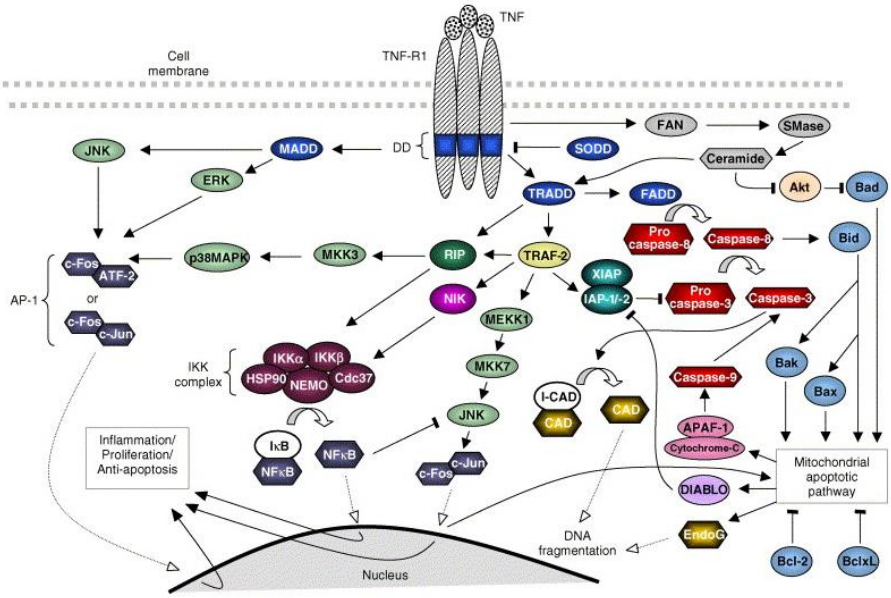

NF-κβ and activating protein-1 pathways[848]

FIGURE 6-71

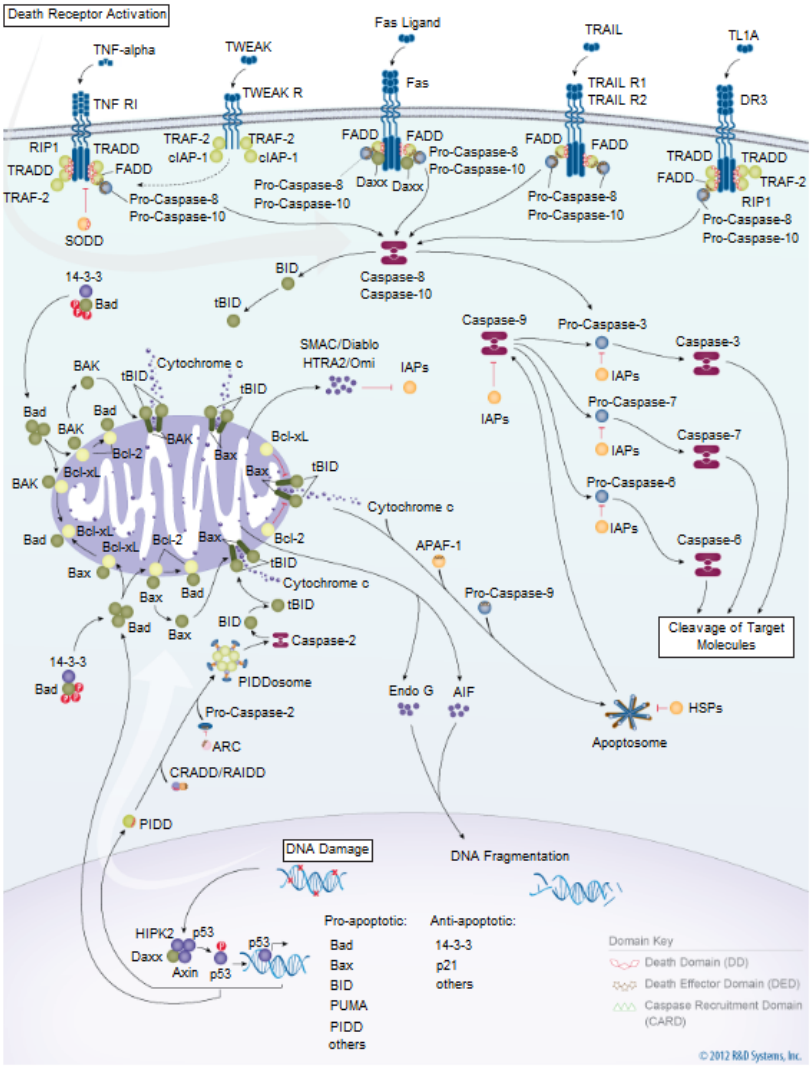

Death receptor activation pathways[785]

7 Galectin as a therapeutic target in endometriosis- therapeutic experimentations

7.1 Introduction

Galectin-3 levels have been documented in endometriosis and levels were found to be elevated in my tissue microarray studies (4.4.3.7). In this study increased level of Cyclin D1 in endometriosis tissues was confirmed. Cyclin D1 is a substrate on which tested therapeutics such as GCS-100 are known to act, increasing the evidence of the potential use of a galectin-3 inhibitor as a novel therapeutic medication (Chapter 7). *In vitro* therapeutic experiments were carried out on primary ovarian and peritoneal endometriosis cells as well as normal uterine endometrial cells taken at laparoscopy to assess for cellular response to GCS-100 in endometriosis.

7.2 Aims

- To explore novel and alternate methods of treatment for endometriosis in an *in vitro* and in vivo setting

7.3 Method

7.3.1 *In vitro* studies on potential therapeutics

Therapeutic studies were performed on fresh patient endometriosis cell samples taken at laparoscopy. Cells were processed as described above (primary patient cellular sample preparation (2.10.2)). They were transferred to a 96 well plate at a concentration of $1x10^5$ viable cells in 80µl of growth medium per well. The 96 well plate was left in the cell incubator overnight at 5% CO_2 and 37°C to allow cells to acclimatise to their new environment and settle at the base of the plate. The ovarian endometriosis, cutaneous/peritoneal endometriosis and normal endometrial uterine cells were placed separately into 96 well plates in preparation for therapeutic studies. 20µl of each drug at a specified concentration was added to each 80µl well containing cells in culture. Each therapeutic experiment was run in triplicate to strengthen result validity. Etoposide was added at different micro molar concentrations in respective wells (0.1µM, 1µM, 5µM, 10µM, 25µM, 50µM) as the standardised control cytotoxic agent to induce cellular death during experimentation. Three wells on each plate contained untreated cells (blank triplicates) to act as positive controls (Table 7-1).

TABLE 7-1

	1	2	3	4	5	6	7	8	9	10	11	12
a	Blank triplicate			Ovarian untreated cells			Ovarian etoposide 0.1			Ovarian etoposide 1		
b	Ovarian etoposide 5			Ovarian etoposide 10			Ovarian etoposide 25			Ovarian etoposide 50		
c	Ovarian treated 10			Ovarian treated 25			Ovarian treated 50			Ovarian treated 100		
d	Ovarian treated 250			Ovarian treated 500			Ovarian treated 750			Ovarian treated 1000		
e	Cutaneous untreated cells			Cutaneous etoposide 0.1			Cutaneous etoposide 1			Cutaneous etoposide 5		
f	Cutaneous etoposide 10			Cutaneous etoposide 25			Cutaneous etoposide 50			Cutaneous treated 10		
g	Cutaneous treated 25			Cutaneous treated 50			Cutaneous treated 100			Cutaneous treated 250		
h	Cutaneous treated 500			Cutaneous treated 750			Cutaneous treated 1000					

An example of the setup of a 96 well plate with 32 triplicate experiments for different therapeutic concentrations. This demonstrates the setup of the plate at initial therapeutic concentrations in µg/mL

Galectin-3 inhibitor (GCS-100) and NADPH oxidase enhancers, (CO-AAW1, PK-11195 and CO-AAW14) were respectively tested on normal uterine endometrial cells, ovarian endometriosis cells and peritoneal endometriosis cells. Each experiment was repeated in triplicate wells over 12, 24, 48 and 72 hours post treatments (7.3.1).The tested drugs were diluted to these respective concentrations (10µg/mL, 25µg/mL, 50µg/mL, 100 µg/mL, 250µg/mL, 500µg/mL, 750µg/mL and 1000µg/mL). The FLUORstar OPTIMA a fully automated 96 fluorescence microplate based multi-detection reader (operating protocol by BMG Labtech) was used to scan the well plates and assesses for cellular viability. This was performed by reading fluorescence output levels that indicate the presence of ATP in viable cells. The 96 well plates were read at 24, 48, 72 and 96 hours respectively to assess for timed therapeutic responses of the treated cells. The fluorescence outputs read by the FLUORstar OPTIMA for each respective well were compared between treated and untreated cells at various concentrations and across the defined timelines. All the output levels of fluorescence were then exported to an excel sheet and graphs plotted with the data. Results of these experiments are plotted and discussed further on in the thesis (Figure 7-6, Figure 7-7, Figure 7-8 and Figure 7-9 in Section 7). Graphs showing the results of percentage cell survival in the treated and untreated groups were plotted below (Figure 7-6)

7.3.2 Zebrafish *in vitro* studies

Attempts at creating in-vivo models of endometriosis using Zebrafish (*Brachydanio rerio* or *Danio rerio*) wild type AB strain as host organisms were performed. If successful, treating host Zebrafish in vivo with the therapeutics identified would give an insight as to in vivo therapeutic effects on disease. Cells from normally sited endometrium (control cells) and endometriosis (case cells) were processed from primary patient samples obtained at surgery (Section 2.10) and stained with Invitrogen™ fluorescent tracker probes for long-term tracing of living cells. A Femtojet microinjector was used for cell injection of sample cells directly into the embryonic tissues. Embryos with cells injected into the bloodstream or yolk sac were excluded as misinterpretation of cellular dissemination through the circulatory route could occur (Figure 7-1, Figure 7-2).

FIGURE 7-1

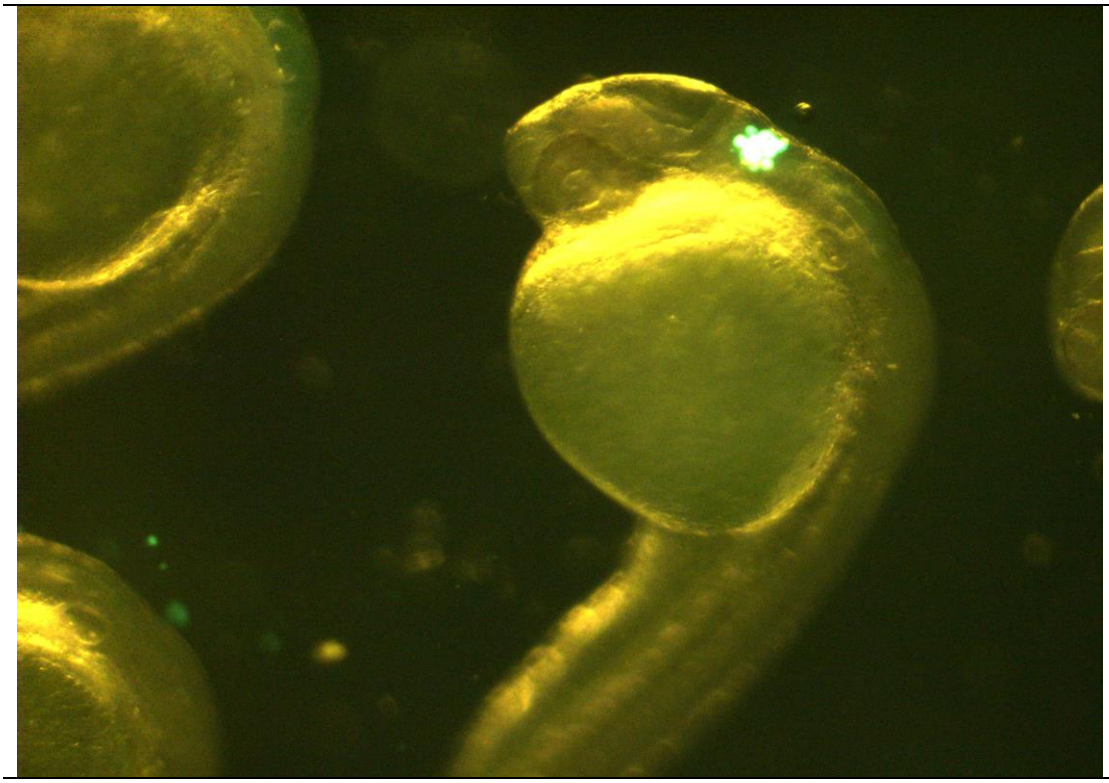

Correctly injected fluorescent labelled endometriosis cells

FIGURE 7-2

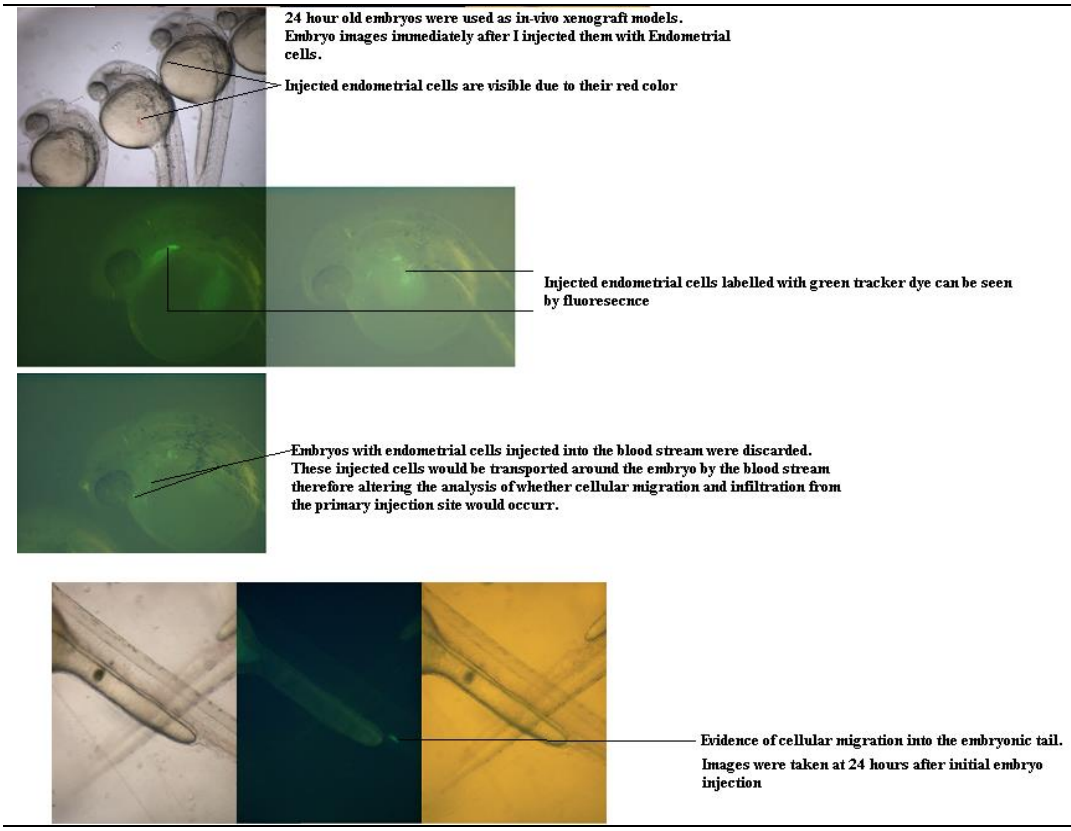

Images of injected fish embryos as seen through the microscope

Non excluded embryos were analysed 24 to 48 hours post injection by fluorescence microscopy to select those which were morphologically normal and containing fluorescent cells. Preliminary images were obtained using the fluorescence stereomicroscope Leica MZ FL III Fluo Combi™ bearing appropriate filters and a fluorescence microscope Leitz Aristoplan coupled with a Leica D-LUX camera. Cellular viability, migration patterns and embryonic infiltration were assessed. Confirmation of the presence of cellular viability and migration was obtained (Figure 7-3, Figure 7-4, Figure 7-5).

FIGURE 7-3

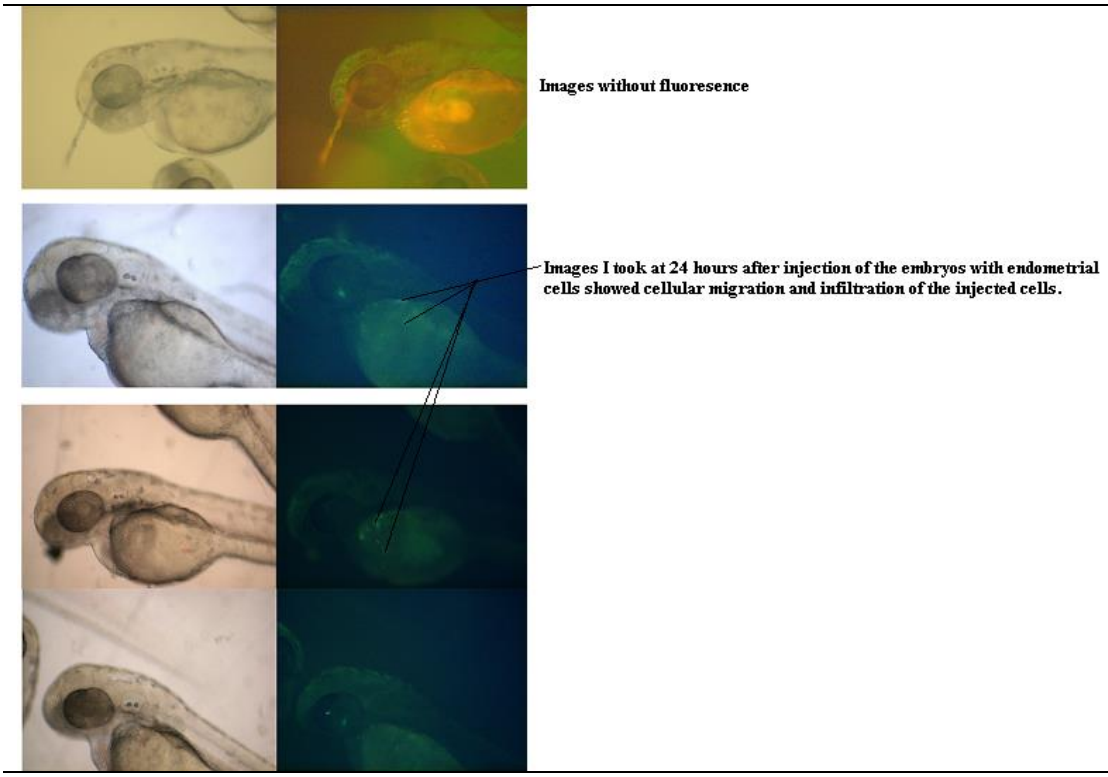

Images of injected fish embryos as seen through the microscope

FIGURE 7-4

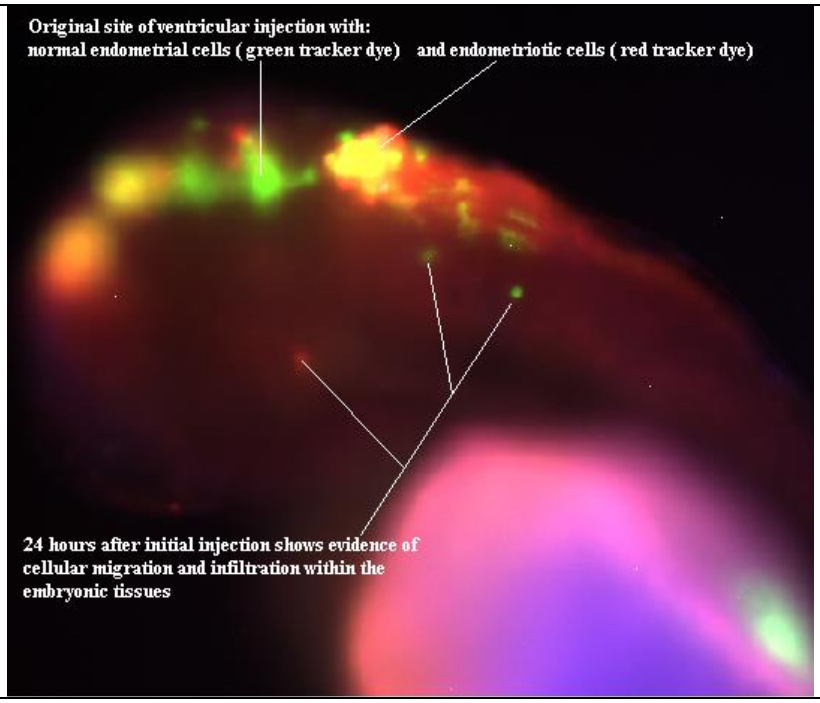

Images of injected fish embryos as seen through the microscope with fluorescent markers

FIGURE 7-5

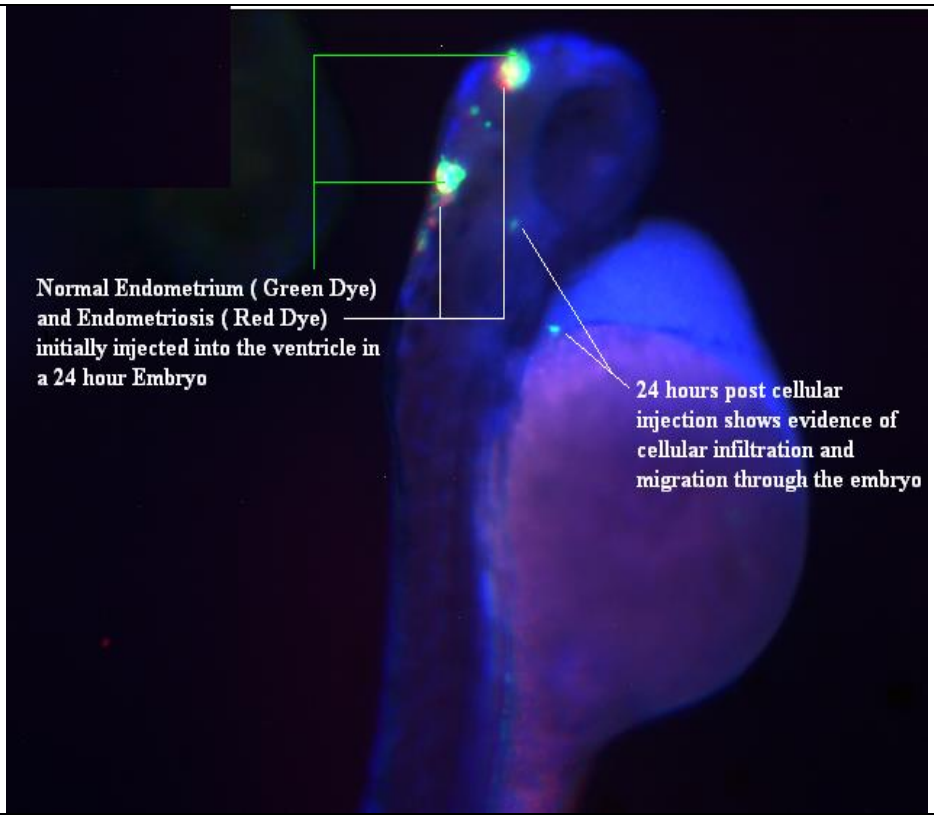

Images of injected fish embryos as seen through the microscope with fluorescent markers

Endometriosis cellular survival could not be maintained over the 24 hour post injection. Whereas tumour cells have the ability of accelerated division and invasion, enabling them to grow successfully in the

zebrafish animal model, endometriosis cells were adherent and slow growing *in vitro*. This could possibly explain why the model could not be maintained. Discussions and collaborations were held with experts in the field and alterations in fish tank water temperature to accommodate for optimal cellular growth conditions resulted in embryonic disfigurement and demise. After multiple unsuccessful attempts at the creation of this in vivo model, a choice was made to continue pursuing the *in vitro* experimentation for therapeutic responses albeit recognising its limits in the mimicking of a living organism.

7.4 Results

From this set of experiments at 72 hours post treatment with GCS-100 there was an observed direct dose dependant relationship between treated endometriosis cells and percentage cell survival (Figure 7-6). Of note, untreated cells maintained viability supporting GCS-100 as a potential future therapeutic in endometriosis. The experiments using alternate compounds CO-AAW1, CO-AAW14 and PK11195 did not show similar tissue responses (Figure 7-7, Figure 7-8, Figure 7-9).

7.4.1 GCS-100

FIGURE 7-6

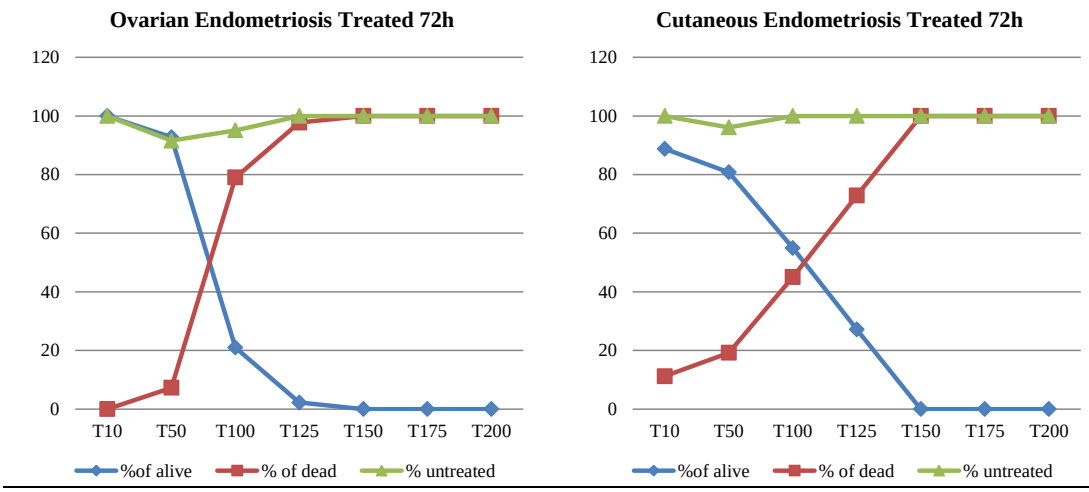

Graphs depicting % cell survival between treated and untreated endometriosis cells with GCS-100

This figure demonstrates a direct dose dependant effect on Ovarian endometriosis cells at 72 hours of culture. Whereas the untreated cells maintain viability throughout the experiment, responses to GCS-100 resulting in cell death are seen from concentrations around 20µg/mL. The cell death % increases proportionally to the drug dose levels reaching almost 100% cell death at 150µg/mL (T150). Further in vivo experimentation could be undertaken as a future body of work to assess GCS-100 as a potential novel therapeutic for endometriosis treatment.

7.4.2 CO-AAW1

FIGURE 7-7

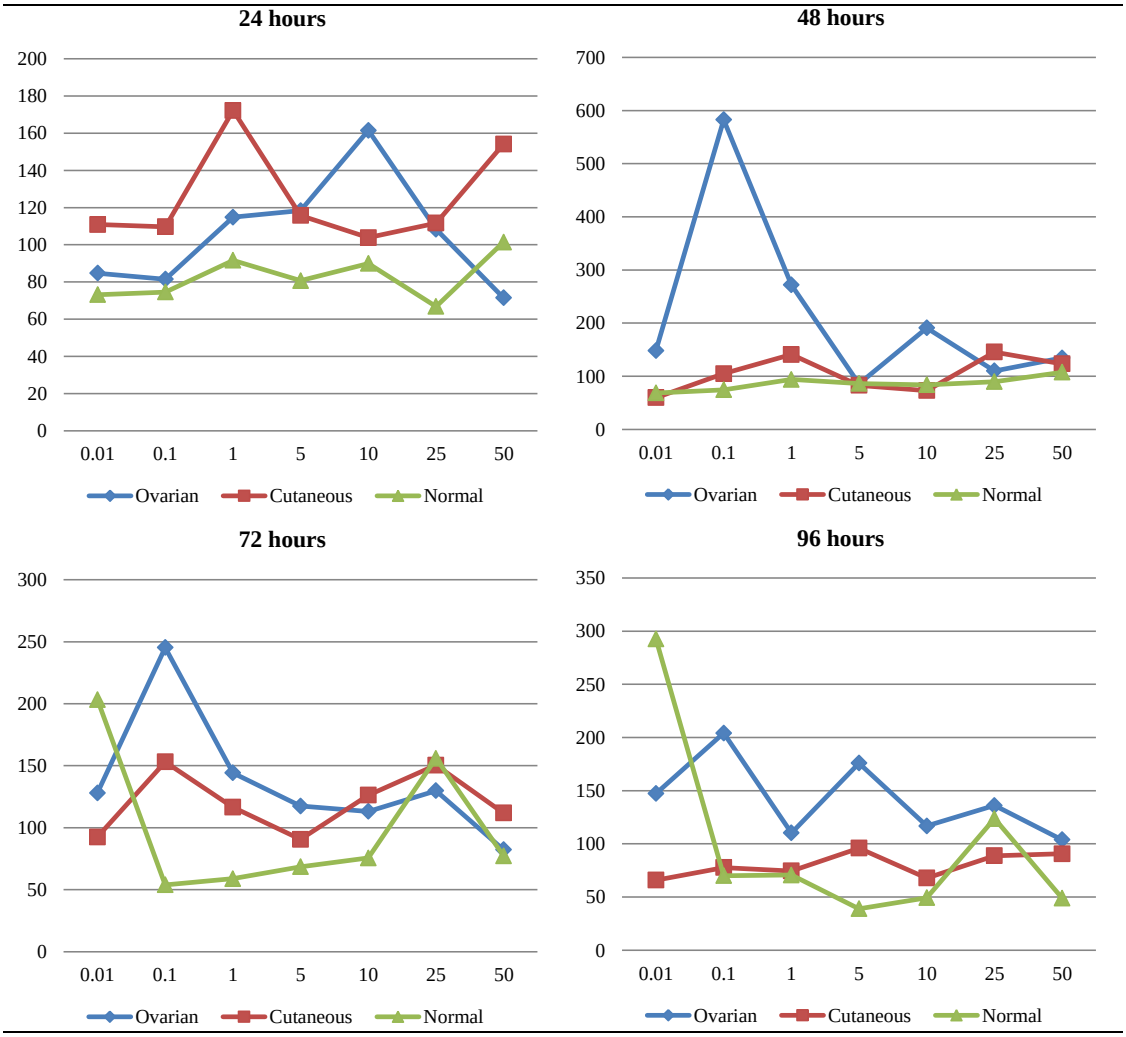

Graphs depicting % cell survival between treated and untreated endometriosis cells with CO-AAW1

These graphs fail to demonstrate a dose dependant effect of treatment with CO-AAW1 on endometriosis. No correlation or response is seen to this drug treatment at any stage of the cellular culture (24 hrs, 48 hrs, 72 hrs or 96 hrs) or to any drug dose. These preliminary tests indicate it is unlikely for CO0AAW1 to have any benefit as a therapeutic in endometriosis.

7.4.3 PK11195

FIGURE 7-8

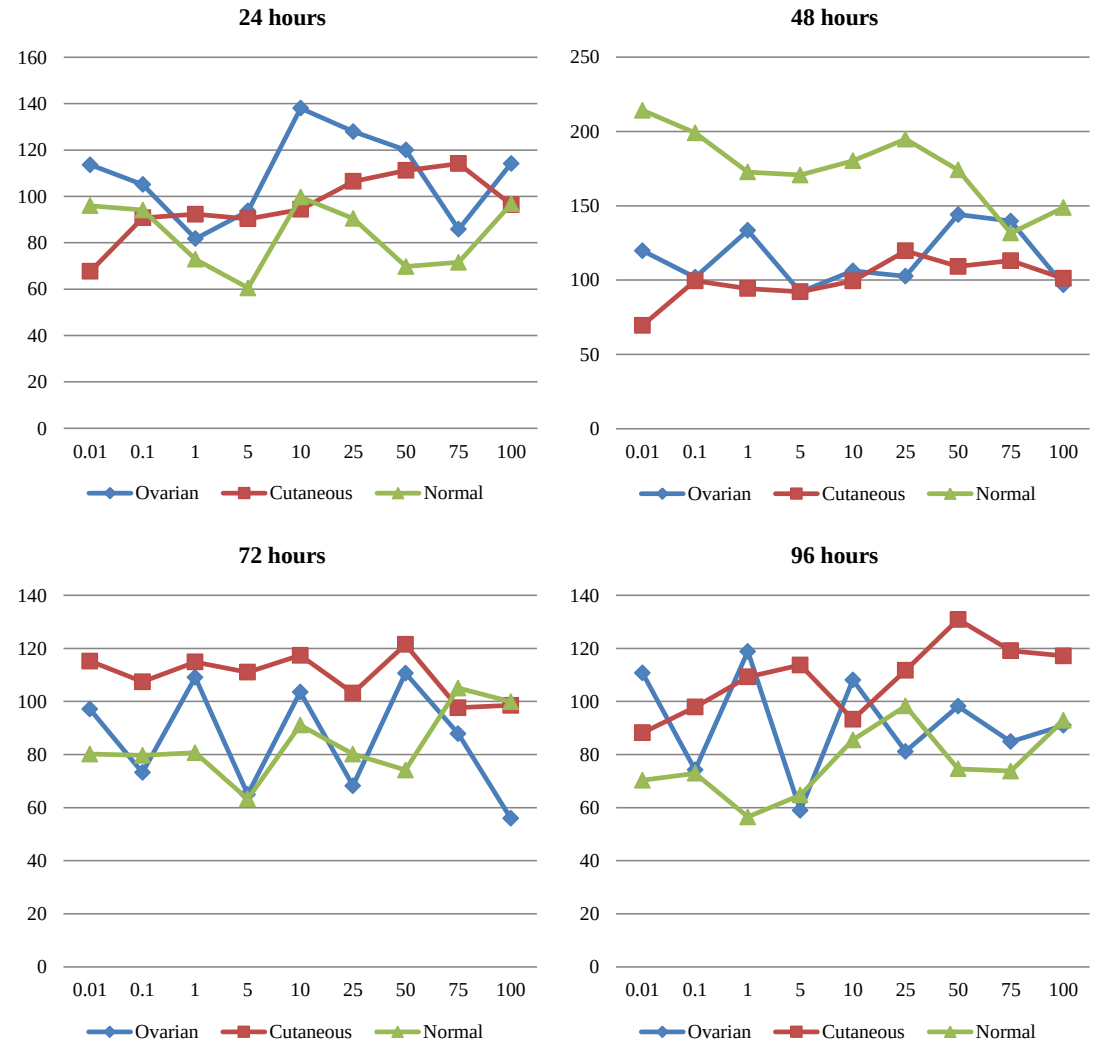

Graphs depicting % cell survival between treated and untreated endometriosis cells with PK11195

These graphs fail to demonstrate a dose dependant effect of treatment with PK11195 on endometriosis. No correlation or response is seen to this drug treatment at any stage of the cellular culture (24 hrs, 48 hrs, 72 hrs or 96 hrs) or to any drug dose. These preliminary tests indicate it is unlikely for PK11195 to have any benefit as a therapeutic in endometriosis.

7.4.4 CO-AAW14

FIGURE 7-9

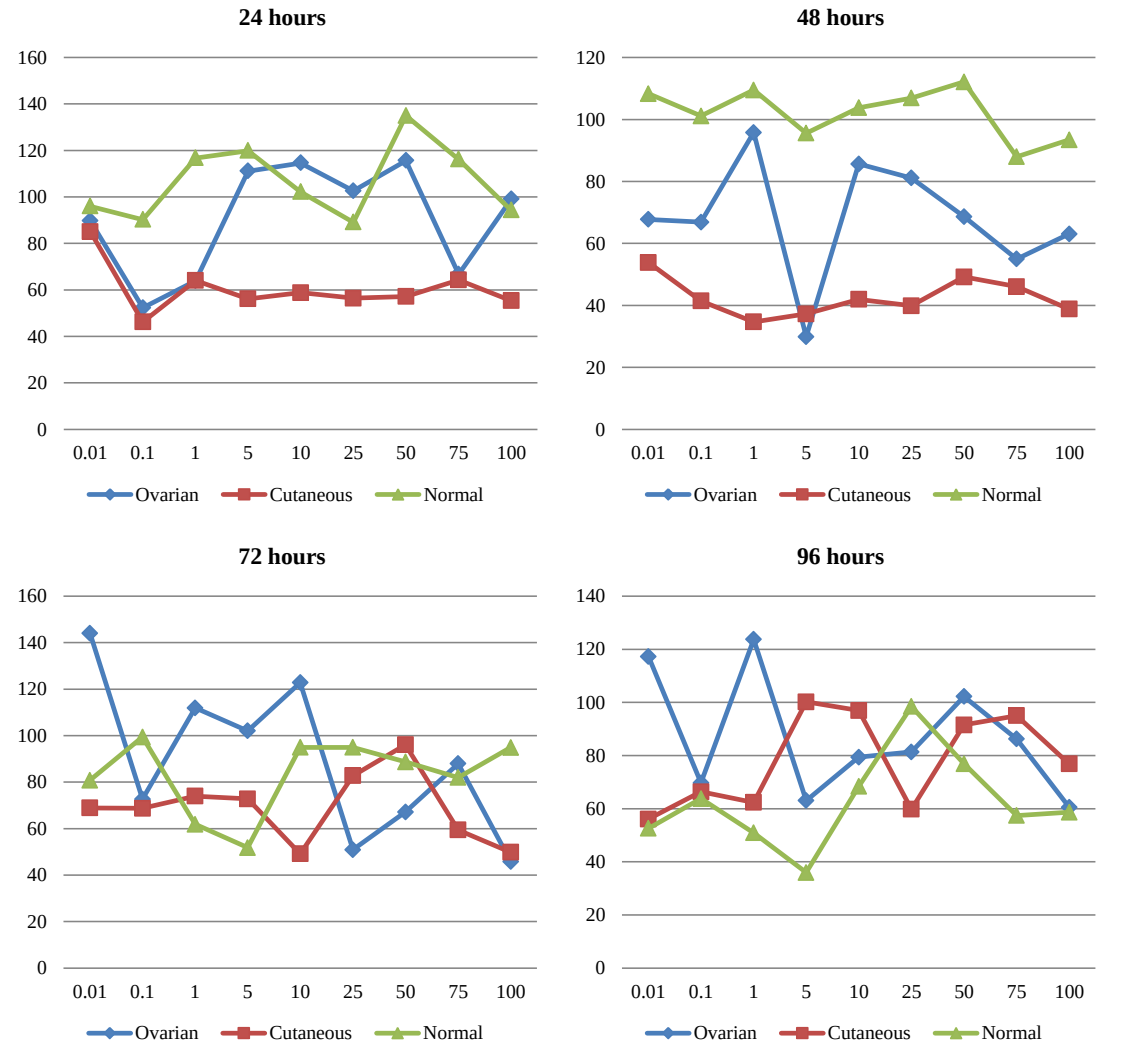

Graphs depicting % cell survival between treated and untreated endometriosis cells with CO-AAW14.

These graphs fail to demonstrate a dose dependant effect of treatment with CO-AAW14 on endometriosis. No correlation or response is seen to this drug treatment at any stage of the cellular culture (24 hrs, 48 hrs, 72 hrs or 96 hrs) or to any drug dose. These preliminary tests indicate it is unlikely for CO-AAW14 to have any benefit as a therapeutic in endometriosis.

7.5 Discussion

7.5.1 GCS-100

GCS-100 is a novel therapeutic that competes against galectin-3, but not galectin-1, off tumour cell surfaces. Manufacturing is required for anti-tumour activity as the unmodified pectin has no anti-tumour activity. GCS-100 binds galectin-3 and has a role in anti-apoptosis, anti-angiogenesis and inhibits cellular migration (Figure 7-10).

FIGURE 7-10

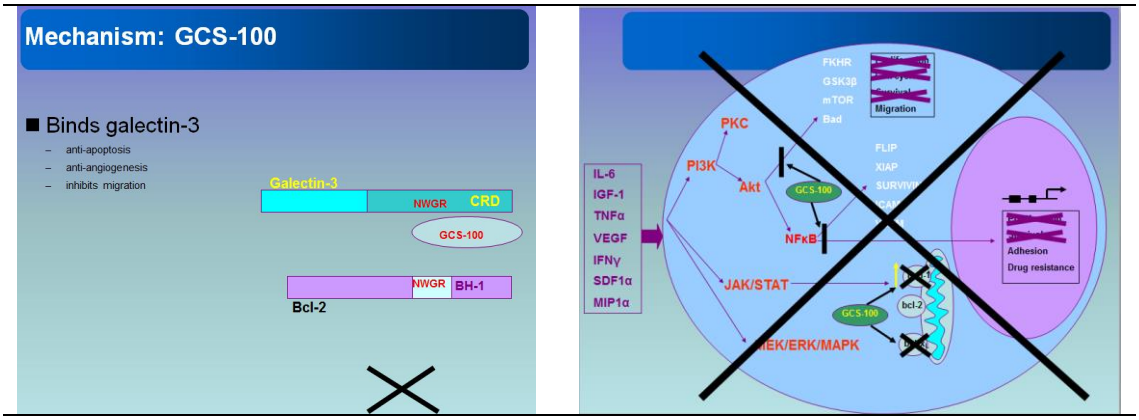

Effects of GCS-100 on cellular function.

In cancers, GCS-100 has a potent anti-myeloma effect where it inhibits cellular proliferation, induces apoptosis, prevents cell cycle progression and reduces mcl-1 and bcl-x_L whilst inducing noxa. It upregulates p21, downregulates cyclin D1, cyclin E2 and interrupts NFκB and akt signalling. The GCS-100 has been identified as a new class of therapeutic molecule as a Galectin 3 antagonist and is already in use for treatment of CLL patients with poor prognostic outlooks who have attempted and not responded optimally to prior therapy. It controls cellular activity related to apoptosis and induces in vivo induction of caspases 8 and 9. It has no myelotoxicity, an acceptable toxicity profile and is also acceptable for elderly CLL. In view of these properties it could be a potentially acceptable treatment in severe forms of endometriosis in women wishing to maintain their fertility. Further trials would be necessary to confirm this in the clinical setting.

FIGURE 7-11

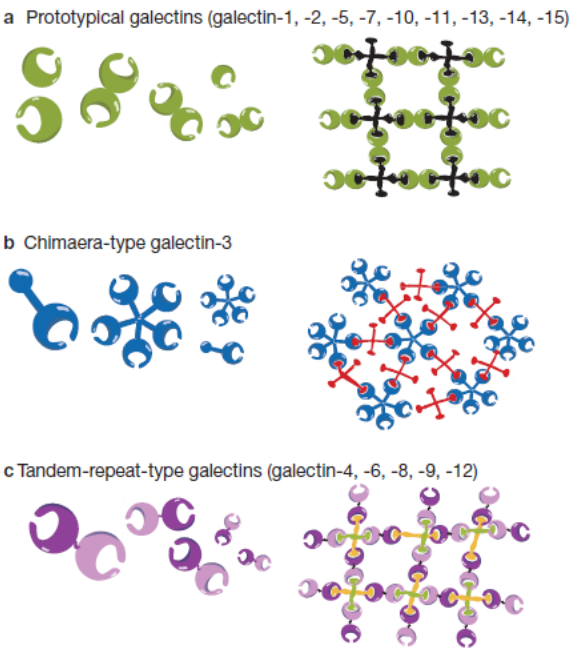

Galectin-glycan lattice formations[849]

Carbohydrates cover the outer cellular surface acting as marker tags to the microenvironment they are in. Carbohydrates are also the trigger for inflammatory reactions within the body and modified or synthetic carbohydrates as well as antibodies have all been used in the attempt of altering cellular functions and controlling disease. Tumorigenic cells utilize carbohydrates to mimic the body's 'normal' cells and escape destruction by the body's immune system. It is once again, these carbohydrates that are involved in inter and intra cellular interactions.

Lectins are highly specific sugar binding proteins, able to detect changes between complex carbohydrate structures[850]. It is this ability that enables them to identify sugars which trigger cellular attachment, migration or invasion[850]. The ability of their monosaccharide units to link in a non-linear fashion at multiple points forming branches enable them to act as cell adhesion and interaction molecules making them an interesting focus for investigations [850].

Galectins are water-soluble proteins and members of the animal lectin family, originating more than 800 million years ago. They were discovered in 1981 in the electric organ of the electric eel Electrophorus electricus[851]. and have conserved their protein architecture and specificity[852] exhibiting specificity for galactosides[852] binding to β-galectosides[849] via their carbohydrate-binding domain (CRD). CRD's are composed of around 130 amino acids responsible for carbohydrate binding. They are able to decipher glycocodes which are sugar structures, triggering certain processes in a given circumstance. Outside the cellular environment they will cause effects on cellular processes by binding to cell surface and extracellular matrix glycans[849] intracellularly. Within the cytosol or cell nucleus, they can regulate cellular functions and intracellular pathways via protein-protein interactions between nucleus and cytosol[849]. Their biological roles are difficult to specify as they correspond to a multitude of diverse biological processes[852]. In total around 15 mammalian galectins have been reported[849,853], of which the best studied are galectin-1 and galectin-3. As yet, there are no characteristic endothelial cell-surface receptors for galectins, though, known ligands include the polylactosamine glycan-containing proteins: laminin, fibronectin, lamp-1, lamp-2, mucin, mac2-binding protein, integrin, CD43, CD45, Cytokeratins and IgE[854].

In 1981, Raz *et al.* observed that cancer cells aggregated in the presence of glycoproteins like asialofetuin and their protein extracts caused haemagglutination[855]. In 1986, the development of a monoclonal antibody to asialofetuin in B16 melanoma cells, inhibited tumour cell aggregation and adhesions[856]. Since then studies showing the expression of galectin-1 and galectin-3 in colon, thyroid and breast carcinomas has been shown, with the expression of galectin-1 being associated with metastatic and poorly differentiated phenotypes. Reports exist showing the association of galectin-3 and head and neck, thyroid, endometrial, gastric, colon and breast cancers. Reports on colon and breast are conflicting[850,857].

FIGURE 7-12

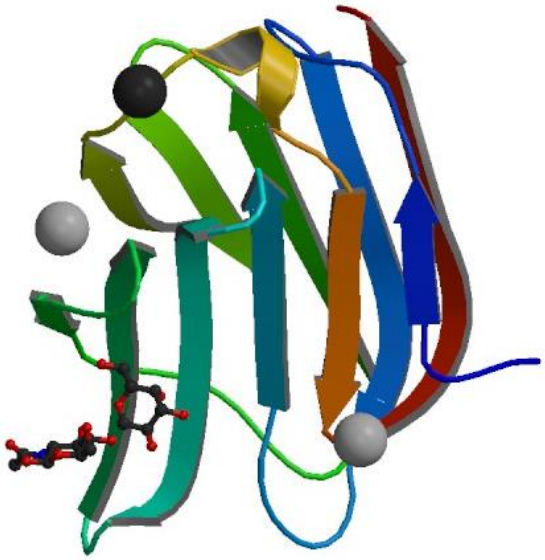

High Resolution X-Ray Structure of Human Galectin-3 in complex with LacNAc (N-Acetyllactosamine)- the key glycocode for galectins[858]

Galectin-3 (Figure 7-12, Figure 7-13) is a member of the family of lectins and is a member of the b-galactose binding protein family. It is structurally, Y shaped making it different to other proteins in its function. It is the only galectin member known so far to have a carbohydrate binding domain (similar to other galectins) with a 20-residue long nonlectin N-terminal [850] and another domain composed of Pro-Gly-Tyr-rich repeating units[850] and is encoded for by the gene LGALS3 on Chromosome 14, locus q21-q22[853,859].

FIGURE 7-13

Galectin-3 structure

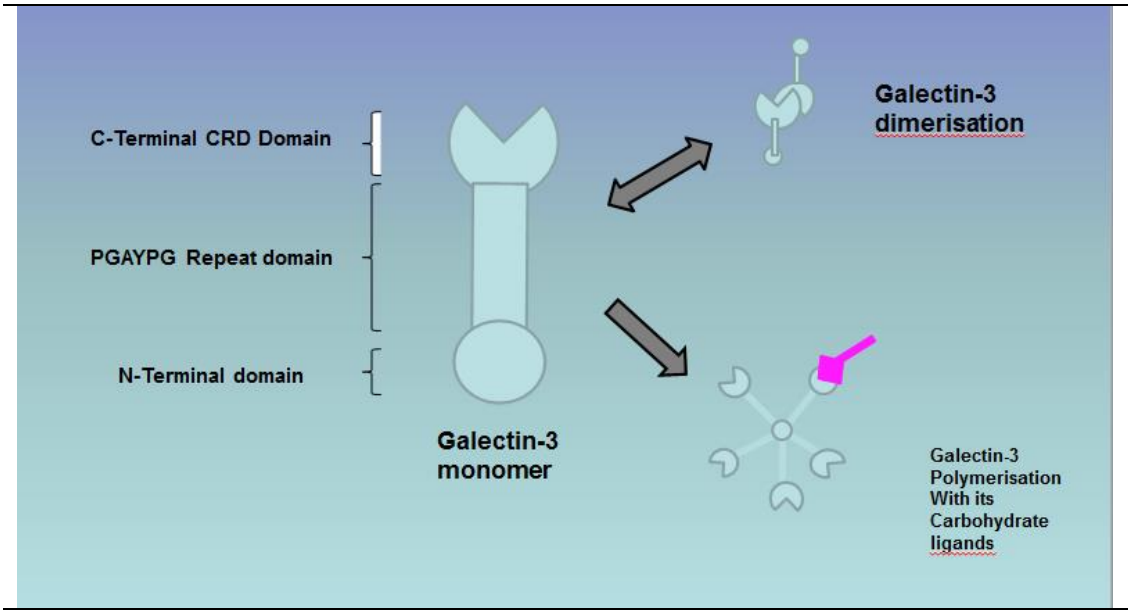

Diagram illustrating the Galectin-3 structure

It is approximately 30kDa and contains a carbohydrate- recognition binding site composed of 130 amino acids which allow the specific binding to β-galactosides[860-862]. The phosphorylation of galectin-3 reduces the binding to its ligands acting as a controlling mechanism for its binding[863].

Galectin 3 is a protein expressed in many types of human cells, especially those of the epithelial and immune systems[864]. It is synthesized in the cytoplasm and shuttles between cytoplasm and nucleus (monomer/dimer). It can be secreted onto the cell surface (multimer) and biological fluids. In the cytoplasm it binds to Bcl-2 to inhibit apoptosis and is involved in Kirsten rat sarcoma viral oncogene homolog (K-Ras) and rat sarcoma viral oncogene homolog (Ras) mediated Akt signalling (dephosphylates AKT). In the nucleus it forms part of the spliceosome assembly via Germin4 and upregulates gene transcription. It is expressed in immune cells, epithelial cells and sensory neurons. MMP-2 and MMP-9 matrix metalloproteases mediate proteolysis of galectin-3 in conjunction with p53.

Galectins, due to their cellular interactions, affect cellular growth and survival and control processes important for the development of invasive pathology. Galectin-3 also has a role in cell cycling and causes Ras activation of Phosphatidylinositide 3-kinases (PI3-K) and Raf-1. It promotes cell cycling by causing b-catenin activation to enhance cyclin D and c-MYC. It has a role in avoidance of immune surveillance by extracellular binding to N-Glycans of monocytes and T cell to induce apoptosis. In metastasis, cells need to detach from the primary tissue, and intravasate into tissues or blood vessels using the cell-matrix adhesion processes. The basement membrane and cell matrix is composed of laminin, fibronectin and collagen IV. Galectin-3 promotes neutrophil attachment to fibronectin and laminin to varying degrees in different tissues[865] with tissues having varied amounts of receptors for galectin-3. It is responsible for tumour adhesion to the extracellular matrix resulting in cytokine release (EGFR, TGFbR). It also binds to transmembrane mucin MUC1 to create ‘nicks’ and cell adhesion in vasculature and results in vascular endothelial growth factor (VEGF) activation. Experiments with Matrigel, a three dimensional matrix derived from basement membrane have shown that Galectin-3 increases cellular invasiveness of breast cancer cells *in vitro*[866] and is also responsible for inducing tumour angiogenesis both *in vitro* and in vivo allowing for cellular dissemination from the original tumour site[867]. Galectin-3 has also been shown to mediate the aggregation of tumour cells forming emboli when induced by the multivalent glycoprotein Asialofetuin[868,869]. It is the only galectin which contains the NWGR domain of the Bcl-2 family which is an anti-apoptotic[870] and may be responsible for the metastatic cell survival of ectopic tissue and infiltrative tumours. Other Galectins such as Galectin-1 induces T-cell apoptosis thereby protecting tumour cells from T-cell destruction[857].

Galectin-3 is over-expressed in human cancer cells of several tissue origins and facilitates their survival, growth, proliferation and migration. It acts as an anti-apoptotic protein protecting cells such as T-cells, macrophages and breast cancer cells from triggers of apoptosis[871]. Studies have indicated that increased levels of circulatory galectin-3 is found in cancer patients and these levels can help in metastasis by enhancing cellular adhesion and avoiding immune surveillance[864]. Over-expression of galectin-3 correlates with tumour aggressiveness and relapse in multiple human cancers and its expression via transfection in animal models increases metastasis. In galectin-$3^{-/-}$ vs. wild-type mice' lung tumorigenesis is reduced. In breast cancer studies, inhibition of Galectin-3 in mouse models showed breast cancer cell

loss of anchorage and serum independent growth. A similar pattern was observed in thyroid papillary cancer models.

Studies assessing for mRNAs have shown that further galectins are implicated in disease and tumour pathology. Colorectal tumours show the presence of galectins-2, 4 and 9[872], neural tumour cell lines express galectin-2 and 4[850] whilst galectin-8 was found in almost all of the tested cell lines[872]. Other galectins such as galectin-12 when expressed ectopically in cancer cells cause cell cycle arrest at the G1 phase and suppress cell growth[873], thereby acting as a regulator for cellular homeostasis (Table 7-2).

TABLE 7-2

Galectin	Associated Pathology
Galectin-1	Tumour astrocyte invasion of the brain parenchyma, Induces T-cell apoptosis[857]
Galectin-2	Fraction of Colorectal tumour cell lines, Neural tumour cell lines
Galectin-3	Breast, Colon, Endometrial, Gastric, Head and Neck, Thyroid, Tumour astrocyte invasion of the brain parenchyma
Galectin-4	Fraction of Colorectal tumour cell lines, Neural tumour cell lines
Galectin-8	Most cell lines[872], Tumour astrocyte invasion of the brain parenchyma
Galectin-9	Fraction of Colorectal tumour cell lines
Galectin-12	Ectopic expression of Galectin-12 in cancer cells causes cell cycle arrest in G1 phase and cell growth suppression[865].

Galectin-3 is seen to be overexpressed in other diseases such as various forms of endometriosis[874]. In this pathology is again believed to play a role in the capacity for cellular invasion, proliferation and angiogenesis similar to tumorigenic mechanisms (Figure 4-23, Figure 4-25).

7.5.2 PK11195, CO-AAW1 and CO-AAW14

Mitochondria have been identified as central players in the process of apoptosis[875] as the Bcl-2 family of proteins preventing apoptosis are localised in the outer mitochondrial membranes and regulate the release of proteins that would enable apoptosis[875]. Carcinoma cells such as cholangiocarcinoma cells are seen to express elevated levels of BcL-X(L) and Mcl-1 antiapoptotic proteins making them resistant to chemo or radiotherapy[875]. Subjects with moderate to severe endometriosis have shown that in the endometrium of women with the disease there is a higher level of expression of Bcl-2, Bax and Mcl-1[876]. These are believed to contribute to prolonged survival of retrograde menstrual cells with the pelvis thus developing the disease.

The use of NADPH oxidase enhancer therapy aims to induce superoxides within mitochondria of tumour cells (independently of the peripheral benzodiazepine receptor) causing their selective apoptosis[877]. Compounds such as PK11195 act on the Caspase 9 apoptosis pathway, interact with mitochondria and result in mitochondrial superoxide generation. PK-11195 is also known as mitochondrial translocator protein (TSPO) and it binds selectively and with high affinity to peripheral benzodiazepine receptors (PBR)[878]. Like Bcl-2 peripheral benzodiazepine receptors (PBRs) reside in the mitochondria and protect cells from apoptotic cell death. PK11195 is seen to chemo sensitise the cells in acute myeloid leukaemias (AML) improving clinical outcomes[879]. CO-AAW1 and CO-AAW14 were other mitochondrial modifiers and NADPH oxidase enhancers which were tested on *in vitro* endometriosis cells. If these compounds

worked effectively on endometrial *in* vitro preliminary studies, they could potentially be explored as novel therapeutics in the field.

As can be viewed from the results (Figure 7-7, Figure 7-8, Figure 7-9) there was no observed cell death response to treatment with CO-AAW1, CO-AAW14 and PK11195 at various concentrations and up to 96 hours post treatments. These do not currently appear promising as potential future therapeutics in endometriosis however their action on eutopic endometrial cells in patients with endometriosis has not been explored. Potentially the reduction of Bcl-2, Bax and Mcl-1 from eutopic endometrial cells could render retrograde menstrual cells less likely to survive and invade, potentially preventing or reducing disease progression rather than causing cellular apoptosis and death.

8 Findings and future work

In this thesis I have shown evidence of the EBV virus being a potential causative factor in the development of endometriosis. EBV-miR-BART2-5p was differentially upregulated in the endometriosis tissue samples when compared to other ectopic and eutopic unaffected tissue. This was confirmed by PCR. In situ hybridisation for EBV on tissue microarrays did not confirm the presence of EBV virus within the endometriotic epithelial cells (Figure 4-19) but 5 of the 42 endometriotic samples on TMA-A gave a positive reading for EBV presence in some of the lymphocytes seen at the base of endometriotic tissue infiltration. Blood taken at surgery was processed and serum and lymphocytes were subsequently separated. RNA extraction with quantitative PCR was performed on the serum lymphocytes to substantiate miRNA tissue findings. PCR on the peripheral blood monocytes confirmed overall higher levels of EBV DNA in the monocytes of people with endometriosis compared to controls. The surgically-confirmed controls showed no EBV presence in the serum (Table 9-39).

The downstream effects of EBV were explored by quantifying expression levels of E-Cadherin, Maspin, BCLAF-1, p53 and cyclin D1 from the endometriosis tissue microarrays. As predicted, E-Cadherin, Maspin and BCLAF-1 are downregulated in endometriosis whereas p53 and Cyclin D1 are elevated in disease. Future studies into the role of EBV and endometriosis could be undertaken. Potentially the exploration and use of a vaccine against EBV could prevent endometriosis formation or regress disease with improvement of the immune response. Immunotherapies for patients with endometriosis are another potential therapeutic route, allowing a healthy immune system to eliminate ectopic cells which develop into endometriosis.

As Galectin-3 is seen to be elevated in many disseminative and metastatic tumours, Galectin-3 expression levels in endometriosis were performed with the aim of potentially using Galectin-3 inhibitors as novel therapeutics for the disease. Galectin-3 was upregulated in endometriotic tissues on my TMA studies. Subsequent *in vitro* endometriosis cellular experimentation from patient primary samples showed a good dose response to the galectin inhibitor GCS-100. This could potentially lead to novel therapeutic approaches to a disease which is as yet only hormonally suppressed but not eliminated. Further *in vitro* and in vivo studies on animal models are required to explore galectin inhibitor potentials as novel therapeutics.

Proteomic antibody studies and miRNA extractions were performed on the serum samples with the aim of identifying a biomarker panel which had enough sensitivity and specificity to be used as a non-invasive test for the presence of disease. Evidence of differential antibody binding between cases and controls were noted and the top eight antibodies were explored at a molecular level to understand their interacting proteins and pathways. The antibodies explored included SH3GL1, aSEPT9, BCAR1, TNFRSF1A, TNFRSF10A, ESR1 and BIRC2.

Endometriosis serum samples were processed for miRNA studies to identify serum miRNAs that were up or down regulated in patients compared to controls. The top 2 downregulated miRNAs by p-value were hsa-miR-150 and hsa-miR-122 whereas the top 2 upregulated miRNAs by p-value included hsa-miR-1224-5p and hsa-miR-4274. Automated logistic regression models were run on the results obtained. A

combined panel composed of a combination of miR-150 and miR-574 and the addition of TPM-1 or RAN (has a marginal improvement) has been identified as a potential non-invasive blood test to identify patients enabling the avoidance of surgery. The panel combining TPM1, hsa-miR-150 and hsa-miR-574p gives a maximum sensitivity of 0.9 and a maximum specificity of 0.75. Care must be taken with any model derived from a small sample set but further studies using this biomarker panel in association with radiological and or clinical findings in the out-patient setting might potentially confirm this panel as a non-invasive diagnostic procedure.

9 Appendix

TABLE 9-1
13 upregulated miRNA in ES samples- follicular phase (*see Section 4.4.1.2.1*)

Name miRNA	P Value
hsa-miR-1	(P=0.0013851)
hsa-miR-22	(P=0.0382426)
hsa-miR-29c	(P=0.0001848)
hsa-miR-99a	(P=0.0031602)
hsa-miR-100	(P=0.0001848)
hsa-miR-126	(P=0.0184264)
hsa-miR-143	(P=0.0031844)
hsa-miR-150	(P=0.0001848)
hsa-miR-193a-5p	(P=0.0189913)
hsa-miR-218	(P=0.0343199)
hsa-miR-376a	(P=0.0327831)
hsa-miR-939	(P=0.0279198)
ebv-miR-BART2-5p	(P=0.0163829)

TABLE 9-2
16 downregulated miRNA in ES samples- follicular phase (*see Section 4.4.1.2.1*)

Name miRNA	P Value
hsa-miR-9	(P=0.0090155)
hsa-miR-96	(P=0.0001848)
hsa-miR-106b	(P=0.0009434)
hsa-miR-135a	(P=0.0382426)
hsa-miR-141	(P=0.0001848)
hsa-miR-183	(P=0.0192309)
hsa-miR-196b	(P=0.0030798)
hsa-miR-200a	(P=0.0021411)
hsa-miR-200b	(P=0.0001848)
hsa-miR-200c	(P=0.0034531)
hsa-miR-203	(P=0.0036471)
hsa-miR-205	(P=0.0090155)
hsa-miR-375	(P=0.0001564)
hsa-miR-429	(P=0.0034531)
hsa-miR-483-3p	(P=0.0009434)
hsa-miR-875-5p	(P=0.0153393)

TABLE 9-3
30 upregulated miRNA in ES samples- luteal phase (*see Section 4.4.1.2.2*)

Name miRNA	P Value
hsa-miR-1	(P=0.0000075)
hsa-miR-10b	(P=0.0422002)
hsa-miR-22	(P=0.0049591)
hsa-miR-23a	(P=0.0007025)
hsa-miR-29c	(P=0.0008691)
hsa-miR-34a	(P=0.0472068)

hsa-miR-95	(P=0.0015269)
hsa-miR-99a	(P=0.0003217)
hsa-miR-100	(P=0.0000001)
hsa-miR-126	(P=0.0002056)
hsa-miR-129-3p	(P=0.0142935)
hsa-miR-133a	(P=0.0240418)
hsa-miR-140-3p	(P=0.0015269)
hsa-miR-140-5p	(P=0.0142935)
hsa-miR-143	(P=0.0000026)
hsa-miR-145	(P=0.0035689)
hsa-miR-146a	(P=0.0013726)
hsa-miR-150	(P=0.0000004)
hsa-miR-152	(P=0.0489491)
hsa-miR-218	(P=0.0087816)
hsa-miR-222	(P=0.0196520)
hsa-miR-223	(P=0.0418717)
hsa-miR-296-5p	(P=0.0108972)
hsa-miR-320a	(P=0.0054891)
hsa-miR-342-3p	(P=0.0215351)
hsa-miR-490-5p	(P=0.0019866)
hsa-miR-520d-3p	(P=0.0051538)
hsa-miR-582-5p	(P=0.0036917)
hsa-miR-623	(P=0.0014631)
hsa-miR-1178	(P=0.0036917)

TABLE 9-4

30 downregulated miRNA in ES samples- luteal phase (*see Section 4.4.1.2.2*)

Name miRNA	P Value
hsa-let-7g	(P=0.0057804)
hsa-miR-9	(P=0.0041952)
hsa-miR-18b	(P=0.0145888)
hsa-miR-19a	(P=0.0498986)
hsa-miR-19b	(P=0.0035689)
hsa-miR-30b	(P=0.0000030)
hsa-miR-30d	(P=0.0036910)
hsa-miR-92a	(P=0.0044340)
hsa-miR-96	(P=0.0000017)
hsa-miR-106b	(P=0.0002197)
hsa-miR-130b	(P=0.0026434)
hsa-miR-141	($P=1.47x10^{-08}$)
hsa-miR-183	(P=0.0077928)
hsa-miR-196b	(P=0.0128738)
hsa-miR-200a	(P=0.0000199)
hsa-miR-200b	(P=0.0000010)
hsa-miR-200c	(P=0.0000146)
hsa-miR-203	(P=0.0000007)
hsa-miR-205	(P=0.0006371)
hsa-miR-210	(P=0.0001025)
hsa-miR-345	(P=0.0017107)
hsa-miR-363	(P=0.0265744)

hsa-miR-375	(P=0.0000004)
hsa-miR-425	(P=0.0061429)
hsa-miR-429	(P=0.0000067)
hsa-miR-449a	(P=0.0299261)
hsa-miR-602	(P=0.0044340)
hsa-miR-646	(P=0.0214837)
hsa-miR-1266	(P=0.0007524)
hsa-miR-1469	(P=0.0498986)

TABLE 9-5

53 upregulated miRNA in OvES samples- follicular phase (*see section 4.4.1.2.4*)

Name miRNA	P Value
hsa-miR-22	(P=0.0269977)
hsa-miR-29c	(P=0.0000081)
hsa-miR-34a	(P=0.0047627)
hsa-miR-99a	(P=0.0240413)
hsa-miR-100	(P=0.0018594)
hsa-miR-146a	(P=0.0012708)
hsa-miR-150	(P=0.0004828)
hsa-miR-154	(P=0.0097972)
hsa-miR-155	(P=0.0004878)
hsa-miR-204	(P=0.0003806)
hsa-miR-211	($P=4.53x10^{-08}$)
hsa-miR-216a	(P=0.0236664)
hsa-miR-223	(P=0.0050572)
hsa-miR-330-5p	(P=0.0000006)
hsa-miR-371-5p	(P=0.0000044)
hsa-miR-376a	(P=0.0003251)
hsa-miR-376c	(P=0.0279803)
hsa-miR-377	(P=0.0033323)
hsa-miR-379	(P=0.0440034)
hsa-miR-421	($P=3.75x10^{-08}$)
hsa-miR-486-3p	(P=0.0023675)
hsa-miR-493	(P=0.0008719)
hsa-miR-507	(P=0.0088743)
hsa-miR-514	(P=0.0013903)
hsa-miR-517a	(P=0.0246943)
hsa-miR-520c-3p	($P=3.10x10^{-09}$)
hsa-miR-520g	(P=0.0282320)
hsa-miR-568	(P=0.0027626)
hsa-miR-569	($P=4.53x10^{-08}$)
hsa-miR-619	(P=0.0178596)
hsa-miR-627	(P=0.0040777)
hsa-miR-629	($P=2.33x10^{-08}$)
hsa-miR-630	(P=0.0000098)
hsa-miR-631	(P=0.0003168)
hsa-miR-635	(P=0.0000154)
hsa-miR-663	(P=0.0047797)
hsa-miR-767-5p	(P=0.0013903)
hsa-miR-939	(P=0.0261161)

hsa-miR-1256	(P=0.0101225)
hsa-miR-1262	(P=0.0018594)
hsa-miR-1263	(P=0.0050428)
hsa-miR-1288	(P=0.0236664)
hsa-miR-1290	(P=0.0086393)
hsa-miR-1297	(P=0.0430781)
hsa-miR-1299	(P=0.0040035)
hsa-miR-1305	(P=0.0035579)
hsa-miR-1975	(P=0.0003998)
hsa-miR-2110	(P=0.0489310)
hsv1-miR-H2-3p	(P=0.0077447)
hsv1-miR-H8	(P=0.0000006)
kshv-miR-K12-4-3p	(P=0.0104343)
kshv-miR-K12-4-5p	(P=0.0081261)
kshv-miR-K12-6-3p	(P=0.0055298)

TABLE 9-6

77 downregulated miRNA in OvES samples- follicular phase (*see section 4.4.1.2.4*)

Name miRNA	P Value
hsa-let-7a	(P=0.0000135)
hsa-let-7d	(P=0.0013903)
hsa-let-7e	($P=2.33x10^{-08}$)
hsa-let-7f	(P=0.0008144)
hsa-let-7g	(P=0.0089419)
hsa-miR-9	(P=0.0003322)
hsa-miR-10a	($P=2.33x10^{-08}$)
hsa-miR-18a	(P=0.0334227)
hsa-miR-18b	(P=0.0071868)
hsa-miR-23b	(P=0.0068376)
hsa-miR-30b	(P=0.0002213)
hsa-miR-31	(P=0.0106252)
hsa-miR-34c-3p	(P=0.0497008)
hsa-miR-34c-5p	(P=0.0026755)
hsa-miR-92b	(P=0.0013903)
hsa-miR-93	(P=0.0033802)
hsa-miR-96	(P=0.0000055)
hsa-miR-106a+hsa-miR-17	(P=0.0156961)
hsa-miR-106b	(P=0.0000081)
hsa-miR-130a	(P=0.0309362)
hsa-miR-130b	(P=0.0113215)
hsa-miR-135a	(P=0.0018594)
hsa-miR-135b	(P=0.0477802)
hsa-miR-139-5p	($P=6.12x10^{-09}$)
hsa-miR-141	($P=6.11x10^{-10}$)
hsa-miR-153	(P=0.0269977)
hsa-miR-183	(P=0.0004793)
hsa-miR-194	(P=0.0021532)
hsa-miR-195	(P=0.0315490)
hsa-miR-196b	(P=0.0000012)
hsa-miR-199b-5p	(P=0.0171636)

hsa-miR-200a	(P=0.0000001)
hsa-miR-200b	($P=3.21x10^{-09}$)
hsa-miR-200c	(P=0.0000001)
hsa-miR-203	(P=0.0000354)
hsa-miR-205	(P=0.0057847)
hsa-miR-219-1-3p	(P=0.0113388)
hsa-miR-219-2-3p	(P=0.0006949)
hsa-miR-219-5p	(P=0.0234177)
hsa-miR-220b	(P=0.0385562)
hsa-miR-221	(P=0.0106250)
hsa-miR-299-5p	(P=0.0308716)
hsa-miR-301a	(P=0.0047474)
hsa-miR-302e	(P=0.0236664)
hsa-miR-323-3p	(P=0.0058083)
hsa-miR-345	(P=0.0009592)
hsa-miR-363	(P=0.0004793)
hsa-miR-375	(P=0.0001810)
hsa-miR-423-3p	(P=0.0002109)
hsa-miR-424	(P=0.0009592)
hsa-miR-425	(P=0.0175318)
hsa-miR-429	(P=0.0000010)
hsa-miR-449a	(P=0.0363696)
hsa-miR-450a	(P=0.0032276)
hsa-miR-454	(P=0.0025762)
hsa-miR-455-3p	(P=0.0060934)
hsa-miR-455-5p	(P=0.0156961)
hsa-miR-483-5p	(P=0.0013038)
hsa-miR-489	(P=0.0035579)
hsa-miR-497	(P=0.0014855)
hsa-miR-505	(P=0.0079510)
hsa-miR-509-3p	(P=0.0153506)
hsa-miR-519d	(P=0.0440034)
hsa-miR-542-3p	(P=0.0035690)
hsa-miR-545	(P=0.0025052)
hsa-miR-588	(P=0.0275377)
hsa-miR-625	(P=0.0004573)
hsa-miR-626	(P=0.0018895)
hsa-miR-720	(P=0.0002386)
hsa-miR-875-5p	(P=0.0440381)
hsa-miR-877	(P=0.0011233)
hsa-miR-1260	(P=0.0089419)
hsa-miR-1266	(P=0.0020872)
hsa-miR-1274a	(P=0.0040035)
hsa-miR-1274b	(P=0.0188569)
hsv1-miR-H1	(P=0.0168708)
kshv-miR-K12-6-5p	(P=0.0269977)

TABLE 9-7

28 upregulated miRNA in OvES samples- luteal phase (*see Section 4.4.1.2.5*)

Name miRNA	P Value
hsa-miR-29c	(P=0.0125318)
hsa-miR-99a	(P=0.0472493)
hsa-miR-100	(P=0.0037619)
hsa-miR-150	(P=0.0305308)
hsa-miR-154	(P=0.0026819)
hsa-miR-199a-3p+hsa-miR-199b-3p	(P=0.0175525)
hsa-miR-211	(P=0.0000008)
hsa-miR-215	(P=0.0357541)
hsa-miR-330-5p	(P=0.0000018)
hsa-miR-337-5p	(P=0.0257030)
hsa-miR-376a	(P=0.0003855)
hsa-miR-376c	(P=0.0026819)
hsa-miR-377	(P=0.0003556)
hsa-miR-379	(P=0.0109079)
hsa-miR-421	($P=4.38x10^{-10}$)
hsa-miR-449b	(P=0.0071211)
hsa-miR-486-3p	(P=0.0410767)
hsa-miR-487a	(P=0.0474365)
hsa-miR-520c-3p	(P=0.0000002)
hsa-miR-569	(P=0.0000019)
hsa-miR-629	(P=0.0000007)
hsa-miR-630	(P=0.0121554)
hsa-miR-635	(P=0.0118206)
hsa-miR-767-5p	(P=0.0001522)
hsa-miR-1262	(P=0.0000005)
hsa-miR-1263	(P=0.0023388)
hsa-miR-1299	(P=0.0129081)
hsv1-miR-H8	(P=0.0000644)

TABLE 9-8

26 downregulated miRNA in OvES samples-luteal phase (*see Section 4.4.1.2.5*)

Name miRNA	P Value
hsa-miR-10a	(P=0.0000393)
hsa-miR-30b	(P=0.0024421)
hsa-miR-30d	(P=0.0363820)
hsa-miR-96	(P=0.0001068)
hsa-miR-106b	(P=0.0001505)
hsa-miR-141	(P=0.0000489)
hsa-miR-183	(P=0.0191037)
hsa-miR-196b	(P=0.0469507)
hsa-miR-200a	(P=0.0001606)
hsa-miR-200b	(P=0.0002046)
hsa-miR-200c	(P=0.0041374)
hsa-miR-203	(P=0.0000393)
hsa-miR-205	(P=0.0257030)
hsa-miR-210	(P=0.0410767)
hsa-miR-375	(P=0.0010806)

hsa-miR-423-3p	(P=0.0026736)
hsa-miR-425	(P=0.0015042)
hsa-miR-429	(P=0.0422405)
hsa-miR-509-3p	(P=0.0111073)
hsa-miR-588	(P=0.0121554)
hsa-miR-642	(P=0.0000154)
hsa-miR-720	(P=0.0035875)
hsa-miR-758	(P=0.0250874)
hsa-miR-1288	(P=0.0000277)
hsa-miR-1911	(P=0.0022848)
hcmv-miR-US33-3p	($P=8.50x10^{-13}$)

TABLE 9-9

Upregulated miRNA in NP from cases- follicular phase (*see Section 4.4.1.2.6*)

Name miRNA	P Value
hsa-miR-211	(P = 0.0208097)

TABLE 9-10

Downregulated miRNA in NP from cases- follicular phase (*see Section 4.4.1.2.6*)

Name miRNA	P Value
hsa-miR-367	(P = 0.0139805)

TABLE 9-11

Significantly expressed miRNA in normal endometrium and fold change (*see Section 4.4.1.3.1*)

Name miRNA	P Value	Fold Change	Log Fold Change
ebv-miR-BART8	(P=0.00505798)	(FC=1.51398464)	(LogFC=0.59835057)
hsa-let-7a	(P=0.00000251)	(FC=1.66597274)	(LogFC=0.73636479)
hsa-let-7b	(P=0.02874230)	(FC=1.19786470)	(LogFC=0.26046497)
hsa-let-7e	(P=0.00057974)	(FC=1.70233796)	(LogFC=0.76751748)
hsa-let-7f	(P=0.00000433)	(FC=1.79790953)	(LogFC=0.84632043)
hsa-let-7g	(P=0.00001000)	(FC=1.76815166)	(LogFC=0.82224203)
hsa-miR-1	(P=0.00000008)	(FC=6.29462395)	(LogFC=-2.65412019)
hsa-miR-100	($P=2.74x10^{-13}$)	(FC=3.44456532)	(LogFC=-1.78432194)
hsa-miR-101	(P=0.04395167)	(FC=1.28667492)	(LogFC=-0.36364760)
hsa-miR-106a+hsa-miR-17	(P=0.00003115)	(FC=1.91814493)	(LogFC=0.93971173)
hsa-miR-106b	($P=3.45x10^{-14}$)	(FC=2.37745983)	(LogFC=1.24942097)
hsa-miR-10a	(P=0.00000007)	(FC=2.05545937)	(LogFC=1.03946086)
hsa-miR-1178	(P=0.01316635)	(FC=1.81625144)	(LogFC=-0.86096394)
hsa-miR-1180	(P=0.01834692)	(FC=1.36879970)	(LogFC=-0.45291135)
hsa-miR-1185	(P=0.01627138)	(FC=1.39505879)	(LogFC=-0.48032592)
hsa-miR-125b	(P=0.03090365)	(FC=1.69368122)	(LogFC=-0.76016236)
hsa-miR-126	(P=0.00000004)	(FC=2.16629361)	(LogFC=-1.11522879)
hsa-miR-1260	(P=0.01864118)	(FC=2.88743529)	(LogFC=1.52978861)
hsa-miR-1262	(P=0.00090990)	(FC=1.53848176)	(LogFC=-0.62150734)
hsa-miR-1263	(P=0.00309516)	(FC=1.31748990)	(LogFC=-0.39779190)
hsa-miR-1266	(P=0.00000007)	(FC=1.70454797)	(LogFC=0.76938920)
hsa-miR-127-3p	(P=0.00342644)	(FC=1.67369141)	(LogFC=-0.74303355)

hsa-miR-1274a	(P=0.00041533)	(FC=4.02352296)	(LogFC=2.00845926)
hsa-miR-1274b	(P=0.00091420)	(FC=3.38463014)	(LogFC=1.75899819)
hsa-miR-1275	(P=0.00026765)	(FC=1.54513439)	(LogFC=0.62773233)
hsa-miR-128	(P=0.01005680)	(FC=1.48242508)	(LogFC=0.56795920)
hsa-miR-1281	(P=0.00946329)	(FC=1.37396588)	(LogFC=-0.45834618)
hsa-miR-129-3p	(P=0.00947061)	(FC=10.94790396)	(LogFC=-3.45258278)
hsa-miR-1299	(P=0.01234786)	(FC=1.42230363)	(LogFC=-0.50822948)
hsa-miR-1305	(P=0.03442910)	(FC=1.44162000)	(LogFC=-0.52769093)
hsa-miR-130b	(P=0.00000588)	(FC=1.70582438)	(LogFC=0.77046912)
hsa-miR-133a	(P=0.00319598)	(FC=2.04985292)	(LogFC=-1.03552040)
hsa-miR-135a	(P=0.00000002)	(FC=3.13844656)	(LogFC=1.65005065)
hsa-miR-135b	(P=0.00000461)	(FC=2.29805013)	(LogFC=1.20041027)
hsa-miR-139-5p	(P=0.00000447)	(FC=2.25767313)	(LogFC=1.17483662)
hsa-miR-140-3p	(P=0.00046038)	(FC=1.57184833)	(LogFC=-0.65246201)
hsa-miR-140-5p	(P=0.01687321)	(FC=1.23734326)	(LogFC=-0.30724578)
hsa-miR-141	($P=1.15x10^{-22}$)	(FC=27.10995536)	(LogFC=4.76075083)
hsa-miR-143	(P=0.00000126)	(FC=2.95555221)	(LogFC=-1.56342771)
hsa-miR-144	(P=0.00729026)	(FC=2.40073058)	(LogFC=1.26347350)
hsa-miR-145	(P=0.00794430)	(FC=2.06035492)	(LogFC=-1.04289288)
hsa-miR-1469	(P=0.00729026)	(FC=1.28232562)	(LogFC=0.35876265)
hsa-miR-146a	(P=0.00000044)	(FC=2.13583598)	(LogFC=-1.09480086)
hsa-miR-148a	(P=0.00680033)	(FC=1.29971423)	(LogFC=-0.37819445)
hsa-miR-148b	(P=0.00710394)	(FC=1.19567568)	(LogFC=-0.25782612)
hsa-miR-150	($P=6.92x10^{-13}$)	(FC=4.99726455)	(LogFC=-2.32113859)
hsa-miR-151-5p	(P=0.00013634)	(FC=1.42348632)	(LogFC=-0.50942862)
hsa-miR-152	(P=0.00003918)	(FC=1.65387694)	(LogFC=-0.72585189)
hsa-miR-154	(P=0.00000014)	(FC=2.07797834)	(LogFC=-1.05518062)
hsa-miR-155	(P=0.00003660)	(FC=1.68026099)	(LogFC=-0.74868534)
hsa-miR-181b+hsa-miR-181d	(P=0.02194210)	(FC=1.20607846)	(LogFC=0.27032376)
hsa-miR-183	(P=0.00000008)	(FC=1.76661962)	(LogFC=0.82099144)
hsa-miR-187	(P=0.01206995)	(FC=1.38144645)	(LogFC=0.46617964)
hsa-miR-18a	(P=0.00000064)	(FC=2.09261706)	(LogFC=1.06530833)
hsa-miR-18b	(P=0.00000007)	(FC=2.21274487)	(LogFC=1.14583712)
hsa-miR-193a-5p	(P=0.00022418)	(FC=1.72439756)	(LogFC=-0.78609243)
hsa-miR-193b	(P=0.00118296)	(FC=1.67671480)	(LogFC=-0.74563731)
hsa-miR-194	(P=0.00051976)	(FC=1.50342974)	(LogFC=0.58825745)
hsa-miR-196b	($P=9.44x10^{-13}$)	(FC=4.07133486)	(LogFC=2.02550189)
hsa-miR-1973	(P=0.01806446)	(FC=1.43412023)	(LogFC=0.52016598)
hsa-miR-1974	(P=0.01302456)	(FC=3.56667486)	(LogFC=1.83457971)
hsa-miR-1975	(P=0.00104324)	(FC=2.06127647)	(LogFC=-1.04353802)
hsa-miR-199b-5p	(P=0.00396826)	(FC=1.51510858)	(LogFC=0.59942119)
hsa-miR-19a	(P=0.00003799)	(FC=1.67866553)	(LogFC=0.74731481)
hsa-miR-19b	(P=0.00000399)	(FC=1.76798464)	(LogFC=0.82210574)
hsa-miR-200a	($P=2.80x10^{-16}$)	(FC=8.36136228)	(LogFC=3.06373801)
hsa-miR-200b	($P=1.50x10^{-21}$)	(FC=15.24448495)	(LogFC=3.93021550)
hsa-miR-200c	($P=3.04x10^{-18}$)	(FC=33.82327084)	(LogFC=5.07994428)
hsa-miR-203	($P=2.36x10^{-11}$)	(FC=2.41024882)	(LogFC=1.26918209)
hsa-miR-204	(P=0.00102080)	(FC=2.43757903)	(LogFC=-1.28544900)
hsa-miR-205	(P=0.00000361)	(FC=2.76944427)	(LogFC=1.46959651)
hsa-miR-20a+hsa-miR-	(P=0.00057185)	(FC=2.56299011)	(LogFC=1.35782791)

20b			
hsa-miR-210	(P=0.00000910)	(FC=2.62326433)	(LogFC=1.39136319)
hsa-miR-211	(P=0.00000250)	(FC=4.55774934)	(LogFC=-2.18832158)
hsa-miR-214	(P=0.04395167)	(FC=1.30330657)	(LogFC=-0.38217649)
hsa-miR-216a	(P=0.01961445)	(FC=1.45760169)	(LogFC=-0.54359653)
hsa-miR-218	(P=0.00124869)	(FC=1.74810606)	(LogFC=-0.80579272)
hsa-miR-219-5p	(P=0.00020553)	(FC=1.46418538)	(LogFC=0.55009822)
hsa-miR-22	(P=0.00000001)	(FC=2.13837562)	(LogFC=-1.09651530)
hsa-miR-220a	(P=0.00609863)	(FC=1.35786358)	(LogFC=-0.44133854)
hsa-miR-220b	(P=0.01022798)	(FC=1.34965902)	(LogFC=0.43259497)
hsa-miR-221	(P=0.00169890)	(FC=1.43940216)	(LogFC=0.52546973)
hsa-miR-222	(P=0.00852146)	(FC=1.28424145)	(LogFC=-0.36091647)
hsa-miR-223	(P=0.00000060)	(FC=6.70247224)	(LogFC=-2.74469334)
hsa-miR-224	(P=0.01058583)	(FC=1.25382357)	(LogFC=-0.32633436)
hsa-miR-23a	(P=0.00000072)	(FC=1.67649015)	(LogFC=-0.74544400)
hsa-miR-23b	(P=0.00087905)	(FC=1.49101153)	(LogFC=0.57629141)
hsa-miR-28-3p	(P=0.01631191)	(FC=1.57218877)	(LogFC=-0.65277445)
hsa-miR-28-5p	(P=0.00272632)	(FC=1.64608020)	(LogFC=-0.71903463)
hsa-miR-296-5p	(P=0.02501809)	(FC=1.23680978)	(LogFC=-0.30662363)
hsa-miR-29c	($P=6.3x10^{-12}$)	(FC=3.06372788)	(LogFC=-1.61528816)
hsa-miR-301a	(P=0.00028807)	(FC=1.40802930)	(LogFC=0.49367736)
hsa-miR-301b	(P=0.00898576)	(FC=1.32002010)	(LogFC=0.40055990)
hsa-miR-302e	(P=0.00680033)	(FC=1.32789486)	(LogFC=0.40914092)
hsa-miR-30b	(P=0.00000011)	(FC=2.34417947)	(LogFC=1.22908303)
hsa-miR-30d	(P=0.02053904)	(FC=1.45193484)	(LogFC=0.53797671)
hsa-miR-31	(P=0.00003557)	(FC=1.98598431)	(LogFC=0.98985422)
hsa-miR-32	(P=0.04257970)	(FC=30.69844914)	(LogFC=4.94009387)
hsa-miR-320a	(P=0.00000011)	(FC=1.69099803)	(LogFC=-0.75787498)
hsa-miR-328	(P=0.04482380)	(FC=1.22842896)	(LogFC=-0.29681443)
hsa-miR-330-5p	(P=0.00000025)	(FC=3.24163632)	(LogFC=-1.69672224)
hsa-miR-337-3p	(P=0.02042418)	(FC=1.38210762)	(LogFC=-0.46686996)
hsa-miR-342-3p	(P=0.02173614)	(FC=1.32852773)	(LogFC=-0.40982834)
hsa-miR-345	(P=0.00000008)	(FC=2.18133862)	(LogFC=1.12521374)
hsa-miR-34a	(P=0.00018088)	(FC=1.58942541)	(LogFC=-0.66850531)
hsa-miR-34c-3p	(P=0.00193474)	(FC=1.54233295)	(LogFC=0.62511424)
hsa-miR-34c-5p	(P=0.00000105)	(FC=2.42715114)	(LogFC=1.27926395)
hsa-miR-363	(P=0.00000629)	(FC=1.69318914)	(LogFC=0.75974314)
hsa-miR-365	(P=0.02469991)	(FC=1.46561829)	(LogFC=-0.55150941)
hsa-miR-371-5p	(P=0.00045085)	(FC=1.69488283)	(LogFC=-0.76118554)
hsa-miR-375	($P=1.87x10^{-14}$)	(FC=6.34376647)	(LogFC=2.66533966)
hsa-miR-376a	(P=0.00000014)	(FC=2.11213730)	(LogFC=-1.07870362)
hsa-miR-376c	(P=0.00027362)	(FC=1.62504948)	(LogFC=-0.70048364)
hsa-miR-377	(P=0.00004983)	(FC=1.84890286)	(LogFC=-0.88666943)
hsa-miR-378	(P=0.00618779)	(FC=1.35163868)	(LogFC=-0.43470954)
hsa-miR-379	(P=0.00015049)	(FC=1.39267807)	(LogFC=-0.47786180)
hsa-miR-381	(P=0.00697682)	(FC=1.49068183)	(LogFC=-0.57597237)
hsa-miR-421	(P=0.00000004)	(FC=2.15076029)	(LogFC=-1.10484674)
hsa-miR-423-3p	(P=0.00000997)	(FC=1.78939141)	(LogFC=0.83946899)
hsa-miR-423-5p	(P=0.00081853)	(FC=1.49420719)	(LogFC=-0.57938021)
hsa-miR-424	(P=0.00004875)	(FC=2.15662398)	(LogFC=1.10877466)
hsa-miR-425	(P=0.00022842)	(FC=1.40247626)	(LogFC=0.48797635)

hsa-miR-429	(P=3.00x10^{-14})	(FC=3.17689769)	(LogFC=1.66761863)
hsa-miR-433	(P=0.01234786)	(FC=1.33707148)	(LogFC=0.41907659)
hsa-miR-449a	(P=0.00000064)	(FC=4.34121499)	(LogFC=2.11809887)
hsa-miR-450a	(P=0.00000716)	(FC=1.94304027)	(LogFC=0.95831580)
hsa-miR-454	(P=0.00025120)	(FC=1.41272601)	(LogFC=0.49848170)
hsa-miR-455-3p	(P=0.00002100)	(FC=1.95771794)	(LogFC=0.96917292)
hsa-miR-455-5p	(P=0.00622594)	(FC=1.77929107)	(LogFC=0.83130254)
hsa-miR-483-3p	(P=0.00000399)	(FC=1.53144924)	(LogFC=0.61489755)
hsa-miR-486-3p	(P=0.00022842)	(FC=1.39297687)	(LogFC=-0.47817130)
hsa-miR-489	(P=0.03313859)	(FC=1.28424696)	(LogFC=0.36092266)
hsa-miR-490-5p	(P=0.00001277)	(FC=1.89015222)	(LogFC=-0.91850242)
hsa-miR-493	(P=0.00113240)	(FC=1.72733529)	(LogFC=-0.78854815)
hsa-miR-495	(P=0.04761080)	(FC=1.32679226)	(LogFC=-0.40794250)
hsa-miR-501-3p	(P=0.00047045)	(FC=1.41586146)	(LogFC=-0.50168011)
hsa-miR-509-3p	(P=0.00001664)	(FC=1.64791112)	(LogFC=0.72063844)
hsa-miR-511	(P=0.01253795)	(FC=1.72851614)	(LogFC=-0.78953408)
hsa-miR-514	(P=0.00092119)	(FC=1.54583722)	(LogFC=-0.62838841)
hsa-miR-518f	(P=0.03006973)	(FC=291.24832021)	(LogFC=8.18610592)
hsa-miR-520c-3p	(P=2.12x10^{-09})	(FC=2.49012180)	(LogFC=-1.31621631)
hsa-miR-520d-3p	(P=0.02062056)	(FC=1.40482132)	(LogFC=-0.49038665)
hsa-miR-532-5p	(P=0.00205317)	(FC=1.43735131)	(LogFC=-0.52341273)
hsa-miR-542-3p	(P=0.00004875)	(FC=1.63741025)	(LogFC=0.71141584)
hsa-miR-542-5p	(P=0.00074125)	(FC=1.48395304)	(LogFC=0.56944544)
hsa-miR-545	(P=0.01243851)	(FC=1.33251796)	(LogFC=0.41415498)
hsa-miR-561	(P=0.02691609)	(FC=302.49915642)	(LogFC=8.24078731)
hsa-miR-569	(P=0.00000002)	(FC=2.63562086)	(LogFC=-1.39814285)
hsa-miR-573	(P=0.02606924)	(FC=1.58470522)	(LogFC=0.66421450)
hsa-miR-574-5p	(P=0.00002085)	(FC=1.55862002)	(LogFC=-0.64026925)
hsa-miR-582-5p	(P=0.00935736)	(FC=1.53014985)	(LogFC=-0.61367294)
hsa-miR-588	(P=0.01565072)	(FC=2.45828384)	(LogFC=1.29765150)
hsa-miR-623	(P=0.00132349)	(FC=1.63377067)	(LogFC=-0.70820548)
hsa-miR-626	(P=0.00000611)	(FC=1.75289086)	(LogFC=0.80973617)
hsa-miR-629	(P=0.00000005)	(FC=1.81536281)	(LogFC=-0.86025791)
hsa-miR-630	(P=0.00000008)	(FC=13.15819204)	(LogFC=-3.71788937)
hsa-miR-631	(P=0.00132349)	(FC=1.53182821)	(LogFC=-0.61525452)
hsa-miR-635	(P=0.00000187)	(FC=2.33055858)	(LogFC=-1.22067578)
hsa-miR-646	(P=0.00020230)	(FC=1.65563126)	(LogFC=0.72738140)
hsa-miR-663	(P=0.00129955)	(FC=2.27550352)	(LogFC=-1.18618582)
hsa-miR-718	(P=0.02830143)	(FC=1.36829178)	(LogFC=-0.45237591)
hsa-miR-720	(P=0.00000150)	(FC=18.57641488)	(LogFC=4.21540019)
hsa-miR-758	(P=0.03839556)	(FC=1.19579837)	(LogFC=0.25797415)
hsa-miR-767-5p	(P=0.00208784)	(FC=1.54925411)	(LogFC=-0.63157379)
hsa-miR-874	(P=0.00011429)	(FC=1.47665695)	(LogFC=-0.56233470)
hsa-miR-875-5p	(P=0.00078619)	(FC=1.34808178)	(LogFC=0.43090802)
hsa-miR-876-3p	(P=0.04478845)	(FC=1.68743170)	(LogFC=0.75482911)
hsa-miR-885-5p	(P=0.00710394)	(FC=1.63775384)	(LogFC=0.71171853)
hsa-miR-891b	(P=0.02514101)	(FC=1.35399557)	(LogFC=0.43722302)
hsa-miR-9	(P=0.00000014)	(FC=2.89372490)	(LogFC=1.53292778)
hsa-miR-92a	(P=0.00312487)	(FC=1.73407725)	(LogFC=0.79416817)
hsa-miR-92b	(P=0.00003723)	(FC=1.79495916)	(LogFC=0.84395102)
hsa-miR-93	(P=0.00002100)	(FC=1.97920113)	(LogFC=0.98491823)

hsa-miR-95	(P=0.00039672)	(FC=1.45269534)	(LogFC=-0.53873217)
hsa-miR-96	(P=$5.25x10^{-14}$)	(FC=2.69472569)	(LogFC=1.43013842)
hsa-miR-98	(P=0.00205317)	(FC=1.44392032)	(LogFC=0.52999113)
hsa-miR-99a	(P=$1.67x10^{-10}$)	(FC=2.39671054)	(LogFC=-1.26105568)
hsv1-miR-H2-3p	(P=0.03442910)	(FC=1.41747184)	(LogFC=-0.50332007)
hsv1-miR-H8	(P=0.00610583)	(FC=1.47639445)	(LogFC=-0.56207822)
kshv-miR-K12-4-5p	(P=0.03794050)	(FC=1.26614194)	(LogFC=-0.34043915)
kshv-miR-K12-6-5p	(P=0.00123390)	(FC=4.48259537)	(LogFC=2.16433428)

TABLE 9-12

Significantly expressed miRNA in normal peritoneum and fold change (*see Section 4.4.1.3.2*)

Name miRNA	P Value	Fold Change	Log Fold Change
ebv-miR-BART15	(P=0.03166570)	(FC=4.44982929)	(LogFC=-2.15374999)
hcmv-miR-UL70-5p	(P=0.03213399)	(FC=1.30856848)	(LogFC=0.38798943)
hcmv-miR-US33-3p	(P=0.00377182)	(FC=1.64159489)	(LogFC=0.71509815)
hsa-let-7c	(P=0.04760847)	(FC=1.46702381)	(LogFC=0.55289229)
hsa-miR-1	(P=0.00007755)	(FC=4.39948016)	(LogFC=2.13733307)
hsa-miR-100	(P=0.00026365)	(FC=1.81437699)	(LogFC=0.85947425)
hsa-miR-10a	(P=0.00000862)	(FC=1.95062707)	(LogFC=0.96393798)
hsa-miR-10b	(P=0.02152117)	(FC=1.46442049)	(LogFC=0.55032986)
hsa-miR-1178	(P=0.03166570)	(FC=1.84276887)	(LogFC=0.88187513)
hsa-miR-1180	(P=0.04760847)	(FC=1.36242964)	(LogFC=0.44618173)
hsa-miR-1246	(P=0.00427491)	(FC=850.56155731)	(LogFC=-9.73227184)
hsa-miR-126	(P=$2.28x10^{-09}$)	(FC=2.65596044)	(LogFC=1.40923366)
hsa-miR-1261	(P=0.04026781)	(FC=1.42943613)	(LogFC=-0.51544616)
hsa-miR-1262	(P=0.00239241)	(FC=1.58374676)	(LogFC=-0.66334167)
hsa-miR-1263	(P=0.04088867)	(FC=1.25645341)	(LogFC=-0.32935717)
hsa-miR-1268	(P=0.01711734)	(FC=1.33957558)	(LogFC=0.42177598)
hsa-miR-1269	(P=0.00498693)	(FC=1.47009977)	(LogFC=0.55591407)
hsa-miR-1290	(P=0.03166570)	(FC=1.86392067)	(LogFC=-0.89834046)
hsa-miR-1299	(P=0.00146646)	(FC=1.66565664)	(LogFC=-0.73609103)
hsa-miR-1305	(P=0.00050420)	(FC=1.95758721)	(LogFC=-0.96907658)
hsa-miR-133a	(P=0.00004862)	(FC=3.15376370)	(LogFC=1.65707457)
hsa-miR-134	(P=0.00073619)	(FC=1.44028363)	(LogFC=0.52635294)
hsa-miR-135a	(P=0.00001016)	(FC=2.67884029)	(LogFC=-1.42160857)
hsa-miR-135b	(P=0.00071256)	(FC=2.00665672)	(LogFC=-1.00479384)
hsa-miR-138	(P=0.01711734)	(FC=1.30080216)	(LogFC=-0.37940156)
hsa-miR-139-5p	(P=0.00000068)	(FC=2.84681614)	(LogFC=1.50934932)
hsa-miR-140-3p	(P=0.00013886)	(FC=1.77409020)	(LogFC=0.82707936)
hsa-miR-140-5p	(P=0.02050398)	(FC=1.27109414)	(LogFC=0.34607088)
hsa-miR-141	(P=$1.87x10^{-13}$)	(FC=8.78104414)	(LogFC=-3.13439250)
hsa-miR-142-5p	(P=0.00508732)	(FC=2.11255675)	(LogFC=-1.07899010)
hsa-miR-143	(P=0.00378696)	(FC=2.06365873)	(LogFC=1.04520441)
hsa-miR-145	(P=0.00155893)	(FC=2.68110576)	(LogFC=1.42282813)
hsa-miR-150	(P=0.00108959)	(FC=2.03478580)	(LogFC=1.02487693)
hsa-miR-151-3p	(P=0.00062258)	(FC=1.45591663)	(LogFC=0.54192774)
hsa-miR-151-5p	(P=0.04474434)	(FC=1.24925157)	(LogFC=0.32106403)
hsa-miR-152	(P=0.04744256)	(FC=1.33653928)	(LogFC=0.41850224)
hsa-miR-1538	(P=0.03236719)	(FC=1.77535290)	(LogFC=0.82810583)
hsa-miR-1539	(P=0.00471221)	(FC=1.55549135)	(LogFC=0.63737037)

hsa-miR-186	(P=0.01711734)	(FC=1.30314068)	(LogFC=0.38199284)
hsa-miR-18a	(P=0.00992899)	(FC=1.53982791)	(LogFC=-0.62276913)
hsa-miR-18b	(P=0.02102226)	(FC=1.45848484)	(LogFC=-0.54447039)
hsa-miR-1915	(P=0.00141685)	(FC=1.59929217)	(LogFC=0.67743353)
hsa-miR-193a-5p	(P=0.00022703)	(FC=1.88059719)	(LogFC=0.91119087)
hsa-miR-195	(P=0.00106319)	(FC=1.58519071)	(LogFC=0.66465642)
hsa-miR-199a-3p+hsa-miR-199b-3p	(P=0.00250134)	(FC=1.49405513)	(LogFC=-0.57923339)
hsa-miR-19a	(P=0.04558562)	(FC=1.35054971)	(LogFC=-0.43354675)
hsa-miR-19b	(P=0.00543809)	(FC=1.47552565)	(LogFC=-0.56122900)
hsa-miR-200a	(P=0.00008231)	(FC=2.46894297)	(LogFC=-1.30389351)
hsa-miR-200b	($P=5.94x10^{-12}$)	(FC=5.59651469)	(LogFC=-2.48452865)
hsa-miR-200c	($P=8.41x10^{-12}$)	(FC=13.73103746)	(LogFC=-3.77936873)
hsa-miR-21	(P=0.00004836)	(FC=2.90353576)	(LogFC=-1.53781080)
hsa-miR-210	(P=0.02033069)	(FC=1.80578908)	(LogFC=-0.85262939)
hsa-miR-211	(P=0.00306621)	(FC=2.93156183)	(LogFC=-1.55166948)
hsa-miR-218	(P=0.00000321)	(FC=2.64151505)	(LogFC=1.40136563)
hsa-miR-219-2-3p	(P=0.00689196)	(FC=2.06366238)	(LogFC=1.04520696)
hsa-miR-22	(P=0.02642698)	(FC=1.37972331)	(LogFC=0.46437897)
hsa-miR-220a	(P=0.00304314)	(FC=1.46084784)	(LogFC=0.54680591)
hsa-miR-222	(P=0.01602688)	(FC=1.30859884)	(LogFC=0.38802289)
hsa-miR-224	(P=0.00002140)	(FC=1.54848879)	(LogFC=0.63086094)
hsa-miR-23a	(P=0.00044730)	(FC=1.50491661)	(LogFC=0.58968355)
hsa-miR-296-5p	(P=0.00002316)	(FC=1.58041221)	(LogFC=0.66030090)
hsa-miR-29c	(P=0.04358816)	(FC=1.40541946)	(LogFC=0.49100078)
hsa-miR-300	(P=0.03166570)	(FC=1.30906842)	(LogFC=0.38854050)
hsa-miR-301a	(P=0.02023188)	(FC=1.29888074)	(LogFC=0.37726897)
hsa-miR-301b	(P=0.01475711)	(FC=1.35535470)	(LogFC=-0.43867046)
hsa-miR-302f	(P=0.03345878)	(FC=1.32181872)	(LogFC=0.40252433)
hsa-miR-31	(P=0.00713714)	(FC=1.67356259)	(LogFC=-0.74292251)
hsa-miR-32	(P=0.00039308)	(FC=759.44619697)	(LogFC=-9.56880395)
hsa-miR-320a	(P=0.00000067)	(FC=1.76339502)	(LogFC=0.81835569)
hsa-miR-328	(P=0.00427006)	(FC=1.38270272)	(LogFC=0.46749101)
hsa-miR-330-5p	(P=0.01399704)	(FC=1.88657227)	(LogFC=-0.91576737)
hsa-miR-34c-5p	(P=0.00263032)	(FC=1.84620376)	(LogFC=-0.88456179)
hsa-miR-361-5p	(P=0.00259442)	(FC=1.68836902)	(LogFC=0.75563026)
hsa-miR-363	(P=0.04853656)	(FC=1.31124026)	(LogFC=0.39093206)
hsa-miR-365	(P=0.00320023)	(FC=1.75953350)	(LogFC=0.81519298)
hsa-miR-371-5p	(P=0.03189548)	(FC=1.46832199)	(LogFC=-0.55416837)
hsa-miR-375	(P=0.00044730)	(FC=2.18842713)	(LogFC=-1.12989434)
hsa-miR-376b	(P=0.00277381)	(FC=1.73438102)	(LogFC=-0.79442088)
hsa-miR-378	(P=0.00000293)	(FC=1.84814554)	(LogFC=0.88607838)
hsa-miR-409-3p	(P=0.02077483)	(FC=1.48187908)	(LogFC=-0.56742773)
hsa-miR-412	(P=0.00277381)	(FC=1.33629271)	(LogFC=0.41823606)
hsa-miR-421	(P=0.00004836)	(FC=1.85311313)	(LogFC=-0.88995096)
hsa-miR-423-5p	(P=0.00027567)	(FC=1.66021005)	(LogFC=0.73136578)
hsa-miR-429	(P=0.00001818)	(FC=1.86460563)	(LogFC=-0.89887053)
hsa-miR-449a	(P=0.00001861)	(FC=4.21583412)	(LogFC=-2.07581810)
hsa-miR-449b	(P=0.00063668)	(FC=1.74437606)	(LogFC=-0.80271109)
hsa-miR-452	(P=0.00907569)	(FC=1.50352235)	(LogFC=0.58834631)
hsa-miR-483-3p	(P=0.04410157)	(FC=1.24435961)	(LogFC=-0.31540347)

hsa-miR-487a	(P=0.03166570)	(FC=1.44122719)	(LogFC=-0.52729777)
hsa-miR-489	(P=0.04358816)	(FC=1.31673202)	(LogFC=0.39696176)
hsa-miR-490-5p	(P=0.00053905)	(FC=1.78129990)	(LogFC=0.83293043)
hsa-miR-493	(P=0.04410157)	(FC=1.50292090)	(LogFC=-0.58776908)
hsa-miR-496	(P=0.03434816)	(FC=1.21155734)	(LogFC=0.27686268)
hsa-miR-497	(P=0.00017353)	(FC=1.48540261)	(LogFC=0.57085402)
hsa-miR-501-3p	(P=0.00001021)	(FC=1.68641188)	(LogFC=0.75395693)
hsa-miR-505	(P=0.02752584)	(FC=1.40256766)	(LogFC=0.48807037)
hsa-miR-509-5p	(P=0.02050398)	(FC=1.52658596)	(LogFC=-0.61030883)
hsa-miR-512-3p	(P=0.04539679)	(FC=1.83121699)	(LogFC=0.87280275)
hsa-miR-517a	(P=0.01550478)	(FC=1.76789342)	(LogFC=-0.82203130)
hsa-miR-519e	(P=0.03033113)	(FC=1.32323486)	(LogFC=0.40406915)
hsa-miR-520c-3p	(P=0.00002140)	(FC=1.99109161)	(LogFC=-0.99355960)
hsa-miR-520d-3p	(P=0.00377182)	(FC=1.61790615)	(LogFC=0.69412793)
hsa-miR-523	(P=0.02033069)	(FC=1.38575601)	(LogFC=0.47067327)
hsa-miR-548i	(P=0.04596312)	(FC=1.40033405)	(LogFC=0.48577102)
hsa-miR-550	(P=0.04720322)	(FC=1.27548667)	(LogFC=0.35104783)
hsa-miR-555	(P=0.02474211)	(FC=1.27395781)	(LogFC=0.34931750)
hsa-miR-568	(P=0.03166570)	(FC=1.38159664)	(LogFC=-0.46633648)
hsa-miR-569	(P=0.00016783)	(FC=2.01589287)	(LogFC=-1.01141897)
hsa-miR-574-5p	(P=0.00693101)	(FC=1.38255987)	(LogFC=0.46734196)
hsa-miR-580	(P=0.00033866)	(FC=1.37352548)	(LogFC=0.45788368)
hsa-miR-582-5p	(P=0.00004862)	(FC=2.14896536)	(LogFC=1.10364222)
hsa-miR-587	(P=0.02642698)	(FC=14.47748321)	(LogFC=3.85573892)
hsa-miR-588	(P=0.00667038)	(FC=3.16315816)	(LogFC=1.66136569)
hsa-miR-609	(P=0.03166570)	(FC=1.28222233)	(LogFC=0.35864644)
hsa-miR-615-5p	(P=0.01711734)	(FC=1.37842810)	(LogFC=0.46302402)
hsa-miR-623	(P=0.00649584)	(FC=1.62717936)	(LogFC=0.70237328)
hsa-miR-625	(P=0.01711734)	(FC=4.71343892)	(LogFC=2.23678003)
hsa-miR-627	(P=0.04760847)	(FC=1.35037162)	(LogFC=-0.43335649)
hsa-miR-629	(P=0.00345662)	(FC=1.41232440)	(LogFC=-0.49807151)
hsa-miR-646	(P=0.02642698)	(FC=1.43122468)	(LogFC=-0.51725017)
hsa-miR-655	(P=0.03166570)	(FC=1.33959340)	(LogFC=0.42179517)
hsa-miR-759	(P=0.00371309)	(FC=1.42582047)	(LogFC=0.51179234)
hsa-miR-767-5p	(P=0.02050398)	(FC=1.48052575)	(LogFC=-0.56610959)
hsa-miR-769-5p	(P=0.00128056)	(FC=1.35360314)	(LogFC=0.43680482)
hsa-miR-802	(P=0.04088867)	(FC=1.31169406)	(LogFC=0.39143127)
hsa-miR-873	(P=0.00158165)	(FC=1.99360769)	(LogFC=0.99538154)
hsa-miR-874	(P=0.01371266)	(FC=1.34256531)	(LogFC=0.42499227)
hsa-miR-888	(P=0.01550478)	(FC=1.35224836)	(LogFC=0.43536015)
hsa-miR-95	(P=0.00108959)	(FC=1.48922696)	(LogFC=0.57456364)
hsa-miR-99a	(P=0.00002316)	(FC=1.82351238)	(LogFC=0.86671999)
hsv1-miR-H4-5p	(P=0.01711734)	(FC=1.23850398)	(LogFC=0.30859851)
hsv1-miR-H8	(P=0.00000007)	(FC=2.54150480)	(LogFC=-1.34568295)
kshv-miR-K12-6-3p	(P=0.02851070)	(FC=1.37485025)	(LogFC=-0.45927449)

TABLE 9-13

Significantly expressed miRNA in peritoneal endometriosis and fold change (*see Section 4.4.1.3.3*)

Name miRNA	P Value	Fold Change	Log Fold Change
ebv-miR-BART2-5p	(P=0.02124769)	(FC=1.44490270)	(LogFC=0.53097235)
hsa-miR-1	(P=0.02013876)	(FC=2.93368027)	(LogFC=1.55271164)
hsa-miR-10a	(P=0.00203621)	(FC=1.70312850)	(LogFC=0.76818729)
hsa-miR-1262	(P=0.02064369)	(FC=1.53933482)	(LogFC=-0.62230707)
hsa-miR-139-5p	(P=0.02142404)	(FC=1.76621442)	(LogFC=0.82066050)
hsa-miR-143	(P=0.02490722)	(FC=2.00499997)	(LogFC=1.00360221)
hsa-miR-145	(P=0.00748715)	(FC=2.70998561)	(LogFC=1.43828519)
hsa-miR-199a-3p+hsa-miR-199b-3p	(P=0.02500682)	(FC=1.44051907)	(LogFC=-0.52658876)
hsa-miR-211	(P=0.01069430)	(FC=3.04857435)	(LogFC=-1.60813473)
hsa-miR-218	(P=0.00120625)	(FC=2.16212172)	(LogFC=1.11244774)
hsa-miR-220a	(P=0.00748715)	(FC=1.50712901)	(LogFC=0.59180292)
hsa-miR-330-5p	(P=0.00572071)	(FC=2.29938576)	(LogFC=-1.20124852)
hsa-miR-421	(P=0.00523286)	(FC=1.65536435)	(LogFC=-0.72714879)
hsa-miR-497	(P=0.01407811)	(FC=1.36887019)	(LogFC=0.45298565)
hsa-miR-520c-3p	(P=0.00258764)	(FC=1.76852812)	(LogFC=-0.82254916)
hsa-miR-564	(P=0.03679057)	(FC=3.87816491)	(LogFC=-1.95537415)
hsa-miR-569	(P=0.00071097)	(FC=2.16693340)	(LogFC=-1.11565482)
hsa-miR-623	(P=0.04123782)	(FC=1.58242248)	(LogFC=0.66213482)
hsa-miR-625	(P=0.03579560)	(FC=5.37709150)	(LogFC=2.42682602)
hsa-miR-629	(P=0.00120625)	(FC=1.57961102)	(LogFC=-0.65956934)
hsa-miR-631	(P=0.01069430)	(FC=1.61059601)	(LogFC=-0.68759467)
hsa-miR-635	(P=0.00523286)	(FC=1.95335047)	(LogFC=-0.96595082)
hsa-miR-767-5p	(P=0.04051340)	(FC=1.53483832)	(LogFC=-0.61808669)
hsa-miR-877	(P=0.02876834)	(FC=16.80983957)	(LogFC=4.07123405)
hsv1-miR-H8	(P=0.00071097)	(FC=1.94775731)	(LogFC=-0.96181393)

TABLE 9-14

Significantly expressed miRNA in ovarian endometriosis and fold change (*see Section 4.4.1.3.4*)

Name miRNA	P Value	Fold Change	Log Fold Change
ebv-miR-BART15	(P=0.04274315)	(FC=9.26498123)	(LogFC=3.21178805)
hcmv-miR-US33-3p	(P=0.00011013)	(FC=2.83049409)	(LogFC=-1.50105391)
hcmv-miR-US33-5p	(P=0.00695055)	(FC=5.00209455)	(LogFC=2.32253233)
hsa-let-7a	(P=0.00005308)	(FC=2.18209584)	(LogFC=-1.12571447)
hsa-let-7d	(P=0.00057564)	(FC=1.64854850)	(LogFC=-0.72119633)
hsa-let-7e	(P=0.00002555)	(FC=3.30773686)	(LogFC=-1.72584447)
hsa-let-7f	(P=0.00172379)	(FC=2.03017362)	(LogFC=-1.02160311)
hsa-let-7g	(P=0.02787527)	(FC=1.68910466)	(LogFC=-0.75625872)
hsa-miR-106a+hsa-miR-17	(P=0.01205552)	(FC=2.05281418)	(LogFC=-1.03760304)
hsa-miR-106b	(P=0.00005627)	(FC=1.97352683)	(LogFC=-0.98077613)
hsa-miR-10a	($P=7.06x10^{-13}$)	(FC=6.82858250)	(LogFC=-2.77158613)
hsa-miR-1185	(P=0.01409928)	(FC=1.84885230)	(LogFC=0.88662998)
hsa-miR-1256	(P=0.00286632)	(FC=3.43541131)	(LogFC=1.78048284)
hsa-miR-1260	(P=0.00723064)	(FC=8.77393890)	(LogFC=-3.13322466)
hsa-miR-1262	(P=0.00000008)	(FC=3.75069011)	(LogFC=1.90715607)
hsa-miR-1263	(P=0.00000838)	(FC=2.15611913)	(LogFC=1.10843689)
hsa-miR-1266	(P=0.01433699)	(FC=1.51655281)	(LogFC=-0.60079574)

hsa-miR-127-3p	(P=0.04274315)	(FC=1.95499755)	(LogFC=0.96716680)
hsa-miR-1274a	(P=0.00541140)	(FC=7.41300549)	(LogFC=-2.89005858)
hsa-miR-1274b	(P=0.04448103)	(FC=4.03859415)	(LogFC=-2.01385317)
hsa-miR-1278	(P=0.03209155)	(FC=1.54443878)	(LogFC=0.62708269)
hsa-miR-128	(P=0.00972947)	(FC=2.05271269)	(LogFC=-1.03753171)
hsa-miR-1290	(P=0.03329579)	(FC=2.63164001)	(LogFC=1.39596215)
hsa-miR-1297	(P=0.01848158)	(FC=3.12675153)	(LogFC=1.64466458)
hsa-miR-1299	(P=0.00001293)	(FC=3.05339394)	(LogFC=1.61041373)
hsa-miR-1305	(P=0.00024794)	(FC=3.03583487)	(LogFC=1.60209332)
hsa-miR-133a	(P=0.01244194)	(FC=3.06779640)	(LogFC=-1.61720274)
hsa-miR-134	(P=0.01351496)	(FC=1.53131307)	(LogFC=-0.61476927)
hsa-miR-139-5p	($P=8.17x10^{-12}$)	(FC=11.35177854)	(LogFC=-3.50484644)
hsa-miR-140-3p	(P=0.04702474)	(FC=1.62467573)	(LogFC=-0.70015180)
hsa-miR-141	(P=0.00001235)	(FC=5.53553258)	(LogFC=-2.46872213)
hsa-miR-142-3p	(P=0.03682150)	(FC=3.13276209)	(LogFC=1.64743521)
hsa-miR-145	(P=0.01129975)	(FC=3.52645942)	(LogFC=-1.81822044)
hsa-miR-1539	(P=0.03300075)	(FC=1.71769594)	(LogFC=-0.78047468)
hsa-miR-154	(P=0.00541140)	(FC=1.95729988)	(LogFC=0.96886481)
hsa-miR-155	(P=0.00001720)	(FC=2.68527870)	(LogFC=1.42507183)
hsa-miR-183	(P=0.01033006)	(FC=1.60345030)	(LogFC=-0.68117963)
hsa-miR-186	(P=0.03205691)	(FC=1.45853255)	(LogFC=-0.54451758)
hsa-miR-194	(P=0.00376535)	(FC=1.86035545)	(LogFC=-0.89557830)
hsa-miR-195	(P=0.00115503)	(FC=2.03698454)	(LogFC=-1.02643503)
hsa-miR-196b	(P=0.00041998)	(FC=2.89640928)	(LogFC=-1.53426548)
hsa-miR-197	(P=0.00631071)	(FC=2.41107277)	(LogFC=-1.26967520)
hsa-miR-1979	(P=0.04970388)	(FC=2.78997168)	(LogFC=-1.48025048)
hsa-miR-199a-3p+hsa-miR-199b-3p	(P=0.00012694)	(FC=2.21277582)	(LogFC=1.14585730)
hsa-miR-200a	(P=0.00001889)	(FC=4.71909595)	(LogFC=-2.23851050)
hsa-miR-200b	(P=0.00001430)	(FC=4.48371093)	(LogFC=-2.16469327)
hsa-miR-200c	(P=0.00113983)	(FC=5.54545860)	(LogFC=-2.47130677)
hsa-miR-203	(P=0.00058047)	(FC=2.04086983)	(LogFC=-1.02918417)
hsa-miR-204	(P=0.00090785)	(FC=5.11456603)	(LogFC=2.35461183)
hsa-miR-21	(P=0.00140219)	(FC=3.64106525)	(LogFC=1.86436060)
hsa-miR-211	($P=1.28x10^{-09}$)	(FC=40.73298962)	(LogFC=5.34812580)
hsa-miR-215	(P=0.03676173)	(FC=1.48354967)	(LogFC=0.56905323)
hsa-miR-218	(P=0.00017217)	(FC=3.26712274)	(LogFC=-1.70802065)
hsa-miR-219-1-3p	(P=0.00667623)	(FC=25.81003296)	(LogFC=-4.68986008)
hsa-miR-219-2-3p	(P=0.00008562)	(FC=5.21336559)	(LogFC=-2.38221503)
hsa-miR-220a	(P=0.01804971)	(FC=1.62143399)	(LogFC=-0.69727029)
hsa-miR-220b	(P=0.00090785)	(FC=1.99775171)	(LogFC=-0.99837729)
hsa-miR-221	(P=0.02635739)	(FC=1.62192245)	(LogFC=-0.69770484)
hsa-miR-223	(P=0.02037932)	(FC=4.84752865)	(LogFC=2.27724943)
hsa-miR-296-3p	(P=0.01351496)	(FC=204.29181029)	(LogFC=-7.67448756)
hsa-miR-296-5p	(P=0.00247925)	(FC=1.65973992)	(LogFC=-0.73095719)
hsa-miR-29a	(P=0.02864948)	(FC=1.83073700)	(LogFC=0.87242455)
hsa-miR-29c	(P=0.00376535)	(FC=2.09582934)	(LogFC=1.06752125)
hsa-miR-301a	(P=0.00050917)	(FC=1.81349031)	(LogFC=-0.85876903)
hsa-miR-30b	(P=0.00034310)	(FC=2.68810940)	(LogFC=-1.42659185)
hsa-miR-31	(P=0.03861175)	(FC=1.89767693)	(LogFC=-0.92423440)
hsa-miR-320c	(P=0.03754534)	(FC=31596.82496976)	(LogFC=14.94749197)

hsa-miR-330-5p	($P=6.35x10^{-10}$)	(FC=14.06208029)	(LogFC=3.81373813)
hsa-miR-337-5p	(P=0.01870955)	(FC=1.93239668)	(LogFC=0.95039128)
hsa-miR-34a	(P=0.00887036)	(FC=1.81003861)	(LogFC=0.85602048)
hsa-miR-361-5p	(P=0.00784110)	(FC=2.07220478)	(LogFC=-1.05116658)
hsa-miR-363	(P=0.00048001)	(FC=2.06715455)	(LogFC=-1.04764626)
hsa-miR-369-3p	(P=0.03767510)	(FC=1.62881316)	(LogFC=0.70382112)
hsa-miR-371-5p	(P=0.00000273)	(FC=3.72049974)	(LogFC=1.89549642)
hsa-miR-376a	(P=0.00008291)	(FC=2.64197179)	(LogFC=1.40161506)
hsa-miR-376c	(P=0.00113843)	(FC=2.19605364)	(LogFC=1.13491330)
hsa-miR-377	(P=0.00015672)	(FC=2.82318381)	(LogFC=1.49732306)
hsa-miR-379	(P=0.01433699)	(FC=1.48152977)	(LogFC=0.56708762)
hsa-miR-409-3p	(P=0.02379735)	(FC=1.83030133)	(LogFC=0.87208119)
hsa-miR-412	(P=0.00331150)	(FC=1.56295392)	(LogFC=-0.64427525)
hsa-miR-421	($P=3.16x10^{-12}$)	(FC=6.59762367)	(LogFC=2.72194649)
hsa-miR-423-3p	(P=0.00000438)	(FC=3.02951545)	(LogFC=-1.59908706)
hsa-miR-424	(P=0.02725434)	(FC=2.18014226)	(LogFC=-1.12442228)
hsa-miR-425	(P=0.03585809)	(FC=1.43772123)	(LogFC=-0.52378396)
hsa-miR-429	(P=0.01278033)	(FC=1.75466486)	(LogFC=-0.81119550)
hsa-miR-449b	(P=0.00239460)	(FC=2.17647818)	(LogFC=1.12199556)
hsa-miR-450b-5p	(P=0.03691754)	(FC=2.04594636)	(LogFC=1.03276832)
hsa-miR-452	(P=0.02646289)	(FC=1.74057844)	(LogFC=-0.79956683)
hsa-miR-454	(P=0.00034310)	(FC=1.84617774)	(LogFC=-0.88454145)
hsa-miR-483-5p	(P=0.00055147)	(FC=4.96787661)	(LogFC=-2.31262934)
hsa-miR-486-3p	(P=0.00113983)	(FC=1.69599243)	(LogFC=0.76212973)
hsa-miR-489	(P=0.00087257)	(FC=1.98093004)	(LogFC=-0.98617793)
hsa-miR-493	(P=0.00004817)	(FC=3.50224887)	(LogFC=1.80828161)
hsa-miR-497	(P=0.00000132)	(FC=2.28158651)	(LogFC=-1.19003736)
hsa-miR-505	(P=0.01173432)	(FC=1.81909493)	(LogFC=-0.86322083)
hsa-miR-507	(P=0.00331150)	(FC=2.07777507)	(LogFC=1.05503948)
hsa-miR-509-3p	(P=0.01205552)	(FC=1.70135718)	(LogFC=-0.76668605)
hsa-miR-514	(P=0.00044094)	(FC=2.31775036)	(LogFC=1.21272518)
hsa-miR-517a	(P=0.00401290)	(FC=2.82193393)	(LogFC=1.49668421)
hsa-miR-517c+hsa-miR-519a	(P=0.01745716)	(FC=1.59580067)	(LogFC=0.67428046)
hsa-miR-519d	(P=0.03205691)	(FC=1.48593033)	(LogFC=-0.57136648)
hsa-miR-520c-3p	($P=6.41x10^{-13}$)	(FC=8.76846963)	(LogFC=3.13232507)
hsa-miR-520g	(P=0.00783409)	(FC=5.36943217)	(LogFC=2.42476953)
hsa-miR-542-3p	(P=0.04376897)	(FC=1.58397276)	(LogFC=-0.66354752)
hsa-miR-545	(P=0.03650825)	(FC=1.56201824)	(LogFC=-0.64341130)
hsa-miR-550	(P=0.02278982)	(FC=1.54209764)	(LogFC=-0.62489411)
hsa-miR-568	(P=0.00331150)	(FC=1.96519682)	(LogFC=0.97467381)
hsa-miR-569	($P=7.06x10^{-13}$)	(FC=11.51319733)	(LogFC=3.52521663)
hsa-miR-576-5p	(P=0.03925952)	(FC=1.37065706)	(LogFC=-0.45486766)
hsa-miR-577	(P=0.00461837)	(FC=1.78629697)	(LogFC=0.83697195)
hsa-miR-580	(P=0.01351496)	(FC=1.41620522)	(LogFC=-0.50203034)
hsa-miR-582-5p	(P=0.00784110)	(FC=2.19718662)	(LogFC=-1.13565741)
hsa-miR-588	(P=0.00029757)	(FC=11.01447486)	(LogFC=-3.46132881)
hsa-miR-604	(P=0.01020216)	(FC=44.96461933)	(LogFC=-5.49071835)
hsa-miR-610	(P=0.01745716)	(FC=1.58835399)	(LogFC=0.66753247)
hsa-miR-619	(P=0.02191077)	(FC=1.82612430)	(LogFC=0.86878497)
hsa-miR-625	(P=0.00011013)	(FC=47.23736529)	(LogFC=-5.56185659)

hsa-miR-626	(P=0.00172379)	(FC=1.99519480)	(LogFC=-0.99652961)
hsa-miR-627	(P=0.00069505)	(FC=2.17518929)	(LogFC=1.12114095)
hsa-miR-629	($P=1.27x10^{-11}$)	(FC=4.04993500)	(LogFC=2.01789875)
hsa-miR-630	(P=0.00000206)	(FC=55.77586944)	(LogFC=5.80156919)
hsa-miR-631	(P=0.00002558)	(FC=2.79663502)	(LogFC=1.48369198)
hsa-miR-635	(P=0.00000001)	(FC=6.64105997)	(LogFC=2.73141353)
hsa-miR-663	(P=0.02284477)	(FC=2.96875903)	(LogFC=1.56986000)
hsa-miR-720	(P=0.00010492)	(FC=64.26142697)	(LogFC=-6.00588111)
hsa-miR-758	(P=0.02379735)	(FC=1.41781663)	(LogFC=-0.50367096)
hsa-miR-767-5p	(P=0.00000230)	(FC=3.52047492)	(LogFC=1.81577006)
hsa-miR-873	(P=0.00469475)	(FC=2.64852072)	(LogFC=-1.40518679)
hsa-miR-876-3p	(P=0.03600156)	(FC=2.67292678)	(LogFC=-1.41842032)
hsa-miR-877	(P=0.00115850)	(FC=191.43675038)	(LogFC=-7.58072400)
hsa-miR-9	(P=0.03948874)	(FC=2.09988134)	(LogFC=-1.07030780)
hsa-miR-92b	(P=0.00383932)	(FC=2.10020022)	(LogFC=-1.07052687)
hsa-miR-96	(P=0.00107762)	(FC=1.88864082)	(LogFC=-0.91734836)
hsv1-miR-H1	(P=0.03948874)	(FC=1.49996142)	(LogFC=-0.58492539)
hsv1-miR-H8	($P=6.22x10^{-12}$)	(FC=7.30849882)	(LogFC=2.86957510)
kshv-miR-K12-6-3p	(P=0.02037932)	(FC=1.68877664)	(LogFC=0.75597853)

TABLE 9-15

T-test results for case vs. control markers sorted by p-value order (*see Section 6.4.3*)

Protein name	p-value	Corrected p-value	Fold change	Log fold change
CCNB1IP1	0.002807	1.00	0.98	**-0.02**
TPM1	0.003941	1.00	1.08	**0.07**
RORC	0.005463	1.00	0.96	**-0.04**
TAOK3	0.006992	1.00	0.98	**-0.02**
HSPD1	0.010996	1.00	0.97	**-0.03**
PAX8	0.011430	1.00	0.97	**-0.03**
NFYA	0.011460	1.00	0.98	**-0.02**
ADSL	0.013800	1.00	1.03	**0.03**
TRAF4	0.013886	1.00	0.98	**-0.02**
GTF2H2	0.014579	1.00	0.98	**-0.02**
USP10	0.016934	1.00	0.97	**-0.03**
SRPK1	0.017187	1.00	0.96	**-0.04**
CLK2	0.019237	1.00	0.98	**-0.02**
CKB	0.021877	1.00	1.02	**0.02**
ZNF41	0.022582	1.00	0.98	**-0.02**
LYL1	0.023566	1.00	0.98	**-0.02**
HRSP12	0.024406	1.00	1.03	**0.03**
RB1	0.025281	1.00	0.98	**-0.02**
AIFM2	0.025824	1.00	1.01	**0.01**
NRAS	0.026865	1.00	1.01	**0.01**
SCP2	0.027430	1.00	0.98	**-0.02**
SOD2	0.027801	1.00	1.04	**0.04**
PYGO2	0.028127	1.00	0.96	**-0.04**
CDK17	0.030821	1.00	0.99	**-0.01**
ALDOA	0.032673	1.00	1.05	**0.05**
NRIP1	0.033093	1.00	0.98	**-0.02**

NAE1	0.033858	1.00	0.98	**-0.02**
PHF1	0.037199	1.00	0.99	**-0.01**
TRAIP	0.039599	1.00	0.98	**-0.02**
FRK	0.039671	1.00	0.99	**-0.01**
UCK2	0.039842	1.00	1.03	**0.03**
TRIM37	0.041163	1.00	1.02	**0.02**
PRPF4	0.042537	1.00	0.99	**-0.01**
ATF3	0.046101	1.00	0.98	**-0.02**
OAS2	0.046106	1.00	0.99	**-0.01**
STUB1	0.047036	1.00	1.04	**0.04**
LDB1	0.048186	1.00	0.99	**-0.01**
SORD	0.050008	1.00	1.03	**0.03**
LDHB	0.051880	1.00	1.05	**0.05**
ZBTB16	0.053215	1.00	0.98	**-0.02**
PLK4	0.053267	1.00	0.99	**-0.01**
CAMKK1	0.053530	1.00	0.99	**-0.01**
FIGF	0.053897	1.00	0.99	**-0.01**
PTRH1	0.055434	1.00	0.99	**-0.01**
NEK3	0.056092	1.00	0.99	**-0.01**
PBK	0.056408	1.00	0.99	**-0.01**
TPM3	0.056646	1.00	1.03	**0.03**
HIPK1	0.057070	1.00	0.98	**-0.02**
FUS	0.058571	1.00	0.99	**-0.01**
PABPC1	0.058655	1.00	1.01	**0.01**
SKAP1	0.059064	1.00	0.99	**-0.01**
TESK2	0.059406	1.00	0.99	**-0.01**
MYCBP	0.062102	1.00	1.04	**0.04**
DNAJA1	0.062594	1.00	0.98	**-0.02**
GATA3	0.062761	1.00	0.99	**-0.01**
RPL32_a	0.063192	1.00	0.99	**-0.01**
POU2F2	0.063701	1.00	0.99	**-0.01**
TBX5	0.063718	1.00	0.98	**-0.02**
RAN	0.064147	1.00	1.04	**0.04**
MRPL55	0.065470	1.00	0.98	**-0.02**
PSMB8	0.066103	1.00	0.98	**-0.02**
ZNF256	0.066803	1.00	0.98	**-0.02**
NEUROD1	0.067362	1.00	1.02	**0.02**
STAU1	0.067895	1.00	0.98	**-0.02**
IRAK1	0.068050	1.00	0.99	**-0.01**
PXK	0.068444	1.00	0.99	**-0.01**
ELMOD1	0.068633	1.00	0.99	**-0.01**
KLHL12	0.069825	1.00	1.01	**0.01**
FGFR2	0.072433	1.00	0.99	**-0.01**
PPP4C	0.073516	1.00	0.98	**-0.02**
ACVR1	0.075101	1.00	0.99	**-0.01**
PMF1	0.076364	1.00	1.02	**0.02**
STAP1	0.079181	1.00	0.97	**-0.04**
MAK	0.079426	1.00	0.99	**-0.01**
MMP2	0.080359	1.00	0.99	**-0.01**
TK1	0.081251	1.00	1.02	**0.02**
AK1	0.082886	1.00	1.03	**0.03**

PHF5A	0.083015	1.00	0.98	**-0.02**
ZNF136	0.084197	1.00	0.99	**-0.01**
SUB1	0.085490	1.00	1.02	**0.02**
C9orf86	0.086850	1.00	0.98	**-0.02**
GOLGA5	0.086962	1.00	0.96	**-0.04**
ULK4	0.088482	1.00	0.99	**-0.01**
GOT1	0.088825	1.00	1.06	**0.06**
PLK2	0.090354	1.00	0.98	**-0.02**
SPEG	0.093581	1.00	1.04	**0.04**
TFAP4	0.094240	1.00	0.99	**-0.01**
NICN1	0.094550	1.00	0.99	**-0.01**
SIX1	0.096227	1.00	0.99	**-0.01**
RUNX1T1	0.096594	1.00	1.05	**0.05**
DUSP11	0.096795	1.00	0.99	**-0.01**
HSBP1	0.096820	1.00	1.03	**0.03**
TEAD2	0.097905	1.00	0.99	**-0.01**
HBG1	0.098070	1.00	1.01	**0.01**
ZNF169	0.098227	1.00	0.99	**-0.01**
SPIB	0.101508	1.00	0.99	**-0.01**
GAS7	0.101595	1.00	1.03	**0.03**
SPIC	0.101600	1.00	0.99	**-0.01**
SEPT9	0.102420	1.00	1.06	**0.06**
MATK	0.102895	1.00	0.97	**-0.03**
ELL3	0.103348	1.00	0.99	**-0.01**
DBNL	0.103447	1.00	0.98	**-0.02**
TOM1	0.104294	1.00	0.96	**-0.04**
PYCR1	0.104565	1.00	1.04	**0.04**
PTK2	0.105873	1.00	0.99	**-0.01**
SH2B1	0.106135	1.00	0.97	**-0.03**
UHMK1	0.106174	1.00	0.99	**-0.01**
TRAF3IP1	0.106483	1.00	0.98	**-0.02**
CKMT2	0.107279	1.00	1.02	**0.02**
CARD8	0.108018	1.00	0.98	**-0.02**
MASTL	0.109469	1.00	0.97	**-0.03**
CBFB	0.109950	1.00	1.02	**0.02**
KLF10	0.110097	1.00	0.99	**-0.01**
TGIF1	0.111268	1.00	0.99	**-0.01**
SRC	0.111374	1.00	0.99	**-0.01**
C19orf50	0.111633	1.00	1.04	**0.04**
ZKSCAN5	0.111805	1.00	0.99	**-0.01**
IL1RN	0.113150	1.00	1.04	**0.04**
RBKS	0.113307	1.00	1.02	**0.02**
PDPK1_a	0.113863	1.00	0.98	**-0.02**
ALOX15	0.114014	1.00	0.99	**-0.02**
CA1	0.114095	1.00	1.04	**0.04**
VPS4A	0.114444	1.00	0.98	**-0.02**
ZKSCAN3	0.116107	1.00	0.99	**-0.01**
IMPA1	0.117900	1.00	1.05	**0.05**
ELF2	0.119761	1.00	0.99	**-0.01**
CSNK1G2_a	0.120027	1.00	0.97	**-0.03**
ZMYM2	0.120208	1.00	0.99	**-0.01**

DNM2_a	0.120485	1.00	0.97	**-0.03**
DR1	0.120701	1.00	1.03	**0.03**
HSP90AA1	0.120812	1.00	1.04	**0.04**
SSBP4	0.122833	1.00	1.02	**0.02**
CASP3	0.122956	1.00	1.01	**0.01**
TCEB3	0.123697	1.00	0.99	**-0.01**
FAF1	0.123772	1.00	1.02	**0.02**
RET_a	0.123843	1.00	0.99	**-0.01**
NFIL3	0.124791	1.00	0.99	**-0.01**
MLLT6	0.125509	1.00	0.97	**-0.03**
BTRC	0.126221	1.00	0.99	**-0.01**
DDB1	0.126661	1.00	1.02	**0.02**
MKNK1	0.127039	1.00	1.02	**0.02**
CASP6	0.128854	1.00	1.04	**0.04**
PHTF1	0.128947	1.00	0.99	**-0.01**
OXSR1	0.129588	1.00	0.99	**-0.01**
PCBD1	0.130100	1.00	1.04	**0.04**
NCF2	0.130350	1.00	1.03	**0.03**
BPI	0.130402	1.00	0.98	**-0.02**
IRF4	0.130919	1.00	0.99	**-0.01**
NUAK2	0.133718	1.00	0.99	**-0.01**
HPRT1	0.133728	1.00	1.02	**0.02**
FOXN2	0.134132	1.00	0.98	**-0.02**
SOX10	0.134402	1.00	0.98	**-0.02**
CTNNB1	0.135058	1.00	1.01	**0.01**
PPP4R1	0.135170	1.00	0.99	**-0.01**
FH	0.135342	1.00	1.01	**0.01**
CASP10	0.136204	1.00	1.04	**0.04**
GCLC	0.136875	1.00	0.99	**-0.01**
TRIP6	0.137645	1.00	1.03	**0.03**
RAC1	0.137871	1.00	0.97	**-0.03**
GNB1	0.139308	1.00	0.99	**-0.01**
PANK3	0.140779	1.00	1.02	**0.02**
CKS1B	0.141110	1.00	1.04	**0.04**
TAF6L	0.142368	1.00	0.99	**-0.01**
NEK11	0.143246	1.00	0.99	**-0.01**
VCL_a	0.143818	1.00	0.98	**-0.03**
SOCS6	0.146584	1.00	0.97	**-0.03**
SIVA1	0.146763	1.00	0.99	**-0.01**
PSME3	0.148445	1.00	1.05	**0.05**
C1D	0.149470	1.00	1.03	**0.03**
LCP1	0.149534	1.00	1.03	**0.03**
TGIF2	0.150022	1.00	0.99	**-0.01**
IL1B	0.150519	1.00	0.98	**-0.02**
MST4	0.152533	1.00	1.01	**0.01**
HSF1	0.152941	1.00	1.01	**0.01**
PDIK1L	0.153873	1.00	0.99	**-0.01**
PPP3CC	0.154156	1.00	0.99	**-0.01**
HES6	0.154676	1.00	0.98	**-0.02**
UBA1	0.155584	1.00	1.02	**0.02**
RPS7	0.156440	1.00	0.99	**-0.01**

CAMKK2	0.156536	1.00	0.98	**-0.02**
PDK3	0.158920	1.00	0.99	**-0.01**
CLK3	0.159879	1.00	0.98	**-0.02**
MGC42105	0.160743	1.00	0.99	**-0.01**
IFIT5	0.161973	1.00	0.99	**-0.01**
ACAT2	0.163506	1.00	1.03	**0.03**
TFDP2	0.163933	1.00	0.99	**-0.01**
NDRG1	0.164144	1.00	0.99	**-0.01**
HEXIM1	0.164628	1.00	0.98	**-0.02**
MEIS3	0.164737	1.00	0.99	**-0.01**
CTBP2	0.165147	1.00	0.99	**-0.01**
MAPK9	0.165644	1.00	0.96	**-0.04**
NME6	0.166358	1.00	0.99	**-0.01**
TFG	0.168621	1.00	1.03	**0.03**
SH3BGRL3	0.169277	1.00	1.04	**0.03**
BRSK2	0.169837	1.00	0.99	**-0.01**
DCLK2	0.170721	1.00	0.97	**-0.03**
APEX1	0.171565	1.00	0.96	**-0.04**
COTL1	0.174623	1.00	1.04	**0.04**
TBPL1	0.175229	1.00	0.99	**-0.01**
CDK2	0.175559	1.00	0.97	**-0.03**
KLF12	0.175740	1.00	0.99	**-0.01**
UTP14A	0.176145	1.00	1.01	**0.01**
ACVR1C	0.177508	1.00	0.99	**-0.01**
BAG3	0.177707	1.00	0.98	**-0.02**
CHST4	0.178392	1.00	0.99	**-0.01**
EIF4A2	0.178909	1.00	1.02	**0.02**
AMOTL2	0.179267	1.00	0.96	**-0.04**
NCOA4	0.180602	1.00	0.99	**-0.01**
PLAGL2	0.180865	1.00	0.99	**-0.01**
LY86	0.181431	1.00	1.01	**0.01**
MTMR2	0.181763	1.00	0.99	**-0.01**
RIOK2	0.182129	1.00	0.99	**-0.01**
PDE4A_a	0.182835	1.00	0.98	**-0.02**
FMNL2	0.183752	1.00	0.99	**-0.01**
PLK1	0.184295	1.00	0.98	**-0.02**
MYST2	0.185678	1.00	0.99	**-0.01**
EIF4EBP1	0.185958	1.00	1.03	**0.03**
ELF5	0.187441	1.00	0.99	**-0.01**
LMNA	0.188709	1.00	0.97	**-0.03**
GNAZ_a	0.188909	1.00	0.98	**-0.02**
NPM1	0.189684	1.00	1.02	**0.02**
ARRB1_a	0.191127	1.00	0.98	**-0.02**
NR1D2	0.192498	1.00	0.98	**-0.02**
TARDBP	0.195030	1.00	1.01	**0.01**
NFKBIA	0.196295	1.00	0.99	**-0.01**
TNFAIP8	0.197579	1.00	1.07	**0.07**
CDK9	0.197952	1.00	0.99	**-0.01**
VDR	0.198109	1.00	0.99	**-0.01**
HIF3A	0.198322	1.00	0.99	**-0.01**
S100A8	0.198542	1.00	1.01	**0.01**

NME7	0.198913	1.00	0.98	**-0.02**
ATF5	0.199253	1.00	0.99	**-0.01**
GNA15	0.199263	1.00	0.99	**-0.01**
DCDC2	0.200802	1.00	0.97	**-0.03**
GSTT1	0.201117	1.00	0.99	**-0.01**
ATF4	0.202754	1.00	0.99	**-0.01**
APOBEC3G	0.203715	1.00	1.02	**0.02**
CASP3_a	0.203715	1.00	0.98	**-0.02**
ZNF346	0.204347	1.00	1.02	**0.02**
ASNA1	0.204865	1.00	1.01	**0.01**
CXXC1	0.205840	1.00	0.99	**-0.01**
MOBKL3	0.206873	1.00	1.02	**0.02**
TPM4	0.207506	1.00	1.04	**0.04**
CDK5R1	0.208172	1.00	0.99	**-0.01**
FAM50B	0.209952	1.00	1.02	**0.02**
ARHGDIB	0.212284	1.00	1.03	**0.03**
IL24	0.213109	1.00	1.01	**0.01**
NRF1	0.213713	1.00	0.99	**-0.01**
GRK5	0.214371	1.00	0.99	**-0.01**
KATNB1	0.214382	1.00	1.02	**0.02**
BAG4	0.214793	1.00	1.02	**0.02**
CUL1	0.215897	1.00	1.03	**0.03**
PIM2	0.216470	1.00	0.98	**-0.02**
ILF2	0.216553	1.00	1.04	**0.04**
PPAT_a	0.217838	1.00	0.98	**-0.02**
IRF2	0.218457	1.00	0.99	**-0.01**
SGK2	0.218552	1.00	0.99	**-0.01**
DNAJA2	0.218925	1.00	0.99	**-0.01**
ZFP36L1	0.219151	1.00	0.99	**-0.01**
AFP	0.220412	1.00	0.99	**-0.01**
HNRNPUL1	0.223207	1.00	1.01	**0.01**
ZKSCAN4	0.223826	1.00	0.99	**-0.01**
SP2	0.224143	1.00	0.99	**-0.01**
KRR1	0.225281	1.00	1.01	**0.01**
HDAC4	0.225701	1.00	0.99	**-0.01**
CCND2	0.226191	1.00	1.01	**0.01**
HNF1B	0.227035	1.00	0.99	**-0.01**
VAX2	0.227357	1.00	0.99	**-0.01**
HSPE1	0.227578	1.00	1.04	**0.04**
COPG2	0.228694	1.00	1.01	**0.01**
ABCF3	0.229033	1.00	0.99	**-0.01**
NR2E1	0.229481	1.00	1.01	**0.01**
TLX2	0.229601	1.00	0.99	**-0.01**
NME4	0.230389	1.00	1.01	**0.01**
ENO1	0.230925	1.00	1.02	**0.02**
TIMP3	0.231112	1.00	1.02	**0.02**
BIRC3	0.231225	1.00	0.99	**-0.01**
PELO	0.232862	1.00	1.01	**0.01**
MCM5_a	0.233507	1.00	0.98	**-0.02**
PHF11	0.233635	1.00	1.02	**0.02**
STK11	0.233734	1.00	0.99	**-0.01**

MAP2K1	0.233928	1.00	1.01	**0.01**
IRAK4	0.234381	1.00	1.01	**0.01**
TADA3	0.235031	1.00	1.02	**0.02**
FLT1_a	0.235351	1.00	0.98	**-0.02**
PPARG	0.236194	1.00	0.99	**-0.01**
HOXD3	0.237273	1.00	0.99	**-0.01**
KLF7	0.238567	1.00	0.99	**-0.01**
CSNK1G1	0.238770	1.00	0.99	**-0.01**
ACTB	0.239192	1.00	0.99	**-0.01**
ZNF207	0.239763	1.00	1.01	**0.01**
TRIM32	0.241159	1.00	0.99	**-0.01**
FEN1	0.241659	1.00	0.98	**-0.02**
RPS6KA1	0.241915	1.00	0.98	**-0.02**
ACVR2A	0.242105	1.00	0.99	**-0.01**
ISG20	0.242188	1.00	1.02	**0.02**
FANCG	0.242202	1.00	0.99	**-0.01**
RFX3	0.242271	1.00	0.99	**-0.01**
GALK1	0.242648	1.00	0.99	**-0.01**
GAS2	0.242988	1.00	1.02	**0.02**
TBL1X_a	0.243173	1.00	0.98	**-0.02**
GRB10	0.243879	1.00	1.01	**0.01**
SRPK2	0.244089	1.00	0.99	**-0.01**
ALOX15B	0.244178	1.00	0.99	**-0.01**
USF1	0.245860	1.00	1.02	**0.02**
RPS2	0.246143	1.00	0.99	**-0.01**
SDHB	0.247070	1.00	0.99	**-0.01**
TBCK	0.247310	1.00	0.99	**-0.01**
ID1	0.247365	1.00	1.03	**0.02**
IP6K1	0.247489	1.00	0.99	**-0.01**
GK2	0.248249	1.00	1.01	**0.01**
GNG3	0.248255	1.00	1.01	**0.01**
DYRK4	0.248427	1.00	0.99	**-0.01**
RBM28	0.248514	1.00	1.03	**0.03**
H2AFY	0.250098	1.00	1.02	**0.02**
GADD45G	0.250202	1.00	0.98	**-0.02**
PCK2	0.251778	1.00	0.99	**-0.01**
VPS45	0.252596	1.00	1.01	**0.01**
LASP1	0.253882	1.00	0.99	**-0.01**
HLX	0.255035	1.00	0.99	**-0.01**
CDC20	0.256359	1.00	0.98	**-0.02**
CSTB	0.257047	1.00	1.01	**0.01**
L3MBTL2	0.257070	1.00	1.03	**0.03**
CYLD	0.257710	1.00	0.99	**-0.01**
SDHC	0.257722	1.00	0.99	**-0.01**
MYBL2	0.258178	1.00	0.98	**-0.02**
STK25	0.258675	1.00	0.97	**-0.03**
RPL37A	0.258800	1.00	1.01	**0.01**
PRC1	0.259279	1.00	1.03	**0.03**
EEF1G	0.260365	1.00	0.99	**-0.01**
NR0B2	0.261395	1.00	0.99	**-0.02**
KIF9	0.261752	1.00	1.01	**0.01**

GGPS1	0.262362	1.00	1.04	**0.04**
PPP2R2C	0.262399	1.00	0.99	**-0.01**
HOPX	0.262492	1.00	1.02	**0.02**
C10orf119	0.263174	1.00	1.04	**0.04**
CDK14	0.264239	1.00	0.99	**-0.01**
NLK	0.264355	1.00	0.99	**-0.01**
MAX	0.265404	1.00	1.02	**0.02**
GNAI2	0.266469	1.00	0.99	**-0.01**
SOD1	0.267661	1.00	1.03	**0.03**
FLT1	0.267760	1.00	0.99	**-0.01**
RDBP	0.268853	1.00	0.97	**-0.03**
MEF2A_a	0.269091	1.00	0.98	**-0.02**
CDK7	0.269164	1.00	1.01	**0.01**
MAPK10	0.269271	1.00	0.99	**-0.01**
GMEB2	0.272224	1.00	0.99	**-0.01**
TBL1X	0.273942	1.00	1.05	**0.04**
PRKRA	0.275423	1.00	0.99	**-0.01**
HK1	0.275489	1.00	0.98	**-0.02**
PSME2	0.276503	1.00	1.01	**0.01**
MAP4K3	0.277721	1.00	0.99	**-0.01**
DVL3	0.278044	1.00	0.99	**-0.01**
SEPT6	0.278198	1.00	0.99	**-0.01**
SRP19	0.279534	1.00	1.02	**0.02**
EAPP	0.279782	1.00	0.98	**-0.02**
XIAP	0.280710	1.00	0.99	**-0.01**
TCEAL1	0.281697	1.00	1.02	**0.02**
MEOX2	0.282380	1.00	0.99	**-0.01**
EEF1A1_a	0.282500	1.00	0.98	**-0.02**
FGFR10P	0.283162	1.00	1.01	**0.01**
NR4A1	0.283478	1.00	0.98	**-0.02**
BRD8	0.283680	1.00	0.99	**-0.01**
RERG	0.284027	1.00	1.01	**0.01**
EPS15	0.286553	1.00	0.98	**-0.02**
DYNC1LI2	0.286588	1.00	1.02	**0.02**
PRDX6_a	0.287558	1.00	0.98	**-0.02**
PHLDA1	0.288883	1.00	1.05	**0.05**
SSX3	0.291727	1.00	0.99	**-0.01**
DSTYK	0.295776	1.00	0.99	**-0.01**
KCMF1	0.296228	1.00	0.99	**-0.01**
STK38L	0.296463	1.00	0.99	**-0.01**
CD96	0.299897	1.00	1.05	**0.05**
PDCD5	0.300040	1.00	1.02	**0.02**
LTV1	0.300333	1.00	1.01	**0.01**
SERPINF2	0.301303	1.00	0.99	**-0.01**
CDK1	0.302697	1.00	0.99	**-0.01**
SNX6	0.303669	1.00	1.01	**0.01**
NSF	0.304829	1.00	1.01	**0.01**
ITK	0.306096	1.00	1.01	**0.01**
NFE2	0.306200	1.00	0.99	**-0.01**
MAPK8	0.307603	1.00	1.01	**0.01**
PIM1	0.307841	1.00	0.99	**-0.01**

STAT3	0.308259	1.00	1.01	**0.01**
RHOXF2	0.308283	1.00	0.98	**-0.02**
DNTT	0.308610	1.00	0.99	**-0.01**
DVL2	0.309030	1.00	0.99	**-0.01**
MAPK8_a	0.309208	1.00	1.01	**0.01**
BFHD	0.309307	1.00	0.98	**-0.02**
RPL18A	0.309732	1.00	1.01	**0.01**
UBE2V1	0.311308	1.00	1.02	**0.02**
NR1I2	0.311496	1.00	0.99	**-0.01**
VEGFB	0.311958	1.00	1.02	**0.02**
MYCBPAP	0.311968	1.00	1.01	**0.01**
SCAND1	0.312826	1.00	1.01	**0.01**
RRAS2_a	0.313036	1.00	0.98	**-0.02**
FBXO9	0.313688	1.00	1.01	**0.01**
VGLL1	0.314042	1.00	1.00	**-0.00**
ZNF143	0.314160	1.00	0.99	**-0.01**
PDE4A	0.316598	1.00	0.99	**-0.01**
SIAH1	0.316773	1.00	0.99	**-0.01**
ELK3	0.318719	1.00	1.01	**0.01**
STK38	0.318770	1.00	0.99	**-0.01**
NAB1	0.318798	1.00	1.00	**0.00**
CDKN2B	0.319710	1.00	1.01	**0.01**
HEYL	0.320843	1.00	0.99	**-0.01**
ANXA1	0.320987	1.00	1.01	**0.01**
PRKCZ	0.321614	1.00	1.06	**0.06**
HSPA1A	0.324047	1.00	1.01	**0.01**
DDR1_int	0.324310	1.00	1.01	**0.01**
PPARD	0.325782	1.00	0.99	**-0.01**
SFRS5	0.326242	1.00	0.99	**-0.01**
STMN1	0.326455	1.00	1.02	**0.02**
CDK16	0.326464	1.00	1.02	**0.02**
GIPC1	0.326820	1.00	0.99	**-0.01**
ENO2	0.326906	1.00	1.03	**0.03**
MAZ	0.327315	1.00	1.02	**0.02**
ZNF165	0.328852	1.00	0.99	**-0.01**
IL1F5	0.328963	1.00	1.01	**0.01**
ABI1	0.329303	1.00	1.02	**0.02**
ZNF323	0.330897	1.00	0.99	**-0.01**
HINFP	0.332253	1.00	0.99	**-0.01**
IL1A	0.332754	1.00	0.98	**-0.02**
IL18	0.333224	1.00	1.02	**0.02**
ZC4H2	0.333994	1.00	0.97	**-0.03**
EPHA10	0.334105	1.00	1.01	**0.01**
PHKG1	0.334214	1.00	0.99	**-0.01**
P4HB	0.334277	1.00	1.01	**0.01**
TLK2	0.334887	1.00	1.01	**0.01**
LYN	0.334940	1.00	0.99	**-0.01**
ELK1	0.335158	1.00	1.02	**0.02**
LIN28A	0.335860	1.00	1.01	**0.01**
RIPK3	0.335948	1.00	0.99	**-0.01**
EEF1A1	0.336404	1.00	1.01	**0.01**

DMRTC2	0.336429	1.00	0.99	**-0.01**
SCYL3	0.336955	1.00	1.01	**0.01**
RHOA	0.338240	1.00	0.99	**-0.01**
CXCR4	0.339171	1.00	1.01	**0.01**
BCL2A1	0.339534	1.00	1.00	**-0.00**
PIR	0.340125	1.00	1.02	**0.02**
PBX3	0.340661	1.00	1.00	**-0.00**
THRB	0.341057	1.00	1.01	**0.01**
MSN	0.342408	1.00	1.02	**0.02**
BMX	0.342979	1.00	1.01	**0.01**
JUNB	0.343519	1.00	1.00	**-0.00**
RPL10	0.343575	1.00	0.99	**-0.01**
ACSL6	0.345259	1.00	0.99	**-0.01**
POLR2I	0.345820	1.00	1.00	**0.00**
CDC25A	0.346295	1.00	0.99	**-0.01**
ESR2	0.347802	1.00	0.99	**-0.01**
PRKX	0.347965	1.00	1.01	**0.01**
ERG	0.348404	1.00	1.01	**0.01**
GMEB1	0.348575	1.00	1.02	**0.02**
RBM6	0.348684	1.00	0.99	**-0.01**
ADRBK1	0.348947	1.00	0.99	**-0.01**
TNFAIP6	0.350418	1.00	0.99	**-0.01**
MAP3K6	0.350723	1.00	0.99	**-0.01**
GNB3	0.351041	1.00	1.00	**-0.00**
PYGB	0.352123	1.00	0.99	**-0.01**
PDGFRB	0.352333	1.00	1.03	**0.03**
ESRRG	0.352655	1.00	1.02	**0.02**
MED4	0.353662	1.00	1.03	**0.03**
HAGHL	0.355442	1.00	1.01	**0.01**
MTO1	0.357787	1.00	1.01	**0.01**
STK32A	0.358100	1.00	1.02	**0.02**
TNFRSF11B	0.358172	1.00	0.99	**-0.01**
ZAK	0.358452	1.00	0.99	**-0.01**
DLX4	0.360079	1.00	1.00	**-0.00**
CLK4	0.361787	1.00	1.01	**0.01**
MKNK2	0.362118	1.00	0.99	**-0.01**
TROVE2	0.362210	1.00	1.02	**0.02**
GTF2A1L	0.363761	1.00	0.99	**-0.01**
PPP2R5A	0.363783	1.00	0.99	**-0.01**
NR4A1_a	0.364085	1.00	0.99	**-0.01**
ZNF394	0.364144	1.00	0.99	**-0.01**
PQBP1	0.367481	1.00	0.99	**-0.01**
CAMK2B	0.368194	1.00	1.02	**0.02**
MXI1	0.368592	1.00	0.99	**-0.01**
HOXA9	0.369732	1.00	1.01	**0.01**
CDK5	0.370789	1.00	0.99	**-0.01**
PHB2	0.371521	1.00	0.99	**-0.01**
RNF7	0.372465	1.00	0.99	**-0.01**
NMRAL1	0.373013	1.00	1.01	**0.01**
CDK10	0.373287	1.00	0.99	**-0.01**
MLLT11	0.373660	1.00	0.99	**-0.01**

ETS2	0.374266	1.00	0.99	**-0.01**
BRSK1	0.374563	1.00	1.01	**0.01**
RPL18	0.375302	1.00	1.01	**0.01**
PDK1	0.375498	1.00	1.00	**0.00**
CRYAB	0.375865	1.00	1.02	**0.02**
DYRK2_a	0.376048	1.00	0.99	**-0.01**
USH1C	0.378336	1.00	0.97	**-0.03**
CUL4A	0.379160	1.00	1.01	**0.01**
FTSJ3	0.379172	1.00	0.99	**-0.01**
PRKAA2	0.379351	1.00	0.99	**-0.01**
NKX2-5	0.380610	1.00	0.99	**-0.01**
MLF1	0.380935	1.00	1.00	**-0.00**
BOP1	0.381218	1.00	1.01	**0.01**
LEF1	0.382495	1.00	0.99	**-0.01**
TWIST2	0.382933	1.00	0.99	**-0.01**
CLUAP1	0.383071	1.00	1.01	**0.01**
MAP2K5_a	0.383229	1.00	0.99	**-0.01**
TXN2	0.383351	1.00	0.99	**-0.01**
PRKAG3	0.383891	1.00	1.01	**0.01**
BMP7	0.383919	1.00	0.99	**-0.01**
HMG20B	0.384246	1.00	0.99	**-0.01**
ADRBK1_a	0.384795	1.00	0.99	**-0.01**
KRT4	0.385373	1.00	0.99	**-0.01**
GPHN	0.385474	1.00	0.99	**-0.01**
PFN2	0.385692	1.00	1.01	**0.01**
HMGN5	0.386276	1.00	0.99	**-0.01**
ZNF19	0.386645	1.00	0.99	**-0.01**
CNOT7	0.386950	1.00	0.99	**-0.01**
CMPK1	0.387429	1.00	1.00	**0.00**
ZSCAN12	0.387846	1.00	0.99	**-0.01**
NAP1L1	0.388526	1.00	1.01	**0.01**
PCBP2	0.388711	1.00	1.01	**0.01**
BIRC5	0.388816	1.00	0.99	**-0.01**
HK2	0.388989	1.00	1.01	**0.01**
LZTR1	0.389454	1.00	0.99	**-0.01**
PAK6	0.390310	1.00	1.02	**0.02**
MAP3K2	0.391681	1.00	1.01	**0.01**
ERCC2	0.391758	1.00	0.99	**-0.01**
DUSP18	0.392509	1.00	1.00	**-0.00**
PFKFB3	0.393114	1.00	1.02	**0.02**
MIF	0.393643	1.00	1.02	**0.02**
RAB11FIP3	0.394288	1.00	0.98	**-0.02**
SYK	0.394591	1.00	1.00	**-0.00**
SAV1	0.395319	1.00	0.99	**-0.01**
ABCF1	0.395622	1.00	1.02	**0.02**
ACTA1	0.395718	1.00	0.99	**-0.01**
MAPK7	0.396163	1.00	0.99	**-0.01**
ME2	0.397022	1.00	0.99	**-0.01**
STK10	0.397273	1.00	0.99	**-0.01**
CCNB1	0.398098	1.00	0.99	**-0.01**
EHMT2	0.398124	1.00	1.01	**0.01**

AIM2	0.398220	1.00	0.99	**-0.01**
SOCS2	0.398231	1.00	1.00	**0.00**
AICDA	0.398591	1.00	1.02	**0.02**
MLLT3	0.398821	1.00	0.99	**-0.01**
AKT1	0.400142	1.00	1.02	**0.02**
PTEN	0.400716	1.00	1.01	**0.01**
MRPS30	0.402233	1.00	1.01	**0.01**
NF2	0.402742	1.00	0.99	**-0.01**
NFIB	0.403244	1.00	0.99	**-0.01**
BLZF1	0.403749	1.00	0.99	**-0.01**
SDCCAG8	0.404459	1.00	0.98	**-0.02**
MITF	0.405052	1.00	1.01	**0.01**
AAK1	0.405198	1.00	1.02	**0.02**
MRPS26	0.405528	1.00	0.99	**-0.01**
METTL3	0.405541	1.00	1.03	**0.03**
CAMKV	0.405904	1.00	1.00	**-0.00**
BDNF	0.406431	1.00	0.99	**-0.01**
ZNF354A	0.406524	1.00	0.99	**-0.01**
PAPSS2	0.406879	1.00	1.01	**0.01**
RBMS1	0.408591	1.00	1.01	**0.01**
SHPK	0.408700	1.00	1.01	**0.01**
SMAD4	0.410416	1.00	1.01	**0.01**
TPD52	0.410432	1.00	0.98	**-0.02**
RPS6KA6	0.411641	1.00	1.01	**0.01**
PTK2_a	0.411644	1.00	1.00	**-0.00**
MLH1	0.411645	1.00	0.98	**-0.03**
DUSP14	0.412199	1.00	0.99	**-0.01**
GTPBP1	0.412808	1.00	0.99	**-0.01**
SGSM3	0.413687	1.00	0.99	**-0.01**
FOSL1	0.413891	1.00	1.00	**-0.00**
ZNF70	0.414508	1.00	1.01	**0.01**
MNAT1	0.414592	1.00	1.02	**0.02**
SUFU	0.415958	1.00	1.01	**0.01**
SOCS5_a	0.416780	1.00	0.99	**-0.01**
FLI1	0.417013	1.00	0.99	**-0.01**
DDR1_ext	0.418507	1.00	1.01	**0.01**
WDR46	0.418591	1.00	0.99	**-0.01**
SORD_a	0.419526	1.00	0.99	**-0.01**
MEF2A	0.420587	1.00	1.02	**0.02**
MED21	0.421009	1.00	1.00	**-0.00**
RRAS	0.421472	1.00	1.00	**-0.00**
RPS6KA5	0.422156	1.00	0.99	**-0.01**
PC_a	0.422656	1.00	0.99	**-0.01**
IFIT3	0.424852	1.00	1.02	**0.02**
WDR45L	0.425047	1.00	0.99	**-0.01**
PRKCI	0.427178	1.00	1.01	**0.01**
PHF17	0.427217	1.00	1.02	**0.02**
CYCS	0.427360	1.00	0.99	**-0.01**
MYF6	0.427375	1.00	1.00	**-0.00**
EZH2	0.428420	1.00	0.99	**-0.01**
NR4A2	0.431811	1.00	0.99	**-0.01**

STK4	0.432684	1.00	0.99	**-0.01**
ITPKB	0.433297	1.00	1.01	**0.01**
STAM	0.436561	1.00	1.00	**-0.00**
ACTR2	0.437699	1.00	1.02	**0.02**
CARHSP1	0.438888	1.00	1.01	**0.01**
ZNF496	0.439070	1.00	0.99	**-0.01**
TRIB2	0.440219	1.00	1.02	**0.02**
ADD1_a	0.440303	1.00	0.99	**-0.01**
FRS2	0.440393	1.00	0.99	**-0.01**
ZNF276	0.441651	1.00	0.99	**-0.01**
NRIP3	0.442162	1.00	1.01	**0.01**
SSX2	0.442212	1.00	1.01	**0.01**
UBE2I	0.442229	1.00	1.02	**0.02**
ZMYND8	0.442311	1.00	1.01	**0.01**
NFE2L2	0.443922	1.00	1.00	**-0.00**
PFKFB4	0.444712	1.00	1.01	**0.01**
KRT19	0.445178	1.00	1.02	**0.02**
KAT2A	0.446384	1.00	0.99	**-0.01**
NDRG2	0.446804	1.00	1.01	**0.01**
CBFA2T3	0.447299	1.00	1.01	**0.01**
ALPK1	0.447511	1.00	1.00	**-0.00**
GTF2E2	0.448449	1.00	1.00	**-0.00**
AK3L1	0.448579	1.00	1.01	**0.01**
THRA	0.452281	1.00	1.00	**-0.00**
TBCB	0.452387	1.00	0.98	**-0.02**
IMPDH1	0.452906	1.00	1.01	**0.01**
FAIM	0.452946	1.00	1.01	**0.01**
PDK4	0.453510	1.00	1.02	**0.02**
PMVK	0.454478	1.00	1.00	**0.00**
CALML4	0.455111	1.00	1.01	**0.01**
SMN1	0.455215	1.00	1.00	**-0.00**
PTP4A1	0.455631	1.00	0.99	**-0.01**
BTG1	0.455801	1.00	0.99	**-0.01**
OGG1	0.455830	1.00	0.99	**-0.01**
ANXA11	0.456744	1.00	1.01	**0.01**
BUB1	0.456783	1.00	1.00	**-0.00**
SMAD5	0.457466	1.00	1.00	**-0.00**
HOOK1	0.458028	1.00	1.01	**0.01**
RPL30	0.458163	1.00	0.98	**-0.02**
MNDA	0.460120	1.00	0.99	**-0.01**
HSPB8	0.460360	1.00	1.02	**0.02**
AURKA	0.460720	1.00	0.99	**-0.01**
YWHAG	0.460981	1.00	1.02	**0.02**
SNCA	0.462131	1.00	1.01	**0.01**
CIDEC	0.462483	1.00	1.00	**0.00**
C1orf57	0.464138	1.00	1.02	**0.02**
PPP3R1	0.464442	1.00	1.00	**-0.00**
MAP2K5	0.465158	1.00	0.99	**-0.01**
PSMD4	0.465667	1.00	0.98	**-0.02**
MYOZ2	0.466402	1.00	1.00	**-0.00**
PAK7	0.467607	1.00	1.00	**0.00**

RAGE	0.467610	1.00	1.00	**-0.00**
SET	0.467693	1.00	1.01	**0.01**
ATG7	0.468084	1.00	1.00	**0.00**
HCFC2	0.470783	1.00	0.99	**-0.01**
LATS1	0.473280	1.00	1.01	**0.01**
RNGTT	0.475696	1.00	0.99	**-0.01**
BUD31	0.475734	1.00	0.99	**-0.01**
PITRM1	0.476560	1.00	1.00	**0.00**
BCKDK	0.476740	1.00	1.01	**0.01**
PPP2R5C	0.476978	1.00	1.00	**0.00**
AURKB	0.477415	1.00	0.99	**-0.01**
NFIA	0.477781	1.00	1.00	**-0.00**
CAMK1	0.477856	1.00	1.01	**0.01**
BLK	0.477985	1.00	1.01	**0.01**
PTPN1	0.477998	1.00	0.99	**-0.01**
DEDD	0.478210	1.00	1.01	**0.01**
CDKN2A	0.479703	1.00	1.01	**0.01**
SCMH1	0.479785	1.00	1.00	**0.00**
TCL1A	0.480925	1.00	1.04	**0.04**
PIAS2	0.481404	1.00	1.00	**0.00**
SSBP3	0.483148	1.00	1.00	**-0.00**
NEK7	0.485359	1.00	1.00	**0.00**
POLR2E	0.487856	1.00	1.01	**0.01**
ALX1	0.487870	1.00	0.99	**-0.01**
ZNF35	0.488004	1.00	1.00	**-0.00**
HAGH	0.488063	1.00	1.01	**0.01**
DUSP4	0.488298	1.00	0.99	**-0.01**
SUPT4H1	0.488782	1.00	1.01	**0.01**
ZSCAN16	0.488994	1.00	0.99	**-0.01**
GRAP2	0.490493	1.00	0.99	**-0.01**
TNK2	0.490594	1.00	0.99	**-0.01**
BATF	0.490633	1.00	1.01	**0.01**
EXOSC10	0.490935	1.00	0.99	**-0.01**
GNG4	0.492058	1.00	1.00	**-0.00**
STK33	0.493094	1.00	1.02	**0.02**
NR2C2	0.493374	1.00	1.00	**0.00**
CD5L	0.493794	1.00	1.00	**-0.00**
STK16	0.495258	1.00	0.99	**-0.01**
GTF2F1	0.495726	1.00	1.00	**-0.00**
MX1	0.495911	1.00	0.98	**-0.02**
FGF13	0.496983	1.00	1.00	**0.00**
STAM2	0.497193	1.00	1.00	**-0.00**
TFEB	0.499042	1.00	0.99	**-0.01**
KIAA0101	0.500682	1.00	1.01	**0.01**
TFCP2	0.504320	1.00	1.00	**-0.00**
TBX6	0.504461	1.00	1.00	**-0.00**
UXT	0.505586	1.00	1.00	**0.00**
YTHDF2	0.506125	1.00	1.00	**0.00**
CKM	0.506235	1.00	1.01	**0.01**
DDB2	0.507191	1.00	1.00	**-0.00**
DLX1	0.508058	1.00	1.00	**-0.00**

SMAD9	0.508678	1.00	1.00	**0.00**
SSX1	0.508872	1.00	1.00	**-0.00**
PTPN11	0.509285	1.00	1.01	**0.01**
CCND1	0.512392	1.00	1.00	**0.00**
CDKN2C	0.512721	1.00	1.00	**-0.00**
FYN	0.513180	1.00	1.00	**-0.00**
PNPT1	0.513687	1.00	0.99	**-0.01**
LDHA	0.514436	1.00	1.00	**0.00**
PPP2R2B	0.515600	1.00	1.00	**-0.00**
ATF1	0.516832	1.00	1.00	**-0.00**
TGFBR2	0.517202	1.00	1.00	**-0.00**
OVOL1	0.517335	1.00	0.99	**-0.01**
HCLS1	0.517843	1.00	1.02	**0.02**
PRELID1	0.518886	1.00	1.01	**0.01**
CDC42	0.519049	1.00	1.00	**0.00**
ODC1	0.519979	1.00	1.02	**0.02**
AK7	0.520170	1.00	1.01	**0.01**
PLUNC	0.520485	1.00	1.01	**0.01**
CDK20	0.520755	1.00	1.00	**-0.00**
POU5F1	0.521833	1.00	1.00	**-0.00**
CASP4	0.522682	1.00	1.00	**-0.00**
TFDP1	0.524699	1.00	0.99	**-0.01**
GK	0.525075	1.00	1.01	**0.01**
TAF5L	0.527766	1.00	1.00	**-0.00**
HUS1	0.529229	1.00	0.99	**-0.01**
ZMAT3	0.529378	1.00	0.99	**-0.01**
CALM2	0.529572	1.00	1.01	**0.01**
SMARCD1	0.529862	1.00	0.99	**-0.01**
BRD3	0.530702	1.00	1.00	**-0.00**
SOX2	0.530900	1.00	1.01	**0.01**
EXOSC8	0.531135	1.00	0.99	**-0.01**
CSNK2A2	0.533480	1.00	0.99	**-0.01**
DGUOK	0.534538	1.00	1.00	**0.00**
PIP4K2B	0.534672	1.00	0.99	**-0.01**
RPL10A	0.535663	1.00	1.00	**-0.00**
MLPH	0.536187	1.00	1.00	**0.00**
PPP2CB	0.536835	1.00	1.00	**-0.00**
MAPKAPK3	0.539811	1.00	1.01	**0.01**
CDK11B	0.540027	1.00	1.01	**0.01**
IKZF1	0.541879	1.00	1.01	**0.01**
SEPT4	0.541979	1.00	1.00	**-0.00**
MTERF	0.542023	1.00	1.01	**0.01**
ARL1	0.544055	1.00	1.01	**0.01**
STYXL1	0.547200	1.00	1.00	**-0.00**
RAD51L1	0.547298	1.00	1.00	**-0.00**
SUMO2	0.548661	1.00	1.00	**0.00**
TTK	0.549639	1.00	0.99	**-0.01**
SECISBP2	0.550112	1.00	1.00	**0.00**
STYX	0.550615	1.00	1.01	**0.01**
NR2C1	0.551363	1.00	1.00	**-0.00**
DUSP12	0.551491	1.00	1.00	**0.00**

CXCR2	0.552459	1.00	1.01	**0.01**
RPS6KL1	0.553231	1.00	1.01	**0.01**
CALM2_a	0.553920	1.00	0.99	**-0.01**
KRAS	0.553920	1.00	1.01	**0.01**
RPL32	0.554014	1.00	1.00	**0.00**
ERCC3	0.554515	1.00	1.00	**-0.00**
MPP1	0.555570	1.00	1.01	**0.01**
FOXA3	0.556459	1.00	1.00	**-0.00**
TUBGCP3	0.556772	1.00	1.01	**0.01**
CDC25C	0.557257	1.00	0.99	**-0.01**
ZNF274	0.558707	1.00	1.00	**0.00**
GATAD2A	0.558823	1.00	1.00	**-0.00**
PTP4A3	0.559127	1.00	1.00	**-0.00**
CSK	0.559495	1.00	1.01	**0.01**
CHEK2	0.560101	1.00	1.00	**0.00**
ARNT	0.560346	1.00	0.99	**-0.01**
KIT_fl	0.560507	1.00	1.00	**-0.00**
GUK1	0.560961	1.00	1.01	**0.01**
RPL28	0.561091	1.00	1.00	**0.00**
EHF	0.561329	1.00	1.00	**-0.00**
CBX5	0.561799	1.00	1.00	**-0.00**
TFCP2L1	0.562150	1.00	1.00	**-0.00**
MUTYH	0.562155	1.00	1.00	**-0.00**
PRKAR1A	0.563217	1.00	1.02	**0.02**
DYRK2	0.563365	1.00	1.00	**-0.00**
CFL1	0.564024	1.00	1.01	**0.01**
CARD9	0.564542	1.00	1.01	**0.01**
SPG20	0.564576	1.00	0.98	**-0.02**
MAP3K14	0.566369	1.00	1.00	**-0.00**
TPI1	0.567914	1.00	1.02	**0.02**
RALBP1	0.568053	1.00	1.00	**0.00**
LTA4H	0.569438	1.00	1.01	**0.01**
TSSK3	0.569472	1.00	1.01	**0.01**
STAT4	0.569656	1.00	0.99	**-0.01**
HMGB2	0.569677	1.00	0.99	**-0.01**
TCEA2	0.569916	1.00	0.99	**-0.01**
SPDEF	0.569935	1.00	1.01	**0.01**
ZBTB25	0.570118	1.00	1.01	**0.01**
GNAI3	0.570546	1.00	1.00	**-0.00**
RRAGC	0.570874	1.00	1.00	**-0.00**
PRKCH	0.571068	1.00	1.01	**0.01**
ZHX2	0.571174	1.00	1.00	**-0.00**
BCL10	0.572295	1.00	0.99	**-0.01**
CRX	0.573457	1.00	1.00	**-0.00**
ILK	0.574033	1.00	1.00	**0.00**
NHLH1	0.574416	1.00	1.01	**0.01**
NR1H2	0.576216	1.00	1.01	**0.01**
CLK1	0.576291	1.00	1.00	**0.00**
DDX5	0.576450	1.00	1.01	**0.01**
FAS	0.578522	1.00	1.01	**0.01**
CAMK1G	0.579800	1.00	0.99	**-0.01**

ARIH2	0.580427	1.00	1.01	**0.01**
DFFA	0.580527	1.00	1.01	**0.01**
SMAD2	0.580636	1.00	1.01	**0.01**
KRT8	0.580637	1.00	0.99	**-0.01**
FAM48A	0.582263	1.00	1.01	**0.01**
EZR	0.582584	1.00	1.01	**0.01**
COPS6	0.582899	1.00	0.99	**-0.01**
LY96	0.583052	1.00	1.00	**-0.00**
RAD23A	0.583869	1.00	1.02	**0.02**
MUSK	0.583900	1.00	1.00	**0.00**
ZMAT2	0.585376	1.00	1.02	**0.02**
FANCC	0.585422	1.00	1.00	**-0.00**
IKBKB	0.585514	1.00	1.00	**-0.00**
EGR2	0.585764	1.00	1.00	**-0.00**
PACSIN3	0.585789	1.00	1.01	**0.01**
PPID	0.587701	1.00	1.00	**-0.00**
AHSG	0.588933	1.00	1.00	**0.00**
CROT	0.589359	1.00	1.00	**0.00**
VHL	0.589846	1.00	1.00	**-0.00**
RAP1GDS1	0.589888	1.00	1.00	**0.00**
COMMD3	0.590031	1.00	1.00	**0.00**
AK2	0.591046	1.00	1.01	**0.01**
CITED1	0.591679	1.00	0.99	**-0.01**
INPP1	0.592145	1.00	1.00	**0.00**
FOLH1	0.592226	1.00	1.00	**-0.00**
UQCRC1	0.592845	1.00	1.01	**0.01**
BMPR1A	0.593016	1.00	1.00	**-0.00**
ING4	0.593204	1.00	1.01	**0.01**
ULK2	0.593282	1.00	0.99	**-0.01**
MAP1S	0.593311	1.00	1.00	**-0.00**
CDKN1A	0.593957	1.00	0.99	**-0.01**
FGF1	0.594506	1.00	1.00	**-0.00**
SOCS5	0.594641	1.00	1.00	**0.00**
EXT2	0.596102	1.00	1.00	**-0.00**
TWF2	0.596561	1.00	0.99	**-0.01**
TRIM25	0.596726	1.00	1.00	**-0.00**
MAP2K7	0.597305	1.00	1.00	**-0.00**
CDH19	0.597833	1.00	0.99	**-0.01**
RAD51	0.598438	1.00	1.00	**-0.00**
CSNK1D	0.599339	1.00	0.99	**-0.01**
SH3GLB1	0.600388	1.00	1.00	**-0.00**
PDGFB	0.600977	1.00	1.00	**-0.00**
ARRB1	0.601610	1.00	1.01	**0.01**
RAD23B	0.602105	1.00	1.02	**0.02**
ABT1	0.602900	1.00	0.99	**-0.01**
NEUROD4	0.605194	1.00	1.00	**-0.00**
NLRP2	0.605443	1.00	1.00	**-0.00**
ZNRD1	0.606846	1.00	1.01	**0.01**
CHIC2	0.612701	1.00	1.00	**-0.00**
BAD	0.612840	1.00	1.01	**0.01**
INPP5B	0.614532	1.00	1.00	**0.00**

YAF2	0.616771	1.00	0.99	**-0.01**
RAPGEF4	0.617383	1.00	1.00	**-0.00**
GTF2F2	0.618546	1.00	1.00	**-0.00**
ZNF45	0.618933	1.00	1.00	**-0.00**
RPL27A	0.619014	1.00	1.00	**-0.00**
RABEP1	0.620552	1.00	1.01	**0.01**
NPY5R	0.620617	1.00	1.00	**0.00**
FLI1_a	0.621660	1.00	1.01	**0.01**
CWC27	0.622158	1.00	0.99	**-0.01**
MAPK12	0.622514	1.00	0.99	**-0.01**
MX2	0.623418	1.00	1.00	**-0.00**
GATA1	0.623511	1.00	1.00	**-0.00**
VAV1	0.623882	1.00	1.00	**0.00**
RBM7	0.624088	1.00	1.00	**-0.00**
AXIN1	0.624358	1.00	1.00	**-0.00**
ZNHIT3	0.624786	1.00	0.99	**-0.01**
EXOSC4	0.624951	1.00	1.00	**-0.00**
CDK16_a	0.625241	1.00	1.01	**0.01**
PKDCC	0.625483	1.00	1.00	**-0.00**
ELF1	0.625821	1.00	1.00	**-0.00**
HDAC3	0.626474	1.00	1.01	**0.01**
E2F6	0.627160	1.00	1.00	**-0.00**
MLKL	0.627974	1.00	0.98	**-0.02**
PTK6	0.628693	1.00	1.00	**-0.00**
DMAP1	0.629399	1.00	1.00	**-0.00**
CCT3	0.630217	1.00	1.00	**-0.00**
FOXM1	0.631294	1.00	1.00	**-0.00**
TSC22D4	0.632461	1.00	1.00	**0.00**
RHOB	0.633693	1.00	1.01	**0.01**
VRK3	0.634775	1.00	1.00	**-0.00**
MCM5	0.636352	1.00	0.99	**-0.01**
CRADD	0.638381	1.00	1.01	**0.01**
PDGFRA_a	0.638419	1.00	1.00	**-0.00**
MTCP1	0.640418	1.00	1.00	**-0.00**
MRTO4	0.642045	1.00	1.00	**0.00**
NTRK3_ext	0.642569	1.00	1.00	**-0.00**
OLIG3	0.642588	1.00	1.00	**-0.00**
STARD7	0.642806	1.00	1.01	**0.01**
CSNK1G2	0.643003	1.00	1.01	**0.01**
RUFY1	0.643980	1.00	1.01	**0.01**
PSMD9	0.644289	1.00	0.99	**-0.01**
STAT5A	0.644494	1.00	1.00	**-0.00**
TP63	0.644511	1.00	0.99	**-0.01**
AXL	0.645410	1.00	1.00	**0.00**
LIMK2	0.645787	1.00	1.00	**-0.00**
PDGFRB_ext	0.646257	1.00	1.00	**0.00**
CAMKV_a	0.646460	1.00	1.00	**-0.00**
SH2D1A	0.646570	1.00	1.00	**0.00**
CNOT8	0.646622	1.00	1.00	**-0.00**
TWF1	0.648711	1.00	0.99	**-0.01**
FOXI1	0.649403	1.00	1.01	**0.01**

MARK4	0.650200	1.00	1.00	**-0.00**
IL21R	0.650800	1.00	1.00	**-0.00**
UCKL1	0.651208	1.00	1.00	**0.00**
MECP2	0.652223	1.00	1.00	**0.00**
IFI16	0.652425	1.00	1.00	**-0.00**
SEPT5	0.652922	1.00	0.99	**-0.01**
ASCL1	0.656185	1.00	1.00	**-0.00**
FOSL2	0.656560	1.00	1.00	**0.00**
PHIP	0.656984	1.00	1.00	**-0.00**
RING1	0.660190	1.00	1.00	**-0.00**
GFAP	0.660610	1.00	0.99	**-0.01**
LRRFIP2	0.660817	1.00	0.99	**-0.01**
CDK18	0.661018	1.00	1.00	**0.00**
IKBKE	0.661721	1.00	1.00	**0.00**
ZSCAN21	0.662612	1.00	0.99	**-0.01**
ETV4	0.663510	1.00	1.01	**0.01**
EIF4E	0.663924	1.00	1.00	**0.00**
IL1F7	0.665081	1.00	1.01	**0.01**
IPMK	0.666962	1.00	1.00	**0.00**
MEF2C	0.667372	1.00	1.00	**0.00**
KLK3	0.667646	1.00	1.00	**0.00**
CASP9	0.667855	1.00	1.00	**-0.00**
DGKA	0.668385	1.00	1.00	**0.00**
TUBA4A	0.669109	1.00	1.00	**-0.00**
VPS24	0.669180	1.00	0.99	**-0.01**
TAF15	0.669977	1.00	1.01	**0.01**
PIK3R1	0.670247	1.00	1.00	**-0.00**
ARAF	0.672054	1.00	1.00	**-0.00**
MAP3K7	0.672260	1.00	1.00	**-0.00**
GNG11	0.674068	1.00	1.00	**0.00**
SGK196	0.674918	1.00	1.00	**0.00**
RPS6KB1	0.676117	1.00	1.01	**0.01**
CHN1	0.676815	1.00	1.00	**0.00**
RPL13A	0.677694	1.00	1.00	**-0.00**
MAPK6	0.680054	1.00	1.00	**-0.00**
CABC1	0.680668	1.00	1.01	**0.01**
SUCLA2	0.680876	1.00	1.00	**-0.00**
ZNF444	0.681233	1.00	1.00	**-0.00**
KLF4	0.682090	1.00	1.00	**0.00**
CTTN	0.682533	1.00	1.00	**-0.00**
KRT15	0.682854	1.00	0.99	**-0.01**
AFF4	0.683141	1.00	1.01	**0.01**
ZNF174	0.683805	1.00	1.00	**-0.00**
PDGFRA_ext	0.684395	1.00	1.00	**0.00**
SP110	0.684857	1.00	1.00	**-0.00**
CDC25B	0.685100	1.00	1.00	**0.00**
MAPKSP1	0.685346	1.00	1.00	**-0.00**
MARK2	0.685603	1.00	1.00	**-0.00**
MAPK14	0.686784	1.00	1.01	**0.01**
BUB1B	0.687300	1.00	1.01	**0.01**
EGFR_ext	0.687550	1.00	1.00	**0.00**

ATXN3	0.688750	1.00	0.99	**-0.01**
MYNN	0.689028	1.00	1.00	**-0.00**
UBA3	0.689044	1.00	1.00	**0.00**
ETV7	0.689189	1.00	1.00	**-0.00**
FASTKD1	0.689530	1.00	1.01	**0.01**
ISL1	0.690163	1.00	1.01	**0.01**
BLK_a	0.691090	1.00	1.00	**-0.00**
RUVBL1	0.692120	1.00	1.00	**0.00**
TBK1	0.692944	1.00	1.00	**-0.00**
IDO1	0.693352	1.00	1.00	**0.00**
RIPK2	0.694485	1.00	0.99	**-0.01**
CXCR6	0.694538	1.00	1.00	**0.00**
GLRX3	0.696050	1.00	1.01	**0.01**
ZNF193	0.696800	1.00	1.00	**0.00**
DTYMK	0.696824	1.00	1.00	**0.00**
PRIM1	0.699440	1.00	1.00	**-0.00**
PDCD6	0.699963	1.00	1.00	**0.00**
WT1	0.701928	1.00	1.00	**-0.00**
CASP1	0.703898	1.00	1.00	**-0.00**
CDKN2D	0.704766	1.00	1.01	**0.01**
AKD1	0.704925	1.00	1.00	**0.00**
STK32B	0.705051	1.00	1.00	**-0.00**
NTRK2	0.706085	1.00	0.99	**-0.01**
PRKD3	0.708080	1.00	1.00	**-0.00**
PTGDR	0.708113	1.00	1.00	**0.00**
STK17B	0.708402	1.00	1.01	**0.01**
INHBA	0.708624	1.00	1.00	**-0.00**
PSME1	0.708688	1.00	0.99	**-0.01**
MAP2K3	0.708975	1.00	0.99	**-0.01**
CALM1	0.709738	1.00	1.01	**0.01**
HOXB7	0.709965	1.00	1.00	**-0.00**
RPS6KA3	0.710614	1.00	1.00	**-0.00**
TIRAP	0.710989	1.00	1.00	**-0.00**
RXRB	0.713595	1.00	1.00	**-0.00**
TSSKIB	0.713943	1.00	1.00	**0.00**
PKLR	0.713974	1.00	1.00	**0.00**
C20orf43	0.714215	1.00	1.00	**-0.00**
PHF7	0.714754	1.00	1.00	**0.00**
FASTK	0.715757	1.00	1.00	**-0.00**
CTAG2	0.716942	1.00	1.00	**0.00**
DLX3	0.717495	1.00	1.00	**0.00**
CEACAM8	0.718896	1.00	1.00	**0.00**
TAF9	0.719691	1.00	1.00	**0.00**
GRB2	0.720259	1.00	1.01	**0.01**
GEM	0.722453	1.00	1.00	**-0.00**
DEK	0.722684	1.00	1.00	**-0.00**
IDI1	0.724177	1.00	1.00	**-0.00**
FOXR2	0.724329	1.00	1.01	**0.01**
IFI35	0.724434	1.00	0.99	**-0.01**
RIPK1	0.725215	1.00	1.00	**0.00**
PRDX6	0.725215	1.00	1.01	**0.01**

BTF3	0.725600	1.00	1.00	**-0.00**
CPA4	0.726381	1.00	1.00	**-0.00**
LASS4	0.727706	1.00	1.00	**0.00**
FKBP3	0.728125	1.00	1.00	**-0.00**
VPS72	0.728527	1.00	1.01	**0.01**
SMARCE1	0.729304	1.00	1.00	**0.00**
GNGT2	0.729537	1.00	0.99	**-0.01**
RCAN1	0.729936	1.00	1.00	**-0.00**
CCNI	0.730244	1.00	1.00	**0.00**
APCS	0.730936	1.00	1.01	**0.01**
CHEK1	0.733956	1.00	1.01	**0.01**
NR3C1	0.734672	1.00	1.00	**0.00**
TRAF2	0.735158	1.00	1.01	**0.01**
DMRTB1	0.735242	1.00	1.00	**0.00**
HOXB6	0.735739	1.00	1.00	**-0.00**
RNF6	0.736155	1.00	1.00	**0.00**
EGFR_int	0.736522	1.00	1.00	**0.00**
MLX	0.737823	1.00	1.01	**0.01**
LIMS1	0.741001	1.00	1.00	**-0.00**
PRKACG	0.741600	1.00	1.00	**0.00**
CAMK2G	0.742475	1.00	1.00	**0.00**
PPM1A	0.742579	1.00	1.01	**0.01**
STRADB	0.743907	1.00	1.00	**-0.00**
EXT1	0.745148	1.00	1.00	**-0.00**
SP1	0.746681	1.00	1.00	**-0.00**
FGFR1_int	0.746825	1.00	1.00	**0.00**
TADA2A	0.746961	1.00	1.00	**0.00**
TXNRD1	0.747104	1.00	1.00	**-0.00**
PDK2	0.747976	1.00	1.00	**-0.00**
PLD2	0.748545	1.00	1.00	**-0.00**
ADCK4	0.749054	1.00	1.00	**-0.00**
IFIT1	0.749071	1.00	1.00	**-0.00**
KIT_int	0.750444	1.00	1.00	**0.00**
CDK19	0.752833	1.00	1.00	**-0.00**
TUBB	0.754032	1.00	1.00	**0.00**
AMD1	0.754876	1.00	1.00	**0.00**
PHB	0.755048	1.00	1.00	**0.00**
SPARC	0.755735	1.00	1.00	**0.00**
TFEC	0.755783	1.00	1.00	**-0.00**
HRAS	0.759403	1.00	1.00	**0.00**
ATG12	0.761487	1.00	1.00	**0.00**
NCOA5	0.762280	1.00	1.00	**0.00**
CSRNP1	0.764044	1.00	1.00	**-0.00**
SOCS3	0.764477	1.00	1.00	**-0.00**
IGHG1	0.765137	1.00	1.01	**0.01**
MEIS2	0.766091	1.00	1.00	**0.00**
ZNF232	0.766694	1.00	1.00	**0.00**
FOS	0.769052	1.00	1.00	**0.00**
TP53	0.769295	1.00	1.01	**0.01**
PECI	0.769361	1.00	1.00	**-0.00**
WAS	0.769496	1.00	1.00	**0.00**

CCM2	0.770647	1.00	1.00	**-0.00**
MAGEA4	0.770820	1.00	1.00	**0.00**
RG9MTD1	0.773555	1.00	1.00	**-0.00**
SGK3	0.774091	1.00	1.00	**0.00**
PPP3CA	0.774216	1.00	1.00	**0.00**
RFK	0.774681	1.00	1.00	**0.00**
EFS	0.774873	1.00	1.00	**-0.00**
OSBPL9	0.775120	1.00	1.01	**0.01**
TFRC	0.775813	1.00	1.00	**-0.00**
VCL	0.775907	1.00	1.00	**-0.00**
PAK2	0.776816	1.00	1.00	**-0.00**
PCGF2	0.777941	1.00	1.00	**0.00**
YWHAE	0.778032	1.00	1.01	**0.01**
BIRC7	0.778061	1.00	0.99	**-0.01**
HOXC8	0.779225	1.00	1.00	**-0.00**
BOLA3	0.779936	1.00	1.00	**-0.00**
CCR5	0.782440	1.00	1.00	**0.00**
C9orf96	0.783403	1.00	1.00	**0.00**
DNMT3L	0.784652	1.00	1.01	**0.01**
NR6A1	0.785182	1.00	1.00	**-0.00**
GPC3	0.786043	1.00	1.00	**0.00**
CAMK4	0.786898	1.00	1.01	**0.00**
PRCC	0.786984	1.00	1.01	**0.01**
ZNF277	0.788928	1.00	1.00	**-0.00**
AKT2	0.789682	1.00	1.00	**0.00**
NDE1	0.790451	1.00	1.01	**0.01**
PRKAA1	0.791096	1.00	1.00	**-0.00**
PRKD2	0.791491	1.00	1.00	**0.00**
PITX2	0.791953	1.00	1.00	**0.00**
ZAP70	0.792079	1.00	1.00	**0.00**
KCNIP3	0.792458	1.00	1.00	**0.00**
NEDD9	0.793083	1.00	1.00	**-0.00**
CDK4	0.793589	1.00	1.00	**-0.00**
DAPK2	0.794910	1.00	1.00	**0.00**
FGFR2_ext	0.795170	1.00	1.00	**-0.00**
ZBTB32	0.796492	1.00	1.00	**0.00**
TCF4	0.797969	1.00	1.00	**-0.00**
SS18L1	0.799288	1.00	1.00	**-0.00**
DNAJB1	0.800643	1.00	1.00	**-0.00**
TFE3	0.801504	1.00	1.00	**0.00**
SLA2	0.802926	1.00	1.00	**-0.00**
BRD2	0.803183	1.00	1.00	**-0.00**
PDXK	0.803226	1.00	1.00	**-0.00**
C21orf2	0.805388	1.00	1.00	**0.00**
XBP1	0.807003	1.00	1.00	**-0.00**
CISH	0.807745	1.00	1.00	**-0.00**
KRT14	0.809712	1.00	1.00	**0.00**
AP2M1	0.810218	1.00	1.00	**-0.00**
EEF1D	0.810548	1.00	1.00	**0.00**
MRPL45	0.810688	1.00	0.99	**-0.01**
PTPN22	0.812129	1.00	1.00	**0.00**

COX6C	0.812429	1.00	1.00	**-0.00**
HSP90AB1	0.812512	1.00	1.00	**0.00**
RAC2	0.812798	1.00	1.00	**0.00**
MAPK1	0.814033	1.00	1.00	**-0.00**
PATZ1	0.814407	1.00	1.00	**-0.00**
EWSR1	0.814787	1.00	1.00	**-0.00**
CAMK2D	0.815685	1.00	1.00	**-0.00**
ATIC	0.817869	1.00	1.00	**-0.00**
ITPK1	0.818699	1.00	1.00	**0.00**
NME5	0.820586	1.00	1.00	**-0.00**
RPL31	0.821071	1.00	1.00	**-0.00**
RLIM	0.821573	1.00	1.00	**0.00**
API5	0.821968	1.00	1.00	**-0.00**
STK32C	0.822283	1.00	1.00	**0.00**
ADRBK2	0.822569	1.00	1.00	**0.00**
SH3GL1	0.822805	1.00	1.01	**0.01**
STIP1	0.823498	1.00	0.99	**-0.01**
FTH1	0.823845	1.00	1.01	**0.01**
CCNH	0.824115	1.00	1.00	**0.00**
MYD88	0.825600	1.00	1.00	**-0.00**
PIP4K2C	0.826025	1.00	1.00	**-0.00**
AARS	0.826324	1.00	1.00	**-0.00**
MOBKL2A	0.827684	1.00	1.00	**-0.00**
PKMYT1	0.828330	1.00	1.00	**-0.00**
TDP2	0.828791	1.00	1.00	**-0.00**
BACH1	0.828917	1.00	0.99	**-0.01**
DMPK	0.829329	1.00	1.00	**-0.00**
PIK3C3	0.830898	1.00	1.00	**-0.00**
EPHB4	0.832105	1.00	1.00	**0.00**
HOXA1	0.832334	1.00	1.00	**-0.00**
GNAO1	0.832519	1.00	1.00	**0.00**
KLF6	0.832912	1.00	1.00	**-0.00**
TRAF5	0.837132	1.00	1.00	**-0.00**
HOMER2	0.837564	1.00	1.00	**0.00**
DPF2	0.838153	1.00	1.00	**0.00**
PTPN4	0.838475	1.00	1.00	**-0.00**
MYOG	0.840501	1.00	1.00	**0.00**
AMT	0.841601	1.00	1.00	**-0.00**
MED24	0.842839	1.00	1.00	**-0.00**
AK3	0.843400	1.00	1.00	**-0.00**
CNOT2	0.843477	1.00	1.00	**0.00**
RPL34	0.843577	1.00	1.00	**0.00**
ELMOD3	0.843671	1.00	1.00	**0.00**
ZNF3	0.843793	1.00	1.00	**0.00**
ASPSCR1	0.844192	1.00	1.01	**0.01**
SLC25A6	0.844355	1.00	1.00	**-0.00**
ZNF202	0.844510	1.00	1.00	**-0.00**
TTF2	0.844964	1.00	1.00	**-0.00**
ABL2	0.846805	1.00	1.00	**-0.00**
COPB2	0.847884	1.00	1.00	**0.00**
STK24	0.847963	1.00	1.00	**0.00**

NDUFAB1	0.848427	1.00	1.00	**0.00**
ETNK2	0.848620	1.00	1.00	**-0.00**
PKNOX1	0.848733	1.00	1.00	**0.00**
CIDEB	0.849027	1.00	1.00	**0.00**
TXNDC3	0.849194	1.00	1.00	**-0.00**
HSFY1	0.850111	1.00	1.00	**0.00**
FN3K	0.850158	1.00	1.00	**0.00**
HOXB13	0.852799	1.00	1.00	**0.00**
PTK7_int	0.852901	1.00	1.00	**-0.00**
LDB2	0.853092	1.00	1.00	**0.00**
NDUFV3	0.853336	1.00	1.00	**0.00**
KIT_ext	0.854693	1.00	1.00	**0.00**
ADD1	0.855033	1.00	1.00	**-0.00**
DDX55	0.856046	1.00	1.00	**0.00**
EPAS1	0.856774	1.00	1.00	**-0.00**
DNM1L	0.857289	1.00	1.00	**-0.00**
PDGFRL	0.858479	1.00	1.00	**0.00**
LCK	0.860462	1.00	1.00	**-0.00**
NAP1L3	0.861203	1.00	0.99	**-0.01**
RARB	0.861751	1.00	1.00	**0.00**
XYLB	0.863708	1.00	1.00	**0.00**
NR2E3	0.863784	1.00	1.00	**0.00**
RRAS2	0.863897	1.00	1.00	**-0.00**
PRKCB	0.863996	1.00	1.00	**-0.00**
ACTR2_a	0.864337	1.00	1.00	**0.00**
DUSP10	0.864663	1.00	1.00	**-0.00**
PTPN6	0.864916	1.00	1.00	**0.00**
PBX1	0.866939	1.00	1.00	**0.00**
ZNF384	0.867415	1.00	1.00	**-0.00**
HTATIP2	0.867648	1.00	1.00	**0.00**
AHCY	0.868759	1.00	1.00	**0.00**
RET_int	0.869696	1.00	1.00	**0.00**
TLK1	0.869849	1.00	1.00	**-0.00**
EEF2K	0.869967	1.00	1.00	**0.00**
ZNF449	0.871103	1.00	1.00	**0.00**
ZNF593	0.871207	1.00	1.00	**-0.00**
CAB39L	0.871831	1.00	1.00	**0.00**
CREB1	0.872058	1.00	1.00	**0.00**
STK3	0.872463	1.00	1.00	**0.00**
PHLDA2	0.873037	1.00	1.00	**-0.00**
PSMB3	0.873855	1.00	1.00	**0.00**
YEATS4	0.873931	1.00	1.00	**0.00**
TRAF6	0.874935	1.00	1.00	**-0.00**
RHOH	0.875331	1.00	1.00	**-0.00**
RET_ext	0.876299	1.00	1.00	**0.00**
GTF2A2	0.876712	1.00	1.00	**-0.00**
PFKP	0.877030	1.00	1.00	**0.00**
SSNA1	0.878696	1.00	1.00	**0.00**
SBDS	0.879670	1.00	1.00	**-0.00**
SOX15	0.879836	1.00	1.00	**0.00**
GNG2	0.880434	1.00	1.00	**-0.00**

MAP2K6	0.881285	1.00	1.00	**0.00**
MARK3	0.882025	1.00	1.00	**-0.00**
SSX4	0.882269	1.00	1.00	**0.00**
GMPS	0.884282	1.00	1.00	**0.00**
PTGER3	0.886250	1.00	1.00	**-0.00**
NUBP2	0.887061	1.00	1.00	**0.00**
S100A6	0.887087	1.00	1.00	**-0.00**
PPP2R4	0.887719	1.00	1.00	**0.00**
DDIT3	0.888496	1.00	1.00	**-0.00**
PTP4A2	0.889386	1.00	1.00	**0.00**
TRIB3	0.889566	1.00	1.00	**-0.00**
RPS6KB2	0.890268	1.00	1.00	**0.00**
ELMO3	0.891504	1.00	1.00	**-0.00**
PC	0.892325	1.00	1.00	**0.00**
TP53RK	0.893286	1.00	1.00	**0.00**
TRAF1	0.894056	1.00	1.00	**-0.00**
RPS6KA2	0.897636	1.00	1.00	**-0.00**
PTPN2	0.898617	1.00	1.00	**0.00**
ELF4	0.898868	1.00	1.00	**0.00**
MED30	0.899680	1.00	1.00	**-0.00**
NRBF2	0.903500	1.00	1.00	**-0.00**
EPHA3_ext	0.903673	1.00	1.00	**0.00**
CEBPG	0.903974	1.00	1.00	**-0.00**
MYC	0.904304	1.00	1.00	**0.00**
CCT5	0.904934	1.00	1.00	**0.00**
C6	0.905031	1.00	1.00	**-0.00**
COL4A3BP	0.905302	1.00	1.00	**0.00**
RNF40	0.906133	1.00	1.00	**-0.00**
FADD	0.907754	1.00	1.00	**-0.00**
DUSP6	0.908155	1.00	1.00	**0.00**
PRPS2	0.908481	1.00	1.00	**0.00**
HAND1	0.908610	1.00	1.00	**0.00**
BIRC2	0.909297	1.00	1.00	**-0.00**
PRKACB	0.909795	1.00	1.00	**-0.00**
RAF1	0.910338	1.00	1.00	**0.00**
ZNF187	0.911419	1.00	1.00	**-0.00**
TOLLIP	0.911963	1.00	1.00	**0.00**
PIN1	0.912420	1.00	1.00	**-0.00**
HDAC1	0.912931	1.00	1.00	**-0.00**
HTR1D	0.912937	1.00	1.00	**0.00**
ANKRD13A	0.913228	1.00	1.00	**0.00**
PPAT	0.914044	1.00	1.00	**-0.00**
RAD51L3	0.914820	1.00	1.00	**0.00**
ASB1	0.915308	1.00	1.00	**-0.00**
NRBP2	0.915795	1.00	1.00	**-0.00**
GNGT1	0.916286	1.00	1.00	**0.00**
AKT3	0.917269	1.00	1.00	**0.00**
MYCL1	0.920854	1.00	1.00	**0.00**
MSC	0.922952	1.00	1.00	**0.00**
IKZF3	0.923242	1.00	1.00	**-0.00**
MAPK3	0.923650	1.00	1.00	**0.00**

DDR1_a	0.924237	1.00	1.00	**0.00**
FGFR4_ext	0.924407	1.00	1.00	**0.00**
DOM3Z	0.924569	1.00	1.00	**0.00**
MAPKAPK5	0.925422	1.00	1.00	**0.00**
BTG3	0.926110	1.00	1.00	**-0.00**
GRB7	0.928009	1.00	1.00	**-0.00**
CASP7	0.928487	1.00	1.00	**-0.00**
VIM	0.928771	1.00	1.00	**0.00**
ERBB3_ext	0.929662	1.00	1.00	**0.00**
CNN1	0.930405	1.00	1.00	**-0.00**
WWTR1	0.932026	1.00	1.00	**0.00**
TCF12	0.932276	1.00	1.00	**-0.00**
RXRG	0.932663	1.00	1.00	**0.00**
TACC1	0.933297	1.00	1.00	**-0.00**
RHOT2	0.935442	1.00	1.00	**-0.00**
TIE1	0.935519	1.00	1.00	**0.00**
CALM3	0.936193	1.00	1.00	**0.00**
BMPR2	0.938581	1.00	1.00	**-0.00**
NUDT2	0.939418	1.00	1.00	**-0.00**
MAPK11	0.940014	1.00	1.00	**0.00**
SGK1	0.940194	1.00	1.00	**-0.00**
PDCD2L	0.941040	1.00	1.00	**-0.00**
CALU	0.941199	1.00	1.00	**0.00**
RPL11	0.942001	1.00	1.00	**-0.00**
GTF2B	0.942211	1.00	1.00	**-0.00**
TRIP11	0.943139	1.00	1.00	**-0.00**
REXO4	0.945209	1.00	1.00	**0.00**
TYRO3	0.945291	1.00	1.00	**-0.00**
ZMYND11	0.945468	1.00	1.00	**0.00**
KIAA1984	0.946669	1.00	1.00	**0.00**
TSG101	0.947213	1.00	1.00	**-0.00**
LSM1	0.948193	1.00	1.00	**-0.00**
LHFP	0.948517	1.00	1.00	**0.00**
GRK6	0.949531	1.00	1.00	**0.00**
PRDM4	0.950451	1.00	1.00	**-0.00**
GTF2H1	0.950944	1.00	1.00	**-0.00**
LNX1	0.951003	1.00	1.00	**-0.00**
ETV6	0.951827	1.00	1.00	**0.00**
TBC1D5	0.957470	1.00	1.00	**0.00**
USF2	0.959791	1.00	1.00	**0.00**
SLA	0.960273	1.00	1.00	**-0.00**
BANK1	0.960930	1.00	1.00	**0.00**
PAK4	0.961147	1.00	1.00	**-0.00**
FOXS1	0.962093	1.00	1.00	**-0.00**
MED17	0.963037	1.00	1.00	**-0.00**
FES	0.963142	1.00	1.00	**0.00**
FGFR4_int	0.963910	1.00	1.00	**0.00**
FKBP5	0.964826	1.00	1.00	**0.00**
MAP4K5	0.966312	1.00	1.00	**0.00**
YARS	0.966446	1.00	1.00	**-0.00**
GNAZ	0.967243	1.00	1.00	**-0.00**

THUMPD1	0.967538	1.00	1.00	**0.00**
FGFR1_ext	0.967872	1.00	1.00	**-0.00**
NFYB	0.968492	1.00	1.00	**-0.00**
STAT1	0.970035	1.00	1.00	**0.00**
PPP1R2P9	0.970043	1.00	1.00	**-0.00**
TEK	0.970504	1.00	1.00	**0.00**
DUSP13	0.970888	1.00	1.00	**-0.00**
IRF5	0.971669	1.00	1.00	**-0.00**
MPP3	0.971741	1.00	1.00	**-0.00**
MSH2	0.973083	1.00	1.00	**-0.00**
FIP1L1	0.974038	1.00	1.00	**-0.00**
ID2	0.974165	1.00	1.00	**0.00**
SERPINB5	0.974677	1.00	1.00	**0.00**
SCFD1	0.975337	1.00	1.00	**0.00**
AIF1	0.976806	1.00	1.00	**0.00**
PTK7_ext	0.977935	1.00	1.00	**0.00**
LMO2	0.979230	1.00	1.00	**0.00**
RPLP1	0.980477	1.00	1.00	**0.00**
MED22	0.980702	1.00	1.00	**-0.00**
HIF1A	0.982107	1.00	1.00	**0.00**
PDCL3	0.982420	1.00	1.00	**-0.00**
HOXC10	0.982621	1.00	1.00	**0.00**
GSK3B	0.984269	1.00	1.00	**0.00**
PKM2	0.984455	1.00	1.00	**-0.00**
S100A9	0.984900	1.00	1.00	**0.00**
HIST1H4I	0.985037	1.00	1.00	**-0.00**
ERCC5	0.985454	1.00	1.00	**0.00**
FGFR2_int	0.986151	1.00	1.00	**-0.00**
FASTK_a	0.986284	1.00	1.00	**0.00**
CSNK2A1	0.986930	1.00	1.00	**-0.00**
RIOK3	0.987442	1.00	1.00	**-0.00**
MAPK13	0.988020	1.00	1.00	**-0.00**
MAFG	0.989557	1.00	1.00	**0.00**
LASS2	0.990424	1.00	1.00	**0.00**
NCK1	0.991657	1.00	1.00	**0.00**
HIF1A_a	0.994344	1.00	1.00	**0.00**
PHKG2	0.995071	1.00	1.00	**-0.00**
CHEK1_a	0.997296	1.00	1.00	**0.00**
RNASEL	0.999426	1.00	1.00	**0.00**
RARA	0.999971	1.00	1.00	0.00

TABLE 9-16
Table showing record of aliquots (see section 5.3)

	Original sample order #	**SampleID**	**Aliquots**	**Box #**	**Disease**	**Location**	**Reproductive phase**
1	24	1546126	5	Box1	Endometriosis	Peritoneal	Mid cycle
2	26	3691029	5	Box1	Endometriosis	Follicular	Follicular
3	40	6791921	5	Box1	Control		Luteal
4	39	503819	5	Box1	Control		Follicular

5	49	3521231	3	Box1	Control		Luteal
6	50	2357654	3	Box2	Control		Luteal
7	21	497197	5	Box2	Endometriosis	Peritoneal	Luteal
8	9	9153343	5	Box2	Endometriosis	Peritoneal	Follicular
9	13	9673929	5	Box2	Endometriosis	Peritoneal	Follicular
10	45	1335891	3	Box2	Control		Luteal
11	10	6707519	5	Box3	Endometriosis	Peritoneal	Follicular
12	22	2183016	5	Box3	Endometriosis	Peritoneal	Mid cycle
13	8	8413629	5	Box3	Endometriosis	Peritoneal	Follicular
14	44	5849813	3	Box3	Control		Luteal
15	28	8973029	5	Box3	Endometriosis	Follicular	Follicular
16	4	227536	4	Box4	Endometriosis	Peritoneal	Follicular
17	51	1286503	3	Box4	Control		Luteal
18	19	3850536	5	Box4	Endometriosis	Peritoneal	Luteal
19	12	811109	3	Box4	Endometriosis	Peritoneal	Follicular
20	2	6170020	2	Box4	Endometriosis	Peritoneal	Follicular
21	15	439356	5	Box5	Endometriosis	Peritoneal	Luteal
22	30	9661629	4	Box5	Endometriosis	Follicular	Follicular
23	3	9066819	5	Box5	Endometriosis	Peritoneal	Follicular
24	31	9410816	5	Box5	Endometriosis	Follicular	Follicular
25	46	6371846	3	Box5	Control		Luteal
26	43	3497512	3	Box6	Control		Luteal
27	20	2487156	5	Box6	Endometriosis	Peritoneal	Luteal
28	1	1602619	3	Box6	Endometriosis	Peritoneal	Follicular
29	6	5938026	5	Box6	Endometriosis	Peritoneal	Follicular
30	38	3140020	5	Box6	Control		Follicular
31	17	9315020		Box7	Endometriosis	Peritoneal	Luteal
32	7	588546	3	Box7	Endometriosis	Peritoneal	Follicular
33	27	2684078	4	Box7	Endometriosis	Follicular	Follicular
34	14	6095346	5	Box7	Endometriosis	Peritoneal	Luteal
35	33	7036506	5	Box7	Endometriosis	Ovarian	Luteal
36	29	8714246	5	Box8	Endometriosis	Follicular	Follicular
37	18	4506746	5	Box8	Endometriosis	Peritoneal	Luteal
38	32	2207656	5	Box8	Endometriosis	Follicular	Follicular
39	23	6220521	5	Box8	Endometriosis	Peritoneal	Mid cycle
40	36	5161629	5	Box8	Endometriosis	Ovarian	Luteal
41	25	8417619	5	Box9	Endometriosis	Follicular	Follicular
42	42	1289895	5	Box9	Control		Luteal
43	47	8361972	3	Box9	Control		Luteal
44	11	6239256	5	Box9	Endometriosis	Peritoneal	Follicular
45	41	1113256	3	Box9	Control		Luteal
46	48	1839711	3	Box10	Control		Luteal
47	34	5044706	5	Box10	Endometriosis	Ovarian	Luteal
48	16	3677410	5	Box10	Endometriosis	Peritoneal	Luteal
49	35	629829	5	Box10	Endometriosis	Ovarian	Luteal
50	5	316919	5	Box10	Endometriosis	Peritoneal	Follicular
51	37	996579	3	Box11	Control		Follicular

TABLE 9-17
Table showing sample identities (see section 5.3)

#	SampleID	Disease	Location	Reproductive phase	Ovarian endometriomas
1	1602619 x	Endometriosis	Peritoneal	Follicular	None
2	6170020 x	Endometriosis	Peritoneal	Follicular	None
3	9066819 x	Endometriosis	Peritoneal	Follicular	None
4	227536 x	Endometriosis	Peritoneal	Follicular	None
5	316919 x	Endometriosis	Peritoneal	Follicular	None
6	5938026 x	Endometriosis	Peritoneal	Follicular	None
7	588546 x	Endometriosis	Peritoneal	Follicular	None
8	8413629 x	Endometriosis	Peritoneal	Follicular	None
9	9153343 x	Endometriosis	Peritoneal	Follicular	None
10	6707519 x	Endometriosis	Peritoneal	Follicular	None
11	6239256 x	Endometriosis	Peritoneal	Follicular	None
12	811109 x	Endometriosis	Peritoneal	Follicular	None
13	9673929 x	Endometriosis	Peritoneal	Follicular	None
14	6095346 x	Endometriosis	Peritoneal	Luteal	None
15	439356 x	Endometriosis	Peritoneal	Luteal	None
16	3677410 x	Endometriosis	Peritoneal	Luteal	None
17	9315020 x	Endometriosis	Peritoneal	Luteal	None
18	4506746 x	Endometriosis	Peritoneal	Luteal	None
19	3850536 x	Endometriosis	Peritoneal	Luteal	None
20	2487156 x	Endometriosis	Peritoneal	Luteal	None
21	497197 x	Endometriosis	Peritoneal	Luteal	None
22	2183016 x	Endometriosis	Peritoneal	Mid cycle	None
23	6220521 x	Endometriosis	Peritoneal	Mid cycle	None
24	1546126 x	Endometriosis	Peritoneal	Mid cycle	None
25	8417619 x	Endometriosis	Ovarian	Follicular	Endometrioma
26	3691029 x	Endometriosis	Ovarian	Follicular	Endometrioma
27	2684078 x	Endometriosis	Ovarian	Follicular	Endometrioma
28	8973029 x	Endometriosis	Ovarian	Follicular	Endometrioma
29	8714246 x	Endometriosis	Ovarian	Follicular	Endometrioma
30	9661629 x	Endometriosis	Ovarian	Follicular	Endometrioma
31	9410816 x	Endometriosis	Ovarian	Follicular	Endometrioma
32	2207656 x	Endometriosis	Ovarian	Follicular	Endometrioma
33	7036506 x	Endometriosis	Ovarian	Luteal	Endometrioma
34	5044706 x	Endometriosis	Ovarian	Luteal	Endometrioma
35	629829 x	Endometriosis	Ovarian	Luteal	Endometrioma
36	5161629 x	Endometriosis	Ovarian	Luteal	Endometrioma
37	996579 x	Control		Follicular	None
38	3140020 x	Control		Follicular	None
39	503819 x	Control		Follicular	None
40	6791921 x	Control		Luteal	None
41	1113256 x	Control		Luteal	None
42	1289895 x	Control		Luteal	None
43	3497512 x	Control		Luteal	None
44	5849813	Control		Luteal	
45	1335891	Control		Luteal	
46	6371846	Control		Luteal	
47	8361972	Control		Luteal	

48	1839711	Control	Luteal
49	3521231	Control	Luteal
50	2357654	Control	Luteal
51	1286503	Control	Luteal

TABLE 9-18

Table showing individual biomarkers for endometriosis (see section 6.5)

No.[(i)]	Symbol[(ii)]	Name[(iii)]	Type
1	ACTB	Homo sapiens actin beta	Auto-antigen
2	ADD1	Homo sapiens adducin 1 (alpha)	Auto-antigen
3	ADSL	Homo sapiens adenylosuccinate lyase	Auto-antigen
4	AK2	Homo sapiens adenylate kinase 2 transcript variant AK2A	Auto-antigen
5	KLK3	Homo sapiens kallikrein 3 (prostate specific antigen) transcript variant 1	Auto-antigen
6	ATF1	Homo sapiens activating transcription factor 1	Auto-antigen
7	CKM	Homo sapiens creatine kinase muscle	Auto-antigen
8	CLK2	Homo sapiens CDC-like kinase 2 transcript variant phclk2	Auto-antigen
9	DDB2	Homo sapiens damage-specific DNA binding protein 2 48kDa	Auto-antigen
10	DTYMK	Homo sapiens deoxythymidylate kinase (thymidylate kinase)	Auto-antigen
11	DUSP4	Homo sapiens dual specificity phosphatase 4 transcript variant 1	Auto-antigen
12	E2F6	Homo sapiens E2F transcription factor 6	Auto-antigen
13	EXT2	Homo sapiens exostoses (multiple) 2	Auto-antigen
14	FGFR4_ext	Homo sapiens fibroblast growth factor receptor 4 transcript variant 3	Auto-antigen
15	FIGF	Homo sapiens c-fos induced growth factor (vascular endothelial growth factor D)	Auto-antigen
16	FKBP3	Homo sapiens FK506 binding protein 3 25kDa	Auto-antigen
17	GALK1	Homo sapiens galactokinase 1	Auto-antigen
18	GK2	Homo sapiens glycerol kinase 2	Auto-antigen
19	GRB7	Homo sapiens growth factor receptor-bound protein 7	Auto-antigen
20	GTF2B	Homo sapiens general transcription factor IIB	Auto-antigen
21	GTF2H1	Homo sapiens general transcription factor IIH polypeptide 1 62kDa	Auto-antigen
22	GTF2H2	Homo sapiens general transcription factor IIH polypeptide 2 44kDa	Auto-antigen
23	HSPD1	Homo sapiens heat shock 60kDa protein 1 (chaperonin)	Auto-antigen
24	IDI1	Homo sapiens isopentenyl-diphosphate delta isomerase	Auto-antigen
25	IFI16	Homo sapiens interferon, gamma-inducible protein 16,	Auto-antigen
26	LDHA	Homo sapiens lactate dehydrogenase A	Auto-antigen
27	LYL1	Homo sapiens lymphoblastic leukemia derived sequence 1	Auto-antigen
28	MARK3	Homo sapiens MAP/microtubule affinity-regulating kinase 3	Auto-antigen
29	MPP3	Homo sapiens membrane protein palmitoylated 3 (MAGUK p55 subfamily member 3)	Auto-antigen
30	TRIM37	Homo sapiens tripartite motif-containing 37,	Auto-antigen
31	NCF2	Homo sapiens neutrophil cytosolic factor 2 (65kDa, chronic granulomatous disease, autosomal 2),	Auto-antigen

32	RPL10A	Homo sapiens ribosomal protein L10a	Auto-antigen
33	NFYA	Homo sapiens nuclear transcription factor Y alpha	Auto-antigen
34	NRAS	Homo sapiens neuroblastoma RAS viral (v-ras) oncogene homolog	Auto-antigen
35	NTRK3_ext	Homo sapiens neurotrophic tyrosine kinase receptor type 3 transcript variant 3	Auto-antigen
36	OAS2	Homo sapiens 2'-5'-oligoadenylate synthetase 2 69/71kDa	Auto-antigen
37	endometriosis	Homo sapiens pyruvate carboxylase	Auto-antigen
38	CDK17	Homo sapiens endometriosisTAIRE protein kinase 2	Auto-antigen
39	PDE4A	Homo sapiens Homo sapiens phosphodiesterase 4A, cAMP-specific (phosphodiesterase E2 dunce homolog, Dro	Auto-antigen
40	PHF1	Homo sapiens PHD finger protein 1 transcript variant 2	Auto-antigen
41	PKM2	Homo sapiens pyruvate kinase muscle transcript variant 1	Auto-antigen
42	MAP2K5	Homo sapiens mitogen-activated protein kinase kinase 5, transcript variant A	Auto-antigen
43	PRPS2	Homo sapiens phosphoribosyl pyrophosphate synthetase 2	Auto-antigen
44	RAN	Homo sapiens RAN member RAS oncogene family	Auto-antigen
45	RB1	Homo sapiens retinoblastoma 1 (including osteosarcoma)	Auto-antigen
46	RBMS1	Homo sapiens Homo sapiens RNA binding motif single stranded interacting protein 1 transcript variant	Auto-antigen
47	RET_a	Homo sapiens ret proto-oncogene (multiple endocrine neoplasia and medullary thyroid carci	Auto-antigen
48	RORC	Homo sapiens RAR-related orphan receptor C	Auto-antigen
49	RPL18	Homo sapiens ribosomal protein L18	Auto-antigen
50	RPL18A	Homo sapiens ribosomal protein L18a	Auto-antigen
51	RPL28	Homo sapiens ribosomal protein L28	Auto-antigen
52	RPL31	Homo sapiens ribosomal protein L31	Auto-antigen
53	RPL32	Homo sapiens ribosomal protein L32	Auto-antigen
54	S100A6	Homo sapiens S100 calcium binding protein A6 (calcyclin)	Auto-antigen
55	SCP2	Homo sapiens sterol carrier protein 2 transcript variant 2	Auto-antigen
56	SIAH1	Homo sapiens seven in absentia homolog 1 (Drosophila) transcript variant 2	Auto-antigen
57	SMARCD1	Homo sapiens SWI/SNF related matrix associated actin dependent regulator of chromatin subfamily d member 1	Auto-antigen
58	SMARCE1	Homo sapiens SWI/SNF related matrix associated actin dependent regulator of chromatin	Auto-antigen
59	SOD2	Homo sapiens superoxide dismutase 2 mitochondrial	Auto-antigen
60	SOX2	Homo sapiens SRY (sex determining region Y)-box 2	Auto-antigen
61	SRPK1	Homo sapiens SFRS protein kinase 1	Auto-antigen
62	TPM1	Homo sapiens tropomyosin 1 (alpha)	Auto-antigen
63	NR2C1	Homo sapiens nuclear receptor subfamily 2 group C member 1	Auto-antigen
64	TRIP6	Homo sapiens thyroid hormone receptor interactor 6,	Auto-antigen
65	UBA1	Homo sapiens Homo sapiens ubiquitin-activating enzyme E1 (A1S9T and BN75 temperature sensitivity compl	Auto-antigen
66	VCL	Homo sapiens vinculin	Auto-antigen
67	ZNF41	Homo sapiens zinc finger protein 41 transcript variant 2	Auto-antigen

68	PAX8	Homo sapiens paired box gene 8 transcript variant PAX8A	Auto-antigen
69	NRIP1	Homo sapiens nuclear receptor interacting protein 1	Auto-antigen
70	PIP4K2B	Homo sapiens phosphatidylinositol-4-phosphate 5-kinase type II beta transcript variant 2	Auto-antigen
71	UXT	Homo sapiens ubiquitously-expressed transcript	Auto-antigen
72	API5	Homo sapiens apoptosis inhibitor 5	Auto-antigen
73	MKNK1	Homo sapiens MAP kinase-interacting serine/threonine kinase 1	Auto-antigen
74	SUCLA2	Homo sapiens succinate-CoA ligase ADP-forming beta subunit	Auto-antigen
75	LDB1	Homo sapiens LIM domain binding 1	Auto-antigen
76	NAE1	Homo sapiens amyloid beta precursor protein binding protein 1 transcript variant 1	Auto-antigen
77	PAPSS2	Homo sapiens 3'-phosphoadenosine 5'-phosphosulfate synthase 2	Auto-antigen
78	USP10	Homo sapiens ubiquitin specific protease 10	Auto-antigen
79	PRPF4	Homo sapiens Homo sapiens PRP4 pre-	Auto-antigen
80	AIM2	Homo sapiens absent in melanoma 2	Auto-antigen
81	TBPL1	Homo sapiens TBP-like 1	Auto-antigen
82	TRAF4	Homo sapiens TNF receptor-associated factor 4 transcript variant 1	Auto-antigen
83	SOCS5	Homo sapiens suppressor of cytokine signaling 5	Auto-antigen
84	ZSCAN12	Homo sapiens zinc finger protein 305	Auto-antigen
85	HDAC4	Homo sapiens cDNA	Auto-antigen
86	KIAA0101	Homo sapiens KIAA0101 gene product	Auto-antigen
87	IP6K1	Homo sapiens inositol hexaphosphate kinase 1	Auto-antigen
88	RNF40	Homo sapiens ring finger protein 40 transcript variant 1	Auto-antigen
89	GPHN	Homo sapiens gephyrin	Auto-antigen
90	HRSP12	Homo sapiens translational inhibitor protein p14.5	Auto-antigen
91	STUB1	Homo sapiens STIP1 homology and U-Box containing protein 1	Auto-antigen
92	TRAIP	Homo sapiens TRAF interacting protein	Auto-antigen
93	PLK4	Homo sapiens serine/threonine kinase 18	Auto-antigen
94	CCNI	Homo sapiens cyclin I	Auto-antigen
95	IL24	Homo sapiens interleukin 24 transcript variant 1	Auto-antigen
96	CDK20	Homo sapiens cell cycle related kinase	Auto-antigen
97	PABendometriosis1	Homo sapiens poly(A) binding protein cytoplasmic 1	Auto-antigen
98	MED4	Homo sapiens vitamin D receptor interacting protein	Auto-antigen
99	NME7	Homo sapiens non-metastatic cells 7 protein expressed in (nucleoside-diphosphate kinase) transcript variant 1	Auto-antigen
100	PHF11	Homo sapiens PHD finger protein 11	Auto-antigen
101	IRAK4	Homo sapiens interleukin-1 receptor-associated kinase 4 mRNA (cDNA clone MGC:13330)	Auto-antigen
102	TXNDC3	Homo sapiens thioredoxin domain containing 3 (spermatozoa)	Auto-antigen
103	TAOK3	Homo sapiens STE20-like kinase	Auto-antigen
104	STYXL1	Homo sapiens dual specificity phosphatase 24 (putative)	Auto-antigen
105	ASB1	Homo sapiens ankyrin repeat and SOCS box-containing 1	Auto-antigen
106	MST4	Homo sapiens Mst3 and SOK1-related kinase (MASK)	Auto-antigen
107	PELO	Homo sapiens pelota homolog (Drosophila)	Auto-antigen
108	ETNK2	Homo sapiens ethanolamine kinase 2	Auto-antigen

109	RFK	Homo sapiens riboflavin kinase	Auto-antigen
110	C9orf86	Homo sapiens chromosome 9 open reading frame 86	Auto-antigen
111	DDX55	Homo sapiens DEAD (Asp-Glu-Ala-Asp) box polypeptide 55	Auto-antigen
112	CCNB1IP1	Homo sapiens cDNA	Auto-antigen
113	KLHL12	Homo sapiens kelch-like protein C3IP1	Auto-antigen
114	SAV1	Homo sapiens salvador homolog 1 (Drosophila)	Auto-antigen
115	CAMKV	Homo sapiens hypothetical protein MGC8407	Auto-antigen
116	NSBP1	Homo sapiens nucleosomal binding protein 1,	Auto-antigen
117	ALPK1	Homo sapiens alpha-kinase 1 mRNA (cDNA clone MGC:71554)	Auto-antigen
118	ELMOD3	Homo sapiens RNA binding motif and ELMO domain 1	Auto-antigen
119	AIFM2	Homo sapiens apoptosis-inducing factor (AIF)-like mitochondrion-associated inducer of death	Auto-antigen
120	RHOT2	Homo sapiens ras homolog gene family member T2	Auto-antigen
121	PYGO2	Homo sapiens pygopus 2	Auto-antigen
122	ebv-miR-BART12	ebv-miR-BART12	miRNA
123	ebv-miR-BART14	ebv-miR-BART14	miRNA
124	ebv-miR-BART16	ebv-miR-BART16	miRNA
125	ebv-miR-BART20-5p	ebv-miR-BART20-5p	miRNA
126	ebv-miR-BART2-5p	ebv-miR-BART2-5p	miRNA
127	MIRLET7B	hsa-let-7b*	miRNA
128	MIRLET7F1	hsa-let-7f	miRNA
129	MIRLET7F2	hsa-let-7f-1*	miRNA
130	MIRLET7G	hsa-let-7g	miRNA
131	MIR103A1	hsa-miR-103a	miRNA
132	MIR10b	hsa-miR-10b	miRNA
133	MIR1183	hsa-miR-1183	miRNA
134	MIR1202	hsa-miR-1202	miRNA
135	MIR1207	hsa-miR-1207-5p	miRNA
136	MIR122	hsa-miR-122	miRNA
137	MIR1224	hsa-miR-1224-5p	miRNA
138	MIR1225	hsa-miR-1225-3p	miRNA
139	MIR1225	hsa-miR-1225-5p	miRNA
140	MIR1226	hsa-miR-1226*	miRNA
141	MIR1228	hsa-miR-1228*	miRNA
142	MIR1234	hsa-miR-1234	miRNA
143	MIR1237	hsa-miR-1237	miRNA
144	MIR1238	hsa-miR-1238	miRNA
145	MIR125a	hsa-miR-125a-5p	miRNA
146	MIR1260A	hsa-miR-1260	miRNA
147	MIR1260b	hsa-miR-1260b	miRNA
148	MIR1280	hsa-miR-1280	miRNA
149	MIR1281	hsa-miR-1281	miRNA
150	MIR1290	hsa-miR-1290	miRNA
151	MIR1291	hsa-miR-1291	miRNA
152	MIR129-1 / MIR129-2	hsa-miR-129-3p	miRNA

153	MIR1301	hsa-miR-1301	miRNA
154	MIR135A1 /	hsa-miR-135a	miRNA
155	MIR135A1 /	hsa-miR-135a*	miRNA
156	MIR141	hsa-miR-141	miRNA
157	MIR142	hsa-miR-142-3p	miRNA
158	MIR149	hsa-miR-149	miRNA
159	MIR150	hsa-miR-150	miRNA
160	MIR150	hsa-miR-150*	miRNA
161	MIR1539	hsa-miR-1539	miRNA
162	MIR181A2	hsa-miR-181a	miRNA
163	MIR1825	hsa-miR-1825	miRNA
164	MIR186	hsa-miR-186	miRNA
165	MIR18a	hsa-miR-18a	miRNA
166	MIR18b	hsa-miR-18b	miRNA
167	MIR191	hsa-miR-191*	miRNA
168	MIR197	hsa-miR-197	miRNA
169	MIR198	hsa-miR-198	miRNA
170	MIR205	hsa-miR-205	miRNA
171	MIR2116	hsa-miR-2116*	miRNA
172	MIR215	hsa-miR-215	miRNA
173	MIR22	hsa-miR-22	miRNA
174	MIR223	hsa-miR-223	miRNA
175	MIR2276	hsa-miR-2276	miRNA
176	MIR23c	hsa-miR-23c	miRNA
177	MIR26A1 / MIR26A2	hsa-miR-26a	miRNA
178	MIR28	hsa-miR-28-3p	miRNA
179	MIR28	hsa-miR-28-5p	miRNA
180	MIR29B1 / MIR29B2	hsa-miR-29b	miRNA
181	MIR30a	hsa-miR-30a	miRNA
182	MIR30b	hsa-miR-30b	miRNA
183	MIR3131	hsa-miR-3131	miRNA
184	MIR3138	hsa-miR-3138	miRNA
185	MIR3149	hsa-miR-3149	miRNA
186	MIR3156-1 / MIR3156-3	hsa-miR-3156-5p	miRNA
187	MIR3180-1 / MIR3180-2 / MIR3180-3 / MIR3180-4 / MIR3180-5	hsa-miR-3180-5p	miRNA
188	MIR3194	hsa-miR-3194-5p	miRNA
189	MIR3195	hsa-miR-3195	miRNA
190	MIR3196	hsa-miR-3196	miRNA
191	MIR32	hsa-miR-32	miRNA
192	MIR320C1 / MIR320C2	hsa-miR-320c	miRNA
193	MIR324	hsa-miR-324-3p	miRNA
194	MIR328	hsa-miR-328	miRNA
195	MIR331	hsa-miR-331-5p	miRNA
196	MIR33b	hsa-miR-33b*	miRNA
197	MIR342	hsa-miR-342-3p	miRNA

198	MIR34a	hsa-miR-34a	miRNA
199	MIR3610	hsa-miR-3610	miRNA
200	MIR3648	hsa-miR-3648	miRNA
201	MIR3652	hsa-miR-3652	miRNA
202	MIR3663	hsa-miR-3663-5p	miRNA
203	MIR3667	hsa-miR-3667-5p	miRNA
204	MIR382	hsa-miR-382	miRNA
205	MIR3911	hsa-miR-3911	miRNA
206	MIR3937	hsa-miR-3937	miRNA
207	MIR4257	hsa-miR-4257	miRNA
208	MIR425	hsa-miR-425*	miRNA
209	MIR4270	hsa-miR-4270	miRNA
210	MIR4274	hsa-miR-4274	miRNA
211	MIR4281	hsa-miR-4281	miRNA
212	MIR4284	hsa-miR-4284	miRNA
213	MIR4286	hsa-miR-4286	miRNA
214	MIR429	hsa-miR-429	miRNA
215	MIR4290	hsa-miR-4290	miRNA
216	MIR4313	hsa-miR-4313	miRNA
217	MIR4323	hsa-miR-4323	miRNA
218	MIR466	hsa-miR-466	miRNA
219	MIR483	hsa-miR-483-3p	miRNA
220	MIR484	hsa-miR-484	miRNA
221	MIR485	hsa-miR-485-3p	miRNA
222	MIR486	hsa-miR-486-5p	miRNA
223	MIR488	hsa-miR-488	miRNA
224	MIR497	hsa-miR-497	miRNA
225	MIR511-1	hsa-miR-511	miRNA
226	MIR511-2	hsa-miR-512	miRNA
227	MIR520c	hsa-miR-520c-3p	miRNA
228	MIR550A1 / MIR550A2 / MIR550A3	hsa-miR-550a	miRNA
229	MIR556	hsa-miR-556-3p	miRNA
230	MIR557	hsa-miR-557	miRNA
231	MIR561	hsa-miR-561	miRNA
232	MIR572	hsa-miR-572	miRNA
233	MIR574	hsa-miR-574-3p	miRNA
234	MIR574	hsa-miR-574-5p	miRNA
235	MIR595	hsa-miR-595	miRNA
236	MIR630	hsa-miR-630	miRNA
237	MIR642b	hsa-miR-642b	miRNA
238	MIR646	hsa-miR-646	miRNA
239	MIR659	hsa-miR-659	miRNA
240	MIR660	hsa-miR-660	miRNA
241	MIR663A	hsa-miR-663	miRNA
242	MIR664	hsa-miR-664	miRNA
243	MIR720	hsa-miR-720	miRNA
244	MIR762	hsa-miR-762	miRNA
245	MIR766	hsa-miR-766	miRNA
246	MIR877	hsa-miR-877*	miRNA

247	MIR888	hsa-miR-888	miRNA
248	MIR933	hsa-miR-933	miRNA
249	MIR940	hsa-miR-940	miRNA
250	MIR95	hsa-miR-95	miRNA
251	hsv1-miR-H1*	hsv1-miR-H1*/ hsv1-miR-H1-3p	miRNA
252	hsv1-miR-H2-3p	hsv1-miR-H2-3p	miRNA
253	hsv1-miR-H6-3p	hsv1-miR-H6-3p	miRNA
254	hsv1-miR-H7*	hsv1-miR-H7*	miRNA
255	hsv1-miR-H8	hsv1-miR-H8	miRNA
256	hsv2-miR-H22	hsv2-miR-H22	miRNA
257	hsv2-miR-H25	hsv2-miR-H25	miRNA
258	hsv2-miR-H6	hsv2-miR-H6	miRNA
259	hsv2-miR-H6*	hsv2-miR-H6*	miRNA
260	kshv-miR-K12-10a	kshv-miR-K12-10a	miRNA
261	kshv-miR-K12-12*	kshv-miR-K12-12*	miRNA
262	kshv-miR-K12-8*	kshv-miR-K12-8*	miRNA
263	MIR564	hsa-miR-564	miRNA
264	MIRLET7D	hsa-let-7d-5p	miRNA
265	MIRLET7D	hsa-let-7d-3p	miRNA
266	MIR29A	hsa-miR-29a	miRNA
267	MIR219	hsa-miR-219-1-3p	miRNA
268	MIR296	hsa-miR-296-3p	miRNA
269	MIR337	hsa-miR-337-5p	miRNA
270	MIR369	hsa-miR-369-3p	miRNA
271	MIR450	hsa-miR-450b-5p	miRNA
272	MIR483	hsa-miR-483-5p	miRNA
273	MIR507	hsa-miR-507	miRNA
274	MIR517C	hsa-miR-517c	miRNA
275	MIR519A	hsa-miR-519a	miRNA
276	MIR519D	hsa-miR-519d	miRNA
277	MIR520G	hsa-miR-520g	miRNA
278	MIR576	hsa-miR-576-5p	miRNA
279	MIR577	hsa-miR-577	miRNA
280	MIR604	hsa-miR-604	miRNA
281	MIR610	hsa-miR-610	miRNA
282	MIR619	hsa-miR-619	miRNA
283	MIR1256	hsa-miR-1256	miRNA
284	MIR1278	hsa-miR-1278	miRNA
285	MIR1297	hsa-miR-1297	miRNA
286	MIRUS33	hcmv-miR-US33-5p	miRNA
287	MIRH1	hsv1-miR-H1-5p	miRNA
288	MIR877	hsa-miR-877	miRNA
289	LET7E	hsa-let-7e-5p	miRNA
290	LET7E	hsa-let-7e-3p	miRNA
291	MIR9	hsa-miR-9	miRNA
292	MIR92B	hsa-miR-92b	miRNA
293	MIR96	hsa-miR-96-5p	miRNA

294	MIR96	hsa-miR-96-3p	miRNA
295	MIR106A	hsa-miR-106a-5p	miRNA
296	MIR106A	hsa-miR-106a-3p	miRNA
297	MIR17	hsa-miR-17-5p	miRNA
298	MIR17	hsa-miR-17-3p	miRNA
299	MIR106B	hsa-miR-106b-5p	miRNA
300	MIR106B	hsa-miR-106b-3p	miRNA
301	MIR127	hsa-miR-127-3p	miRNA
302	MIR128	hsa-miR-128	miRNA
303	MIR154	hsa-miR-154	miRNA
304	MIR155	hsa-miR-155	miRNA
305	MIR183	hsa-miR-183-5p	miRNA
306	MIR183	hsa-miR-183-3p	miRNA
307	MIR194	hsa-miR-194	miRNA
308	MIR196B	hsa-miR-196b-5p	miRNA
309	MIR196B	hsa-miR-196b-3p	miRNA
310	MIR203	hsa-miR-203	miRNA
311	MIR204	hsa-miR-204	miRNA
312	MIR221	hsa-miR-221-5p	miRNA
313	MIR221	hsa-miR-221-3p	miRNA
314	MIR376	hsa-miR-376a	miRNA
315	MIR376C	hsa-miR-376c	miRNA
316	MIR377	hsa-miR-377	miRNA
317	MIR379	hsa-miR-379	miRNA
318	MIR423	hsa-miR-423-3p	miRNA
319	MIR424	hsa-miR-424-5p	miRNA
320	MIR424	hsa-miR-424-3p	miRNA
321	MIR425	hsa-miR-425-5p	miRNA
322	MIR425	hsa-miR-425-3p	miRNA
323	MIR454	hsa-miR-454-5p	miRNA
324	MIR454	hsa-miR-454-3p	miRNA
325	MIR486	hsa-miR-486-3p	miRNA
326	MIR509	hsa-miR-509-3p	miRNA
327	MIR514	hsa-miR-514	miRNA
328	MIR542	hsa-miR-542-3p	miRNA
329	MIR545	hsa-miR-545-5p	miRNA
330	MIR545	hsa-miR-545-3p	miRNA
331	MIR626	hsa-miR-626	miRNA
332	MIR758	hsa-miR-758-5p	miRNA
333	MIR758	hsa-miR-758-3p	miRNA
334	MIR876	hsa-miR-876-3p	miRNA
335	MIR1185	hsa-miR-1185	miRNA
336	MIR1266	hsa-miR-1266-5p	miRNA
337	MIR1266	hsa-miR-1266-3p	miRNA
338	MIR199A	hsa-miR-199a-3p	miRNA
339	MIR199B	hsa-miR-199b-3p	miRNA
340	MIR625	hsa-miR-625-5p	miRNA
341	MIR625	hsa-miR-625-3p	miRNA
342	MIR631	hsa-miR-631	miRNA
343	MIR635	hsa-miR-635	miRNA

(i) This number is the SEQ ID NO as shown in the sequence listing. For an auto-antigen biomarker, the SEQ ID

NO in the sequence listing provides the coding sequence for the auto-antigen biomarker. For a miRNA biomarker, the SEQ ID NO in the sequence listing provides the sequence of the mature, expressed miRNA biomarker.

(ii) The "Symbol" column gives the gene symbol which has been approved by the HGNC. The HGNC aims to give unique and meaningful names to every miRNA and human gene. An additional dash-number suffix indicates pre-miRNAs that lead to identical mature miRNAs but that are located at different places in the genome.

(iii) The names for auto-antigens are taken from the Official Full Name provided by NCBI. An auto-antigen may have been referred to by one or more pseudonyms in the prior art. The invention relates to these auto-antigens regardless of their nomenclature. The names of the miRNA are taken from the specialist database, miRBase, according to version 16 (released, August 2010).

TABLE 9-19

Autoantibody biomarkers identified from serum studies of subjects suffering from endometriosis (see section 6.5)

No.[i]	Symbol	ID[iii]	Name[vi]	HGNC[v]	GI[vi]
1	ACTB	60	Homo sapiens actin beta	132	12654910
2	ADD1	118	Homo sapiens adducin 1 (alpha)	243	33869910
3	ADSL	158	Homo sapiens adenylosuccinate lyase	291	12652984
4	AK2	204	Homo sapiens adenylate kinase 2 transcript variant AK2A	362	39645192
5	KLK3	354	Homo sapiens kallikrein 3 (prostate specific antigen) transcript variant 1	6364	34193547
6	ATF1	466	Homo sapiens activating transcription factor 1	783	20810444
7	CKM	1158	Homo sapiens creatine kinase muscle	1994	13938618
8	CLK2	1196	Homo sapiens CDC-like kinase 2 transcript variant phclk2	2069	33873844
9	DDB2	1643	Homo sapiens damage-specific DNA binding protein 2 48kDa	2718	34783036
10	DTYMK	1841	Homo sapiens deoxythymidylate kinase (thymidylate kinase)	3061	38114725
11	DUSP4	1846	Homo sapiens dual specificity phosphatase 4 transcript variant 1	3070	33869553
12	E2F6	1876	Homo sapiens E2F transcription factor 6	3120	14249933
13	EXT2	2132	Homo sapiens exostoses (multiple) 2	3513	14603195
14	FGFR4_e	2264	Homo sapiens fibroblast growth factor receptor 4 transcript variant 3	3691	33873872
15	FIGF	2277	Homo sapiens c-fos induced growth factor (vascular endothelial growth factor D)	3708	20379761
16	FKBP3	2287	Homo sapiens FK506 binding protein 3 25kDa	3719	16740853
17	GALK1	2584	Homo sapiens galactokinase 1	4118	12654656
18	GK2	2712	Homo sapiens glycerol kinase 2	4291	20987489
19	GRB7	2886	Homo sapiens growth factor receptor-bound protein 7	4567	33870450
20	GTF2B	2959	Homo sapiens general transcription factor IIB	4648	18088836
21	GTF2H1	2965	Homo sapiens general transcription factor IIH polypeptide 1 62kDa	4655	33991027
22	GTF2H2	2966	Homo sapiens general transcription factor IIH polypeptide 2 44kDa	4656	40674449
23	HSPD1	3329	Homo sapiens heat shock 60kDa protein 1 (chaperonin)	5261	38197215
24	IDI1	3422	Homo sapiens isopentenyl-diphosphate delta isomerase	5387	34782883
25	IFI16	3428	Homo sapiens interferon, gamma-	5395	16877621

			inducible protein 16,		
26	LDHA	3939	Homo sapiens lactate dehydrogenase A	6535	45501321
27	LYL1	4066	Homo sapiens lymphoblastic leukemia derived sequence 1	6734	33988028
28	MARK3	4140	Homo sapiens MAP/microtubule affinity- regulating kinase 3	6897	19353235
29	MPP3	4356	Homo sapiens membrane protein palmitoylated 3 (MAGUK p55 subfamily member 3)	7221	34785138
30	TRIM37	4591	Homo sapiens tripartite motif-containing 37,	7523	23271191
31	NCF2	4688	Homo sapiens neutrophil cytosolic factor 2 (65kDa, chronic granulomatous disease, autosomal 2),	7661	12804408
32	RPL10A	4736	Homo sapiens ribosomal protein L10a	10299	13905015
33	NFYA	4800	Homo sapiens nuclear transcription factor Y alpha	7804	24660183
34	NRAS	4893	Homo sapiens neuroblastoma RAS viral (v- ras) oncogene homolog	7989	13528839
35	NTRK3_e	4916	Homo sapiens neurotrophic tyrosine kinase receptor type 3 transcript variant 3	8033	15489167
36	OAS2	4939	Homo sapiens 2'-5'-oligoadenylate synthetase 2 69/71kDa	8087	29351562
37	endometriosis	5091	Homo sapiens pyruvate carboxylase	8636	33871110
38	CDK17	5128	Homo sapiens endometriosisTAIRE protein kinase 2	8750	21542570
39	PDE4A	5141	Homo sapiens Homo sapiens phosphodiesterase 4A, cAMP-specific (phosphodiesterase E2 dunce homolog, Dro	8780	18043808
40	PHF1	5252	Homo sapiens PHD finger protein 1 transcript variant 2	8919	33874006
41	PKM2	5315	Homo sapiens pyruvate kinase muscle transcript variant 1	9021	14043290
42	MAP2K5	5607	Homo sapiens mitogen-activated protein kinase kinase 5, transcript variant A	6845	33871775
43	PRPS2	5634	Homo sapiens phosphoribosyl pyrophosphate synthetase 2	9465	26251732
44	RAN	5901	Homo sapiens RAN member RAS oncogene family	9846	33871120
45	RB1	5925	Homo sapiens retinoblastoma 1 (including osteosarcoma)	9884	24660139
46	RBMS1	5937	Homo sapiens Homo sapiens RNA binding motif single stranded interacting protein 1 transcript variant	9907	33869903
47	RET_a	5979	Homo sapiens ret proto-oncogene (multiple endocrine neoplasia and medullary thyroid carci	9967	13279040
48	RORC	6097	Homo sapiens RAR-related orphan receptor C	10260	21594879
49	RPL18	6141	Homo sapiens ribosomal protein L18	10310	38197133
50	RPL18A	6142	Homo sapiens ribosomal protein L18a	10311	38196939
51	RPL28	6158	Homo sapiens ribosomal protein L28	10330	15079502
52	RPL31	6160	Homo sapiens ribosomal protein L31	10334	40226052
53	RPL32	6161	Homo sapiens ribosomal protein L32	10336	15079341
54	S100A6	6277	Homo sapiens S100 calcium binding protein A6 (calcyclin)	10496	33876209

55	SCP2	6342	Homo sapiens sterol carrier protein 2 transcript variant 2	10606	45501107
56	SIAH1	6477	Homo sapiens seven in absentia homolog 1 (Drosophila) transcript variant 2	10857	27503513
57	SMARCD	6602	Homo sapiens SWI/SNF related matrix associated actin dependent regulator of chromatin subfamily d member 1	11106	33874464
58	SMARCE	6605	Homo sapiens SWI/SNF related matrix associated actin dependent regulator of chromatin	11109	13937940
59	SOD2	6648	Homo sapiens superoxide dismutase 2 mitochondrial	11180	15214594
60	SOX2	6657	Homo sapiens SRY (sex determining region Y)-box 2	11195	33869633
61	SRPK1	6732	Homo sapiens SFRS protein kinase 1	11305	23468344
62	TPM1	7168	Homo sapiens tropomyosin 1 (alpha)	12010	33873609
63	NR2C1	7181	Homo sapiens nuclear receptor subfamily 2 group C member 1	7971	25304018
64	TRIP6	7205	Homo sapiens thyroid hormone receptor interactor 6,	12311	13436460
65	UBA1	7317	Homo sapiens Homo sapiens ubiquitin- activating enzyme E1 (A1S9T and BN75 temperature sensitivity compl	12469	33989140
66	VCL	7414	Homo sapiens vinculin	12665	24657578
67	ZNF41	7592	Homo sapiens zinc finger protein 41 transcript variant 2	13107	21955337
68	PAX8	7849	Homo sapiens paired box gene 8 transcript variant PAX8A	8622	33987990
69	NRIP1	8204	Homo sapiens nuclear receptor interacting protein 1	8001	25955638
70	PIP4K2B	8396	Homo sapiens phosphatidylinositol-4-phosphate 5-kinase type II beta transcript variant 2	8998	20071965
71	UXT	8409	Homo sapiens ubiquitously-expressed transcript	12641	14424496
72	API5	8539	Homo sapiens apoptosis inhibitor 5	594	17389324
73	MKNK1	8569	Homo sapiens MAP kinase-interacting serine/threonine kinase 1	7110	33877125
74	SUCLA2	8803	Homo sapiens succinate-CoA ligase ADP- forming beta subunit	11448	34783884
75	LDB1	8861	Homo sapiens LIM domain binding 1	6532	38197167
76	NAE1	8883	Homo sapiens amyloid beta precursor protein binding protein 1 transcript variant 1	621	38197227
77	PAPSS2	9060	Homo sapiens 3'-phosphoadenosine 5'- phosphosulfate synthase 2	8604	33869502
78	USP10	9100	Homo sapiens ubiquitin specific protease 10	12608	12653004
79	PRPF4	9128	Homo sapiens Homo sapiens PRP4 pre-	17349	33876345
80	AIM2	9447	Homo sapiens absent in melanoma 2	357	15012076
81	TBPL1	9519	Homo sapiens TBP-like 1	11589	33988482
82	TRAF4	9618	Homo sapiens TNF receptor-associated factor 4 transcript variant 1	12034	12804686
83	SOCS5	9655	Homo sapiens suppressor of cytokine signaling 5	16852	23273933
84	ZSCAN12	9753	Homo sapiens zinc finger protein 305	13172	27371192

85	HDAC4	9759	Homo sapiens cDNA	14063	25058272
86	KIAA0101	9768	Homo sapiens KIAA0101 gene product	28961	33873244
87	IP6K1	9807	Homo sapiens inositol hexaphosphate kinase 1	18360	15277916
88	RNF40	9810	Homo sapiens ring finger protein 40 transcript variant 1	16867	13543993
89	GPHN	10243	Homo sapiens gephyrin	15465	34783414
90	HRSP12	10247	Homo sapiens translational inhibitor protein p14.5	16897	16307462
91	STUB1	10273	Homo sapiens STIP1 homology and U-Box containing protein 1	11427	14043118
92	TRAIP	10293	Homo sapiens TRAF interacting protein	30764	17939476
93	PLK4	10733	Homo sapiens serine/threonine kinase 18	11397	23243308
94	CCNI	10983	Homo sapiens cyclin I	1595	38197480
95	IL24	11009	Homo sapiens interleukin 24 transcript variant 1	11346	16307184
96	CDK20	23552	Homo sapiens cell cycle related kinase	21420	33988018
97	PABendo metriosis 1	26986	Homo sapiens poly(A) binding protein cytoplasmic 1	8554	33872187
98	MED4	29079	Homo sapiens vitamin D receptor interacting protein	17903	13528773
99	NME7	29922	Homo sapiens non-metastatic cells 7 protein expressed in (nucleoside-diphosphate kinase) transcript variant 1	20461	13937770
100	PHF11	51131	Homo sapiens PHD finger protein 11	17024	33880652
101	IRAK4	51135	Homo sapiens interleukin-1 receptor-associated kinase 4 mRNA (cDNA clone MGC:13330)	17967	15426431
102	TXNDC3	51314	Homo sapiens thioredoxin domain containing 3 (spermatozoa)	16473	22477641
103	TAOK3	51347	Homo sapiens STE20-like kinase	18133	33877128
104	STYXL1	51657	Homo sapiens dual specificity phosphatase 24 (putative)	18165	33869206
105	ASB1	51665	Homo sapiens ankyrin repeat and SOCS box- containing 1	16011	33878672
106	MST4	51765	Homo sapiens Mst3 and SOK1-related kinase (MASK)	na	109633024
107	PELO	53918	Homo sapiens pelota homolog (Drosophila)	8829	33870521
108	ETNK2	55224	Homo sapiens ethanolamine kinase 2	25575	33873304
109	RFK	55312	Homo sapiens riboflavin kinase	30324	13937919
110	C9orf86	55684	Homo sapiens chromosome 9 open reading frame 86	24703	18089263
111	DDX55	57696	Homo sapiens DEAD (Asp-Glu-Ala-Asp) box polypeptide 55	20085	34190861
112	CCNB1IP	57820	Homo sapiens cDNA	19437	12654750
113	KLHL12	59349	Homo sapiens kelch-like protein C3IP1	19360	13112018
114	SAV1	60485	Homo sapiens salvador homolog 1 (Drosophila)	17795	18088227
115	CAMKV	79012	Homo sapiens hypothetical protein MGC8407	28788	33875513
116	NSBP1	79366	Homo sapiens nucleosomal binding protein 1,	8013	13529139
117	ALPK1	80216	Homo sapiens alpha-kinase 1 mRNA (cDNA clone MGC:71554)	20917	38174241

118	ELMOD3	84173	Homo sapiens RNA binding motif and ELMO domain 1	26158	33877554
119	AIFM2	84883	Homo sapiens apoptosis-inducing factor (AIF)-like mitochondrion-associated inducer of death	21411	13543963
120	RHOT2	89941	Homo sapiens ras homolog gene family member T2	21169	15928946
121	PYGO2	90780	Homo sapiens pygopus 2	30257	33991480

(i) This number is the SEQ ID NO: for the coding sequence for the auto-antigen biomarker, as shown in the sequence listing.

(ii)The "ID" column shows the Entrez GeneID number for the antigen marker. An Entrez GeneID value is unique across all taxa.

(iii)The "Symbol" column gives the gene symbol which has been approved by the HGNC. The HGNC aims to give unique and meaningful names to every miRNA and human gene.

(iv) This name is taken from the Official Full Name provided by NCBI. An auto-antigen may have been referred to by one or more pseudonyms in the prior art. The invention relates to these auto-antigens regardless of their nomenclature.

(v) The HUGO Gene Nomenclature Committee aims to give unique and meaningful names to every human gene. The HGNC number thus identifies a unique human gene. An additional dash-number suffix indicates pre-miRNAs that lead to identical mature miRNAs but that are located at different places in the genome.

(vi)A "GI" number, or "GenInfo Identifier", is a series of digits assigned consecutively to each sequence record processed by NCBI when sequences are added to its databases. The GI number bears no resemblance to the accession number of the sequence record. When a sequence is updated (e.g. for correction, or to add more annotation or information) it receives a new GI number. Thus the sequence associated with a given GI number is never changed.

TABLE 9-20

Table listing relevant miRNAs (see section 6.5)

No.[(i)]	miRNA name[(ii)]	Symbol[(iii)]	HGNC[(iv)]	Sequence
122	ebv-miR-BART12	ebv-miR-BART12		UCCUGUGGUGUUUGGUGUGGUU
123	ebv-miR-BART14	ebv-miR-BART14		UAAAUGCUGCAGUAGUAGGGAU
124	ebv-miR-BART16	ebv-miR-BART16		UUAGAUAGAGUGGGUGUGUGCUCU
125	ebv-miR-BART20-5p	ebv-miR-BART20-5p		UAGCAGGCAUGUCUUCAUUCC
126	ebv-miR-BART2-5p	ebv-miR-BART2-5p		UAUUUUCUGCAUUCGCCCUUGC
127	hsa-let-7b*	MIRLET7B	HGNC:31479	UGAGGUAGUAGGUUGUGUGGUU
128	hsa-let-7f	MIRLET7F1	HGNC:31483	UGAGGUAGUAGAUUGUAUAGUU
129	hsa-let-7f-1*	MIRLET7F2	HGNC:31484	UGAGGUAGUAGAUUGUAUAGUU
130	hsa-let-7g	MIRLET7G	HGNC:31485	UGAGGUAGUAGUUUGUACAGUU
131	hsa-miR-103a	MIR103A1	HGNC:31490	AGCAGCAUUGUACAGGGCUAUGA
132	hsa-miR-10b	MIR10b	HGNC:31498	UACCCUGUAGAACCGAAUUUGUG
133	hsa-miR-1183	MIR1183	HGNC:35264	CACUGUAGGUGAUGGUGAGAGUGGGCA
134	hsa-miR-1202	MIR1202	HGNC:35268	GUGCCAGCUGCAGUGGGGGAG
135	hsa-miR-1207-5p	MIR1207	HGNC:35273	UGGCAGGGAGGCUGGGAGGGG
136	hsa-miR-122	MIR122	HGNC:31501	UGGAGUGUGACAAUGGUGUUUG
137	hsa-miR-1224-5p	MIR1224	HGNC:33923	GUGAGGACUCGGGAGGUGG
138	hsa-miR-1225-3p	MIR1225	HGNC:33931	GUGGGUACGGCCCAGUGGGGGG
139	hsa-miR-1225-5p	MIR1225	HGNC:33931	GUGGGUACGGCCCAGUGGGGGG
140	hsa-miR-1226*	MIR1226	HGNC:33922	UCACCAGCCCUGUGUUCCCUAG
141	hsa-miR-1228*	MIR1228	HGNC:33928	UCACACCUGCCUCGCCCCCC
142	hsa-miR-1234	MIR1234	HGNC:33926	UCGGCCUGACCACCCACCCCAC
143	hsa-miR-1237	MIR1237	HGNC:33927	UCCUUCUGCUCCGUCCCCCAG
144	hsa-miR-1238	MIR1238	HGNC:33933	CUUCCUCGUCUGUCUGCCCC
145	hsa-miR-125a-5p	MIR125a	HGNC:31505	UCCCUGAGACCCUUUAACCUGUGA
146	hsa-miR-1260	MIR1260A	HGNC:35325	AUCCCACCUCUGCCACCA
147	hsa-miR-1260b	MIR1260b	HGNC:38258	AUCCCACCACUGCCACCAU
148	hsa-miR-1280	MIR1280	HGNC:35368	UCCCACCGCUGCCACCC

149	hsa-miR-1281	MIR1281	HGNC:35359	UCGCCUCCUCCUCUCCC
150	hsa-miR-1290	MIR1290	HGNC:35283	UGGAUUUUUGGAUCAGGGA
151	hsa-miR-1291	MIR1291	HGNC:35284	UGGCCCUGACUGAAGACCAGCAGU
152	hsa-miR-129-3p	MIR129-1/ MIR129-2	HGNC:31512/ 31513	CUUUUUGCGGUCUGGGCUUGC
153	hsa-miR-1301	MIR1301	HGNC:35253	UUGCAGCUGCCUGGGAGUGACUUC
154	hsa-miR-135a	MIR135A1/ MIR135A2	HGNC:31520/ 31521	UAUGGCUUUUUAUUCCUAUGUGA
155	hsa-miR-135a*	MIR135A1/ MIR135A2	HGNC:31520/ 31521	UAUGGCUUUUUAUUCCUAUGUGA
156	hsa-miR-141	MIR141	HGNC:31528	UAACACUGUCUGGUAAAGAUGG
157	hsa-miR-142-3p	MIR142	HGNC:31529	CAUAAAGUAGAAAGCACUACU
158	hsa-miR-149	MIR149	HGNC:31536	UCUGGCUCCGUGUCUUCACUCCC
159	hsa-miR-150	MIR150	HGNC:31537	UCUCCCAACCCUUGUACCAGUG
160	hsa-miR-150*	MIR150	HGNC:31537	UCUCCCAACCCUUGUACCAGUG
161	hsa-miR-1539	MIR1539	HGNC:35383	UCCUGCGCGUCCCAGAUGCCC
162	hsa-miR-181a	MIR181A2	HGNC:31549	AACAUUCAACGCUGUCGGUGAGU
163	hsa-miR-1825	MIR1825	HGNC:35389	UCCAGUGCCCUCCUCUCC
164	hsa-miR-186	MIR186	HGNC:31557	CAAAGAAUUCUCCUUUUGGGCU
165	hsa-miR-18a	MIR18a	HGNC:31548	UAAGGUGCAUCUAGUGCAGAUAG
166	hsa-miR-18b	MIR18b	HGNC:32025	UAAGGUGCAUCUAGUGCAGUUAG
167	hsa-miR-191*	MIR191	HGNC:31561	CAACGGAAUCCCAAAAGCAGCUG
168	hsa-miR-197	MIR197	HGNC:31569	UUCACCACCUUCUCCACCCAGC
169	hsa-miR-198	MIR198	HGNC:31570	GGUCCAGAGGGGAGAUAGGUUC
170	hsa-miR-205	MIR205	HGNC:31583	UCCUUCAUUCCACCGGAGUCUG
171	hsa-miR-2116*	MIR2116	HGNC:37310	GGUUCUUAGCAUAGGAGGUCU
172	hsa-miR-215	MIR215	HGNC:31592	AUGACCUAUGAAUUGACAGAC
173	hsa-miR-22	MIR22	HGNC:31599	AAGCUGCCAGUUGAAGAACUGU
174	hsa-miR-223	MIR223	HGNC:31603	UGUCAGUUUGUCAAAUACCCCA
175	hsa-miR-2276	MIR2276	HGNC:37313	UCUGCAAGUGUCAGAGGCGAGG
176	hsa-miR-23c	MIR23c	HGNC:38913	AUCACAUUGCCAGUGAUUACCC
177	hsa-miR-26a	MIR26A1/ MIR26A2	HGNC:31610/ 31611	UUCAAGUAAUCCAGGAUAGGCU
178	hsa-miR-28-3p	MIR28	HGNC:31615	AAGGAGCUCACAGUCUAUUGAG

179	hsa-miR-28-5p	MIR28	HGNC:31615	AAGGAGCUCACAGUCUAUUGAG
180	hsa-miR-29b	MIR29B1/ MIR29B2	HGNC:31619/ 31620	UAGCACCAUUUGAAAUCAGUGUU
181	hsa-miR-30a	MIR30a	HGNC:31624	UGUAAACAUCCUCGACUGGAAG
182	hsa-miR-30b	MIR30b	HGNC:31625	UGUAAACAUCCUACACUCAGCU
183	hsa-miR-3131	MIR3131	HGNC:38347	UCGAGGACUGGUGGAAGGGCCUU
184	hsa-miR-3138	MIR3138	HGNC:38341	UGUGGACAGUGAGGUAGAGGGAGU
185	hsa-miR-3149	MIR3149	HGNC:38251	UUUGUAUGGAUAUGUGUGUGUAU
186	hsa-miR-3156-5p	MIR3156-1/ MIR3156-2/ MIR3156-3	HGNC:38241/ 38213/ 38229	AAAGAUCUGGAAGUGGGAGACA
187	hsa-miR-3180-5p	MIR3180-1/ MIR3180-2/ MIR3180-3/ MIR3180-4/ MIR3180-5	HGNC:38382/ 38343/ 38239/ 38920/ 38969	UGGGGCGGAGCUUCCGGAG
188	hsa-miR-3194-5p	MIR3194	HGNC:38346	GGCCAGCCACCAGGAGGGCUG
189	hsa-miR-3195	MIR3195	HGNC:38250	CGCGCCGGGCCCGGGUU
190	hsa-miR-3196	MIR3196	HGNC:38198	CGGGGCGGCAGGGGCCUC
191	hsa-miR-32	MIR32	HGNC:31631	UAUUGCACAUUACUAAGUUGCA
192	hsa-miR-320c	MIR320C1/ MIR320C2	HGNC:35248/ 35387	AAAAGCUGGGUUGAGAGGGU
193	hsa-miR-324-3p	MIR324	HGNC:31767	CGCAUCCCCUAGGGCAUUGGUGU
194	hsa-miR-328	MIR328	HGNC:31770	CUGGCCCUCUCUGCCCUUCCGU
195	hsa-miR-331-5p	MIR331	HGNC:31772	CUAGGUAUGGUCCCAGGGAUCC
196	hsa-miR-33b*	MIR33b	HGNC:32791	GUGCAUUGCUGUUGCAUUGC
197	hsa-miR-342-3p	MIR342	HGNC:31778	AGGGGUGCUAUCUGUGAUUGA
198	hsa-miR-34a	MIR34a	HGNC:31635	UGGCAGUGUCUUAGCUGGUUGU
199	hsa-miR-3610	MIR3610	HGNC:38942	GAAUCGGAAAGGAGGCGCCG
200	hsa-miR-3648	MIR3648	HGNC:38941	AGCCGCGGGGAUCGCCGAGGG
201	hsa-miR-3652	MIR3652	HGNC:38894	CGGCUGGAGGUGUGAGGA
202	hsa-miR-3663-5p	MIR3663	HGNC:38958	GCUGGUCUGCGUGGUGCUCGG
203	hsa-miR-3667-5p	MIR3667	HGNC:38990	AAAGACCCAUUGAGGAGAAGGU
204	hsa-miR-382	MIR382	HGNC:31875	GAAGUUGUUCGUGGUGGAUUCG
205	hsa-miR-3911	MIR3911	HGNC:38962	UGUGUGGAUCCUGGAGGAGGCA

206	hsa-miR-3937	MIR3937	HGNC:38970	ACAGGCGGCUGUAGCAAUGGGGG
207	hsa-miR-4257	MIR4257	HGNC:38312	CCAGAGGUGGGGACUGAG
208	hsa-miR-425*	MIR425	HGNC:31882	AAUGACACGAUCACUCCCGUUGA
209	hsa-miR-4270	MIR4270	HGNC:38377	UCAGGGAGUCAGGGGAGGGC
210	hsa-miR-4274	MIR4274	HGNC:38194	CAGCAGUCCCUCCCCCUG
211	hsa-miR-4281	MIR4281	HGNC:38357	GGGUCCCGGGGAGGGGGG
212	hsa-miR-4284	MIR4284	HGNC:38322	GGGCUCACAUCACCCCAU
213	hsa-miR-4286	MIR4286	HGNC:38186	ACCCCACUCCUGGUACC
214	hsa-miR-429	MIR429	HGNC:13784	UAAUACUGUCUGGUAAAACCGU
215	hsa-miR-4290	MIR4290	HGNC:38360	UGCCCUCCUUUCUUCCCUC
216	hsa-miR-4313	MIR4313	HGNC:38310	AGCCCCCUGGCCCCAAACCC
217	hsa-miR-4323	MIR4323	HGNC:38394	CAGCCCCACAGCCUCAGA
218	hsa-miR-466	MIR466	HGNC:38359	AUACACAUACACGCAACACACAU
219	hsa-miR-483-3p	MIR483	HGNC:32340	AAGACGGGAGGAAAGAAGGGAG
220	hsa-miR-484	MIR484	HGNC:32341	UCAGGCUCAGUCCCCUCCCGAU
221	hsa-miR-485-3p	MIR485	HGNC:32067	AGAGGCUGGCCGUGAUGAAUUC
222	hsa-miR-486-5p	MIR486	HGNC:32342	UCCUGUACUGAGCUGCCCCGAG
223	hsa-miR-488	MIR488	HGNC:32073	UUGAAAGGCUAUUUCUUGGUC
224	hsa-miR-497	MIR497	HGNC:32088	CAGCAGCACACUGUGGUUUGU
225	hsa-miR-511	MIR511-1	HGNC:32077	GUGUCUUUUGCUCUGCAGUCA
226	hsa-miR-512	MIR511-2	HGNC:32078	GUGUCUUUUGCUCUGCAGUCA
227	hsa-miR-520c-3p	MIR520c	HGNC:32108	CUCUAGAGGGAAGCACUUUCUG
228	hsa-miR-550a	MIR550A1/ MIR550A2/ MIR550A3	HGNC:32804/ 32805/ 41870	AGUGCCUGAGGGAGUAAGAGCCC
229	hsa-miR-556-3p	MIR556	HGNC:32812	GAUGAGCUCAUUGUAAUAUGAG
230	hsa-miR-557	MIR557	HGNC:32813	GUUUGCACGGGUGGGCCUUGUCU
231	hsa-miR-561	MIR561	HGNC:32817	CAAAGUUUAAGAUCCUUGAAGU
232	hsa-miR-572	MIR572	HGNC:32828	GUCCGCUCGGCGGUGGCCCA
233	hsa-miR-574-3p	MIR574	HGNC:32830	UGAGUGUGUGUGUGUGAGUGUGU
234	hsa-miR-574-5p	MIR574	HGNC:32830	UGAGUGUGUGUGUGUGAGUGUGU

235	hsa-miR-595	MIR595	HGNC:32851	GAAGUGUGCCGUGGUGUGUCU
236	hsa-miR-630	MIR630	HGNC:32886	AGUAUUCUGUACCAGGGAAGGU
237	hsa-miR-642b	MIR642b	HGNC:38902	AGACACAUUUGGAGAGGGACCC
238	hsa-miR-646	MIR646	HGNC:32902	AAGCAGCUGCCUCUGAGGC
239	hsa-miR-659	MIR659	HGNC:32915	CUUGGUUCAGGGAGGGUCCCCA
240	hsa-miR-660	MIR660	HGNC:32916	UACCCAUUGCAUAUCGGAGUUG
241	hsa-miR-663	MIR663A	HGNC:32919	AGGCGGGGCGCCGCGGGACCGC
242	hsa-miR-664	MIR664	HGNC:35370	UAUUCAUUUAUCCCCAGCCUACA
243	hsa-miR-720	MIR720	HGNC:35375	UCUCGCUGGGGCCUCCA
244	hsa-miR-762	MIR762	HGNC:37303	GGGGCUGGGGCCGGGGCCGAGC
245	hsa-miR-766	MIR766	HGNC:33139	ACUCCAGCCCCACAGCCUCAGC
246	hsa-miR-877*	MIR877	HGNC:33660	GUAGAGGAGAUGGCGCAGGG
247	hsa-miR-888	MIR888	HGNC:33648	UACUCAAAAAGCUGUCAGUCA
248	hsa-miR-933	MIR933	HGNC:33676	UGUGCGCAGGGAGACCUCUCCC
249	hsa-miR-940	MIR940	HGNC:33683	AAGGCAGGGCCCCCGCUCCCC
250	hsa-miR-95	MIR95	HGNC:31647	UUCAACGGGUAUUUAUUGAGCA
251	hsv1-miR-H1*/ hsv1-miR-H1-3p	hsv1-miR-H1*		UACACCCCCCUGCCUUCCACCCU
252	hsv1-miR-H2-3p	hsv1-miR-H2-3p		CCUGAGCCAGGGACGAGUGCGACU
253	hsv1-miR-H6-3p	hsv1-miR-H6-3p		CACUUCCCGUCCUUCCAUCCC
254	hsv1-miR-H7*	hsv1-miR-H7*		UUUGGAUCCCGACCCCUCUUC
255	hsv1-miR-H8	hsv1-miR-H8		UAUAUAGGGUCAGGGGGUUC
256	hsv2-miR-H22	hsv2-miR-H22		AGGGGUCUGGACGUGGGUGGGC
257	hsv2-miR-H25	hsv2-miR-H25		CUGCGCGGCGGAGACCGGGAC
258	hsv2-miR-H6	hsv2-miR-H6		AAUGGAAGGCGAGGGGAUGC
259	hsv2-miR-H6*	hsv2-miR-H6*		CCCAUCUUCUGCCCUUCCAUCCU
260	kshv-miR-K12-10a	kshv-miR-K12-10a		UAGUGUUGUCCCCCCGAGUGGC
261	kshv-miR-K12-12*	kshv-miR-K12-12*		UGGGGGAGGGUGCCCUGGUUGA
262	kshv-miR-K12-8*	kshv-miR-K12-8*		ACUCCCUCACUAACGCCCCGCU

(i) The SEQ ID NO: for the sequence of the mature, expressed miRNA biomarker.

(ii) The "miRNA name" column gives the name of the human miRNA as provided by the specialist database, miRBase, according to version 16 (released, August 2010).

(iii) The "Symbol" column gives the gene symbol which has been approved by the HGNC. The HGNC aims to give unique and meaningful names to every miRNA and human gene. An additional dash-number suffix indicates premiRNAs that lead to identical mature miRNAs but that are located at different places in the genome.

(iv) The HGNC aims to give unique and meaningful names to every miRNA (and human gene). The HGNC number thus identifies a unique human gene. Inclusion on to HUGO is for human genes only.

TABLE 9-21

Table listing identified miRNAs (see section 6.5)

No.	miRNA name[(i)]	Symbol[(ii)]	HGNC[(iii)]	Sequence
126	ebv-miR-BART2-5p	ebv-miR-BART2-5p	N/A	UAUUUUCUGCAUUCGCCCUUGC
263	hsa-miR-564	MIR564	32820	AGGCACGGUGUCAGCAGGC
264	hsa-let-7d-5p	MIRLET7D	31481	AGAGGUAGUAGGUUGCAUAGUU
265	hsa-let-7d-3p	MIRLET7D	31481	CUAUACGACCUGCUGCCUUUCU
266	hsa-miR-29a	MIR29A	31616	UAGCACCAUCUGAAAUCGGUUA
157	hsa-miR-142-3p	MIR142	31529	CAUAAAGUAGAAAGCACUACU
168	hsa-miR-197	MIR197	31569	UUCACCACCUUCUCCACCCAGC
172	hsa-miR-215	MIR215	31592	AUGACCUAUGAAUUGACAGAC
267	hsa-miR-219-1-3p	MIR-219-1	31597	AGAGUUGAGUCUGGACGUCCCG
268	hsa-miR-296-3p	MIR296	31617	GAGGGUUGGGUGGAGGCUCUCC
192	hsa-miR-320c	MIR320C	35248	AAAAGCUGGGUUGAGAGGGU
269	hsa-miR-337-5p	MIR337	31774	GAACGGCUUCAUACAGGAGUU
270	hsa-miR-369-3p	MIR369	31783	AAUAAUACAUGGUUGAUCUUU
271	hsa-miR-450b-5p	MIR450B	33642	UUUUGCAAUAUGUUCCUGAAUA
272	hsa-miR-483-5p	MIR483	32340	AAGACGGGAGGAAAGAAGGGAG
273	hsa-miR-507	MIR507	32144	UUUUGCACCUUUUGGAGUGAA
274	hsa-miR-517c	MIR517C	32124	AUCGUGCAUCCUUUUAGAGUGU
275	hsa-miR-519a	MIR519A1/ MIR519A2	32128/ 32132	AAAGUGCAUCCUUUUAGAGUGU
276	hsa-miR-519d	MIR519D	32112	CAAAGUGCCUCCCUUUAGAGUG

277	hsa-miR-520g	MIR520G	32116	ACAAAGUGCUUCCCUUUAGAGUGU
278	hsa-miR-576-5p	MIR576	32832	AUUCUAAUUUCUCCACGUCUUU
279	hsa-miR-577	MIR577	32833	UAGAUAAAAUAUUGGUACCUG
280	hsa-miR-604	MIR604	32860	AGGCUGCGGAAUUCAGGAC
281	hsa-miR-610	MIR610	32866	UGAGCUAAAUGUGUGCUGGGA
282	hsa-miR-619	MIR619	32875	GACCUGGACAUGUUUGUGCCCAGU
283	hsa-miR-1256	MIR1256	35321	AGGCAUUGACUUCUCACUAGCU
284	hsa-miR-1278	MIR1278	35356	UAGUACUGUGCAUAUCAUCUAU
285	hsa-miR-1297	MIR1297	35289	UUCAAGUAAUUCAGGUG
286	hcmv-miR-US33-5p	N/A	N/A	GAUUGUGCCCGGACCGUGGGCG
287	hsv1-miR-H1-5p	N/A	N/A	GAUGGAAGGACGGGAAGUGGA
288	hsa-miR-877	MIR877	33660	GUAGAGGAGAUGGCGCAGGG
289	hsa-let-7e-5p	MIRLET7E	31482	UGAGGUAGGAGGUUGUAUAGUU
290	hsa-let-7e-3p	MIRLET7E	31482	CUAUACGGCCUCCUAGCUUUCC
128	hsa-let-7f	MIRLET7F1	31483	UGAGGUAGUAGAUUGUAUAGUU
130	hsa-let-7g	MIRLET7G	31485	UGAGGUAGUAGUUUGUACAGUU
291	hsa-miR-9	MIR9-1/ MIR9-2/ MIR9-3	31641/ 31642/ 31646	UCUUUGGUUAUCUAGCUGUAUGA
182	hsa-miR-30b	MIR30a	31624	UGUAAACAUCCUCGACUGGAAG
198	hsa-miR-34a	MIR34A	31635	UGGCAGUGUCUUAGCUGGUUGU
292	hsa-miR-92b	MIR92B	32920	UAUUGCACUCGUCCCGGCCUCC
293	hsa-miR-96-5p	MIR96	31648	UUUGGCACUAGCACAUUUUUGCU
294	hsa-miR-96-3p	MIR96	31648	AAUCAUGUGCAGUGCCAAUAUG
295	hsa-miR-106a-5p	MIR106A	31494	AAAAGUGCUUACAGUGCAGGUAG
296	hsa-miR-106a-3p	MIR106A	31494	CUGCAAUGUAAGCACUUCUUAC
297	hsa-miR-17-5p	MIR17	31547	CAAAGUGCUUACAGUGCAGGUAG
298	hsa-miR-17-3p	MIR17	31547	ACUGCAGUGAAGGCACUUGUAG
299	hsa-miR-106b-5p	MIR106B	31495	UAAAGUGCUGACAGUGCAGAU
300	hsa-miR-106b-3p	MIR106B	31495	CCGCACUGUGGGUACUUGCUGC
301	hsa-miR-127-3p	MIR127	31509	UCGGAUCCGUCUGAGCUUGGCU
302	hsa-miR-128	MIR128-1/MIR128-2	31510/31511	UCACAGUGAACCGGUCUCUUU

303	hsa-miR-154	MIR154	31541	UAGGUUAUCCGUGUUGCCUUCG
304	hsa-miR-155	MIR155	31542	UUAAUGCUAAUCGUGAUAGGGGU
305	hsa-miR-183-5p	MIR183	31554	UAUGGCACUGGUAGAAUUCACU
306	hsa-miR-183-3p	MIR183	31554	GUGAAUUACCGAAGGGCCAUAA
307	hsa-miR-194	MIR194-1/ MIR194-2	31564/ 31565	UGUAACAGCAACUCCAUGUGGA
308	hsa-miR-196b-5p	MIR196B	31790	UAGGUAGUUUCCUGUUGUUGGG
309	hsa-miR-196b-3p	MIR196B	31790	UCGACAGCACGACACUGCCUUC
310	hsa-miR-203	MIR203	31581	GUGAAAUGUUUAGGACCACUAG
311	hsa-miR-204	MIR204	31582	UUCCCUUUGUCAUCCUAUGCCU
312	hsa-miR-221-5p	MIR221	31601	ACCUGGCAUACAAUGUAGAUUU
313	hsa-miR-221-3p	MIR221	31601	AGCUACAUUGUCUGCUGGGUUUC
174	hsa-miR-223	MIR223	31603	UGUCAGUUUGUCAAAUACCCCA
314	hsa-miR-376a	MIR376A1/ MIR376A2	31869/ 32532	AUCAUAGAGGAAAAUCCACGU
315	hsa-miR-376c	MIR376C	31782	AACAUAGAGGAAAUUCCACGU
316	hsa-miR-377	MIR377	31870	AUCACACAAAGGCAACUUUUGU
317	hsa-miR-379	MIR379	31872	UGGUAGACUAUGGAACGUAGG
318	hsa-miR-423-3p	MIR423	31880	AGCUCGGUCUGAGGCCCCUCAGU
319	hsa-miR-424-5p	MIR424	31881	CAGCAGCAAUUCAUGUUUUGAA
320	hsa-miR-424-3p	MIR424	31881	CAAAACGUGAGGCGCUGCUAU
321	hsa-miR-425-5p	MIR425	31882	AAUGACACGAUCACUCCCGUUGA
322	hsa-miR-425-3p	MIR425	31882	AUCGGGAAUGUCGUGUCCGCCC
323	hsa-miR-454-5p	MIR454	33137	ACCCUAUCAAUAUUGUCUCUGC
324	hsa-miR-454-3p	MIR454	33137	UAGUGCAAUAUUGCUUAUAGGGU
325	hsa-miR-486-3p	hsa-miR-486/ MIR486	32342	CGGGGCAGCUCAGUACAGGAU
326	hsa-miR-509-3p	MIR509-3	33675	UGAUUGGUACGUCUGUGGGUAG
327	hsa-miR-514	MIR514-1/ MIR514-2/ MIR514-3	32148/ 32149/ 32150	AUUGACACUUCUGUGAGUAGA
328	hsa-miR-542-3p	MIR542	32534	UGUGACAGAUUGAUAACUGAAA
329	hsa-miR-545-5p	MIR545	32531	UCAGUAAAUGUUUAUUAGAUGA
330	hsa-miR-545-3p	MIR545	32531	UCAGCAAACAUUUAUUGUGUGC
331	hsa-miR-626	MIR626	32882	AGCUGUCUGAAAAUGUCUU

236	hsa-miR-630	MIR630	32886	AGUAUUCUGUACCAGGGAAGGU
241	hsa-miR-663	MIR663A	32919	AGGCGGGGCGCCGCGGGACCGC
243	hsa-miR-720	MIR720	35375	UCUCGCUGGGGCCUCCA
332	hsa-miR-758-5p	MIR758	33133	GAUGGUUGACCAGAGAGCACAC
333	hsa-miR-758-3p	MIR758	33133	UUUGUGACCUGGUCCACUAACC
334	hsa-miR-876-3p	MIR876	33653	UGGUGGUUUACAAAGUAAUUCA
335	hsa-miR-1185	MIR1185-1 /MIR1185-2	35257 /35254	AGAGGAUACCCUUUGUAUGUU
146	hsa-miR-1260	MIR1260A	35325	AUCCCACCUCUGCCACCA
336	hsa-miR-1266-5p	MIR1266	35334	CCUCAGGGCUGUAGAACAGGGCU
337	hsa-miR-1266-3p	MIR1266	35334	CCCUGUUCUAUGCCCUGAGGGA
338	hsa-miR-199a-3p	MIR199A1 /MIR199A2	31571 /31572	ACAGUAGUCUGCACAUUGGUUA
339	hsa-miR-199b-3p	MIR199B	31573	ACAGUAGUCUGCACAUUGGUUA
224	hsa-miR-497	MIR497	32088	CAGCAGCACACUGUGGUUUGU
340	hsa-miR-625-5p	MIR625	32881	AGGGGGAAAGUUCUAUAGUCC
341	hsa-miR-625-3p	MIR625	32881	GACUAUAGAACUUUCCCCCUCA
342	hsa-miR-631	MIR631	32887	AGACCUGGCCCAGACCUCAGC
343	hsa-miR-635	MIR635	32891	ACUUGGGCACUGAAACAAUGUCC

(i) The SEQ ID NO: for the sequence of the mature, expressed miRNA biomarker.

(ii) The "miRNA name" column gives the name of the human miRNA as provided by the specialist database, miRBase, according to version 16 (released, August 2010).

(iii) The "Symbol" column gives the gene symbol which has been approved by the HGNC. The HGNC aims to give unique and meaningful names to every miRNA and human gene. An additional dash-number suffix indicates premiRNAs that lead to identical mature miRNAs but that are located at different places in the genome.

(iv) The HGNC aims to give unique and meaningful names to every miRNA (and human gene). The HGNC number thus identifies a unique human gene. Inclusion on to HUGO is for human genes only.

TABLE 9-22

Table listing relevant genes (see section 6.5)

No.[i]	Symbol[ii]	ID[iii]	Name[iv]	HGNC[v]	GI[vi]
344	CDC42	998	Homo sapiens cell division cycle 42 (GTP binding protein 25kDa) transcript variant 1	1736	33990903
345	EGFR_int	1956	Homo sapiens epidermal growth factor receptor (erythroblastic leukemia viral (v-erb- b) oncogene homolog avian)	3236	63101669
346	KIT_ext	3815	Homo sapiens v-kit Hardy-Zuckerman 4 feline sarcoma viral oncogene homolog	6342	47938801
347	PPARG	5468	Homo sapiens peroxisome proliferative activated receptor gamma transcript variant 3	9236	13905055
348	WT1	7490	Homo sapiens Wilms tumor 1	12796	34190661

(i) This number is the SEQ ID NO: for the coding sequence for the auto-antigen biomarker, as shown in the sequence listing.

(ii) The "ID" column shows the Entrez GeneID number for the antigen marker. An Entrez GeneID value is unique across all taxa.

(iii) The "Symbol" column gives the gene symbol which has been approved by the HGNC. The HGNC aims to give unique and meaningful names to every miRNA and human gene.

(iv) This name is taken from the Official Full Name provided by NCBI. An auto-antigen may have been referred to by one or more pseudonyms in the prior art. The invention relates to these auto-antigens regardless of their nomenclature.

(v) The HUGO Gene Nomenclature Committee aims to give unique and meaningful names to every human gene. The HGNC number thus identifies a unique human gene. An additional dash-number suffix indicates pre-miRNAs that lead to identical mature miRNAs but that are located at different places in the genome.

(vi) A "GI" number, or "GenInfo Identifier", is a series of digits assigned consecutively to each sequence record processed by NCBI when sequences are added to its databases. The GI number bears no resemblance to the accession number of the sequence record. When a sequence is updated (e.g. for correction, or to add more annotation or information) it receives a new GI number. Thus the sequence associated with a given GI number is never changed.

TABLE 9-23

Table listing identified genes/proteins (see section 6.5)

Symbol[i]	ID[ii]	P. Value[iii]	Expression[iv]
CCNB1IP1	57820	0.000000816	Down
HSPD1	3329	0.00000196	Down
PRPF4	9128	0.00000296	Down
STYXL1	51657	0.0000222	Down
ETNK2	55224	0.0000223	Down
GALK1	2584	0.0000275	Down
RNF40	9810	0.0000295	Down
NTRK3_ext	4916	0.0000498	Down
UBA1	7317	0.0000854	Up
GTF2H1	2965	0.0000923	Down
PDE4A	5141	0.000115	Down
SMARCE1	6605	0.000133	Up
TBPL1	9519	0.000197	Down
PIP4K2B	8396	0.000252	Down
LDB1	8861	0.000304	Down
RHOT2	89941	0.00037	Down
SMARCD1	6602	0.000384	Down

SAV1	60485	0.000403	Down
ZSCAN12	9753	0.000412	Down
ASB1	51665	0.000414	Down
KLHL12	59349	0.000428	Up
UXT	8409	0.000642	Down
E2F6	1876	0.000747	Up
RBMS1	5937	0.000829	Up
MAP2K5	5607	0.000909	Down
PAPSS2	9060	0.001015	Down
RAN	5901	0.001377	Up
STUB1	10273	0.015531	Up
TPM1	7168	0.022489	Up

(i) The "ID" column shows the Entrez GeneID number for the antigen marker. An Entrez GeneID value is unique across all taxa.

(ii) The "Symbol" column gives the gene symbol which has been approved by the HGNC. The HGNC aims to give 5 unique and meaningful names to every miRNA and human gene.

(iii) The "p-value" represents the p-value of a microarray T-test derived from comparing case with control, as determined in study 1.

(iv) The biomarkers can be up-regulated (i.e. an increase in fold-change, when compared to control samples) or down-regulated (i.e. a decrease in fold-change, when compared to control samples), as determined in study 1.

TABLE 9-24
Table listing identified genes/proteins (see section 6.5)

Symbol[(i)]	**ID[(ii)]**	**P. Value[(iii)]**	**Expression[(iv)]**
TPM1	7168	0.002915091	Up
RORC	6097	0.006178466	Down
HSPD1	3329	0.008954673	Down
SRPK1	6732	0.015397291	Down
PYGO2	90780	0.024303172	Down
SOD2	6648	0.028978148	Up
STUB1	10273	0.039435959	Up
RAN	5901	0.02988746	Up

(i) The "ID" column shows the Entrez GeneID number for the antigen marker. An Entrez GeneID value is unique across all taxa.

(ii) The "Symbol" column gives the gene symbol which has been approved by the HGNC. The HGNC aims to give 5 unique and meaningful names to every miRNA and human gene.

(iii) The "p-value" represents the p-value of a microarray T-test derived from comparing case with control, as determined in study 1.

(iv) The biomarkers can be up-regulated (i.e. an increase in fold-change, when compared to control samples) or down-regulated (i.e. a decrease in fold-change, when compared to control samples), as determined in study 1.

TABLE 9-25
Table listing identified miRNAs(see section 6.5)

miRNA Name[(i)]	**P. Value[(ii)]**	**Expression[(iii)]**
hsa-miR-150	0.00006394	Down
hsa-miR-122	0.02533983	Down
hsa-miR-342-3p	0.00003342	Down
hsa-miR-3648	0.00558781	Up

hsa-miR-574-5p	0.00002921	Down
hsa-miR-1224-5p	0.00565712	Up
hsa-miR-483-3p	0.00000011	Down
hsa-miR-1290	0.02750229	Down
hsa-miR-630	0.00000073	Down
hsa-miR-4284	0.00000622	Down
hsa-miR-4274	0.00578241	Down
hsa-miR-1539	0.01689898	Down
hsa-miR-484	0.00005860	Down
hsa-miR-150*	0.00015240	Up
hsa-miR-103a	0.00015153	Down
hsa-miR-595	0.00000370	Down
hsa-let-7f	0.01103692	Down
hsa-miR-2116*	0.00966057	Down
hsa-let-7g	0.01804877	Down
hsa-miR-10b	0.00037142	Up
hsa-miR-557	0.00171716	Up
hsa-miR-574-3p	0.00001553	Down
hsa-miR-29b	0.02130244	Down
hsa-miR-3675-3p	0.02426579	Down
hsa-miR-3196	0.00077761	Up
hsa-miR-142-3p	0.00184763	Down
hsa-miR-762	0.00310027	Up
hsv2-miR-H22	0.01761904	Up
hsa-miR-1260	0.00000231	Down
hsv1-miR-H17	0.04790461	Up
hsa-miR-1281	0.00000779	Down
hsa-miR-720	0.00001081	Down
ebv-miR-BART12	0.00005959	Down
hsa-miR-146a	0.04352182	Down
hsa-miR-1183	0.01111370	Up
hsa-miR-1228*	0.00000083	Down
hsa-miR-3131	0.00077353	Up
hsa-miR-1825	0.00000149	Down
hsa-miR-30b	0.00644932	Down
kshv-miR-K12-12*	0.00002874	Down
hsv2-miR-H6	0.00825432	Up
hsa-miR-26a	0.00002875	Down
hsa-miR-4281	0.00008771	Up
hsa-miR-3911	0.01275802	Up
ebv-miR-BART16	0.00004541	Down
hsv1-miR-H1*	0.00000324	Down
hsa-miR-1202	0.00055105	Up
hsa-miR-3610	0.00687590	Up
hsv1-miR-H6-3p	0.00004842	Down
hsa-miR-3138	0.00899372	Up
hsa-miR-1207-5p	0.00281946	Up
hsa-miR-3149	0.00009532	Down
hsa-miR-4270	0.00004371	Up
hsa-miR-3195	0.00682325	Up
hsv1-miR-H8	0.00202682	Down

hsa-miR-4257	0.00287878	Down
hsa-miR-1225-5p	0.00003946	Up
hsa-miR-142-5p	0.02297944	Down
hsa-miR-320c	0.00490620	Up
hsa-miR-466	0.00012439	Down
hsa-miR-3665	0.02194315	Down
hsa-miR-3180-5p	0.00000784	Down
hsa-miR-572	0.00003356	Down
hsa-miR-498	0.03899671	Down
hsv1-miR-H7*	0.00000153	Down
hsa-miR-4290	0.00008972	Down
hsa-miR-766	0.00005281	Down
hsa-miR-550a	0.00000246	Down
hsa-miR-642b	0.00038856	Up
hiv1-miR-H1	0.02389090	Up
hsa-miR-4286	0.00000972	Down
hsa-miR-1275	0.02853258	Up
hsa-miR-328	0.00000589	Down
hsa-miR-940	0.00085814	Down
hsa-miR-425*	0.00000196	Down
hsa-miR-877*	0.00000197	Down
hsa-miR-1237	0.00473766	Down
hsa-miR-197	0.00689774	Down
hsa-miR-30a	0.00237993	Up
hsa-miR-23c	0.00008162	Down
hsa-miR-3652	0.00008498	Down
hsa-miR-22	0.00512710	Up
hsa-miR-181a	0.00132119	Down
hsa-miR-3663-3p	0.02216322	Up
hsv2-miR-H25	0.01841174	Up
hsa-miR-485-3p	0.00003097	Down
hsa-miR-324-3p	0.00034769	Down
hsa-miR-486-5p	0.00864165	Up
hsa-miR-1238	0.00119172	Down
hsa-miR-1280	0.00021707	Down
hsa-miR-129*	0.02477021	Down
hsa-miR-1225-3p	0.00018305	Down
hsa-let-7f-1*	0.01068060	Down
hsa-miR-4313	0.00072572	Down
hsa-miR-4323	0.00014421	Down
hsa-miR-149	0.00009577	Down
hsa-miR-199a-5p	0.03839473	Down
hsa-miR-19b	0.03402975	Up
hsa-miR-92a	0.03160700	Up
hsv2-miR-H6*	0.00006381	Down
hsa-miR-16-2*	0.03334112	Up
hsa-miR-933	0.00000019	Down
hsa-miR-660	0.00700913	Up
hsa-miR-494	0.04910243	Down
hsa-miR-1260b	0.00050477	Down
hsa-miR-33b*	0.00000225	Down

hsa-miR-186	0.02114488	Up
hsa-let-7b*	0.00029688	Down
hsa-miR-424	0.02888965	Up
kshv-miR-K12-8*	0.00002078	Down
hsa-miR-191*	0.00253484	Down
hsa-miR-1234	0.00947810	Down

(i) The "miRNA name" column gives the name of the human miRNA as provided by the specialist database, miRBase, according to version 16 (released, August 2010).

(ii) The "p-value" represents the p-value of a microarray T-test derived from comparing case with control, as determined in study 1.

(iii) The biomarkers can be up-regulated (i.e. an increase in fold-change, when compared to control samples) or down-regulated (i.e. a decrease in fold-change, when compared to control samples), as determined in study 1.

TABLE 9-26
Table listing identified miRNAs (see section 6.5)

miRNA Name[(i)]	**P. Value[(ii)]**	**Expression[(iii)]**
hsa-miR-150	0.000731818	Down
hsa-miR-122	0.001736842	Down
hsa-miR-1224-5p	0.005657118	Up
hsa-miR-342-3p	0.007122454	Down
hsa-miR-3648	0.038141456	Up
hsa-miR-574-5p	0.043514783	Down

(i) The "miRNA name" column gives the name of the human miRNA as provided by the specialist database, miRBase, according to version 16 (released, August 2010).

(ii) The "p-value" represents the p-value of a microarray T-test derived from comparing case with control, as determined in study 1.

(iii) The biomarkers can be up-regulated (i.e. an increase in fold-change, when compared to control samples) or down-regulated (i.e. a decrease in fold-change, when compared to control samples), as determined in study 1.

TABLE 9-27
Table listing identified biomarkers (see section 6.5)

Biomarker	**AUC**	**S+S[(i)]**	**Sensitivity[(ii)]**	**Specificity[(iii)]**	**Assay[(iv)]**
hsa-miR-122	0.66	1.25	0.4	0.85	qPCR
hsa-miR-122	0.65	1.19	0.55	0.65	microarray
hsa-miR-150	0.8	1.44	0.8	0.65	microarray
hsa-miR-150	0.69	1.31	0.47	0.85	qPCR
hsa-miR-342-3p	0.78	1.42	0.66	0.76	microarray
hsa-miR-342-3p	0.62	1.14	0.76	0.38	qPCR
hsa-miR-1224-5p	0.48	1.06	0.06	1	microarray
hsa-miR-3194-5p	0.62	1.14	0.68	0.46	qPCR
hsa-miR-3648	0.63	1.21	0.85	0.35	microarray
hsa-miR-3663-5p	0.7	1.26	0.41	0.85	qPCR
hsa-miR-574-5p	0.8	1.43	0.73	0.71	microarray
HSPD1	0.62	1.15	0.81	0.33	autoAb
RAN	0.54	1.1	0.87	0.22	autoAb
STUB1	0.66	1.21	0.65	0.56	autoAb
TPM1	0.67	1.25	0.69	0.56	autoAb

(i) S+S is the sum of the sensitivity and specificity columns, as determined in study 1.

(ii) and (iii) These two columns show the sensitivity and specificity of a test based solely on the relevant biomarker (or, for Tables 11-15, panel) shown in the left-hand column in the same row when applied to the samples used in study 1.

(iv) For miRNA analysis, data was generated using either a microarray ("microarray") or qPCR ("qPCR") platform, as described in study 1. Autoantbody ("autoAb") biomarkers were identified using the protein array platform described in study 1. Where panels were developed incorporating both miRNA and autoantibody biomarkers as variables (see study 1), these are described as "combiAbMir".

TABLE 9-28

Table listing identified biomarkers (panel of two combinations) (see section 6.5)

Panel	AUC	S+S[(i)]	Sensitivity[(ii)]	Specificity[(iii)]	Assay[(iv)]
hsa-miR-150, hsa-miR-574-5p	0.9100	1.6300	0.8600	0.7600	microarray
hsa-miR-342-3p, hsa-miR-574-5p	0.8600	1.5200	0.7600	0.7600	microarray
hsa-miR-122, hsa-miR-574-5p	0.8400	1.5100	0.7500	0.7600	microarray
hsa-miR-3648, hsa-miR-574-5p	0.8300	1.4900	0.7900	0.7100	microarray
hsa-miR-150, hsa-miR-342-3p	0.8100	1.4500	0.6800	0.7600	microarray
TPM1, hsa-miR-150	0.8119	1.4825	0.8575	0.6250	combiAbMir
hsa-miR-342-3p, hsa-miR-3648	0.8100	1.4500	0.6900	0.7600	microarray
RAN, hsa-miR-574-5p	0.8102	1.4306	0.8056	0.6250	combiAbMir
HSPD1, hsa-miR-342-3p	0.8092	1.4506	0.5756	0.8750	combiAbMir
RAN, hsa-miR-342-3p	0.8078	1.4594	0.7094	0.7500	combiAbMir
TPM1, hsa-miR-342-3p	0.8064	1.4456	0.6956	0.7500	combiAbMir
hsa-miR-1224-5p, hsa-miR-342-3p	0.8000	1.4500	0.6800	0.7600	microarray
TPM1, hsa-miR-574-5p	0.7964	1.4350	0.8100	0.6250	combiAbMir
HSPD1, hsa-miR-150	0.7956	1.4288	0.6788	0.7500	combiAbMir
RAN, hsa-miR-150	0.7841	1.3856	0.7606	0.6250	combiAbMir
hsa-miR-1224-5p, hsa-miR-574-5p	0.7800	1.4200	0.6600	0.7600	microarray
hsa-miR-150, hsa-miR-3648	0.7800	1.3900	0.7400	0.6500	microarray
hsa-miR-150, hsa-miR-1224-5p	0.7800	1.3900	0.6800	0.7100	microarray
STUB1, hsa-miR-150	0.7773	1.4044	0.6544	0.7500	combiAbMir
HSPD1, hsa-miR-574-5p	0.7750	1.3875	0.7625	0.6250	combiAbMir
STUB1, hsa-miR-342-3p	0.7745	1.4113	0.6613	0.7500	combiAbMir
hsa-miR-122, hsa-miR-342-3p	0.7700	1.4000	0.6300	0.7600	microarray
STUB1, hsa-miR-574-5p	0.7697	1.3800	0.6300	0.7500	combiAbMir
hsa-miR-150, hsa-miR-122	0.7700	1.3800	0.6100	0.7600	microarray
hsa-miR-122, hsa-miR-3663-5p	0.7600	1.3700	0.6000	0.7700	qPCR
hsa-miR-150, hsa-miR-3663-5p	0.7500	1.3500	0.5000	0.8500	qPCR
hsa-miR-342-3p, hsa-miR-3663-5p	0.7200	1.3000	0.6000	0.6900	qPCR

TPM1, hsa-miR-122	0.6947	1.2813	0.6563	0.6250	combiAbMir
TPM1, HSPD1	0.6900	1.2800	0.8400	0.4400	autoAb
TPM1, hsa-miR-3648	0.6842	1.2400	0.7400	0.5000	combiAbMir
HSPD1, hsa-miR-3648	0.6727	1.2544	0.7544	0.5000	combiAbMir
hsa-miR-150, hsa-miR-3194-5p	0.6700	1.2800	0.4300	0.8500	qPCR
hsa-miR-122, hsa-miR-3648	0.6700	1.2300	0.8200	0.4100	microarray
STUB1, hsa-miR-122	0.6611	1.2650	0.6400	0.6250	combiAbMir
RAN, hsa-miR-3648	0.6611	1.2556	0.8806	0.3750	combiAbMir
TPM1, STUB1	0.6600	1.2500	0.8100	0.4400	autoAb
hsa-miR-3663-5p, hsa-miR-3194-5p	0.6600	1.1800	0.6400	0.5400	qPCR
HSPD1, STUB1	0.6500	1.1900	0.6400	0.5600	autoAb
hsa-miR-342-3p, hsa-miR-3194-5p	0.6400	1.1800	0.3300	0.8500	qPCR
STUB1, hsa-miR-3648	0.6398	1.2013	0.8263	0.3750	combiAbMir
TPM1, hsa-miR-1224-5p	0.6395	1.1956	0.5706	0.6250	combiAbMir
HSPD1, hsa-miR-122	0.6391	1.1925	0.4425	0.7500	combiAbMir
hsa-miR-122, hsa-miR-3194-5p	0.6400	1.2600	0.4100	0.8500	qPCR
HSPD1, RAN	0.6300	1.1700	0.8400	0.3300	autoAb
hsa-miR-150, hsa-miR-122	0.6300	1.2100	0.3600	0.8500	qPCR
hsa-miR-150, hsa-miR-342-3p	0.6300	1.2100	0.3600	0.8500	qPCR
TPM1, RAN	0.6300	1.1800	0.7300	0.4400	autoAb
hsa-miR-122, hsa-miR-342-3p	0.6200	1.2000	0.3500	0.8500	qPCR
RAN, hsa-miR-122	0.6178	1.1594	0.5344	0.6250	combiAbMir
STUB1, hsa-miR-1224-5p	0.6122	1.1731	0.4231	0.7500	combiAbMir
hsa-miR-122, hsa-miR-1224-5p	0.5900	1.1100	0.7000	0.4100	microarray
HSPD1, hsa-miR-1224-5p	0.5870	1.1206	0.6206	0.5000	combiAbMir
RAN, STUB1	0.5900	1.1500	0.8200	0.3300	autoAb
hsa-miR-1224-5p, hsa-miR-3648	0.5800	1.1100	0.8100	0.2900	microarray
RAN, hsa-miR-1224-5p	0.5373	1.0844	0.8344	0.2500	combiAbMir

(i) S+S is the sum of the sensitivity and specificity columns, as determined in study 1.

(ii) and (iii) These two columns show the sensitivity and specificity of a test based solely on the relevant biomarker (or, for Tables 11-15, panel) shown in the left-hand column in the same row when applied to the samples used in study 1.

(iv) For miRNA analysis, data was generated using either a microarray ("microarray") or qPCR ("qPCR") platform, as described in study 1. Autoantbody ("autoAb") biomarkers were identified using the protein array platform described in study 1. Where panels were developed incorporating both miRNA and autoantibody biomarkers as variables (see study 1), these are described as "combiAbMir".

TABLE 9-29

Table listing identified biomarkers (panel of three combinations) (see section 6.5)

Panel	AUC	S+S[(i)]	Sensitivity[(ii)]	Specificity[(iii)]	Assay[(iv)]
RAN, hsa-miR-150, hsa-miR-574-5p	0.92359	1.65750	0.78250	0.87500	combiAbMir
TPM1, hsa-miR-150, hsa-miR-574-5p	0.92359	1.65500	0.90500	0.75000	combiAbMir
hsa-miR-150, hsa-miR-342-3p, hsa-miR-574-5p	0.90000	1.61000	0.85000	0.76000	microarray
STUB1, hsa-miR-150, hsa-miR-574-5p	0.90078	1.61625	0.86625	0.75000	combiAbMir
hsa-miR-150, hsa-miR-122, hsa-miR-574-5p	0.90000	1.60000	0.83000	0.76000	microarray
HSPD1, hsa-miR-150, hsa-miR-574-5p	0.89719	1.60063	0.85063	0.75000	combiAbMir
hsa-miR-122, hsa-miR-342-3p, hsa-miR-574-5p	0.90000	1.60000	0.78000	0.82000	microarray
TPM1, hsa-miR-342-3p, hsa-miR-574-5p	0.89297	1.57125	0.69625	0.87500	combiAbMir
hsa-miR-150, hsa-miR-1224-5p, hsa-miR-574-5p	0.89000	1.59000	0.83000	0.76000	microarray
hsa-miR-150, hsa-miR-3648, hsa-miR-574-5p	0.89000	1.59000	0.83000	0.76000	microarray
RAN, hsa-miR-342-3p, hsa-miR-574-5p	0.87891	1.55375	0.67875	0.87500	combiAbMir
hsa-miR-1224-5p, hsa-miR-342-3p, hsa-miR-574-5p	0.88000	1.57000	0.81000	0.76000	microarray
TPM1, hsa-miR-122, hsa-miR-574-5p	0.87234	1.55000	0.80000	0.75000	combiAbMir
STUB1, hsa-miR-342-3p, hsa-miR-574-5p	0.86703	1.53500	0.78500	0.75000	combiAbMir
RAN, hsa-miR-122, hsa-miR-574-5p	0.86422	1.52875	0.77875	0.75000	combiAbMir
hsa-miR-342-3p, hsa-miR-3648, hsa-miR-574-5p	0.86000	1.54000	0.77000	0.76000	microarray
HSPD1, hsa-miR-342-3p, hsa-miR-574-5p	0.86266	1.51875	0.76875	0.75000	combiAbMir
RAN, hsa-miR-3648, hsa-miR-574-5p	0.86078	1.51563	0.76563	0.75000	combiAbMir
hsa-miR-122, hsa-miR-3648, hsa-miR-574-5p	0.85000	1.51000	0.75000	0.76000	microarray
TPM1, hsa-miR-3648, hsa-miR-574-5p	0.84250	1.51813	0.76813	0.75000	combiAbMir

TPM1, RAN, hsa-miR-574-5p	0.82516	1.45875	0.70875	0.75000	combiAbMir
hsa-miR-122, hsa-miR-1224-5p, hsa-miR-574-5p	0.82000	1.49000	0.72000	0.76000	microarray
HSPD1, hsa-miR-122, hsa-miR-574-5p	0.82172	1.46125	0.71125	0.75000	combiAbMir
STUB1, hsa-miR-122, hsa-miR-574-5p	0.81938	1.47125	0.72125	0.75000	combiAbMir
TPM1, RAN, hsa-miR-342-3p	0.81578	1.45750	0.58250	0.87500	combiAbMir
HSPD1, RAN, hsa-miR-574-5p	0.81406	1.45500	0.83000	0.62500	combiAbMir
RAN, hsa-miR-342-3p, hsa-miR-3648	0.81109	1.43875	0.68875	0.75000	combiAbMir
TPM1, STUB1, hsa-miR-574-5p	0.81094	1.45438	0.82938	0.62500	combiAbMir
TPM1, RAN, hsa-miR-150	0.81063	1.47500	0.85000	0.62500	combiAbMir
TPM1, HSPD1, hsa-miR-342-3p	0.80969	1.47313	0.72313	0.75000	combiAbMir
RAN, hsa-miR-1224-5p, hsa-miR-574-5p	0.80875	1.45625	0.70625	0.75000	combiAbMir
hsa-miR-1224-5p, hsa-miR-3648, hsa-miR-574-5p	0.81000	1.44000	0.74000	0.71000	microarray
HSPD1, hsa-miR-342-3p, hsa-miR-3648	0.80344	1.44000	0.69000	0.75000	combiAbMir
RAN, hsa-miR-150, hsa-miR-342-3p	0.80281	1.45688	0.58188	0.87500	combiAbMir
TPM1, hsa-miR-150, hsa-miR-342-3p	0.80219	1.43688	0.68688	0.75000	combiAbMir
TPM1, HSPD1, hsa-miR-574-5p	0.80203	1.43500	0.81000	0.62500	combiAbMir
TPM1, hsa-miR-342-3p, hsa-miR-3648	0.80109	1.43938	0.68938	0.75000	combiAbMir
TPM1, HSPD1, hsa-miR-150	0.80063	1.45375	0.82875	0.62500	combiAbMir
STUB1, hsa-miR-3648, hsa-miR-574-5p	0.80047	1.42563	0.67563	0.75000	combiAbMir
hsa-miR-150, hsa-miR-1224-5p, hsa-miR-342-3p	0.80000	1.42000	0.65000	0.76000	microarray
HSPD1, RAN, hsa-miR-150	0.79984	1.44000	0.69000	0.75000	combiAbMir
HSPD1, hsa-miR-150, hsa-miR-342-3p	0.79922	1.41938	0.66938	0.75000	combiAbMir
RAN, hsa-miR-122, hsa-miR-342-3p	0.79828	1.43125	0.68125	0.75000	combiAbMir
TPM1, hsa-miR-1224-5p, hsa-miR-574-5p	0.79813	1.45188	0.82688	0.62500	combiAbMir
RAN, STUB1, hsa-miR-574-5p	0.79750	1.41563	0.66563	0.75000	combiAbMir
TPM1, STUB1, hsa-miR-342-3p	0.79719	1.43563	0.68563	0.75000	combiAbMir
TPM1, hsa-miR-122, hsa-miR-342-3p	0.79672	1.42313	0.54813	0.87500	combiAbMir
TPM1, hsa-miR-150, hsa-miR-3648	0.79406	1.46250	0.83750	0.62500	combiAbMir
TPM1, hsa-miR-1224-5p, hsa-miR-342-3p	0.79391	1.44375	0.56875	0.87500	combiAbMir
HSPD1, RAN, hsa-miR-342-3p	0.79328	1.44688	0.57188	0.87500	combiAbMir

RAN, hsa-miR-1224-5p, hsa-miR-342-3p	0.79313	1.42563	0.55063	0.87500	combiAbMir
HSPD1, STUB1, hsa-miR-342-3p	0.79250	1.43250	0.68250	0.75000	combiAbMir
HSPD1, hsa-miR-150, hsa-miR-1224-5p	0.79078	1.41938	0.66938	0.75000	combiAbMir
STUB1, hsa-miR-342-3p, hsa-miR-3648	0.78688	1.40875	0.65875	0.75000	combiAbMir
HSPD1, hsa-miR-3648, hsa-miR-574-5p	0.78156	1.38938	0.88938	0.50000	combiAbMir
STUB1, hsa-miR-1224-5p, hsa-miR-574-5p	0.78141	1.40438	0.65438	0.75000	combiAbMir
STUB1, hsa-miR-122, hsa-miR-342-3p	0.78125	1.42063	0.54563	0.87500	combiAbMir
RAN, hsa-miR-150, hsa-miR-1224-5p	0.78125	1.39000	0.76500	0.62500	combiAbMir
TPM1, hsa-miR-150, hsa-miR-122	0.77844	1.43688	0.81188	0.62500	combiAbMir
TPM1, STUB1, hsa-miR-150	0.77750	1.42438	0.79938	0.62500	combiAbMir
hsa-miR-150, hsa-miR-342-3p, hsa-miR-3648	0.78000	1.40000	0.63000	0.76000	microarray
hsa-miR-150, hsa-miR-122, hsa-miR-342-3p	0.78000	1.40000	0.64000	0.76000	microarray
STUB1, hsa-miR-1224-5p, hsa-miR-342-3p	0.77594	1.39563	0.52063	0.87500	combiAbMir
RAN, hsa-miR-150, hsa-miR-3648	0.77516	1.38125	0.75625	0.62500	combiAbMir
TPM1, hsa-miR-150, hsa-miR-1224-5p	0.77406	1.42250	0.79750	0.62500	combiAbMir
hsa-miR-122, hsa-miR-1224-5p, hsa-miR-342-3p	0.77000	1.38000	0.61000	0.76000	microarray
STUB1, hsa-miR-150, hsa-miR-342-3p	0.77094	1.39813	0.64813	0.75000	combiAbMir
HSPD1, hsa-miR-150, hsa-miR-3648	0.76953	1.38375	0.75875	0.62500	combiAbMir
HSPD1, STUB1, hsa-miR-574-5p	0.76672	1.35500	0.73000	0.62500	combiAbMir
RAN, STUB1, hsa-miR-342-3p	0.76484	1.38375	0.63375	0.75000	combiAbMir
HSPD1, hsa-miR-1224-5p, hsa-miR-342-3p	0.76453	1.37375	0.49875	0.87500	combiAbMir
HSPD1, hsa-miR-122, hsa-miR-342-3p	0.76344	1.39313	0.51813	0.87500	combiAbMir
hsa-miR-1224-5p, hsa-miR-342-3p, hsa-miR-3648	0.76000	1.37000	0.72000	0.65000	microarray
hsa-miR-122, hsa-miR-342-3p, hsa-miR-3648	0.76000	1.36000	0.71000	0.65000	microarray
HSPD1, hsa-miR-150, hsa-miR-122	0.76109	1.36875	0.61875	0.75000	combiAbMir
HSPD1, STUB1, hsa-miR-150	0.76094	1.38250	0.75750	0.62500	combiAbMir
STUB1, hsa-miR-150, hsa-miR-122	0.76063	1.36438	0.73938	0.62500	combiAbMir
hsa-miR-150, hsa-miR-1224-5p, hsa-miR-3648	0.76000	1.35000	0.71000	0.65000	microarray
RAN, hsa-miR-150, hsa-miR-122	0.75563	1.35875	0.73375	0.62500	combiAbMir
HSPD1, hsa-miR-1224-5p, hsa-miR-574-5p	0.75469	1.36188	0.73688	0.62500	combiAbMir

RAN, STUB1, hsa-miR-150	0.75453	1.37188	0.74688	0.62500	combiAbMir
STUB1, hsa-miR-150, hsa-miR-1224-5p	0.75422	1.37063	0.74563	0.62500	combiAbMir
STUB1, hsa-miR-150, hsa-miR-3648	0.74891	1.35188	0.72688	0.62500	combiAbMir
hsa-miR-150, hsa-miR-122, hsa-miR-1224-5p	0.75000	1.35000	0.65000	0.71000	microarray
hsa-miR-150, hsa-miR-122, hsa-miR-3648	0.75000	1.35000	0.71000	0.65000	microarray
hsa-miR-150, hsa-miR-3663-5p, hsa-miR-3194-5p	0.74000	1.34000	0.65000	0.69000	qPCR
TPM1, HSPD1, hsa-miR-122	0.73094	1.34688	0.72188	0.62500	combiAbMir
hsa-miR-122, hsa-miR-3663-5p, hsa-miR-3194-5p	0.72000	1.32000	0.47000	0.85000	qPCR
hsa-miR-150, hsa-miR-122, hsa-miR-3663-5p	0.72000	1.31000	0.46000	0.85000	qPCR
hsa-miR-122, hsa-miR-342-3p, hsa-miR-3663-5p	0.72000	1.32000	0.63000	0.69000	qPCR
hsa-miR-150, hsa-miR-342-3p, hsa-miR-3663-5p	0.72000	1.31000	0.61000	0.69000	qPCR
hsa-miR-342-3p, hsa-miR-3663-5p, hsa-miR-3194-5p	0.70000	1.28000	0.59000	0.69000	qPCR
TPM1, HSPD1, hsa-miR-3648	0.70000	1.28063	0.78063	0.50000	combiAbMir
TPM1, RAN, hsa-miR-3648	0.69766	1.25813	0.75813	0.50000	combiAbMir
TPM1, hsa-miR-122, hsa-miR-3648	0.69375	1.25750	0.75750	0.50000	combiAbMir
HSPD1, RAN, hsa-miR-3648	0.68813	1.28813	0.91313	0.37500	combiAbMir
HSPD1, STUB1, hsa-miR-3648	0.68641	1.24875	0.74875	0.50000	combiAbMir
TPM1, HSPD1, RAN	0.68000	1.28000	0.83000	0.44000	autoAb
TPM1, HSPD1, STUB1	0.68000	1.29000	0.84000	0.44000	autoAb
TPM1, STUB1, hsa-miR-122	0.68078	1.28938	0.78938	0.50000	combiAbMir
RAN, hsa-miR-122, hsa-miR-3648	0.68000	1.26313	0.88813	0.37500	combiAbMir
TPM1, hsa-miR-1224-5p, hsa-miR-3648	0.68000	1.23500	0.73500	0.50000	combiAbMir
STUB1, hsa-miR-122, hsa-miR-3648	0.67938	1.25750	0.75750	0.50000	combiAbMir
HSPD1, hsa-miR-122, hsa-miR-3648	0.67453	1.21875	0.71875	0.50000	combiAbMir
TPM1, hsa-miR-122, hsa-miR-1224-5p	0.67438	1.26813	0.64313	0.62500	combiAbMir
TPM1, STUB1, hsa-miR-3648	0.66438	1.23438	0.73438	0.50000	combiAbMir
RAN, STUB1, hsa-miR-3648	0.66359	1.24563	0.87063	0.37500	combiAbMir
TPM1, HSPD1, hsa-miR-1224-5p	0.66188	1.22125	0.72125	0.50000	combiAbMir
TPM1, RAN, hsa-miR-122	0.65563	1.24000	0.74000	0.50000	combiAbMir
HSPD1, RAN, hsa-miR-122	0.65563	1.18375	0.80875	0.37500	combiAbMir

hsa-miR-150, hsa-miR-342-3p, hsa-miR-3194-5p	0.65000	1.25000	0.41000	0.85000	qPCR
hsa-miR-150, hsa-miR-122, hsa-miR-342-3p	0.65000	1.21000	0.36000	0.85000	qPCR
HSPD1, RAN, STUB1	0.65000	1.21000	0.76000	0.44000	autoAb
HSPD1, STUB1, hsa-miR-122	0.64828	1.20875	0.58375	0.62500	combiAbMir
hsa-miR-122, hsa-miR-1224-5p, hsa-miR-3648	0.64000	1.17000	0.82000	0.35000	microarray
hsa-miR-150, hsa-miR-122, hsa-miR-3194-5p	0.64000	1.25000	0.41000	0.85000	qPCR
TPM1, STUB1, hsa-miR-1224-5p	0.63531	1.20438	0.70438	0.50000	combiAbMir
HSPD1, STUB1, hsa-miR-1224-5p	0.63375	1.19938	0.69938	0.50000	combiAbMir
RAN, hsa-miR-1224-5p, hsa-miR-3648	0.63266	1.19188	0.81688	0.37500	combiAbMir
RAN, STUB1, hsa-miR-122	0.62906	1.19688	0.57188	0.62500	combiAbMir
TPM1, RAN, STUB1	0.62000	1.19000	0.64000	0.56000	autoAb
TPM1, RAN, hsa-miR-1224-5p	0.61922	1.15188	0.65188	0.50000	combiAbMir
hsa-miR-122, hsa-miR-342-3p, hsa-miR-3194-5p	0.62000	1.22000	0.37000	0.85000	qPCR
STUB1, hsa-miR-122, hsa-miR-1224-5p	0.61469	1.18250	0.55750	0.62500	combiAbMir
HSPD1, hsa-miR-122, hsa-miR-1224-5p	0.61406	1.15813	0.40813	0.75000	combiAbMir
HSPD1, RAN, hsa-miR-1224-5p	0.61328	1.17250	0.79750	0.37500	combiAbMir
STUB1, hsa-miR-1224-5p, hsa-miR-3648	0.60922	1.15500	0.78000	0.37500	combiAbMir
HSPD1, hsa-miR-1224-5p, hsa-miR-3648	0.60438	1.15000	0.90000	0.25000	combiAbMir
RAN, hsa-miR-122, hsa-miR-1224-5p	0.59906	1.11625	0.61625	0.50000	combiAbMir
RAN, STUB1, hsa-miR-1224-5p	0.57453	1.13688	0.76188	0.37500	combiAbMir

(i) S+S is the sum of the sensitivity and specificity columns, as determined in study 1.

(ii) and (iii) These two columns show the sensitivity and specificity of a test based solely on the relevant biomarker (or, for Tables 11-15, panel) shown in the left-hand column in the same row when applied to the samples used in study 1.

(iv) For miRNA analysis, data was generated using either a microarray ("microarray") or qPCR ("qPCR") platform, as described in study 1. Autoantbody ("autoAb") biomarkers were identified using the protein array platform described in study 1. Where panels were developed incorporating both miRNA and autoantibody biomarkers as variables (see study 1), these are described as "combiAbMir".

TABLE 9-30

Table listing identified biomarkers (panel of four combinations) (see section 6.5)

Panel	AUC	S+S (i)	Sensitivity[(ii)]	Specificity[(iii)]	Assay[(iv)]
TPM1, hsa-miR-150, hsa-miR-342-3p, hsa-miR-574-5p	0.928594	1.652500	0.902500	0.750000	combiAbMir
TPM1, hsa-miR-150, hsa-miR-122, hsa-miR-574-5p	0.928125	1.649375	0.899375	0.750000	combiAbMir
RAN, hsa-miR-150, hsa-miR-3648, hsa-miR-574-5p	0.925469	1.646250	0.771250	0.875000	combiAbMir
TPM1, RAN, hsa-miR-150, hsa-miR-574-5p	0.923125	1.646875	0.896875	0.750000	combiAbMir
TPM1, STUB1, hsa-miR-150, hsa-miR-574-5p	0.919844	1.635000	0.760000	0.875000	combiAbMir
RAN, hsa-miR-150, hsa-miR-122, hsa-miR-574-5p	0.914375	1.635000	0.760000	0.875000	combiAbMir
TPM1, hsa-miR-150, hsa-miR-3648, hsa-miR-574-5p	0.913594	1.612500	0.862500	0.750000	combiAbMir
RAN, STUB1, hsa-miR-150, hsa-miR-574-5p	0.913438	1.635625	0.760625	0.875000	combiAbMir
TPM1, hsa-miR-150, hsa-miR-1224-5p, hsa-miR-574-5p	0.913438	1.631875	0.881875	0.750000	combiAbMir
HSPD1, RAN, hsa-miR-150, hsa-miR-574-5p	0.912031	1.623750	0.748750	0.875000	combiAbMir
RAN, hsa-miR-150, hsa-miR-342-3p, hsa-miR-574-5p	0.908594	1.619375	0.869375	0.750000	combiAbMir
RAN, hsa-miR-150, hsa-miR-1224-5p, hsa-miR-574-5p	0.906719	1.618125	0.868125	0.750000	combiAbMir
TPM1, hsa-miR-122, hsa-miR-342-3p, hsa-miR-574-5p	0.906563	1.611250	0.861250	0.750000	combiAbMir
TPM1, HSPD1, hsa-miR-150, hsa-miR-574-5p	0.906406	1.612500	0.862500	0.750000	combiAbMir
HSPD1, hsa-miR-150, hsa-miR-342-3p, hsa-miR-574-5p	0.903906	1.607500	0.857500	0.750000	combiAbMir
STUB1, hsa-miR-150, hsa-miR-342-3p, hsa-miR-574-5p	0.902031	1.615625	0.865625	0.750000	combiAbMir
TPM1, RAN, hsa-miR-342-3p, hsa-miR-574-5p	0.901406	1.584375	0.834375	0.750000	combiAbMir
hsa-miR-150, hsa-miR-122, hsa-miR-3648,hsa-miR-574-5p	0.900000	1.610000	0.840000	0.760000	microarray
HSPD1, hsa-miR-150, hsa-miR-122, hsa-miR-574-5p	0.900625	1.593125	0.843125	0.750000	combiAbMir
HSPD1, hsa-miR-150, hsa-miR-1224-5p, hsa-miR-574-5p	0.898125	1.605625	0.855625	0.750000	combiAbMir
hsa-miR-150, hsa-miR-122, hsa-miR-342-3p,hsa-miR-574-5p	0.900000	1.590000	0.830000	0.760000	microarray
TPM1, HSPD1, hsa-miR-342-3p, hsa-miR-574-5p	0.895781	1.586250	0.836250	0.750000	combiAbMir
HSPD1, STUB1, hsa-miR-150, hsa-miR-574-5p	0.895313	1.600000	0.850000	0.750000	combiAbMir
TPM1, STUB1, hsa-miR-342-3p, hsa-miR-574-5p	0.893125	1.579375	0.829375	0.750000	combiAbMir
STUB1, hsa-miR-150, hsa-miR-3648, hsa-miR-574-5p	0.891563	1.595000	0.845000	0.750000	combiAbMir
HSPD1, hsa-miR-122, hsa-miR-342-3p, hsa-miR-574-5p	0.890938	1.607500	0.732500	0.875000	combiAbMir
STUB1, hsa-miR-150, hsa-miR-122, hsa-miR-574-5p	0.890625	1.583750	0.833750	0.750000	combiAbMir

HSPD1, hsa-miR-150, hsa-miR-3648, hsa-miR-574-5p	0.889063	1.592500	0.842500	0.750000	combiAbMir
STUB1, hsa-miR-122, hsa-miR-342-3p, hsa-miR-574-5p	0.888594	1.585625	0.835625	0.750000	combiAbMir
RAN, hsa-miR-122, hsa-miR-342-3p, hsa-miR-574-5p	0.886719	1.600000	0.725000	0.875000	combiAbMir
hsa-miR-150, hsa-miR-1224-5p, hsa-miR-3648, hsa-miR-574-5p	0.890000	1.570000	0.810000	0.760000	microarray
RAN, hsa-miR-342-3p, hsa-miR-3648, hsa-miR-574-5p	0.884375	1.560625	0.810625	0.750000	combiAbMir
STUB1, hsa-miR-150, hsa-miR-1224-5p, hsa-miR-574-5p	0.882344	1.575625	0.825625	0.750000	combiAbMir
hsa-miR-150, hsa-miR-342-3p, hsa-miR-3648,hsa-miR-574-5p	0.880000	1.570000	0.800000	0.760000	microarray
RAN, STUB1, hsa-miR-342-3p, hsa-miR-574-5p	0.881250	1.555625	0.680625	0.875000	combiAbMir
hsa-miR-150, hsa-miR-122, hsa-miR-1224-5p,hsa-miR-574-5p	0.880000	1.560000	0.800000	0.760000	microarray
TPM1, hsa-miR-342-3p, hsa-miR-3648, hsa-miR-574-5p	0.880313	1.555625	0.805625	0.750000	combiAbMir
TPM1, hsa-miR-122, hsa-miR-3648, hsa-miR-574-5p	0.877813	1.572500	0.822500	0.750000	combiAbMir
TPM1, hsa-miR-1224-5p, hsa-miR-342-3p,hsa-miR-574-5p	0.877813	1.556875	0.806875	0.750000	combiAbMir
hsa-miR-150, hsa-miR-1224-5p, hsa-miR-342-3p, hsa-miR-574-5p	0.880000	1.570000	0.810000	0.760000	microarray
hsa-miR-122, hsa-miR-342-3p, hsa-miR-3648,hsa-miR-574-5p	0.880000	1.560000	0.800000	0.760000	microarray
HSPD1, STUB1, hsa-miR-342-3p, hsa-miR-574-5p	0.874688	1.546250	0.796250	0.750000	combiAbMir
RAN, hsa-miR-1224-5p, hsa-miR-342-3p, hsa-miR-574-5p	0.872031	1.565000	0.690000	0.875000	combiAbMir
HSPD1, hsa-miR-1224-5p, hsa-miR-342-3p,hsa-miR-574-5p	0.870156	1.552500	0.802500	0.750000	combiAbMir
HSPD1, RAN, hsa-miR-342-3p, hsa-miR-574-5p	0.870000	1.546875	0.671875	0.875000	combiAbMir
hsa-miR-122, hsa-miR-1224-5p, hsa-miR-342-3p, hsa-miR-574-5p	0.870000	1.550000	0.730000	0.820000	microarray
TPM1, RAN, hsa-miR-3648, hsa-miR-574-5p	0.862500	1.542500	0.792500	0.750000	combiAbMir
TPM1, hsa-miR-122, hsa-miR-1224-5p, hsa-miR-574-5p	0.861094	1.536875	0.786875	0.750000	combiAbMir
STUB1, hsa-miR-1224-5p, hsa-miR-342-3p,hsa-miR-574-5p	0.859844	1.530625	0.780625	0.750000	combiAbMir
hsa-miR-1224-5p, hsa-miR-342-3p, hsa-miR-3648, hsa-miR-574-5p	0.860000	1.520000	0.760000	0.760000	microarray
STUB1, hsa-miR-342-3p, hsa-miR-3648, hsa-miR-574-5p	0.855156	1.502500	0.752500	0.750000	combiAbMir
RAN, hsa-miR-122, hsa-miR-3648, hsa-miR-574-5p	0.854219	1.500000	0.750000	0.750000	combiAbMir
TPM1, HSPD1, hsa-miR-122, hsa-miR-574-5p	0.852969	1.500000	0.750000	0.750000	combiAbMir
HSPD1, hsa-miR-342-3p, hsa-miR-3648, hsa-miR-574-5p	0.850625	1.506250	0.756250	0.750000	combiAbMir
TPM1, RAN, hsa-miR-122, hsa-miR-574-5p	0.848281	1.497500	0.747500	0.750000	combiAbMir
TPM1, STUB1, hsa-miR-122, hsa-miR-574-5p	0.847813	1.509375	0.759375	0.750000	combiAbMir
HSPD1, hsa-miR-122, hsa-miR-3648, hsa-miR-574-5p	0.846719	1.496875	0.621875	0.875000	combiAbMir

STUB1, hsa-miR-122, hsa-miR-3648, hsa-miR-574-5p	0.841406	1.498750	0.748750	0.750000	combiAbMir
HSPD1, RAN, hsa-miR-122, hsa-miR-574-5p	0.839531	1.470625	0.720625	0.750000	combiAbMir
RAN, hsa-miR-122, hsa-miR-1224-5p, hsa-miR-574-5p	0.837969	1.503750	0.753750	0.750000	combiAbMir
HSPD1, hsa-miR-122, hsa-miR-1224-5p, hsa-miR-574-5p	0.837188	1.492500	0.617500	0.875000	combiAbMir
hsa-miR-122, hsa-miR-1224-5p, hsa-miR-3648, hsa-miR-574-5p	0.830000	1.500000	0.730000	0.760000	microarray
TPM1, HSPD1, RAN, hsa-miR-342-3p	0.832656	1.505000	0.755000	0.750000	combiAbMir
HSPD1, RAN, hsa-miR-3648, hsa-miR-574-5p	0.832656	1.440625	0.690625	0.750000	combiAbMir
TPM1, RAN, hsa-miR-150, hsa-miR-342-3p	0.832188	1.486875	0.736875	0.750000	combiAbMir
RAN, hsa-miR-1224-5p, hsa-miR-3648, hsa-miR-574-5p	0.830625	1.468125	0.718125	0.750000	combiAbMir
TPM1, RAN, hsa-miR-342-3p, hsa-miR-3648	0.828125	1.485000	0.735000	0.750000	combiAbMir
TPM1, STUB1, hsa-miR-3648, hsa-miR-574-5p	0.827969	1.476875	0.726875	0.750000	combiAbMir
RAN, STUB1, hsa-miR-122, hsa-miR-574-5p	0.827500	1.470625	0.720625	0.750000	combiAbMir
HSPD1, STUB1, hsa-miR-122, hsa-miR-574-5p	0.826563	1.470625	0.720625	0.750000	combiAbMir
RAN, STUB1, hsa-miR-3648, hsa-miR-574-5p	0.823125	1.428125	0.678125	0.750000	combiAbMir
TPM1, HSPD1, STUB1, hsa-miR-342-3p	0.822656	1.483125	0.733125	0.750000	combiAbMir
TPM1, hsa-miR-1224-5p, hsa-miR-3648, hsa-miR-574-5p	0.822031	1.467500	0.717500	0.750000	combiAbMir
TPM1, HSPD1, hsa-miR-122, hsa-miR-342-3p	0.821563	1.485625	0.735625	0.750000	combiAbMir
TPM1, HSPD1, RAN, hsa-miR-150	0.818906	1.473750	0.848750	0.625000	combiAbMir
TPM1, HSPD1, hsa-miR-342-3p, hsa-miR-3648	0.817813	1.453750	0.703750	0.750000	combiAbMir
TPM1, HSPD1, hsa-miR-3648, hsa-miR-574-5p	0.817031	1.443750	0.818750	0.625000	combiAbMir
TPM1, HSPD1, hsa-miR-150, hsa-miR-342-3p	0.815938	1.477500	0.727500	0.750000	combiAbMir
TPM1, HSPD1, RAN, hsa-miR-574-5p	0.815000	1.430625	0.805625	0.625000	combiAbMir
TPM1, HSPD1, STUB1, hsa-miR-574-5p	0.812656	1.433125	0.808125	0.625000	combiAbMir
HSPD1, RAN, hsa-miR-342-3p, hsa-miR-3648	0.810781	1.438750	0.688750	0.750000	combiAbMir
TPM1, HSPD1, hsa-miR-150, hsa-miR-122	0.810625	1.455625	0.830625	0.625000	combiAbMir
TPM1, RAN, STUB1, hsa-miR-150	0.810156	1.470625	0.845625	0.625000	combiAbMir
TPM1, RAN, hsa-miR-1224-5p, hsa-miR-342-3p	0.806094	1.448750	0.698750	0.750000	combiAbMir
TPM1, RAN, hsa-miR-150, hsa-miR-1224-5p	0.805469	1.469375	0.844375	0.625000	combiAbMir
RAN, hsa-miR-150, hsa-miR-342-3p, hsa-miR-3648	0.805000	1.424375	0.674375	0.750000	combiAbMir
TPM1, STUB1, hsa-miR-122, hsa-miR-342-3p	0.803438	1.449375	0.699375	0.750000	combiAbMir

RAN, hsa-miR-150, hsa-miR-122, hsa-miR-342-3p	0.802188	1.434375	0.559375	0.875000	combiAbMir
STUB1, hsa-miR-122, hsa-miR-1224-5p, hsa-miR-574-5p	0.801875	1.463125	0.713125	0.750000	combiAbMir
HSPD1, RAN, hsa-miR-150, hsa-miR-1224-5p	0.800781	1.457500	0.707500	0.750000	combiAbMir
TPM1, hsa-miR-122, hsa-miR-342-3p, hsa-miR-3648	0.800781	1.434375	0.684375	0.750000	combiAbMir
TPM1, RAN, hsa-miR-1224-5p, hsa-miR-574-5p	0.800000	1.426250	0.801250	0.625000	combiAbMir
TPM1, HSPD1, hsa-miR-1224-5p, hsa-miR-342-3p	0.799375	1.443750	0.693750	0.750000	combiAbMir
TPM1, RAN, STUB1, hsa-miR-574-5p	0.798281	1.415000	0.790000	0.625000	combiAbMir
TPM1, HSPD1, hsa-miR-150, hsa-miR-3648	0.796875	1.451250	0.826250	0.625000	combiAbMir
HSPD1, RAN, hsa-miR-1224-5p, hsa-miR-574-5p	0.795938	1.431250	0.806250	0.625000	combiAbMir
HSPD1, RAN, hsa-miR-150, hsa-miR-342-3p	0.795625	1.449375	0.574375	0.875000	combiAbMir
TPM1, HSPD1, STUB1, hsa-miR-150	0.794844	1.441250	0.816250	0.625000	combiAbMir
HSPD1, hsa-miR-150, hsa-miR-342-3p, hsa-miR-3648	0.793750	1.419375	0.669375	0.750000	combiAbMir
HSPD1, STUB1, hsa-miR-3648, hsa-miR-574-5p	0.792813	1.402500	0.777500	0.625000	combiAbMir
HSPD1, hsa-miR-150, hsa-miR-122, hsa-miR-342-3p	0.792656	1.426875	0.551875	0.875000	combiAbMir
HSPD1, hsa-miR-1224-5p, hsa-miR-3648, hsa-miR-574-5p	0.792500	1.416875	0.791875	0.625000	combiAbMir
RAN, STUB1, hsa-miR-342-3p, hsa-miR-3648	0.792500	1.411250	0.661250	0.750000	combiAbMir
TPM1, RAN, hsa-miR-150, hsa-miR-3648	0.792344	1.432500	0.807500	0.625000	combiAbMir
HSPD1, RAN, STUB1, hsa-miR-574-5p	0.790938	1.400625	0.775625	0.625000	combiAbMir
TPM1, hsa-miR-150, hsa-miR-342-3p, hsa-miR-3648	0.790469	1.405625	0.780625	0.625000	combiAbMir
TPM1, HSPD1, hsa-miR-150, hsa-miR-1224-5p	0.790313	1.421875	0.796875	0.625000	combiAbMir
TPM1, HSPD1, hsa-miR-1224-5p, hsa-miR-574-5p	0.790313	1.415625	0.790625	0.625000	combiAbMir
HSPD1, STUB1, hsa-miR-150, hsa-miR-342-3p	0.790156	1.431250	0.681250	0.750000	combiAbMir
HSPD1, RAN, STUB1, hsa-miR-342-3p	0.788438	1.424375	0.549375	0.875000	combiAbMir
TPM1, STUB1, hsa-miR-150, hsa-miR-342-3p	0.788281	1.413750	0.663750	0.750000	combiAbMir
TPM1, hsa-miR-150, hsa-miR-1224-5p, hsa-miR-342-3p	0.787500	1.406875	0.781875	0.625000	combiAbMir
HSPD1, STUB1, hsa-miR-150, hsa-miR-122	0.787031	1.435625	0.685625	0.750000	combiAbMir
HSPD1, STUB1, hsa-miR-342-3p, hsa-miR-3648	0.785938	1.414375	0.664375	0.750000	combiAbMir
RAN, hsa-miR-150, hsa-miR-1224-5p, hsa-miR-342-3p	0.785313	1.420000	0.545000	0.875000	combiAbMir
TPM1, STUB1, hsa-miR-342-3p, hsa-miR-3648	0.785313	1.403750	0.653750	0.750000	combiAbMir
HSPD1, hsa-miR-1224-5p, hsa-miR-342-3p,hsa-miR-3648	0.785156	1.410625	0.660625	0.750000	combiAbMir

hsa-miR-150, hsa-miR-122, hsa-miR-342-3p,hsa-miR-3648	0.780000	1.390000	0.750000	0.650000	microarray
TPM1, STUB1, hsa-miR-1224-5p, hsa-miR-342-3p	0.783906	1.424375	0.674375	0.750000	combiAbMir
STUB1, hsa-miR-1224-5p, hsa-miR-3648, hsa-miR-574-5p	0.783750	1.404375	0.654375	0.750000	combiAbMir
HSPD1, hsa-miR-150, hsa-miR-122, hsa-miR-1224-5p	0.783281	1.419375	0.669375	0.750000	combiAbMir
hsa-miR-150, hsa-miR-1224-5p, hsa-miR-342-3p, hsa-miR-3648	0.780000	1.400000	0.750000	0.650000	microarray
TPM1, STUB1, hsa-miR-1224-5p, hsa-miR-574-5p	0.782188	1.431250	0.681250	0.750000	combiAbMir
HSPD1, RAN, hsa-miR-1224-5p, hsa-miR-342-3p	0.782188	1.427500	0.552500	0.875000	combiAbMir
TPM1, hsa-miR-150, hsa-miR-122, hsa-miR-342-3p	0.782188	1.407500	0.657500	0.750000	combiAbMir
HSPD1, RAN, hsa-miR-122, hsa-miR-342-3p	0.782188	1.405625	0.530625	0.875000	combiAbMir
TPM1, RAN, hsa-miR-122, hsa-miR-342-3p	0.781875	1.418125	0.543125	0.875000	combiAbMir
RAN, STUB1, hsa-miR-1224-5p, hsa-miR-574-5p	0.781719	1.413125	0.663125	0.750000	combiAbMir
HSPD1, RAN, hsa-miR-150, hsa-miR-3648	0.781719	1.396875	0.771875	0.625000	combiAbMir
TPM1, hsa-miR-1224-5p, hsa-miR-342-3p,hsa-miR-3648	0.780938	1.396250	0.771250	0.625000	combiAbMir
RAN, STUB1, hsa-miR-1224-5p, hsa-miR-342-3p	0.780469	1.396875	0.646875	0.750000	combiAbMir
TPM1, RAN, STUB1, hsa-miR-342-3p	0.780313	1.408125	0.658125	0.750000	combiAbMir
RAN, hsa-miR-122, hsa-miR-342-3p, hsa-miR-3648	0.779063	1.376250	0.751250	0.625000	combiAbMir
HSPD1, STUB1, hsa-miR-150, hsa-miR-1224-5p	0.778125	1.401250	0.651250	0.750000	combiAbMir
TPM1, hsa-miR-122, hsa-miR-1224-5p, hsa-miR-342-3p	0.777969	1.409375	0.659375	0.750000	combiAbMir
HSPD1, RAN, hsa-miR-150, hsa-miR-122	0.777188	1.395000	0.770000	0.625000	combiAbMir
HSPD1, hsa-miR-150, hsa-miR-1224-5p, hsa-miR-342-3p	0.776875	1.395625	0.645625	0.750000	combiAbMir
TPM1, hsa-miR-150, hsa-miR-1224-5p, hsa-miR-3648	0.773281	1.415625	0.790625	0.625000	combiAbMir
RAN, hsa-miR-122, hsa-miR-1224-5p, hsa-miR-342-3p	0.772344	1.406250	0.531250	0.875000	combiAbMir
HSPD1, RAN, STUB1, hsa-miR-150	0.772344	1.384375	0.634375	0.750000	combiAbMir
HSPD1, STUB1, hsa-miR-122, hsa-miR-342-3p	0.772188	1.381875	0.506875	0.875000	combiAbMir
TPM1, STUB1, hsa-miR-150, hsa-miR-122	0.770469	1.426875	0.801875	0.625000	combiAbMir
HSPD1, hsa-miR-122, hsa-miR-342-3p, hsa-miR-3648	0.770156	1.370625	0.620625	0.750000	combiAbMir
RAN, hsa-miR-1224-5p, hsa-miR-342-3p, hsa-miR-3648	0.769688	1.381250	0.756250	0.625000	combiAbMir
RAN, hsa-miR-150, hsa-miR-1224-5p, hsa-miR-3648	0.769063	1.373750	0.748750	0.625000	combiAbMir
hsa-miR-150, hsa-miR-122, hsa-miR-1224-5p,hsa-miR-342-3p	0.770000	1.380000	0.620000	0.760000	microarray
TPM1, hsa-miR-150, hsa-miR-122, hsa-miR-1224-5p	0.768750	1.406250	0.781250	0.625000	combiAbMir

HSPD1, STUB1, hsa-miR-1224-5p, hsa-miR-342-3p	0.768125	1.398125	0.523125	0.875000	combiAbMir
RAN, STUB1, hsa-miR-122, hsa-miR-342-3p	0.767969	1.378750	0.628750	0.750000	combiAbMir
HSPD1, hsa-miR-150, hsa-miR-122, hsa-miR-3648	0.767344	1.376250	0.751250	0.625000	combiAbMir
HSPD1, STUB1, hsa-miR-1224-5p, hsa-miR-574-5p	0.766094	1.378125	0.628125	0.750000	combiAbMir
TPM1, RAN, hsa-miR-150, hsa-miR-122	0.765938	1.405000	0.780000	0.625000	combiAbMir
TPM1, STUB1, hsa-miR-150, hsa-miR-1224-5p	0.764219	1.415000	0.790000	0.625000	combiAbMir
HSPD1, hsa-miR-122, hsa-miR-1224-5p, hsa-miR-342-3p	0.763594	1.373750	0.498750	0.875000	combiAbMir
RAN, STUB1, hsa-miR-150, hsa-miR-1224-5p	0.763281	1.385000	0.760000	0.625000	combiAbMir
HSPD1, hsa-miR-150, hsa-miR-1224-5p, hsa-miR-3648	0.758438	1.370000	0.745000	0.625000	combiAbMir
RAN, STUB1, hsa-miR-150, hsa-miR-342-3p	0.757813	1.376875	0.501875	0.875000	combiAbMir
STUB1, hsa-miR-122, hsa-miR-1224-5p, hsa-miR-342-3p	0.757344	1.351875	0.601875	0.750000	combiAbMir
RAN, STUB1, hsa-miR-150, hsa-miR-3648	0.755781	1.373125	0.748125	0.625000	combiAbMir
hsa-miR-122, hsa-miR-1224-5p, hsa-miR-342-3p, hsa-miR-3648	0.760000	1.360000	0.660000	0.710000	microarray
TPM1, STUB1, hsa-miR-150, hsa-miR-3648	0.755469	1.392500	0.767500	0.625000	combiAbMir
RAN, hsa-miR-150, hsa-miR-122, hsa-miR-1224-5p	0.753594	1.351250	0.726250	0.625000	combiAbMir
TPM1, hsa-miR-150, hsa-miR-122, hsa-miR-3648	0.753438	1.376250	0.751250	0.625000	combiAbMir
RAN, STUB1, hsa-miR-150, hsa-miR-122	0.752500	1.355000	0.730000	0.625000	combiAbMir
STUB1, hsa-miR-122, hsa-miR-342-3p, hsa-miR-3648	0.752500	1.343750	0.593750	0.750000	combiAbMir
STUB1, hsa-miR-150, hsa-miR-122, hsa-miR-342-3p	0.751250	1.353750	0.603750	0.750000	combiAbMir
STUB1, hsa-miR-150, hsa-miR-1224-5p, hsa-miR-342-3p	0.749688	1.346250	0.471250	0.875000	combiAbMir
HSPD1, STUB1, hsa-miR-150, hsa-miR-3648	0.748750	1.352500	0.727500	0.625000	combiAbMir
STUB1, hsa-miR-150, hsa-miR-122, hsa-miR-3648	0.748750	1.343750	0.718750	0.625000	combiAbMir
STUB1, hsa-miR-1224-5p, hsa-miR-342-3p,hsa-miR-3648	0.746406	1.344375	0.719375	0.625000	combiAbMir
STUB1, hsa-miR-150, hsa-miR-342-3p, hsa-miR-3648	0.742969	1.332500	0.582500	0.750000	combiAbMir
RAN, hsa-miR-150, hsa-miR-122, hsa-miR-3648	0.740938	1.323125	0.698125	0.625000	combiAbMir
hsa-miR-150, hsa-miR-122, hsa-miR-1224-5p,hsa-miR-3648	0.740000	1.320000	0.680000	0.650000	microarray
STUB1, hsa-miR-150, hsa-miR-122, hsa-miR-1224-5p	0.736719	1.325000	0.575000	0.750000	combiAbMir
STUB1, hsa-miR-150, hsa-miR-1224-5p, hsa-miR-3648	0.730313	1.313750	0.688750	0.625000	combiAbMir
hsa-miR-150, hsa-miR-122, hsa-miR-3663-5p,hsa-miR-3194-5p	0.730000	1.300000	0.450000	0.850000	qPCR
hsa-miR-150, hsa-miR-122, hsa-miR-342-3p,hsa-miR-3663-5p	0.720000	1.310000	0.470000	0.850000	qPCR

hsa-miR-150, hsa-miR-342-3p, hsa-miR-3663-5p, hsa-miR-3194-5p	0.720000	1.310000	0.610000	0.690000	qPCR
TPM1, RAN, hsa-miR-122, hsa-miR-3648	0.720156	1.309375	0.809375	0.500000	combiAbMir
TPM1, HSPD1, RAN, hsa-miR-122	0.718438	1.318125	0.693125	0.625000	combiAbMir
TPM1, HSPD1, RAN, hsa-miR-3648	0.715469	1.281250	0.781250	0.500000	combiAbMir
TPM1, RAN, hsa-miR-1224-5p, hsa-miR-3648	0.710156	1.280625	0.780625	0.500000	combiAbMir
TPM1, hsa-miR-122, hsa-miR-1224-5p, hsa-miR-3648	0.709063	1.278750	0.778750	0.500000	combiAbMir
hsa-miR-122, hsa-miR-342-3p, hsa-miR-3663-5p, hsa-miR-3194-5p	0.710000	1.290000	0.600000	0.690000	qPCR
TPM1, HSPD1, STUB1, hsa-miR-3648	0.704531	1.276250	0.776250	0.500000	combiAbMir
TPM1, HSPD1, hsa-miR-122, hsa-miR-3648	0.697500	1.283125	0.658125	0.625000	combiAbMir
TPM1, HSPD1, STUB1, hsa-miR-122	0.696719	1.298125	0.673125	0.625000	combiAbMir
HSPD1, RAN, hsa-miR-122, hsa-miR-3648	0.692656	1.270625	0.770625	0.500000	combiAbMir
TPM1, HSPD1, hsa-miR-1224-5p, hsa-miR-3648	0.688281	1.258750	0.758750	0.500000	combiAbMir
TPM1, STUB1, hsa-miR-122, hsa-miR-3648	0.687656	1.269375	0.769375	0.500000	combiAbMir
TPM1, HSPD1, RAN, STUB1	0.690000	1.280000	0.830000	0.440000	autoAb
TPM1, HSPD1, hsa-miR-122, hsa-miR-1224-5p	0.684063	1.286250	0.661250	0.625000	combiAbMir
HSPD1, RAN, hsa-miR-1224-5p, hsa-miR-3648	0.682656	1.234375	0.734375	0.500000	combiAbMir
TPM1, HSPD1, STUB1, hsa-miR-1224-5p	0.682344	1.286250	0.786250	0.500000	combiAbMir
TPM1, RAN, STUB1, hsa-miR-3648	0.680000	1.250000	0.750000	0.500000	combiAbMir
HSPD1, STUB1, hsa-miR-122, hsa-miR-3648	0.678125	1.249375	0.749375	0.500000	combiAbMir
RAN, STUB1, hsa-miR-122, hsa-miR-3648	0.669531	1.255000	0.755000	0.500000	combiAbMir
TPM1, RAN, STUB1, hsa-miR-122	0.669219	1.273125	0.773125	0.500000	combiAbMir
HSPD1, RAN, STUB1, hsa-miR-3648	0.669063	1.235000	0.860000	0.375000	combiAbMir
STUB1, hsa-miR-122, hsa-miR-1224-5p, hsa-miR-3648	0.668750	1.234375	0.734375	0.500000	combiAbMir
TPM1, HSPD1, RAN, hsa-miR-1224-5p	0.666094	1.242500	0.742500	0.500000	combiAbMir
HSPD1, RAN, STUB1, hsa-miR-122	0.663281	1.237500	0.737500	0.500000	combiAbMir
TPM1, STUB1, hsa-miR-1224-5p, hsa-miR-3648	0.661250	1.200000	0.700000	0.500000	combiAbMir
TPM1, STUB1, hsa-miR-122, hsa-miR-1224-5p	0.657500	1.270625	0.770625	0.500000	combiAbMir
TPM1, RAN, hsa-miR-122, hsa-miR-1224-5p	0.651406	1.221875	0.596875	0.625000	combiAbMir
HSPD1, hsa-miR-122, hsa-miR-1224-5p, hsa-miR-3648	0.649219	1.192500	0.817500	0.375000	combiAbMir
hsa-miR-150, hsa-miR-122, hsa-miR-342-3p,hsa-miR-3194-5p	0.650000	1.250000	0.410000	0.850000	qPCR

HSPD1, STUB1, hsa-miR-122, hsa-miR-1224-5p	0.642031	1.193750	0.568750	0.625000	combiAbMir
HSPD1, STUB1, hsa-miR-1224-5p, hsa-miR-3648	0.631250	1.166250	0.791250	0.375000	combiAbMir
HSPD1, RAN, hsa-miR-122, hsa-miR-1224-5p	0.628438	1.147500	0.647500	0.500000	combiAbMir
RAN, STUB1, hsa-miR-1224-5p, hsa-miR-3648	0.622656	1.210625	0.835625	0.375000	combiAbMir
HSPD1, RAN, STUB1, hsa-miR-1224-5p	0.618906	1.156875	0.781875	0.375000	combiAbMir
RAN, hsa-miR-122, hsa-miR-1224-5p, hsa-miR-3648	0.617656	1.180000	0.805000	0.375000	combiAbMir
TPM1, RAN, STUB1, hsa-miR-1224-5p	0.614531	1.177500	0.802500	0.375000	combiAbMir
RAN, STUB1, hsa-miR-122, hsa-miR-1224-5p	0.603125	1.141875	0.516875	0.625000	combiAbMir

(i) S+S is the sum of the sensitivity and specificity columns, as determined in study 1.

(ii) and (iii) These two columns show the sensitivity and specificity of a test based solely on the relevant biomarker (or, for Tables 11-15, panel) shown in the left-hand column in the same row when applied to the samples used in study 1.

(iv) For miRNA analysis, data was generated using either a microarray ("microarray") or qPCR ("qPCR") platform, as described in study 1. Autoantbody ("autoAb") biomarkers were identified using the protein array platform described in study 1. Where panels were developed incorporating both miRNA and autoantibody biomarkers as variables (see study 1), these are described as "combiAbMir".

TABLE 9-31

Table listing identified biomarkers (panel of five combinations) (see section 6.5)

Panel	**AUC**	**S+S[(i)]**	**Sensitivity[(ii)]**	**Specificity[(iii)]**	**Assay[(iv)]**
hsa-miR-150, hsa-miR-122, hsa-miR-1224-5p,hsa-miR-342-3p, hsa-miR-574-5p	0.9	1.59	0.77	0.82	microarray
hsa-miR-150, hsa-miR-122, hsa-miR-342-3p,hsa-miR-3648, hsa-miR-574-5p	0.89	1.57	0.8	0.76	microarray
hsa-miR-150, hsa-miR-122, hsa-miR-1224-5p,hsa-miR-3648, hsa-miR-574-5p	0.88	1.57	0.8	0.76	microarray
hsa-miR-122, hsa-miR-1224-5p, hsa-miR-342-3p, hsa-miR-3648, hsa-miR-574-5p	0.88	1.57	0.81	0.76	microarray
hsa-miR-150, hsa-miR-1224-5p, hsa-miR-342-3p, hsa-miR-3648, hsa-miR-574-5p	0.88	1.56	0.8	0.76	microarray
hsa-miR-150, hsa-miR-122, hsa-miR-1224-5p,hsa-miR-342-3p, hsa-miR-3648	0.77	1.38	0.73	0.65	microarray
hsa-miR-150, hsa-miR-122, hsa-miR-342-3p,hsa-miR-3663-5p, hsa-miR-3194-5p	0.71	1.28	0.44	0.85	qPCR

(i) S+S is the sum of the sensitivity and specificity columns, as determined in study 1.

(ii) and (iii) These two columns show the sensitivity and specificity of a test based solely on the relevant biomarker (or, for Tables 11-15, panel) shown in the left-hand column in the

same row when applied to the samples used in study 1.

(iv) For miRNA analysis, data was generated using either a microarray ("microarray") or qPCR ("qPCR") platform, as described in study 1. Autoantbody ("autoAb") biomarkers were identified using the protein array platform described in study 1. Where panels were developed incorporating both miRNA and autoantibody biomarkers as variables (see study 1), these are described as "combiAbMir".

TABLE 9-32

Table listing identified biomarkers (panel of six combinations) (see section 6.5)

Panel	**AUC**	**S+S[(i)]**	**Sensitivity[(ii)]**	**Specificity[(iii)]**	**Assay[(iv)]**
hsa-miR-150, hsa-miR-122, hsa-miR-1224-5p, hsa-miR-342-3p, hsa-miR-3648, hsa-miR-574-5p	0.89	1.58	0.81	0.76	microarray

TABLE 9-33
The levels of expression of the following 2 miRNAs are significantly different in ES samples compared to that in OvES, NE and NP samples (see Section 4.4.1.1)

miRNA	Expression in ES samples compared to that in OvES, NE and NP samples
ebv-miR-BART2-5p	Up
hsa-miR-564	Down

TABLE 9-34
The levels of expression of the following miRNAs are significantly different in OvES samples compared to that in ES, NE and NP samples (see Section 4.4.1.1)

miRNA	Expression in OvES samples compared to that in ES, NE and NP samples
hsa-let-7d-5p/3p	Up
hsa-miR-29a	Down
hsa-miR-142-3p	Down
hsa-miR-197	Up
hsa-miR-215	Down
hsa-miR-219-1-3p	Up
hsa-miR-296-3p	Up
hsa-miR-320c	Down
hsa-miR-337-5p	Down
hsa-miR-369-3p	Down
hsa-miR-450b-5p	Down
hsa-miR-483-5p	Up
hsa-miR-507	Down
hsa-miR-517c / hsa-miR-519a	Down
hsa-miR-519d	Up
hsa-miR-520g	Down
hsa-miR-576-5p	Up
hsa-miR-577	Down
hsa-miR-604	Up
hsa-miR-610	Down
hsa-miR-619	Down
hsa-miR-1256	Down
hsa-miR-1278	Down
hsa-miR-1297	Down
hcmv-miR-US33-5p	Down
hsv1-miR-H1-5p	Up

TABLE 9-35
The level of expression of the following miRNA in OvES and ES samples is significantly different from that in NE and NP samples (see Section 4.4.1.1)

miRNA	Expression in OvES and ES samples compared to that in NE and NP samples
hsa-miR-877	Down

TABLE 9-36
The levels of expression of the following miRNAs in OvES and NE samples are significantly different from that in ES and NP samples (see Section 4.4.1.1)

miRNA	Expression in OvES and NE samples compared to that in ES and NP samples

hsa-let-7e-5p/3p	Up
hsa-let-7f	Up
hsa-let-7g	Up
hsa-miR-9	Up
hsa-miR-30b	Up
hsa-miR-34a	Up
hsa-miR-92b	Up
hsa-miR-96-5p/3p	Up
hsa-miR-106a-5p/3p	Up
hsa-miR-17-5p/3p	Up
hsa-miR-106b-5p/3p	Up
hsa-miR-127-3p	Up
hsa-miR-128	Up
hsa-miR-154	Up
hsa-miR-155	Up
hsa-miR-183-5p/3p	Up
hsa-miR-194	Up
hsa-miR-196b-5p/3p	Up
hsa-miR-203	Up
hsa-miR-204	Up
hsa-miR-221-5p/3p	Up
hsa-miR-223	Up
hsa-miR-376a	Up
hsa-miR-376c	Up
hsa-miR-377	Up
hsa-miR-379	Up
hsa-miR-423-3p	Up
hsa-miR-424-5p/3p	Up
hsa-miR-425-5p/3p	Up
hsa-miR-454-5p/3p	Up
hsa-miR-486-3p	Up
hsa-miR-509-3p	Up
hsa-miR-514	Up
hsa-miR-542-3p	Up
hsa-miR-545-5p/3p	Up
hsa-miR-626	Up
hsa-miR-630	Up
hsa-miR-663	Up
hsa-miR-720	Up
hsa-miR-758-5p/3p	Up
hsa-miR-876-3p	Up
hsa-miR-1185	Up
hsa-miR-1260	Up
hsa-miR-1266-5p/3p	Up

TABLE 9-37
The levels of expression of the following miRNAs are significantly different in OvES, ES and NP samples compared to that in NE samples (see Section 4.4.1.1)

miRNA	**Expression in OvES, ES and NP compared to that in NE samples**
hsa-miR-199a-3p	Up

hsa-miR-199b-3p	Up
hsa-miR-497	Up
hsa-miR-625-5p/3p	Up

TABLE 9-38

The levels of expression of the following miRNAs are significantly different in OvES, ES and NE samples compared to that in NP samples (see Section 4.4.1.1)

miRNA	Expression in OvES, ES and NE samples compared to that in NP samples
hsa-miR-631	Up
hsa-miR-635	Up

TABLE 9-39

Table showing the results for EBV PCR from patient peripheral blood lymphocytes (see Section 4.5.2.1)

Case	Control	Phase of menstrual cycle	Coding	DNA ng/microl	260/280	260/230	PCR
	S Control	Follicular	503819	38.00	1.88	2.21	0
	S Control	Follicular	2573709	27.70	1.92	1.62	0
	S Control	Luteal	6371846	49.30	1.95	2.44	0
	S Control	Luteal	2839865	44.40	1.87	2.31	0
	S Control	Luteal	6471336	63.70	2.00	2.30	0
	S Control	Luteal	1624876	87.90	1.92	2.28	0
	S Control	Follicular	3140020	74.00	1.90	2.29	0
	S Control	Follicular	1872461	43.10	1.99	2.28	0
	Control	Follicular	1577512	51.20	1.95	2.35	45
	Control	Follicular	7891234	31.50	2.12	1.94	82
	Control	Luteal	9155193	49.60	1.92	2.29	118
	Control	Luteal	9123853	58.30	1.97	2.23	162
	Control		7891234	31.50	2.12	1.94	82
Case		Follicular	1602619	61.70	1.94	2.09	0
Case		Follicular	6170020	32.60	1.74	0.27	1,041
Case		Follicular	9066819	33.00	1.73	1.80	469
Case		Follicular	227536	72.00	1.89	1.96	35
Case		Follicular	316919	91.70	1.88	1.77	0
Case		Follicular	5938026	9.10	1.72	0.76	76
Case		Follicular	588546	63.40	1.90	1.93	1,843
Case		Follicular	8413629	192.00	1.86	1.77	0
Case		Follicular	8947629	11.80	2.02	1.52	0
Case		Follicular	811109	54.90	2.01	2.11	6,594
Case		Follicular	6707519	30.00	2.01	1.53	0
Case		Follicular	8417619	39.70	1.95	0.81	51
Case		Follicular	3691029	21.00	2.21	2.80	59
Case Ov		Follicular	8973029	26.70	2.17	2.55	3,014
Case Ov		Follicular	8714246	33.10	1.84	2.47	56
Case		Follicular	1802116	6.70	1.26	0.38	0
Case		Luteal	6095346	83.00	1.85	2.10	0
Case		Luteal	439356	5.80	2.01	0.35	0
Case		Luteal	3677410	28.80	1.85	1.71	0
Case		Luteal	4506746	61.30	1.99	2.45	51

Case	Luteal	3850536	50.00	1.77	1.66	0
Case Ov	Luteal	7036506	20.10	2.27	2.35	0
Case Ov	Luteal	5044706	57.40	1.98	0.93	76
Case	Mid Cycle	2183016	71.00	1.91	0.68	0
Case	Luteal	2207656	333.80	1.87	1.48	147
Case	Mid Cycle	6220521	14.20	1.86	1.05	76
Case	Mid Cycle	1546126	10.40	1.67	0.96	0
Case	Mid Cycle	2487156	27.50	1.96	2.27	64

Bibliography

1. Dhillon AS, Hagan S, Rath O, Kolch W. MAP kinase signalling pathways in cancer. *Oncogene*. 2007;26(22):3279-3290.
2. Bieging KT, Mello SS, Attardi LD. Unravelling mechanisms of p53-mediated tumour suppression. *Nat Rev Cancer*. 2014;14(5):359-370.
3. Strathy JH, Molgaard CA, Coulam CB, Melton LJ, 3rd. Endometriosis and infertility: a laparoscopic study of endometriosis among fertile and infertile women. *Fertil Steril*. 1982;38(6):667-672.
4. Nnoaham KE, Hummelshoj L, Webster P, et al. Impact of endometriosis on quality of life and work productivity: a multicenter study across ten countries. *Fertil Steril*. 2011;96(2):366-373 e368.
5. Hadfield R, Mardon H, Barlow D, Kennedy S. Delay in the diagnosis of endometriosis: a survey of women from the USA and the UK. *Hum Reprod*. 1996;11(4):878-880.
6. centre Er. Understanding endometriosis: past present and future. The National women's health information council; 2005.
7. Nnoaham KE, Sivananthan S, Hummelshoj L, et al. Session 05: Endometriosis: Impact, Diagnosis and Surgery / O-021 Global study of women's health: a multi-centre study of the global impact of endometriosis / O-022 Evaluation of 28 different plasma biomarkers for potential non-invasive diagnosis of endometriosis / O-023 Complete surgical removal of minimal and mild endometriosis improves outcome of subsequent assisted reproduction treatment / O-024 Laparoscopic nerve sparing surgery of deep infiltrating endometriosis; description of the technique, patient outcome and revue of the literature / O-025 Endometrioma-related damage to ovarian reserve: insights from IVF cycles / O-026 The impact of endometriosis on cancer survival. *Human Reproduction*. 2010;25(suppl 1):i9-i11.
8. Augoulea A, Mastorakos G, Lambrinoudaki I, Christodoulakos G, Creatsas G. The role of the oxidative-stress in the endometriosis-related infertility. *Gynecol Endocrinol*. 2009;25(2):75-81.
9. Missmer SA, Cramer DW. The epidemiology of endometriosis. *Obstet Gynecol Clin North Am*. 2003;30(1):1-19, vii.
10. Moen MH, Schei B. Epidemiology of endometriosis in a Norwegian county. *Acta Obstet Gynecol Scand*. 1997;76(6):559-562.
11. Vercellini P, Fedele L, Aimi G, Pietropaolo G, Consonni D, Crosignani PG. Association between endometriosis stage, lesion type, patient characteristics and severity of pelvic pain symptoms: a multivariate analysis of over 1000 patients. *Hum Reprod*. 2007;22(1):266-271.
12. Huang H, Li C, Zarogoulidis P, et al. Endometriosis of the lung: report of a case and literature review. *Eur J Med Res*. 2013;18:13.
13. Kazakov DV, Ondic O, Zamecnik M, et al. Morphological variations of scar-related and spontaneous endometriosis of the skin and superficial soft tissue: a study of 71 cases with emphasis on atypical features and types of mullerian differentiations. *J Am Acad Dermatol*. 2007;57(1):134-146.
14. Risk factors for pelvic endometriosis in women with pelvic pain or infertility. Gruppo Italiano per lo Studio dell' endometriosi. *Eur J Obstet Gynecol Reprod Biol*. 1999;83(2):195-199.
15. Missmer SA, Hankinson SE, Spiegelman D, Barbieri RL, Michels KB, Hunter DJ. In utero exposures and the incidence of endometriosis. *Fertil Steril*. 2004;82(6):1501-1508.
16. Parazzini F, Ferraroni M, Fedele L, Bocciolone L, Rubessa S, Riccardi A. Pelvic endometriosis: reproductive and menstrual risk factors at different stages in Lombardy, northern Italy. *J Epidemiol Community Health*. 1995;49(1):61-64.
17. Missmer SA, Hankinson SE, Spiegelman D, et al. Reproductive history and endometriosis among premenopausal women. *Obstet Gynecol*. 2004;104(5 Pt 1):965-974.
18. Moen MH, Magnus P. The familial risk of endometriosis. *Acta Obstet Gynecol Scand*. 1993;72(7):560-564.

19. Moen MH. Endometriosis in monozygotic twins. *Acta Obstet Gynecol Scand*. 1994;73(1):59-62.
20. Vessey MP, Villard-Mackintosh L, Painter R. Epidemiology of endometriosis in women attending family planning clinics. *BMJ*. 1993;306(6871):182-184.
21. Vitonis AF, Hankinson SE, Hornstein MD, Missmer SA. Adult physical activity and endometriosis risk. *Epidemiology*. 2010;21(1):16-23.
22. Sangi-Haghpeykar H, Poindexter AN, 3rd. Epidemiology of endometriosis among parous women. *Obstet Gynecol*. 1995;85(6):983-992.
23. Koninckx PR, Braet P, Kennedy SH, Barlow DH. Dioxin pollution and endometriosis in Belgium. *Hum Reprod*. 1994;9(6):1001-1002.
24. Sinaii N, Cleary SD, Ballweg ML, Nieman LK, Stratton P. High rates of autoimmune and endocrine disorders, fibromyalgia, chronic fatigue syndrome and atopic diseases among women with endometriosis: a survey analysis. *Hum Reprod*. 2002;17(10):2715-2724.
25. Matalliotakis I, Cakmak H, Fragouli Y, Zervoudis S, Neonaki M, Arici A. Association of endometriosis with family history of non-Hodgkin's lymphoma: presentation of 10 cases. *J BUON*. 2009;14(4):699-701.
26. Kvaskoff M, Mesrine S, Clavel-Chapelon F, Boutron-Ruault MC. Endometriosis risk in relation to naevi, freckles and skin sensitivity to sun exposure: the French E3N cohort. *Int J Epidemiol*. 2009;38(4):1143-1153.
27. Hornstein MD, Thomas PP, Sober AJ, Wyshak G, Albright NL, Frisch RE. Association between endometriosis, dysplastic naevi and history of melanoma in women of reproductive age. *Hum Reprod*. 1997;12(1):143-145.
28. Tesone M, Bilotas M, Baranao RI, Meresman G. The role of GnRH analogues in endometriosis-associated apoptosis and angiogenesis. *Gynecol Obstet Invest*. 2008;66 Suppl 1:10-18.
29. May K, Becker CM. Endometriosis and angiogenesis. *Minerva Ginecol*. 2008;60(3):245-254.
30. Laschke MW, Menger MD. In vitro and in vivo approaches to study angiogenesis in the pathophysiology and therapy of endometriosis. *Hum Reprod Update*. 2007;13(4):331-342.
31. Kennedy S, Bergqvist A, Chapron C, et al. ESHRE guideline for the diagnosis and treatment of endometriosis. *Hum Reprod*. 2005;20(10):2698-2704.
32. Lin YJ, Lai MD, Lei HY, Wing LY. Neutrophils and macrophages promote angiogenesis in the early stage of endometriosis in a mouse model. *Endocrinology*. 2006;147(3):1278-1286.
33. Burlev VA, Il'yasova NA, Dubinskaya ED. Proliferative activity of microvessels and angiogenesis in eutopic endometrium in patients with peritoneal endometriosis. *Bull Exp Biol Med*. 2005;139(6):727-731.
34. Buyalos RP, Agarwal SK. Endometriosis-associated infertility. *Curr Opin Obstet Gynecol*. 2000;12(5):377-381.
35. DC S. Disputatio Inauguralis Medica de Ulceribus Uteri. University of Jena, Literis Krebsianis: University of Jena; 1690.
36. Lundeberg T. Is there a role for acupuncture in endometriosis pain, or 'endometrialgia'? . In: Lund FfAaABTMSHSSI ed. Depanmcni of Pbysiokigy and Pharmacology Karolinska Institute! Stockholm, Sweden Depanmcni of Pbysiokigy and Pharmacology Karolinska Institute! Stockholm, .Sweden 2008.
37. RE B. Emergence of endometriosis in North America: a study in the history of ideas. Faculty of the graduate school of the Universty of Buffalo. New York: State University of New York; 2008:109-113.
38. C R. Uber Uterusdrusen-Neubildung in Uterus- und Ovarial- Sarcomen. *Zeitschr gesellschaft der Aerzte in Wien*. 1860;16:577-581.
39. F VR. Die Adenomyomata und Cystadenomata der Uterus und Tubenwandung: Ihre Abkunft von Resten des Wolffischen Koerpers. August Hirschwald Verlag. Berlin; 1896.
40. Cullen TS. Adenomyoma of the Uterus. WB Saunders. Philadelphia; 1908.

41. Sampson JA. Perforating haemorrhagic (chocolate) cysts of Ovary: their importance and especially their relation to pelvic adenomas of endometriotic type ('adenomyoma' of the Uterus, rectovaginal septum,sigmoid,etc.). *Arch Surg*. 1921;3:245-261.
42. Sampson JA. Metastatic or Embolic Endometriosis, due to the Menstrual Dissemination of Endometrial Tissue into the Venous Circulation. *Am J Pathol*. 1927;3(2):93-110 143.
43. Benagiano G, Brosens I. The history of endometriosis: identifying the disease. *Hum Reprod*. 1991;6(7):963-968.
44. Ota H, Igarashi S, Tanaka T. Expression of gamma delta T cells and adhesion molecules in endometriotic tissue in patients with endometriosis and adenomyosis. *Am J Reprod Immunol*. 1996;35(5):477-482.
45. Bird CC, Willis RA. The production of smooth muscle by the endometrial stroma of the adult human uterus. *J Pathol Bacteriol*. 1965;90(1):75-81.
46. Winkel CA. Evaluation and management of women with endometriosis. *Obstet Gynecol*. 2003;102(2):397-408.
47. Gould D. Endometriosis. *Nurs Stand*. 2003;17(27):47-53; quiz 54-45.
48. Gambone JC, Mittman BS, Munro MG, Scialli AR, Winkel CA. Consensus statement for the management of chronic pelvic pain and endometriosis: proceedings of an expert-panel consensus process. *Fertil Steril*. 2002;78(5):961-972.
49. Nap AW, Griffioen AW, Dunselman GA, et al. Antiangiogenesis therapy for endometriosis. *J Clin Endocrinol Metab*. 2004;89(3):1089-1095.
50. Propst AM, Laufer MR. Endometriosis in adolescents. Incidence, diagnosis and treatment. *J Reprod Med*. 1999;44(9):751-758.
51. Koninckx PR, Meuleman C, Oosterlynck D, Cornillie FJ. Diagnosis of deep endometriosis by clinical examination during menstruation and plasma CA-125 concentration. *Fertil Steril*. 1996;65(2):280-287.
52. Jiang W, Roma AA, Lai K, Carver P, Xiao SY, Liu X. Endometriosis involving the mucosa of the intestinal tract: a clinicopathologic study of 15 cases. *Mod Pathol*. 2013;26(9):1270-1278.
53. Vilos GA, Hollett-Caines J, Abu-Rafea B, Ahmad R, Mazurek MF. Resolution of catamenial epilepsy after goserelin therapy and oophorectomy: case report of presumed cerebral endometriosis. *J Minim Invasive Gynecol*. 2011;18(1):128-130.
54. Adamson GD. Endometriosis classification: an update. *Curr Opin Obstet Gynecol*;23(4):213-220.
55. Beecham CT. Classification of endometriosis. *Obstet Gynecol*. 1966;28(3):437.
56. Acosta AA, Buttram VC, Jr., Besch PK, Malinak LR, Franklin RR, Vanderheyden JD. A proposed classification of pelvic endometriosis. *Obstet Gynecol*. 1973;42(1):19-25.
57. Buttram VC, Jr. An expanded classification of endometriosis. *Fertil Steril*. 1978;30(2):240-242.
58. Revised American Society for Reproductive Medicine classification of endometriosis: 1996. *Fertil Steril*. 1997;67(5):817-821.
59. Chapron C, Fauconnier A, Vieira M, et al. Anatomical distribution of deeply infiltrating endometriosis: surgical implications and proposition for a classification. *Hum Reprod*. 2003;18(1):157-161.
60. D'Hooghe TM, Debrock S, Hill JA, Meuleman C. Endometriosis and subfertility: is the relationship resolved? *Semin Reprod Med*. 2003;21(2):243-254.
61. Koninckx PR, Meuleman C, Demeyere S, Lesaffre E, Cornillie FJ. Suggestive evidence that pelvic endometriosis is a progressive disease, whereas deeply infiltrating endometriosis is associated with pelvic pain. *Fertil Steril*. 1991;55(4):759-765.
62. Porpora MG, Koninckx PR, Piazze J, Natili M, Colagrande S, Cosmi EV. Correlation between endometriosis and pelvic pain. *J Am Assoc Gynecol Laparosc*. 1999;6(4):429-434.
63. Chapron C, Fauconnier A, Dubuisson JB, Barakat H, Vieira M, Breart G. Deep infiltrating endometriosis: relation between severity of dysmenorrhoea and extent of disease. *Hum Reprod*. 2003;18(4):760-766.

64. Classification of endometriosis. The American Fertility Society. *Fertil Steril*. 1979;32(6):633-634.
65. Guzick DS, Bross DS, Rock JA. Assessing the efficacy of The American Fertility Society's classification of endometriosis: application of a dose-response methodology. *Fertil Steril*. 1982;38(2):171-176.
66. Adamson GD, Frison L, Lamb EJ. Endometriosis: studies of a method for the design of a surgical staging system. *Fertil Steril*. 1982;38(6):659-666.
67. Buttram VC, Jr. Evolution of the revised American Fertility Society classification of endometriosis. *Fertil Steril*. 1985;43(3):347-350.
68. Candiani GB. The classification of endometriosis: historical evolution, critical review and present state of the art. *Acta Eur Fertil*. 1986;17(2):85-92.
69. Canis M, Pouly JL, Wattiez A, Manhes H, Mage G, Bruhat MA. Incidence of bilateral adnexal disease in severe endometriosis (revised American Fertility Society [AFS], stage IV): should a stage V be included in the AFS classification? *Fertil Steril*. 1992;57(3):691-692.
70. Pal L, Shifren JL, Isaacson KB, Chang Y, Leykin L, Toth TL. Impact of varying stages of endometriosis on the outcome of in vitro fertilization-embryo transfer. *J Assist Reprod Genet*. 1998;15(1):27-31.
71. Redwine DB. Age-related evolution in color appearance of endometriosis. *Fertil Steril*. 1987;48(6):1062-1063.
72. Redwine DB. The distribution of endometriosis in the pelvis by age groups and fertility. *Fertil Steril*. 1987;47(1):173-175.
73. Canis M, Bouquet De Jolinieres J, Wattiez A, et al. Classification of endometriosis. *Baillieres Clin Obstet Gynaecol*. 1993;7(4):759-774.
74. Hornstein MD, Gleason RE, Orav J, et al. The reproducibility of the revised American Fertility Society classification of endometriosis. *Fertil Steril*. 1993;59(5):1015-1021.
75. Rock JA. The revised American Fertility Society classification of endometriosis: reproducibility of scoring. ZOLADEX Endometriosis Study Group. *Fertil Steril*. 1995;63(5):1108-1110.
76. Adamson GD, Hurd SJ, Pasta DJ, Rodriguez BD. Laparoscopic endometriosis treatment: is it better? *Fertil Steril*. 1993;59(1):35-44.
77. Vercellini P, Trespidi L, De Giorgi O, Cortesi I, Parazzini F, Crosignani PG. Endometriosis and pelvic pain: relation to disease stage and localization. *Fertil Steril*. 1996;65(2):299-304.
78. Fedele L, Bianchi S, Bocciolone L, Di Nola G, Parazzini F. Pain symptoms associated with endometriosis. *Obstet Gynecol*. 1992;79(5 (Pt 1)):767-769.
79. Guzick DS, Silliman NP, Adamson GD, et al. Prediction of pregnancy in infertile women based on the American Society for Reproductive Medicine's revised classification of endometriosis. *Fertil Steril*. 1997;67(5):822-829.
80. Management of endometriosis in the presence of pelvic pain. The American Fertility Society. *Fertil Steril*. 1993;60(6):952-955.
81. Martin DC, Batt RE. Retrocervical, retrovaginal pouch, and rectovaginal septum endometriosis. *J Am Assoc Gynecol Laparosc*. 2001;8(1):12-17.
82. Signorile PG, Baldi F, Bussani R, D'Armiento M, De Falco M, Baldi A. Ectopic endometrium in human foetuses is a common event and sustains the theory of mullerianosis in the pathogenesis of endometriosis, a disease that predisposes to cancer. *J Exp Clin Cancer Res*. 2009;28:49.
83. Sanfilippo JS, Wakim NG, Schikler KN, Yussman MA. Endometriosis in association with uterine anomaly. *Am J Obstet Gynecol*. 1986;154(1):39-43.
84. Simpson JL, Bischoff FZ, Kamat A, Buster JE, Carson SA. Genetics of endometriosis. *Obstet Gynecol Clin North Am*. 2003;30(1):21-40, vii.
85. Levander G, Normann P. The pathogenesis of endometriosis; an experimental study. *Acta Obstet Gynecol Scand*. 1955;34(4):366-398.

86. Javert CT. Pathogenesis of endometriosis based on endometrial homeoplasia, direct extension, exfoliation and implantation, lymphatic and hematogenous metastasis, including five case reports of endometrial tissue in pelvic lymph nodes. *Cancer*. 1949;2(3):399-410.
87. Gargett CE. Uterine stem cells: what is the evidence? *Hum Reprod Update*. 2007;13(1):87-101.
88. Donnez J, Squifflet J, Casanas-Roux F, Pirard C, Jadoul P, Van Langendonckt A. Typical and subtle atypical presentations of endometriosis. *Obstet Gynecol Clin North Am*. 2003;30(1):83-93, viii.
89. Garai J, Molnar V, Varga T, Koppan M, Torok A, Bodis J. Endometriosis: harmful survival of an ectopic tissue. *Front Biosci*. 2006;11:595-619.
90. Noble LS, Simpson ER, Johns A, Bulun SE. Aromatase expression in endometriosis. *J Clin Endocrinol Metab*. 1996;81(1):174-179.
91. Taylor RN, Yu J, Torres PB, et al. Mechanistic and therapeutic implications of angiogenesis in endometriosis. *Reprod Sci*. 2009;16(2):140-146.
92. Oosterlynck DJ, Cornillie FJ, Waer M, Vandeputte M, Koninckx PR. Women with endometriosis show a defect in natural killer activity resulting in a decreased cytotoxicity to autologous endometrium. *Fertil Steril*. 1991;56(1):45-51.
93. Vinatier D, Orazi G, Cosson M, Dufour P. Theories of endometriosis. *Eur J Obstet Gynecol Reprod Biol*. 2001;96(1):21-34.
94. Tabibzadeh S, Kong QF, Satyaswaroop PG, Babaknia A. Heat shock proteins in human endometrium throughout the menstrual cycle. *Hum Reprod*. 1996;11(3):633-640.
95. Lessey BA, Castelbaum AJ, Sawin SW, et al. Aberrant integrin expression in the endometrium of women with endometriosis. *J Clin Endocrinol Metab*. 1994;79(2):643-649.
96. Sharpe-Timms KL, Keisler LW, McIntush EW, Keisler DH. Tissue inhibitor of metalloproteinase-1 concentrations are attenuated in peritoneal fluid and sera of women with endometriosis and restored in sera by gonadotropin-releasing hormone agonist therapy. *Fertil Steril*. 1998;69(6):1128-1134.
97. McLaren J, Dealtry G, Prentice A, Charnock-Jones DS, Smith SK. Decreased levels of the potent regulator of monocyte/macrophage activation, interleukin-13, in the peritoneal fluid of patients with endometriosis. *Hum Reprod*. 1997;12(6):1307-1310.
98. van der Linden PJ. Theories on the pathogenesis of endometriosis. *Hum Reprod*. 1996;11 Suppl 3:53-65.
99. Fujii S. Secondary mullerian system and endometriosis. *Am J Obstet Gynecol*. 1991;165(1):219-225.
100. Cramer DW, Wilson E, Stillman RJ, et al. The relation of endometriosis to menstrual characteristics, smoking, and exercise. *JAMA*. 1986;255(14):1904-1908.
101. Kruitwagen RF, Poels LG, Willemsen WN, de Ronde IJ, Jap PH, Rolland R. Endometrial epithelial cells in peritoneal fluid during the early follicular phase. *Fertil Steril*. 1991;55(2):297-303.
102. Koks CA, Dunselman GA, de Goeij AF, Arends JW, Evers JL. Evaluation of a menstrual cup to collect shed endometrium for in vitro studies. *Fertil Steril*. 1997;68(3):560-564.
103. Halme J, Hammond MG, Hulka JF, Raj SG, Talbert LM. Retrograde menstruation in healthy women and in patients with endometriosis. *Obstet Gynecol*. 1984;64(2):151-154.
104. Szlachter NB, Moskowitz J, Bigelow B, Weiss G. Iatrogenic endometriosis: substantiation of the Sampson hypothesis. *Obstet Gynecol*. 1980;55(3 Suppl):52S-53S.
105. Jenkins S. Endometriosis: pathogenic implications of the anatomic distribution. *obstet Ginecol*. 1968;67:355-358.
106. Vercellini P, Abbiati A, Vigano P, et al. Asymmetry in distribution of diaphragmatic endometriotic lesions: evidence in favour of the menstrual reflux theory. *Hum Reprod*. 2007;22(9):2359-2367.
107. Al-Fozan H, Tulandi T. Left lateral predisposition of endometriosis and endometrioma. *Obstet Gynecol*. 2003;101(1):164-166.
108. Ridley A. The histogenesis of endometriosis. *obstet Ginecol*. 1968;23:1-35.

109. Lauchlan SC. The secondary Mullerian system. *Obstet Gynecol Surv*. 1972;27(3):133-146.
110. Batt RE, Smith RA, Buck Louis GM, et al. Mullerianosis. *Histol Histopathol*. 2007;22(10):1161-1166.
111. Nawroth F, Rahimi G, Nawroth C, Foth D, Ludwig M, Schmidt T. Is there an association between septate uterus and endometriosis? *Hum Reprod*. 2006;21(2):542-544.
112. Mok-Lin EY, Wolfberg A, Hollinquist H, Laufer MR. Endometriosis in a patient with Mayer-Rokitansky-Kuster-Hauser syndrome and complete uterine agenesis: evidence to support the theory of coelomic metaplasia. *J Pediatr Adolesc Gynecol*. 2010;23(1):e35-37.
113. Klattig J, Englert C. The Mullerian duct: recent insights into its development and regression. *Sex Dev*. 2007;1(5):271-278.
114. Zheng W, Li N, Wang J, et al. Initial endometriosis showing direct morphologic evidence of metaplasia in the pathogenesis of ovarian endometriosis. *Int J Gynecol Pathol*. 2005;24(2):164-172.
115. Novak E. Pelvic Endometriosis. Spontaneous rupture of Endometrial cysts, with a report of Three cases. *Am J Obstet Gynecol*. 1931;22:826-837.
116. Nakayama K, Masuzawa H, Li SF, et al. Immunohistochemical analysis of the peritoneum adjacent to endometriotic lesions using antibodies for Ber-EP4 antigen, estrogen receptors, and progesterone receptors: implication of peritoneal metaplasia in the pathogenesis of endometriosis. *Int J Gynecol Pathol*. 1994;13(4):348-358.
117. Suginami H. A reappraisal of the coelomic metaplasia theory by reviewing endometriosis occurring in unusual sites and instances. *Am J Obstet Gynecol*. 1991;165(1):214-218.
118. Decenzo JA. Iatrogenic endometriosis caused by uterine morcellation during a supracervical hysterectomy. *Obstet Gynecol*. 2004;103(3):583; author reply 583-584.
119. Brown RL. Iatrogenic endometriosis caused by uterine morcellation during a supracervical hysterectomy. *Obstet Gynecol*. 2004;103(3):583; author reply 583-584.
120. Sepilian V, Della Badia C. Iatrogenic endometriosis caused by uterine morcellation during a supracervical hysterectomy. *Obstet Gynecol*. 2003;102(5 Pt 2):1125-1127.
121. Chi T, Yang CC. Iatrogenic abdominal scar endometriosis: a case report. *Zhonghua Yi Xue Za Zhi (Taipei)*. 1999;62(4):236-238.
122. Akbulut S, Sevinc MM, Bakir S, Cakabay B, Sezgin A. Scar endometriosis in the abdominal wall: a predictable condition for experienced surgeons. *Acta Chir Belg*;110(3):303-307.
123. Barlas D, Bozkurt S, Kaya MA, Celik F. [Scar endometriosis in the rectus abdominis muscle]. *Ulus Travma Acil Cerrahi Derg*;16(4):371-372.
124. Brouha PC, de Lange DW, Broekhuysen CL, Scholten E, Schipper ME, Kon M. [Iatrogenic cicatricial endometriosis]. *Ned Tijdschr Geneeskd*. 1997;141(15):740-743.
125. Medeiros FC, Cavalcante DI, Medeiros MA, Eleuterio J, Jr. Fine-needle aspiration cytology of scar endometriosis: study of seven cases and literature review. *Diagn Cytopathol*;39(1):18-21.
126. Goel P, Devi L, Tandon R, Saha PK, Dalal A. Scar endometriosis - A series of six patients. *Int J Surg*;9(1):39-40.
127. Merrill JA. Endometrial Induction of Endometriosis across millipore filters. *Am J Obstet Gynecol*. 1996;94:780-789.
128. Kennedy S, Mardon H, Barlow D. Familial endometriosis. *Journal of Assisted Reproduction and Genetics*. 1995;12(1):32-34.
129. Lamb K, Hoffmann RG, Nichols TR. Family trait analysis: a case-control study of 43 women with endometriosis and their best friends. *Am J Obstet Gynecol*. 1986;154(3):596-601.
130. Crosignani PG, De Cecco L, Gastaldi A, et al. Leuprolide in a 3-monthly versus a monthly depot formulation for the treatment of symptomatic endometriosis: a pilot study. *Hum Reprod*. 1996;11(12):2732-2735.

131. Semino C, Semino A, Pietra G, et al. Role of major histocompatibility complex class I expression and natural killer-like T cells in the genetic control of endometriosis. *Fertil Steril*. 1995;64(5):909-916.
132. Venturini PL, Semino A, De Cecco L. The biological basis of medical treatment of endometriosis. *Gynecol Endocrinol*. 1995;9(3):259-266.
133. Semino G, Alessandri A. [Statistical contribution to the clinical study of endometriosis]. *Pathologica*. 1961;53:125-139.
134. Kitawaki J, Obayashi H, Kado N, et al. Association of HLA class I and class II alleles with susceptibility to endometriosis. *Hum Immunol*. 2002;63(11):1033-1038.
135. Simoens S, Dunselman G, Dirksen C, et al. The burden of endometriosis: costs and quality of life of women with endometriosis and treated in referral centres. *Hum Reprod*;27(5):1292-1299.
136. Conroy SE, Sasieni PD, Amin V, et al. Antibodies to heat-shock protein 27 are associated with improved survival in patients with breast cancer. *Br J Cancer*. 1998;77(11):1875-1879.
137. Gurbuxani S, Bruey JM, Fromentin A, et al. Selective depletion of inducible HSP70 enhances immunogenicity of rat colon cancer cells. *Oncogene*. 2001;20(51):7478-7485.
138. Garrido C, Fromentin A, Bonnotte B, et al. Heat shock protein 27 enhances the tumorigenicity of immunogenic rat colon carcinoma cell clones. *Cancer Res*. 1998;58(23):5495-5499.
139. Protti MP, Heltai S, Bellone M, Ferrarini M, Manfredi AA, Rugarli C. Constitutive expression of the heat shock protein 72 kDa in human melanoma cells. *Cancer Lett*. 1994;85(2):211-216.
140. Udelsman R, Blake MJ, Stagg CA, Holbrook NJ. Endocrine control of stress-induced heat shock protein 70 expression in vivo. *Surgery*. 1994;115(5):611-616.
141. Kanerud L, Scheynius A, Nord CE, Hafstrom I. Effect of sulphasalazine on gastrointestinal microflora and on mucosal heat shock protein expression in patients with rheumatoid arthritis. *Br J Rheumatol*. 1994;33(11):1039-1048.
142. Stratton P, Winkel CA, Sinaii N, Merino MJ, Zimmer C, Nieman LK. Location, color, size, depth, and volume may predict endometriosis in lesions resected at surgery. *Fertil Steril*. 2002;78(4):743-749.
143. Soliman AS, Levin B, El-Badawy S, et al. Planning cancer prevention strategies based on epidemiologic characteristics: an Egyptian example. *Public Health Rev*. 2001;29(1):1-11.
144. Badawy SZ, Etman A, Singh M, Murphy K, Mayelli T, Philadelphia M. Uterine artery embolization: the role in obstetrics and gynecology. *Clin Imaging*. 2001;25(4):288-295.
145. Morgan CJ, Badawy AA. Alcohol-induced euphoria: exclusion of serotonin. *Alcohol Alcohol*. 2001;36(1):22-25.
146. Badawy AA. Happy New Year, congratulations, thank you and welcome. *Alcohol Alcohol*. 2001;36(1):1.
147. Acien P, Quereda F, Campos A, Gomez-Torres MJ, Velasco I, Gutierrez M. Use of intraperitoneal interferon alpha-2b therapy after conservative surgery for endometriosis and postoperative medical treatment with depot gonadotropin-releasing hormone analog: a randomized clinical trial. *Fertil Steril*. 2002;78(4):705-711.
148. Acien P. Obstructive mullerian anomalies. *Am J Obstet Gynecol*. 2002;186(4):854.
149. Takeuchi S, Minoura H, Shibahara T, Shen X, Futamura N, Toyoda N. In vitro fertilization and intracytoplasmic sperm injection for couples with unexplained infertility after failed direct intraperitoneal insemination. *J Assist Reprod Genet*. 2000;17(9):515-520.
150. Gomez-Torres MJ, Acien P, Campos A, Velasco I. Embryotoxicity of peritoneal fluid in women with endometriosis. Its relation with cytokines and lymphocyte populations. *Hum Reprod*. 2002;17(3):777-781.
151. Tollner B, Roth J, Storr B, Martin D, Voigt K, Zeisberger E. The role of tumor necrosis factor (TNF) in the febrile and metabolic responses of rats to intraperitoneal injection of a high dose of lipopolysaccharide. *Pflugers Arch*. 2000;440(6):925-932.

152. Yim HJ, Robinson DL, White ML, et al. Dissociation between the time course of ethanol and extracellular dopamine concentrations in the nucleus accumbens after a single intraperitoneal injection. *Alcohol Clin Exp Res*. 2000;24(6):781-788.
153. Ali AFM, Fateen B, Ezzet A, Badawy H, Ramadan A, El-tobge A. Laparoscopic intraperitoneal injection of human interferon-Î±2b in the treatment of pelvic endometriosis: a new modality. *Obstetrics & Gynecology*. 2000;95(4, Supplement 1):S47-S48.
154. Birgersdotter A, Baumforth KR, Wei W, et al. Connective tissue growth factor is expressed in malignant cells of Hodgkin lymphoma but not in other mature B-cell lymphomas. *Am J Clin Pathol*;133(2):271-280.
155. Walboomers JM, Jacobs MV, Manos MM, et al. Human papillomavirus is a necessary cause of invasive cervical cancer worldwide. *J Pathol*. 1999;189(1):12-19.
156. William C. McBee, Amy S. Gardiner, Robert P. Edwards, et al. MicroRNA Analysis in Human Papillomavirus (HPV)-Associated Cervical Neoplasia and Cancer
Journal of Carcinogenesis and Mutagenesis. 2011;1:114

157. de Villiers EM, Fauquet C, Broker TR, Bernard HU, zur Hausen H. Classification of papillomaviruses. *Virology*. 2004;324(1):17-27.
158. Ho GY, Bierman R, Beardsley L, Chang CJ, Burk RD. Natural history of cervicovaginal papillomavirus infection in young women. *N Engl J Med*. 1998;338(7):423-428.
159. Oppelt P, Renner SP, Strick R, et al. Correlation of high-risk human papilloma viruses but not of herpes viruses or Chlamydia trachomatis with endometriosis lesions. *Fertil Steril*;93(6):1778-1786.
160. Volinia S, Calin GA, Liu CG, et al. A microRNA expression signature of human solid tumors defines cancer gene targets. *Proc Natl Acad Sci U S A*. 2006;103(7):2257-2261.
161. Zhang L, Huang J, Yang N, et al. microRNAs exhibit high frequency genomic alterations in human cancer. *Proc Natl Acad Sci U S A*. 2006;103(24):9136-9141.
162. Vinatier D, Dufour P, Oosterlynck D. Immunological aspects of endometriosis. *Hum Reprod Update*. 1996;2(5):371-384.
163. Shamji MF, Maziak DE, Shamji FM, Matzinger FR, Perkins DG. Surgical staple metalloptysis after apical bullectomy: a reaction to bovine pericardium? *Ann Thorac Surg*. 2002;74(1):258-261.
164. Gati A, Guerra N, Giron-Michel J, et al. Tumor cells regulate the lytic activity of tumor-specific cytotoxic t lymphocytes by modulating the inhibitory natural killer receptor function. *Cancer Res*. 2001;61(8):3240-3244.
165. Binder RJ, Han DK, Srivastava PK. CD91: a receptor for heat shock protein gp96. *Nat Immunol*. 2000;1(2):151-155.
166. Doody AD, Kovalchin JT, Mihalyo MA, Hagymasi AT, Drake CG, Adler AJ. Glycoprotein 96 can chaperone both MHC class I- and class II-restricted epitopes for in vivo presentation, but selectively primes CD8+ T cell effector function. *J Immunol*. 2004;172(10):6087-6092.
167. Chishima F, Hayakawa S, Hirata Y, et al. Peritoneal and peripheral B-1-cell populations in patients with endometriosis. *J Obstet Gynaecol Res*. 2000;26(2):141-149.
168. Gupta S, Goldberg JM, Aziz N, Goldberg E, Krajcir N, Agarwal A. Pathogenic mechanisms in endometriosis-associated infertility. *Fertil Steril*. 2008;90(2):247-257.
169. Ota H, Igarashi S. Expression of major histocompatibility complex class II antigen in endometriotic tissue in patients with endometriosis and adenomyosis. *Fertil Steril*. 1993;60(5):834-838.
170. Prefumo F, Semino C, Melioli G, Venturini PL. A defective expression of ICAM-1 (CD54) on secretory endometrial cells is associated with endometriosis. *Immunol Lett*. 2002;80(1):49-53.
171. Vigano P, Gaffuri B, Somigliana E, Busacca M, Di Blasio AM, Vignali M. Expression of intercellular adhesion molecule (ICAM)-1 mRNA and protein is enhanced in endometriosis versus endometrial stromal cells in culture. *Mol Hum Reprod*. 1998;4(12):1150-1156.

172. Ehrnsperger M, Graber S, Gaestel M, Buchner J. Binding of non-native protein to Hsp25 during heat shock creates a reservoir of folding intermediates for reactivation. *EMBO J*. 1997;16(2):221-229.
173. Schmitt E, Gehrmann M, Brunet M, Multhoff G, Garrido C. Intracellular and extracellular functions of heat shock proteins: repercussions in cancer therapy. *J Leukoc Biol*. 2007;81(1):15-27.
174. Arnold-Schild D, Hanau D, Spehner D, et al. Cutting edge: receptor-mediated endocytosis of heat shock proteins by professional antigen-presenting cells. *J Immunol*. 1999;162(7):3757-3760.
175. Basu S, Binder RJ, Ramalingam T, Srivastava PK. CD91 is a common receptor for heat shock proteins gp96, hsp90, hsp70, and calreticulin. *Immunity*. 2001;14(3):303-313.
176. Sondermann H, Becker T, Mayhew M, Wieland F, Hartl FU. Characterization of a receptor for heat shock protein 70 on macrophages and monocytes. *Biol Chem*. 2000;381(12):1165-1174.
177. Schild H, Rammensee HG. gp96--the immune system's Swiss army knife. *Nat Immunol*. 2000;1(2):100-101.
178. Jaattela M. Over-expression of hsp70 confers tumorigenicity to mouse fibrosarcoma cells. *Int J Cancer*. 1995;60(5):689-693.
179. Lemieux P, Oesterreich S, Lawrence JA, et al. The small heat shock protein hsp27 increases invasiveness but decreases motility of breast cancer cells. *Invasion Metastasis*. 1997;17(3):113-123.
180. Ota H, Igarashi S, Hatazawa J, Tanaka T. Distribution of heat shock proteins in eutopic and ectopic endometrium in endometriosis and adenomyosis. *Fertil Steril*. 1997;68(1):23-28.
181. Nip MM, Miller D, Taylor PV, Gannon MJ, Hancock KW. Expression of heat shock protein 70 kDa in human endometrium of normal and infertile women. *Hum Reprod*. 1994;9(7):1253-1256.
182. Nanbu K, Konishi I, Mandai M, et al. Prognostic significance of heat shock proteins HSP70 and HSP90 in endometrial carcinomas. *Cancer Detect Prev*. 1998;22(6):549-555.
183. Lambrinoudaki IV, Augoulea A, Christodoulakos GE, et al. Measurable serum markers of oxidative stress response in women with endometriosis. *Fertil Steril*. 2009;91(1):46-50.
184. Khan KN, Kitajima M, Imamura T, et al. Toll-like receptor 4-mediated growth of endometriosis by human heat-shock protein 70. *Hum Reprod*. 2008;23(10):2210-2219.
185. Moretta A, Bottino C, Vitale M, et al. Activating receptors and coreceptors involved in human natural killer cell-mediated cytolysis. *Annu Rev Immunol*. 2001;19:197-223.
186. Gagne D, Rivard M, Page M, Shazand K, Hugo P, Gosselin D. Blood leukocyte subsets are modulated in patients with endometriosis. *Fertil Steril*. 2003;80(1):43-53.
187. Hassa H, Tanir HM, Tekin B, Kirilmaz SD, Sahin Mutlu F. Cytokine and immune cell levels in peritoneal fluid and peripheral blood of women with early- and late-staged endometriosis. *Arch Gynecol Obstet*. 2009;279(6):891-895.
188. Gross C, Hansch D, Gastpar R, Multhoff G. Interaction of heat shock protein 70 peptide with NK cells involves the NK receptor CD94. *Biol Chem*. 2003;384(2):267-279.
189. Gross C, Schmidt-Wolf IG, Nagaraj S, et al. Heat shock protein 70-reactivity is associated with increased cell surface density of CD94/CD56 on primary natural killer cells. *Cell Stress Chaperones*. 2003;8(4):348-360.
190. Evers JL. Female subfertility. *Lancet*. 2002;360(9327):151-159.
191. Ozkan S, Murk W, Arici A. Endometriosis and infertility: epidemiology and evidence-based treatments. *Ann N Y Acad Sci*. 2008;1127:92-100.
192. Mahmood TA, Templeton A. Prevalence and genesis of endometriosis. *Hum Reprod*. 1991;6(4):544-549.
193. Hull MG, Glazener CM, Kelly NJ, et al. Population study of causes, treatment, and outcome of infertility. *Br Med J (Clin Res Ed)*. 1985;291(6510):1693-1697.
194. Guo SW, Wang Y. The prevalence of endometriosis in women with chronic pelvic pain. *Gynecol Obstet Invest*. 2006;62(3):121-130.

195. Meuleman C, Vandenabeele B, Fieuws S, Spiessens C, Timmerman D, D'Hooghe T. High prevalence of endometriosis in infertile women with normal ovulation and normospermic partners. *Fertil Steril*. 2009;92(1):68-74.
196. Ilangavan K, Kalu E. High prevalence of endometriosis in infertile women with normal ovulation and normospermic partners. *Fertil Steril*. 2010;93(3):e10; author reply e12.
197. Guo SW, Wang Y. Sources of heterogeneities in estimating the prevalence of endometriosis in infertile and previously fertile women. *Fertil Steril*. 2006;86(6):1584-1595.
198. infertility PCotASfRMEa. Endometriosis and infertility. *Fertil Steril*. 2004;82(suppl1):S40-45.
199. Waller KG, Lindsay P, Curtis P, Shaw RW. The prevalence of endometriosis in women with infertile partners. *Eur J Obstet Gynecol Reprod Biol*. 1993;48(2):135-139.
200. Arumugam K, Mahmood TA, Kong YF. The association of anovulation and endometriosis in the infertile female. *Aust N Z J Obstet Gynaecol*. 1989;29(3 Pt 2):350-351.
201. Soules MR, Makinak LR, Bury R, Poindexter A. Endometriosis and anovulation: a coexisting problem in the infertile female. *Am J Obstet Gynecol*. 1976;125(3):412-417.
202. Koninckx PR. Biases in the endometriosis literature. Illustrated by 20 years of endometriosis research in Leuven. *Eur J Obstet Gynecol Reprod Biol*. 1998;81(2):259-271.
203. Martin DC, Hubert GD, Vander Zwaag R, el-Zeky FA. Laparoscopic appearances of peritoneal endometriosis. *Fertil Steril*. 1989;51(1):63-67.
204. Arruda MS, Petta CA, Abrao MS, Benetti-Pinto CL. Time elapsed from onset of symptoms to diagnosis of endometriosis in a cohort study of Brazilian women. *Hum Reprod*. 2003;18(4):756-759.
205. Husby GK, Haugen RS, Moen MH. Diagnostic delay in women with pain and endometriosis. *Acta Obstet Gynecol Scand*. 2003;82(7):649-653.
206. McArthur JW, Ulfelder H. The effect of pregnancy upon endometriosis. *Obstet Gynecol Surv*. 1965;20(5):709-733.
207. D'Hooghe TM, Bambra CS, De Jonge I, Lauweryns JM, Raeymaekers BM, Koninckx PR. The effect of pregnancy on endometriosis in baboons (Papio anubis, Papio cynocephalus). *Arch Gynecol Obstet*. 1997;261(1):15-19.
208. Schenken RS, Williams RF, Hodgen GD. Effect of pregnancy on surgically induced endometriosis in cynomolgus monkeys. *Am J Obstet Gynecol*. 1987;157(6):1392-1396.
209. Barragan JC, Brotons J, Ruiz JA, Acien P. Experimentally induced endometriosis in rats: effect on fertility and the effects of pregnancy and lactation on the ectopic endometrial tissue. *Fertil Steril*. 1992;58(6):1215-1219.
210. Cornish J, Tan E, Teare J, et al. A meta-analysis on the influence of inflammatory bowel disease on pregnancy. *Gut*. 2007;56(6):830-837.
211. Skomsvoll JF, Ostensen M, Irgens LM, Baste V. Obstetrical and neonatal outcome in pregnant patients with rheumatic disease. *Scand J Rheumatol Suppl*. 1998;107:109-112.
212. Thomson F, Shanbhag S, Templeton A, Bhattacharya S. Obstetric outcome in women with subfertility. *BJOG*. 2005;112(5):632-637.
213. Brosens IA, Robertson WB, Dixon HG. The role of the spiral arteries in the pathogenesis of preeclampsia. *Obstet Gynecol Annu*. 1972;1:177-191.
214. Hadfield RM, Lain SJ, Raynes-Greenow CH, Morris JM, Roberts CL. Is there an association between endometriosis and the risk of pre-eclampsia? A population based study. *Hum Reprod*. 2009;24(9):2348-2352.
215. Fernando S, Breheny S, Jaques AM, Halliday JL, Baker G, Healy D. Preterm birth, ovarian endometriomata, and assisted reproduction technologies. *Fertil Steril*. 2009;91(2):325-330.
216. Stephansson O, Kieler H, Granath F, Falconer H. Endometriosis, assisted reproduction technology, and risk of adverse pregnancy outcome. *Hum Reprod*. 2009;24(9):2341-2347.
217. Karck U, Reister F, Schafer W, Zahradnik HP, Breckwoldt M. PGE2 and PGF2 alpha release by human peritoneal macrophages in endometriosis. *Prostaglandins*. 1996;51(1):49-60.

218. Ametzazurra A, Matorras R, Garcia-Velasco JA, et al. Endometrial fluid is a specific and non-invasive biological sample for protein biomarker identification in endometriosis. *Hum Reprod*. 2009;24(4):954-965.
219. Beier HM, Beier-Hellwig K. Molecular and cellular aspects of endometrial receptivity. *Hum Reprod Update*. 1998;4(5):448-458.
220. Arribas J, Borroto A. Protein ectodomain shedding. *Chem Rev*. 2002;102(12):4627-4638.
221. Blobel CP. Remarkable roles of proteolysis on and beyond the cell surface. *Curr Opin Cell Biol*. 2000;12(5):606-612.
222. Lessey BA. The role of the endometrium during embryo implantation. *Hum Reprod*. 2000;15 Suppl 6:39-50.
223. Lessey BA, Castelbaum AJ, Wolf L, et al. Use of integrins to date the endometrium. *Fertil Steril*. 2000;73(4):779-787.
224. Meseguer M, Pellicer A, Simon C. MUC1 and endometrial receptivity. *Mol Hum Reprod*. 1998;4(12):1089-1098.
225. Diedrich K, Fauser BC, Devroey P, Griesinger G. The role of the endometrium and embryo in human implantation. *Hum Reprod Update*. 2007;13(4):365-377.
226. Evers JL, Land JA, Dunselman GA, van der Linden PJ, Hamilton JC. "The Flemish Giant", reflections on the defense against endometriosis, inspired by Professor Emeritus Ivo A. Brosens. *Eur J Obstet Gynecol Reprod Biol*. 1998;81(2):253-258.
227. Wiegerinck MA, Van Dop PA, Brosens IA. The staging of peritoneal endometriosis by the type of active lesion in addition to the revised American Fertility Society classification. *Fertil Steril*. 1993;60(3):461-464.
228. Jansen RP. Minimal endometriosis and reduced fecundability: prospective evidence from an artificial insemination by donor program. *Fertil Steril*. 1986;46(1):141-143.
229. Jansen RP, Russell P. Nonpigmented endometriosis: clinical, laparoscopic, and pathologic definition. *Am J Obstet Gynecol*. 1986;155(6):1154-1159.
230. Stripling MC, Martin DC, Chatman DL, Zwaag RV, Poston WM. Subtle appearance of pelvic endometriosis. *Fertil Steril*. 1988;49(3):427-431.
231. Koninckx PR, Martin DC. Deep endometriosis: a consequence of infiltration or retraction or possibly adenomyosis externa? *Fertil Steril*. 1992;58(5):924-928.
232. Chapron C, Dumontier I, Dousset B, et al. Results and role of rectal endoscopic ultrasonography for patients with deep pelvic endometriosis. *Hum Reprod*. 1998;13(8):2266-2270.
233. Chapron C, Vieira M, Chopin N, et al. Accuracy of rectal endoscopic ultrasonography and magnetic resonance imaging in the diagnosis of rectal involvement for patients presenting with deeply infiltrating endometriosis. *Ultrasound Obstet Gynecol*. 2004;24(2):175-179.
234. Hughesdon PE. The endometrial identity of benign stromatosis of the ovary and its relation to other forms of endometriosis. *J Pathol*. 1976;119(4):201-209.
235. Brosens IA, Puttemans PJ, Deprest J. The endoscopic localization of endometrial implants in the ovarian chocolate cyst. *Fertil Steril*. 1994;61(6):1034-1038.
236. Hudelist G, English J, Thomas AE, Tinelli A, Singer CF, Keckstein J. Diagnostic accuracy of transvaginal ultrasound for non-invasive diagnosis of bowel endometriosis: systematic review and meta-analysis. *Ultrasound Obstet Gynecol*;37(3):257-263.
237. Moore J, Copley S, Morris J, Lindsell D, Golding S, Kennedy S. A systematic review of the accuracy of ultrasound in the diagnosis of endometriosis. *Ultrasound Obstet Gynecol*. 2002;20(6):630-634.
238. Hricak H, Alpers C, Crooks LE, Sheldon PE. Magnetic resonance imaging of the female pelvis: initial experience. *AJR Am J Roentgenol*. 1983;141(6):1119-1128.
239. Togashi K, Nishimura K, Kimura I, et al. Endometrial cysts: diagnosis with MR imaging. *Radiology*. 1991;180(1):73-78.

240. Champaneria R, Abedin P, Daniels J, Balogun M, Khan KS. Ultrasound scan and magnetic resonance imaging for the diagnosis of adenomyosis: systematic review comparing test accuracy. *Acta Obstet Gynecol Scand*;89(11):1374-1384.
241. Bast RC, Jr., Xu FJ, Yu YH, Barnhill S, Zhang Z, Mills GB. CA 125: the past and the future. *Int J Biol Markers*. 1998;13(4):179-187.
242. Mol BW, Bayram N, Lijmer JG, et al. The performance of CA-125 measurement in the detection of endometriosis: a meta-analysis. *Fertil Steril*. 1998;70(6):1101-1108.
243. Krasnicki D. [Serum and peritoneal fluid CA-125 concentration in women with endometriosis]. *Ginekol Pol*. 2001;72(12A):1365-1369.
244. Agic A, Djalali S, Wolfler MM, Halis G, Diedrich K, Hornung D. Combination of CCR1 mRNA, MCP1, and CA125 measurements in peripheral blood as a diagnostic test for endometriosis. *Reprod Sci*. 2008;15(9):906-911.
245. Kitawaki J, Kusuki I, Koshiba H, Tsukamoto K, Honjo H. Expression of aromatase cytochrome P450 in eutopic endometrium and its application as a diagnostic test for endometriosis. *Gynecol Obstet Invest*. 1999;48 Suppl 1:21-28.
246. Geist. Androgen therapy in Gynaecology. *JAMA*. 1941;117:2207-2215.
247. Hirst JC. Favorable response of advanced Endometriosis to Testosterone Propionate Therapy. *Am J Obstet Gynecol*. 1943;46:97-102.
248. Karnaky KJ. The use of stilbestrol for endometriosis; preliminary report. *South Med J*. 1948;41(12):1109-1111.
249. Kistner RW. The use of newer progestins in the treatment of endometriosis. *Am J Obstet Gynecol*. 1958;75(2):264-278.
250. Bergqvist A, Ljungberg O, Myhre E. Human endometrium and endometriotic tissue obtained simultaneously: a comparative histological study. *Int J Gynecol Pathol*. 1984;3(2):135-145.
251. Moghissi KS. Treatment of endometriosis with estrogen-progestin combination and progestogens alone. *Clin Obstet Gynecol*. 1988;31(4):823-828.
252. Vercellini P, Crosignani PG, Somigliana E, Berlanda N, Barbara G, Fedele L. Medical treatment for rectovaginal endometriosis: what is the evidence? *Hum Reprod*. 2009;24(10):2504-2514.
253. Daguati R, Somigliana E, Vigano P, Vercellini P. [Progestogens and estroprogestins in the treatment of pelvic pain associated with endometriosis]. *Minerva Ginecol*. 2006;58(6):499-510.
254. Fedele L, Berlanda N. Emerging drugs for endometriosis. *Expert Opin Emerg Drugs*. 2004;9(1):167-177.
255. Guo SW. Emerging drugs for endometriosis. *Expert Opin Emerg Drugs*. 2008;13(4):547-571.
256. Ulrich U, Hucke J, Schweppe KW. [Recommendations for diagnosis and treatment of endometriosis]. *Zentralbl Gynakol*. 2005;127(5):338-345.
257. Vercellini P, Vigano P, Somigliana E. The role of the levonorgestrel-releasing intrauterine device in the management of symptomatic endometriosis. *Curr Opin Obstet Gynecol*. 2005;17(4):359-365.
258. Creus M, Fabregues F, Carmona F, del Pino M, Manau D, Balasch J. Combined laparoscopic surgery and pentoxifylline therapy for treatment of endometriosis-associated infertility: a preliminary trial. *Hum Reprod*. 2008;23(8):1910-1916.
259. Badawy SZ, Etman A, Cuenca V, Montante A, Kaufman L. Effect of interferon alpha-2b on endometrioma cells in vitro. *Obstet Gynecol*. 2001;98(3):417-420.
260. Kauppila A, Ronnberg L. Naproxen sodium in dysmenorrhea secondary to endometriosis. *Obstet Gynecol*. 1985;65(3):379-383.
261. Kauppila A, Puolakka J, Ylikorkala O. Prostaglandin biosynthesis inhibitors and endometriosis. *Prostaglandins*. 1979;18(4):655-661.

262. Vercellini P, Aimi G, Panazza S, De Giorgi O, Pesole A, Crosignani PG. A levonorgestrel-releasing intrauterine system for the treatment of dysmenorrhea associated with endometriosis: a pilot study. *Fertil Steril*. 1999;72(3):505-508.
263. Davis L, Kennedy SS, Moore J, Prentice A. Modern combined oral contraceptives for pain associated with endometriosis. *Cochrane Database Syst Rev*. 2007(3):CD001019.
264. Moore J, Kennedy S, Prentice A. Modern combined oral contraceptives for pain associated with endometriosis. *Cochrane Database Syst Rev*. 2000(2):CD001019.
265. Schweppe KW. [Guidelines for the use of GnRH-analogues in the treatment of endometriosis]. *Zentralbl Gynakol*. 2005;127(5):308-313.
266. Lindheim SR. Chronic pelvic pain: presumptive diagnosis and therapy using GnRH agonists. *Int J Fertil Womens Med*. 1999;44(3):131-138.
267. Garry R. The effectiveness of laparoscopic excision of endometriosis. *Curr Opin Obstet Gynecol*. 2004;16(4):299-303.
268. RCOG. Endometriosis, Investigation and Management Green top guideline 24; 2013.
269. Hayrabedyan S, Kyurkchiev S, Kehayov I. FGF-1 and S100A13 possibly contribute to angiogenesis in endometriosis. *J Reprod Immunol*. 2005;67(1-2):87-101.
270. Wright J, Lotfallah H, Jones K, Lovell D. A randomized trial of excision versus ablation for mild endometriosis. *Fertil Steril*. 2005;83(6):1830-1836.
271. Sutton CJ, Ewen SP, Whitelaw N, Haines P. Prospective, randomized, double-blind, controlled trial of laser laparoscopy in the treatment of pelvic pain associated with minimal, mild, and moderate endometriosis. *Fertil Steril*. 1994;62(4):696-700.
272. Jones KD, Sutton C. Patient satisfaction and changes in pain scores after ablative laparoscopic surgery for stage III-IV endometriosis and endometriotic cysts. *Fertil Steril*. 2003;79(5):1086-1090.
273. Cibula D, Kuzel D, Fucikova Z, et al. [Long-term follow-up after complete treatment of peritoneal endometriosis with the CO2 laser]. *Ceska Gynekol*. 2003;68(2):63-68.
274. Vercellini P, Aimi G, Busacca M, Apolone G, Uglietti A, Crosignani PG. Laparoscopic uterosacral ligament resection for dysmenorrhea associated with endometriosis: results of a randomized, controlled trial. *Fertil Steril*. 2003;80(2):310-319.
275. Candiani GB, Fedele L, Vercellini P, Bianchi S, Di Nola G. Presacral neurectomy for the treatment of pelvic pain associated with endometriosis: a controlled study. *Am J Obstet Gynecol*. 1992;167(1):100-103.
276. Crosignani PG, Vercellini P, Biffignandi F, Costantini W, Cortesi I, Imparato E. Laparoscopy versus laparotomy in conservative surgical treatment for severe endometriosis. *Fertil Steril*. 1996;66(5):706-711.
277. Vercellini P, De Giorgi O, Pisacreta A, Pesole AP, Vicentini S, Crosignani PG. Surgical management of endometriosis. *Baillieres Best Pract Res Clin Obstet Gynaecol*. 2000;14(3):501-523.
278. Johnson NP, Farquhar CM, Crossley S, et al. A double-blind randomised controlled trial of laparoscopic uterine nerve ablation for women with chronic pelvic pain. *BJOG*. 2004;111(9):950-959.
279. Rapkin AJ. Neuroanatomy, neurophysiology, and neuropharmacology of pelvic pain. *Clin Obstet Gynecol*. 1990;33(1):119-129.
280. Khan KS, Khan SF, Nwosu CR, Dwarakanath LS, Chien PFW. Laparoscopic uterosacral nerve ablation in chronic pelvic pain: an overview. *Gynaecological Endoscopy*. 1999;8(5):257-265.
281. Sutton C, Pooley AS, Jones KD, Dover RW, Haines P. A prospective, randomized, double-blind controlled trial of laparoscopic uterine nerve ablation in the treatment of pelvic pain associated with endometriosis. *Gynaecological Endoscopy*. 2001;10(4):217-222.
282. Proctor ML, Latthe PM, Farquhar CM, Khan KS, Johnson NP. Surgical interruption of pelvic nerve pathways for primary and secondary dysmenorrhoea. *Cochrane Database Syst Rev*. 2005(4):CD001896.

283. Fedele L, Marchini M, Acaia B, Garagiola U, Tiengo M. Dynamics and significance of placebo response in primary dysmenorrhea. *Pain*. 1989;36(1):43-47.
284. Jacobson TZ, Duffy JM, Barlow D, Farquhar C, Koninckx PR, Olive D. Laparoscopic surgery for subfertility associated with endometriosis. *Cochrane Database Syst Rev*. 2010(1):CD001398.
285. Werbrouck E, Spiessens C, Meuleman C, D'Hooghe T. No difference in cycle pregnancy rate and in cumulative live-birth rate between women with surgically treated minimal to mild endometriosis and women with unexplained infertility after controlled ovarian hyperstimulation and intrauterine insemination. *Fertil Steril*. 2006;86(3):566-571.
286. Fourquet J, Baez L, Figueroa M, Iriarte RI, Flores I. Quantification of the impact of endometriosis symptoms on health-related quality of life and work productivity. *Fertil Steril*. 2011;96(1):107-112.
287. Lemaire GS. More than just menstrual cramps: symptoms and uncertainty among women with endometriosis. *J Obstet Gynecol Neonatal Nurs*. 2004;33(1):71-79.
288. Low WY, Edelmann RJ, Sutton C. A psychological profile of endometriosis patients in comparison to patients with pelvic pain of other origins. *J Psychosom Res*. 1993;37(2):111-116.
289. Greco CD. Management of adolescent chronic pelvic pain from endometriosis: a pain center perspective. *J Pediatr Adolesc Gynecol*. 2003;16(3 Suppl):S17-19.
290. Wanyonyi SZ, Sequeira E, Mukono SG. Correlation between laparoscopic and histopathologic diagnosis of endometriosis. *Int J Gynaecol Obstet*. 2011;115(3):273-276.
291. Overton C, Park C. Endometriosis. More on the missed disease. *BMJ*. 2010;341:c3727.
292. Fauconnier A, Chapron C, Dubuisson JB, Vieira M, Dousset B, Breart G. Relation between pain symptoms and the anatomic location of deep infiltrating endometriosis. *Fertil Steril*. 2002;78(4):719-726.
293. Vercellini P, Crosignani PG, Abbiati A, Somigliana E, Vigano P, Fedele L. The effect of surgery for symptomatic endometriosis: the other side of the story. *Hum Reprod Update*. 2009;15(2):177-188.
294. EuroQol--a new facility for the measurement of health-related quality of life. The EuroQol Group. *Health Policy*. 1990;16(3):199-208.
295. McHorney CA, Ware JE, Jr., Lu JF, Sherbourne CD. The MOS 36-item Short-Form Health Survey (SF-36): III. Tests of data quality, scaling assumptions, and reliability across diverse patient groups. *Med Care*. 1994;32(1):40-66.
296. Zigmond AS, Snaith RP. The Hospital Anxiety and Depression Scale. *Acta Psychiatrica Scandinavica*. 1983;67(6):361-370.
297. Garratt AM, Torgerson DJ, Wyness J, Hall MH, Reid DM. Measuring sexual functioning in premenopausal women. *BJOG: An International Journal of Obstetrics & Gynaecology*. 1995;102(4):311-316.
298. Ballweg ML. Blaming the victim. The psychologizing of endometriosis. *Obstet Gynecol Clin North Am*. 1997;24(2):441-453.
299. Whitney ML. Importance of lay organizations for coping with endometriosis. *J Reprod Med*. 1998;43(3 Suppl):331-334.
300. Lessey BA. Medical management of endometriosis and infertility. *Fertil Steril*. 2000;73(6):1089-1096.
301. Surrey E. An economically rational method of managing early-stage endometriosis. *Med Interface*. 1997;10(3):119-124.
302. Mathias SD, Kuppermann M, Liberman RF, Lipschutz RC, Steege JF. Chronic pelvic pain: prevalence, health-related quality of life, and economic correlates. *Obstet Gynecol*. 1996;87(3):321-327.
303. Chopin N, Vieira M, Borghese B, et al. Operative management of deeply infiltrating endometriosis: results on pelvic pain symptoms according to a surgical classification. *J Minim Invasive Gynecol*. 2005;12(2):106-112.

304. Martin CE, Johnson E, Wechter ME, Leserman J, Zolnoun DA. Catastrophizing: a predictor of persistent pain among women with endometriosis at 1 year. *Human Reproduction*. 2011;26(11):3078-3084.
305. Denny E. Women's experience of endometriosis. *Journal of Advanced Nursing*. 2004;46(6):641-648.
306. Berube S, Marcoux S, Langevin M, Maheux R. Fecundity of infertile women with minimal or mild endometriosis and women with unexplained infertility. The Canadian Collaborative Group on Endometriosis. *Fertil Steril*. 1998;69(6):1034-1041.
307. Marcoux S, Maheux R, Berube S. Laparoscopic surgery in infertile women with minimal or mild endometriosis. Canadian Collaborative Group on Endometriosis. *N Engl J Med*. 1997;337(4):217-222.
308. Milingos S, Mavrommatis C, Elsheikh A, et al. Fecundity of infertile women with minimal or mild endometriosis. A clinical study. *Arch Gynecol Obstet*. 2002;267(1):37-40.
309. Tulandi T, al-Took S. Reproductive outcome after treatment of mild endometriosis with laparoscopic excision and electrocoagulation. *Fertil Steril*. 1998;69(2):229-231.
310. Healey M, Ang WC, Cheng C. Surgical treatment of endometriosis: a prospective randomized double-blinded trial comparing excision and ablation. *Fertil Steril*. 2010;94(7):2536-2540.
311. Ferrero S, Anserini P, Abbamonte LH, Ragni N, Camerini G, Remorgida V. Fertility after bowel resection for endometriosis. *Fertil Steril*. 2009;92(1):41-46.
312. Opoien HK, Fedorcsak P, Byholm T, Tanbo T. Complete surgical removal of minimal and mild endometriosis improves outcome of subsequent IVF/ICSI treatment. *Reprod Biomed Online*. 2011;23(3):389-395.
313. Laschke MW, Elitzsch A, Vollmar B, Menger MD. In vivo analysis of angiogenesis in endometriosis-like lesions by intravital fluorescence microscopy. *Fertil Steril*. 2005;84 Suppl 2:1199-1209.
314. Simoens S, Hummelshoj L, D'Hooghe T. Endometriosis: cost estimates and methodological perspective. *Hum Reprod Update*. 2007;13(4):395-404.
315. Levy AR, Osenenko KM, Lozano-Ortega G, et al. Economic burden of surgically confirmed endometriosis in Canada. *J Obstet Gynaecol Can*. 2011;33(8):830-837.
316. Gao X, Outley J, Botteman M, Spalding J, Simon JA, Pashos CL. Economic burden of endometriosis. *Fertil Steril*. 2006;86(6):1561-1572.
317. Philips Z, Barraza-Llorens M, Posnett J. Evaluation of the relative cost-effectiveness of treatments for infertility in the UK. *Hum Reprod*. 2000;15(1):95-106.
318. Winkel CA. Modeling of medical and surgical treatment costs of chronic pelvic pain: new paradigms for making clinical decisions. *Am J Manag Care*. 1999;5(5 Suppl):S276-290.
319. L C. Cell Based Assays: the Cell Cycle, Cell Proliferation and Cell Death. MATER METHODS 2013;3:172: Labome; 2014.
320. Wikipedia. Signal transduction pathways
In: http://en.wikipedia.org/wiki/File:Signal_transduction_v1.png ed. File:Signal_transduction_pathways_(zh-cn)svg </wiki/File:Signal_transduction_pathways_(zh-cn)svg>
2010.
321. Perfettini JL, Kroemer G. Caspase activation is not death. *Nat Immunol*. 2003;4(4):308-310.
322. Zhao H, Bauzon F, Fu H, et al. Skp2 Deletion Unmasks a p27 Safeguard that Blocks Tumorigenesis in the Absence of pRb and p53 Tumor Suppressors. *Cancer Cell*. 2013;24(5):645-659.
323. Gezginc ST, Celik C, Dogan NU, Toy H, Tazegul A, Colakoglu MC. Expression of cyclin A, cyclin E and p27 in normal, hyperplastic and frankly malignant endometrial samples. *J Obstet Gynaecol*. 2013;33(5):508-511.
324. Ying TH, Tseng CJ, Tsai SJ, et al. Association of p53 and CDKN1A genotypes with endometriosis. *Anticancer Res*. 2011;31(12):4301-4306.

325. Healy DL, Rogers PA, Hii L, Wingfield M. Angiogenesis: a new theory for endometriosis. *Hum Reprod Update*. 1998;4(5):736-740.
326. Haney AF. Endometriosis, macrophages, and adhesions. *Prog Clin Biol Res*. 1993;381:19-44.
327. Bergqvist A, Bruse C, Carlberg M, Carlstrom K. Interleukin 1beta, interleukin-6, and tumor necrosis factor-alpha in endometriotic tissue and in endometrium. *Fertil Steril*. 2001;75(3):489-495.
328. Akira S, Kishimoto T. IL-6 and NF-IL6 in acute-phase response and viral infection. *Immunol Rev*. 1992;127:25-50.
329. Febbraio M, Hajjar DP, Silverstein RL. CD36: a class B scavenger receptor involved in angiogenesis, atherosclerosis, inflammation, and lipid metabolism. *J Clin Invest*. 2001;108(6):785-791.
330. Chuang PC, Lin YJ, Wu MH, Wing LY, Shoji Y, Tsai SJ. Inhibition of CD36-dependent phagocytosis by prostaglandin E2 contributes to the development of endometriosis. *Am J Pathol*;176(2):850-860.
331. Somigliana E, Vigano P, Parazzini F, Stoppelli S, Giambattista E, Vercellini P. Association between endometriosis and cancer: a comprehensive review and a critical analysis of clinical and epidemiological evidence. *Gynecol Oncol*. 2006;101(2):331-341.
332. Sato N, Tsunoda H, Nishida M, et al. Loss of heterozygosity on 10q23.3 and mutation of the tumor suppressor gene PTEN in benign endometrial cyst of the ovary: possible sequence progression from benign endometrial cyst to endometrioid carcinoma and clear cell carcinoma of the ovary. *Cancer Res*. 2000;60(24):7052-7056.
333. Fukunaga M, Nomura K, Ishikawa E, Ushigome S. Ovarian atypical endometriosis: its close association with malignant epithelial tumours. *Histopathology*. 1997;30(3):249-255.
334. Prefumo F, Todeschini F, Fulcheri E, Venturini PL. Epithelial abnormalities in cystic ovarian endometriosis. *Gynecol Oncol*. 2002;84(2):280-284.
335. Olson JE, Cerhan JR, Janney CA, Anderson KE, Vachon CM, Sellers TA. Postmenopausal cancer risk after self-reported endometriosis diagnosis in the Iowa Women's Health Study. *Cancer*. 2002;94(5):1612-1618.
336. Borgfeldt C, Andolf E. Cancer risk after hospital discharge diagnosis of benign ovarian cysts and endometriosis. *Acta Obstet Gynecol Scand*. 2004;83(4):395-400.
337. Venn A, Watson L, Bruinsma F, Giles G, Healy D. Risk of cancer after use of fertility drugs with in-vitro fertilisation. *Lancet*. 1999;354(9190):1586-1590.
338. Schairer C, Persson I, Falkeborn M, Naessen T, Troisi R, Brinton LA. Breast cancer risk associated with gynecologic surgery and indications for such surgery. *Int J Cancer*. 1997;70(2):150-154.
339. Slavin RE, Krum R, Van Dinh T. Endometriosis-associated intestinal tumors: a clinical and pathological study of 6 cases with a review of the literature. *Hum Pathol*. 2000;31(4):456-463.
340. Heaps JM, Nieberg RK, Berek JS. Malignant neoplasms arising in endometriosis. *Obstet Gynecol*. 1990;75(6):1023-1028.
341. Reimnitz C, Brand E, Nieberg RK, Hacker NF. Malignancy arising in endometriosis associated with unopposed estrogen replacement. *Obstet Gynecol*. 1988;71(3 Pt 2):444-447.
342. Gucer F, Pieber D, Arikan MG. Malignancy arising in extraovarian endometriosis during estrogen stimulation. *European journal of gynaecological oncology*. 1998;19(1):39-41.
343. Vercellini P, Scarfone G, Bolis G, Stellato G, Carinelli S, Crosignani PG. Site of origin of epithelial ovarian cancer: the endometriosis connection. *BJOG*. 2000;107(9):1155-1157.
344. McMeekin DS, Burger RA, Manetta A, DiSaia P, Berman ML. Endometrioid adenocarcinoma of the ovary and its relationship to endometriosis. *Gynecol Oncol*. 1995;59(1):81-86.
345. Erzen M, Rakar S, Klancnik B, Syrjanen K. Endometriosis-associated ovarian carcinoma (EAOC): an entity distinct from other ovarian carcinomas as suggested by a nested case-control study. *Gynecol Oncol*. 2001;83(1):100-108.

346. Erzen M, Kovacic J. Relationship between endometriosis and ovarian cancer. *Eur J Gynaecol Oncol*. 1998;19(6):553-555.
347. Clement PB. The pathology of endometriosis: a survey of the many faces of a common disease emphasizing diagnostic pitfalls and unusual and newly appreciated aspects. *Adv Anat Pathol*. 2007;14(4):241-260.
348. Prowse AH, Manek S, Varma R, et al. Molecular genetic evidence that endometriosis is a precursor of ovarian cancer. *Int J Cancer*. 2006;119(3):556-562.
349. Jiang X, Hitchcock A, Bryan EJ, et al. Microsatellite analysis of endometriosis reveals loss of heterozygosity at candidate ovarian tumor suppressor gene loci. *Cancer Res*. 1996;56(15):3534-3539.
350. Dinulescu DM, Ince TA, Quade BJ, Shafer SA, Crowley D, Jacks T. Role of K-ras and Pten in the development of mouse models of endometriosis and endometrioid ovarian cancer. *Nat Med*. 2005;11(1):63-70.
351. Akahane T, Sekizawa A, Purwosunu Y, Nagatsuka M, Okai T. The role of p53 mutation in the carcinomas arising from endometriosis. *Int J Gynecol Pathol*. 2007;26(3):345-351.
352. Bischoff FZ, Heard M, Simpson JL. Somatic DNA alterations in endometriosis: high frequency of chromosome 17 and p53 loss in late-stage endometriosis. *J Reprod Immunol*. 2002;55(1-2):49-64.
353. Nezhat FR, Kalir T. Comparative immunohistochemical studies of endometriosis lesions and endometriotic cysts. *Fertil Steril*. 2002;78(4):820-824.
354. Sainz de la Cuesta R, Izquierdo M, Canamero M, Granizo JJ, Manzarbeitia F. Increased prevalence of p53 overexpression from typical endometriosis to atypical endometriosis and ovarian cancer associated with endometriosis. *Eur J Obstet Gynecol Reprod Biol*. 2004;113(1):87-93.
355. Vercellini P, Trecca D, Oldani S, Fracchiolla NS, Neri A, Crosignani PG. Analysis of p53 and ras gene mutations in endometriosis. *Gynecol Obstet Invest*. 1994;38(1):70-71.
356. Bayramoglu H, Duzcan E. Atypical epithelial changes and mutant p53 gene expression in ovarian endometriosis. *Pathol Oncol Res*. 2001;7(1):33-38.
357. Wiegand KC, Shah SP, Al-Agha OM, et al. ARID1A mutations in endometriosis-associated ovarian carcinomas. *N Engl J Med*. 2010;363(16):1532-1543.
358. Al-Jefout M, Dezarnaulds G, Cooper M, et al. Diagnosis of endometriosis by detection of nerve fibres in an endometrial biopsy: a double blind study. *Hum Reprod*. 2009;24(12):3019-3024.
359. Bedaiwy MA, Falcone T, Sharma RK, et al. Prediction of endometriosis with serum and peritoneal fluid markers: a prospective controlled trial. *Hum Reprod*. 2002;17(2):426-431.
360. Somigliana E, Vigano P, Tirelli AS, et al. Use of the concomitant serum dosage of CA 125, CA 19-9 and interleukin-6 to detect the presence of endometriosis. Results from a series of reproductive age women undergoing laparoscopic surgery for benign gynaecological conditions. *Hum Reprod*. 2004;19(8):1871-1876.
361. Martinez S, Garrido N, Coperias JL, et al. Serum interleukin-6 levels are elevated in women with minimal-mild endometriosis. *Hum Reprod*. 2007;22(3):836-842.
362. Seeber B, Sammel MD, Fan X, et al. Panel of markers can accurately predict endometriosis in a subset of patients. *Fertil Steril*. 2008;89(5):1073-1081.
363. Othman Eel D, Hornung D, Salem HT, Khalifa EA, El-Metwally TH, Al-Hendy A. Serum cytokines as biomarkers for nonsurgical prediction of endometriosis. *Eur J Obstet Gynecol Reprod Biol*. 2008;137(2):240-246.
364. Mihalyi A, Gevaert O, Kyama CM, et al. Non-invasive diagnosis of endometriosis based on a combined analysis of six plasma biomarkers. *Hum Reprod*. 2010;25(3):654-664.
365. Agic A, Xu H, Rehbein M, Wolfler MM, Ebert AD, Hornung D. Cognate chemokine receptor 1 messenger ribonucleic acid expression in peripheral blood as a diagnostic test for endometriosis. *Fertil Steril*. 2007;87(4):982-984.
366. Cho S, Cho H, Nam A, et al. Neutrophil-to-lymphocyte ratio as an adjunct to CA-125 for the diagnosis of endometriosis. *Fertil Steril*. 2008;90(6):2073-2079.

367. Zachariah R, Schmid S, Radpour R, et al. Circulating cell-free DNA as a potential biomarker for minimal and mild endometriosis. *Reprod Biomed Online*. 2009;18(3):407-411.
368. Florio P, Reis FM, Torres PB, et al. Plasma urocortin levels in the diagnosis of ovarian endometriosis. *Obstet Gynecol*. 2007;110(3):594-600.
369. Florio P, Reis FM, Torres PB, et al. High serum follistatin levels in women with ovarian endometriosis. *Hum Reprod*. 2009;24(10):2600-2606.
370. Vodolazkaia A, El-Aalamat Y, Popovic D, et al. Evaluation of a panel of 28 biomarkers for the non-invasive diagnosis of endometriosis. *Hum Reprod*. 2012;27(9):2698-2711.
371. Gagne D, Rivard M, Page M, et al. Development of a nonsurgical diagnostic tool for endometriosis based on the detection of endometrial leukocyte subsets and serum CA-125 levels. *Fertil Steril*. 2003;80(4):876-885.
372. Kitawaki J, Kusuki I, Koshiba H, Tsukamoto K, Fushiki S, Honjo H. Detection of aromatase cytochrome P-450 in endometrial biopsy specimens as a diagnostic test for endometriosis. *Fertil Steril*. 1999;72(6):1100-1106.
373. Dheenadayalu K, Mak I, Gordts S, et al. Aromatase P450 messenger RNA expression in eutopic endometrium is not a specific marker for pelvic endometriosis. *Fertil Steril*. 2002;78(4):825-829.
374. Wu Y, Halverson G, Basir Z, Strawn E, Yan P, Guo SW. Aberrant methylation at HOXA10 may be responsible for its aberrant expression in the endometrium of patients with endometriosis. *Am J Obstet Gynecol*. 2005;193(2):371-380.
375. Kim JJ, Taylor HS, Lu Z, et al. Altered expression of HOXA10 in endometriosis: potential role in decidualization. *Mol Hum Reprod*. 2007;13(5):323-332.
376. Lee B, Du H, Taylor HS. Experimental murine endometriosis induces DNA methylation and altered gene expression in eutopic endometrium. *Biol Reprod*. 2009;80(1):79-85.
377. Wu Y, Strawn E, Basir Z, Halverson G, Guo SW. Promoter hypermethylation of progesterone receptor isoform B (PR-B) in endometriosis. *Epigenetics*. 2006;1(2):106-111.
378. Jichan N, Xishi L, Guo SW. Promoter hypermethylation of progesterone receptor isoform B (PR-B) in adenomyosis and its rectification by a histone deacetylase inhibitor and a demethylation agent. *Reprod Sci*. 2010;17(11):995-1005.
379. Izawa M, Harada T, Taniguchi F, Ohama Y, Takenaka Y, Terakawa N. An epigenetic disorder may cause aberrant expression of aromatase gene in endometriotic stromal cells. *Fertil Steril*. 2008;89(5 Suppl):1390-1396.
380. Izawa M, Taniguchi F, Uegaki T, et al. Demethylation of a nonpromoter cytosine-phosphate-guanine island in the aromatase gene may cause the aberrant up-regulation in endometriotic tissues. *Fertil Steril*. 2011;95(1):33-39.
381. Xue Q, Lin Z, Cheng YH, et al. Promoter methylation regulates estrogen receptor 2 in human endometrium and endometriosis. *Biol Reprod*. 2007;77(4):681-687.
382. Xue Q, Lin Z, Yin P, et al. Transcriptional activation of steroidogenic factor-1 by hypomethylation of the 5' CpG island in endometriosis. *J Clin Endocrinol Metab*. 2007;92(8):3261-3267.
383. Wu Y, Starzinski-Powitz A, Guo SW. Trichostatin A, a histone deacetylase inhibitor, attenuates invasiveness and reactivates E-cadherin expression in immortalized endometriotic cells. *Reprod Sci*. 2007;14(4):374-382.
384. Pan Q, Luo X, Toloubeydokhti T, Chegini N. The expression profile of micro-RNA in endometrium and endometriosis and the influence of ovarian steroids on their expression. *Mol Hum Reprod*. 2007;13(11):797-806.
385. Ohlsson Teague EM, Van der Hoek KH, Van der Hoek MB, et al. MicroRNA-regulated pathways associated with endometriosis. *Mol Endocrinol*. 2009;23(2):265-275.
386. Filigheddu N, Gregnanin I, Porporato PE, et al. Differential expression of microRNAs between eutopic and ectopic endometrium in ovarian endometriosis. *J Biomed Biotechnol*;2010:369549.

387. Burney RO, Talbi S, Hamilton AE, et al. Gene expression analysis of endometrium reveals progesterone resistance and candidate susceptibility genes in women with endometriosis. *Endocrinology*. 2007;148(8):3814-3826.
388. Toloubeydokhti T, Pan Q, Luo X, Bukulmez O, Chegini N. The expression and ovarian steroid regulation of endometrial micro-RNAs. *Reprod Sci*. 2008;15(10):993-1001.
389. Burney RO, Hamilton AE, Aghajanova L, et al. MicroRNA expression profiling of eutopic secretory endometrium in women with versus without endometriosis. *Mol Hum Reprod*. 2009;15(10):625-631.
390. Aghajanova L, Giudice LC. Molecular evidence for differences in endometrium in severe versus mild endometriosis. *Reprod Sci*. 2011;18(3):229-251.
391. Kyama CM, Mihalyi A, Gevaert O, et al. Evaluation of endometrial biomarkers for semi-invasive diagnosis of endometriosis. *Fertil Steril*. 2011;95(4):1338-1343 e1331-1333.
392. Kyama CM, T'Jampens D, Mihalyi A, et al. ProteinChip technology is a useful method in the pathogenesis and diagnosis of endometriosis: a preliminary study. *Fertil Steril*. 2006;86(1):203-209.
393. Fassbender A, Simsa P, Kyama CM, et al. TRIzol treatment of secretory phase endometrium allows combined proteomic and mRNA microarray analysis of the same sample in women with and without endometriosis. *Reprod Biol Endocrinol*. 2010;8:123.
394. Fassbender A, Waelkens E, Verbeeck N, et al. Proteomics analysis of plasma for early diagnosis of endometriosis. *Obstet Gynecol*. 2012;119(2 Pt 1):276-285.
395. Jing J, Qiao Y, Suginami H, Taniguchi F, Shi H, Wang X. Two novel serum biomarkers for endometriosis screened by surface-enhanced laser desorption/ionization time-of-flight mass spectrometry and their change after laparoscopic removal of endometriosis. *Fertil Steril*. 2009;92(4):1221-1227.
396. Liu H, Lang J, Zhou Q, Shan D, Li Q. Detection of endometriosis with the use of plasma protein profiling by surface-enhanced laser desorption/ionization time-of-flight mass spectrometry. *Fertil Steril*. 2007;87(4):988-990.
397. Seeber B, Sammel MD, Fan X, et al. Proteomic analysis of serum yields six candidate proteins that are differentially regulated in a subset of women with endometriosis. *Fertil Steril*. 2010;93(7):2137-2144.
398. Wolfler MM, Schwamborn K, Otten D, Hornung D, Liu H, Rath W. Mass spectrometry and serum pattern profiling for analyzing the individual risk for endometriosis: promising insights? *Fertil Steril*. 2009;91(6):2331-2337.
399. Zhang H, Feng J, Chang XH, Li ZX, Wu XY, Cui H. Effect of surface-enhanced laser desorption/ionization time-of-flight mass spectrometry on identifing biomarkers of endometriosis. *Chin Med J (Engl)*. 2009;122(4):373-376.
400. Wang L, Zheng W, Ding XY, Yu JK, Jiang WZ, Zhang SZ. Identification biomarkers of eutopic endometrium in endometriosis using artificial neural networks and protein fingerprinting. *Fertil Steril*. 2010;93(7):2460-2462.
401. Ding X, Wang L, Ren Y, Zheng W. Detection of mitochondrial biomarkers in eutopic endometria of endometriosis using surface-enhanced laser desorption/ionization time-of-flight mass spectrometry. *Fertil Steril*. 2010;94(7):2528-2530.
402. Fassbender A, Verbeeck N, Bornigen D, et al. Combined mRNA microarray and proteomic analysis of eutopic endometrium of women with and without endometriosis. *Hum Reprod*. 2012;27(7):2020-2029.
403. Brennecke J, Hipfner DR, Stark A, Russell RB, Cohen SM. bantam encodes a developmentally regulated microRNA that controls cell proliferation and regulates the proapoptotic gene hid in Drosophila. *Cell*. 2003;113(1):25-36.
404. Xu P, Vernooy SY, Guo M, Hay BA. The Drosophila microRNA Mir-14 suppresses cell death and is required for normal fat metabolism. *Curr Biol*. 2003;13(9):790-795.
405. Bartel DP. MicroRNAs: genomics, biogenesis, mechanism, and function. *Cell*. 2004;116(2):281-297.

406. Lewis BP, Shih IH, Jones-Rhoades MW, Bartel DP, Burge CB. Prediction of mammalian microRNA targets. *Cell*. 2003;115(7):787-798.
407. Friedman RC, Farh KK, Burge CB, Bartel DP. Most mammalian mRNAs are conserved targets of microRNAs. *Genome Res*. 2009;19(1):92-105.
408. Takamizawa J, Konishi H, Yanagisawa K, et al. Reduced expression of the let-7 microRNAs in human lung cancers in association with shortened postoperative survival. *Cancer Res*. 2004;64(11):3753-3756.
409. Orom UA, Nielsen FC, Lund AH. MicroRNA-10a binds the 5'UTR of ribosomal protein mRNAs and enhances their translation. *Mol Cell*. 2008;30(4):460-471.
410. Garzon R, Fabbri M, Cimmino A, Calin GA, Croce CM. MicroRNA expression and function in cancer. *Trends Mol Med*. 2006;12(12):580-587.
411. Miranda KC, Huynh T, Tay Y, et al. A pattern-based method for the identification of MicroRNA binding sites and their corresponding heteroduplexes. *Cell*. 2006;126(6):1203-1217.
412. Creighton CJ, Benham AL, Zhu H, et al. Discovery of novel microRNAs in female reproductive tract using next generation sequencing. *PLoS One*;5(3):e9637.
413. Lee RC, Feinbaum RL, Ambros V. The C. elegans heterochronic gene lin-4 encodes small RNAs with antisense complementarity to lin-14. *Cell*. 1993;75(5):843-854.
414. Wightman B, Burglin TR, Gatto J, Arasu P, Ruvkun G. Negative regulatory sequences in the lin-14 3'-untranslated region are necessary to generate a temporal switch during Caenorhabditis elegans development. *Genes Dev*. 1991;5(10):1813-1824.
415. Lagos-Quintana M, Rauhut R, Lendeckel W, Tuschl T. Identification of novel genes coding for small expressed RNAs. *Science*. 2001;294(5543):853-858.
416. Lau NC, Lim LP, Weinstein EG, Bartel DP. An abundant class of tiny RNAs with probable regulatory roles in Caenorhabditis elegans. *Science*. 2001;294(5543):858-862.
417. Lee RC, Ambros V. An extensive class of small RNAs in Caenorhabditis elegans. *Science*. 2001;294(5543):862-864.
418. Reinhart BJ, Slack FJ, Basson M, et al. The 21-nucleotide let-7 RNA regulates developmental timing in Caenorhabditis elegans. *Nature*. 2000;403(6772):901-906.
419. Slack FJ, Basson M, Liu Z, Ambros V, Horvitz HR, Ruvkun G. The lin-41 RBCC gene acts in the C. elegans heterochronic pathway between the let-7 regulatory RNA and the LIN-29 transcription factor. *Mol Cell*. 2000;5(4):659-669.
420. Aukerman MJ, Sakai H. Regulation of flowering time and floral organ identity by a MicroRNA and its APETALA2-like target genes. *Plant Cell*. 2003;15(11):2730-2741.
421. Reinhart BJ, Weinstein EG, Rhoades MW, Bartel B, Bartel DP. MicroRNAs in plants. *Genes Dev*. 2002;16(13):1616-1626.
422. Mourelatos Z, Dostie J, Paushkin S, et al. miRNPs: a novel class of ribonucleoproteins containing numerous microRNAs. *Genes Dev*. 2002;16(6):720-728.
423. Pasquinelli AE, Reinhart BJ, Slack F, et al. Conservation of the sequence and temporal expression of let-7 heterochronic regulatory RNA. *Nature*. 2000;408(6808):86-89.
424. Lim LP, Lau NC, Weinstein EG, et al. The microRNAs of Caenorhabditis elegans. *Genes Dev*. 2003;17(8):991-1008.
425. Guo L, Lu Z. Global expression analysis of miRNA gene cluster and family based on isomiRs from deep sequencing data. *Comput Biol Chem*. 2010;34(3):165-171.
426. Lim LP, Glasner ME, Yekta S, Burge CB, Bartel DP. Vertebrate microRNA genes. *Science*. 2003;299(5612):1540.
427. Voight BF, Kudaravalli S, Wen X, Pritchard JK. A map of recent positive selection in the human genome. *PLoS Biol*. 2006;4(3):e72.
428. Houbaviy HB, Murray MF, Sharp PA. Embryonic stem cell-specific MicroRNAs. *Dev Cell*. 2003;5(2):351-358.
429. Seitz H, Youngson N, Lin SP, et al. Imprinted microRNA genes transcribed antisense to a reciprocally imprinted retrotransposon-like gene. *Nat Genet*. 2003;34(3):261-262.
430. Aravin AA, Lagos-Quintana M, Yalcin A, et al. The small RNA profile during Drosophila melanogaster development. *Dev Cell*. 2003;5(2):337-350.

431. Kim J, Krichevsky A, Grad Y, et al. Identification of many microRNAs that copurify with polyribosomes in mammalian neurons. *Proc Natl Acad Sci U S A*. 2004;101(1):360-365.
432. Rodriguez A, Griffiths-Jones S, Ashurst JL, Bradley A. Identification of mammalian microRNA host genes and transcription units. *Genome Res*. 2004;14(10A):1902-1910.
433. Lai EC, Tomancak P, Williams RW, Rubin GM. Computational identification of Drosophila microRNA genes. *Genome Biol*. 2003;4(7):R42.
434. Lee Y, Jeon K, Lee JT, Kim S, Kim VN. MicroRNA maturation: stepwise processing and subcellular localization. *EMBO J*. 2002;21(17):4663-4670.
435. Zeng Y, Yi R, Cullen BR. MicroRNAs and small interfering RNAs can inhibit mRNA expression by similar mechanisms. *Proc Natl Acad Sci U S A*. 2003;100(17):9779-9784.
436. Lu J, Getz G, Miska EA, et al. MicroRNA expression profiles classify human cancers. *Nature*. 2005;435(7043):834-838.
437. Lujambio A, Calin GA, Villanueva A, et al. A microRNA DNA methylation signature for human cancer metastasis. *Proc Natl Acad Sci U S A*. 2008;105(36):13556-13561.
438. Croce CM, Calin GA. miRNAs, cancer, and stem cell division. *Cell*. 2005;122(1):6-7.
439. Calin GA, Ferracin M, Cimmino A, et al. A MicroRNA signature associated with prognosis and progression in chronic lymphocytic leukemia. *N Engl J Med*. 2005;353(17):1793-1801.
440. Pelch KE, Sharpe-Timms KL, Nagel SC. Mouse model of surgically-induced endometriosis by auto-transplantation of uterine tissue. *J Vis Exp*(59):e3396.
441. Pelch KE, Schroder AL, Kimball PA, Sharpe-Timms KL, Davis JW, Nagel SC. Aberrant gene expression profile in a mouse model of endometriosis mirrors that observed in women. *Fertil Steril*;93(5):1615-1627 e1618.
442. Hull ML, Escareno CR, Godsland JM, et al. Endometrial-peritoneal interactions during endometriotic lesion establishment. *Am J Pathol*. 2008;173(3):700-715.
443. Flores I, Rivera E, Ruiz LA, Santiago OI, Vernon MW, Appleyard CB. Molecular profiling of experimental endometriosis identified gene expression patterns in common with human disease. *Fertil Steril*. 2007;87(5):1180-1199.
444. Hever A, Roth RB, Hevezi P, et al. Human endometriosis is associated with plasma cells and overexpression of B lymphocyte stimulator. *Proc Natl Acad Sci U S A*. 2007;104(30):12451-12456.
445. Marsh EE, Lin Z, Yin P, Milad M, Chakravarti D, Bulun SE. Differential expression of microRNA species in human uterine leiomyoma versus normal myometrium. *Fertil Steril*. 2008;89(6):1771-1776.
446. Wilkins M. Proteomics data mining. *Expert Rev Proteomics*. 2009;6(6):599-603.
447. Wilkins MR, Arthur JW, Junius FK, et al. Information management for proteomics: a perspective. *Expert Rev Proteomics*. 2008;5(5):663-678.
448. Baveja G, Saini S, Sangwan K, Arora DR. A study of bacterial pathogens in acute pelvic inflammatory disease. *J Commun Dis*. 2001;33(2):121-125.
449. Kozak KR, Amneus MW, Pusey SM, et al. Identification of biomarkers for ovarian cancer using strong anion-exchange ProteinChips: potential use in diagnosis and prognosis. *Proc Natl Acad Sci U S A*. 2003;100(21):12343-12348.
450. Kozak KR, Su F, Whitelegge JP, Faull K, Reddy S, Farias-Eisner R. Characterization of serum biomarkers for detection of early stage ovarian cancer. *Proteomics*. 2005;5(17):4589-4596.
451. Tabibzadeh S, Becker JL, Parsons AK. Endometriosis is associated with alterations in the relative abundance of proteins and IL-10 in the peritoneal fluid. *Front Biosci*. 2003;8:a70-78.
452. Ferrero S, Gillott DJ, Remorgida V, et al. Proteomic analysis of peritoneal fluid in women with endometriosis. *J Proteome Res*. 2007;6(9):3402-3411.
453. Fowler PA, Tattum J, Bhattacharya S, et al. An investigation of the effects of endometriosis on the proteome of human eutopic endometrium: a heterogeneous tissue with a complex disease. *Proteomics*. 2007;7(1):130-142.

454. Ten Have S, Fraser I, Markham R, Lam A, Matsumoto I. Proteomic analysis of protein expression in the eutopic endometrium of women with endometriosis. *Proteomics Clin Appl*. 2007;1(10):1243-1251.
455. Casado-Vela J, Rodriguez-Suarez E, Iloro I, et al. Comprehensive proteomic analysis of human endometrial fluid aspirate. *J Proteome Res*. 2009;8(10):4622-4632.
456. Hsu CC, Yang BC, Wu MH, Huang KE. Enhanced interleukin-4 expression in patients with endometriosis. *Fertil Steril*. 1997;67(6):1059-1064.
457. Scholes D, Stergachis A, Heidrich FE, Andrilla H, Holmes KK, Stamm WE. Prevention of pelvic inflammatory disease by screening for cervical chlamydial infection. *N Engl J Med*. 1996;334(21):1362-1366.
458. Oral E, Olive DL, Arici A. The peritoneal environment in endometriosis. *Hum Reprod Update*. 1996;2(5):385-398.
459. Iwabe T, Harada T, Terakawa N. Role of cytokines in endometriosis-associated infertility. *Gynecol Obstet Invest*. 2002;53 Suppl 1:19-25.
460. Taketani Y, Kuo TM, Mizuno M. Comparison of cytokine levels and embryo toxicity in peritoneal fluid in infertile women with untreated or treated endometriosis. *Am J Obstet Gynecol*. 1992;167(1):265-270.
461. Ho HN, Wu MY, Chao KH, et al. Decrease in interferon gamma production and impairment of T-lymphocyte proliferation in peritoneal fluid of women with endometriosis. *Am J Obstet Gynecol*. 1996;175(5):1236-1241.
462. Shimoya K, Moriyama A, Ogata I, et al. Increased concentrations of secretory leukocyte protease inhibitor in peritoneal fluid of women with endometriosis. *Mol Hum Reprod*. 2000;6(9):829-834.
463. Cheong YC, Shelton JB, Laird SM, et al. IL-1, IL-6 and TNF-alpha concentrations in the peritoneal fluid of women with pelvic adhesions. *Hum Reprod*. 2002;17(1):69-75.
464. Bedaiwy MA, Falcone T. Peritoneal fluid environment in endometriosis. Clinicopathological implications. *Minerva Ginecol*. 2003;55(4):333-345.
465. Rossi D, Zlotnik A. The biology of chemokines and their receptors. *Annu Rev Immunol*. 2000;18:217-242.
466. Hornung D, Bentzien F, Wallwiener D, Kiesel L, Taylor RN. Chemokine bioactivity of RANTES in endometriotic and normal endometrial stromal cells and peritoneal fluid. *Mol Hum Reprod*. 2001;7(2):163-168.
467. Wieser F, Dogan S, Klingel K, Diedrich K, Taylor RN, Hornung D. Expression and regulation of CCR1 in peritoneal macrophages from women with and without endometriosis. *Fertil Steril*. 2005;83(6):1878-1881.
468. Ryan IP, Tseng JF, Schriock ED, Khorram O, Landers DV, Taylor RN. Interleukin-8 concentrations are elevated in peritoneal fluid of women with endometriosis. *Fertil Steril*. 1995;63(4):929-932.
469. Pellicer A, Albert C, Mercader A, Bonilla-Musoles F, Remohi J, Simon C. The follicular and endocrine environment in women with endometriosis: local and systemic cytokine production. *Fertil Steril*. 1998;70(3):425-431.
470. Pizzo A, Salmeri FM, Ardita FV, Sofo V, Tripepi M, Marsico S. Behaviour of cytokine levels in serum and peritoneal fluid of women with endometriosis. *Gynecol Obstet Invest*. 2002;54(2):82-87.
471. Diamond M, Osteen KG, Pittaway DE. Serum markers of endometrium and endometriosis (ed **Publication date:** 20 Nov 1997): John Wiley and Sons Ltd Blackwell Science Inc.; 1997.
472. Harada T, Kubota T, Aso T. Usefulness of CA19-9 versus CA125 for the diagnosis of endometriosis. *Fertil Steril*. 2002;78(4):733-739.
473. Aghaizu A, Adams EJ, Turner K, et al. What is the cost of pelvic inflammatory disease and how much could be prevented by screening for Chlamydia trachomatis? Cost analysis of the Prevention Of Pelvic Infection (POPI) trial. *Sex Transm Infect*.

474. Robinson AJ, Greenhouse P. Prevention of recurrent pelvic infection by contact tracing: a commonsense approach. *Br J Obstet Gynaecol*. 1996;103(9):859-861.
475. Bevan CD, Johal BJ, Mumtaz G, Ridgway GL, Siddle NC. Clinical, laparoscopic and microbiological findings in acute salpingitis: report on a United Kingdom cohort. *Br J Obstet Gynaecol*. 1995;102(5):407-414.
476. Oakeshott P, Kerry S, Atherton H, et al. Community-based trial of screening for Chlamydia trachomatis to prevent pelvic inflammatory disease: the POPI (prevention of pelvic infection) trial. *Trials*. 2008;9:73.
477. Kyama CM, Mihalyi A, Gevaert O, et al. Evaluation of endometrial biomarkers for semi-invasive diagnosis of endometriosis. *Fertil Steril*;95(4):1338-1343 e1331-1333.
478. Hu J, Coombes KR, Morris JS, Baggerly KA. The importance of experimental design in proteomic mass spectrometry experiments: some cautionary tales. *Brief Funct Genomic Proteomic*. 2005;3(4):322-331.
479. Liu HY, Zheng YH, Zhang JZ, et al. [Establishment of endometriosis diagnostic model using plasma protein profiling]. *Zhonghua Fu Chan Ke Za Zhi*. 2009;44(8):601-604.
480. Wink M. An introduction to Molecular Biotechnology : Molecular Fundamentals, methods and application in Modern Biotechnology. Germany: Wiley-VCH; 2006.
481. Cseke LJ, Kaufmann PB, Podila GK, Tsai. Handbook of Molecular and cellular methods in Biology and Medicine (ed 2nd). USA: CRC Press; 2004.
482. Dinh HK, Zhao B, Schuschereba ST, Merrill G, Bowman PD. Gene expression profiling of the response to thermal injury in human cells. *Physiol Genomics*. 2001;7(1):3-13.
483. Fan H, Gulley ML. RNA extraction from fresh or frozen tissues. *Methods Mol Med*. 2001;49:11-14.
484. Botling J, Edlund K, Segersten U, et al. Impact of thawing on RNA integrity and gene expression analysis in fresh frozen tissue. *Diagn Mol Pathol*. 2009;18(1):44-52.
485. Technologies A. Agilent Technologies miRNA Microarray System with miRNA Complete Labelling and Hyb Kit protocol (Version 2.4). 2013.
486. Battifora H. The multitumor (sausage) tissue block: novel method for immunohistochemical antibody testing. *Lab Invest*. 1986;55(2):244-248.
487. Battifora H, Mehta P. The checkerboard tissue block. An improved multitissue control block. *Lab Invest*. 1990;63(5):722-724.
488. Kononen J, Bubendorf L, Kallioniemi A, et al. Tissue microarrays for high-throughput molecular profiling of tumor specimens. *Nat Med*. 1998;4(7):844-847.
489. Cresson CM. Vi-Cell XR Cell Viability Analyzer, User Instructions; 2006.
490. Bodnar AG, Ouellette M, Frolkis M, et al. Extension of life-span by introduction of telomerase into normal human cells. *Science*. 1998;279(5349):349-352.
491. Freshney RI ed Culture of Animal Cells. In: Edition F ed: Wiley-Liss; 2005.
492. Deguara CS, Pepas L, Davis C. Does minimally invasive surgery for endometriosis improve pelvic symptoms and quality of life? *Curr Opin Obstet Gynecol*. 2012;24(4):241-244.
493. Perie S, Meyers M, Mazzaschi O, De Crouy Chanel O, Baujat B, Lacau St Guily J. Epidemiology and anatomy of head and neck cancers. *Bull Cancer*. 2014;101(5):404-410.
494. Pellegrini C, Gori I, Achtari C, et al. The expression of estrogen receptors as well as GREB1, c-MYC, and cyclin D1, estrogen-regulated genes implicated in proliferation, is increased in peritoneal endometriosis. *Fertil Steril*. 2012;98(5):1200-1208.
495. Kalaany NY, Sabatini DM. Tumours with PI3K activation are resistant to dietary restriction. *Nature*. 2009;458(7239):725-731.
496. Program PC. Genetic and molecular pathways; 2013.
497. Velarde MC, Aghajanova L, Nezhat CR, Giudice LC. Increased mitogen-activated protein kinase kinase/extracellularly regulated kinase activity in human endometrial stromal fibroblasts of women with endometriosis reduces 3',5'-cyclic adenosine 5'-monophosphate inhibition of cyclin D1. *Endocrinology*. 2009;150(10):4701-4712.

498. Nachmani D, Stern-Ginossar N, Sarid R, Mandelboim O. Diverse herpesvirus microRNAs target the stress-induced immune ligand MICB to escape recognition by natural killer cells. *Cell Host Microbe*. 2009;5(4):376-385.
499. Cullen BR. Viral and cellular messenger RNA targets of viral microRNAs. *Nature*. 2009;457(7228):421-425.
500. Pfeffer S, Zavolan M, Grasser FA, et al. Identification of virus-encoded microRNAs. *Science*. 2004;304(5671):734-736.
501. Pfeffer S, Sewer A, Lagos-Quintana M, et al. Identification of microRNAs of the herpesvirus family. *Nat Methods*. 2005;2(4):269-276.
502. Jonjic S, Babic M, Polic B, Krmpotic A. Immune evasion of natural killer cells by viruses. *Curr Opin Immunol*. 2008;20(1):30-38.
503. Powers C, DeFilippis V, Malouli D, Fruh K. Cytomegalovirus immune evasion. *Curr Top Microbiol Immunol*. 2008;325:333-359.
504. Cesarman E. The role of Kaposi's sarcoma-associated herpesvirus (KSHV/HHV-8) in lymphoproliferative diseases. *Recent Results Cancer Res*. 2002;159:27-37.
505. Cesarman E. Epstein-Barr virus (EBV) and lymphomagenesis. *Front Biosci*. 2002;7:e58-65.
506. Bartel DP. MicroRNAs: target recognition and regulatory functions. *Cell*. 2009;136(2):215-233.
507. Gottwein E, Cullen BR. Viral and Cellular MicroRNAs as Determinants of Viral Pathogenesis and Immunity. *Cell Host & Microbe*. 2008;3(6):375-387.
508. Skalsky RL, Corcoran DL, Gottwein E, et al. The viral and cellular microRNA targetome in lymphoblastoid cell lines. *PLoS Pathog*. 2012;8(1):e1002484.
509. Thorley-Lawson DA, Allday MJ. The curious case of the tumour virus: 50 years of Burkitt's lymphoma. *Nat Rev Microbiol*. 2008;6(12):913-924.
510. Hecht JL, Aster JC. Molecular biology of Burkitt's lymphoma. *J Clin Oncol*. 2000;18(21):3707-3721.
511. Brooks L, Yao QY, Rickinson AB, Young LS. Epstein-Barr virus latent gene transcription in nasopharyngeal carcinoma cells: coexpression of EBNA1, LMP1, and LMP2 transcripts. *J Virol*. 1992;66(5):2689-2697.
512. Fahraeus R, Fu HL, Ernberg I, et al. Expression of Epstein-Barr virus-encoded proteins in nasopharyngeal carcinoma. *Int J Cancer*. 1988;42(3):329-338.
513. Wilson AD, Morgan AJ. Primary immune responses by cord blood CD4(+) T cells and NK cells inhibit Epstein-Barr virus B-cell transformation in vitro. *J Virol*. 2002;76(10):5071-5081.
514. Rokah OH, Granot G, Ovcharenko A, et al. Downregulation of miR-31, miR-155, and miR-564 in chronic myeloid leukemia cells. *PLoS One*. 2012;7(4):e35501.
515. Wang Z, Zhang H, Zhang P, Li J, Shan Z, Teng W. Upregulation of miR-2861 and miR-451 expression in papillary thyroid carcinoma with lymph node metastasis. *Med Oncol*. 2013;30(2):577.
516. Zeng X, Yin F, Liu X, et al. Upregulation of E2F transcription factor 3 is associated with poor prognosis in hepatocellular carcinoma. *Oncol Rep*. 2014.
517. Ren XS, Yin MH, Zhang X, et al. Tumor-suppressive microRNA-449a induces growth arrest and senescence by targeting E2F3 in human lung cancer cells. *Cancer Lett*. 2013.
518. Karlseder J, Rotheneder H, Wintersberger E. Interaction of Sp1 with the growth- and cell cycle-regulated transcription factor E2F. *Mol Cell Biol*. 1996;16(4):1659-1667.
519. Cheng JQ, Godwin AK, Bellacosa A, et al. AKT2, a putative oncogene encoding a member of a subfamily of protein-serine/threonine kinases, is amplified in human ovarian carcinomas. *Proc Natl Acad Sci U S A*. 1992;89(19):9267-9271.
520. Ocheni S, Olusina DB, Oyekunle AA, et al. EBV-Associated Malignancies. *The Open Infectious Diseases Journal*. 2010;4(4):101-112.
521. Butel JS. Viral carcinogenesis: revelation of molecular mechanisms and etiology of human disease. *Carcinogenesis*. 2000;21(3):405-426.

522. Carbone A, Gloghini A, Dotti G. EBV-associated lymphoproliferative disorders: classification and treatment. *Oncologist*. 2008;13(5):577-585.
523. Baumforth KR, Birgersdotter A, Reynolds GM, et al. Expression of the Epstein-Barr virus-encoded Epstein-Barr virus nuclear antigen 1 in Hodgkin's lymphoma cells mediates Up-regulation of CCL20 and the migration of regulatory T cells. *Am J Pathol*. 2008;173(1):195-204.
524. Baumforth KR, Young LS, Flavell KJ, Constandinou C, Murray PG. The Epstein-Barr virus and its association with human cancers. *Mol Pathol*. 1999;52(6):307-322.
525. Leung SY, Yuen ST, Chung LP, Kwong WK, Wong MP, Chan SY. Epstein-Barr virus is present in a wide histological spectrum of sinonasal carcinomas. *Am J Surg Pathol*. 1995;19(9):994-1001.
526. Analysis KP. Kegg Pathways; 2013.
527. Kutok JL, Wang F. Spectrum of Epstein-Barr virus-associated diseases. *Annu Rev Pathol*. 2006;1:375-404.
528. Hoagland RJ. The transmission of infectious mononucleosis. *Am J Med Sci*. 1955;229(3):262-272.
529. Liu YJ, Arpin C. Germinal center development. *Immunol Rev*. 1997;156:111-126.
530. Gruhne B, Sompallae R, Masucci MG. Three Epstein-Barr virus latency proteins independently promote genomic instability by inducing DNA damage, inhibiting DNA repair and inactivating cell cycle checkpoints. *Oncogene*. 2009;28(45):3997-4008.
531. Raptis S, Bapat B. Genetic instability in human tumors. *EXS*. 2006(96):303-320.
532. Uchida J, Yasui T, Takaoka-Shichijo Y, et al. Mimicry of CD40 signals by Epstein-Barr virus LMP1 in B lymphocyte responses. *Science*. 1999;286(5438):300-303.
533. Klein G. Constitutive activation of oncogenes by chromosomal translocations in B-cell derived tumors. *AIDS Res*. 1986;2 Suppl 1:S167-176.
534. Tierney RJ, Steven N, Young LS, Rickinson AB. Epstein-Barr virus latency in blood mononuclear cells: analysis of viral gene transcription during primary infection and in the carrier state. *J Virol*. 1994;68(11):7374-7385.
535. Khanna R, Burrows SR. Role of cytotoxic T lymphocytes in Epstein-Barr virus-associated diseases. *Annu Rev Microbiol*. 2000;54:19-48.
536. Wikipedia. Epstein–Barr virus; 2013.
537. Aman P, Ehlin-Henriksson B, Klein G. Epstein-Barr virus susceptibility of normal human B lymphocyte populations. *J Exp Med*. 1984;159(1):208-220.
538. Thorley-Lawson DA, Mann KP. Early events in Epstein-Barr virus infection provide a model for B cell activation. *J Exp Med*. 1985;162(1):45-59.
539. Yates JL, Warren N, Sugden B. Stable replication of plasmids derived from Epstein-Barr virus in various mammalian cells. *Nature*. 1985;313(6005):812-815.
540. Ling PD, Hsieh JJ, Ruf IK, Rawlins DR, Hayward SD. EBNA-2 upregulation of Epstein-Barr virus latency promoters and the cellular CD23 promoter utilizes a common targeting intermediate, CBF1. *J Virol*. 1994;68(9):5375-5383.
541. Thorley-Lawson DA. Epstein-Barr virus: exploiting the immune system. *Nat Rev Immunol*. 2001;1(1):75-82.
542. Kaiser C, Laux G, Eick D, Jochner N, Bornkamm GW, Kempkes B. The proto-oncogene c-myc is a direct target gene of Epstein-Barr virus nuclear antigen 2. *J Virol*. 1999;73(5):4481-4484.
543. Inoue J, Ishida T, Tsukamoto N, et al. Tumor necrosis factor receptor-associated factor (TRAF) family: adapter proteins that mediate cytokine signaling. *Exp Cell Res*. 2000;254(1):14-24.
544. Baker SJ, Reddy EP. Transducers of life and death: TNF receptor superfamily and associated proteins. *Oncogene*. 1996;12(1):1-9.
545. Kilger E, Kieser A, Baumann M, Hammerschmidt W. Epstein-Barr virus-mediated B-cell proliferation is dependent upon latent membrane protein 1, which simulates an activated CD40 receptor. *EMBO J*. 1998;17(6):1700-1709.

546. Zimber-Strobl U, Kempkes B, Marschall G, et al. Epstein-Barr virus latent membrane protein (LMP1) is not sufficient to maintain proliferation of B cells but both it and activated CD40 can prolong their survival. *EMBO J*. 1996;15(24):7070-7078.
547. Gires O, Zimber-Strobl U, Gonnella R, et al. Latent membrane protein 1 of Epstein-Barr virus mimics a constitutively active receptor molecule. *EMBO J*. 1997;16(20):6131-6140.
548. Lam KP, Kuhn R, Rajewsky K. In vivo ablation of surface immunoglobulin on mature B cells by inducible gene targeting results in rapid cell death. *Cell*. 1997;90(6):1073-1083.
549. Esquela-Kerscher A, Slack FJ. Oncomirs - microRNAs with a role in cancer. *Nat Rev Cancer*. 2006;6(4):259-269.
550. Pegtel DM, Cosmopoulos K, Thorley-Lawson DA, et al. Functional delivery of viral miRNAs via exosomes. *Proc Natl Acad Sci U S A*. 2010;107(14):6328-6333.
551. Mobius W, Ohno-Iwashita Y, van Donselaar EG, et al. Immunoelectron microscopic localization of cholesterol using biotinylated and non-cytolytic perfringolysin O. *J Histochem Cytochem*. 2002;50(1):43-55.
552. Thery C, Zitvogel L, Amigorena S. Exosomes: composition, biogenesis and function. *Nat Rev Immunol*. 2002;2(8):569-579.
553. Raposo G, Nijman HW, Stoorvogel W, et al. B lymphocytes secrete antigen-presenting vesicles. *J Exp Med*. 1996;183(3):1161-1172.
554. Yuan A, Farber EL, Rapoport AL, et al. Transfer of microRNAs by embryonic stem cell microvesicles. *PLoS One*. 2009;4(3):e4722.
555. Verweij FJ, van Eijndhoven MA, Middeldorp J, Pegtel DM. Analysis of Viral MicroRNA Exchange via Exosomes In Vitro and In Vivo. *Methods Mol Biol*. 2013;1024:53-68.
556. Assil S, Decembre E, Dreux M. [Exosomes are carriers for immunostimulatory viral RNA]. *Med Sci (Paris)*. 2013;29(1):104-106.
557. Dukers DF, Meij P, Vervoort MB, et al. Direct immunosuppressive effects of EBV-encoded latent membrane protein 1. *J Immunol*. 2000;165(2):663-670.
558. Mittelbrunn M, Sanchez-Madrid F. Intercellular communication: diverse structures for exchange of genetic information. *Nat Rev Mol Cell Biol*. 2012;13(5):328-335.
559. Thery C. Exosomes: secreted vesicles and intercellular communications. *F1000 Biol Rep*. 2011;3:15.
560. Thery C, Ostrowski M, Segura E. Membrane vesicles as conveyors of immune responses. *Nat Rev Immunol*. 2009;9(8):581-593.
561. Teles A, Zenclussen AC. How Cells of the Immune System Prepare the Endometrium for Implantation. *Semin Reprod Med*. 2014;32(5):358-364.
562. Mathur SP. Autoimmunity in endometriosis: relevance to infertility. *Am J Reprod Immunol*. 2000;44(2):89-95.
563. Hopwood P, Crawford DH. The role of EBV in post-transplant malignancies: a review. *J Clin Pathol*. 2000;53(4):248-254.
564. Arnon TI, Markel G, Mandelboim O. Tumor and viral recognition by natural killer cells receptors. *Semin Cancer Biol*. 2006;16(5):348-358.
565. Glas R, Franksson L, Une C, et al. Recruitment and activation of natural killer (NK) cells in vivo determined by the target cell phenotype. An adaptive component of NK cell-mediated responses. *J Exp Med*. 2000;191(1):129-138.
566. Oosterlynck DJ, Meuleman C, Waer M, Vandeputte M, Koninckx PR. The natural killer activity of peritoneal fluid lymphocytes is decreased in women with endometriosis. *Fertil Steril*. 1992;58(2):290-295.
567. Xin Y, Xu X, Ling H. [Expression of major histocompatibility complex-class I antigen on endometrial stroma cells in patients with endometriosis]. *Zhonghua Fu Chan Ke Za Zhi*. 2000;35(9):530-532.
568. Lee KS, Baek DW, Kim KH, et al. IL-10-dependent down-regulation of MHC class II expression level on monocytes by peritoneal fluid from endometriosis patients. *Int Immunopharmacol*. 2005;5(12):1699-1712.

569. Kasof GM, Goyal L, White E. Btf, a novel death-promoting transcriptional repressor that interacts with Bcl-2-related proteins. *Mol Cell Biol*. 1999;19(6):4390-4404.
570. Bai X, Hosler G, Rogers BB, Dawson DB, Scheuermann RH. Quantitative polymerase chain reaction for human herpesvirus diagnosis and measurement of Epstein-Barr virus burden in posttransplant lymphoproliferative disorder. *Clin Chem*. 1997;43(10):1843-1849.
571. Heslop HE, Slobod KS, Pule MA, et al. Long-term outcome of EBV-specific T-cell infusions to prevent or treat EBV-related lymphoproliferative disease in transplant recipients. *Blood*. 2010;115(5):925-935.
572. Comoli P, Labirio M, Basso S, et al. Infusion of autologous Epstein-Barr virus (EBV)-specific cytotoxic T cells for prevention of EBV-related lymphoproliferative disorder in solid organ transplant recipients with evidence of active virus replication. *Blood*. 2002;99(7):2592-2598.
573. Rooney CM, Roskrow MA, Smith CA, Brenner MK, Heslop HE. Immunotherapy for Epstein-Barr virus-associated cancers. *J Natl Cancer Inst Monogr*. 1998(23):89-93.
574. Kawada J, Zou P, Mazitschek R, Bradner JE, Cohen JI. Tubacin kills Epstein-Barr virus (EBV)-Burkitt lymphoma cells by inducing reactive oxygen species and EBV lymphoblastoid cells by inducing apoptosis. *J Biol Chem*. 2009;284(25):17102-17109.
575. Biosystems A. Protocol for Creating Custom RT and Preamplification Pools using TaqMan® MicroRNA Assays; 2013.
576. 9.05 SP. Known Genetic and Protein associations; 2013.
577. NCBI. RefSeq: NCBI Reference Sequence Database; 2013.
578. Database WIoS-O. Gene Cards-The Human gene Compendium; 2013.
579. Zhang H, Berezov A, Wang Q, et al. ErbB receptors: from oncogenes to targeted cancer therapies. *J Clin Invest*. 2007;117(8):2051-2058.
580. Harris SL, Levine AJ. The p53 pathway: positive and negative feedback loops. *Oncogene*. 2005;24(17):2899-2908.
581. Verit FF, Yucel O. Endometriosis, leiomyoma and adenomyosis: the risk of gynecologic malignancy. *Asian Pac J Cancer Prev*. 2013;14(10):5589-5597.
582. Robinson DR, Wu YM, Lin SF. The protein tyrosine kinase family of the human genome. *Oncogene*. 2000;19(49):5548-5557.
583. Zwick E, Bange J, Ullrich A. Receptor tyrosine kinase signalling as a target for cancer intervention strategies. *Endocr Relat Cancer*. 2001;8(3):161-173.
584. Dorsam RT, Gutkind JS. G-protein-coupled receptors and cancer. *Nat Rev Cancer*. 2007;7(2):79-94.
585. Audigier Y, Picault FX, Chaves-Almagro C, Masri B. G Protein-Coupled Receptors in cancer: biochemical interactions and drug design. *Prog Mol Biol Transl Sci*. 2013;115:143-173.
586. Ogawa K, Sun C, Horii A. Exploration of genetic alterations in human endometrial cancer and melanoma: distinct tumorigenic pathways that share a frequent abnormal PI3K/AKT cascade. *Oncol Rep*. 2005;14(6):1481-1485.
587. Wu G, Guo Z, Chang X, et al. LOXL1 and LOXL4 are epigenetically silenced and can inhibit ras/extracellular signal-regulated kinase signaling pathway in human bladder cancer. *Cancer Res*. 2007;67(9):4123-4129.
588. Garcia-Velasco JA, Arici A, Zreik T, Naftolin F, Mor G. Macrophage derived growth factors modulate Fas ligand expression in cultured endometrial stromal cells: a role in endometriosis. *Mol Hum Reprod*. 1999;5(7):642-650.
589. Wang DB, Xu YL, Chen P, Chen YH, Li Y. Silencing Cofilin-1 blocks PDGF-induced proliferation in eutopic endometrium of endometriosis patients. *Cell Biol Int*. 2013;37(8):799-804.
590. Bilotas M, Baranao RI, Buquet R, Sueldo C, Tesone M, Meresman G. Effect of GnRH analogues on apoptosis and expression of Bcl-2, Bax, Fas and FasL proteins in endometrial epithelial cell cultures from patients with endometriosis and controls. *Hum Reprod*. 2007;22(3):644-653.

591. Lustig B, Behrens J. The Wnt signaling pathway and its role in tumor development. *J Cancer Res Clin Oncol*. 2003;129(4):199-221.
592. Wikigenes. Wikigenes online genetic database; 2014.
593. Niikura T, Hirata R, Weil SC. A novel interferon-inducible gene expressed during myeloid differentiation. *Blood Cells Mol Dis*. 1997;23(3):337-349.
594. Zhou X, Michal JJ, Zhang L, et al. Interferon induced IFIT family genes in host antiviral defense. *Int J Biol Sci*. 2013;9(2):200-208.
595. Kohno T, Takakura S, Yamada T, Okamoto A, Tanaka T, Yokota J. Alterations of the PPP1R3 gene in human cancer. *Cancer Res*. 1999;59(17):4170-4174.
596. Hayashida Y, Goi T, Hirono Y, Katayama K, Urano T, Yamaguchi A. PPP1R3 gene (protein phosphatase 1) alterations in colorectal cancer and its relationship to metastasis. *Oncol Rep*. 2005;13(6):1223-1227.
597. Alcoser SY, Hara M, Bell GI, Ehrmann DA. Association of the (AU)AT-rich element polymorphism in PPP1R3 with hormonal and metabolic features of polycystic ovary syndrome. *J Clin Endocrinol Metab*. 2004;89(6):2973-2976.
598. Inoue K, Kohno T, Takakura S, et al. Alterations of the PPP1R3 gene in hematological malignancies. *Int J Oncol*. 2000;17(4):717-721.
599. Yang G, Cao K, Wu L, Wang R. Cystathionine gamma-lyase overexpression inhibits cell proliferation via a H2S-dependent modulation of ERK1/2 phosphorylation and p21Cip/WAK-1. *J Biol Chem*. 2004;279(47):49199-49205.
600. Moore LE, Malats N, Rothman N, et al. Polymorphisms in one-carbon metabolism and trans-sulfuration pathway genes and susceptibility to bladder cancer. *Int J Cancer*. 2007;120(11):2452-2458.
601. Moreau C, Froment P, Tosca L, Moreau V, Dupont J. Expression and regulation of the SCD2 desaturase in the rat ovary. *Biol Reprod*. 2006;74(1):75-87.
602. Ambrosio MR, Piccaluga PP, Ponzoni M, et al. The alteration of lipid metabolism in Burkitt lymphoma identifies a novel marker: adipophilin. *PLoS One*. 2012;7(8):e44315.
603. Chi RJ, Torres OT, Segarra VA, et al. Role of Scd5, a protein phosphatase-1 targeting protein, in phosphoregulation of Sla1 during endocytosis. *J Cell Sci*. 2012;125(Pt 20):4728-4739.
604. Thomas Shenk JDR, Josh Munger, Bryson Bennett. Treatment of viral infections by modulation of host cell metabolic pathways EP 2572712 A2. In: University TtoP ed; 2013.
605. Miyashita H, Sato Y. Metallothionein 1 is a downstream target of vascular endothelial zinc finger 1 (VEZF1) in endothelial cells and participates in the regulation of angiogenesis. *Endothelium*. 2005;12(4):163-170.
606. Aitsebaomo J, Kingsley-Kallesen ML, Wu Y, Quertermous T, Patterson C. Vezf1/DB1 is an endothelial cell-specific transcription factor that regulates expression of the endothelin-1 promoter. *J Biol Chem*. 2001;276(42):39197-39205.
607. Qiagen. Sample essays, Technologies and pathways; 2013.
608. Liu Y, Bourgeois CF, Pang S, et al. The germ cell nuclear proteins hnRNP G-T and RBMY activate a testis-specific exon. *PLoS Genet*. 2009;5(11):e1000707.
609. Ehrmann I, Dalgliesh C, Tsaousi A, et al. Haploinsufficiency of the germ cell-specific nuclear RNA binding protein hnRNP G-T prevents functional spermatogenesis in the mouse. *Hum Mol Genet*. 2008;17(18):2803-2818.
610. pathways Ms. 2013.
611. Fitzgibbon J, Neat MJ, Foot N, Hill AS, Lister TA, Gupta RK. Assignment of brain acid-soluble protein 1 (BASP1) to human chromosome 5p15.1-->p14, differential expression in human cancer cell lines as a result of alterations in gene dosage. *Cytogenet Cell Genet*. 2000;89(3-4):147-149.
612. Hartl M, Nist A, Khan MI, Valovka T, Bister K. Inhibition of Myc-induced cell transformation by brain acid-soluble protein 1 (BASP1). *Proc Natl Acad Sci U S A*. 2009;106(14):5604-5609.

613. Grinberg M, Schwarz M, Zaltsman Y, et al. Mitochondrial carrier homolog 2 is a target of tBID in cells signaled to die by tumor necrosis factor alpha. *Mol Cell Biol*. 2005;25(11):4579-4590.
614. Gross A. Mitochondrial carrier homolog 2: a clue to cracking the BCL-2 family riddle? *J Bioenerg Biomembr*. 2005;37(3):113-119.
615. Yu K, Ganesan K, Tan LK, et al. A precisely regulated gene expression cassette potently modulates metastasis and survival in multiple solid cancers. *PLoS Genet*. 2008;4(7):e1000129.
616. Delahanty RJ, Beeghly-Fadiel A, Xiang YB, et al. Association of obesity-related genetic variants with endometrial cancer risk: a report from the Shanghai Endometrial Cancer Genetics Study. *Am J Epidemiol*. 2011;174(10):1115-1126.
617. Yu HG, Nam JO, Miller NL, et al. p190RhoGEF (Rgnef) promotes colon carcinoma tumor progression via interaction with focal adhesion kinase. *Cancer Res*. 2011;71(2):360-370.
618. Sokolowski B, Orchard S, Harvey M, Sridhar S, Sakai Y. Conserved BK channel-protein interactions reveal signals relevant to cell death and survival. *PLoS One*. 2011;6(12):e28532.
619. Zhao R, Zhao ZJ. Dissecting the interaction of SHP-2 with PZR, an immunoglobulin family protein containing immunoreceptor tyrosine-based inhibitory motifs. *J Biol Chem*. 2000;275(8):5453-5459.
620. Zannettino AC, Roubelakis M, Welldon KJ, et al. Novel mesenchymal and haematopoietic cell isoforms of the SHP-2 docking receptor, PZR: identification, molecular cloning and effects on cell migration. *Biochem J*. 2003;370(Pt 2):537-549.
621. Roubelakis MG, Martin-Rendon E, Tsaknakis G, Stavropoulos A, Watt SM. The murine ortholog of the SHP-2 binding molecule, PZR accelerates cell migration on fibronectin and is expressed in early embryo formation. *J Cell Biochem*. 2007;102(4):955-969.
622. Kalma Y, Granot I, Gnainsky Y, et al. Endometrial biopsy-induced gene modulation: first evidence for the expression of bladder-transmembranal uroplakin Ib in human endometrium. *Fertil Steril*. 2009;91(4):1042-1049, 1049 e1041-1049.
623. . !!! INVALID CITATION !!!
624. Bradel-Tretheway BG, Mattiacio JL, Krasnoselsky A, et al. Comprehensive proteomic analysis of influenza virus polymerase complex reveals a novel association with mitochondrial proteins and RNA polymerase accessory factors. *J Virol*. 2011;85(17):8569-8581.
625. Munier S, Rolland T, Diot C, Jacob Y, Naffakh N. Exploration of binary virus-host interactions using an infectious protein complementation assay. *Mol Cell Proteomics*. 2013.
626. Gosens I, Sessa A, den Hollander AI, et al. FERM protein EPB41L5 is a novel member of the mammalian CRB-MPP5 polarity complex. *Exp Cell Res*. 2007;313(19):3959-3970.
627. Schulz WA, Ingenwerth M, Djuidje CE, Hader C, Rahnenfuhrer J, Engers R. Changes in cortical cytoskeletal and extracellular matrix gene expression in prostate cancer are related to oncogenic ERG deregulation. *BMC Cancer*. 2010;10:505.
628. Little NA, Hastie ND, Davies RC. Identification of WTAP, a novel Wilms' tumour 1-associating protein. *Hum Mol Genet*. 2000;9(15):2231-2239.
629. Small TW, Pickering JG. Nuclear degradation of Wilms tumor 1-associating protein and survivin splice variant switching underlie IGF-1-mediated survival. *J Biol Chem*. 2009;284(37):24684-24695.
630. Kim SH, Lubec G. Decreased alpha-endosulfine, an endogenous regulator of ATP-sensitive potassium channels, in brains from adult Down syndrome patients. *J Neural Transm Suppl*. 2001(61):1-9.
631. Wang H, Craig RL, Schay J, et al. Alpha-endosulfine, a positional and functional candidate gene for type 2 diabetes: molecular screening, association studies, and role in reduced insulin secretion. *Mol Genet Metab*. 2004;81(1):9-15.
632. Kansaku A, Hirabayashi S, Mori H, et al. Ligand-of-Numb protein X is an endocytic scaffold for junctional adhesion molecule 4. *Oncogene*. 2006;25(37):5071-5084.
633. Wai Wong C, Dye DE, Coombe DR. The role of immunoglobulin superfamily cell adhesion molecules in cancer metastasis. *Int J Cell Biol*. 2012;2012:340296.
634. foundation KAW. The Human Protein Atlas; 2013.

635. Gorodeski GI. Estrogen decrease in tight junctional resistance involves matrix-metalloproteinase-7-mediated remodeling of occludin. *Endocrinology*. 2007;148(1):218-231.
636. Rao RK, Basuroy S, Rao VU, Karnaky Jr KJ, Gupta A. Tyrosine phosphorylation and dissociation of occludin-ZO-1 and E-cadherin-beta-catenin complexes from the cytoskeleton by oxidative stress. *Biochem J*. 2002;368(Pt 2):471-481.
637. Tobioka H, Isomura H, Kokai Y, Tokunaga Y, Yamaguchi J, Sawada N. Occludin expression decreases with the progression of human endometrial carcinoma. *Hum Pathol*. 2004;35(2):159-164.
638. Jones NP, Katan M. Role of phospholipase Cgamma1 in cell spreading requires association with a beta-Pix/GIT1-containing complex, leading to activation of Cdc42 and Rac1. *Mol Cell Biol*. 2007;27(16):5790-5805.
639. Hsu RM, Tsai MH, Hsieh YJ, Lyu PC, Yu JS. Identification of MYO18A as a novel interacting partner of the PAK2/betaPIX/GIT1 complex and its potential function in modulating epithelial cell migration. *Mol Biol Cell*. 2010;21(2):287-301.
640. Duband-Goulet I, Courvalin JC, Buendia B. LBR, a chromatin and lamin binding protein from the inner nuclear membrane, is proteolyzed at late stages of apoptosis. *J Cell Sci*. 1998;111 (Pt 10):1441-1451.
641. LIN H-c. Screening for membrane proteins differentially expressed between the lung adenocarcinoma cell lines with high- and low-metastatic potential using iTRAQ technology. *Tumor*. 2013;33(2):150-156.
642. Teng CH, Huang WN, Meng TC. Several dual specificity phosphatases coordinate to control the magnitude and duration of JNK activation in signaling response to oxidative stress. *J Biol Chem*. 2007;282(39):28395-28407.
643. Keyse SM. Dual-specificity MAP kinase phosphatases (MKPs) and cancer. *Cancer Metastasis Rev*. 2008;27(2):253-261.
644. Yao Q, Qu X, Yang Q, Wei M, Kong B. CLIC4 mediates TGF-beta1-induced fibroblast-to-myofibroblast transdifferentiation in ovarian cancer. *Oncol Rep*. 2009;22(3):541-548.
645. Shukla A, Edwards R, Yang Y, et al. CLIC4 regulates TGF-beta-dependent myofibroblast differentiation to produce a cancer stroma. *Oncogene*. 2013.
646. Chen CB, Ng JK, Choo PH, Wu W, Porter AG. Mammalian sterile 20-like kinase 3 (MST3) mediates oxidative-stress-induced cell death by modulating JNK activation. *Biosci Rep*. 2009;29(6):405-415.
647. Lu TJ, Lai WY, Huang CY, et al. Inhibition of cell migration by autophosphorylated mammalian sterile 20-like kinase 3 (MST3) involves paxillin and protein-tyrosine phosphatase-PEST. *J Biol Chem*. 2006;281(50):38405-38417.
648. Ripka S, Konig A, Buchholz M, et al. WNT5A--target of CUTL1 and potent modulator of tumor cell migration and invasion in pancreatic cancer. *Carcinogenesis*. 2007;28(6):1178-1187.
649. Xu H, He JH, Xiao ZD, et al. Liver-enriched transcription factors regulate microRNA-122 that targets CUTL1 during liver development. *Hepatology*. 2010;52(4):1431-1442.
650. Hu L, Zhu YT, Qi C, Zhu YJ. Identification of Smyd4 as a potential tumor suppressor gene involved in breast cancer development. *Cancer Res*. 2009;69(9):4067-4072.
651. Kudo LC, Parfenova L, Ren G, et al. Puromycin-sensitive aminopeptidase (PSA/NPEPPS) impedes development of neuropathology in hPSA/TAU(P301L) double-transgenic mice. *Hum Mol Genet*. 2011;20(9):1820-1833.
652. Green MR, Aya-Bonilla C, Gandhi MK, et al. Integrative genomic profiling reveals conserved genetic mechanisms for tumorigenesis in common entities of non-Hodgkin's lymphoma. *Genes Chromosomes Cancer*. 2011;50(5):313-326.
653. Kee HJ, Koh JT, Kim MY, et al. Expression of brain-specific angiogenesis inhibitor 2 (BAI2) in normal and ischemic brain: involvement of BAI2 in the ischemia-induced brain angiogenesis. *J Cereb Blood Flow Metab*. 2002;22(9):1054-1067.
654. Bennett RL, Blalock WL, Abtahi DM, Pan Y, Moyer SA, May WS. RAX, the PKR activator, sensitizes cells to inflammatory cytokines, serum withdrawal, chemotherapy, and viral infection. *Blood*. 2006;108(3):821-829.

655. Takada Y, Ichikawa H, Pataer A, Swisher S, Aggarwal BB. Genetic deletion of PKR abrogates TNF-induced activation of IkappaBalpha kinase, JNK, Akt and cell proliferation but potentiates p44/p42 MAPK and p38 MAPK activation. *Oncogene*. 2007;26(8):1201-1212.
656. Yoshino O, Osuga Y, Hirota Y, et al. Possible pathophysiological roles of mitogen-activated protein kinases (MAPKs) in endometriosis. *Am J Reprod Immunol*. 2004;52(5):306-311.
657. Ghosh S, Ghosh A, Maiti GP, et al. Alterations of 3p21.31 tumor suppressor genes in head and neck squamous cell carcinoma: Correlation with progression and prognosis. *Int J Cancer*. 2008;123(11):2594-2604.
658. da Costa Prando E, Cavalli LR, Rainho CA. Evidence of epigenetic regulation of the tumor suppressor gene cluster flanking RASSF1 in breast cancer cell lines. *Epigenetics*. 2011;6(12):1413-1424.
659. Mitra S, Mazumder Indra D, Basu PS, et al. Alterations of RASSF1A in premalignant cervical lesions: clinical and prognostic significance. *Mol Carcinog*. 2012;51(9):723-733.
660. Chiang Y, Chou CY, Hsu KF, Huang YF, Shen MR. EGF upregulates Na+/H+ exchanger NHE1 by post-translational regulation that is important for cervical cancer cell invasiveness. *J Cell Physiol*. 2008;214(3):810-819.
661. Shi Y, Kim D, Caldwell M, Sun D. The role of Na(+)/h (+) exchanger isoform 1 in inflammatory responses: maintaining H(+) homeostasis of immune cells. *Adv Exp Med Biol*. 2013;961:411-418.
662. Zhang X, Wu M, Xiao H, et al. Methylation of a single intronic CpG mediates expression silencing of the PMP24 gene in prostate cancer. *Prostate*. 2010;70(7):765-776.
663. Fletcher JM, Jordan MA, Snelgrove SL, et al. Congenic analysis of the NKT cell control gene Nkt2 implicates the peroxisomal protein Pxmp4. *J Immunol*. 2008;181(5):3400-3412.
664. Laird KM, Briggs LL, Boss JM, Summers MF, Garvie CW. Solution structure of the heterotrimeric complex between the interaction domains of RFX5 and RFXAP from the RFX gene regulatory complex. *J Mol Biol*. 2010;403(1):40-51.
665. Mudhasani R, Fontes JD. Multiple interactions between BRG1 and MHC class II promoter binding proteins. *Mol Immunol*. 2005;42(6):673-682.
666. Nagarajan UM, Long AB, Harreman MT, Corbett AH, Boss JM. A hierarchy of nuclear localization signals governs the import of the regulatory factor X complex subunits and MHC class II expression. *J Immunol*. 2004;173(1):410-419.
667. Backofen B, Jacob R, Serth K, Gossler A, Naim HY, Leeb T. Cloning and characterization of the mammalian-specific nicolin 1 gene (NICN1) encoding a nuclear 24 kDa protein. *Eur J Biochem*. 2002;269(21):5240-5245.
668. Pavsic M, Vito T, Lenarcic B. Purification and characterization of a recombinant human testican-2 expressed in baculovirus-infected Sf9 insect cells. *Protein Expr Purif*. 2008;58(1):132-139.
669. Ren F, Wang DB, Li T. [Epigenetic inactivation of SPOCK2 in the malignant transformation of ovarian endometriosis]. *Zhonghua Fu Chan Ke Za Zhi*. 2011;46(11):822-825.
670. Signorile PG, Baldi F, Bussani R, et al. Embryologic origin of endometriosis: analysis of 101 human female fetuses. *J Cell Physiol*. 2012;227(4):1653-1656.
671. Goldwyn RM. Gray's anatomy. *Plast Reconstr Surg*. 1985;76(1):147-148.
672. Loeb LA, Loeb KR, Anderson JP. Multiple mutations and cancer. *Proc Natl Acad Sci U S A*. 2003;100(3):776-781.
673. Perkins ND. Integrating cell-signalling pathways with NF-kappaB and IKK function. *Nat Rev Mol Cell Biol*. 2007;8(1):49-62.
674. Clarke DJ. Proteolysis and the cell cycle. *Cell Cycle*. 2002;1(4):233-234.
675. Alberts B JA, Lewis J, et al. Molecular Biology of the Cell 4th Edition: New York: Garland Science; 2002.
676. Jackson AM, Boutell J, Cooley N, He M. Cell-free protein synthesis for proteomics. *Brief Funct Genomic Proteomic*. 2004;2(4):308-319.

677. Gnjatic S, Wheeler C, Ebner M, et al. Seromic analysis of antibody responses in non-small cell lung cancer patients and healthy donors using conformational protein arrays. *J Immunol Methods*. 2009;341(1-2):50-58.
678. Pappworth IY, Kulik L, Haluszczak C, Reuter JW, Holers VM, Marchbank KJ. Increased B cell deletion and significantly reduced auto-antibody titre due to premature expression of human complement receptor 2 (CR2, CD21). *Mol Immunol*. 2009;46(6):1042-1049.
679. Fanarraga ML, Bellido J, Jaen C, Villegas JC, Zabala JC. TBCD links centriologenesis, spindle microtubule dynamics, and midbody abscission in human cells. *PLoS One*. 2010;5(1):e8846.
680. Zhao F, Siu MK, Jiang L, et al. Overexpression of dedicator of cytokinesis I (Dock180) in ovarian cancer correlated with aggressive phenotype and poor patient survival. *Histopathology*. 2011;59(6):1163-1172.
681. Hage-Sleiman R, Herveau S, Matera EL, Laurier JF, Dumontet C. Tubulin binding cofactor C (TBCC) suppresses tumor growth and enhances chemosensitivity in human breast cancer cells. *BMC Cancer*. 2010;10:135.
682. Yokoyama Y, Sato S, Futagami M, et al. Prognostic significance of vascular endothelial growth factor and its receptors in endometrial carcinoma. *Gynecol Oncol*. 2000;77(3):413-418.
683. Konno R, Sato S, Yajima A. A questionnaire survey on current surgical procedures for endometrial cancer in Japan. *Tohoku J Exp Med*. 2000;190(3):193-203.
684. Sagona AP, Stenmark H. Cytokinesis and cancer. *FEBS Lett*. 2010;584(12):2652-2661.
685. Chen Y, Deng L, Maeno-Hikichi Y, et al. Formation of an endophilin-Ca2+ channel complex is critical for clathrin-mediated synaptic vesicle endocytosis. *Cell*. 2003;115(1):37-48.
686. Wu X, Gan B, Yoo Y, Guan JL. FAK-mediated src phosphorylation of endophilin A2 inhibits endocytosis of MT1-MMP and promotes ECM degradation. *Dev Cell*. 2005;9(2):185-196.
687. Sounni NE, Devy L, Hajitou A, et al. MT1-MMP expression promotes tumor growth and angiogenesis through an up-regulation of vascular endothelial growth factor expression. *FASEB J*. 2002;16(6):555-564.
688. Shankar J, Messenberg A, Chan J, Underhill TM, Foster LJ, Nabi IR. Pseudopodial actin dynamics control epithelial-mesenchymal transition in metastatic cancer cells. *Cancer Res*;70(9):3780-3790.
689. Defilippi P, Di Stefano P, Cabodi S. p130Cas: a versatile scaffold in signaling networks. *Trends Cell Biol*. 2006;16(5):257-263.
690. Birgegard A, Bjorck C, Norring C, Sohlberg S, Clinton D. Anorexic self-control and bulimic self-hate: differential outcome prediction from initial self-image. *Int J Eat Disord*. 2009;42(6):522-530.
691. Le Masne Q, Pothier H, Birge NO, Urbina C, Esteve D. Asymmetric noise probed with a josephson junction. *Phys Rev Lett*. 2009;102(6):067002.
692. Rivard RL, Birger M, Gaston KJ, Howe AK. AKAP-independent localization of type-II protein kinase A to dynamic actin microspikes. *Cell Motil Cytoskeleton*. 2009;66(9):693-709.
693. Terada R, Yasutake T, Nakamura S, et al. Evaluation of metastatic potential of gastric tumors by staining for proliferating cell nuclear antigen and chromosome 17 numerical aberrations. *Ann Surg Oncol*. 2001;8(6):525-532.
694. Cabodi S, Tinnirello A, Di Stefano P, et al. p130Cas as a new regulator of mammary epithelial cell proliferation, survival, and HER2-neu oncogene-dependent breast tumorigenesis. *Cancer Res*. 2006;66(9):4672-4680.
695. Zhang RJ, Wild RA, Ojago JM. Effect of tumor necrosis factor-alpha on adhesion of human endometrial stromal cells to peritoneal mesothelial cells: an in vitro system. *Fertil Steril*. 1993;59(6):1196-1201.
696. Chen DB, Yang ZM, Hilsenrath R, Le SP, Harper MJ. Stimulation of prostaglandin (PG) F2 alpha and PGE2 release by tumour necrosis factor-alpha and interleukin-1 alpha in cultured human luteal phase endometrial cells. *Hum Reprod*. 1995;10(10):2773-2780.

697. Wortzman M, Watts TH. Workshop summary: functions of the TNF family in infectious disease. *Adv Exp Med Biol*;691:171-175.
698. Gonzalez-Ramos R, Donnez J, Defrere S, et al. Nuclear factor-kappa B is constitutively activated in peritoneal endometriosis. *Mol Hum Reprod*. 2007;13(7):503-509.
699. Perkins ND. NF-kappaB: tumor promoter or suppressor? *Trends Cell Biol*. 2004;14(2):64-69.
700. Tergaonkar V, Pando M, Vafa O, Wahl G, Verma I. p53 stabilization is decreased upon NFkappaB activation: a role for NFkappaB in acquisition of resistance to chemotherapy. *Cancer Cell*. 2002;1(5):493-503.
701. Stern RC, Dash R, Bentley RC, Snyder MJ, Haney AF, Robboy SJ. Malignancy in endometriosis: frequency and comparison of ovarian and extraovarian types. *Int J Gynecol Pathol*. 2001;20(2):133-139.
702. Dahlman-Wright K, Cavailles V, Fuqua SA, et al. International Union of Pharmacology. LXIV. Estrogen receptors. *Pharmacol Rev*. 2006;58(4):773-781.
703. Matsuzaki S, Murakami T, Uehara S, Canis M, Sasano H, Okamura K. Expression of estrogen receptor alpha and beta in peritoneal and ovarian endometriosis. *Fertil Steril*. 2001;75(6):1198-1205.
704. Druckmann R, Rohr UD. IGF-1 in gynaecology and obstetrics: update 2002. *Maturitas*. 2002;41 Suppl 1:S65-83.
705. Hinds MG, Norton RS, Vaux DL, Day CL. Solution structure of a baculoviral inhibitor of apoptosis (IAP) repeat. *Nat Struct Biol*. 1999;6(7):648-651.
706. Bertrand MJ, Milutinovic S, Dickson KM, et al. cIAP1 and cIAP2 facilitate cancer cell survival by functioning as E3 ligases that promote RIP1 ubiquitination. *Mol Cell*. 2008;30(6):689-700.
707. Karin M, Cao Y, Greten FR, Li ZW. NF-kappaB in cancer: from innocent bystander to major culprit. *Nat Rev Cancer*. 2002;2(4):301-310.
708. Vallabhapurapu S, Matsuzawa A, Zhang W, et al. Nonredundant and complementary functions of TRAF2 and TRAF3 in a ubiquitination cascade that activates NIK-dependent alternative NF-kappaB signaling. *Nat Immunol*. 2008;9(12):1364-1370.
709. Liu Z, Li H, Wu X, et al. Detachment-induced upregulation of XIAP and cIAP2 delays anoikis of intestinal epithelial cells. *Oncogene*. 2006;25(59):7680-7690.
710. Hamanaka RB, Bobrovnikova-Marjon E, Ji X, Liebhaber SA, Diehl JA. PERK-dependent regulation of IAP translation during ER stress. *Oncogene*. 2009;28(6):910-920.
711. Tang HY, Beer LA, Tanyi JL, Zhang R, Liu Q, Speicher DW. Protein isoform-specific validation defines multiple chloride intracellular channel and tropomyosin isoforms as serological biomarkers of ovarian cancer. *J Proteomics*. 2013;89:165-178.
712. Aalberse JA, Kapitein B, de Roock S, et al. Cord blood CD4+ T cells respond to self heat shock protein 60 (HSP60). *PLoS One*. 2011;6(9):e24119.
713. Pockley AG. The heat shock protein Hsp60 as an intercellular signalling molecule. Expert Rev Mol Med: Cambridge Journals; 2001:http://journals.cambridge.org/fulltext_content/ERM/ERM3_23/S1462399401003556sup1462399401003003.pdf.
714. Wikipedia. Online Encyclopedia; 2013.
715. Ye T, Zhang X. Involvement of Ran in the regulation of phagocytosis against virus infection in S2 cells. *Dev Comp Immunol*. 2013;41(4):491-497.
716. Wang S, Li Y, Hu YH, et al. STUB1 is essential for T-cell activation by ubiquitinating CARMA1. *Eur J Immunol*. 2013;43(4):1034-1041.
717. Ruckova E, Muller P, Nenutil R, Vojtesek B. Alterations of the Hsp70/Hsp90 chaperone and the HOP/CHIP co-chaperone system in cancer. *Cell Mol Biol Lett*. 2012;17(3):446-458.
718. Li D, Marchenko ND, Schulz R, et al. Functional inactivation of endogenous MDM2 and CHIP by HSP90 causes aberrant stabilization of mutant p53 in human cancer cells. *Mol Cancer Res*. 2011;9(5):577-588.

719. Huttner WB, Schmidt A. Lipids, lipid modification and lipid-protein interaction in membrane budding and fission--insights from the roles of endophilin A1 and synaptophysin in synaptic vesicle endocytosis. *Curr Opin Neurobiol*. 2000;10(5):543-551.
720. Ren G, Vajjhala P, Lee JS, Winsor B, Munn AL. The BAR domain proteins: molding membranes in fission, fusion, and phagy. *Microbiol Mol Biol Rev*. 2006;70(1):37-120.
721. Owens LV, Xu L, Craven RJ, et al. Overexpression of the focal adhesion kinase (p125FAK) in invasive human tumors. *Cancer Res*. 1995;55(13):2752-2755.
722. Cance WG, Harris JE, Iacocca MV, et al. Immunohistochemical analyses of focal adhesion kinase expression in benign and malignant human breast and colon tissues: correlation with preinvasive and invasive phenotypes. *Clin Cancer Res*. 2000;6(6):2417-2423.
723. Kornberg LJ. Focal adhesion kinase and its potential involvement in tumor invasion and metastasis. *Head Neck*. 1998;20(8):745-752.
724. Rajashekhar G, Traktuev DO, Roell WC, et al. IFATS collection: Adipose stromal cell differentiation is reduced by endothelial cell contact and paracrine communication: role of canonical Wnt signaling. *Stem Cells*. 2008;26(10):2674-2681.
725. Kluin-Nelemans HC, Hoster E, Hermine O, et al. Treatment of older patients with mantle-cell lymphoma. *N Engl J Med*;367(6):520-531.
726. Mu L, Zheng W, Wang L, Chen X, Yang J. Focal adhesion kinase expression in ovarian endometriosis. *Int J Gynaecol Obstet*. 2008;101(2):161-165.
727. Mu L, Zheng W, Wang L, Chen XJ, Zhang X, Yang JH. Alteration of focal adhesion kinase expression in eutopic endometrium of women with endometriosis. *Fertil Steril*. 2008;89(3):529-537.
728. Birge RB, Kalodimos C, Inagaki F, Tanaka S. Crk and CrkL adaptor proteins: networks for physiological and pathological signaling. *Cell Commun Signal*. 2009;7:13.
729. Philippeaux MM, Piguet PF. Expression of tumor necrosis factor-alpha and its mRNA in the endometrial mucosa during the menstrual cycle. *Am J Pathol*. 1993;143(2):480-486.
730. Calhaz-Jorge C, Costa AP, Barata M, Santos MC, Melo A, Palma-Carlos ML. Tumour necrosis factor alpha concentrations in the peritoneal fluid of infertile women with minimal or mild endometriosis are lower in patients with red lesions only than in patients without red lesions. *Hum Reprod*. 2000;15(6):1256-1260.
731. Hunt JS, Chen HL, Hu XL, Tabibzadeh S. Tumor necrosis factor-alpha messenger ribonucleic acid and protein in human endometrium. *Biol Reprod*. 1992;47(1):141-147.
732. Guicciardi ME, Gores GJ. Life and death by death receptors. *FASEB J*. 2009;23(6):1625-1637.
733. Watts TH. TNF/TNFR family members in costimulation of T cell responses. *Annu Rev Immunol*. 2005;23:23-68.
734. Rojas-Cartagena C, Appleyard CB, Santiago OI, Flores I. Experimental intestinal endometriosis is characterized by increased levels of soluble TNFRSF1B and downregulation of Tnfrsf1a and Tnfrsf1b gene expression. *Biol Reprod*. 2005;73(6):1211-1218.
735. Falconer H, Mwenda JM, Chai DC, et al. Treatment with anti-TNF monoclonal antibody (c5N) reduces the extent of induced endometriosis in the baboon. *Hum Reprod*. 2006;21(7):1856-1862.
736. D'Hooghe TM, Nugent NP, Cuneo S, et al. Recombinant human TNFRSF1A (r-hTBP1) inhibits the development of endometriosis in baboons: a prospective, randomized, placebo- and drug-controlled study. *Biol Reprod*. 2006;74(1):131-136.
737. SABiosciences. Estrogen Pathway; 2013.
738. Kitawaki J, Obayashi H, Ishihara H, et al. Oestrogen receptor-alpha gene polymorphism is associated with endometriosis, adenomyosis and leiomyomata. *Hum Reprod*. 2001;16(1):51-55.
739. Wieser F, Schneeberger C, Tong D, Tempfer C, Huber JC, Wenzl R. PROGINS receptor gene polymorphism is associated with endometriosis. *Fertil Steril*. 2002;77(2):309-312.
740. Bulun SE, Zeitoun KM, Takayama K, Sasano H. Estrogen biosynthesis in endometriosis: molecular basis and clinical relevance. *J Mol Endocrinol*. 2000;25(1):35-42.

741. Baranova H, Canis M, Ivaschenko T, et al. Possible involvement of arylamine N-acetyltransferase 2, glutathione S-transferases M1 and T1 genes in the development of endometriosis. *Mol Hum Reprod*. 1999;5(7):636-641.
742. Hadfield RM, Manek S, Weeks DE, Mardon HJ, Barlow DH, Kennedy SH. Linkage and association studies of the relationship between endometriosis and genes encoding the detoxification enzymes GSTM1, GSTT1 and CYP1A1. *Mol Hum Reprod*. 2001;7(11):1073-1078.
743. Nakago S, Hadfield RM, Zondervan KT, et al. Association between endometriosis and N-acetyl transferase 2 polymorphisms in a UK population. *Mol Hum Reprod*. 2001;7(11):1079-1083.
744. Bulun SE, Zeitoun KM, Kilic G. Expression of dioxin-related transactivating factors and target genes in human eutopic endometrial and endometriotic tissues. *Am J Obstet Gynecol*. 2000;182(4):767-775.
745. Lukanova A, Zeleniuch-Jacquotte A, Lundin E, et al. Prediagnostic levels of C-peptide, IGF-I, IGFBP -1, -2 and -3 and risk of endometrial cancer. *Int J Cancer*. 2004;108(2):262-268.
746. Hu S, Yang X. Cellular inhibitor of apoptosis 1 and 2 are ubiquitin ligases for the apoptosis inducer Smac/DIABLO. *J Biol Chem*. 2003;278(12):10055-10060.
747. Wang CY, Mayo MW, Korneluk RG, Goeddel DV, Baldwin AS, Jr. NF-kappaB antiapoptosis: induction of TRAF1 and TRAF2 and c-IAP1 and c-IAP2 to suppress caspase-8 activation. *Science*. 1998;281(5383):1680-1683.
748. Karin M, Lin A. NF-kappaB at the crossroads of life and death. *Nat Immun*. 2002;3(3):221-227.
749. Siebenlist U, Brown K, Claudio E. Control of lymphocyte development by nuclear factor-kappaB. *Nat Rev Immunol*. 2005;5(6):435-445.
750. Liu Z, Li H, Derouet M, et al. ras Oncogene triggers up-regulation of cIAP2 and XIAP in intestinal epithelial cells: epidermal growth factor receptor-dependent and -independent mechanisms of ras-induced transformation. *J Biol Chem*. 2005;280(45):37383-37392.
751. Dai Z, Zhu WG, Morrison CD, et al. A comprehensive search for DNA amplification in lung cancer identifies inhibitors of apoptosis cIAP1 and cIAP2 as candidate oncogenes. *Hum Mol Genet*. 2003;12(7):791-801.
752. Lau R, Pratt MA. The opposing roles of cellular inhibitor of apoptosis proteins in cancer. *ISRN Oncol*. 2012;2012:928120.
753. Zhu S, Wu H, Wu F, Nie D, Sheng S, Mo YY. MicroRNA-21 targets tumor suppressor genes in invasion and metastasis. *Cell Res*. 2008;18(3):350-359.
754. Varga AE, Stourman NV, Zheng Q, et al. Silencing of the Tropomyosin-1 gene by DNA methylation alters tumor suppressor function of TGF-beta. *Oncogene*. 2005;24(32):5043-5052.
755. Hjerpe E, Egyhazi S, Carlson J, et al. HSP60 predicts survival in advanced serous ovarian cancer. *Int J Gynecol Cancer*. 2013;23(3):448-455.
756. Schneider J, Jimenez E, Marenbach K, Romero H, Marx D, Meden H. Immunohistochemical detection of HSP60-expression in human ovarian cancer. Correlation with survival in a series of 247 patients. *Anticancer Res*. 1999;19(3A):2141-2146.
757. Lebret T, Watson RW, Molinie V, et al. Heat shock proteins HSP27, HSP60, HSP70, and HSP90: expression in bladder carcinoma. *Cancer*. 2003;98(5):970-977.
758. Zhang L, Koivisto L, Heino J, Uitto VJ. Bacterial heat shock protein 60 may increase epithelial cell migration through activation of MAP kinases and inhibition of alpha6beta4 integrin expression. *Biochem Biophys Res Commun*. 2004;319(4):1088-1095.
759. Noda T, Murakami T, Terada Y, Yaegashi N, Okamura K. Increased production of tumor necrosis factor-alpha by peritoneal fluid mononuclear cells induced by 60-kDa heat shock protein in women with minimal to mild endometriosis. *Am J Reprod Immunol*. 2003;50(5):427-432.
760. Sampson ER, Yeh SY, Chang HC, et al. Identification and characterization of androgen receptor associated coregulators in prostate cancer cells. *J Biol Regul Homeost Agents*. 2001;15(2):123-129.

761. Li H, Ren CP, Tan XJ, et al. Identification of genes related to nasopharyngeal carcinoma with the help of pathway-based networks. *Acta Biochim Biophys Sin (Shanghai)*. 2006;38(12):900-910.
762. Yuen HF, Gunasekharan VK, Chan KK, et al. RanGTPase: a candidate for Myc-mediated cancer progression. *J Natl Cancer Inst*. 2013;105(7):475-488.
763. Jan CI, Yu CC, Hung MC, et al. Tid1, CHIP and ErbB2 interactions and their prognostic implications for breast cancer patients. *J Pathol*. 2011;225(3):424-437.
764. Rual JF, Venkatesan K, Hao T, et al. Towards a proteome-scale map of the human protein-protein interaction network. *Nature*. 2005;437(7062):1173-1178.
765. Breton S. The cellular physiology of carbonic anhydrases. *JOP*. 2001;2(4 Suppl):159-164.
766. Helmholtz. Patent EP2384766 A1- Novel antibody to a carbonic anhydrase. Vol. EP2384766 A1. Germany; 2010.
767. Nordfors K, Haapasalo J, Korja M, et al. The tumour-associated carbonic anhydrases CA II, CA IX and CA XII in a group of medulloblastomas and supratentorial primitive neuroectodermal tumours: an association of CA IX with poor prognosis. *BMC Cancer*. 2010;10:148.
768. Manokaran S, Berg A, Zhang X, Chen W, Srivastava DK. Modulation of Ligand Binding Affinity of Tumorigenic Carbonic Anhydrase XII upon Interaction with Cationic CdTe Quantum Dots. *J Biomed Nanotechnol*. 2008;4(4):491-498.
769. Brinton DA, Quattrociocchi-Longe TM, Kiechle FL. Endometriosis: identification by carbonic anhydrase autoantibodies and clinical features. *Ann Clin Lab Sci*. 1996;26(5):409-420.
770. Kiechle FL, Quattrociocchi-Longe TM, Brinton DA. Carbonic anhydrase antibody in sera from patients with endometriosis. *Am J Clin Pathol*. 1994;101(5):611-615.
771. D'Cruz OJ, Wild RA, Haas GG, Jr., Reichlin M. Antibodies to carbonic anhydrase in endometriosis: prevalence, specificity, and relationship to clinical and laboratory parameters. *Fertil Steril*. 1996;66(4):547-556.
772. Walter M, Berg H, Leidenberger FA, Schweppe KW, Northemann W. Autoreactive epitopes within the human alpha-enolase and their recognition by sera from patients with endometriosis. *J Autoimmun*. 1995;8(6):931-945.
773. Reimand K, Talja I, Metskula K, Kadastik U, Matt K, Uibo R. Autoantibody studies of female patients with reproductive failure. *J Reprod Immunol*. 2001;51(2):167-176.
774. Hoogsteen IJ, Marres HA, Wijffels KI, et al. Colocalization of carbonic anhydrase 9 expression and cell proliferation in human head and neck squamous cell carcinoma. *Clin Cancer Res*. 2005;11(1):97-106.
775. Tonks A, Pearn L, Mills KI, Burnett AK, Darley RL. The sensitivity of human cells expressing RUNX1-RUNX1T1 to chemotherapeutic agents. *Leukemia*. 2006;20(10):1883-1885.
776. Lam K, Zhang DE. RUNX1 and RUNX1-ETO: roles in hematopoiesis and leukemogenesis. *Front Biosci*. 2012;17:1120-1139.
777. Yeh KT, Chen TH, Yang HW, et al. Aberrant TGFbeta/SMAD4 signaling contributes to epigenetic silencing of a putative tumor suppressor, RunX1T1 in ovarian cancer. *Epigenetics*. 2011;6(6):727-739.
778. Leu YW, Yan PS, Fan M, et al. Loss of estrogen receptor signaling triggers epigenetic silencing of downstream targets in breast cancer. *Cancer Res*. 2004;64(22):8184-8192.
779. Schonwasser DC, Marais RM, Marshall CJ, Parker PJ. Activation of the mitogen-activated protein kinase/extracellular signal-regulated kinase pathway by conventional, novel, and atypical protein kinase C isotypes. *Mol Cell Biol*. 1998;18(2):790-798.
780. Monick MM, Carter AB, Flaherty DM, Peterson MW, Hunninghake GW. Protein kinase C zeta plays a central role in activation of the p42/44 mitogen-activated protein kinase by endotoxin in alveolar macrophages. *J Immunol*. 2000;165(8):4632-4639.
781. Samuels Y, Waldman T. Oncogenic mutations of PIK3CA in human cancers. *Curr Top Microbiol Immunol*. 2010;347:21-41.
782. UniProt. Protein Knowledgebase; 2013.

783. Lin CC, Chen LC, Tseng VS, et al. Malignant pleural effusion cells show aberrant glucose metabolism gene expression. *Eur Respir J*. 2011;37(6):1453-1465.
784. Reuters T. Pathway Maps; 2013.
785. R&D. Apoptosis Pathways; 2013.
786. Fernandes-Alnemri T, Armstrong RC, Krebs J, et al. In vitro activation of CPP32 and Mch3 by Mch4, a novel human apoptotic cysteine protease containing two FADD-like domains. *Proc Natl Acad Sci U S A*. 1996;93(15):7464-7469.
787. Gajate C, Mollinedo F. Cytoskeleton-mediated death receptor and ligand concentration in lipid rafts forms apoptosis-promoting clusters in cancer chemotherapy. *J Biol Chem*. 2005;280(12):11641-11647.
788. Wang J, Chun HJ, Wong W, Spencer DM, Lenardo MJ. Caspase-10 is an initiator caspase in death receptor signaling. *Proc Natl Acad Sci U S A*. 2001;98(24):13884-13888.
789. Micheau O, Tschopp J. Induction of TNF receptor I-mediated apoptosis via two sequential signaling complexes. *Cell*. 2003;114(2):181-190.
790. Zheng L, Schickling O, Peter ME, Lenardo MJ. The death effector domain-associated factor plays distinct regulatory roles in the nucleus and cytoplasm. *J Biol Chem*. 2001;276(34):31945-31952.
791. Muhlethaler-Mottet A, Flahaut M, Bourloud KB, et al. Individual caspase-10 isoforms play distinct and opposing roles in the initiation of death receptor-mediated tumour cell apoptosis. *Cell Death Dis*;2:e125.
792. Nakayama K, Toki T, Zhai YL, et al. Demonstration of focal p53 expression without genetic alterations in endometriotic lesions. *Int J Gynecol Pathol*. 2001;20(3):227-231.
793. Rikhof B, Corn PG, El-Deiry WS. Caspase 10 levels are increased following DNA damage in a p53-dependent manner. *Cancer Biol Ther*. 2003;2(6):707-712.
794. Wiemer AJ, Wiemer DF, Hohl RJ. Geranylgeranyl diphosphate synthase: an emerging therapeutic target. *Clin Pharmacol Ther*. 2011;90(6):804-812.
795. Graaf MR, Richel DJ, van Noorden CJ, Guchelaar HJ. Effects of statins and farnesyltransferase inhibitors on the development and progression of cancer. *Cancer Treat Rev*. 2004;30(7):609-641.
796. Zhao TT, Le Francois BG, Goss G, Ding K, Bradbury PA, Dimitroulakos J. Lovastatin inhibits EGFR dimerization and AKT activation in squamous cell carcinoma cells: potential regulation by targeting rho proteins. *Oncogene*. 2010;29(33):4682-4692.
797. Hendrix A, Maynard D, Pauwels P, et al. Effect of the secretory small GTPase Rab27B on breast cancer growth, invasion, and metastasis. *J Natl Cancer Inst*. 2010;102(12):866-880.
798. Artz JD, Dunford JE, Arrowood MJ, et al. Targeting a uniquely nonspecific prenyl synthase with bisphosphonates to combat cryptosporidiosis. *Chem Biol*. 2008;15(12):1296-1306.
799. Singh AP, Zhang Y, No JH, Docampo R, Nussenzweig V, Oldfield E. Lipophilic bisphosphonates are potent inhibitors of Plasmodium liver-stage growth. *Antimicrob Agents Chemother*. 2010;54(7):2987-2993.
800. Vennstrom B, Sheiness D, Zabielski J, Bishop JM. Isolation and characterization of c-myc, a cellular homolog of the oncogene (v-myc) of avian myelocytomatosis virus strain 29. *J Virol*. 1982;42(3):773-779.
801. Nesbit CE, Tersak JM, Prochownik EV. MYC oncogenes and human neoplastic disease. *Oncogene*. 1999;18(19):3004-3016.
802. Schneider J, Jimenez E, Rodriguez F, del Tanago JG. c-myc, c-erb-B2, nm23 and p53 expression in human endometriosis. *Oncol Rep*. 1998;5(1):49-52.
803. Dang CV. c-Myc target genes involved in cell growth, apoptosis, and metabolism. *Mol Cell Biol*. 1999;19(1):1-11.
804. Steiner P, Philipp A, Lukas J, et al. Identification of a Myc-dependent step during the formation of active G1 cyclin-cdk complexes. *EMBO J*. 1995;14(19):4814-4826.
805. Pelengaris S, Khan M, Evan G. c-MYC: more than just a matter of life and death. *Nat Rev Cancer*. 2002;2(10):764-776.

806. Tiso N, Pallavicini A, Muraro T, et al. Chromosomal localization of the human genes, CPP32, Mch2, Mch3, and Ich-1, involved in cellular apoptosis. *Biochem Biophys Res Commun*. 1996;225(3):983-989.
807. Siegel RM. Caspases at the crossroads of immune-cell life and death. *Nat Rev Immunol*. 2006;6(4):308-317.
808. Wang XJ, Cao Q, Liu X, et al. Crystal structures of human caspase 6 reveal a new mechanism for intramolecular cleavage self-activation. *EMBO Rep*. 2010;11(11):841-847.
809. Hengartner MO. The biochemistry of apoptosis. *Nature*. 2000;407(6805):770-776.
810. Richards S, Watanabe C, Santos L, Craxton A, Clark EA. Regulation of B-cell entry into the cell cycle. *Immunol Rev*. 2008;224:183-200.
811. Chun HJ, Zheng L, Ahmad M, et al. Pleiotropic defects in lymphocyte activation caused by caspase-8 mutations lead to human immunodeficiency. *Nature*. 2002;419(6905):395-399.
812. Olson NE, Graves JD, Shu GL, Ryan EJ, Clark EA. Caspase activity is required for stimulated B lymphocytes to enter the cell cycle. *J Immunol*. 2003;170(12):6065-6072.
813. Wang JJ, Li YF, Jin YY, Wang X, Chen TX. Effects of Epstein-Barr virus on the development of dendritic cells derived from cord blood monocytes: an essential role for apoptosis. *Braz J Infect Dis*. 2012;16(1):19-26.
814. Cowling V, Downward J. Caspase-6 is the direct activator of caspase-8 in the cytochrome c-induced apoptosis pathway: absolute requirement for removal of caspase-6 prodomain. *Cell Death Differ*. 2002;9(10):1046-1056.
815. Nakagawa T, Tsuruma K, Uehara T, Nomura Y. GMEB1, a novel endogenous caspase inhibitor, prevents hypoxia- and oxidative stress-induced neuronal apoptosis. *Neurosci Lett*. 2008;438(1):34-37.
816. Zhang S, Zhang Y, Wei X, et al. Expression and regulation of a novel identified TNFAIP8 family is associated with diabetic nephropathy. *Biochim Biophys Acta*. 2010;1802(11):1078-1086.
817. Liu T, Gao H, Yang M, Zhao T, Liu Y, Lou G. Correlation of TNFAIP8 overexpression with the proliferation, metastasis, and disease-free survival in endometrial cancer. *Tumour Biol*. 2014;35(6):5805-5814.
818. Kumar D, Whiteside TL, Kasid U. Identification of a novel tumor necrosis factor-alpha-inducible gene, SCC-S2, containing the consensus sequence of a death effector domain of fas-associated death domain-like interleukin- 1beta-converting enzyme-inhibitory protein. *J Biol Chem*. 2000;275(4):2973-2978.
819. You Z, Ouyang H, Lopatin D, Polver PJ, Wang CY. Nuclear factor-kappa B-inducible death effector domain-containing protein suppresses tumor necrosis factor-mediated apoptosis by inhibiting caspase-8 activity. *J Biol Chem*. 2001;276(28):26398-26404.
820. Kumar D, Gokhale P, Broustas C, Chakravarty D, Ahmad I, Kasid U. Expression of SCC-S2, an antiapoptotic molecule, correlates with enhanced proliferation and tumorigenicity of MDA-MB 435 cells. *Oncogene*. 2004;23(2):612-616.
821. Zhang C, Chakravarty D, Sakabe I, et al. Role of SCC-S2 in experimental metastasis and modulation of VEGFR-2, MMP-1, and MMP-9 expression. *Mol Ther*. 2006;13(5):947-955.
822. Dong QZ, Zhao Y, Liu Y, et al. Overexpression of SCC-S2 correlates with lymph node metastasis and poor prognosis in patients with non-small-cell lung cancer. *Cancer Sci*. 2010;101(6):1562-1569.
823. Sadacharan SK, Cavanagh AC, Gupta RS. Immunoelectron microscopy provides evidence for the presence of mitochondrial heat shock 10-kDa protein (chaperonin 10) in red blood cells and a variety of secretory granules. *Histochem Cell Biol*. 2001;116(6):507-517.
824. Cappello F, Bellafiore M, David S, Anzalone R, Zummo G. Ten kilodalton heat shock protein (HSP10) is overexpressed during carcinogenesis of large bowel and uterine exocervix. *Cancer Lett*. 2003;196(1):35-41.
825. Jia H, Halilou AI, Hu L, Cai W, Liu J, Huang B. Heat shock protein 10 (Hsp10) in immune-related diseases: one coin, two sides. *Int J Biochem Mol Biol*. 2011;2(1):47-57.

826. Macario AJ, Conway de Macario E. Sick chaperones, cellular stress, and disease. *N Engl J Med*. 2005;353(14):1489-1501.
827. Corrao S, Campanella C, Anzalone R, et al. Human Hsp10 and Early Pregnancy Factor (EPF) and their relationship and involvement in cancer and immunity: current knowledge and perspectives. *Life Sci*. 2010;86(5-6):145-152.
828. Gupta S, Knowlton AA. HSP60 trafficking in adult cardiac myocytes: role of the exosomal pathway. *Am J Physiol Heart Circ Physiol*. 2007;292(6):H3052-3056.
829. Cheng SJ, Zheng ZQ. Early pregnancy factor in cervical mucus of pregnant women. *Am J Reprod Immunol*. 2004;51(2):102-105.
830. Vanags D, Williams B, Johnson B, et al. Therapeutic efficacy and safety of chaperonin 10 in patients with rheumatoid arthritis: a double-blind randomised trial. *Lancet*. 2006;368(9538):855-863.
831. Athanasas-Platsis S, Zhang B, Hillyard NC, et al. Early pregnancy factor suppresses the infiltration of lymphocytes and macrophages in the spinal cord of rats during experimental autoimmune encephalomyelitis but has no effect on apoptosis. *J Neurol Sci*. 2003;214(1-2):27-36.
832. al VVMe. Prognostic effect of EIF4EBP1 on ovarian cancer: A single gene biomarker for overall survival and platinum response; 2013.
833. Jovicic A, Zaldivar Jolissaint JF, Moser R, Silva Santos Mde F, Luthi-Carter R. MicroRNA-22 (miR-22) overexpression is neuroprotective via general anti-apoptotic effects and may also target specific Huntington's disease-related mechanisms. *PLoS One*. 2013;8(1):e54222.
834. Wagner EF, Nebreda AR. Signal integration by JNK and p38 MAPK pathways in cancer development. *Nat Rev Cancer*. 2009;9(8):537-549.
835. Makker A, Goel MM, Das V, Agarwal A. PI3K-Akt-mTOR and MAPK signaling pathways in polycystic ovarian syndrome, uterine leiomyomas and endometriosis: an update. *Gynecol Endocrinol*. 2012;28(3):175-181.
836. Richard M, Drouin R, Beaulieu AD. ABC50, a novel human ATP-binding cassette protein found in tumor necrosis factor-alpha-stimulated synoviocytes. *Genomics*. 1998;53(2):137-145.
837. Hlavata I, Mohelnikova-Duchonova B, Vaclavikova R, et al. The role of ABC transporters in progression and clinical outcome of colorectal cancer. *Mutagenesis*. 2012;27(2):187-196.
838. Yi YC, Wang SC, Chao CC, Su CL, Lee YL, Chen LY. Evaluation of serum autoantibody levels in the diagnosis of ovarian endometrioma. *J Clin Lab Anal*. 2010;24(5):357-362.
839. Kikuchi Y, Momose E, Kizawa I, Kuki E, Kato K. Elevated serum alpha-hydroxybutyrate dehydrogenase in patients with ovarian carcinoma. *Acta Obstet Gynecol Scand*. 1985;64(7):553-556.
840. Slomovitz BM, Coleman RL. The PI3K/AKT/mTOR pathway as a therapeutic target in endometrial cancer. *Clin Cancer Res*. 2012;18(21):5856-5864.
841. Zha X, Wang F, Wang Y, et al. Lactate dehydrogenase B is critical for hyperactive mTOR-mediated tumorigenesis. *Cancer Res*. 2011;71(1):13-18.
842. de Haas T, Hasselt N, Troost D, et al. Molecular risk stratification of medulloblastoma patients based on immunohistochemical analysis of MYC, LDHB, and CCNB1 expression. *Clin Cancer Res*. 2008;14(13):4154-4160.
843. Rodrigues AJ, Coppola G, Santos C, et al. Functional genomics and biochemical characterization of the C. elegans orthologue of the Machado-Joseph disease protein ataxin-3. *FASEB J*. 2007;21(4):1126-1136.
844. al Sje. The deubiquitylase Ataxin-3 restricts PTEN transcription in lung cancer cells. Oncogene; 2013.
845. Seet LF, Liu N, Hanson BJ, Hong W. Endofin recruits TOM1 to endosomes. *J Biol Chem*. 2004;279(6):4670-4679.
846. Yamakami M, Yokosawa H. Tom1 (target of Myb 1) is a novel negative regulator of interleukin-1- and tumor necrosis factor-induced signaling pathways. *Biol Pharm Bull*. 2004;27(4):564-566.

847. Shaulian E, Karin M. AP-1 in cell proliferation and survival. *Oncogene*. 2001;20(19):2390-2400.
848. Mocellin S, Rossi CR, Pilati P, Nitti D. Tumor necrosis factor, cancer and anticancer therapy. *Cytokine Growth Factor Rev*. 2005;16(1):35-53.
849. Yang RY, Rabinovich GA, Liu FT. Galectins: structure, function and therapeutic potential. *Expert Rev Mol Med*. 2008;10:e17.
850. Nangia-Makker P, Conklin J, Hogan V, Raz A. Carbohydrate-binding proteins in cancer, and their ligands as therapeutic agents. *Trends Mol Med*. 2002;8(4):187-192.
851. Levi G, Teichberg VI. Isolation and physicochemical characterization of electrolectin, a beta-D-galactoside binding lectin from the electric organ of Electrophorus electricus. *J Biol Chem*. 1981;256(11):5735-5740.
852. Kasai K, Hirabayashi J. Galectins: a family of animal lectins that decipher glycocodes. *J Biochem*. 1996;119(1):1-8.
853. Dumic J, Dabelic S, Flogel M. Galectin-3: an open-ended story. *Biochim Biophys Acta*. 2006;1760(4):616-635.
854. Van den Brule F, Castronovo V eds. Laminin binding lectins during invasion and metastasis In: Publishers HA ed: Harwood Academic Publishers; 1999.
855. Raz A, Lotan R. Lectin-like activities associated with human and murine neoplastic cells. *Cancer Res*. 1981;41(9 Pt 1):3642-3647.
856. Meromsky L, Lotan R, Raz A. Implications of endogenous tumor cell surface lectins as mediators of cellular interactions and lung colonization. *Cancer Res*. 1986;46(10):5270-5275.
857. Perillo NL, Marcus ME, Baum LG. Galectins: versatile modulators of cell adhesion, cell proliferation, and cell death. *J Mol Med (Berl)*. 1998;76(6):402-412.
858. Bank RPd. High Resolution X-Ray Structure of Human Galectin-3 in complex with LacNAc
RCSB Protein data Bank; 2011.
859. Raimond J, Zimonjic DB, Mignon C, et al. Mapping of the galectin-3 gene (LGALS3) to human chromosome 14 at region 14q21-22. *Mamm Genome*. 1997;8(9):706-707.
860. Liu FT, Patterson RJ, Wang JL. Intracellular functions of galectins. *Biochim Biophys Acta*. 2002;1572(2-3):263-273.
861. Cooper DN. Galectinomics: finding themes in complexity. *Biochim Biophys Acta*. 2002;1572(2-3):209-231.
862. Henderson NC, Sethi T. The regulation of inflammation by galectin-3. *Immunol Rev*. 2009;230(1):160-171.
863. Mazurek N, Conklin J, Byrd JC, Raz A, Bresalier RS. Phosphorylation of the beta-galactoside-binding protein galectin-3 modulates binding to its ligands. *J Biol Chem*. 2000;275(46):36311-36315.
864. Yu LG. Circulating galectin-3 in the bloodstream: An emerging promoter of cancer metastasis. *World J Gastrointest Oncol*. 2010;2(4):177-180.
865. Kuwabara I, Liu FT. Galectin-3 promotes adhesion of human neutrophils to laminin. *J Immunol*. 1996;156(10):3939-3944.
866. Warfield PR, Makker PN, Raz A, Ochieng J. Adhesion of human breast carcinoma to extracellular matrix proteins is modulated by galectin-3. *Invasion Metastasis*. 1997;17(2):101-112.
867. Nangia-Makker P, Honjo Y, Sarvis R, et al. Galectin-3 induces endothelial cell morphogenesis and angiogenesis. *Am J Pathol*. 2000;156(3):899-909.
868. Dam TK, Gabius H-J, AndrÃ© S, Kaltner H, Lensch M, Brewer CF. Galectins Bind to the Multivalent Glycoprotein Asialofetuin with Enhanced Affinities and a Gradient of Decreasing Binding Constantsâ€ *Biochemistry*. 2005;44(37):12564-12571.
869. Inohara H, Raz A. Functional evidence that cell surface galectin-3 mediates homotypic cell adhesion. *Cancer Res*. 1995;55(15):3267-3271.

870. Matarrese P, Tinari N, Semeraro ML, Natoli C, Iacobelli S, Malorni W. Galectin-3 overexpression protects from cell damage and death by influencing mitochondrial homeostasis. *FEBS Lett*. 2000;473(3):311-315.
871. Hoyer KK, Pang M, Gui D, et al. An anti-apoptotic role for galectin-3 in diffuse large B-cell lymphomas. *Am J Pathol*. 2004;164(3):893-902.
872. Lahm H, Andre S, Hoeflich A, et al. Comprehensive galectin fingerprinting in a panel of 61 human tumor cell lines by RT-PCR and its implications for diagnostic and therapeutic procedures. *J Cancer Res Clin Oncol*. 2001;127(6):375-386.
873. Yang RY, Hsu DK, Yu L, Ni J, Liu FT. Cell cycle regulation by galectin-12, a new member of the galectin superfamily. *J Biol Chem*. 2001;276(23):20252-20260.
874. Noel JC, Chapron C, Borghese B, Fayt I, Anaf V. Galectin-3 is overexpressed in various forms of endometriosis. *Appl Immunohistochem Mol Morphol*. 2011;19(3):253-257.
875. Okaro AC, Fennell DA, Corbo M, Davidson BR, Cotter FE. Pk11195, a mitochondrial benzodiazepine receptor antagonist, reduces apoptosis threshold in Bcl-X(L) and Mcl-1 expressing human cholangiocarcinoma cells. *Gut*. 2002;51(4):556-561.
876. Korkmaz D, Bastu E, Dural O, Yasa C, Yavuz E, Buyru F. Apoptosis through regulation of Bcl-2, Bax and Mcl-1 expressions in endometriotic cyst lesions and the endometrium of women with moderate to severe endometriosis. *J Obstet Gynaecol*. 2013;33(7):725-728.
877. Finbarr Cotter DF. Peripheral benzodiazepine receptor independent superoxide generation. Vol. US20060111288 A1. US; 2006.
878. Pike VW, Halldin C, Crouzel C, et al. Radioligands for PET studies of central benzodiazepine receptors and PK (peripheral benzodiazepine) binding sites--current status. *Nucl Med Biol*. 1993;20(4):503-525.
879. Banker DE, Cooper JJ, Fennell DA, Willman CL, Appelbaum FR, Cotter FE. PK11195, a peripheral benzodiazepine receptor ligand, chemosensitizes acute myeloid leukemia cells to relevant therapeutic agents by more than one mechanism. *Leuk Res*. 2002;26(1):91-106.